8th Young Geotechnical Professionals Conference

Wellington, New Zealand
5th-8th November 2008

8YGPC

Conference Proceedings

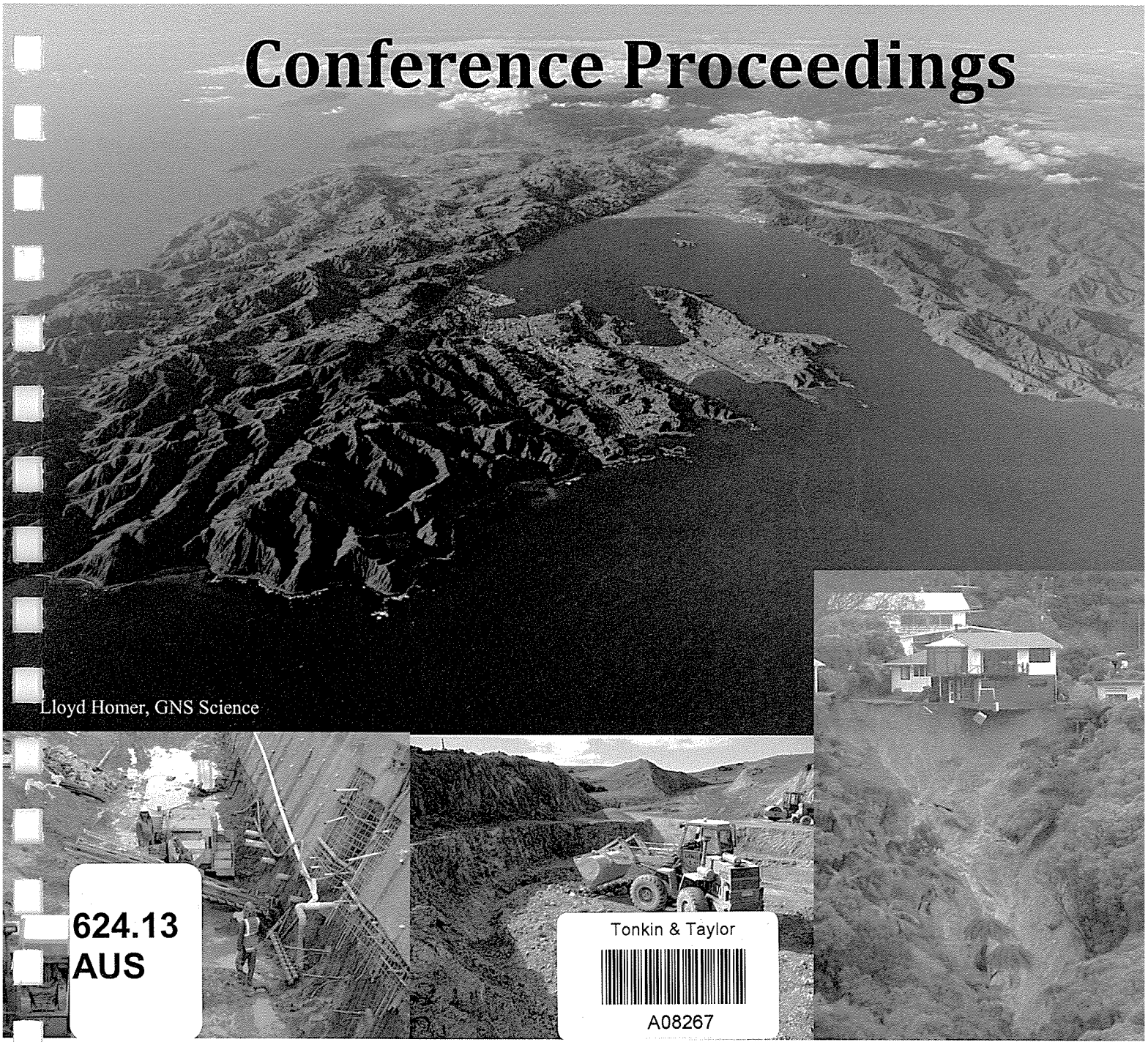

Lloyd Homer, GNS Science

EARTHQUAKE COMMISSION
KŌMIHANA RŪWHENUA

ENGINEERS
AUSTRALIA

IPENZ
ENGINEERS NEW ZEALAND

8YGPC

Proceedings of the 8th New Zealand - Australia Young Geotechnical Professionals Conference

Copthorne Hotel, Wellington, November 5th - 8th 2008

ORGANISING COMMITTEE:
Elisabeth Bowman, Lucy Coe, Beverley Curley, Paul Fletcher, Andrew Kennedy, Ross Kendrick

EQC
EARTHQUAKE COMMISSION
KŌMIHANA RŪWHENUA

ENGINEERS AUSTRALIA

IPENZ
ENGINEERS NEW ZEALAND

Welcome

Welcome to the Eighth Australia & New Zealand Young Geotechnical Professionals Conference, Wellington, New Zealand, 2008. Following on from previous successful conferences held in Sydney 1994, Auckland 1996, Melbourne 1998, Perth 2000, Rotorua 2002, the Gold Coast 2004 and Adelaide 2006, this biannual event is a joint initiative of the New Zealand Geotechnical Society and the Australian Geomechanics Society.

The aims of the conference are to:

- Promote the professional development of delegates through sharing experience and ideas, and by presenting a paper to senior professionals and peers
- Expand and strengthen the lines of communication between young professionals within the field of geomechanics
- Promote an enhanced perspective of the varied roles, responsibilities and opportunities encompassed by the geotechnical profession

The specific goal of the organising committee has been to prepare an interesting, meaningful, informative and enjoyable conference from which delegates can gain an enhanced understanding of their profession.

As with all previous YGP conferences, support of the geotechnical community is very important to ensure a successful event. We would like to thank all the companies and individuals that have provided assistance to committee members in our preparation of the conference over the past two years. Thanks also to the various employers of the committee members (many of whom are also event sponsors) for their support in releasing staff to organise and attend this conference.

A big thanks goes to Nick Perrin, Dick Beetham and Rob Langridge from GNS Science for designing and accompanying us on the field trip.

Bruce Symmans and Gavin Alexander will be acting as senior mentors along with Elisabeth Bowman, Ross Kendrick and our guest speaker will be Prof John Atkinson. Without such valuable input, the conference would lack much of what makes it such a success.

It is hoped that delegates will interact with their peers openly, make some new friends and maximise their exposure to the geotechnical community during the conference. A short question time has been allocated to each talk and we hope that delegates will take this opportunity to ask questions and learn more about the topics on offer.

Most of all we hope you have a rewarding time at the conference. The organising committee members look forward to meeting you all and joining you in an informative and enjoyable three days.

Elisabeth Bowman
Proceedings Editor
8YGPC Committee

Sponsors

The organising committee would like to gratefully acknowledge the financial support from the following sponsors:

Platinum:

The Earthquake Commission

Gold:

Beca Geotechnical,
Coffey Geotechnics,
Golder Associates (double gold),
Griffiths Drilling,
Tonkin & Taylor Consultants

Silver:

Broons Hire,
Riley Consultants (double silver),
Connell Wagner Consultants,
Geotechnics,
Geotek Services,
Maunsell AECOM,
Opus International Consultants (double silver),
Pro-Drill,
Websters Drilling & Exploration

Imagine the view from the top

Be part of Beca Geotechnical's 40-strong team, working on some of the biggest infrastructure projects around, aiming to solve some of the most complex problems in the ground.

Engineering Geology / Hydrogeology / Geotechnical Engineering

Auckland // Tauranga // Wellington // Christchurch // Singapore

www.beca.com

Beca
Geotechnical

Coffey Geotechnics is a specialist ground engineering consultancy, helping clients manage the earth.

We specialise in providing solutions from initial site investigation through to analysis, design and construction monitoring of ground conditions for major infrastructure, buildings and mines.

Connected to a global network of specialists, we add value to projects around the world from our offices in New Zealand, Australia, Canada and the United Kingdom.

Our New Zealand offices are located in Newmarket, Silverdale, Tauranga and Christchurch.

If you are interested in finding out more about opportunities with Coffey in New Zealand and around the world, visit coffey.com

coffey geotechnics
SPECIALISTS MANAGING THE EARTH

coffey.com

Seeking Challenges? Looking for Inspiring and Exciting Projects? Want to Explore the World?

Golder Associates is currently looking for **Geotechnical Engineers and Engineering Geologists** of all levels to join our specialist teams in Australia and New Zealand.

At Golder we know that the pursuit of excellence requires diversity, challenge, innovation and opportunities at every step. We offer a great working environment, cutting edge projects and the chance to collaborate with leading specialists around the world.

Own shares in the company. Focus on your professional development with courses in leadership, management and technical development. Make use of a gym membership subsidy and take advantage of work life balance initiatives such as extra leave entitlements.

Golder Associates is an internationally renowned consultancy and a leader in the field of geotechnical engineering, environmental sciences and ground engineering. With over 7,000 employees working out of 150 offices worldwide, we provide a truly global presence and great opportunities for international exposure.

There is more to life at Golder.

Golder Associates

Enquiries:

Perth & Adelaide | Jake Leahy | jleahy@golder.com.au | + 61 8 9213 7600
Queensland | Cate Clark | cclark@golder.com.au | + 61 7 3721 5400
Melbourne & Sydney | Melanie Neal | mneal@golder.com.au | + 61 3 8862 3500
New Zealand | Jill Bond | jbond@golder.co.nz | +64 3 377 5696

BRW. CLIENT CHOICE AWARDS 2008

www.golder.com

solutions@golder.com

OPUS

BROONS

RILEY CONSULTANTS

Connell Wagner

PRO-DRILL

MAUNSELL | AECOM

CONTENTS

Geotechnical Challenges for Road Construction in the Hamilton Area

Sarah Amoore
Opus International Consultants, Hamilton, New Zealand

Keywords: Hamilton, liquefaction, compressible soils, peat soils, gully instability, high water level.

ABSTRACT

The geology in the Hamilton area consists of peat deposits in low lying flat areas. The peat overlies the Hinuera formation (cross bedded pumice sand, silt and gravel) and the Walton Subgroup, (pumiceous silt, dense sand and gravel interbedded with peat).

There are many challenges in the geology of the Waikato area due to the subsurface geology. With the fine sands in the Hinuera formation there is potential for liquefaction in a large earthquake. The high water table in the Waikato causes problems with cuts. The soft soils of the peat deposits, Hinuera Formation and Walton subgroup cause ongoing challenges with settlement. Due to the soft, interbedded soils we also have many issues with gully instability, and we also have challenges of reusing cut material as fill.

1 INTRODUCTION

Opus Hamilton are involved in a large number of roading projects in the Hamilton area. These projects provide numerous geotechnical challenges. This paper focuses on the following challenges, peat soils, soft soils, liquefaction, high water level and gully instability. Examples have been used from Cambridge Bypass, Piako Road, and Te Rapa Bypass. This paper discusses how these issues were investigated and mitigated.

2 HAMILTON GEOLOGY

The geology of the Hamilton area consists of young extensive peat deposits, the Hinuera formation and associated alluvial sediments, and the Walton subgroup (Puketoka formation) (Figure 1).

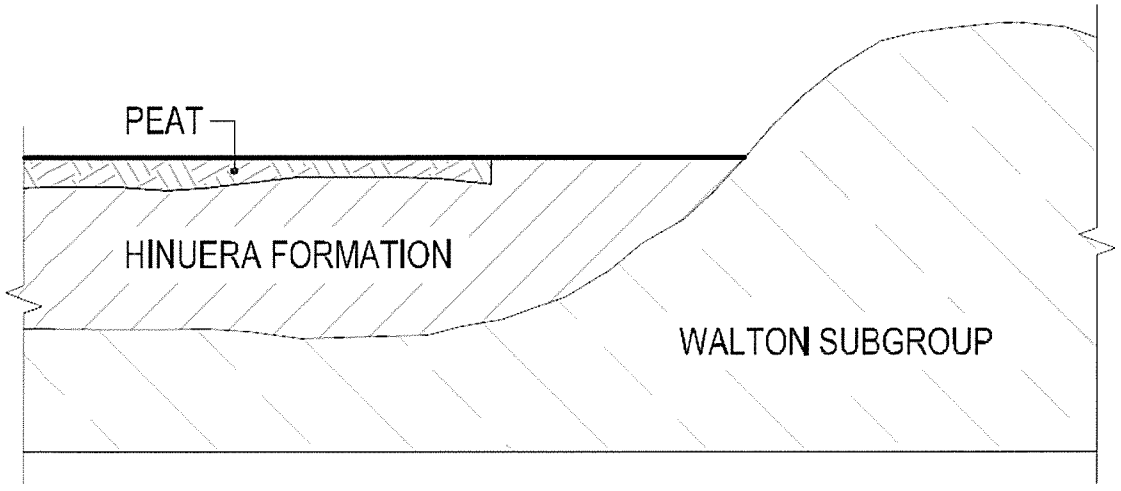

Figure 1: Showing the soft peat soils overlying the Hinuera Formation, and the lower Walton Subgroup forming the hills.

The extensive peat deposits are a Holocene deposit and predominately consist of soft, dark brown to black organic rich mud, muddy peat and woody peat. The Peat deposits are mainly found in the low lying areas on the outskirts of Hamilton.

The Hinuera Formation was deposited in the late Pleistocene Epoch. It is up to 90m thick and comprises of cross-bedded pumiceous sands, silts, and gravels (Figure 2), interbedded with peat. The Hinuera Formation is the result of deposition of typically volcanic deposits from the Taupo Volcanic Zone by a braided ancestral Waikato River.

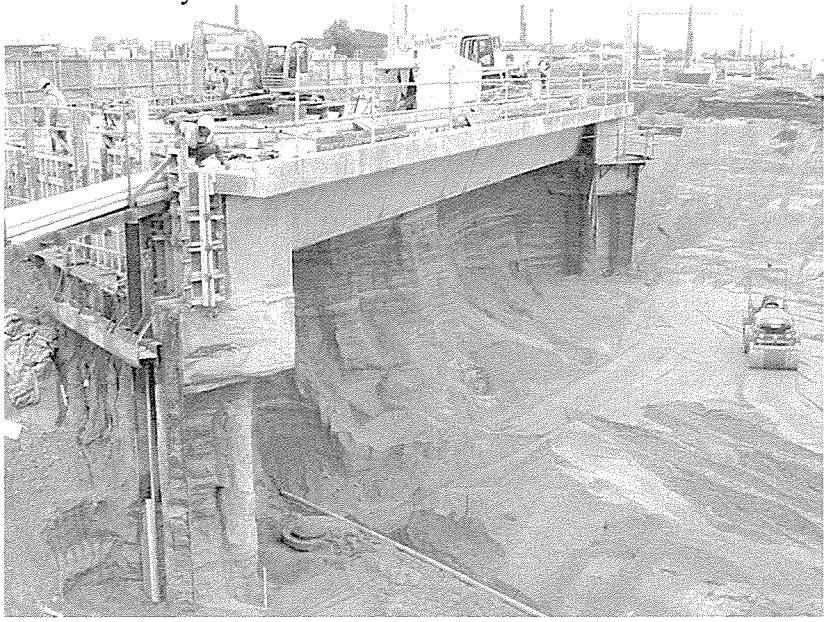

Figure 2: Showing the interbedded sands and silts of the Hinuera Formation

The Walton Subgroup is an early Pleistocene deposit and predominately consists of highly weathered pumiceous silt and sand interbedded with peat. The Walton subgroup is mostly subsurface in the Hamilton lowlands, but forms prominent low hills, up to 100m above sea level.

The Walton subgroup appears as two layers: a silt/clay layer which is more noticeable on hills, and a fine to coarse dense sand, which is located generally under the Hinuera formation on the lowlands.

3 CHALLENGES

3.1 Organic Soils

The Waikato area has many organic soils, some overlying the Hinuera Formation and some throughout the Hinuera Formation and Walton subgroup. Large settlements are a problem in Organic soils but they also cause other problems, such as creep deformation, and very low shear strength.

Peats have a very high compressibility and settlement in peat is usually a two stage process – consolidation followed by creep. This means that they have ongoing issues with continuous settlement. They also experience volume change due to water content changes, lateral spreading which causes reduced bearing capacity, and a very low shear strength which limits potential embankment heights. They also provide a poor subgrade for roading.

3.4.1 Case study

The Piako Road area has approximately 3m of soft to very soft peat under the road which overlays the Hinuera formation, it has experienced many ongoing problems. A 2km section of the road has cracked longitudinally; it has poor surface quality, and has incurred high maintenance costs. The road has a deep drain on one side and a shallower drain on the other side.

This road has numerous ongoing problems (cracking and requiring ongoing maintenance) with differential settlement due to the lower groundwater level on either side of the road, and lateral spreading of the embankment.

It is thought that some of the cracking was due to the willow trees over summer that were located on one side of the road, reducing the water content and therefore causing differential settlement, or the fact that the drainage on one side of the road is deeper than the other side of the road. Thee problems on Piako Road could be fixed by either: pavement reconstruction, excavation and replacement of the peat, piling through the soft peat, stabilisation of the peat soils, or heavy tamping.

3.2 Soft Soils

The Hamilton area has many soft compressible soils, the silts of the Hinuera formation as well as the top silty unit of the Walton Park sub-group. Soft soils are associated with settlement, as they are very compressible and the time over which settlement occurs can be long, settlement can lead to problems with weak subgrade for pavement design and embankment stability problems.

Factors which affect the amount of settlement are: the load applied to the soil, soil compressibility, the depth of compressible soils. The time for settlement is dependent on the soil parameters and the length of the drainage path.

3.2.1 Settlement Mitigation

The need for mitigation of settlement depends on the time we have for construction and the amount of settlement acceptable at the end of construction. If this can be accommodated for in construction, then no settlement mitigation is required

There are numerous ways to mitigate settlement these include preloading, surcharging, wick drains and undercutting.

Preloading involves constructing fill to the finished surface level with additional fill to allow for the expected settlement. The preload is then removed to subgrade level once settlement is within 50mm of the expected final level before constructing the pavement. Some topping up of the embankment may be needed if actual settlement exceeds our predictions. Monitoring of settlement is required to assess when it is appropriate to remove the preload or if topping is required.

Surcharging involves temporarily applying additional height to the embankment to accelerate settlement. The embankment is constructed to the finished level with additional fill to allow for settlement then surcharged typically 1m to 2m. The surcharge is removed to subgrade level when sufficient settlement has occurred. Surcharging may also be used to mitigate creep settlement in organic soils.

Wick drains are pre-fabricated vertical drains installed into the compressible ground to shorten drainage paths and accelerate settlement. The wick drains should penetrate the full depth of compressible soils.

Undercutting involves digging out the compressible ground and replacing it with stiffer fill to reduce the amount of settlement.

3.2.2 Soft soils of the Te Rapa Bypass

On Te Rapa bypass we encountered layers near bridge foundations where mitigation of settlement was required, in some areas we had expected settlement of 150mm over 4.5 years. We recommended wick drains be installed to accelerate this settlement to about 6 months.

In some areas we were required to undercut the soft organic soils at the base of a gully by 3m, we then applied a surcharge for 3 months to reduce the settlement risks.

3.3 Earthquake Liquefaction

The Waikato area consists of many potentially liquefiable soils. Liquefaction occurs predominately in saturated, loose, fine sands and silts. Gradings of sand sampled throughout the Hamilton region show that the sands within the Hinuera formation generally have a particle distribution that is susceptible to liquefaction.

Liquefaction is caused by rapid cyclic shearing of the soil such that pore water pressures build up and the soil loses strength and encounters possible settlement after excess pore pressures dissipate. With roading we are mainly interested in the reduced bearing capacity of piles and retaining walls, as there is a large cost involved with these structures, liquefaction can also create sand boils disrupting the ground, and reduced lateral spreading, buoyancy of buried services, subsidence.

The potential for earthquake induced liquefaction is primarily dependent on the earthquake magnitude, amplitude and duration characteristics, soil particle size distribution, soil density and over-burden stress. There is also some evidence that the age and the history of the deposit are a factor. If deposits have been shaken before they are less likely to liquefy.

We use various methods for investigating whether the sands are susceptible to liquefaction, we use lab testing from gradings, density from SPTs and conventional CPTs, and seismic CPTs.

We assess the potential for liquefaction to occur during the design earthquake using the cyclic stress approach NCEER method. To mitigate the effects of liquefaction ground improvement is used in the way of stone columns or driving piles through the liquefiable layers.

3.3.1 Liquefaction for the Te Rapa Project

The recent alluvial deposits from the Hinuera Formation have been identified as liquefiable on the Te Rapa Bypass project, this has affected design of the bridge approach and foundations. Due to liquefaction on this project we have recommended stone columns under bridge approaches.

3.4 High Groundwater levels

The Hamilton area has a high groundwater level in the Cambridge Bypass region. The depth to ground water level is between 1.2m at the shallowest to 8m at the deepest point.

High groundwater makes excavation of sands very difficult, as it reduces the stability of the cuts. This affects both undercuts and cuts, because the sand material is collapsing in to the cut. It also gives pavements a reduced life due to the wet subgrade.

To deal with a high water table, you can avoid doing cuts in the area, or support all excavations possibly with sheet piles, or undertake dewatering in the area of the excavation either permanently or for the short term.

3.5 Gully Instability

With the interbedded sands and silts of the Hinuera formation, there are numerous issues with gully instability. The steeps sides of a gully through the Hinuera formation can cause slips and erosion.

The Karapiro Stream gully has 40 degree slopes and is 200m wide at the top (Figure 3), the Cambridge Bypass will cross this gully. The Karapiro gully was created by incision of a small stream in the base. Because the gully slopes are within the interbedded sands and silts of the Hinuera formation they encounter many problems with seepage through the silt layers causing slumps.

These problems can lead to slips on the gully slopes which can damage piers and undermine abutments. To mitigate these issues we need to extend the bridge further past the gully than normal, and increase the number of piles.

Figure 3: Cambridge Bypass proposed crossing of Karapiro Gully Stream

3.6 Suitability of Cut Material for Fill

With all roading jobs there are areas of cut and fill required at all points, and finding suitable fill is always a problem. The ability to use clayey or silty soils as fill is generally dependent on there natural water content, the water content range over which the soils can be compacted, and the effort required to change the water content, the sensitivity of soils to disturbance, and the shear strength during compaction

With most of the cuts in the Hamilton area being in the Hinuera Formation, or the small hills in the Walton subgroup, there is a general lack of suitable cut material. The interbedded nature of the Hinuera Formation generally rules out cut to fill as an option, as it is difficult to separate the sands and the silts. It is also easy to underestimate the percentage not suitable as fill material. The silts of the upper part of the Walton Subgroup also have a high water content and are quite sensitive therefore replacing the soils without drying them is not an option. This makes cutting to fill very costly for this material.

3.6.1 Investigation

Field investigations of Test Pits and PQ Size boreholes are used to get suitable quantities of samples for Laboratory Testing. These samples are then used for optimum water content/dry density curves. This allows us to establish how much of this material is suitable in its current state for cut to fill, or how much effort is required for the material to be used.

3.6.2 Te Rapa Bypass Cut Slopes for Fill Example

Most of the fill excavated as part of the Te Rapa Bypass will be from the Onion Road cut. This fill has been examined through lab testing and it is too wet or sensitive to be used as fill. The extra cut material is from further north in the job and this is through Hinuera Formation consisting of mainly sand deposits, although this material is too wet there is minimal effort required to make this soil useful and therefore will be dried and placed as fill.

4 CONCLUSIONS

Due to the highly variable soils found in the Waikato Region there are many geotechnical challenges. The Peat deposits are very compressible and cause numerous problems in roading, the best solution for peat soils is removal. The Hinuera Formation sands create gully instability problems where extra stabilisation is required, they are also liquefiable so major roading structures require ground improvement. The soft soils of the Hinuera Formation and Walton Subgroup are compressible and often require mitigation for settlement to be completed in the construction timeframe. The use of the interbedded silts and sands for cut to fill material is generally not suitable. More allowance should be made when estimating cut to waste.

The high groundwater level throughout the Hamilton region makes cuts difficult and also reduces pavement life.

REFERENCES

Edbrooke, S.W. (2005) *Geology of the Waikato area. Institute of Geological and Nuclear Sciences 1:250 000 geological map 4.* Institute of Geological and Nuclear Sciences Limited, Lower Hutt, New Zealand.

Edger, N. (2000) *Piako Road Geotechnical Assessment of Road Cracking*, Report No G2138 to Matamata Piako District Council. (Unpublished) Opus International Consultants Ltd, Hamilton, New Zealand.

Keepa, C. (2008) *Te Rapa Bypass Geotechnical Assessment,* Report No. G2448 to Transit New Zealand. (Unpublished). Opus International Consultants Ltd, Hamilton, New Zealand.

Results of tests performed on ~1 Ma distal reworked Kidnappers eruption volcaniclastics in the Tauranga Harbour area

James M. Arthurs
Geology Programme (SGGES) and IESE, University of Auckland, NZ

Keywords: sensitivity, triaxial testing, variability, Atterberg limits, index properties, volcaniclastic

ABSTRACT

Index and shear strength parameters often vary within deposits of a similar age and geologic origin. In the case of sensitive soils in the Tauranga Harbour area, variations occur at outcrop scale within a single geologic unit. This study focuses on a volcaniclastic clayey silt, which is typically exposed near sea level. Although this deposit was generated during one eruptive episode at ~1 Ma, variations in deposition processes and subsequent weathering have contributed to a diversity of geomechanical properties. Samples were collected from several Tauranga locations and used for drained and undrained triaxial, ring shear, and Atterberg limits tests. These test results show variability of material properties on a decimetre scale. The tests also show unexpected stress-strain relationships for materials which are dominated by silt-sized particles (as all these materials were originally, at the time of deposition). Some drained triaxial test results show increases in strength after 20% strain or more. Further work is underway to better define the relationship between shear strength parameters and index properties, and to examine the untypical behaviour of these soils.

1 INTRODUCTION

1.1 Geology and Setting

The eruption of the Kidnappers ignimbrite approximately one million years ago blanketed much of the North Island in pyroclastic material (Wilson et al., 1995). Immediately after deposition, this material was reworked and redeposited, typically by fluvial action. The effects of reworking vary from very faint bedding and lamination within near-intact deposits to complete remobilization with loss of the fine particles. The materials of focus in this study are reworked fine grained deposits from the early ash-fall stages of the Kidnappers eruption. These soils are typically exposed above a lignite or other organic rich palaeosol. Sand and gravel sized pyroclastic materials (ignimbrite, or its reworked equivalent) are exposed on top of the silty materials. Above these are further pyroclastic deposits interbedded with pedogenic soils ("Hamilton Ash"). At many locations, the 61 ka Rotoehu ash is exposed near the top of the sequence.

The fine-grained ash from the Kidnappers eruption is preserved in a number of locations near the Tauranga Harbour, particularly on the four peninsulas west of the city centre. Samples for this study were collected from the Otemoetai, Omokoroa, Te Puna, and Pahoia peninsulas (Figure 1).

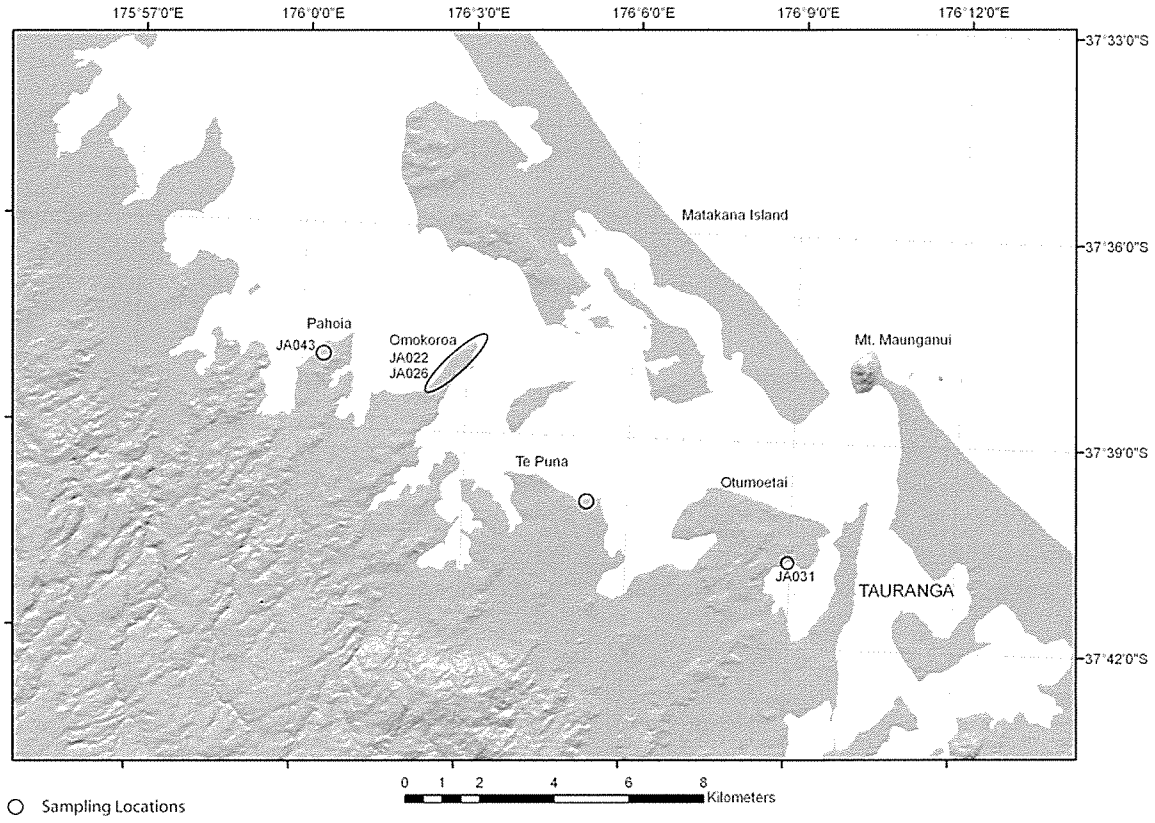

Figure 1 - Map of sampling locations

2 METHODS

Field exposures were described using guidelines from the New Zealand Geotechnical Society (2005). Shear strength was measured using a hand shear vane in accordance with ASTM D 2573-01 (2001). Samples of material were collected using standard 38 mm diameter brass tubes, pushed into the soil by hand. In cases where the soil was too stiff for tubes to be pushed by hand, a large block sample was collected in the field and taken back to the lab to be trimmed and tested. In all cases, samples were stored in plastic zipper bags or wrapped in plastic cling wrap to prevent the loss of natural moisture. "Undisturbed" samples were trimmed to size in the lab and tested in a triaxial strength cell. Remoulded material was tested in a Bromhead style ring shear apparatus (Bromhead, 1979). The Atterberg limits for samples were determined according to NZ 4402:1986 Tests 2.1-2.4 (Standards Association of New Zealand, 1986).

3 RESULTS

3.1 Field description of deposits observed

The samples collected for this study are fine-grained (silty clays or clayey silts), high plasticity soils. In outcrop, most of the deposits are wet or saturated and moderately to highly sensitive (sensitivity of 4-30). The colour of deposits varies, but is typically white, grey, or yellow. Mottling of red due to iron oxides and hydroxides is also common. The deposits are dominated by glass and its clay alteration products with some pumice fragments and crystals. Crystal species are typically quartz, plagioclase, and hydromica. Ferro-manganese nodules are common, but are inferred to result from in situ weathering. Results of field shear vane testing is reported in Table 1. A general trend of increasing strength with decreasing natural water is noted.

Table 1 - Summary of field shear vane tests

Peak Shear Strength (kPa)	Remolded Shear Strength (kPa)	Sensitivity	Natural Moisture Content
120	24	5	65.8%
56	4	14	76.8%
136	16	8.5	71.1%
68	3	22.66667	87.9%
80	1	80	69.8%
116	6	19.33333	95.8%
136	18	7.555556	58.6%
140	12	11.66667	65.6%
260	16	16.25	50.8%

3.2 Lab testing results

Results from laboratory testing are presented as charts in Figures 2–6. The deposits have a peak friction angle ranging from 29° to 64° (Figure 2), and residual friction angle ranging from 15° to 30° (Figure 4). The results of peak shear strength testing for samples JA031 and JA043 closely overlap. Results from a single consolidated drained triaxial test are shown in Figure 3. The test shown in Figure 3 shows dilatant behaviour and an increase in shear stress well beyond 20% strain is evident. The cause of this is not clear but may be related to the interaction of fine-grained crystals and glass shards. The undrained shear strength was determined from the average of three samples from location JA022 is 160 kPa, which is in line with the average results from the field shear vane at the sampling location (136 kPa).

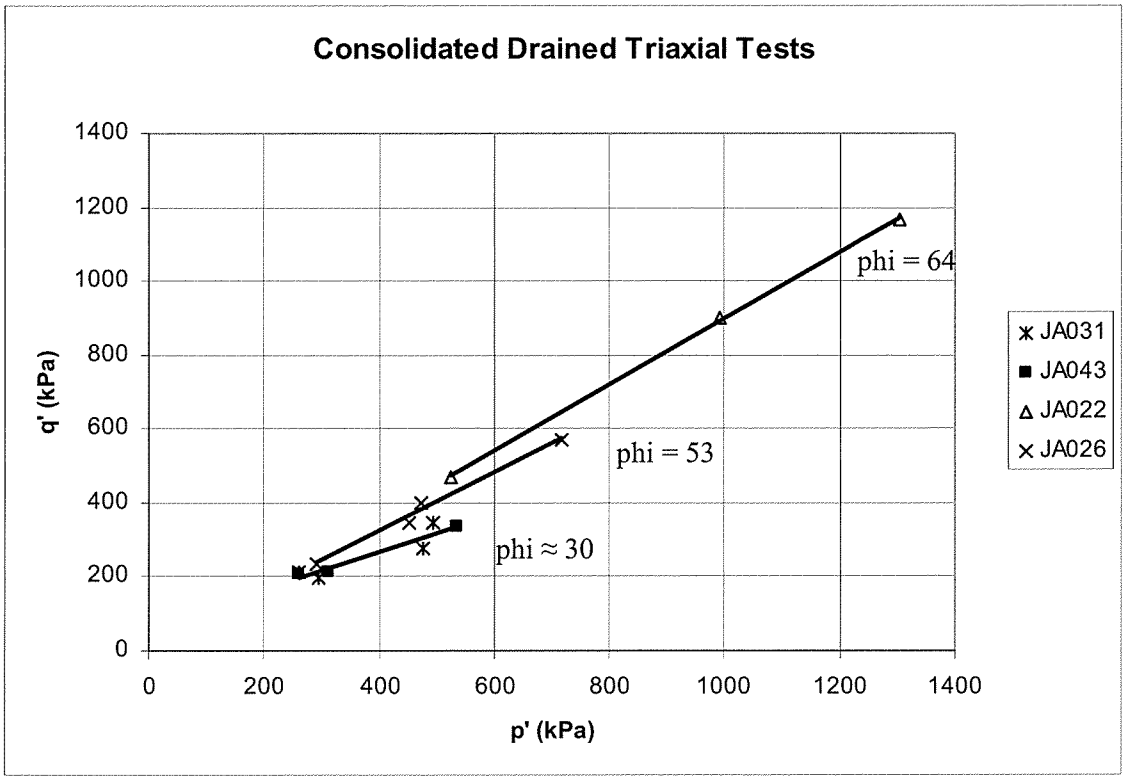

Figure 2 - Summary of consolidated-drained triaxial tests

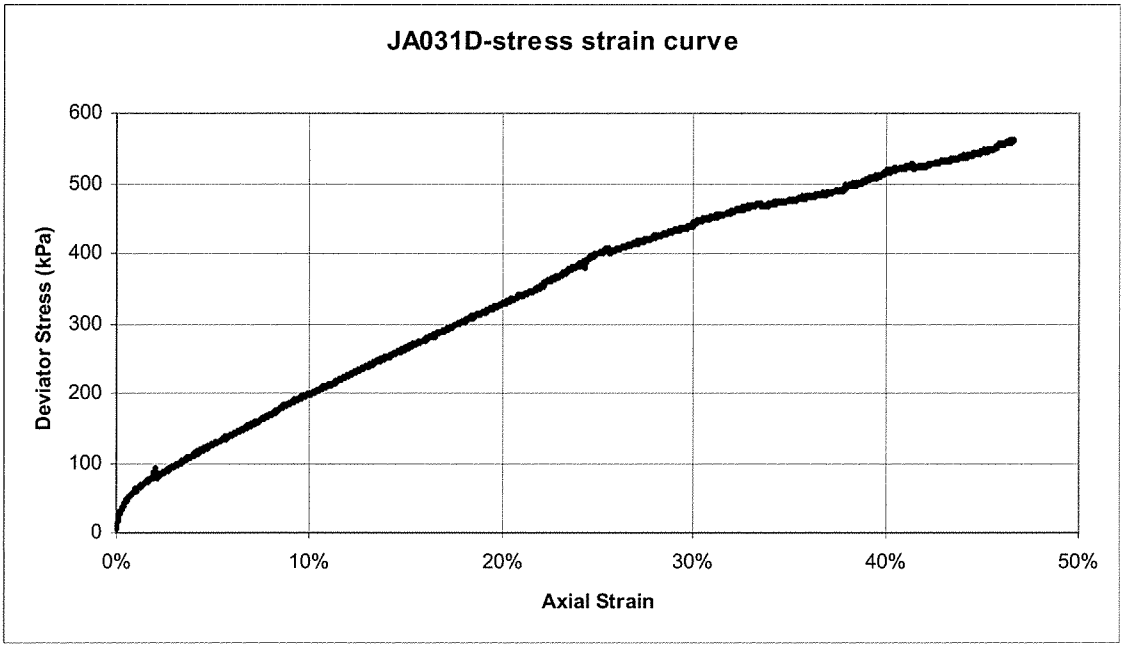

Figure 3 - Example of a stress strain plot for a drained triaxial test

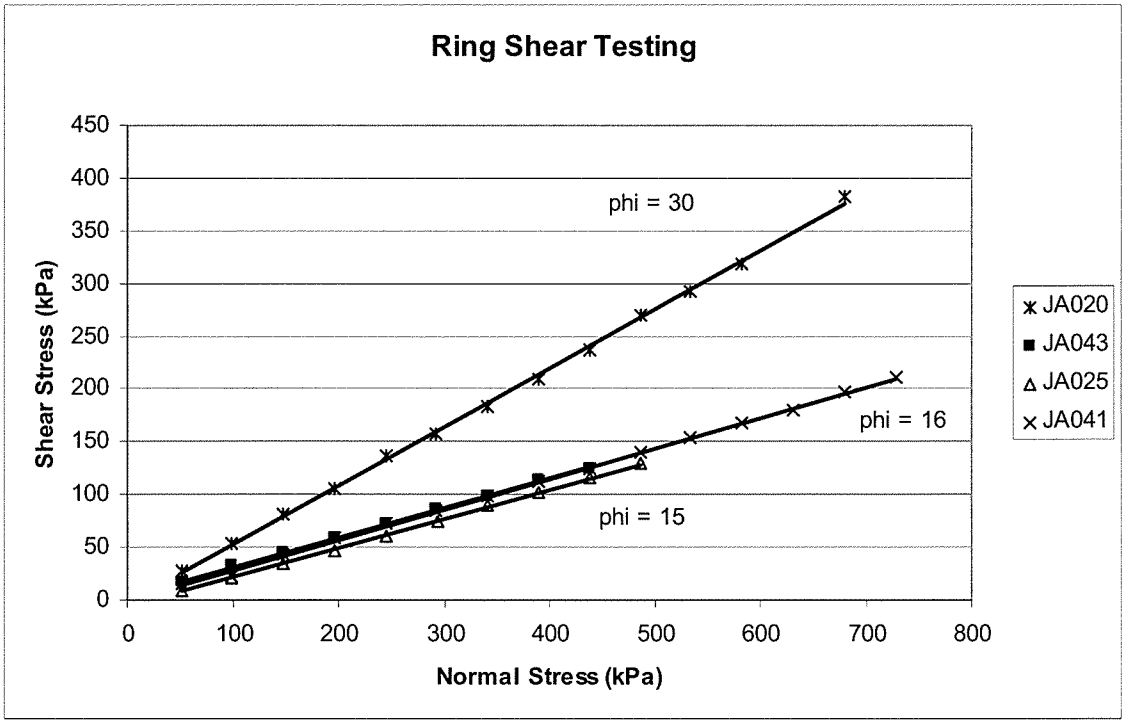

Figure 4 - Summary of ring shear tests

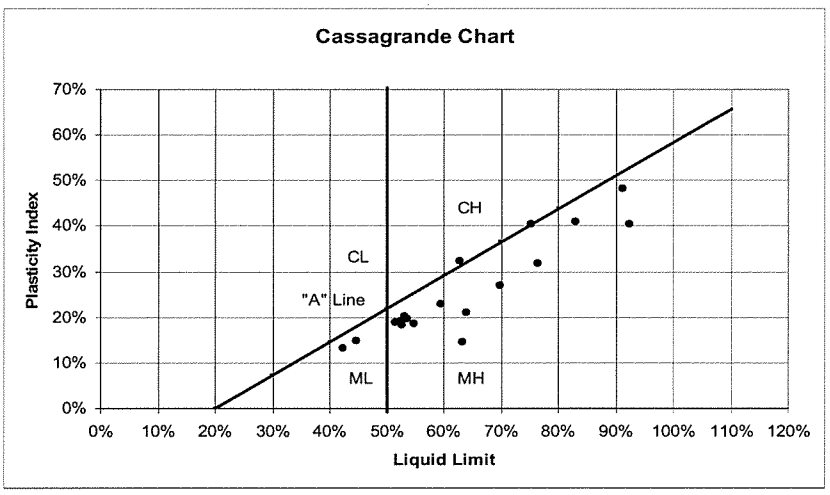

Figure 5 - Summary of Atterberg limits tests.

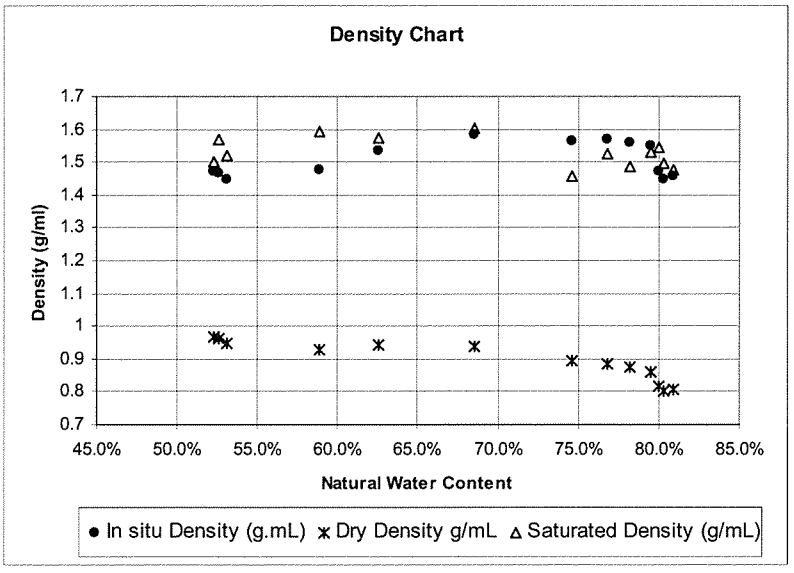

Figure 6 - Summary of sample density based on measurement of triaxial specimens

4 DISCUSSION

The variation in these samples is easily noted from the results of the lab tests, however a few properties tie these materials together in a common classification. Most of the samples plot near to the A-line of the Cassagrande chart (Figure 5), and could therefore be described as silty clays or clayey silts. In addition, the water content of many samples is above the measured liquid limit *in situ*, as seen in liquidity index values above 1.0 in Figure 7.

Dry density and shear strength increase with decreasing natural moisture content (Table 1 and Figure 6). This is probably related to the method of testing shear strength. A material with lower dry density is likely to have a higher porosity and, therefore, be able to hold more water per volume at saturation (Figure 6). There is not a strong trend in *in situ* or saturated density, except for a possible peak at 1.6 g/mL. The field shear vane does not create an undrained condition in the soil, although the shear strength measured by this method is typically assumed to be an undrained strength. Therefore, lower natural water content will result in a higher strength reading due to lower induced pore pressures during the test.

The sensitivity of samples is calculated as the ratio of peak to remoulded shear strength determined by use of the field shear vane. Although there are a number of outliers within the data set, a vague trend of increasing sensitivity to increasing liquidity index is present (Figure 7). In this case, the liquidity index is used as a measure of relative moisture content to compare samples with varying saturation values.

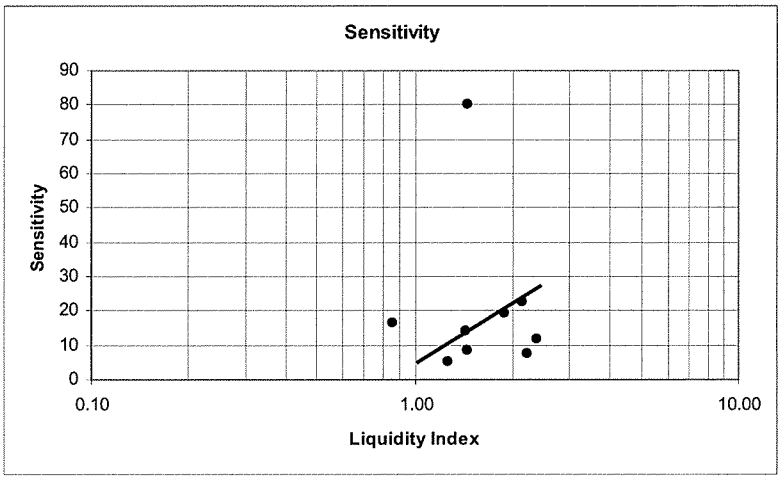

Figure 7 - Sensitivity (ratio of peak to remolded shear strength) of samples from Tauranga measured by field shear vane.

5 CONCLUSIONS

- Much of the variation in strength of these soils is likely to be related to variations of *in situ* water content, which in turn may be related to the clay content, porosity of the material, and sampling location.
- Causes of variation in these soils are under investigation. These causes may relate to the original particle size; the porosity; the microfabric controlling weathering of the soil particles; and to the conversion of volcanic glass to clay.

ACKNOWLEDGEMENTS

Funding for this research was provided by the Earthquake Commission through the Institute of Earth Science and Engineering. The author would like to acknowledge the contributions of C. Wilson, W. Prebble, and J. St. George for guidance and advice, and an anonymous reviewer who helped to improve the manuscript.

REFERENCES

American Society for Testing and Materials (2001) *Annual Book of ASTM Standards*. American Society for Testing and Materials, Philadelphia.

Bromhead, E. N. (1979) A simple ring shear apparatus. *Ground Engineering* Vol. 12, No. 5, pp 40-44.

New Zealand Geotechnical Society (2005) Field Description of Soil and Rock: Guideline for the field classification and description of soil and rock for engineering purposes. New Zealand Geotechnical Society, Wellington

Standards Association of New Zealand (1986) *Methods of Testing Soils for Civil Engineering Purposes*. Standards Association of New Zealand, Wellington.

Wilson, C. J. N., Houghton, B.F., Kamp, P. J. J. & McWilliams, M. O. (1995) An exceptionally widespread ignimbrite with implications for pyroclastic flow emplacement. *Nature* Vol. 378, pp 605-607.

Pile foundations in liquefiable soil – A case study of a bridge foundation

Hayden Bowen
Tonkin & Taylor Ltd., Christchurch, NZ

Keywords: Pile, liquefaction, lateral spreading, effective stress analysis, pseudo-static analysis

ABSTRACT

Soil liquefaction has caused major damage to pile foundations in previous earthquakes, particularly during the 1964 Niigata and 1995 Kobe events. Since pile foundations are primarily designed to transfer vertical loads from the superstructure to the bearing stratum, they are relatively vulnerable to lateral loads, such as those imposed by ground shaking during earthquakes. In the case of soil liquefaction, this vulnerability is particularly pronounced since the loss of strength and stiffness in the liquefied soil results in a near complete loss of lateral support for the embedded piles.

In this paper the seismic assessment of a bridge founded on piles in liquefiable soils is presented. The effects of liquefaction, lateral spreading and soil-structure interaction on the bridge during a predicted future earthquake are examined using two different analytical approaches. First, a simplified, pseudo-static beam-spring method is used. This analysis can be performed using common site investigation data such as the SPT blow count, yet it captures the essential features of pile behaviour. Secondly, a detailed finite element time-history analysis based on the effective stress principle is conducted. This analysis can simulate the process of pore pressure build up and the associated stress-strain behaviour of soils in great detail, giving a rigorous evaluation of pile performance.

1 INTRODUCTION

The loading of piles in liquefiable soils during earthquake shaking is a complex phenomenon involving interaction between the soil, pile and superstructure. During intense ground shaking and liquefaction of saturated sandy soils, rapid changes occur in the soil stiffness and strength, and the pile is subject to large ground deformations and inertial loads from the superstructure.

Based on observations from damage to piles in previous earthquakes, two phases in the seismic response of piles in liquefied soil have been recognised: firstly a cyclic phase during the ground shaking and development of liquefaction, and secondly lateral spreading following the liquefaction. The soil-pile interaction in the cyclic phase is characterised by dynamic loads on the pile from both ground movements and inertial loads from the superstructure. Lateral spreading can develop where driving shear stresses exist in the ground, such as sloping ground, riverbanks or backfills behind quay walls, and primarily occurs after the liquefaction has developed. It is characterised by large unilateral ground displacements and relatively small inertial effects. During this phase the stiffness and strength of liquefied soils are very low, reflecting features of a completely liquefied soil.

This paper describes an assessment of the seismic response of the Fitzgerald Avenue Twin Bridges over the Avon River in Christchurch, New Zealand. In conjunction with the University of Canterbury, Tonkin & Taylor has considered the two phases in the earthquake response; the cyclic phase during intense ground shaking, and the lateral spreading of soil toward the river. For the purposes of this paper only the response of the midspan piles during the cyclic phase, calculated using both a simplified design orientated analysis and an advanced dynamic finite element analysis, is presented. Analysis of the abutment piles response to lateral spreading is presented elsewhere (Bowen and Cubrinovski 2008a).

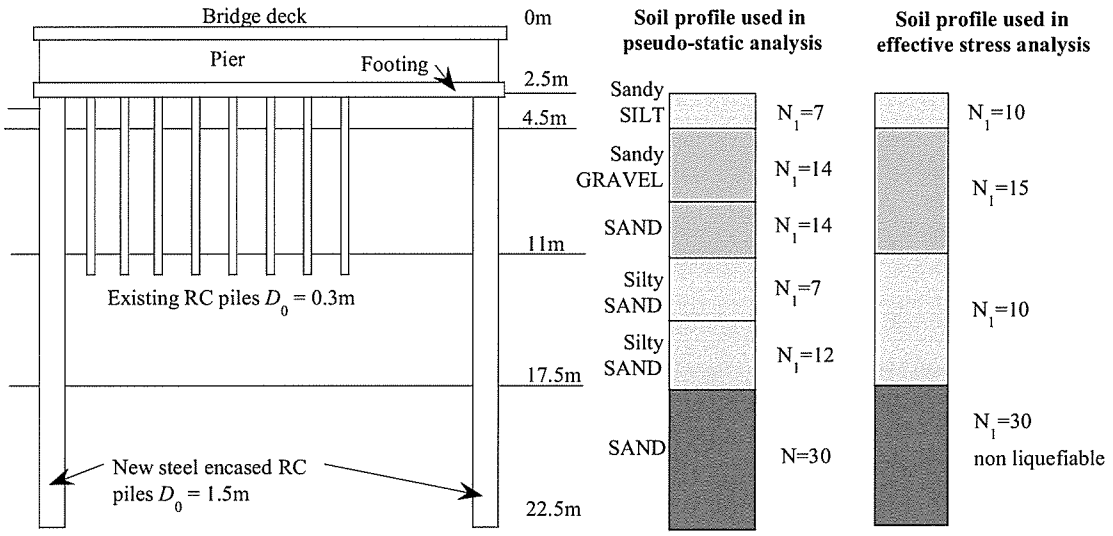

Figure 1: Central pier of the bridge, showing foundation layout and soil properties used for the effective stress and pseudo-static analysis

2 FITZGERALD AVENUE BRIDGES

The Fitzgerald Avenue Twin Bridges have been identified as an important lifeline for post-disaster emergency services and recovery operations. To avoid structural failure of the foundations or loss of function of the bridge in an anticipated strong earthquake affecting the Canterbury region, a structural retrofit has been proposed by the Christchurch City Council. In conjunction with bridge widening, this retrofit involves strengthening of the foundation with new large diameter bored piles. These piles have been designed to take the full gravity and seismic loads of the widened bridge. A cross section at the mid span of one of the bridges is shown in Figure 1 where both existing piles and new piles are shown. The existing bridges are supported by piled abutments on the banks and with a central piled pier at the mid-span. The existing piles are founded on potentially liquefiable soils, at about 11 m depth below the ground surface. The new retrofit piles will be connected rigidly to the existing foundation and superstructure at each end of the pile cap, and founded into deeper strata consisting of non-liquefiable soils, as shown in Figure 1.

3 PSEUDO-STATIC ANALYSIS

3.1 Model

The analytical model used in the pseudo-static analysis consists of a beam connected to a series of springs representing the lateral stiffness of the soil. The effects of liquefaction on the soil are accounted for by degrading the stiffness of the soil springs in the liquefied layers. The complex dynamic forces applied to piles in liquefied soil are approximated by the sum of two static loads applied to the pile:

(1) Kinematic loads from the soil movement are applied through free field ground displacements acting on a series of soil springs. This displacement represents the maximum cyclic ground displacements due to soil liquefaction and ground shaking. Note that this is a free field ground displacement unaffected by the presence or response of the pile foundation.

(2) Inertial loads from the superstructure are modelled as a lateral point load applied at the pile head. It was adopted in the analysis that this load acts in the same direction as the applied ground displacement.

3.2 Parametric Study

Cubrinovski and Ishihara (2004) identified the following key parameters affecting the pile response in liquefied soils:

- The stiffness degradation factor due to liquefaction, β
- The ultimate pressure exerted by the crust layer (if present)
- The magnitude of the lateral ground displacement, U_G
- The inertial load applied at the pile head from the superstructure

When designing piles to account for liquefaction, the selection of these parameters is very difficult as nearly all of them are subject to large variation throughout the course of pore pressure build up and eventual liquefaction. These intrinsic uncertainties associated with piles in liquefiable ground are directly reflected on these key parameters. Therefore for the analysis of the Fitzgerald Avenue Bridges these parameters were not uniquely determined; rather a range of values were considered. Full details of the parametric study are given in Bowen and Cubrinovski (2008a), where all of the above parameters are addressed. Here only the first parameter, the stiffness degradation due to liquefaction, is addressed.

The stiffness degradation of the soil due to liquefaction is quantified by multiplying the lateral stiffness of the soil by a constant β. Based on case studies and experimental tests, the stiffness degradation of liquefied soils can be assumed to vary between β = 1/10 and 1/50 during the cyclic phase. Figure 2 shows the results two analysis cases with β = 1/20 and β = 1/50. Both cases were analysed assuming the soil profile shown in Figure 1 and external loads consisting of the free field ground displacement shown in Figure 2b and an inertial load at the pile head. The free field ground displacement was determined using the method of Tokimatsu and Asaka (1998) assuming a peak ground acceleration of 0.4g. The magnitude of the inertial load at the pile head was calculated as the tributary bridge mass supported the pile multiplied by the peak ground acceleration.

Figure 2 shows that for both cases the maximum bending moments occur at the pile head and at the interface between the liquefied and non-liquefied soil layers. With regard to the pile displacements the β = 1/50 case demonstrates stiffer pile behaviour, where relatively stiff pile resists the movement of the surrounding ground. For the β = 1/20 case the liquefied soil is softer, the pile shows more flexible behaviour and the pile displacement and bending moment is higher than the β = 1/50 case.

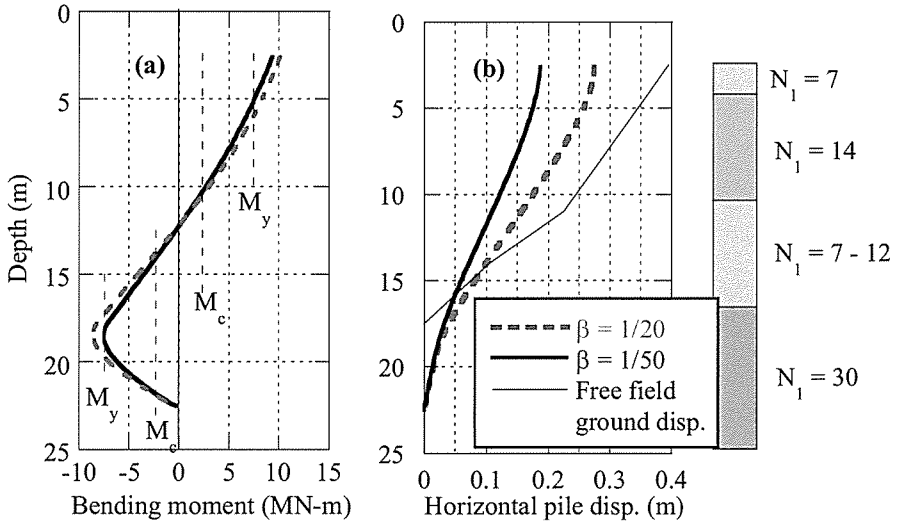

Figure 2: Variation of pile response due to liquefied layer soil stiffness; (a) pile bending moment, (b) pile displacement

4 EFFECTIVE STRESS ANALYSIS

4.1 Model

A fully coupled effective stress method was used to analyse the soil-pile-bridge system. This is an advanced analysis that permits consideration of excess pore water pressure, flow of pore water through the soil and detailed modelling of the stress-strain behaviour of soils. Conventional liquefaction modelling techniques model the foundation system using post-liquefaction soil properties, liquefaction induced ground displacements and inertial loads from the superstructure that have been determined using very approximate empirical correlations. In contrast, effective stress analysis, based on a detailed model of the initial state of the soil and foundation, calculates these parameters throughout the course of earthquake shaking.

The accuracy of the analysis has been extensively verified through case studies and large-scale shake table tests. The 2-D numerical model used in this study is 160m x 30m in size. Solid elements are employed for the soil and bridge superstructure, while beam elements are used for the piles and footing. The piles were modelled as non-linear members with a moment-curvature relationship approximated using the hyperbolic model. The footing, bridge deck and pier were all modelled as elastic materials with an appropriate tributary mass. The soil elements were modelled as two phase solid elements using an advanced constitutive model, which uses an elasto-plastic deformation law for sandy soils. Further details are provided in Bowen and Cubrinovski (2008b).

The finite-element model was subjected to a base input motion with similar general attributes to those relevant for the seismic hazard of Christchurch. An acceleration record obtained during the 1995 Kobe earthquake (M=7.2) was used as an input motion in the effective stress analysis; this motion was recorded 50km away from the epicentre in a down-hole array at a depth of 25m. The motion was scaled to have a peak acceleration of 0.4g. Needless to say, the adopted input motion is neither representative for the source mechanism nor for the path effects specific to Canterbury, but rather it was considered a relevant input motion that represents the general features of the earthquake event considered in this study.

4.2 Ground and Pile Response

First we will examine the computed ground response in the free field, which is not affected by the presence of the pile foundation. Figure 3a shows computed time histories of excess pore water pressure at two different depths throughout the soil profile in the free field. Here z = 9.5 m and z = 15.7 m depths correspond to the top parts of the second layer (N_1=15) and the third layer (N_1=10) respectively.

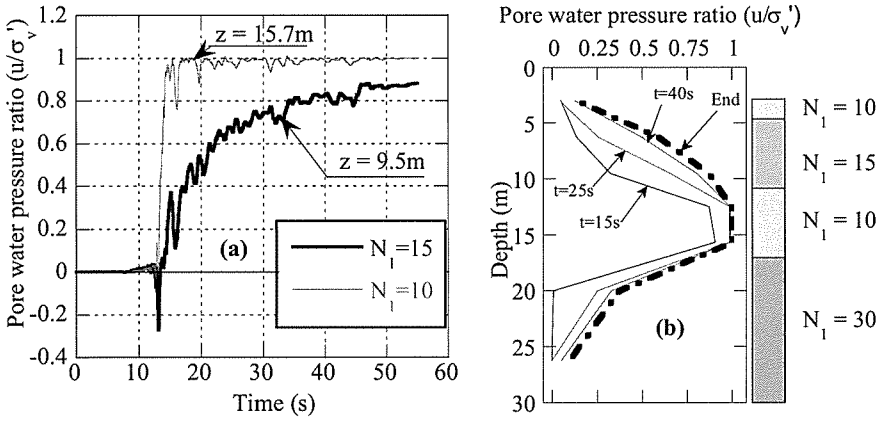

Figure 3: Excess pore water pressures in the free field; (a) time histories showing the development of pore pressure and eventual liquefaction at different depths, (b) distribution of excess pore water pressure ratio throughout the depth of the profile at different times

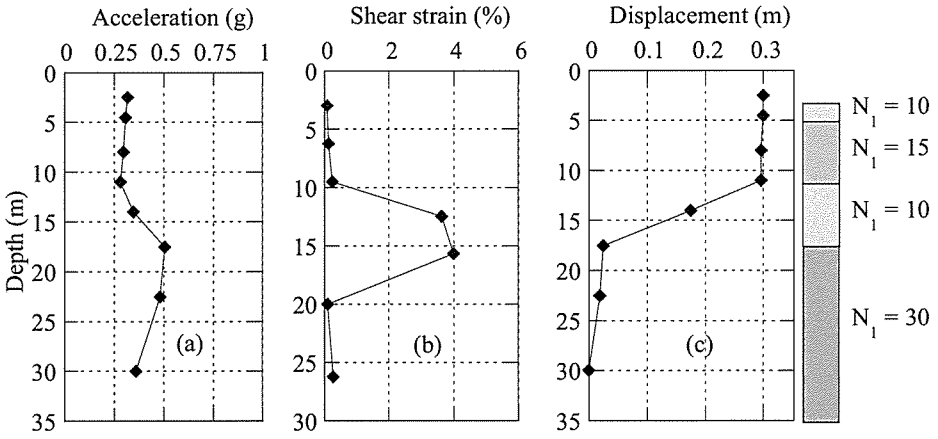

Figure 4: Maximum free field response: (a) accelerations, (b) shear strains, (c) ground displacements

In the weaker layer (N_1=10), liquefaction occurs straight after the first cycle of strong shaking, as indicated by the rapid increase in the pore water pressure ratio (u/σ'_v) in Figure 3a. In the stronger layer (N_1=15), however, the excess pore pressures build up gradually with the application of cyclic shear stresses and liquefaction does not fully develop; the pore pressure ratio reaches a value of about 0.88 at the end of the shaking (t = 55 seconds). Note that here a pore pressure ratio of unity indicates complete liquefaction. Figure 3b illustrates the development of the excess pore pressure throughout the depth of the deposit by depicting snapshots of the pore pressure ratio values and hence the extent of liquefaction at different stages of shaking or time sections. This plot shows that the looser sand layer (N_1=10) completely liquefied whereas in the denser sand layer (N_1=15) the peak pore pressure ratio was in the range between 0.4 and 0.9 at the end of the shaking.

The maximum values of the ground acceleration, shear strain and ground displacement, plotted in Figure 4, clearly display the effects of liquefaction on the free field ground response. Figure 4a shows a decrease in acceleration above the weaker layer that liquefied rapidly; this phenomenon has been observed in down-hole array records during past earthquakes and in many shake-table experiments on scaled-down models of relatively loose sands that do not exhibit cyclic mobility. Figure 4b and Figure 4c show that the majority of the ground deformation occurs in the mid layer with N_1=10, where the peak shear strains reach about 4%. The strains in the shallow part of the deposit are well below 1%, which is consistent with the lower excess pore water pressures generated in these layers. Clearly, the response of the weaker layer significantly affects and, in this case, practically governs the response of the layers above.

In general terms, the pile foundation provides a stiffening effect to the surrounding foundation soil. This effect is apparent in Figure 5, where time histories of horizontal ground displacements in the foundation soil and free field are compared. The peak horizontal displacement in the free field reaches 0.3 m whereas the peak displacement of the foundation soil is less than 0.2 m.

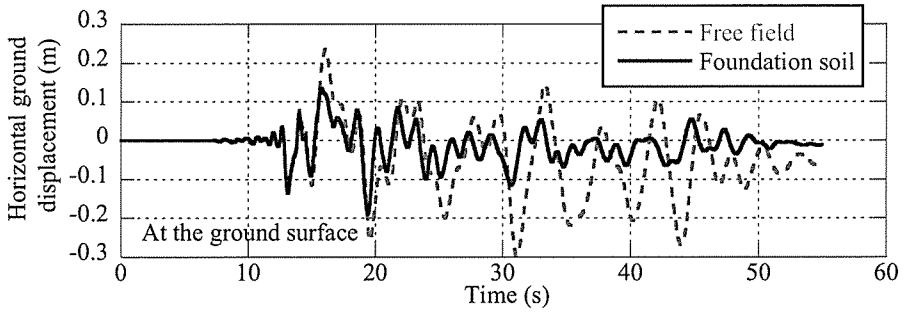

Figure 5: Comparison of the horizontal displacement at the ground surface for locations in the free field and in between the piles

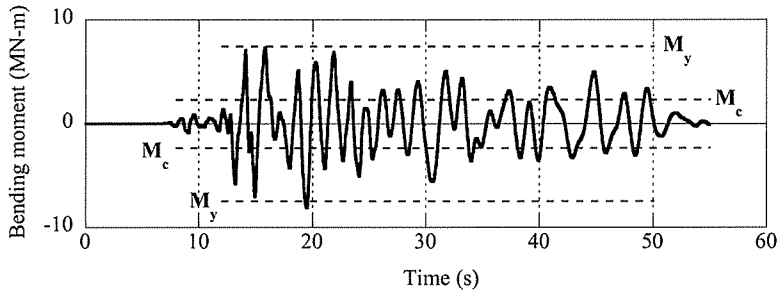

Figure 6: Bending moment time history at the pile head

A time history of the bending moment at the pile head is presented in Figure 6, showing that throughout the most intense part of the shaking the pile response is well above the cracking moment (M_c) of the pile. The yielding moment (M_y) of the pile is approached a number of times throughout the shaking and is exceeded at approximately $t = 19$ seconds for the particular input motion used in this study.

5 CONCLUSIONS

The seismic response of the Fitzgerald Avenue Bridges, including the effects of liquefaction and lateral spreading, was analysed using both an advanced effective stress analysis and a simplified pseudo-static analysis. The two approaches focus on different issues and play complimentary roles in providing a comprehensive assessment of the bridge foundation response to a major earthquake.

Due to its simple and design orientated nature, the pseudo-static analysis is well suited to conduct parametric analyses in order to account for the significant uncertainties inherent in liquefaction problems. For the response of the midspan piles to the cyclic phase of liquefaction, it was shown that the liquefied soil stiffness has a large bearing on the analysis result. Thus for design of piles in liquefiable soils, it is essential to consider the large aleatoric uncertainties present. Parametric studies using pseudo-static analysis are therefore recommended in practice.

This case study demonstrated the capability of the effective stress analysis to capture important features of the soil-pile interaction in liquefying soils, including:

- Detailed development of excess pore water pressure through time and space including effects of soil density and complex interaction between intensity of shaking, pore pressures and associated ground deformation, and;
- A rigorous evaluation of pile performance, determined by taking into account the highly complex dynamic nature of loads and soil-pile interaction.

Therefore this analysis methodology can provide a rigorous evaluation of the seismic performance of pile foundations of important structures. It can explain complex features of the response and verify design assumptions, and hence, it provides a unique contribution in the assessment and design of piles.

REFERENCES

Bowen, H. and Cubrinovski, M. (2008a). "Pseudo-static analysis of piles in liquefied soils: Parametric evaluation of liquefied layer properties" *Bulletin of the New Zealand Society for Earthquake Engineering*, (submitted).

Bowen, H. and Cubrinovski, M. (2008b). "Effective stress analysis of piles in liquefiable soil: a case study of a bridge foundation" *Bulletin of the New Zealand Society for Earthquake Engineering*, (submitted).

Tokimatsu, K., and Asaka, Y. (1998). "Effects of liquefaction induced ground displacements on pile performance in the 1995 Hyogoken-Nambu Earthquake." *Soils and Foundations* (Special Issue), 163-177.

Catastrophic failures – and a few other reasons to use instrumentation to monitor performance

Paul Burton
Geotechnics Ltd, Tauranga, New Zealand

Keywords: geotechnical, instrumentation, construction, performance

ABSTRACT

Construction projects in New Zealand are utilising geotechnical instruments to monitor performance on an ever increasing scale. Our urban centres are providing more challenges for our engineers as they design for constrained areas with concern for neighbouring land use. The integration of geotechnical instrumentation providers into our project teams has seen project timelines reduced, safety increased and our clients receiving better value with a superior understanding of their risk. Our requirement to minimise the impact of our project to all affected parties is now paramount to our success.

This paper will outline the benefits of monitoring construction performance and provide some examples of the benefits gained for all stakeholders.

1 INTRODUCTION

There are few cases as catastrophic in the public domain such as the Vajont Dam and reservoir landslide. There have been many studies reviewing the events of 9th October 1963, most concluding that a 5 – 15cm layer of clay within the limestone provided the slip surface. The known landslide was being carefully managed by adjusting the water levels in the reservoir whilst monitoring the movements. The fateful dropping of the water level induced hydraulic pressures as water in the jointed limestone tried to drain. The stresses imparted led to massive destruction and loss of life as the structure failed.

Appreciating that this was in 1963, we can use hindsight to consider how different it could be in the modern world. The ability to measure pore pressures at significant depth very accurately and in very discreet layers has provided the modern engineer with options that were unavailable at Vajont [Petley, D 2001]. The development of consumer electronics has allowed the geotechnical instrumentation industry to access cheap(er), smaller and more accurate instruments than ever before - we must consider these benefits to our projects.

2 INSTRUMENTATION AND RISK

Large construction projects require major investment. In modern times such investment requires a detailed understanding of the risks surrounding the geotechnical parameters.

Worldwide, geotechnical engineering is considered one of the highest risk disciplines within the engineering field. [Houchen, D.] Clients and investors in projects of this nature are innately risk-averse and the more we can do to reduce the risk, the happier they will be. There are many ways that the geotechnical professional can calculate risk and allow a client to make informed decisions. The calculated risks can provide pre-construction reference, but through construction there will always be "unforeseen circumstances". In a geological setting there will always be a requirement to provide educated assumptions to create models. In reality, we find that ground conditions can often change very quickly, much to the designers' astonishment and dismay. This astonishment in the engineer's mind needs to be converted to "peace of mind" when they attend the client update meeting. It could be fair to assume that astonishment would not be the only issue on the client's mind.

The use of geotechnical instrumentation to monitor construction performance can provide an up to date understanding of ground conditions and how the calculated risks have changed or not. The geotechnical engineer gains confidence in their predictions and models, and this assurance is inevitably passed on to their client.

The author freely admits that this scenario is perhaps viewed through rose-tinted spectacles. However, there is significant evidence in many projects throughout New Zealand to suggest that projects with adequate geotechnical instrumentation to monitor construction performance result in very good client relationships. Due to the litigious nature of many projects with significant geotechnical problems, the ability to use case studies from recent times is very limited.

The risks, when understood fully, can be monitored to provide legal backing should conflict arise between stakeholders. The provision of accurate data to show compliance is commonplace in projects, especially in our urban centres. The potential impacts that our projects can have on a significant range of stakeholders has increased as our green field developments decrease and our brown field developments increase.

2.1 Risk example

An example of managing risk through the use of geotechnical instrumentation is the monitoring of in-situ bridge piers during construction.

Current engineering designs allow for retro-fitting of bridges with "clip-ons" or twinning with replica parallel aligned new bridges. Bridges over waterways will inherently be founded in alluvial, fluvial and estuarine deposits. These deposits will in general, but not always, exhibit seismic risks, not only from tectonic movement but from percussive installation of new piles, caisson or temporary staging.

To ensure security of the existing bridge structures which will commonly be in use throughout the construction phase, we can place tiltmeters on the pile caps. The use of tiltmeters in a wireless mesh network can provide near real-time data of existing structures, including piles. Alarm levels can be set to ensure that notifications are made to the engineer should construction methodologies affect the existing structures.

The initial risk of damaging or affecting the performance of an existing structure can be carefully monitored throughout the project lifetime. All stakeholders can make informed decisions about how they wish to proceed with a quantified risk in comparison to a calculated one.

3 INSTRUMENTATION AND TIMELINES

I am yet to meet a successful geotechnical engineer who doesn't have significant time constraints on his/her projects. As we are all aware, timeliness has an impact on the cost and quality of a project. It is imperative that project scoping allows for a suitable balance of all three: time, quality and cost.

Our modern project management systems include such wondrous tools as milestones and critical paths. The project success can rest, not on the use of these management tools but on construction performance and essentially the engineer's expertise in managing timelines. Geotechnical instrumentation can provide engineers with very accurate data to support their decisions on construction programme. The ability for engineers to know their construction performance in comparison to an "assumed" performance will provide their clients (and their representatives) with confidence and assurance that their project is in good hands.

3.1 Timelines Example

A suitable example for increasing knowledge of construction performance over calculations could be the use of hydrostatic profile gauges (see Figure 1) to measure settlement in conjunction with vibrating wire piezometers (see Figure 2) for pore pressure. As New Zealand's towns and cities develop, the roads and infrastructure required to support that growth need to be built. Prime land is almost always consumed by the residential and industrial sector of construction, leaving marginal land for the infrastructure. The marginal land in many towns and cities consists of estuarine, alluvial, colluvial or organic deposits (commonly dunes interspersed with peat). These ground conditions provide significant challenges to the geotechnical engineer when considering the timeline of projects.

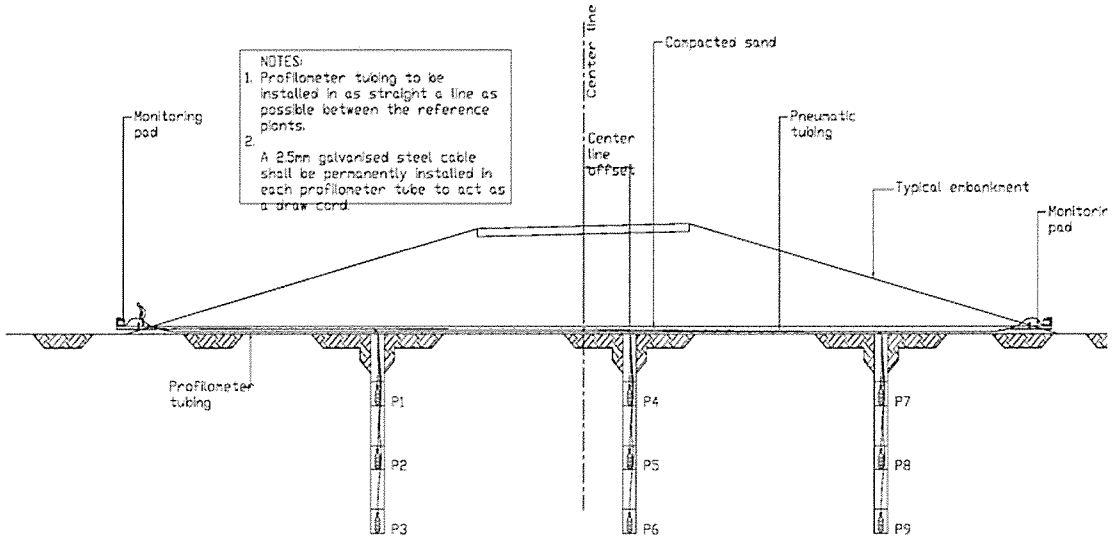

Figure 1: Typical profilometer tubing installation beneath an embankment (including piezometer)

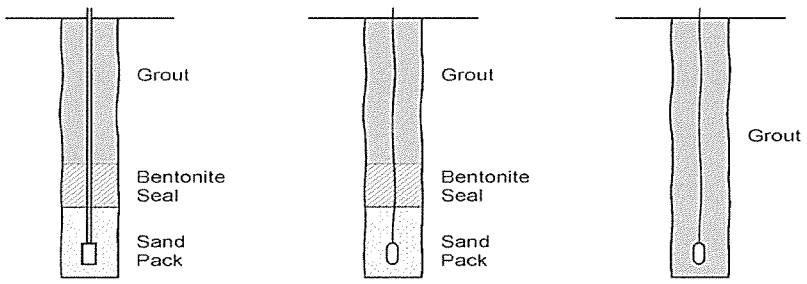

(a) **(b)** **(c)**

Figure 2(a): Traditional standpipe piezometer with sand pack
Figure 2(b): Diaphragm piezometer with sand pack
Figure 2(c): Fully grouted piezometer [Contreras, I.A. et al 2007]

One of the most significant issues will be settlement of the ground with specific consideration to consolidation and pore pressure dissipation. In the past, a significant amount of calculation and a reasonable amount of conservatism were used to ensure pre-load activities achieved their

aims. In more recent times we have seen fill quantities, density calculations and survey provide a more accurate picture. The use of a hydrostatic profilometer in conjunction with heavy duty vibrating wire piezometers can now provide significant improvements in timelines for all stakeholders (see Figure 3 below).

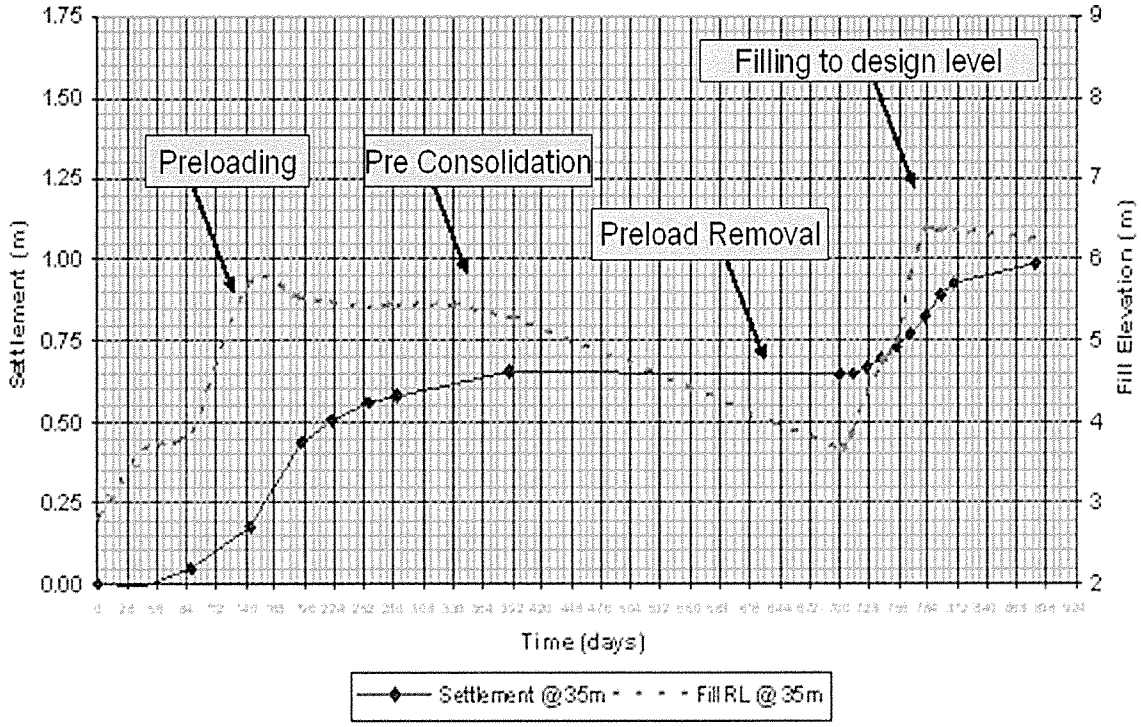

Figure 3: Profile tube settlement versus time (0 – 924 days) [O'Connor, V.P. et al 2003]

The comparative methods below (Table 1) show significant reasons any of the options should be considered. The choice of method would, however, depend on the size of the project. It is clear that if the programme timeline can be reduced, the hydrostatic profilometer & piezometer combination will provide full assurance to the engineer and the client that the construction is performing to the required standard.

Table 1: Comparison of construction performance monitoring methods

Method	Pros	Cons
Calculations & conservatism	Cheap (in the short term)	Assumptions galore Higher construction costs
Fill quantities & survey of settlement plates	Provides the engineer with known performance from single points in fill and surface	Impedes Construction Construction damage likely Single point measurements at depth
Hydrostatic profile gauges & vibrating wire piezometers	Provides full cross section at original ground level All instrumentation away from construction traffic Provides assurance of all pore pressure & settlement parameters	Relatively expensive for set-up Requires specialist technicians

4 INSTRUMENTATION AND SAFETY

The integration of safety into the construction process and final product has become imperative to project success.

Project stakeholders may include national and local government, public and private companies, and the end users including the general public. The Health and Safety in Employment Act 1992 section 19(b) states "That no action or inaction of the employee while at work causes harm to any other person.". This is a very important statement to understand when major projects have our staff, construction staff and the public involved.

It should be noted that the Act views engineers' responsibilities at a higher level than the general public. Section 2A(2) states "a person required by this Act to take all practicable steps is required to take those steps only in respect of circumstances that the person knows or ought reasonably to know about.". It must be noted that this includes action or in-action for site activities as well as design requirements. There may also be implications surrounding the registration of the engineers covered in the Chartered Professional Engineers Act 2002.

The use of geotechnical instrumentation on major projects can provide a near real-time understanding of any hazards which might affect stakeholders and be detrimental to the project success.

4.1 Safety Example

A suitable example of this is an inner-city roading project. There are numerous public stakeholders, from current road-users through to owners and visitors to large high-rise buildings. The implications of cut-slope failures can vary from structural damage through to injury or even death. There are very few geotechnical engineers who would like to have any of these litigations on their CV.

Although geotechnical instrumentation will not stop any cut-slope failures (in normal circumstances and quantities), the ability for an engineer to make informed decisions as soon as parameters reach critical levels can minimize and even eliminate any damage or injury.

An engineer can specify to install vertical inclinometers or ShapeAccelArray™ prior to any works being carried out on site. These instruments can provide accurate measurements of lateral deviation at any depth specified along with direction of movement. In the case of ShapeAccelArray™ we can also measure dynamic acceleration which in New Zealand is very important with the seismic risks we have. The correlation of this data along with construction activity can provide a very good understanding of whether initial design parameters are being met or exceeded. The use of alarm levels for construction development will provide surety to all stakeholders that the programme can be met, or not, as the case may be.

5 CONCLUSION

The use of geotechnical instrumentation should always be considered, no matter what size of project is being scoped. The use of a systematic approach to planning monitoring programs is encouraged with Dunnicliff [1988] providing a 20 step approach to planning a monitoring programme.

The suitability of instrumentation and the technology levels required will normally be dependent on project size and thus budget. Although this paper lists the examples of higher technologies it should be noted that the use of the humble crackmeter and/or survey markers can be just as effective when monitoring construction performance.

A note of caution should also be raised when dealing with complex technologies and complex engineering tasks. I would recommend that we do not simply dismiss the reliance on calculations for construction performance but blend the two methods into a hybrid. The prediction of construction performance alongside measured parameters can then be used for review throughout the project lifetime. A significant use of the "observational method" [Peck 1969[a], 1972] should also be considered to provide back-up to any measured responses to construction.

Unfortunately the geotechnical instrumentation can also highlight the performance of the geotechnical engineer and how safe their position is with their client due to their predictions for construction performance. I would therefore suggest a close working relationship with the geotechnical instrumentation team. An understanding of their work will pay dividends to project success.

ACKNOWLEDGEMENTS

Dunnicliff, J.	Instrumentation Engineer, Review and Encouragement
Houchen, D.	General Manager, Professional Risk AON. Insurance Consultants to CEAS.
Kriel, I. & O'Connor, V.P.	Geotechnics Ltd, Encouragement and Review

REFERENCES

Barnes, G.E. (2000) *Soil Mechanics, Principles and Practice.* MacMillan Press, London.

Dunnicliff, J. (1988-93) *Geotechnical Instrumentation for monitoring field performance.* Wiley-Interscience.

Contreras, I.A. et al (2007) The use of the fully-grouted method for piezometer installation. FMGM2007: *Sevent International Symposium on Field Measurements in Geomechanics.*

Marr, W.A. (2007) Why monitor geotechnical Performance? FMGM 2007: *Seventh International Symposium on Field Measurements in Geomechanics.* Boston, ASCE

O'Connor, V.P. et al (2003) Mercer to Longswamp Expressway and Project PJK Instrumentation and monitoring.
NZIHT TNZ Symposium, Oct. 2003

Peck, R.B. (1969a) Advantage and Limitations of the observational method in Applied Soil mechanics. *Geotechnique,*
Vol. 19, No.2 pp171-187

Peck, R.B. (1972) Observation and Instrumentation: some elementary considerations.
Highway Focus, USPOT, FHWA Vol. 4, No.2 pp1-5

Petley, D. (2001) The Vajont Landslide. Summary – www.land-man-net/vajont

Chartered Professional Engineers Act, New Zealand Statutes (2002)

Health and Safety Employment Act, New Zealand Statutes §19 (1992)

Case study – Suitability of hollow core soil nails as a permanent slope stabilisation method in granular fill

James Cherubin
Maunsell AECOM Pty Ltd, Melbourne

Keywords: soil nail, hollow core, granular, fill, drilling, grouting

ABSTRACT

This paper focuses on a soil nail wall to be constructed in loose and medium dense granular fill on the Southern Link Upgrade (SLU) project, Melbourne. The suitability of utilising hollow core self drilling soil nails was investigated. Hollow core soil nails can be installed into potentially unstable material without the need for temporary casing to provide borehole support. However, the use of hollow core soil nails for permanent slope stabilisation is a relatively new concept and not widely accepted due to concerns regarding corrosion protection. A review of limited available literature; an assessment of subsurface conditions (including soil aggressivity); and, the performance of pullout testing were used to assess the suitability of hollow core soil nails as a permanent slope stabilisation method for the SLU project.

1 INTRODUCTION

The use of conventional soil nailing as a slope stabilisation technique has become increasingly common in Australian infrastructure projects over the past 10 to 15 years. Conventional (drill and grout) soil nailing involves the drilling of a borehole and the insertion of a soil nail which is then grouted in place, involving three construction stages. The advantages of soil nailing are its top down construction methodology, its cost effectiveness and its suitability in a wide range of ground conditions (FHWA, 2003). However the advantages of conventional soil nailing techniques have limitations and its attractive characteristics mentioned above may be reduced where potentially unstable soils are present.

The SLU project in Melbourne involves the widening of a 5 kilometre section of City Link. As a brownfield site in the inner suburbs of Melbourne, there is limited space available to widen the section of the tollway. Hence as part of the SLU project an existing soil nail wall constructed in 1997 is to be demolished and reconstructed (See Figure 1 below). The proposed wall is approximately 84 metres in length and has a maximum height of 5.1m.

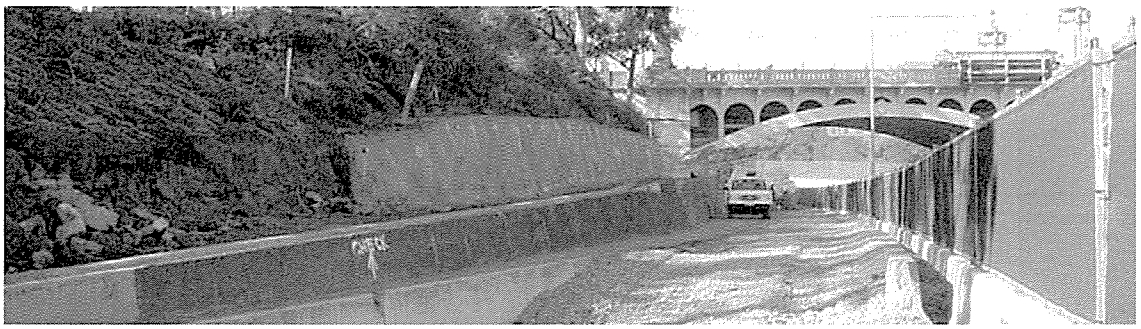

Figure 1: The existing wall following partial demolition and excavation of the first bench of the new wall.

The geotechnical site investigation identified uncontrolled loose and medium dense sand fill. These soil conditions are often indicative of borehole instability, however due to a range of other site constraints, a soil nail wall was identified as the most appropriate slope stabilisation technique for the SLU project. During the preliminary design phase, the need for casing to provide temporary support was identified. All test holes drilled for the SLU project collapsed, proving that ground conditions were as anticipated in design. In addition to this, evidence of the

use of steel casing was observed during the demolition of the existing wall. Due to the significant construction cost of drilling with temporary casing (as a result of very low production rates and significant manual labour) the suitability of utilising hollow core soil nails as a permanent slope stabilisation method was investigated.

1.1 Subsurface Conditions

The geotechnical information indicated the sub surface conditions to be uncontrolled fill between 5.5 and 9.5 metres thick, comprising loose to medium dense sand, silty sand and silty gravel and stiff to very stiff sandy clay. Bricks were encountered at varying depths. The fill was underlain by the geologically recent alluvial/estuarine deposit, Coode Island Silt, the thickness of which was anticipated to be approximately 7 metres. Testing for pH, Chloride and Sulphate was undertaken on a number of soil samples to aid in the estimation of corrosion rates.

1.2 Site constraints

Despite the unfavourable ground conditions a soil nail wall was identified as the most appropriate slope stabilisation technique. Alternative retaining systems and slope treatments were considered including: a gravity wall; various forms of piled retaining systems (including contiguous piles and soldier piles); and, battering. However, a number of constraints made these options unfeasible. This included; the presence of mature native trees of significant value to the community and stakeholders; high voltage electricity cables near the crest of the proposed wall (with significant relocation costs); space restrictions due to live traffic at the top and bottom of the proposed wall; and, soft ground beneath the proposed wall.

1.3 Hollow core self drilling soil nails

The use of hollow core soil nails is a relatively new technique as a permanent slope stabilisation method. They have been used in the United States for approximately 10 years (FHWA, 2006). They were initially utilised in temporary applications, and it is understood that this is still the primary function. However, support is increasing for the method to be utilised wherever possible for permanent applications (FHWA, 2006).

Hollow core soil nails allow the drilling of boreholes in potentially unstable soils without casing, because the hollow, threaded bar acts as the drilling rod, the soil nail and the grout tube. The sacrificial drill bit, which screws onto the threaded hollow core bar, has grout ports on its side (See Figure 2 below). As drilling proceeds, "flushing" grout is circulated through the hollow bar and the drill bit and back out of the borehole, providing continuous drilling, flushing, and grouting during the nail installation. The "flushing" grout flushes cuttings out of the borehole as drilling proceeds and also acts as a drilling mud providing borehole support in potentially unstable soils (See Figure 3 below).

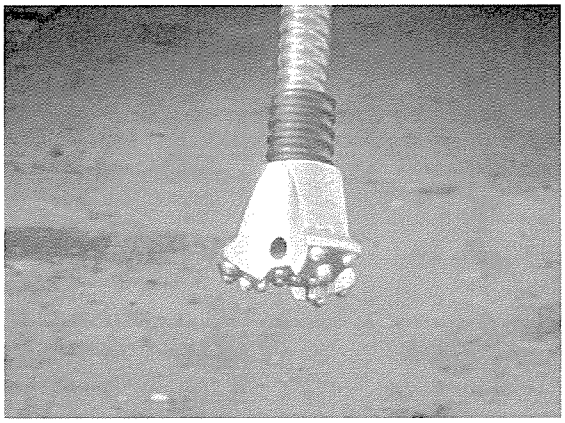

Figure 2: A hollow core soil nail, drill bit adaptor and sacrificial drill bit.

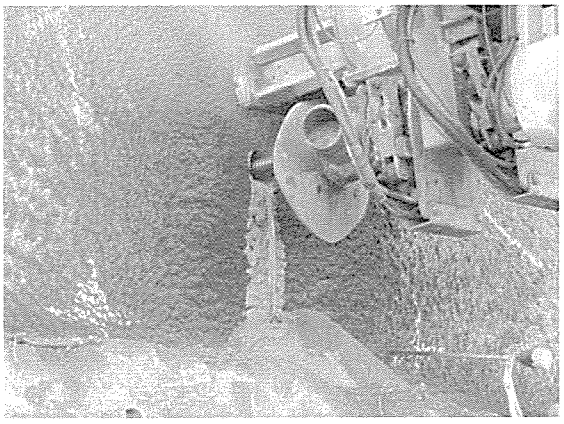

Figure 3: The simultaneous drilling and grouting process.

A "final" (thicker) grout is circulated through the borehole once the target depth is reached. The final grout displaces the flushing grout and remaining cuttings, provides the required bond between the soil and the anchor and (where sufficient cover is achieved), it provides the first level of corrosion protection. The technique reduces construction stages making it an efficient soil nailing method in unstable soils. However, the durability of hollow core soil nails is a key issue as grout cover cannot be guaranteed. This issue is discussed in more detail below.

2 ESTIMATING THE ULTIMATE GROUT-TO-GROUND ADHESION

2.1 The use of the effective stress method

The interaction between soil strength, soil weight, nail strength, pullout capacity and nail head capacity was analysed using the software package SLIDE. The aim of the analysis using a first principles approach was to achieve a target Factor of Safety (FoS) of 1.5 on the global stability of the soil nail reinforced slope. In-situ soil test results were used to estimate strength parameters such as the effective cohesion (c') and friction angle (ϕ') of the soil while the grout-to-ground adhesion was calculated by estimating the frictional resistance along the nail as a result of the effective overburden stress using Equation 1 below.

$$P_{ult} = K \sigma_v \tan\delta \quad (1)$$

Where;

P_{ult} = ultimate grout-to-ground adhesion (kPa)
K = coefficient of friction due to constrained dilation
σ_v = vertical effective stress
δ = effective friction angle between grout and soil

The effective stress method is thought to underestimate the ultimate grout-to-ground adhesion of conventional soil nails in granular material (CIRIA, 2005). This is considered to be due to the effect known as "constrained dilation" whereby radial stresses on the nail are increased as the surrounding soil restricts dilation caused by extension and movement as the nail is loaded. However, the influence of constrained dilation may be limited where loose sands are present (CIRIA, 2005) and when the soil nail is installed by drilling and grouting (Schlosser, 1982). Values published in CIRIA (2005) range between K=0.5 for fine, loose sands and silts, K=1.0 for fine, dense sands to K=2.3 for medium dense to dense sandy gravels. Due to the potential variation in density of the uncontrolled fill, the presence of bricks and gravel, and using a drill and grout installation method, it was decided to adopt a value of K=1 in the design.

2.2 The effects of simultaneous drilling and grouting

According to FHWA (2006), hollow core soil nailing in granular soils generally achieves a better grout-to-ground adhesion than conventional soil nails due to the grouting process. Continuous grouting in permeable granular soils allows grout to permeate into the surrounding material further than would be expected under the conventional drill and grout method. The extent of the permeation zone is dependent on the soil type and its properties, such as; its hydraulic conductivity; whether the material is cohesive or granular; and, its density (FHWA, 2006). Also, in granular fill material it is not unreasonable to expect that the drilled hole will vary in diameter along its length. This is due not only to the permeation zone, but also to localised or possibly extensive soil collapse creating an undulating, irregular and rough grout column.

In addition to this, utilising a simultaneous drilling and grouting method creates the potential for the grout flow to erode away the surrounding material. Once again the extent of erosion will be dictated by the soil properties and also the grouting velocity. Research into the ratio between the borehole diameter and the drill bit diameter in granular soils (including sands, sandy silts and gravels) when installing hollow core soil nails has been undertaken by FHWA (2006). The

results suggested that the borehole will be at least the diameter of the drill bit and in some cases up to 1.5 to 2 times the diameter of the drill bit.

2.3 Pullout testing on sacrificial nails

Pullout testing on six sacrificial hollow core soil nails was undertaken for the SLU project. The design test load was based on the highest average (50kPa) grout-to-ground adhesion estimated by the effective stress method described in Equation 1 multiplied by a factor of 1.5. The estimated grout-to-ground adhesion varied along the length of the wall due to the varying height of overburden. The maximum test load was 90% of the yield strength of the 38mm diameter hollow core bar. Table 1 provides further details of the six pullout test nails.

Table 1: Sacrificial test nail installation details

Test Number	Material	Drill Bit Diameter	Grouted Length	Free Length	Design* Test Load	90% Yield Strength (nail)
Test 1	FILL: Sand	115mm	3.0m	1.5m	81kN	360kN
Test 2	FILL: Sand	115mm	3.0m	3m	81kN	360kN
Test 3	FILL: Sand	115mm	3.0m	3m	81kN	360kN
Test 4	FILL: Sand	115mm	3.0m	3m	81kN	360kN
Test 5	FILL: Sand	115mm	4.0m	2m	105kN	360kN
Test 6	FILL: Sand	115mm	3.0m	3m	81kN	360kN

* 1.5 x Pult (average) x π x D x Lgrouted

Due to the simultaneous drilling and grouting technique, achieving the desired grouted and free lengths for the tests was found to be difficult and a potential area for error in the pullout test results. To achieve the free length (simulating the "active zone"), the grout was flushed out of each borehole with water by inserting a hose to the depth of the desired free length. In unstable soils it was observed that this method may not always be practical or produce trustworthy results due to borehole cave in. Inserting slightly undersized temporary PVC casing to achieve the free length was also trialled and in this instance found to be impractical. The presence of bricks within the fill restricted the insertion of the PVC casing. Further consideration needs to be given to a suitable method of achieving the desired free length in potentially unstable soils. It is suitable to ignore the free length and fully grout the sacrificial test nail for the purposes of proving the grout-to-ground adhesion, provided that the loading jack reaction system is located beyond the passive failure wedge.

The recorded total nail extensions for all six tests were deemed acceptable based on their elastic performance. The test results indicated nail extension rather than mobilisation of the grout-to-ground adhesion. Under the applied loading, nail extensions did not reflect the change in height of overburden along the length of the wall, which is likely to be a result of not loading the nails to the point of bond failure. Recorded nail extensions at the nominated load increments and 90% yield strength of the nail are presented in Figure 4 below. The lower-bound mobilised adhesion C_a^{ult} (calculated from Equation 2 and 3 (Ims & McDonald, 2006) below) was at least five times greater than P_{ult} estimated using the effective stress method in the design.

$$L_{effective} = 2AE\delta m/Fo - 2L_{free} \quad (2)$$

$$C_a^{ult} = Fo/(\pi d L_{effective}) \quad (3)$$

Where;

A = Cross-sectional area of the nail
E = Modulus of Elasticity of nail
δm = Measured extension at the maximum test load
Fo = Maximum test load
L_{free} = Un-grouted or free length of test nail

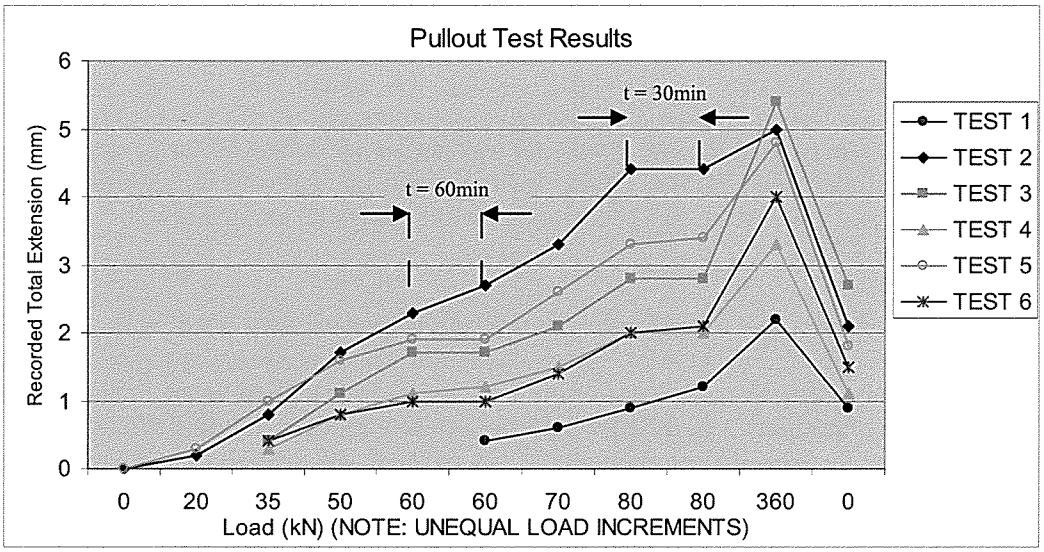

Figure 4: Pullout test results on hollow core soil nails

The design undertaken for the conventional soil nail solution using the effective overburden stress method was deemed to be satisfactory to be applied directly to hollow core soil nails. The grout-to-ground adhesion estimated using Equation 1 was overconservative when compared to the mobilised grout-to-ground adhesion calculated from the pullout test results. It is considered that this is predominantly due to the borehole being irregular, rough and larger than the drill bit diameter. Constrained dilation may have also contributed to the underestimation.

3 ADDRESSING DURABILITY

The perceived hesitation amongst the engineering industry to utilise hollow core self drilling soil nails in permanent applications is predominantly due to concerns regarding long term durability. The installation method, while being advantageous in many regards, also has its disadvantages. Firstly, there is no way of confirming the amount of grout cover achieved using the simultaneous drilling and grouting method. Also, where nails are to be installed in potentially unstable soil and where long nail lengths are required, it is likely that there will be areas where little or no grout cover will be achieved. It is worth noting at this point that galvanising of a hollow core soil nail was trialled. However, the available soil nails and attachments were not sized to allow for the additional thickness created by galvanising.

3.1 Sacrificial steel

One approach to address durability concerns is to estimate the likely corrosion rate of steel and increase the specified steel cross-sectional area depending on the intended design life of the structure. On SLU, testing of pH and Chloride concentrations indicated that the soil was in the non-aggressive range, in accordance with AS2159 (1995). However, a slightly elevated sulphate concentration placed the ground conditions within the lower bound of mild with a corresponding corrosion rate between 20 and 40μm per year. Therefore an allowance of between 2 and 4mm off the radius of the soil nail is required to service the design stresses for the required 100 year design life. This corrosion allowance was taken into consideration when specifying the required hollow core soil nail to meet the required tensile capacity.

3.2 Epoxy coating

Although the tensile capacity of the soil nail is maintained through the allowance of sacrificial steel, it does not address loss of bond between the grout and nail due to spalling when insufficient grout cover is achieved. The application of a Fusion Bonded Epoxy (FBE) coating to the hollow core soil nails reduces the risk of systematic corrosion and spalling. A FBE coating has significant advantages over other forms of epoxy coating in that its powder coat or

dipping application method is very controlled providing a reasonably consistent thickness. It forms a hard, durable coating which minimises the potential for damage during drilling. During nail installation, some damage to the epoxy coating was noted. The damage was incurred (predominantly at the free end of the nail) during un-coupling of the drill head from the hollow core nail. Localised damage to the epoxy coating was not a major concern due to the significant allowance of sacrificial steel. FHWA (2006) indicated that on a limited number of test cases, FBE epoxy coatings were observed to be undamaged following nail exhumation.

3.3 Centralisers

Conventional centralisers are not suitable for this application as they need to be sufficiently robust to withstand the drilling process. Specialized steel star centralisers are available for use on hollow core nails. However, steel star centralisers were not specified in the final design as it is considered that centralisers may restrict the flow of grout and the removal of cuttings. Also, centralisers in granular soils do not guarantee grout cover as the centraliser is likely to embed itself into the bottom of the borehole during drilling.

4 CONCLUSION

On SLU, cost savings as a result of relatively high production rates, when compared to conventional soil nailing necessitating temporary casing, meant that hollow core soil nailing was a viable option. Providing suitable corrosion protection for permanent applications (design life of 100yrs) is the major concern when considering the suitability of hollow core soil nails. However, in relatively non aggressive ground conditions, durability can be addressed through the adoption of sacrificial steel and epoxy coating. The ultimate grout-to-ground adhesion is likely to have been significantly underestimated by the effective stress method (in the fill material), predominantly due to the grout column irregularity and also the potentially enlarged borehole diameter. Pullout testing confirmed that the ultimate grout-to-ground adhesion was at least five times greater than that estimated in the design.

It is recommended that further research into a number of aspects of hollow core soil nailing be undertaken. Research should endeavour to include an assessment of the performance of steel star centralisers in granular soils; an assessment of the toughness of the fusion bonded epoxy coating during installation; a development of a practical method to achieve the free length on test nails; and the undertaking of a program of nail installation and exhumation to observe and record borehole and grout conditions in differing soil types.

ACKNOWLEDGMENTS

I would like to thank Ian Cookson and Brian Chandler of Maunsell AECOM for their advice, guidance and support. I would also like to thank the Southern Link Upgrade Alliance, and in particular Transurban Pty Ltd, for their willingness to support the development of the hollow core soil nail concept.

REFERENCES

AS 2159. (1995) Piling – Design and Installation. *Australian Standard.* Standards Australia, Homebush.

CIRIA. (2005) Soil nailing – best practice guidance. *Report C637.* CIRIA , London.

FHWA. (2003) Geotechnical Engineering Circular No.7 – Soil nail walls. *US Department of Transportation, Federal Highway Adminstration*, FHWA0-IF-03-017, Washington D.C.

FHWA. (2006) Hollow core soil nails – state of the practice. *US Department of Transportation, Federal Highway Administration.* FHWA, Washington D.C.

McDonald, P. & Ims, B. (2006) Soil nailed retention – a practical approach to field verification, *Australian Geomechanics*, Vol 41 No 3, September.

Schlosser, F. (1982) Behaviour and design of soil nailing, *Symposium of recent developments in ground improvement techniques*, Bangkok.

Distinct element modelling of slope stability: application to the Tutupan coal mine

Cecile Coll
Golder Associates, Brisbane, Australia

Anthony Dutton
Golder Associates, Brisbane, Australia

Keywords: open pit, slope stability, discontinuum model, UDEC.

ABSTRACT

Located in South Kalimantan (Borneo, Indonesia), the Tutupan Coal Mine is one of the largest coal open pits in the world, with an annual production of 40 million tonnes. The proposed final pit is 18 km long and up to 400 m deep. The open pit is developing a multi-seam deposit with coal seams up to 50 meters thick dipping from 20° to 70°. Interburden and overburden materials are soft rocks, mainly mudstone and weakly cemented sandstone. Low shear strength bedding parallel sheared zones are present throughout the deposit, particularly at the coal-carbonaceous mudstone interfaces. The geotechnical assessment being undertaken by Golder Associates includes complex numerical modelling to simulate the behaviour of the proposed interim and final pits to determine optimum pit wall angles. Numerical analyses are carried out using UDEC (Universal Distinct Element Code, Itasca) to account for the discontinuities within the rockmass. The paper describes the methodology used in the analyses, the influence of geological and groundwater variations on the results and the behaviour of large open pit walls excavated in low strength jointed soft rocks.

1 INTRODUCTION

Tutupan coal mine is a large open pit located in South Kalimantan (Borneo, Indonesia). The mine is owned and managed by Pt Adaro Indonesia. The mine produces about 40 million tonnes of coal per year and generates about 160 million tonnes of waste per year. The pit works a multi-seam deposit over a length of 18 km (Figure 1). The current maximum depth is about 180 m. The proposed final pit is up to 300m deep with consideration being given to a 400 m deep pit.

Understanding of the hydromechanical behaviour of the rock mass to assess pit wall stability requires the development of combination of geological, geotechnical and hydrogeological models. Those models are supported by geotechnical and hydrogeological investigations including field observation of slope behaviour, mapping, drilling, piezometer installation and laboratory testing undertaken during the past 10 years. Site conditions are complex and variable along strike and down dip with low strength jointed interburden rocks, the presence of bedding shears, variable bedding dip (20° to 70°), faulting and pore pressure distributions strongly influenced by rock type.

Simplified numerical models have been developed and implemented in UDEC (Universal Distinct Element Code, Itasca) in order to simulate the behaviour of the proposed interim and final pits to determine overall slope angles.

This paper presents the geotechnical model used to assess wall stability issues for the southern portion of the Tutupan coal mine. Model complexity is discussed and failure examples of both high wall and low wall are given.

Figure 1: View of part of the Tutupan Coal Mine.

Figure 2: Bedding shear at the interface between a coal seam and a mudstone unit.

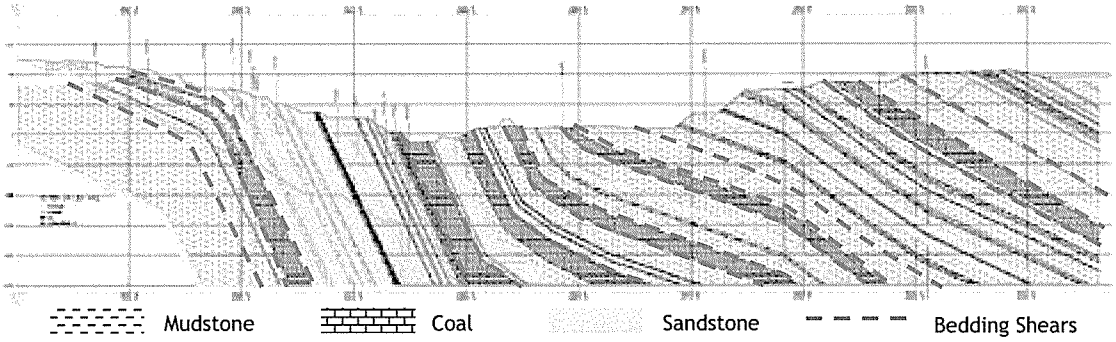

Figure 3: Example of stratigraphy sequence at the Tutupan Coal Mine.

2 GEOLOGY

The coal deposit at Tutupan is of Tertiary age and is characterised by multiple coal seams interbedded with sandstone and mudstone. Major coal seams are 20 to 50 m thick and dip from 20° to 70°. Mudstones are predominant in the upper part of the stratigraphic sequence whereas sandstones are dominant in part of the lower stratigraphic sequence (Figure 2).
Much of the sandstones are weakly cemented and consequently can have low shear strength and are easily crushed. Mudstones are carbonaceous or sandy in places and can include numerous slickensided structures due to past large strains from folding and faulting. The dominant clay mineral is kaolinite.

Bedding parallel sheared zones (bedding shears) are present throughout the sequence, particularly along the coal – mudstone contacts (Figure 2). Bedding shears are typically composed of 10 – 500 mm of sheared carbonaceous mudstone, clay and pulverised coal.
Some cross cutting faults are present, particularly in the northern portion of the mine.

3 GEOTECHNICAL INVESTIGATIONS

Extensive geotechnical investigations have been carried out over the past 10 years to determine rock mass strength and characterise the discontinuities encountered at Tutupan. Investigations

are ongoing as the potential for a deeper pit is assessed. The following sections provide data regarding the southern portion of the mine.

3.1 Geotechnical data

Geotechnical data has been obtained from boreholes, pit mapping, laboratory testing and back analysis of slope failures. Over 100 geotechnical boreholes have been drilled together with 300 + geotechnical mapping stations and numerous piezometers installed to monitor water levels in the mining area. Laboratory testing is predominantly uniaxial compression tests to determine intact rock strength and stiffness and direct shear tests to determine the shear strength of bedding shears, faults, cleat and joints.

3.2 Geotechnical model – Rock mass properties

3.2.1 Discontinuities

The following discontinuities are present in the deposit:

- bedding partings and contacts between adjacent units. Most of the sandstone - mudstone contacts are intact;
- bedding shears are often present at the coal - mudstone contacts and within carbonaceous mudstone units;
- coal cleat, usually organised in two sets;
- joints cutting across bedding are present in both the mudstone and sandstone but are more obvious in some of the sandstone units;
- normal, reverse and strike-slip faults of various throws are present in the deposit but are more common in the northern portion of the mine; and
- numerous, partly healed, slickensided surfaces are present in some of the mudstone beds particularly those near a bedding shear.

The range in peak strength values derived from laboratory direct shear tests are presented in Table 1. The bedding shear friction angles are considerably lower than bedding dip resulting in the potential for low wall stability issues and movements along these weak layers.

Table 1: peak strength values for discontinuities

Discontinuity Type	c'_{peak} [kPa]	φ'_{peak} [°]
Bedding shear	10 (0 – 40)	15.4 (10.0 – 26.0)
Cleat	11 (3 – 30)	30.6 (25 – 34)
Joint in Mudstone	3.6 (0 – 9)	30.1 (25 – 36)
Fault	20	19

3.2.2 Rock mass strength

Geotechnical borehole logs, mapping data and laboratory testing indicate a high degree of variability in intact rock strength and stiffness and rock mass conditions within a particular stratigraphic unit and between different stratigraphic units. No consistent trends were identified along strike or down dip within specific stratigraphic units. There is a general trend of increasing strength for the interburden materials with depth in the stratigraphy. Coal strength is similar for all seams albeit with a high range of values. The mean and range in unconfined compressive strength (UCS) for the different material types are presented in Table 2. The interburden rocks are classified as *soft rocks* according to ISSMFE (International Society for Soil Mechanics and Foundation Engineering).

Elastic properties and shear strength of the rock mass have been estimated using the "GSI approach" described in Hoek *et al.*, 2002. GSI values have been estimated based on mapping data and detailed core logs (Table 2).

Table 2: UCS and GSI values for soft rocks at Tutupan (southern portion of the mine)

Rock	UCS [MPa]	GSI
Coal	9.0 (0.3 – 22.5)	35 (25 - 49)
Mudstone	2.7 (0.01 – 17.2)	52 (39 – 63)
Sandstone	2.3 (0.01 – 16.3)	62 (54 – 71)

High quality testing conditions are needed in order to get reliable results. Sampling and storage conditions are important, especially when dealing with mudstone (strong hydromechanical coupling). Although very important, water content preservation is difficult to ensure and testing on dryer specimens may lead to an overestimation of strengths.

4 STABILITY ANALYSIS

4.1 Possible failure mechanisms

The most likely low wall failure mechanism is an active-passive wedge with the active wedge sliding down a bedding shear(s) and rock mass shearing / buckling in the passive wedge at the toe of the slope. Bedding dip and the presence of weaker materials near the toe of the wall will determine whether failure will occur. Both small scale and overall failure may occur by this mechanism.

Potential high wall failure mechanisms include rock mass shearing / circular failure in flatter dipping areas and flexural toppling in steeper dipping areas particularly where weaker materials are present. Block toppling may occur where unfavourable jointing is present.

Stability issues are highly sensitive to pore pressure as they may reduce considerably the material strength of the rock mass. Rapid unloading during mining induces stress redistribution and consequently dilation and development of fractures leading to changes in pore water pressures affecting (reducing) the mechanical strength of the rock.

4.2 Numerical Analysis: discontinuum model

Numerical analyses of 2D cross sections, subject to plane strain conditions, have been carried out using the distinct element code UDEC (Itasca group) in order to investigate both the possible failure mechanisms and the geometry for the proposed pit walls at different locations along the pit. Model dimensions depend upon the section being analysed and specifically the pit profiles being simulated. The planned size of the pit (up to 400 m deep) required the set up of extensive models which are time consuming to run (days/weeks to run).

4.2.1 Model description

A model includes both the low wall and high wall with the boundaries placed sufficiently remote from the open pit to avoid influencing the behaviour of the rock mass in the vicinity of the pit walls. Each model is divided into an array of blocks by stratigraphic unit contacts, bedding shears, cleat in coal, cross cutting joints (if present) in the interburden and glued joints to simulate the mining sequence.

The rock mass is modelled as an elasto-plastic material with strain softening and a Mohr-Coulomb failure criterion. Cohesion, friction angle, tension and dilation angle reduce linearly from their peak values to the residual values at 4% plastic strain. Discontinuities are described with a Coulomb slip model with residual strength.

The in situ stress state has not been measured at Tutupan Mine, nor is Golder aware of any nearby stress measurements that could be used. As such the in situ stress state was assumed to

be composed of compressive vertical and horizontal principal stresses whose magnitudes increase linearly with depth of cover (K_0=1).

Groundwater pressure in the models is based solely on the vertical depth below a defined water table, and thus remained constant at a given location during an analysis until the water table was altered in response to mining. This is a major and potentially problematic assumption that the water pressures remain constant whilst the rock mass is undergoing volumetric changes due to stress redistribution from mining. Pore pressure is expected to drop in the damaged zones due to dilation and the formation of new fractures. In most of the analyses the groundwater pressure was applied solely to the joints. No coupling was considered between the mechanical behaviour of joints and the pore water pressure (i.e. the hydraulic conductivity is independent of the joint aperture). The groundwater pressure value is however used to calculate the effective stress state acting on the joints.

4.2.2 Case study: example

Figure 4 presents stability issues for a section characterised by a very steep bedding dip (> 60°) changing across the section with a kink present behind the low wall. The pit design comprises a low wall with an 18° overall slope angle and a stepped high wall that has a 53 m wide bench separating a 35° lower slope and a 20° upper slope. Slope instabilities initiate in both walls as a pit depth of 200 m to 250 m, these instabilities lead to large scale failures. The failure mechanisms are flexural toppling along a circular base in the high wall and active-passive wedge failure in the low wall. The low wall failure involves sliding down a bedding shear to the kink in bedding where the resulting stress concentration initiates the development of rock mass shearing through to the toe of the slope and buckling in the lower part of the slope. According to these results, the design in this portion of the pit has been revised to a 16° low wall with the high wall composed of a 50 m wide bench separating a 25°lower slope from a 17° upper slope.

5 CONCLUSION

Extensive geotechnical investigations have allowed the development of complex geotechnical models for the Tutupan coal mine. The reliability of these models is dependent upon an accurate geological model and high quality sampling and testing.

Numerical models were built in UDEC to assess slope behaviour, potential failure mechanisms and to design the proposed final pit walls. An example of a particular section has been presented. UDEC allows the modelling of complex configurations and to trial different scenarios. These analyses are based on some major assumptions regarding groundwater pressures and in situ stress state. Further sensitivity analysis is required to quantify the impact of these assumptions on the pit stability and hence wall design.

ACKNOWLEDGEMENTS

The authors gratefully acknowledge Pt Adaro Indonesia for their assistance with geotechnical data collection and permission to publish analysis results.

REFERENCES

Hoek E., Carranza-Torres C. & Corkum B. (2002) *Hoek-Brown Failure Criterium – 2002 Edition.*

Hoek E. and Diederichs M.S. (2006), *Empirical Estimation of Rock Mass Modulus,* Int. J. Rock Mech. & Min. Sciences, Vol 43.

Itasca Consulting Group, Inc. 2004 *UDEC manuals – Universal Distinct Element Code, Version 4.0*, Minneapolis.

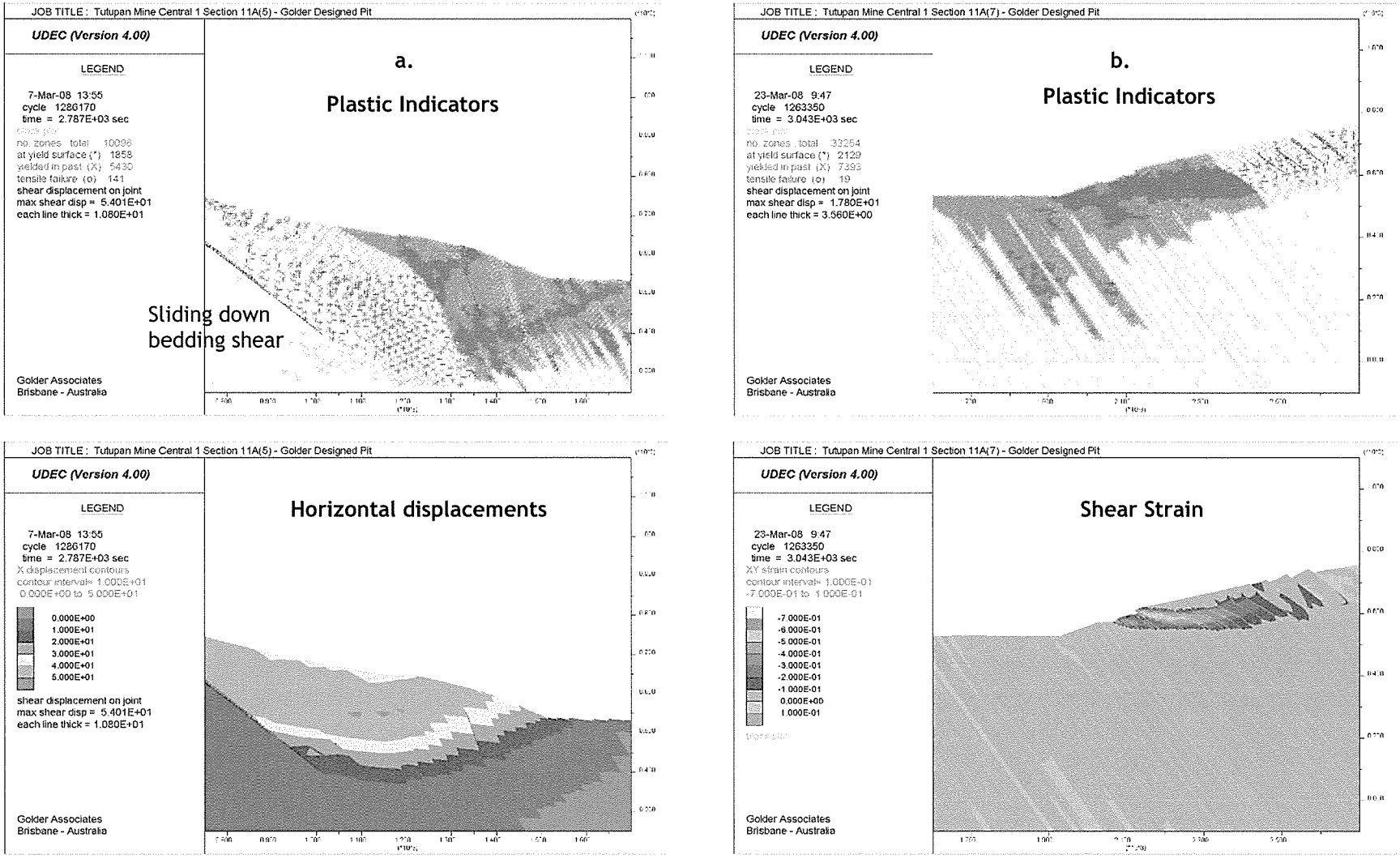

Figure 4: Example of failure in a. low wall, b. high wall

Bored belled piles within Wellington alluvium

Timothy Croad
Tonkin & Taylor Ltd, Wellington, NZ

Keywords: Bored Piles, Wellington, Alluvium

ABSTRACT

Most of Central Wellington is situated on alluvial materials. Generally, the top 30m of alluvium consist of gravels and sands interbeded with layers of silt. The nature in which alluvium is deposited means layers may differ significantly over a small distance (2-3m). Developments within the region are predominantly multiple storeys leading to high structural loads being taken by the foundation systems. These loads dictate the use of pile foundations with the most common form of these being bored belled piles. When setting founding depths for piles it is ideal to found within the gravel layers in order to provide sufficient end bearing and minimise settlement. However these gravel layers often include silt beds of 50mm to 1m thickness. Silt beds within the gravel reduce bearing capacity and increase settlement potential. Special consideration for the presence and strength of these silt beds must be taken into account when designing these piles. This paper discusses design and construction monitoring methodologies developed to address these issues.

1 INTRODUCTION

Much of the development within the Wellington region recently has been within the CBD where the increasing demand for land dictates taller buildings. Taller buildings create larger loads to be supported by the foundations. This paper discusses the design of these foundations with specific consideration of the variable interbeded nature of the underlying alluvium.

2 GEOLOGICAL SETTING

Wellington is located on the intersection of the Indo-Australian and Pacific plates which push together to create hills and pose a risk of earthquakes.

2.1 Wellington Geology

The Wellington landscape is dominated by hills comprising Greywacke rock. The more desirable flat alluvial plains making up the Wellington CBD and the Hutt Valley are underlain by large depths of alluvial soil over the bedrock.

2.2 Geological properties of the Wellington alluvium

The Wellington alluvium varies in grading and consistency. The alluvium has originated from the Greywacke Sandstone and Siltstone found within the Wellington hills. Wellington alluvium consists mainly of a mixture of sands, gravels and silts. The alluvium principally comprise layers of sand or gravel however silt layers are often located between these layers. Silt layers are commonly found to be from 100mm to 5m thick. The layering profile and consistency of this profile varies significantly around Wellington and can be extremely variable across a single building site.

3 FOUNDATION OPTIONS

3.1 Shallow foundations

Shallow foundations are often used in Wellington for lightly loaded structures and in some cases can be used to take large structural loads in areas underlain by alluvial deposits. Shallow foundations have been used for this purpose on projects where deep foundations cannot reach stronger bearing layers than those immediately below the site due to constraints on the depth foundations may extend. This is often the case because resource consent constricts the depth foundations may extend as is the case within the Hutt Valley basin where penetration of the Whaiwhetu aquifer is prohibited. Foundations in cases like this must be relatively rigid to reduce the risk of differential settlement posed from the lack of continuity of alluvial deposits below the site. Shallow foundations often require some form of ground improvement when used to take larger loads. This can increase bearing capacity, reduce settlement potential and reduce the potential for liquefaction. Ground improvement is discussed further in the deep foundations section below.

3.2 Deep foundations

Deep foundations are the primary method of transferring large structural loads to the ground in Wellington. Deep foundations have the ability to resist significant downward and upward loads along with reducing the risk of damage from liquefiable layers below the structure.
The general idea of deep foundations is to transfer loads from the structure to layers within the ground, which have better bearing capabilities than the soil immediately below the ground surface.
The following deep foundations are often used within Wellington depending on site conditions and Resource Consent requirements.

3.2.1 Bored Piles

These are covered in more detail in section 4. These are primarily used as end bearing piles in Wellington due to relatively low skin friction. Belled pile bases are commonly used to increase pile capacity.

3.2.2 Driven piles

A driven piles capacity is achieved through either end bearing, skin friction or a combination of the two. Various different driving and construction methods can be used and a range of different pile sections depending on the ground conditions and capacity requirements.
Driven piles are fast to construct. Their capacity can be efficiently verified by driving formula or pile driving analysis (PDA) testing. Driving construction noise and vibration often precludes their use in built up areas.

3.2.3 Screw piles

The capacity of a screw pile is gained purely in end bearing as it is commonly recognized that the friction from the disturbed soil around the relatively small shaft is negligible. This structural system is useful on sites where strong bearing layers are located within the top 10m and is relatively cheap and easy to construct.
Care must be taken when used on sites within Wellington alluvium as the purely end bearing nature of these piles exposes them to the risk of settlement if compressible layers are located below the bearing layer.

3.2.4 Micro piles

Micro piles are miniature bored piles, often as small as 100mm in diameter. Micro piles rely mainly on shaft friction and are relatively simple to construct. These piles have relatively low capacity.

3.2.5 Ground improvement

Common ground improvement methods include gravel columns and Cement Soil Mixing (CSM). These methods improve the strength characteristics and can reduce the liquefaction and settlement potential of the soils they are applied to.

4 BORED PILE DESIGN

Bored and cast piles are the most common form of deep foundation used for highly loaded structures within the Wellington Region. This is because the noise and vibration associated with large driven piles is unacceptable in built up areas and belling allows the bored piles to carry high loads making these a cost effective solution.

4.1 Site Investigation

Due to the variable nature of the alluvial deposits it is important that extensive data of the subsurface is obtained. Site investigations generally comprise boreholes with SPTs, since CPTs refuse on dense layers within the alluvium. The borehole investigation are normally carried out in two stages. The first stage to provide an initial estimate of founding depth and pile capacity.
The second stage of investigation is undertaken to design specific pile foundation depths. The number and location of the boreholes required are determined by considering the consistency of the alluvial deposits and the spacing and loading of the piles. It is not uncommon on highly variable sites to undertake one borehole per pile. SPTs in these boreholes are undertaken at 1m intervals until a sufficient thickness (3 x pile bell diameters) of appropriate bearing material is identified above and below the proposed founding level. The wash drilling cuttings are monitored carefully during drilling to identify any silt lenses between the SPT sampling.

4.2 Downward capacity

Piles in Wellington alluvium are often designed individually with pile specific downward loads being considered. Ultimate limit state loads are considered relative to the design capacity of the pile and serviceability limit state loads are considered in checking settlement potential. The failure mechanism assumed under ultimate limit state downward loads is shown in figure 1. Founding level and bearing capacity of individual piles are assessed from borehole and SPT data adjoining the pile location.
Bearing capacities within the Wellington alluvium have been assessed by a number of published methods. Based on this assessment and engineering judgment a standardised formula has been developed as outlined below. Bearing capacity is assessed on the basis of soil type and density (SPT 'N' value). In granular soils the bearing capacity in kPa is taken as 115 times the average SPT N count with a maximum of 5,000 kPa. Where non-plastic silts are present and judged to influence bearing capacity, a value in kPa of 80 times the average SPT N is assumed. A bearing capacity of 45 times the average SPT N is assumed from plastic silt beds, however these are generally avoided due to their high settlement potential. The average SPT N count is taken over the bearing influence area which is approximately three bell diameters above and below the founding level. The influence of differing materials on bearing capacity must be considered when deciding upon the bearing capacity available for a pile.
Skin friction will vary based on material type and density, however for simplicity only one or two different skin friction values are generally applied for different layers located along the

length of shaft providing skin friction. Skin friction has been based on a number of different papers and methods and engineering judgement. Pile pull out tests within Wellington Alluvium have been undertaken and generally confirm a skin friction of more than 2 times the average SPT N count over the length of shaft providing skin friction. Skin friction should not be considered over the length of the pile shaft which is located within the end bearing area of influence which is approximately three bell diameters above the founding level. This is because the soil within this length will not provide skin friction on the shaft of the pile once a failure bulb has been formed. When seismic loads are being considered it is important to consider liquefiable layers within the piles shaft as having no skin friction.

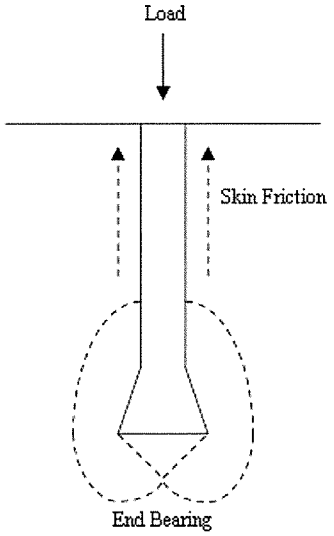

Figure 1: Downward bearing capacity failure

4.3 Upward capacity

Large upward loads on piles within Wellington are generally due to earthquake imposed actions. Buoyancy forces on basements can also impose upward loads. Design considers two potential mechanisms of uplift failure on bored and belled piles. These are a bearing capacity failure around the annulus above the bell plus the shaft resistance, and a projected cylinder failure as shown in figure 2. When uplift loads are imposed from seismic design it is important to discard friction from any layers prone to liquefaction.

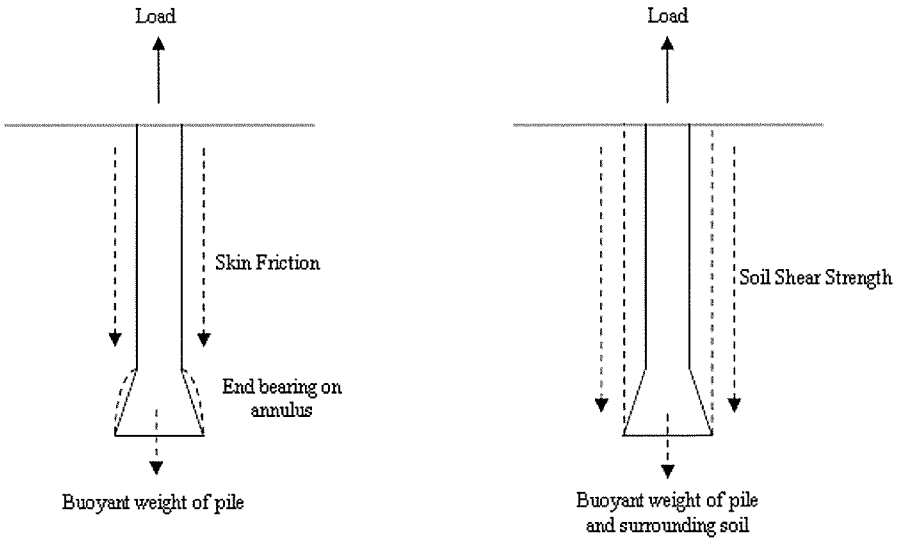

Figure 2: Upward bearing capacity failure and projected cylinder failure

4.4 Settlement

Consolidation of the silt beds beneath piles presents a risk of settlement. Settlement of a pile has structural implications and must be minimised. Allowable settlements should be agreed with the structural engineer. When looking at founding levels for a pile it is preferable to find a bearing layer which does not contain compressible silts below the base of the bell. This is not always possible and a founding level which minimises the settlement potential from compressible silts is looked for by undertaking settlement analysis of piles under serviceability limit state loads.
The serviceability limit state load on a pile is taken by both skin friction and end bearing. However, the skin friction component has less of an impact on the settlement potential than the end bearing component because the pile base must move if any settlement is to occur. The load critical to settlement is therefore the load transferred to the base of the pile. The load transferred to the base is taken as the serviceability limit state load less the load taken by the skin friction. Settlement potential of the pile is taken as that of the base of the pile.

5 CONSTRUCTION OF BORED PILES

Pile construction within Wellington alluvium varies depending on specific site conditions. The most prominent risk when constructing bored piles within Wellington alluvium is collapse of the exposed pile excavation and bell. On some sites the materials retain sufficient undrained shear strength when exposed for piles to be constructed by drilling under dry conditions. Water seepage into the excavation can be pumped and the pile can be poured with minimal risk of collapse. Where conditions are less favourable, soils either do not retain sufficient undrained shear strength or do not have sufficient undrained shear strength to start. Once exposed these soils often collapse. Piles must then be drilled under water which provides hydrostatic head and reduces the drainage of water from the surrounding soil. Most sites fitting into this category have high water tables (approx 5m below ground level) and seepage of water into the surrounding fluid from the pile excavation does not occur. The hydrostatic head provides limited support to the pile excavation and bell while the soils do not drain and loose there undrained shear strength, reducing the risk of collapse. On the most difficult sites, pile excavations and bells are prone to collapse even when a hydrostatic head is present and alternative construction techniques must be used. A method recently used to allow pile construction in these relatively unstable conditions is excavation under water with a polymer additive. Use of polymer is discussed further below.

5.1 Methodology

Two main methods for constructing bored and belled piles have been developed to reduce the risks of collapse of exposed excavations and bells. The use of these methods generally depends upon the length of the pile to be constructed and the temporary stability of the soils being constructed in.
In the first method the casing is temporary and is driven into the ground through the use of a vibratory hammer. Ideally the casing will extend to the top of the bell. The pile is drilled and a bell is formed and cleaned. Reinforcing is added and the pile is ready for concrete. The pile is either tremmie poured or top poured depending upon the degree of water seepage into the pile. The casing is removed using a vibratory hammer which vibrates the concrete.
The second method has been developed recently for use on sites where either the length of pile makes use of a temporary casing difficult, or impossible, or where there is a high risk of the bell of a pile collapsing. A temporary casing is installed through the upper weaker soils. The pile is then drilled with the pile full with water mixed with a polymer additive which increases the liquids viscosity. The high viscosity of the liquid reduces the washing effects on the un-cased pile excavation and reduces any seepage between the soil and the pile excavation while the hydrostatic pressure provides some support. This reduces the likelihood of excavation collapse

within and above the bell. The pile is drilled and prepared the same as in the first method and the pile is tremmie poured.

5.2 Construction monitoring

When monitoring the construction of bored and belled piles it is important to be confident that a well formed bell is present and that sediment on the base of the pile both within the annulus and spigit of the bell is minimised. Sediment from the construction process settles on the bottom of the pile and if left, poses a significant risk of compressing once load is applied. Some of this sediment will be displaced from the pile's bottom by tremmie pour. However, it is important ensure that the contractor's equipment and techniques are such that the annulus of the bell is swept into the spigit where it can be removed by a cleaning bucket. The effectiveness of the belling tool sweeping the annulus clean cannot be tested. It is therefore important to develop a full understanding of the processes and tools being used to judge this. Monitoring engineers should also check that the spigit is cleaned sufficiently. The thickness of sediment within the spigit can be felt using a tape measure weighted at the end. The sediment can often be viewed using a camera under dry conditions. In addition to the information from the boreholes the design engineer can confirm the design ground conditions by inspection of samples taken within the founding depth during the drilling of a pile.

6 CONCLUSIONS

The materials of the Wellington alluvium are generally granular in nature however the variability in strength and presence of silt beds both with depth and across a site has dictated that design is specific to an individual pile. Piles are designed based on individual loadings and borehole data most relevant to the pile. It is not uncommon for piles very close together and with similar loads to have different founding levels.
Settlement of piles must be considered in cases where silt beds below the base of the pile cannot be avoided and this often governs design.
Contractors have had to come up with some innovative ways of mitigating the risks from pile excavation and bell collapse.

ACKNOWLEDGEMENTS

This paper was written with the support of Tonkin & Taylor. Assistance and review was provided by Stuart Palmer.

REFERENCES

Loney, G. Langbein, A. and Sinclair, T. (2008) Tonkin & Taylor Ltd - Shallow Foundations Training Course.

Palmer, S. and Langbein, A. (2008) Tonkin & Taylor Ltd – Design and Construction of Deep Foundations presentation.

Residential Land Development on Organic Soils, Takanini, Auckland, New Zealand

Chris Edwards
Coffey Geotechnics (NZ) Limited, Auckland, New Zealand

Keywords: Organic soils, settlement, preload, foundation design, Takanini

ABSTRACT

Takanini is a suburb situated within the Papakura District and located approximately 25km south of the Auckland CBD. The geological setting of this area comprises alluvial sediments of the Tauranga Group deposited during the Pleistocene period consisting of consolidated clays, silts and sands, with layers of peat and organic clay.

The geology of this area provides geotechnical issues for residential, commercial and industrial land development. The Addison Block residential subdivision is located within this area and when finished will consist of medium to high density two and three storied dwellings along with commercial precincts, recreational reserves and associated infrastructure.

Geotechnical involvement includes, predicting settlement rates of building and fill loads, and monitoring post earthworks and building construction settlements. Impermeable surfaces are designed to recharge the groundwater regime to minimise groundwater drawdown and associated settlement. The construction of road pavements and service lines is generally by undercutting nominal depths, lining with geotextile cloth and replacing with sand and hardfill.

1. INTRODUCTION

Addison Block residential subdivision is an irregular shaped block of predominantly flat land made up of several stages. It is situated within Takanini, a suburb of South Auckland area and is identified within the Takanini Structure Plan as an area of high expected growth, situated near both light rail and motorways and approximately 25km south of the Auckland CBD.

Stages completed and proposed consist of 2 to 3 level dwellings comprising of stiffened raft foundations to evenly disperse foundation loads. The subdivision is a medium to high density development consisting of approximately 20 dwellings per hectare and surrounded with public parks. A commercial centre and retirement village are also proposed as part of the development.

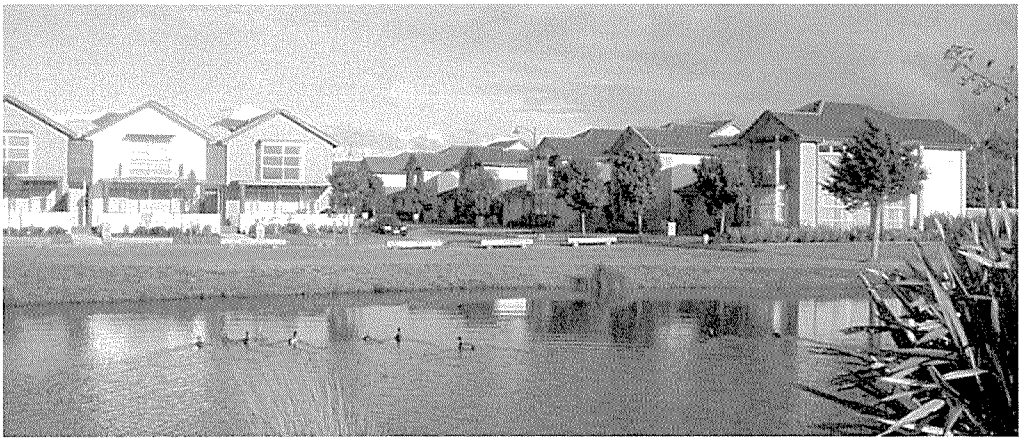

Figure 1: Addison Block

2. GEOLOGICAL SETTING

The Takanini area is situated within a depositional basin of shallow alluvial sediments of the Tauranga Group, deposited within the Pleistocene period. The deposits comprise an inorganic layer typically between 1 and 3 metres thick of pre-consolidated clays, silts and sands, this layer is generally described as the inorganic "raft". The thickness and consistency of this raft governs building foundation options. This is underlain by layers of amorphous peat and organic clay to varying depths. The engineering properties of these peat/ organic clay layers vary over the site, but are typically very soft to firm, moderately to highly compressible, highly organic and generally have water contents around 150%.

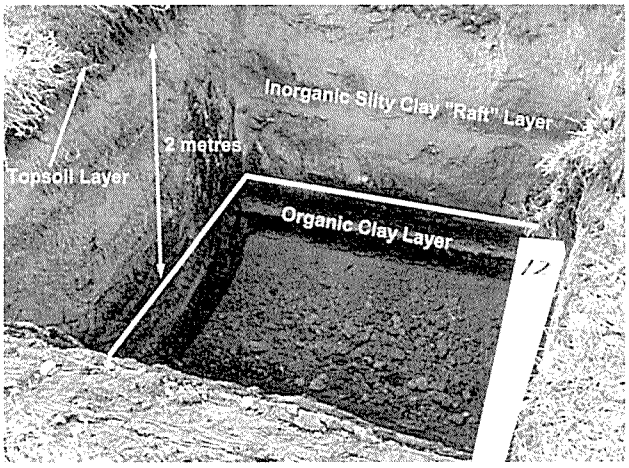

Figure 2: Typical Soil Profile

Below these deposits are gently dipping Waitemata Group bedrock sandstones and mudstones of the Miocene Age. As can be seen on Figure 3, Waitemata Group outcrops border the northern and southern reaches of the Takanini Basin. Within the subject area this bedrock is located at depths typically between 10 and 30 metres.

This geological setting formed as a result of the area being below sea level during the Pleistocene age and as a result a deep embayment of the Waitemata Group strata was formed. This resulted in the formation of a depositional basin and infilling by Pleistocene alluvial sediments. Shallow waters resulting from this and the inducement of estuarine and lacustrine environmental conditions formed the interbedded alluvial and carbonaceous deposits existing today.

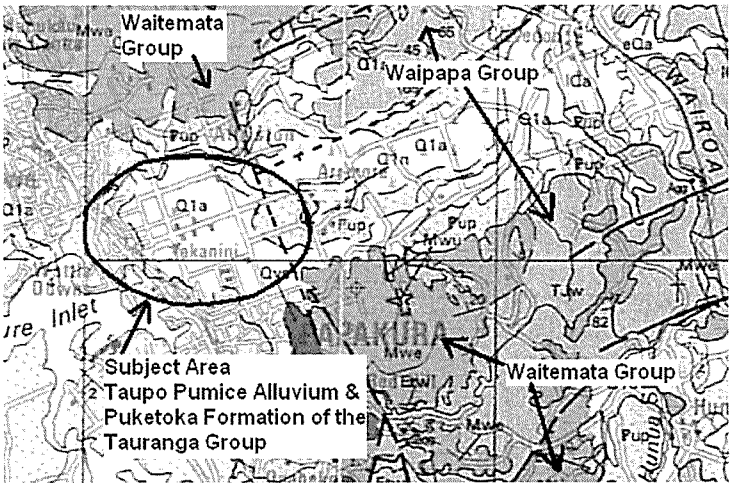

Figure 3: Geology of the Takanini Area (adapted from GNS 1:250,000 Geological Map 3)

3. SETTLEMENT PREDICTION AND MONITORING

Cuts and fills are undertaken on site to create level building platforms. Due to soft subsoils, fill depths are kept to a minimum and are typically on average less than 400mm and generally comprise cut balance material.

Fill and building induced settlement is first predicted through settlement calculations and preload trials using available laboratory and field data. During development, settlement monitoring of fill areas and constructed dwellings is then undertaken.

3.1 Preliminary Settlement Predictions

Settlement calculations were initially based on consolidation parameters derived from laboratory consolidation testing and from the assumption that the depth to relatively incompressible inorganic substrata is approximately 15 metres. This represents worst case scenario soil conditions on site.

Settlement calculations took into account wide spread fill loads of 7kPa representing a scenario of 400mm height of subdivisional filling placed and uniform floor loads of up to 10 kPa.
From this, settlements of up to 200mm were calculated as possible under worst case soil conditions, but it was assessed that settlements may be closer to 100mm on account that lenses of less compressible inorganic sands and silts are most likely present within the organic clays and peat. (Coffey Geotechnics (NZ) Limited 2008).

3.2 Preload Trials

To validate settlement prediction calculations a preload trial area was selected within an area of site defined as having worst case scenario subsoils (Foundation Class C). The preload trial consisted of approximately 1 metre height of hardfill placed over a levelled area of approximately 18 by 18 metres. As shown in Table 1, monitoring results from the 2 year preload trial showed settlement of up to 135 mm under 1 metre of hardfill with over 90% of settlement induced within the first year. (Coffey Geotechnics (NZ) Limited 2008).

Table 1: 1 Metre Preload Settlement Trial – Foundation Class C

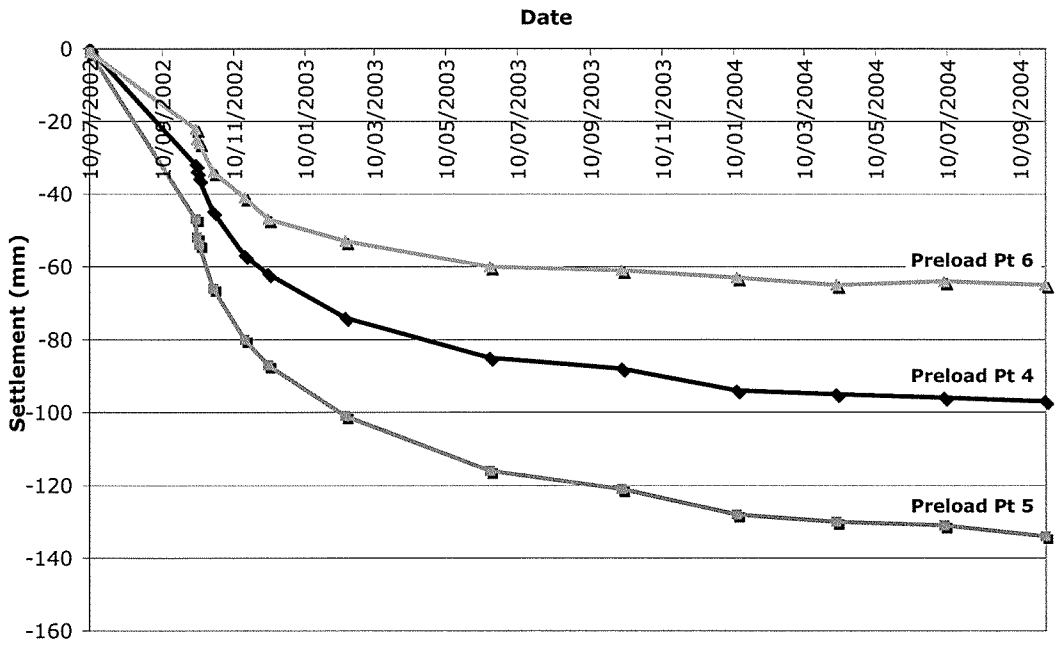

3.3 Foundation Class Settlement Predictions

The preload settlement data was then used to refine and validate preliminary settlement calculations under worst case scenario soils. From adjusted calculations a figure of 13.5mm of settlement per 100mm of filling was expected in worst case scenario soils (Foundation Class C) and subsequently rounded up to 15mm settlement per 100mm of filling. Under more competent soil classes (Foundation Classes A and B) a lower settlement value of 10mm per 100mm was assumed. (Coffey Geotechnics (NZ) Limited 2008).

3.4 House Settlement

The preload data was then used to calibrate the original settlement calculations and applied to a house platform with dimensions of 8.5 by 8.5 metres applying a net pressure of 9kPa to the soil, this replicates the proposed two level Addison Block dwellings. Building settlements were subsequently calculated as 45mm, and rounded up to 50mm to make allowance for subfloor hardfilling. (Coffey Geotechnics (NZ) Limited 2008).

Differential building settlements were calculated to be less than 25mm over 6 metres length in building and within the New Zealand Building Code limits. Differential building settlement from subdivisional fill can usually be disregarded through allowing elapsed lengths of time (usually in the order of at least a year) for fill induced settlement to occur before allowing building construction to commence. Settlement monitoring (as discussed in 3.5 below) is also used to confirm that settlement has elapsed before building construction commences.

3.5 Settlement Monitoring

Prior to earthworks commencing, settlement monitoring markers are installed at selected fill locations. The levels and locations of the settlement markers are then surveyed to get pre-development levels. Subdivisional filling is then placed up to and around the markers and regular measurement of the marker levels undertaken until it is assessed that the majority of fill induced settlement has occurred.

Within constructed stages, survey monitoring points have also been set on the foundations of selected dwellings to monitor settlement post development and ensure settlement of dwellings and underlain fill is within predicted limits.

4. SOIL CLASSIFICATION FOR RESIDENTIAL FOUNDATIONS

Foundation design for the dwellings is affected by the specific ground conditions. The soils present within Addison Block are therefore zoned into three specific classes' (as depicted on figure 4 below) dependant on the consistency and thickness of the inorganic raft layer, composition of the underlying organic soils and subsequent settlement prediction as discussed in section 3 above. Preliminary foundation classification is undertaken during site investigation stage and confirmed within the Geotechnical Completion Report for the subdivision prior to building construction. The general specifications of these foundation classifications are described below but are also adjusted between stages where subsoil conditions vary. (Foundation Engineering Consultants Limited 2003).

4.1 Foundation Class A

- Mainly inorganic overburden soils through out influence of shallow building foundations (inorganic raft greater than 2 metres thick).
- Soils strengths less than required by NZS 3604 for 'good ground'.
- Best suited for uniformly spread building loads constructed at or near original ground level or shallow pile foundation systems.

- Roofing systems can be tile or iron, brittle exterior cladding should have regular construction joints.
- Geotechnical Ultimate Bearing Pressures limited to 180kPa.
- Approximately 20mm of settlement expected under uniform building loads.
- 10mm of additional settlement per 100mm thickness of subdivisional filling.

4.2 Foundation Class B

- Up to 1 metre of topsoil and inorganic raft overlying soft organic clays.
- Best suited for uniformly spread building loads constructed at or near original ground level.
- Roofing systems may be tile or iron and brittle exterior cladding must have construction joints.
- Geotechnical Ultimate Bearing Pressures limited to 90kPa.
- Approximately 30mm of settlement may be expected under uniform building loads.
- 10mm of additional settlement per 100mm thickness of subdivisional filling.

4.3 Foundation Class C

- Minimal thickness of topsoil and/or inorganic clay raft (less than one metre thick) overlying very soft organic clays.
- Best suited for low pressure uniformly spread building loads constructed at or near original ground level.
- Roofing systems should be lightweight and exterior cladding flexible and contain adequate control joints.
- Geotechnical Ultimate Bearing Pressures limited to 50kPa.
- Approximately 50mm of settlement may be expected under uniform building loads.
- 15mm of additional settlement per 100mm thickness of subdivisional filling.

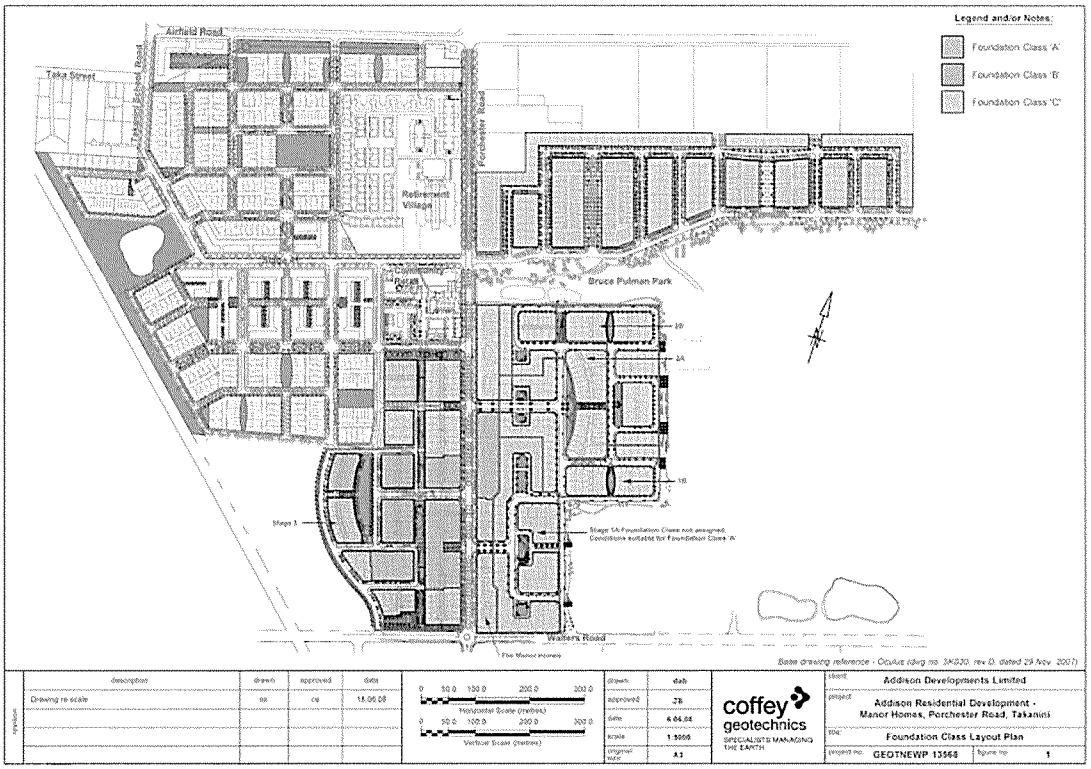

Figure 4: Foundation Class Zone Plan of Addison Block

5. GROUNDWATER

Measured fluctuations in the groundwater table typically trend within 3 metres of the surface. The development of land can have a large impact on the resulting groundwater regime due to increased impervious surfaces mainly from dwellings and roads reducing recharge of the groundwater table. Impacts of this can theoretically drawdown the groundwater table and possibly induce consolidation and degradation of the organic subsoils.

The majority of stormwater collected from impermeable surfaces (i.e. roofs and roads) is therefore recharged back into the ground via stormwater ponds, rain gardens, swales and soakage pits. Piezometers installed within the subdivision are monitored regularly, apart from seasonal fluctuations in the groundwater regime, monitoring has shown no groundwater drawdown trend from the development of the land.

6. ROAD AND SERVICE LINE CONSTRUCTION

The strength of subgrades within roads and service trenches varies between the soil foundation classes. Ground improvement undercuts to provide adequate bearing strength for sealed roads and service pipes is therefore undertaken. Construction methodology is generally as follows:

1. Road subgrades are undercut by 300mm to 700mm (undercut depth dependant on foundation class and CBR testing), geotextile cloth placed over subgrade and up faces of undercut excavations.
2. Road undercuts are then backfilled with Woodhill black sand capped with a 150 mm hardfill layer to confine the top of the sand
3. The roads are also used for truck haulage to help induce settlement during construction.
4. Service lines (stormwater and sanitary sewer) are then installed where crossing or within influence of road subgrades. A general undercut below the invert of the pipes of between 300mm and 450mm is undertaken (undercut depth dependant on foundation class, trench depth and pipe size), geotextile laid and the undercuts backfilled with hardfill.
5. Roads are then sealed.

7. CONCLUSIONS

Development of land within the Takanini area presents issues due to relatively soft and organic subsoils. Settlement prediction and monitoring is therefore undertaken and careful design and construction methodology is required to minimise the potential effects of settlement on dwellings and infrastructure.

REFERENCES

Coffey Geotechnics (NZ) Limited (2008). *Geotechnical Design and Construction Summary for The Manor Homes, Porchester Road, Takanini.*

Foundation Engineering Consultants Limited (2003). *Geotechnical Investigation Report on Addison Residential Development, Stages 1B and 2, Takanini.*

Institute of Geological and Nuclear Sciences Limited (2001). *Auckland 1:125,000 Geological Map 3.*

The Cutter Soil Mixer Method for Ground Improvement

Heather Enright
Coffey Geotechnics (NZ) Limited, Auckland, New Zealand

Keywords: Cutter Soil Mixer, cut-off wall, inground wall, slope stability

ABSTRACT

The Cutter Soil Mixer (CSM) Method for ground improvement is new to New Zealand, and brings with it new construction possibilities for retaining walls, cut-off walls, building foundations and slope stabilisation.

The CSM method involves the formation of a vertical panel in the ground by using rotary cutting heads to break up the soil and intermix it with a cement slurry.
Recently the CSM method was used to construct a temporary retaining wall to facilitate a single level basement excavation in downtown Auckland. The panels were successfully constructed to 9 metres depth through four distinct lithologies, including reclamation fill, marine sediments, residual Waitemata Group soils and Waitemata Group bedrock.

A CSM slope stabilisation method has also been proposed for a future residential subdivision in Northcote where conventional shear key construction and bulk earthworks are difficult due to access, limited available area for fill conditioning and material handling, and silt control constraints. The CSM method offers solutions to these issues, with the added benefit of speed in a season-driven industry.

The CSM method is showing success in a range of applications across several different soil types. This paper outlines the CSM method and machinery, using case studies to illustrate some of its capabilities and efficiency.

1. INTRODUCTION

The Cutter Soil Mixer (CSM) Method for ground improvement uses a set of cutter wheels mounted on a mixer head to mix a cement slurry with the insitu soils to create an inground panel. The technique is predominantly used for retaining walls and cut-off walls, and can result in significant cost and time savings when compared to conventional wall construction and deep mixing methods.

The German innovation is new to New Zealand, and has been involved in many successful projects. It has been used to create inground walls and for ground improvement, and has been proposed for slope stabilisation purposes.

2. THE CUTTER SOIL MIXER METHOD

The CSM machinery comprises a mixing head mounted on a Kelly bar manipulated by a large track rig. The Kelly bar is typically circular for shallow depths of up to 12 metres, with a rectangular shaft used for depths of up to 35 metres. The mixing head features two cutter wheels that rotate about a horizontal axis, cutting and loosening the soil and mixing it with a concrete slurry. The mixing head currently used in New Zealand produces a panel measuring 550mm by 2400mm, mounted on a rig that can install a panel to depths of up to 18 metres. Larger mixing heads and rigs are available with a potential panel depth of up to 80 metres.

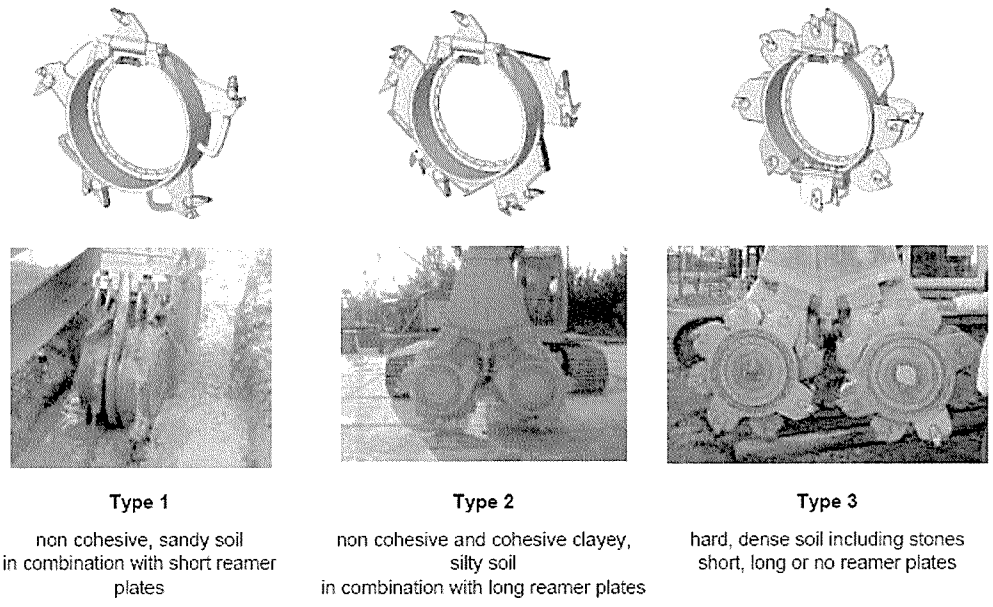

Figure 1: Cutter Wheels (Bauer Maschinen, 2005)

The cutter wheels used vary depending on the soil to be mixed. Non-cohesive sandy soils utilise a wheel primarily designed for mixing, while mixing in dense and cohesive soils requires a greater cutting component (Figure 1). The cutter wheels are the only moving parts in the mixing head, allowing instruments to be mounted within the unit to monitor information such as verticality during the construction process (Fiorotto et al., 2005). The operator can correct any deviations by varying the speeds of the independent cutter wheels if necessary.

CSM production rates are influenced by a variety of factors. In general, uniform non-cohesive soils mix most efficiently while dense to very dense soils and weak rock require a longer cutting phase. In addition, long straight sections to depths of greater than 10 metres are more cost efficient than irregular wall layouts and panels to shallow depths due to the impact of non-productive periods such as moving and setting up (Bauer Maschinen, 2005).

During the construction process the cutter wheels break up and mix the soil while a nozzle set between the wheels injects the cement slurry. Penetration rates are dependent on the soil type and machinery used, typically reaching 200 mm – 600 mm/min. The cutter wheels can rotate in both directions, with the preferred direction from outside inwards (Bauer Maschinen, 2005). The wheels force the soil material up through a set of fixed shear plates, forcing it to break down and combine with the slurry to form a homogenous mix. Construction is typically carried out in a shallow pre-excavated trench to collect surplus slurry. The slurry is removed by an excavator to be trucked off site.

The binder used in the CSM process typically comprises cement, bentonite and water. Other additives may be used if required. The mix design depends on the application of the panels and the soil conditions, with mix proportions determined by suitability testing prior to construction.

The primary use of the CSM technique has been to install cut-off and retaining walls. Creating a continuous low permeability wall involves installing a row of primary panels spaced at approximately 4.2 metre centres (dependent on the dimensions of the mixing head used) followed by a series of interlocking secondary panels (Figure 2). Overlapping may be carried out immediately following primary panel installation ("fresh-in-fresh") or following work interruption or weekend breaks ("hard-in-hard").

Reinforcement in the form of steel beams or cages may be inserted into the wet panel to add strength to the completed wall. These generally penetrate under their own weight, or with the assistance of a light vibrator.

The CSM technique has significant advantages over other deep mixing techniques:

- The existing soil is used as a construction material, resulting in minimal generation of spoil and runoff. This is particularly suited to use in contaminated sites or areas where silt control is critical.
- A continuous wall formed with interlocking panels has a greater overall strength than interlocking columns as there are fewer joints within the structure. In addition, the technique is more cost effective as it uses less binder than a secant pile wall where pile diameter must be much greater than the panel width to achieve an equivalent surface area (Figure 3).
- Monitoring equipment within the immobile mixing head provides the operator with real-time information on the mixing progress.
- Ground disturbance and vibration is minimal, allowing for construction directly adjacent to existing structures.

Design of a CSM wall involves conventional steel cantilever wall calculations, finite element analyses and arching calculations. Modelling software such as *Wallap* or *Phase*^{2} is used to calculate likely deflections.

Mix design is determined in the laboratory using samples of the soils to be mixed. In general, coarse-grained soils such as sand and silty sand are faster and easier to mix and yield higher strengths than cohesive clayey soils. Organic soils are inherently weak and generally do not react well to the addition of cement. Mixed samples are tested for strength following setting periods of 7 and 28 days, with the mix design yielding the required strength being used in construction.

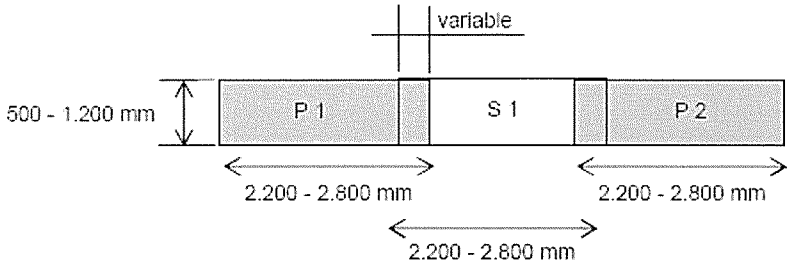

Figure 2: Forming a continuous wall (Bauer Maschinen, 2005)

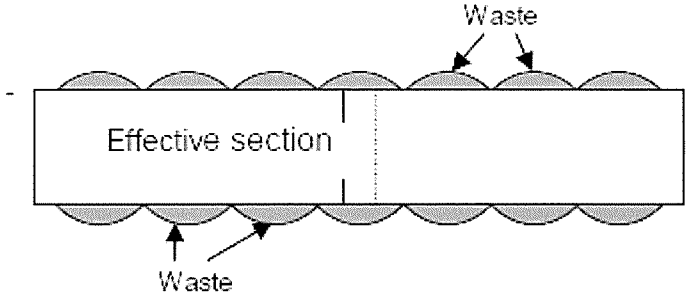

Figure 3: Comparison of mixed areas (Fiorotto et al., 2005)

Quality control and monitoring measures should be put in place during the construction process. A series of laboratory testing including unconfined compressive strength (UCS) and effective stress triaxial (EST) tests may be carried out to determine the nature of the insitu mix and strength of the CSM panels to ensure that its design strength requirements have been met. In addition, deflection monitoring in the form of survey markers and/or inclinometer installation allows for ongoing monitoring following construction and acts as an early warning system if trigger levels (set at the design stage) are reached.

3. CSM FOR CUT-OFF AND RETAINING WALLS

The CSM technique is widely utilised for inground wall construction. It was used in downtown Auckland to create a temporary retaining wall to support a basement excavation. The wall was to be embedded 4.3 metres with a retained height of 3.2 metres. Interlocking CSM panels to depths of 9 metres formed the wall around the perimeter, with construction carried out directly adjacent to busy main roads and a neighbouring building. A small portion of the wall was formed using sheet piles where services were excavated and realigned while the CSM rig was operating on another portion of the wall (Figure 4).

The panels were mixed through four distinct material layers. The surficial reclamation fill comprised construction debris, sands and silts, and other miscellaneous materials. Soft marine sediments were encountered beneath the fill, overlying residual Waitemata Group clays and silts and Waitemata Group bedrock. Mixing was completed within two weeks. To resist bending moments 310UB46 beams were inserted into the panels at 1 metre centres while the slurry mix was fresh. The beams sank under their own weight.

Wall construction was quick and cost effective, with basement excavation and construction now complete. Monitoring instrumentation shows minimal deflection of the walls, indicating that the mix design and reinforcement were correctly determined for the job.

CSM walls may also be used to support gravity loads to contribute to foundation design and construction.

Figure 4: Sheet pile and CSM wall at Fanshawe Street, Auckland

4. CSM FOR SLOPE STABILITY

The CSM technique has been proposed for use in slope stabilisation by constructing an array of panels to act as a shear key. The panels are oriented with the long axis downslope in a grid pattern arranged to treat a percentage of the slope as determined by stability analyses. Specifics for panel parameters, dimensions and array are determined by using a slope stability analysis programme such as *Slide, Phase*^{2} or similar. The advantages of the CSM technique over conventional bulk earthworks and shear key construction include savings in time and materials, and less onerous silt control requirements.

A proposed residential subdivision in Northcote, Auckland, requires a shear key to be constructed at the downslope boundary of four residential lots where signs of geomorphic instability have been identified. Conventional shear key construction beneath these lots will be onerous as the only viable fill conditioning area is on the western portion of the site, one hundred metres away across a gully that will need to be bridged and stabilised to allow the passage of heavy earthmoving equipment. In addition, the construction area is directly adjacent to dense native vegetation and an existing water course on which strict setbacks and silt control measures are placed.

The proposed shear key design involves excavating, working and replacing approximately 12,000m^3 of material and associated stability benching. Confined conditions will limit the number of machines in the excavation, prolonging the construction time. Construction of the shear key may potentially run over two earthworks seasons at a considerable cost.

The proposed CSM design involves the construction of approximately 230 panels to depths of up to 9 metres along a 17 metre wide zone at the lower boundary of the affected lots. This design treats 15% of the slope, the volume required in this case to minimise slope instability. The panels will be aligned in a grid with the long axis oriented downslope and each row offset from the rows above and below by 0.9 metres. These parameters were established by modelling the section in *Slide* and *Phase*^{2} to achieve a factor of safety of 1.5 (Figure 6). Following the establishment of an appropriate model, further analyses were carried out using *Phase*^{2} to calculate the required mix design strengths.

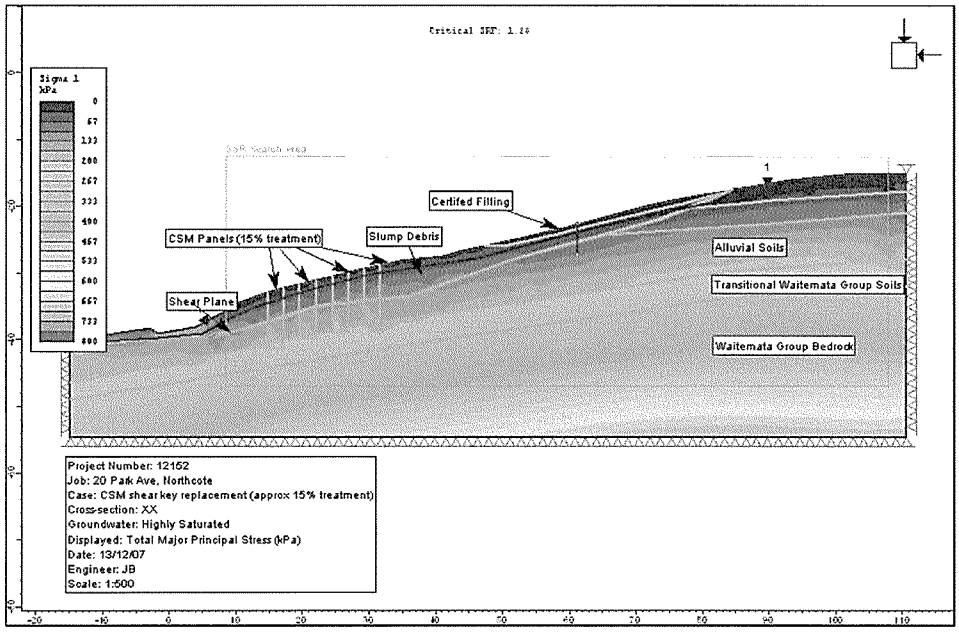

Figure 6: *Phase*^{2} analysis for CSM slope stability design at Park Avenue, Northcote

The CSM rig and associated pumps can be set up and run within the confined construction area. Panel formation produces minimal overflow which is collected by a trench system and removed, dramatically reducing the requirement for silt control measures. With a mixing rate of up to 200m^2 per day, construction can be completed in approximately 2 weeks, allowing a further 30 days for the mix to completely set. These time savings are passed on to the client who can develop the lots in a much shorter timeframe.

5. CONCLUSION

The CSM technique is new to New Zealand and has already shown success in a variety of inground wall applications. The technique presents significant time and cost savings, with the advantage of operating in confined spaces adjacent to existing structures with minimal disturbance. The mixing is most successful in granular soils, with lower strengths achieved in soils with a high organic content.

The technique has yet to be used for slope stability purposes, but shows promise and the potential to minimise time spent on conventional bulk earthworks operations. As outlined above, the technique is particularly suited to sites where contaminated soils and/or silt control restrictions are imposed.

ACKNOWLEDGEMENTS

The author would like to thank James L. Beaumont of Coffey Geotechnics (NZ) Limited for his assistance in compiling this paper, and Civil Works Limited and Birkenhead Properties Limited for their permission to use their sites as case studies.

REFERENCES

Bauer Maschinen (2005) *CSM Cutter Soil Mixing: Equipment, Construction Procedure. Product information 49e.* Bauer Maschinen GmbH, Schrobenhausen, Germany.

Beaumont, J. L. (2008) Personal communication.

Fiorotto, R et al. (2005) *Cutter Soil Mixing (C.S.M.): An innovation in Soil mixing for creating Cut-off and Retaining walls.* Bauer Maschinen, Schrobenhausen, Germany.

Stoetzer, E et al. (2006) *CSM Cutter Soil Mixing – A New Technique for the Construction of Subterranean Walls, Initial Experiences Gained on Completed Projects.* Bauer Maschinen, Schrobenhausen, Germany.

Revised Temporary CSM Retaining Wall Design at 1 Fanshawe Street, Auckland City (ref 13573, dated September 2007) Coffey Geotechnics (NZ) Limited.

Geotechnical Investigation Report on Proposed Residential Subdivision at 20 and 34 Park Avenue, Northcote (ref 12152, dated December 2007) Coffey Geotechnics (NZ) Limited.

Silverstream "Class A" landfill: Lining solutions for leachate control

Carys Everett
Tonkin & Taylor Ltd., Wellington, NZ

Keywords: landfill, lining, leachate

ABSTRACT

The engineering design and construction of modern landfills to meet environmental requirements, particularly at steep or challenging sites, is complex. The growing awareness regarding environmental protection means the prevention of contamination leaching from refuse and entering surface or ground water is a critical element in modern landfill design. Silverstream landfill Stage 2 upgrade involves a 23 hectare extension in a steep sided valley downstream from the existing landfill. The Stage 2 upgrade is planned to be constructed in five phases over a period of thirty to forty years. The geology and geometry of the site and the objective to optimise capacity resulted in new and innovative lining methods for steep slopes. This paper summarises the construction challenges of installation of both standard lining components and the use of "no fines" concrete in the liner system on steep slopes.

1 INTRODUCTION

Silverstream landfill is located in the eastern hills of the Hutt Valley on the boundary between Upper Hutt and Hutt City. The landfill has been operating since 1972, serving a population of over 125,000 and receiving approximately 115,000 tonnes of residential, industrial and commercial refuse each year. In 2001, Tonkin & Taylor began preliminary design for an extension to the Silverstream municipal solid waste landfill. The increased capacity provided by the extension will allow the landfill to continue receiving waste for an additional period of up to 50 years. The extension also provided the opportunity to upgrade the landfill to provide the Wellington region's only "Class A" landfill. Higher environmental standards are required to achieve "Class A" status, which means that less stringent controls can be applied to the waste accepted. The "Class A" classification is awarded for compliance with 20 performance requirements. Those requirements that had the greatest impact on the design of the Silverstream landfill are listed below and discussed in more detail in this paper.

- Avoid contamination of a viable groundwater supply
- Remove all risks from active faults on the containment system
- Waste, landfill gas, and leachate containment systems must be in place.

The Stage 2 extension (the focus of this paper) will be developed as a number of phases to distribute the capital required for the construction (Figure 1). The first part of the Stage 2 development, namely Phase 1; base and slopes 1 & 2, is currently under construction. Tonkin & Taylor are employed by Hutt City Council, as the designer of the landfill, to administer the construction contract and provide construction monitoring services.

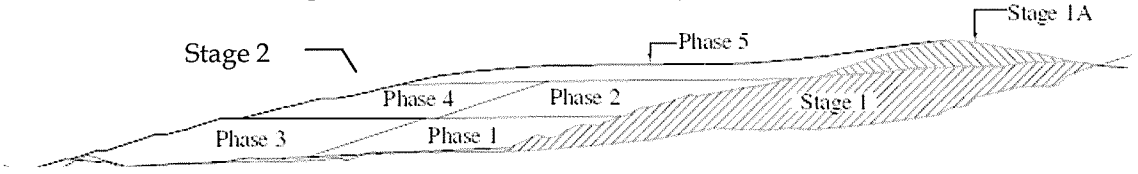

Figure 1: Phases of landfill development

1.1 Site Geology

An interbedded sandstone and mudstone sequence known as "Greywacke" underlies the entire site. Within Stage 2, this is overlain with alluvium (in the valley floor), colluvium, residual soil and non-engineered fill (Tonkin & Taylor, 2003).

The Silverstream landfill site is located in a seismically active area and contains several known "relic" faults. The site is located between two significant active faults, the Wellington Fault situated approximately 1km to the northwest of the proposed landfill toe and the Whitemans Valley Fault, located 4km to the southeast (Figure 2). Groundwater drainage and liner systems have been designed with consideration to the potential for sympathetic movements along the "relic" faults as a result of regional seismicity. A comprehensive groundwater drainage system with inbuilt redundancy was installed as part of the basegrade construction. This drainage system would act as a back up leachate collection system in the event of liner damage of the leachate drainage systems.

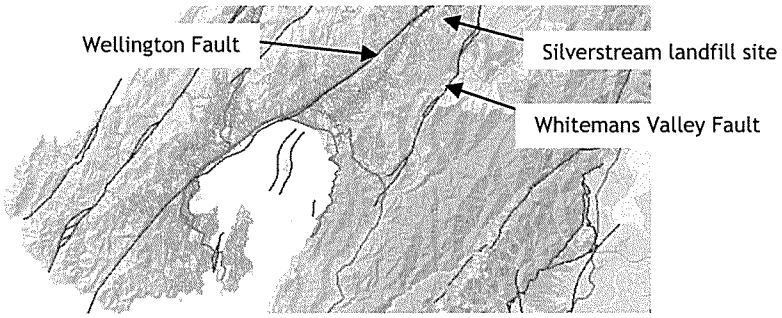

Figure 2: Active faults

The rock beneath the site, whilst heavily fractured, is of low permeability and often has a significant weathered mantle. It therefore provides a good level of natural containment. The Stage 1 landfill operates with no engineered liner system. No significant detrimental effect has been observed to local surface water or the regionally important Hutt groundwater aquifer, whose catchment area underlies the site. To reflect improving environmental standards, the Stage 2 landfill has been designed with an engineering liner system that complies with the "Class A" requirements without relying on natural containment.

Temporary slopes above the Phase 1; base and slopes 1 & 2 have been excavated to the maximum permissible angles, to delay capital expenditure and serve as a slope stability trial. Water ingress during rainfall events has caused some landslips along joint defects, as the rock relaxes over time. Failures on these slopes have not been repaired with structural engineered solutions. These slopes are temporary and will be re-profiled in future development phases.

2 LINER DESIGN

2.1 Overview

The liner system has been designed to accommodate the site's variable geology and steep topography and to prevent stresses to the liner through:

- A regular system of slopes and benches avoiding sharp transitions in slope direction and gradient
- Re-profiling, to remove sharp ridges and infill deeply incised gullies with engineered earth and rockfill embankment to create a regular basegrade on which to place liner
- Four different liner systems to suit the basegrade slope

The installation of the HDPE geomembrane with textured lower surface and smooth upper surface with a geotextile above introduces a defined slip surface. This surface will reduce stresses in the HDPE liner as the refuse consolidates and settles. The reinforcement geogrid distributes the stresses and facilitates placement of leachate collection gravel.

The liner system constructed at Silverstream includes a number of elements being used for the first time in New Zealand. This presented a number of challenges for the main contractor and

the lining subcontractor – a focus of this paper in terms of lessons learned. The following sections focus on the innovative aspects of the design and related construction issues, with reference also to some issues encountered with standard liner components.

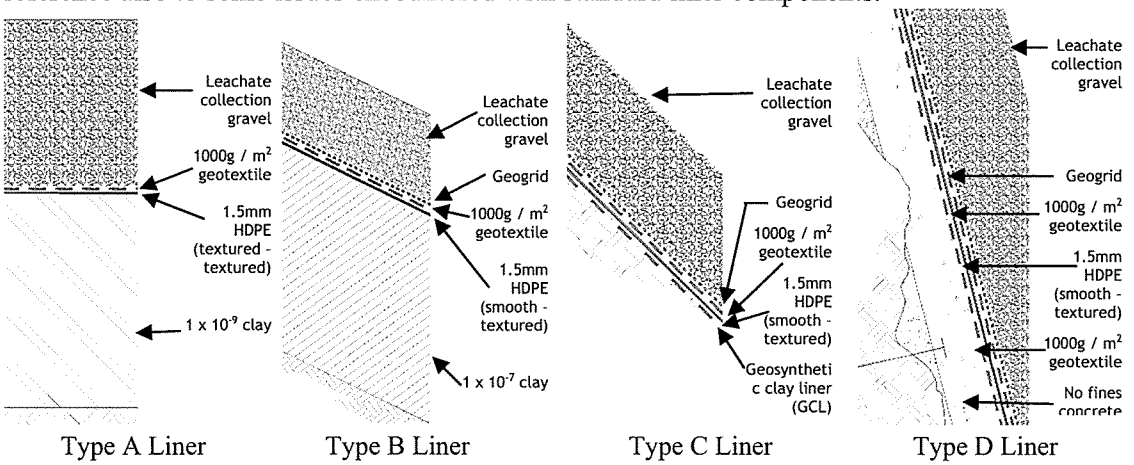

Figure 3: Liner systems

2.2 Type A and B Liner

Types A and B liner are very similar (Figure 3), and are located where hydraulic retention is the key design requirement. The liners comprise of a conventional low permeability compacted clay soil and HDPE geomembrane combination. Type A liner is used in the base areas and has an increased thickness of leachate drainage gravel. Type B liner is placed on the lower slopes and the slopes overlying the existing Stage 1 landfill. These slopes have a gradient lower than 2 horizontal to 1 vertical (2H:1V) to facilitate clay liner construction. The low permeability liner is a residually weathered clayey silt soil derived from the more deeply weathered greywacke rock on the upper ridges of the site.

2.3 Type C Liner

The Type C liner system (Figure 3) was used on transition slopes between the shallow soil fill slopes and the steep rock slopes (2H:1V to 1H:1V). Installation of a compacted clay soil liner is difficult on slopes of this gradient, therefore the low permeability component utilised was geosynthetic clay liner (GCL).

2.4 Type D Liner

Liner constructability for the steep upper side slopes (steeper than 1H:1V) meant that traditional landfill liner design was not practical. A technique not previously employed in New Zealand was adopted based on experience of landfills in Hong Kong. A "no fines" concrete drainage blanket is installed behind the HDPE liner (Figure 3). The design ensures that no ground water pressure can build up behind the liner and creates a smooth surface for placement of the HDPE. The grade of the slopes in combination with the layer of leachate drainage gravel above the HDPE creates a preferential flow path to the leachate collection system and prevents an increase of leachate head.

3 LINER CONSTRUCTION CHALLENGES

3.1 Type A and B Liner - Compacted clay

Clay on the slopes was placed in small lengths with ramps at either end to prevent overworking from excessive trafficking by construction machinery. For ease of construction, the clay liner was placed significantly thicker than specified, allowing safe access for all plant (Figure 4). The sacrificial clay assisted in preventing desiccation cracking and the formation of surface water scour channels in the trimmed surface during hot weather and significant rainfall events. The excess clay was trimmed and the clay surface prepared immediately prior to HDPE lining.

A close working relationship between the lining subcontractor and the earthwork contractor ensured that the trimmed clay surface was not left unprotected for longer than necessary.

Figure 4: Low permeability compacted clay soil installation

To create a homogeneous clay liner, compaction was generally achieved with a wedge foot compaction roller. Towards the end of the clay placement this roller was moved off site and compaction continued using a smooth drum compaction roller. Following compaction, the surface of each clay layer was scarified using the blade and tracks of the bull dozer. Despite the contractor being diligent, final trimming of the slope revealed an area with a series of smooth horizontal surfaces. The clay immediately beneath the surface was densely compacted, and the clay above was less compacted. The smooth surface allowed surface runoff water to flow along the dense clay layer, further softening the clay above. Geotechnical investigations concluded the clay met strength and stability criteria. A layer of GCL was placed over the clay to ensure permeability requirements were satisfied.

The time required to process laboratory permeability tests resulted in a reliance on visual selection of the material, with nuclear densometer and shear vane results to confirm compaction and shear strength. When the moisture content of the clay exceeded optimum, achieving specified compaction without evidence of weave was difficult. The clay was mixed with lower moisture content clay and / or left to dry sufficiently to be reworked.

3.2 Type C Liner - Geosynthetic Clay Liner (GCL)

Subgrade was prepared to ensure a smooth and dry surface, with areas of groundwater seepage being connected into the groundwater drainage system. GCL was placed on completely dry subgrade and covered immediately to prevent excessive unrestrained hydration of the GCL prior to the loading of the liner. It was placed directly from the roll using a crane and spreader bar to prevent damage to the liner. Overlaps were arranged in a shingle pattern with upslope panels laid on top of downslope panels to prevent leachate draining through the joint.

3.3 Type D Liner - "No fines" concrete

The risk of overbreak during preparation of the rock subgrade was identified in the contract documents and up to 200mm of overbreak was predicted based on rock type. The prepared subgrade was inspected prior to the "no fines" concrete installation. Any overbreaks larger than 200mm were measured and the contractor was entitled to payment for additional "no fines" concrete required in these areas due to unforeseen ground conditions.

During preparation of the subgrade, "relic" faults and potential areas of instability were encountered. These areas were secured with specifically designed passive rock anchors and sprayed concrete retaining walls prior to installation of the "no fines" concrete. The rock anchors in this area caused difficulty to the contractor during the "no fines" concrete installation. The standard detail of localised thickening of the concrete around the anchor plates

caused a bulge in the slope profile. To address this and to comply with the specification, the shutters were moved away from the wall to ensure a minimum "no fines" concrete thickness of 100mm over the anchor heads and maintain the specified angle. This resulted in an increase in the volume of "no fines" concrete required. The design specification was relaxed to reduce the minimum thickness to 60mm and some tolerance to angle change permitted. The outcome was workable and satisfactory.

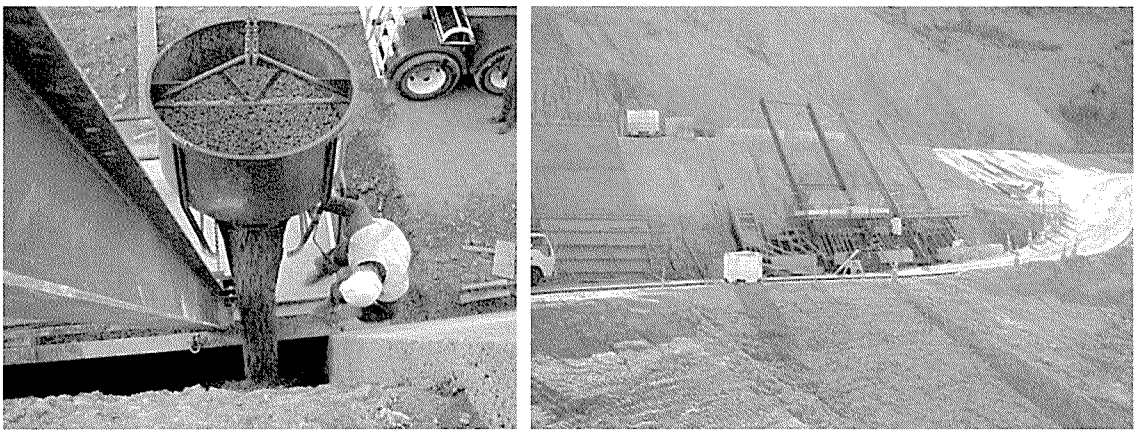

Figure 5: "No fines" concrete installation

Specially designed formwork and shutters were fabricated for installation of the "no fines" concrete. At the transition areas the gradient changed from the 1H:2V to 1V:1H, the prefabricated shutters could not be used and timber formwork was used to create the correct profile (Figure 5). Several patches in the transition areas required handwork to achieve the specified surface finish as the concrete did not flow easily due to the reduced gradient and because mechanical vibration of the concrete was not permitted (to prevent segregation of the cement and gravel).

3.4 HDPE installation

HDPE installation requires a very carefully prepared subgrade, which is free from all rocks, loose soil, sticks, stones, sharp objects and any debris larger than 10mm in diameter. As the HDPE is loaded with drainage gravel and refuse, debris beneath the liner could create stresses and potentially puncture the liner. Prior to HDPE lining, an inspection with the contractor, lining subcontractor and Engineer was carried out to ensure subgrade suitability.

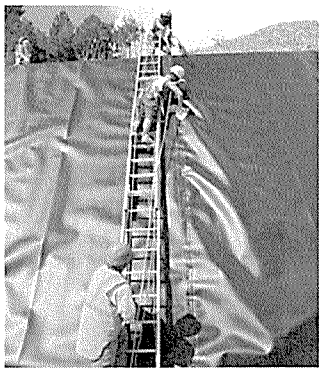

Figure 6A: HDPE liner fusion welding

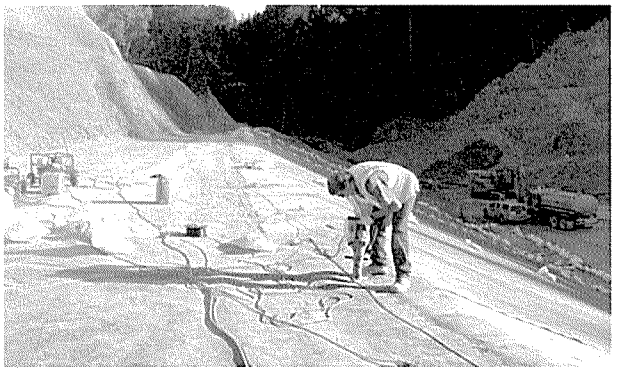

Figure 6B: HDPE liner extrusion welding

Panels of HDPE were primarily welded using double track fusion welding (Figure 6A), ensuring that critical overlaps on the base of the landfill were shingled to allow leachate to flow over the joint and not through it. Fusion seams were air tested to ensure that the weld was completed and no holes or mis-welded areas were present. The Slope 2 HDPE was extrusion

welded onto the Slope 1 HDPE on the bench (Figure 6B), after allowing sufficient time for the slope 2 HDPE to adjust to the local environment. Critical Slope 1 to Slope 2 HDPE panels were welded when the liner was fully contracted in the cool mornings to prevent subsequent lift forming voids beneath the liner. However as the majority of the slope 2 HDPE liner was placed during summer, some lifting occurred during the cooler winter months and it was necessary to cut, patch and re weld the HDPE in these locations.

To ensure the HDPE was not damaged during backfilling of anchor trenches, surface water channel formation and sprayed concrete application, careful construction practices were employed. Once installed the liner required sand bag ballast to prevent wind uplift. Sandbags were strung together in lines and placed down the slopes and along liner edges.

4 CONCLUSIONS

The challenges of liner construction at Silverstream were significant and increased as the weather deteriorated at the end of the construction period. Key points evident from construction monitoring of the complex liner installation are:

- Careful monitoring is essential in order to ensure that contractors comply with approved method statements. Any change in construction method needs to be carefully assessed and approved to avoid design compromises and possible re-work.
- Timely provision of method statements and quality plans by contractors is essential to ensure that construction work is not delayed by the approval process. The contractor needs to be aware of the expected amount of detail required for a method statement before approval can be given. Communication between the main contractor and sub-contractors is important as method statements often require input from several parties.
- During the design phase and when ordering variations, it is important to consider all implications of any proposed design changes in order to prevent unnecessary risk. Even very minor omissions on the design drawings can have major implication in terms of constructability and cost.
- "As built" surveys and testing for critical items should be undertaken prior to any covering or approval, to avoid remedial works and deviation from the specification.
- Practicalities of construction often create situations which can compromise the design intent. Working through and coming up with a practical working method that achieves the design intent is one of the most challenging and rewarding aspects of being involved in construction monitoring.

ACKNOWLEDGEMENTS

This paper was written with the support of Tonkin & Taylor Ltd. Assistance and review was provided by Tony Kortegast and Gary Smith. I would also like to thank Hutt City Council for permission to publish this paper.

REFERENCES

Ministry for the Environment. (2004) *Module 2 Hazardous Waste Guidelines Landfill waste acceptance criteria and landfill classification.* Ministry for the Environment, Wellington, New Zealand.

Tonkin & Taylor Ltd. (2003) *Silverstream Landfill: Stage 2 Appendix C: Geotechnical Investigation Report ref. 83091.002.*

Tonkin & Taylor Ltd. (2006) *Silverstream Landfill Stage 2: Phase 1 Base, Slopes 1 & 2: Design Report ref. 83091.402.*

Kortegast, A.P. et al (2006) Silverstream Landfill – The Transition to a "Class A" Facility. *Proceedings of the Conference: Waste Management Institute of New Zealand (WasteMINZ).*

Cut and Cover Tunnelling: Drawdown, Damming and Contaminant Migration

Sian France
Beca Infrastructure Ltd, Auckland, NZ.

Keywords: Vic Park Tunnel, cut and cover, groundwater modelling, SEEP/W, Visual Modflow Pro, tunnelling, drawdown, damming, contaminant migration, consolidation settlement

ABSTRACT

The Vic Park Tunnel project will see the construction of a new 460 m long, northbound 3-lane tunnel beneath Victoria Park, downtown Auckland, to meet objectives for upgrading the motorway between the Auckland Harbour Bridge and the Central Motorway Junction.

The tunnel, to be constructed by cut and cover techniques, will cross low-lying reclaimed land. Reclamation was constructed progressively from the early 1900's and comprises variable materials to depths of up to 10 m, locally containing hydrocarbons in the near surface. The fill overlies compressible clayey silts and interbedded weak sandstone and siltstone.

Long term the tunnel will be lined to limit groundwater seepage, but the excavation will need to be dewatered during construction. The dewatering period is expected to be 6 months.

Both 2D seepage and 3D groundwater flow modelling were undertaken to assess the extent and magnitude of drawdown (up to 4.0 m adjacent to the tunnel), the potential for contaminant migration to be induced by dewatering, and in the longer term, the extent to which the tunnel might act as a 'dam' to groundwater flow. Classical 1D consolidation settlement analyses were used together with reviews of foundation records to identify the likely impact of settlement on existing structures.

1 INTRODUCTION

The Vic Park Tunnel (VPT) project comprises improvements to SH1 between Wellington Street and the Auckland Harbour Bridge and includes the construction of a new 460 m long, 3 lane north-bound tunnel through Victoria Park (Figure 1a). The tunnel, to be constructed by cut and cover methods, will be located to the west of the existing Victoria Park flyover with a maximum depth to underside of floor slab of 12 m; some 11 m below the groundwater table. Retaining walls supporting the excavation will extend up to 6 m into competent Waitemata Group rock.

In the long term the tunnel will be lined (and groundwater seepage limited to a practical minimum) however the excavation will need to be dewatered to allow construction. Excavation of the tunnel will move progressively forward from a 'mined' face with sump pumps to control groundwater inflow over the expected 6-month dewatering period. Both 2D and 3D groundwater flow modelling was undertaken to assess the drawdown, and related environmental effects that could occur due to excavation dewatering.

The key issues under consideration during excavation dewatering are:

- Volume of groundwater inflows for consenting and engineering design purposes;
- The magnitude and extent of drawdown;
- The potential for settlement associated with a reduction in pore pressure (particularly relevant for the large number of historic buildings in this area); and

- The potential for contaminant migration or saline intrusion due to changes in groundwater flow and direction.

This paper describes the hydrogeological assessment required to support resource consent applications (but not detailed design) for the take and diversion of groundwater from the tunnel excavation.

2 CONCEPTUAL HYDROGEOLOGICAL MODEL

The motorway corridor generally occupies low-lying reclaimed land within the original Freemans Bay embayment and St Mary's Bay foreshore, as well as naturally in-filled drainage gullies and channels originating from the surrounding elevated land and former shoreline cliffs to the south and southwest (Figure 1a). A schematic cross-section that identifies the main geological units, as confirmed by site investigation (Beca, 2006a; Beca, 2006b) is given in Figure 1b.

2.1 Sub-surface Profile

2.1.1 Fill

Hydraulic fill, comprising very soft silts and sands up to 5 m thick, occurs along much of the alignment. Pockets of construction fill (including gravel, packed organics and building waste) are also encountered. Hydrocarbons, resulting from the former industrial use of the surrounding area and other associated contaminants are found in the fill. In-situ testing indicated a hydraulic conductivity of 4×10^{-7} m/s for the hydraulic fill.

2.1.2 Tauranga Group Alluvium

The fill is underlain by a variable thickness of compressible Tauranga Group sediments that include upper, very soft or loose, recently deposited silty and sandy marine sediments, and lower estuarine and terrestrial, undifferentiated alluvium of soft to very stiff clay, peat, silt and sand. In-situ testing suggests a horizontal hydraulic conductivity (k_h) of 2×10^{-7} m/s; given the stratified nature of this unit a vertical to horizontal conductivity ratio (k_v/k_h) of 0.1 was adopted.

2.1.3 Waitemata Group Sandstone / Siltstone

Waitemata Group East Coast Bays Formation, interbedded sandstone and siltstone, forms the bedrock in the study area and outcrops along the old cliff line and foreshore throughout St Mary's Bay. The pre-reclamation shoreline follows the approximate boundary of Victoria Park. Secondary hydraulic conductivity is dominant in this unit, with groundwater flow occurring preferentially along joints, and bedding plane interfaces. In-situ testing indicated a mean hydraulic conductivity of 5×10^{-7} m/s; with values up to 5×10^{-6} m/s. These higher hydraulic conductivities are coincident with areas of lower groundwater levels and are inferred to indicate more significant fractures within paleo valleys.

2.2 Groundwater Levels

Recorded groundwater levels indicate a north to north-easterly gradient dropping from about 10 m above sea level (asl) in the south to sea-level at the coast. The presence of preferred drainage pathways is inferred, with lower water levels corresponding to those locations where above average Waitemata Group hydraulic conductivities were measured.

A delayed and muted tidal influence (up to 50 – 100 mm over a tidal cycle) is recorded in some boreholes indicating some hydraulic connection between the harbour and the Waitemata Group.

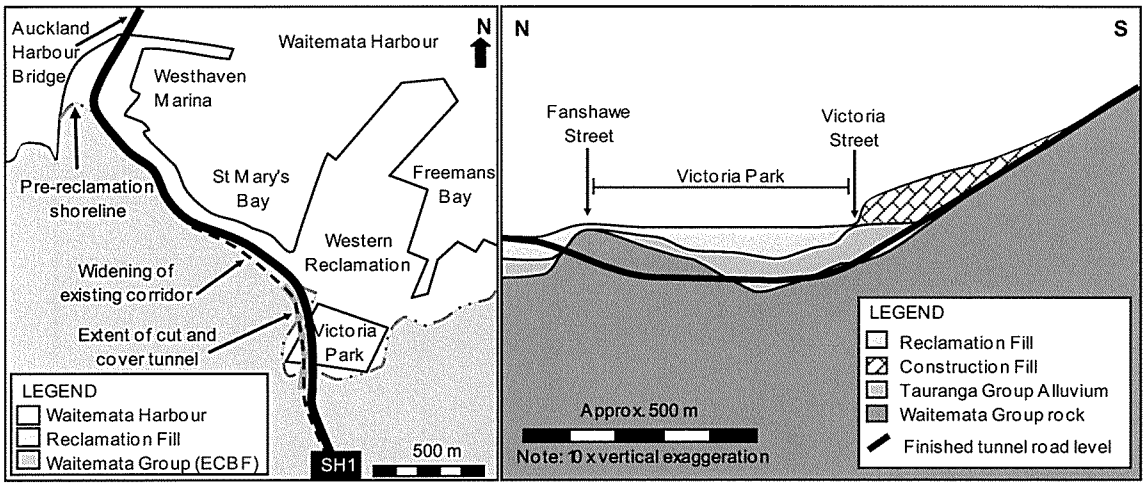

Figure 1a: Schematic Site Map **Figure 1b: Schematic Geological Long Section**

3 NUMERICAL GROUNDWATER MODELLING

3.1 Approach to Groundwater Modelling

A 3D model was developed (using the USGS MODFLOW code (Harbaugh et al, 2000) and the pre/post-processing software Visual Modflow (Schlumberger)) to provide an assessment of the regional groundwater effects and to examine 3D flow effects associated with the construction and long term performance of the tunnel.

A series of 3 No. 2D groundwater models were developed in SEEP/W to assess tunnel drainage volumes, the magnitude and extent of drawdown, uplift pressures on the floor slab and the feasibility of mitigation measures.

3.2 Results of Numerical Modelling

3.2.1 Construction

Both 3D and 2D groundwater modelling suggest that immediately adjacent to the tunnel excavation an average drawdown of up to 4 m may be expected (Figure 2). The drawdown reduces to less than 0.5 m at a distance of 100 m. Measurable drawdown is predicted to extend some 200 m to 500 m from the tunnel. The extent of drawdown at any location is dependent on heterogeneity of the units, and may be greater than expected should areas of higher hydraulic conductivity be interconnected.

As a result of draining the tunnel excavation, the groundwater flow is reversed over some 300 m down-gradient of the tunnel, allowing groundwater to enter the tunnel from both the western and eastern sides.

The majority of groundwater entering the tunnel enters from the Waitemata Group rock. A series of analyses were run to check the sensitivity of Waitemata Group hydraulic conductivities to discharge volumes. A realistic range of inflow to the 600 m length of tunnel and below grade approaches, assuming 6 m deep cut-off piles, was considered to be 5 – 50 cubic metres per day (m^3/d).

3.2.2 Long Term

In the long term, the tunnel will be lined and groundwater levels will generally return to pre-construction levels, except in close proximity to the tunnel where drawdown of up to 1.0 m is

predicted down-gradient of the tunnel. Because the cut-off walls will block groundwater flow, a comparable level of damming is expected immediately up-gradient.

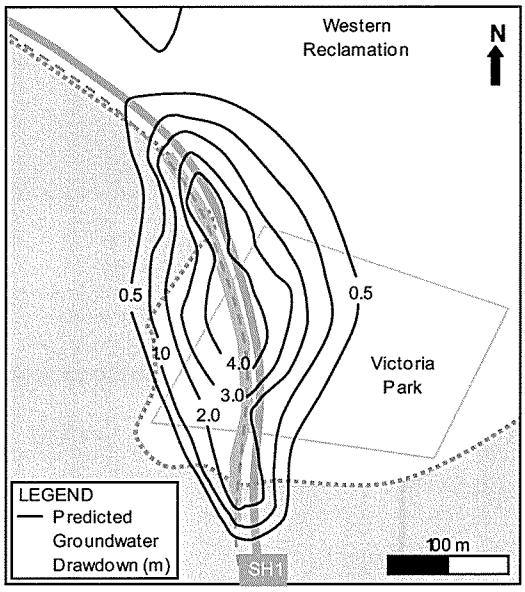

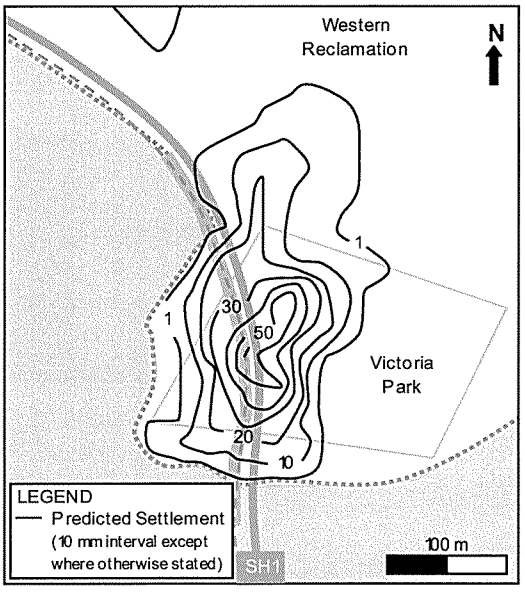

Figure 2: Predicted Construction Drawdown Figure 3: Predicted Construction Settlement

4 ASSESSMENT OF ENVIRONMENTAL EFFECTS

4.1 Changes in Groundwater Quality

4.1.1 Contaminant Migration

Groundwater modelling indicates a local steepening of the hydraulic gradient around the tunnel. Depending on contaminant mobility properties this steepening could result in vertical migration of the contaminants from the fill into the Waitemata Group, and the tunnel drainage system.

Seepage modelling indicates that the rate of groundwater flow in the soils is slow. Consequently, if it were assumed that contaminants travel at the same speed as groundwater, contaminants would migrate less than 0.1 m in the 6-month dewatering period. Migration of contaminants is therefore unlikely to be significantly affected by the project.

4.1.2 Saline Intrusion

Modelling suggests that dewatering of the excavation could result in a reversal of the groundwater flow down-gradient of the tunnel. However the flow reversal at 6 months is predicted to extend only 40 m to 100 m down-gradient of the tunnel. Given that the tunnel is generally at least 100 m from the coast, saline intrusion should not occur as a result of the project.

4.2 Settlement

Although the Tauranga Group soils are not completely dewatered as a result of tunnel construction, a reduction in pore water pressure of up to 25 kPa may be expected. This reduction in pore pressure causes an increase in effective stress that can result in settlement of compressible soils.

Classical 1D consolidation analyses were undertaken to assess the likely magnitude and extent of settlement. A model consisting of sub-layers between 0.5 and 1.0 m thick was analysed with

allowance for time dependent drainage (using the pore pressure gradients obtained from the 2D models). Consolidation parameters, assessed from lab testing and recent projects in similar material, are given in Table 1.

Table 1: Adopted Settlement Parameters

Geological Unit	Unit Weight γ (kM/m^3)	Compression Ratio $C_c/1+e_0$	Recompression Ratio $C_r/1+e_0$	Preconsolidation Pressure (kPa)
Fill	17	0.2	0.03	0
Tauranga Group (< 7 m depth)	15	0.2	0.03	0 – 20
Tauranga Group (>7 m depth)	15	0.2	0.03	0 - 100

Settlements of up to 50 mm were calculated immediately adjacent to the tunnel excavation, where the thickness of compressible soils is greatest, reducing to less than 15 mm at the boundary of Victoria Park (Figure 3). Ground settlements in the range of 2 mm to 15 mm could occur beneath some buildings surrounding the park.

In addition to groundwater related settlement, immediate ground settlements of up to 50 mm extending to about 30 m distance (i.e. wholly contained within Victoria Park) are anticipated as a result of ground retention structures taking up load and deflecting following excavation.

Settlement impacts could potentially affect 21 buildings and other structures. The age and condition of structures surrounding the park varies from multi-storey apartment buildings (less than 10 years old) to heritage listed buildings such as Victoria Park Market and the old Gasworks. Settlement effects will also extend to pavements and services including the existing large stormwater pipe through Victoria Park.

In order to assess the consequence of the predicted settlements, building foundation details were reviewed for 14 potentially affected buildings (recent and historic). Half of the buildings reviewed are founded on piles into Waitemata Group rock and are therefore not considered susceptible to settlement. The remaining buildings are on shallow pad foundations on fill or residual soils and are susceptible to settlement.

The predicted settlements for these buildings are less than typical maximum allowable design settlements, of the order of 25 mm for isolated pads and 50 mm for rafts (Tomlinson, 1995). The settlements will occur over a broad area and average rotation profiles may not be severe, however localised differential settlements could occur, due in particular to the variable nature of the fill deposits; however these effects are considered to be no more than minor.

5 MITIGATION AND MONITORING

Predicted construction related settlements are expected to be within tolerable limits over a significant area, consequently very limited mitigation is required. The following mitigation methods were considered:

1. Develop a programme of monitoring and identify mitigation measures such as underpinning of buildings or re-levelling of services that might be implemented should greater than anticipated drawdown or settlement occur.
2. Recharge by introduction of abstracted water adjacent to the excavation to reduce the magnitude of drawdown, saline intrusion and settlement, but not contaminant migration as vertical groundwater movement would still occur.
3. Construction of a deep cut-off such as a slurry trench or grouted bentonite curtain to cut off flow. This would reduce the magnitude of groundwater drawdown hence

reducing the potential for contaminant migration, saline intrusion and settlement. However this was considered likely to be ineffective due to the nature of materials underlying the site.

Given the relatively short construction time frames and limited potential for adverse settlement or water quality effects, Option 1 was adopted, an approach commonly used during the construction phase of deep excavations. A monitoring programme was developed that includes multi-level piezometers, inclinometers at excavation crests, ground and building settlement pin arrays, flow meters at collection sumps and water quality testing.

Preliminary modelling suggests that, if necessary, recharge wells could be used to re-inject water into the Waitemata Group reducing the potential for adverse effects where groundwater drawdown or settlement exceeds that predicted.

In addition to these measures, the tunnel design is expected to comprise elements that are typical to engineering practice such as low permeability secant pile or diaphragm type construction to limit groundwater inflow through sidewalls, remedial grouting of construction joints and passive groundwater bypasses around the tunnel.

6 CONCLUSIONS

2D and 3D groundwater modelling has been used to demonstrate that construction of a cut and cover tunnel through Victoria Park is likely to result in groundwater drawdown of up to 4.0 m within the compressible Tauranga Group soils, which might result in settlements of 50 mm immediately adjacent to the tunnel, reducing to below tolerable limits at adjacent properties. The drawdown is largely limited to Victoria Park. Contaminant migration and saline intrusion are expected to be limited.

Given the limited potential adverse effects due to dewatering, an extensive monitoring programme was developed to monitor changes in groundwater levels, flow and quality and to trigger appropriate remedial measures if required.

ACKNOWLEDGEMENTS

The writer would like to thank Transit New Zealand for permission to publish details of the proposed Vic Park Tunnel Project, and Ann Williams and Gavin Alexander (Beca Infrastructure Ltd) and Patrick Kelly (Transit New Zealand) for reviewing this paper.

The writer would also like to thank the late Dr Keith Simpson for his guidance, support and encouragement throughout the project.

REFERENCES

Beca (2006a) *Vic Park Tunnel Project – Hydrogeological and Engineering Assessment Report.* prepared for Transit New Zealand.

Beca (2006b) *VPT Addendum Report – Hydrogeological and Engineering Assessment.* prepared for Transit New Zealand.

Harbaugh, A.W., Banta, E.R., Hill, M.C., and McDonald, M.G. (2000) *MODFLOW-2000, the U.S. Geological Survey modular groundwater model.* Open File Report 00-92. U.S. Geological Survey 121 p.

Tomlinson, M.J. (1995) *Foundation Design and Construction, 6th edition.* Longman

Relationship between observed failure mechanisms and the rate of coastal recession

Camilla Gibbons,
Connell Wagner, Christchurch, NZ

Keywords: Coastal recession, Landslip, Failure Mechanism, Holderness, Glacial till

ABSTRACT

This paper investigates the rate of coastal recession to determine if correlations can be established between rates of recession and observed failure mechanisms. Correlations are shown by way of example on a stretch of coastline in Holderness in the UK. The Holderness Coastline, in the north east of England, has one of the fastest rates of coastal recession observed in Europe, with an average of 1.55m per annum. The cliffs comprise stiff gravelly clay of the Basement, Skipsea, Withernsea and Hessle Glacial Tills, deposited during the Devensian and Saale Glaciations. Eight different sections with varying recession rates along the 61km stretch of coastline were investigated. Geomorphological maps were produced, beach profiles were measured and failure mechanisms were mapped for each section, in addition to observations of a number of other factors. This paper describes the fieldwork undertaken and details the analysis of data. Correlations between recession and slip mechanisms are described and data is used to determine if similar conclusions may be drawn for other coastal areas.

1 INTRODUCTION

The Holderness coastline is in the east of Yorkshire, in the north east of England. The coastline is one of the fastest eroding coastlines in Europe with an average recession rate of 1.55m/yr along the 61 kilometres between Bridlington in the north and Spurn Point in the south. Records suggest at least 30 towns and villages have been lost along this stretch of coastline in the last 550 years (LOIS).

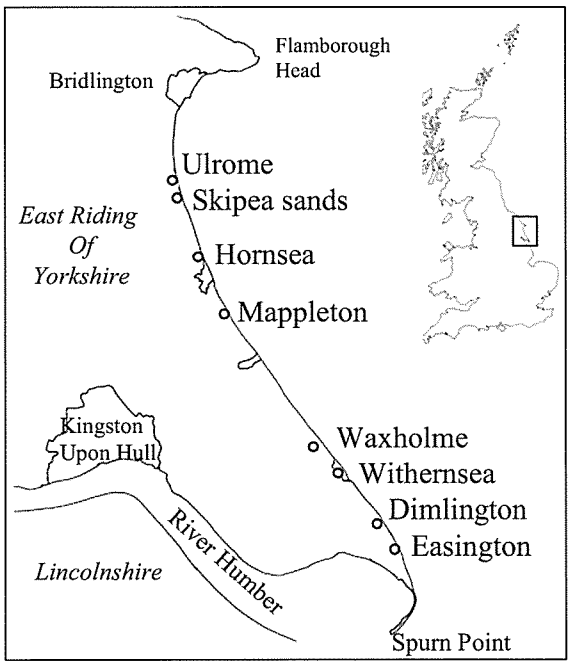

Figure 1: Map of the Holderness Coastline

1.1 Geology

The geology of the Holderness coast predominantly comprises lodgement till with minor flow tills and outwash tills. Lodgement till is formed by the deposition of debris from the lower layers of the glacier, it is consequently often over-consolidated and very stiff. Four tills are present along this section of the coastline, the Skipsea, Withernsea and Hessle Tills were deposited 13-18 thousand years ago during the late Devensian Glaciation. The Basement till was deposited 175-300 thousand years ago during the Saale glaciation. The tills are all stiff to very stiff over consolidated, matrix dominated, gap-graded gravelly clays with minor sand; they have low to medium plasticity with low moisture contents and an effective angle of friction of 25-30° (Bell, 2000).

Prior to the glaciations, the cliffs comprised chalk from the Mesozoic; this was partially eroded by the glaciers and the tills deposited. The boundary between the chalk and till is now several kilometres inland at the furthest point. Refer to the geology maps in Figure 2.

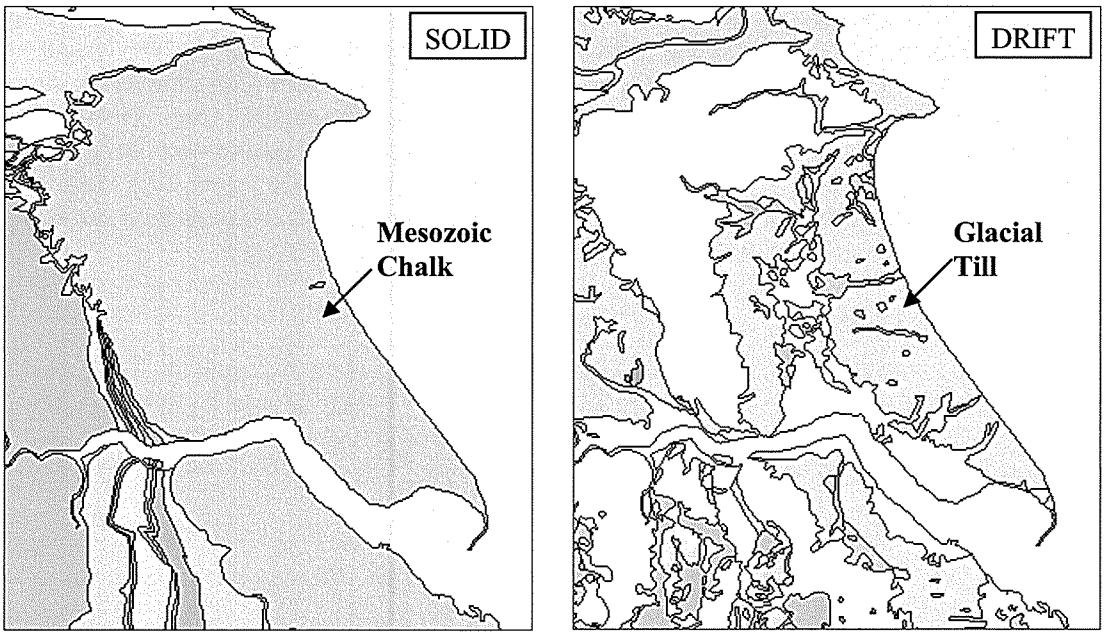

Figure 2: Solid and Drift Geology Maps of the Region (British Geological Survey)

2 OBSERVED COASTAL RECESSION

The rates of recession at Holderness are historically very rapid and to investigate these, the coastal processes and factors affecting recession must be considered.

The cliff height varies along the coast from 5.2 mAOD (above ordnance datum) to 35.1 mAOD. The higher the cliff, the larger the volume of material must be removed to achieve the same erosion rate. The geology also varies, however the four glacial tills found along the Holderness coastline are all of similar composition and stiffness and this is therefore not considered to have a significant influence on the varying rate of recession along the coastline.

The proximity of the base of the cliff to the high tide is important. Valentin (1971) suggested wave action was the most important factor controlling the rate of erosion. Additionally, the more beach material there is, the more protection the cliff will have from the full force of the waves. The composition of the beach material will also affect the amount of energy dissipation from the waves and therefore the sediment and force of the waves directed at the cliffs. Robinson (1977) observed that when there was backshore material moving at the base of the cliff, the cliff erosion rates were 15 to 18.5 times higher than if there was no backshore material.

There are two sea walls and several groynes along the coast. Immediately to the south of the two sea walls, the recession rates are significantly higher than immediately to the north. The predominant wave direction is from the north east, with long-shore drift acting from north to south; it is therefore suggested that the presence of the walls reduce the volume of material moving southwards, by reducing the erosion and therefore less material is available to protect the cliffs immediately to the south of the walls.

3 FIELDWORK

A field work programme was undertaken to investigate many of the factors that may be affecting the rates of recession. Eight sections of 100 metres in length were chosen for further investigation.

3.1 Sections

The sections covered areas with different recession rates using the recession rate data from the East Riding of Yorkshire Council records, refer to Figure 3. The sections covered the different till lithologies and locations where two or more of the tills are exposed in the cliff, to determine whether till lithology has a significant impact on the recession rates. Additionally, a variety of cliff heights were included in the sections to determine the affect this has on the recession. The sites were at a distance from areas where man's intervention is likely affecting recession rates.

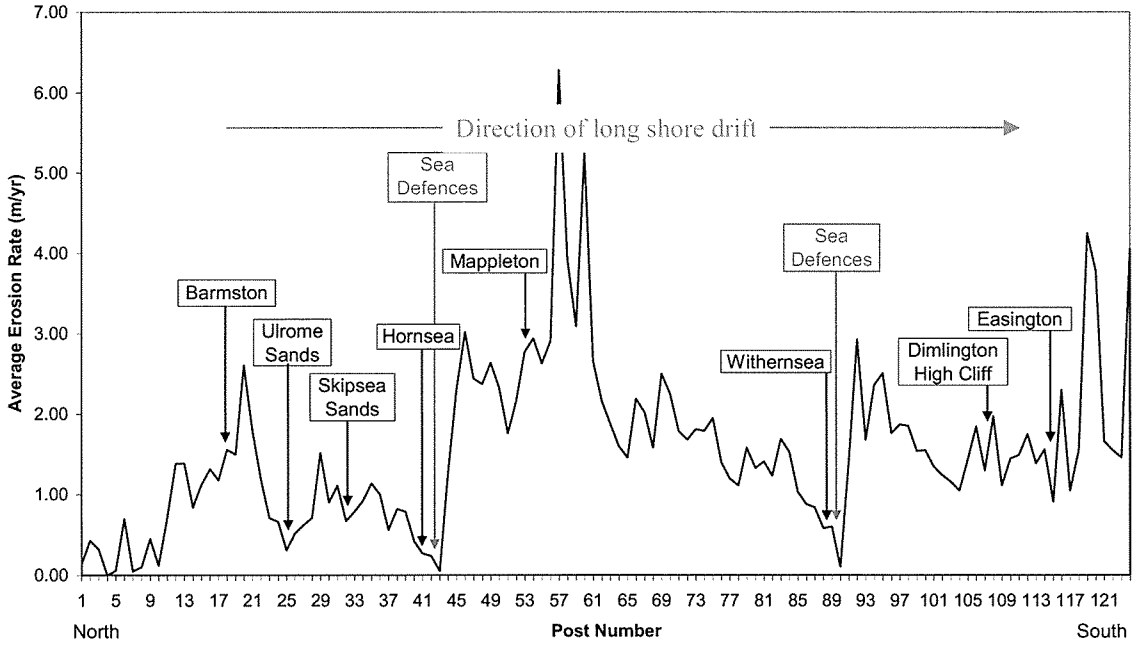

Figure 3: Average Erosion Rates along the Coastline (data from the East Riding Of Yorkshire Council)

3.2 Observations

At each location, detailed geomorphological mapping including photograph documentation was undertaken to investigate the types of failures present and how these related to the different till lithologies exposed in the cliff face.

The height of the exposed cliff was measured; and every 10 metres along the section a topographical beach profile was measured. The profiles were continued for 60 metres out from the cliff as possible. The beach profiles were recorded to establish the shape of the beach from the base of the cliff.

The third main piece of information obtained from each site was a series of shear vane and pocket penetrometer readings. These were taken at a variety of locations along the profile and average shear and compressive strengths for each of the tills at each location was determined.

3.3 Interpretation

Using all the information gained in the fieldwork, the geomorphological maps were zoned by failure mechanism. The percentage by area of each failure mechanism was measured (Table 1). Additionally the beach profiles were plotted and the maximum and minimum height difference between the foot of the cliff and the end of the profile was calculated.

Table 1: The percentage area of the different failure mechanisms in the 8 sections

Location	% Translational Slide	% Rotational Slide	% Flow	% Spread	% Topple	% Fall
Easington	0.00	0.00	0.00	0.00	0.00	100.00
Dimlington	23.52	53.46	19.85	0.00	1.02	2.78
Withernsea	35.33	59.08	6.40	0.00	0.00	0.00
Waxholme	23.66	0.00	0.00	0.00	0.62	76.51
Mappleton	28.75	46.35	2.75	9.89	0.00	11.34
Hornsea	63.30	22.14	0.00	15.84	0.00	0.00
Skipsea	57.35	12.50	20.86	0.00	0.00	10.42
Ulrome	0.00	0.00	1.35	0.00	0.00	98.81

4 ANALYSIS

Multiple Linear Regression analyses were performed on the results to determine the link between the various factors affecting and the rate of the recession. Much of the literature refers to a link between the rate of recession and the height of the cliff, a simple linear regression test was performed and our investigations indicated that for the selected sections, this strong relationship was not evident. The computed coefficient of determination (r^2) value is 0.02 with a probability (p) value of 0.73. This suggests there is no significant correlation between the height of the cliff and the recession rate.

Further, the link between the recession rates and the distance from Flamborough Head and the orientation of the coast with respect to north was analysed. Both tests indicated no significant correlation, with r^2 values of 0 and 0.02 respectively; the p-values were 0.89 and 0.74.

The recession rates were then compared with the distance of the mean high tide from the cliff, used as an analogy for the average number of times each year the water touched the base of the cliff. A more significant relationship was found, with an r^2 value of 0.28 and a p-value of 0.179. This is more relevant than the previous factors that were tested as the waves appear to have a direct influence on the rate of erosion; however, the cliff height, the distance from Flamborough Head and the orientation of the coast with respect to north are consequential effects of the erosion rates. When all four factors are analysed together, the results show a relatively significant and moderately good relationship, with an r^2 value of 0.55 and a p-value of 0.56.

The next group of variables analysed were the maximum and minimum drop in the beach height over 60 metres, and the distance of the mean high tide level from the base of the cliff. These variables were correlated and the multi-linear regression test, comparing them with the recession rate suggests they do have a significant affect on the rates of recession. The r^2 for the test was 0.63 and the p-value was 0.22.

The analysis was then concentrated on the failure mode. The area of each section was calculated from the geomorphological map, including the total area of a particular failure mechanism. The percentages of each failure mechanism were calculated based on the whole area of the section and then normalised to the area of identifiable active landslides (Table 1).

Individual simple linear regression tests were conducted comparing the rate of recession with the eight different failure mechanisms and the results of these tests are summarised in Table 2.

Table 2: Results of the analyses comparing the recession rate and the failure mechanisms

Analysis of recession and failure mechanism	r^2	p-value
% Flow	0.05	0.60
% Spread	0.03	0.70
% Translational slide	0.26	0.19
% Rotational slide	0.00	0.98
% Topple	0.04	0.65
% Fall	0.07	0.53
All Failure mechanisms	0.998	0.07

The results indicate that translational slides have by far the greatest impact on the observed recession rates, although the r^2 value is only 0.26. Rotational slides, in comparison have little effect on the observed recession rates. Apart from the above main types, other failure types and the recession rates show little correlation.

Certain types of failures often occurred in combination with other types, for example the translational and rotational slides were generally observed in the same sections and on two occasions where toppling was observed, it was in association will fall failures. It is highly likely that there is an interaction between these failure mechanisms with respect to the affect on the recession rates and this was shown by the multi linear regression test. The test computed an r^2 value of 0.9987 with a p-value of 0.0686. This result indicates the type of failure has a strong influence on the observed recession rates. The relationship was determined as follows:

Erosion Rate = 77.623 + (-0.77TS) + (-0.77RS) + (-0.72Fl) + (-0.70S) + (-0.92T) + (-0.76F) (1)
Where TS= Translational Slide, RS= Rotational Slide, Fl= Flow, S = Slide, T= Topple, F= Fall

The type of failures present in the cliff was also closely related to the height of the cliff, an analysis indicated an r^2 of 0.9996 and a p-value of 0.037.

5 CONCLUSIONS

A large range of data and observations has been obtained for the eight sections studied for this project. The aims of the project were to firstly investigate the rate of recession along the Holderness coastline and secondly, to determine a link between the recession rates and the failure mechanisms of the landslides along the coastline.

The observations that have been made in the field have provided data for a statistical analysis. The most significant outcome of this study is that a relationship exists between the mode of failure and the observed rate of coastal recession. Secondly, that no relationship was observed between the height of the cliff and the observed rate of recession. However, this study indicates that a complex relationship exists between coastal erosion, subsequent recession and tidal processes.

Further, it has calculated that the mode of failure is likely to dictate the volume and form of the failed material at the base of the cliff. For example, the material resulting from a fall is more

likely to be blocks of varying sizes scattered over the beach. The material from a slide is more likely to be a large mass, which has slid down the cliff by a distance in the range of a few metres; this will consequently be slumped at the base of the cliff. The material from a fall makes a more dramatic difference to the morphology of the beach and as the waves flow around the blocks they will be eroded from all sides of the block. The material resulting from a sliding failure will make a lesser impact to the morphology of the beach and although the waves are likely to be in contact with the material more frequently that the intact cliff, the material can only be eroded from one predominant direction. Thus, the faster the material at the toe is removed, the quicker the waves can begin to attack the base of the cliff once more.

The scenarios described suggest that the mode of failure of a particular stretch of coastline will not vary significantly over long periods of time, as sliding failures generally give rise to conditions favourable for further sliding failures, and falls will give rise to the conditions favourable for falls to occur. It is likely that the cycles of failure, ensuing debris removal, which in turn leads to erosion and subsequent failure will occur at different rates. This theory is supported by the relationship between the recession rates and the distance of the mean high tide mark from the foot of the cliff.

The key finding is that the rate of debris removal is likely to have a significant affect on coastal recession. Further, this project has shown that many factors affect the rate of coastal recession and it is very unlikely that there exists one single contributory factor.

ACKNOWLEDGEMENTS

This research was undertaken at the University of Leeds in the UK. I acknowledge Mr Neil McLachlan of East Riding of Yorkshire council for providing the coastal recession data. I also thank Miss Lucy Philip of the University of Leeds for her assistance with this project and Dr Jan Kupec of Connell Wagner for reviewing this paper. Finally, I would like to thank the Natural Environment Research Council in the UK for funding the fieldwork, and Connell Wagner for supporting my research.

REFERENCES

Bell (2000) Engineering Properties of Soils and Rocks, 4th Ed., Blackwell Science, UK

British Geological Survey, http://www.bgs.ac.uk

East Riding of Yorkshire Council, (2004). *Coastal Information Pack, East Riding of Yorkshire's Coastline, Flamborough Head to Spurn Point*, Beverley.

Land Ocean Interaction Study, http://www.nerc.ac.uk/lois/coastl.shtm

Ordnance Survey, (1998-1999). Kingston Upon Hull, Beverley and Driffield. Ordnance Survey, Southampton.

Robinson, L. A., (1977). Marine erosive processes at the cliff foot. *Marine Geology*, 23: 257-271.

Valentin, H., (1971). Land loss at Holderness. *In*: J. A. Steers (Editor), *Applied Coastal Geomorphology*. MacMillan, London, pp. 116-137.

The remediation of an unstable soil nail wall in South Eastern Queensland

Patrick Gibbons
Coffey Geotechnics, Brisbane, Australia

Keywords: Soil nail wall, Slope/W, instability, weakly cemented sandstone, remediation

ABSTRACT

The construction of a soil nail wall was instigated as part of a major interchange upgrade project in the south east Queensland area. The geology of the area consists of a claystone of the Raceview Formation and sandstone of the Darra formation, with two geological faults crossing the wall site. The near vertical soil nail wall was designed using Geoslope Slope/W™ software and a 'top down' method of construction was proposed using vertical lift heights of 1.2 m so as to prevent potential block failures along shear joints in the claystone. During excavation of the wall, a layer of weakly cemented sandstone began to slump forward from the soil face. Survey measurements of the wall showed horizontal movement of the wall face and tension cracking at the batter slope above the wall indicated instability. This paper discusses the design of the soil nail wall, causes of the instability and the remediation measures taken to stabilise the wall.

1. INTRODUCTION

Phear et al. (2005) provides a comprehensive guide to the design methodology (bond resistance) of soil nail walls which include design methods using empirical correlation and charts, design by using pull out load test results, undrained shear strength design, effective stress methods and determination of bond resistance using pressuremeter tests. The bond resistance used in the design of the soil nail wall described in this paper was determined using the effective stress method which has been described in Watkins & Powell (1992) and Phear et al. (2005)

Soil nailing is a passive system of soil reinforcement, so some degree of movement is required in order to mobilise the bond resistance of soil nails. Wong et al. (1997) showed that lateral movement of up to 15 mm occurred in a soil nail wall with residual soil. Murray (1993) suggests that movement (vertical or lateral) of 0.1% in sands and gravels or 0.4% in clay is expected. Briaud and Lim (1997) found that up to 18 mm of lateral movement occurred in a 4.7 m high soil nailed wall which formed part of a piled bridge abutment in embankment fill.

2. SITE DESCRIPTION & GEOLOGICAL CONDITIONS

The construction of a vertical soil nail wall was instigated as part of a major interchange upgrade project in the south east Queensland area. The soil nail wall that was proposed forms part of a piled bridge abutment.

The ground conditions at the soil nail reinforced wall is characterised by two geological units, the Tertiary Age Darra Formation overlying the Triassic Age Raceview Formation strata – the latter falling within the Ipswich Coal Measures Group. Preliminary cuttings that were excavated within 25 m to the north of the finished profile in July 2007 enabled the outcrop to be mapped.

The Darra Formation is characterised by weakly cemented (or non cemented) slightly clayey medium grained sand with distinctive subrounded cobbles of quartzitic sandstone. Published information indicates that the Formation also includes thinly interbedded sandstone and mudstone. In this location cuttings revealed a distinct unconformity between the sand and cobbles stratum overlying a moderately dipping interbedded stratum and here the latter is interpreted to represent the Raceview Formation.

The Raceview Formation is characterised by feldspathic and quartzose sandstone, siltstone and mudstone/ shale, with thin coal seams that together form a relatively competent bedrock. Observations made in the cutting revealed a distinct sequence of massive or (thickly) cross bedded sandstone, grading to interbedded mudstone and shale with minor sandstone beds beneath.

Review of the borehole data indicated a distinct variation in rock type (competency) at the wall location. Towards the western part of the wall, borehole data indicated predominantly sand overlying mudstone and siltstone strata that were recovered from the boreholes as soils. Towards the east, borehole data are interpreted to represent typically low strength sandstone. Preliminary cuttings made in the vicinity revealed a WNW to ESE trending low angle fault where mudstone and siltstone strata appear to be thrust onto the sandstone. Some poorly cemented sand was revealed within the fault. This sand was partially water bearing when the cutting was first made, although it appeared to become fully drained within a matter of days.

3. GEOTECHNICAL DESIGN

3.1 Geotechnical Parameters

The design is based on compilation of the information obtained from field and laboratory testing together with site observations. Critical to the behaviour of the bedrock will be the frequency and orientation of bedding, joints and faults that represent defects within the rock mass, as well as the condition of the defects, such as their aperture, roughness, weathered state and infill type. Geotechnical parameters are shown in Table 1.

Table 1: Original and revised geotechnical design parameters

Engineered Fill/Darra Formation Strata*		**Original**	**Revised**
Typically a medium dense clayey sand	Drained friction angle (ϕ')	30°	30°
	Effective Cohesion (c')	5 kPa	5 kPa
	Bulk density (γ_b)	19 kN/m^3	19 kN/m^3
Bedrock (Raceview Formation sedimentary rocks)			
Interbedded mudstone and siltstone with minor sandstone, Feldspathic sandstone	Drained friction angle (ϕ')	42°	42°
	Effective Cohesion (c')	10 kPa	10 kPa
	Bulk density (γ_b)	21 kN/m^3	21 kN/m^3
Claystone (underlying distinctively interbedded strata) – competent mudstone	Drained friction angle (ϕ')	40°	40°
	Effective Cohesion (c')	10 kPa	10 kPa
	Bulk density (γ_b)	21 kN/m^3	21 kN/m^3
Massive sandstone	Drained friction angle (ϕ')	42°	42°
	Effective Cohesion (c')	2 kPa	2 kPa
	Bulk density (γ_b)	20 kN/m^3	20 kN/m^3
Uncemented sandstone	Drained friction angle (ϕ')	N/A	35°
	Effective Cohesion (c')		0 kPa
	Bulk density (γ_b)		20 kN/m^3

*Part of the slope comprises cutting into *in situ* Darra Formation strata, which, for the purposes of design is conservatively assumed to have similar engineering properties to the fill.

3.2 Groundwater

The borehole logs did not include accurate records on observation of groundwater conditions. During excavation groundwater seepage was recorded at discrete points and from larger defects within the strata – notably at faults.

The design allowed for a depressed phreatic surface, drainage from the face and horizontal drainage drilled into the soil and bedrock profile.

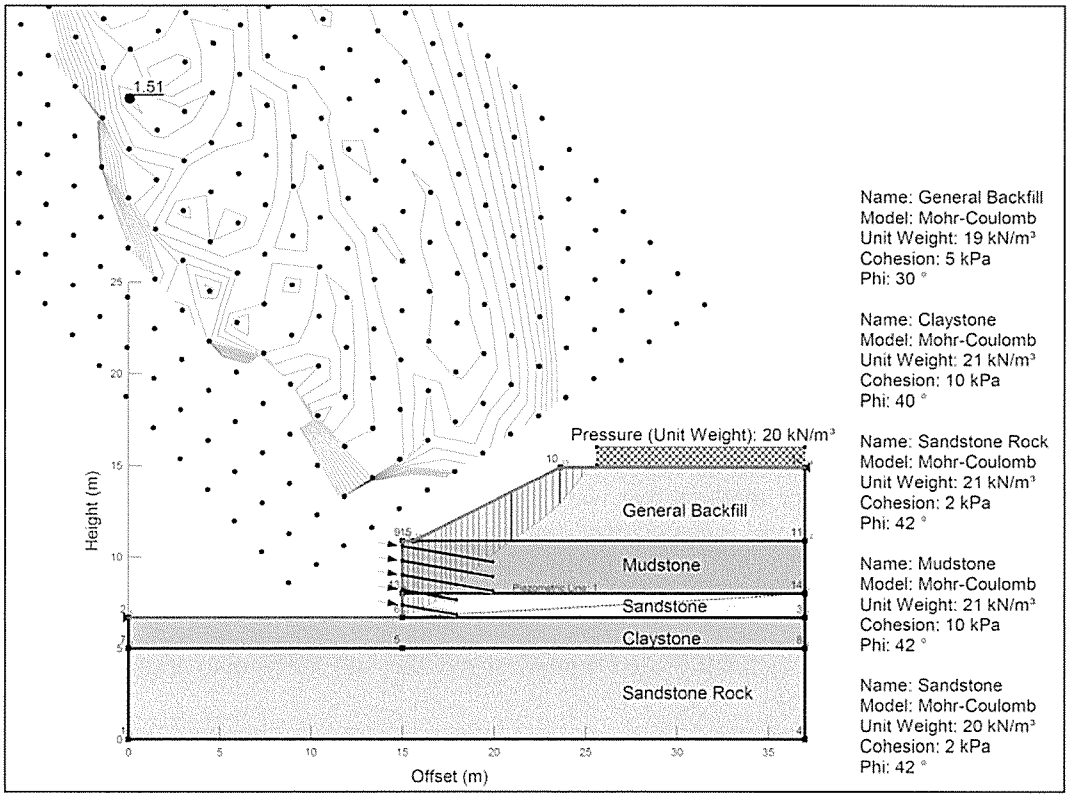

Figure 1: Original design

3.3 Geotechnical design

Soil nail reinforcement design was undertaken with the use of the proprietary software Geostudio Slope/W. The soil nail bond capacity was modelled as a function of the effective overburden stress using the following expression:

$$\text{Bond resistance} = (c' + \text{overburden stress} \times \tan \phi') \times \text{interface factor} \quad (1)$$

The analysis showed that for a 4.2 m high section of wall, three rows of nails 5 m in length and two rows of nails 3 m in length were required. The required bar size was 20 mm and the grouted hole diameter was 130 mm. The vertical spacing of the nails of 0.8 m and the horizontal spacing of 1.5 m were chosen to provide the required capacity. The design output from Slope/W is shown in Figure 1.

4. CONSTRUCTION & REMEDIATION

4.1 Construction methodology and observations

The initial design advice recommended that 'top-down' construction at 1.2m vertical lifts be carried out. After the nails were grouted, steel mesh was placed on the slope face and shotcrete was sprayed over the face of the slope to a thickness of 170 mm (minimum).

Initial observations of the cut slope revealed a slightly clayey sand from the Darra formation. As the slope excavation increased and proceeded into the Raceview Formation, the slope face was mapped and the mudstone was deemed to have better shear strength characteristics than

originally anticipated. Seepage was initially noted at a height of some 1.5 m above the toe of the cutting both in the preliminary cuttings, and during excavation of the reinforced cutting. The seepage was noted to reduce to the base of the cutting over a period of days.

Approximately 1.5 m above the toe of the reinforced slope, a weakly cemented sandstone layer was encountered. After excavation, movement took place where the weakly cemented material was able to slump from the toe of the excavation at a time when the depth of excavation was nearing completion. This occurred where a specific bed of water bearing, non-cemented or poorly cemented sandstone was exposed as a specific stratum within the bedded Raceview Formation geological unit. This had a shorter 'stand-up' time than anticipated. At the time of construction, it was recommended that the 3 m nails that were designed be replaced with longer 5 m nails, to account for the lower internal angle of friction in the sandstone. The void that was created as a result of the slumping of the weakly cemented sandstone was filled with cement grout.

4.2 Geotechnical reassessment and design

Monitoring of the wall face markers that were placed on the shotcrete revealed that significant movement of up to 100 mm, had occurred (shown in Figure 2). Visual observations of the embankment batter also revealed some tension cracks up to 10 mm wide, probably due to instability caused by the slumping of the weakly cemented sandstone. Figure 3 shows the location of the monitoring points, slumping of the sandstone and the tension cracks in the embankment batter. The instability also compromised the sub-horizontal drainage that was installed.

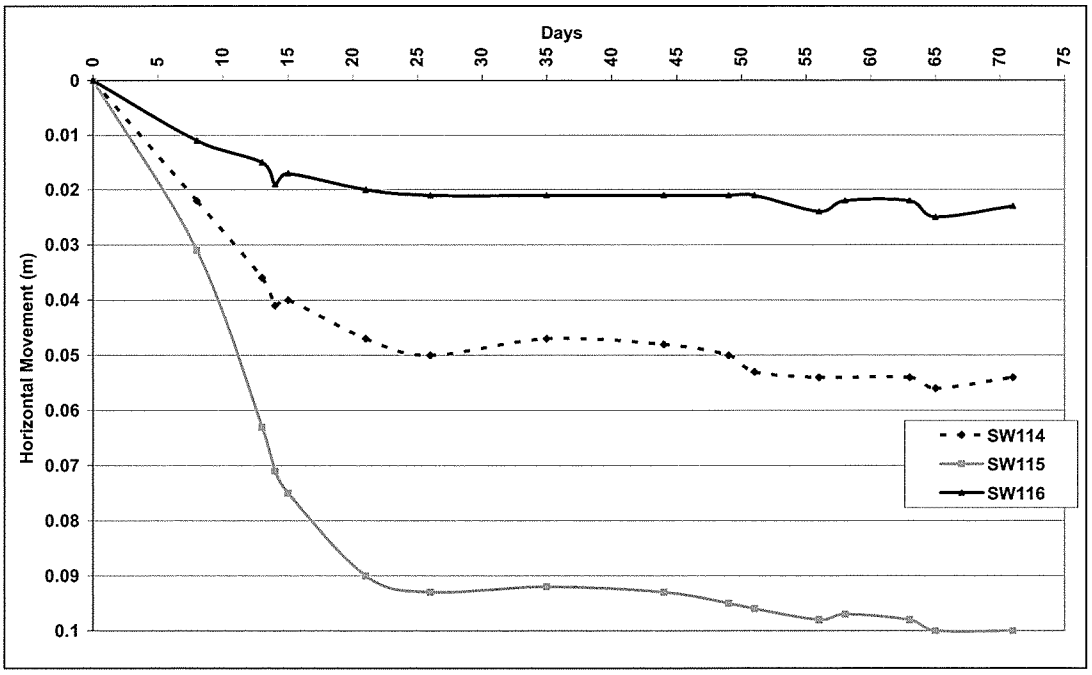

Figure 2: Survey monitoring data showing extent of lateral movement

This was likely to have occurred as a result of movement of soil mass as opposed to single nails and as a consequence, it was recommended that this soil mass be anchored to the slope. It was proposed to install two rows of 10 m long 25 mm diameter nails with a grouted hole size of 130mm, along the unstable section.

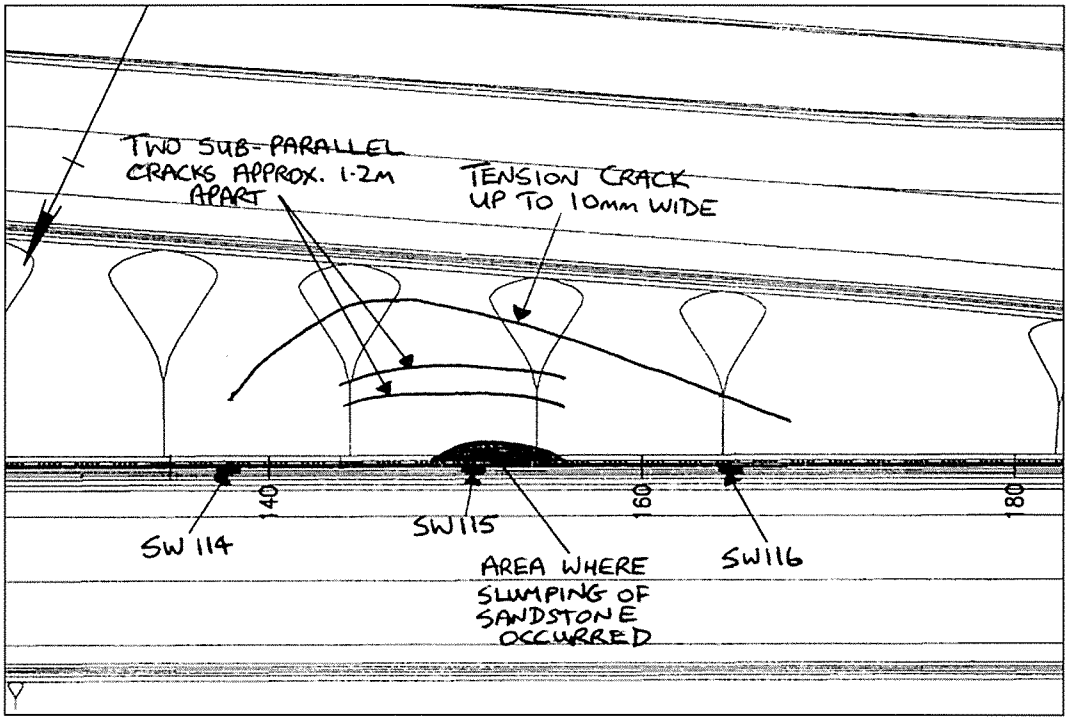

Figure 3: Location of monitoring points, area of slumping and tension cracks

The geotechnical model was revised (revised values are shown in Table 1) based on visual observations during construction of the wall and these values were used to design the length of remediation nails.

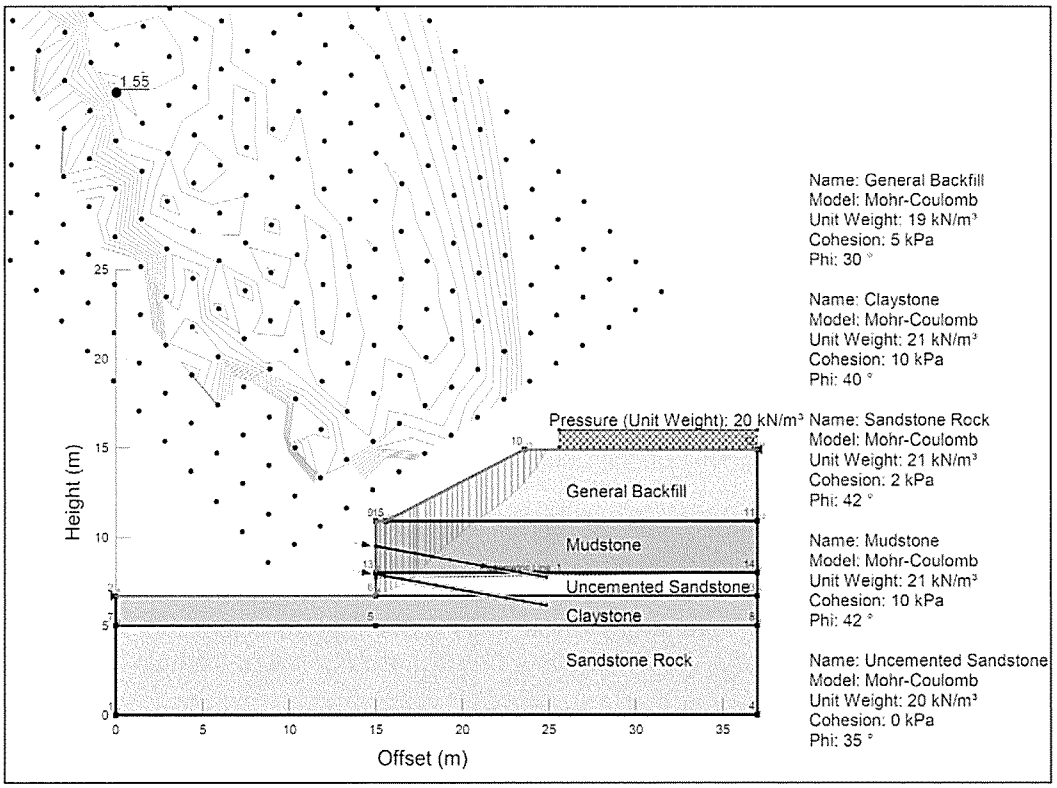

Figure 4: Design of remediation nails

During the design of remedial works, the effect of the initially designed 5 m long nails was ignored. During construction of the 10 m long nails, water was encountered when drilling. The presence of the water was due to the fact that during grouting of the void, some of the drainage was compromised. As a result, an extra row of sub-horizontal drains was recommended to ensure adequate drainage of the wall.

Monitoring data of the wall suggests that movement has ceased indicating that the remediation nails were successful in stabilising the wall.

5 CONCLUSIONS

During excavation for a soil nailed wall, instability of the wall and embankment above it occurred due to the presence of a weakly cemented layer of sandstone and groundwater. Parameters used in the original design were reassessed and remedial soil nails were designed and extra horizontal drainage was also recommended.

The presence of groundwater combined with the weakly cemented sandstone layer meant that the 'stand-up' time for an unsupported vertical face was much shorter than expected. Where such a situation exists after excavation, it would be recommended to place mesh and shotcrete prior to installation of nails and grout; this will enhance the stability of the vertical face in the short term. Sub-horizontal drains could also be installed after placing of shotcrete. This isn't always practical, but the extra time and expense required to carry out this method of construction can prevent potentially costly remediation measures.

ACKNOWLEDGEMENTS

The author gratefully acknowledges the assistance from Chris Bridges and Iain Turner from Coffey Geotechnics in preparing this paper.

REFERENCES

Briaud, J.L. and Lim, Y (1997) Soil nailed wall under piled bridge abutment: simulation and guidelines. *Journal of Geotechnical and Geoenvironmental engineering*. Volume 123 No.11.

Murray, R.T. (1993). "The development of specifications for soil nailing," *Research Report 380,* Transportation Research Laboratory, Crowthorne, UK.

Phear, A; Dew, C; Ozsoy, B; Wharmby, N J; Judge, J; Barley, A D (2005) Soil Nailing – best practice guidance. *CIRIA C637* London 2005

Watkins, A.T. & Powell, G.E. (1992) Soil nailing to existing slopes as landslip preventative works. *Hong Kong engineer*, March, pp 20–27

Wong, I.H.; Low, B.K.; Pang, P.Y. and Raju, G.V.R. (1997). Field performance of a soil nailed wall in residual soil. *Journal of Performance of Constructed Facilities*. Volume 11 No. 3.

Predicted site behaviour of geogrid encased stone columns

Joel Gniel & Abdelmalek Bouazza
Department of Civil Engineering, Monash University, Clayton, Victoria, Australia.

Keywords: ground improvement, stone columns, geogrid

ABSTRACT

Where lightly loaded structures such as embankments are to be founded on soft compressible soils, stone columns are often used to improve the engineering properties of the bearing layer. Stone column treatment can provide a significant reduction in the magnitude of both primary and creep settlement, in addition to accelerating consolidation. With recent research aimed at reinforcing columns with geosynthetics, a technique of partial encasement using geogrid has been investigated to further reduce settlements. Small-scale testing of model columns has indicated that significant reductions in vertical settlement can be achieved by steadily increasing the percent encased length of the column. Based on these findings, a parametric study using numerical modelling was undertaken, indicating that similar reductions in vertical settlement may be achieved in full-scale. It is expected that geogrid encasement could be used to extend stone column treatment to sites with strict settlement control or to reduce the 'step' in differential creep settlement that can occur off piled structures such as bridge abutments.

1 INTRODUCTION

In recent years, geotextile has been used to provide additional lateral confinement to stone columns, extending their use to very soft soils. The technique has been employed on numerous projects throughout Europe (Raithel et al., 2005) and more recently, South America (De Mello et al., 2008). Research is currently being undertaken at Monash University to investigate the use of geogrid as an encasement material. Geogrid is expected to be more robust than geotextile, allowing column material to be compacted to a greater density during installation and enabling the use of crushed rock rather than only sand.

Small-scale testing was undertaken on encased model sand columns installed in clay to investigate the impact of geogrid encasement on column behaviour. Despite scale effects, past authors have shown that model columns can adequately represent stone column behaviour in many cases (McKelvey et al., 2004). Emphasis was placed on investigating whether partial encasement of the upper section of the column could provide a similar reduction in settlement to fully-encased columns.

Finite element modelling (FEM) using the software PLAXIS® (v8) was then undertaken to reproduce the results observed in small-scale testing. This was achieved by modelling individual materials based on laboratory strength/deformation tests, then combining these models to simulate column tests. Numerical models were then scaled up to reproduce typical site conditions and predict full-scale column behaviour, including the impact of varying parameters such as geogrid stiffness and encased length. This paper discusses the laboratory testing, numerical study and possible practical applications for geogrid encased columns.

2 SMALL-SCALE LABORATORY TESTING

Kaolin slurry was initially consolidated in three custom-built cells, at a vertical pressure of about 50 kPa, to create very soft beds of clay, measuring about 300 mm in height and 155 mm in diameter. The clay had an undrained shear strength of about 5 kPa, representing the type of soil strength in which encased columns may be installed. A vertical cylindrical hole measuring

51 mm in diameter was then excavated at the centre of the clay and a pre-prepared frozen sand column (compacted to a relative density of about 90%) of similar diameter was placed within it. Although somewhat idealised, the adopted installation represented a replacement technique (using casing) that may be used to install stone columns on site. Where geogrid encasement was required, a fibreglass mesh with similar scaled properties to geogrid was used. Other aspects of testing including column geometry and particle size were also appropriately scaled.

The column and surrounding clay were loaded with a piston, forming the boundary conditions of a 'unit-cell', a concept often used to simplify column group behaviour to that of a single column (Barksdale & Bachus, 1983). Samples were loaded in several stages, up to a pressure of about 300kPa. Consolidation was completed between stages, simulating staged construction. Testing was undertaken on clay and non-encased samples to provide base data for encased column tests. Tests were then undertaken on columns with the upper 25%, 50%, 75% and 100% encased with fibreglass mesh. Photographs of the test equipment and samples are presented in Figure 1. Further details of testing are provided by Gniel & Bouazza (2008a).

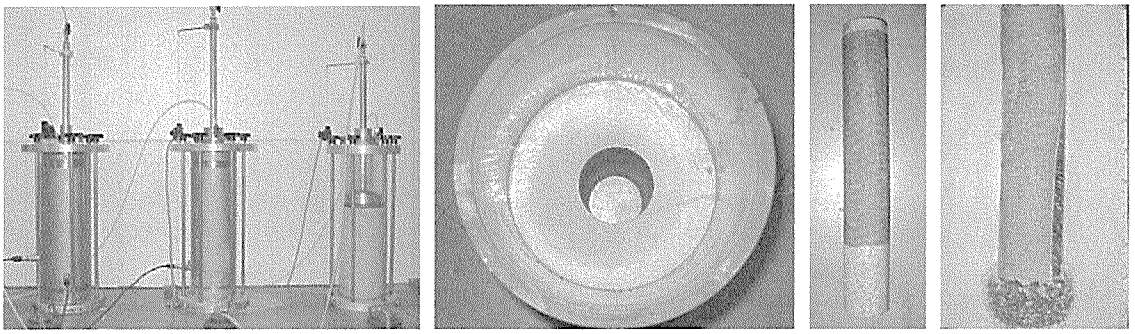

Figure 1: Photographs of small-scale testing (from left); custom-built consolidation cells, column installation, frozen sand column (75% encased), extruded sample (75% encased)

Although various aspects of encased column behaviour were investigated as part of ongoing research, settlement reduction is only considered in this paper. The relationship between pressure and vertical strain for the column tests is presented in Figure 2 and compared to the results of FEM (discussed later). Results indicated that vertical strain was significantly reduced through the use of non-encased sand columns, as expected. By steadily increasing the percent encased length from 25% to 75%, a further reduction in vertical strain was realised. Fully encased columns were observed to provide a dramatic reduction in sample strain when compared to non-encased and partially-encased columns.

3 NUMERICAL MODELLING

A numerical study was used to replicate the results of small-scale testing in order to establish a method of modelling column installation and column behaviour based on basic laboratory strength/deformation tests. Following this, the modelling process was scaled up to predict the behaviour of columns installed on site, including the impact of varying different parameters.

3.1 Small-scale modelling technique

Oedometer and shear box tests were undertaken on samples of clay and sand in order to define their strength and deformation properties. These properties were then used to develop a numerical soil model in PLAXIS that reproduced the test behaviour, hence calibrating the numerical model to test data. For clay, the 'Soft Soil' model in PLAXIS most closely matched the compressibility observed in oedometer tests. For sand, the 'Hardening Soil' model most closely matched test behaviour. The fibreglass mesh was modelled using an elastic tensile element with tensile strength and stiffness derived from uniaxial tensile testing of the mesh.

Having calibrated the separate numerical models to the results of strength-deformation testing, they were combined to model the behaviour of sand column tests. An axi-symmetric model of the cell geometry was created with the relevant stress history applied to the clay. The excavation of clay and installation of the frozen sand column was modelled by replacing the clay cluster within the excavation zone with sand. As the small-scale installation method was not considered to significantly affect the lateral stresses within the clay, the numerical installation method was considered a reasonable approximation. The relevant load stages were then applied to the model and settlements were compared to the small-scale tests. Further details of the numerical modelling process are provided by Gniel & Bouazza (2008b).

3.2 Comparison to small-scale testing

The vertical stress-strain behaviour of the numerical models are compared to small-scale tests in Figure 2. Results show that the numerical models closely match the small-scale tests, with the modelling process able to capture the general trend in strain reduction observed with increased column encasement. Other aspects of small-scale test behaviour including lateral deformation, geogrid hoop forces and consolidation time rate were closely matched by the PLAXIS models.

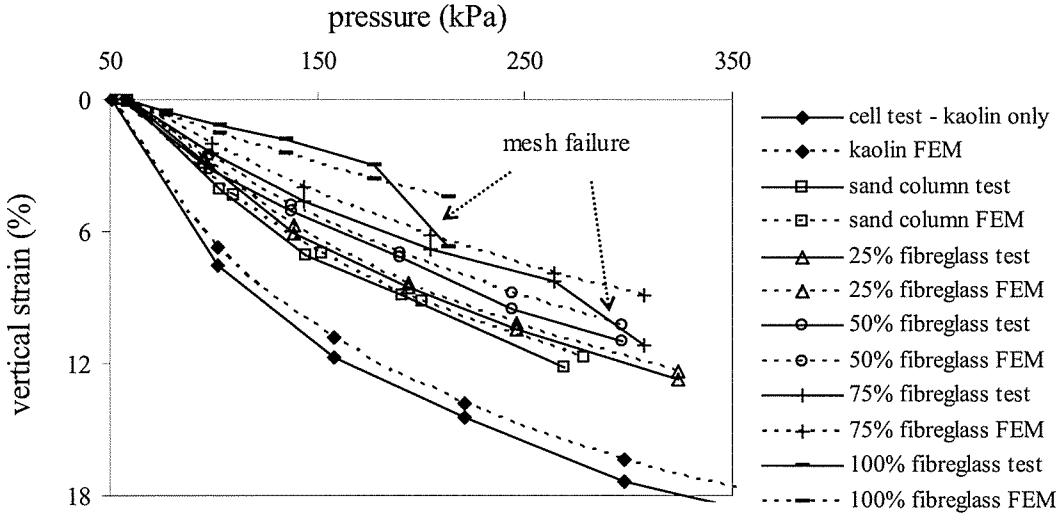

Figure 2: Comparison of FEM to small-scale laboratory test results

3.3 Scaled up modelling

Based on the results of the small-scale study, the numerical model was scaled up to full size with some confidence that (i) models calibrated to the behaviour of laboratory tests would adequately represent the behaviour of the clay deposit from which they were sampled, and (ii) column installation using a replacement technique could be modelled with reasonable accuracy.

The base model used for the full-scale study comprised an 8 m thick deposit of soft, compressible clay modelled in axi-symmetric half space. The properties of Coode Island Silt (CIS) were used for this model. CIS is of Quaternary Age, near-normally consolidated and deposited in the Yarra Delta region of Melbourne, with properties considered typical of soft clay. In addition, the engineering properties of CIS have been well documented. Typical strength and compressibility parameters for CIS are presented in Table 1, taken from Ervin (1992). Using these parameters, an 8 m surcharge was applied to the base model and consolidated, resulting in 1.55 m of settlement. This settlement compared favourably to case studies with similar surcharge loads, including that of Day & Woods (2007).

Stone column installation was then modelled using a replacement technique. Columns were assumed to receive minimal compaction during installation and were assigned the properties of

the loose to medium dense granular material presented in Table 1. Furthermore, the column was modelled as a Mohr-Coulomb material due to convergence problems running the non-linear 'Hardening Soil' and 'Soft Soil' models in full-scale. As there was little difference between the performance of the 'Hardening Soil' and 'Mohr-Coulomb' models in small-scale (at least at lower stresses), the change was not considered to significantly impact the results.

Table 1: CIS and stone column properties used in numerical modelling

Coode Island Silt		Granular Column Material	
Properties	**Value**	**Properties**	**Value**
Unit weight	16 kN/m^3	**Unit weight**	21 kN/m^3
Friction angle, ϕ'	30°	**Friction angle, ϕ'**	37°
Dilation, ψ	0°	**Dilation, ψ**	6°
Cohesion, c'	2 kPa	**Cohesion, c'**	0.1 kPa
Initial void ratio, e_0	2.0	**Young's modulus, E'**	11 MPa
Compression index, C_c	0.8	**Poisson's ratio, ν**	0.3
Recompression index, C_r	0.08		

The column diameter was kept constant at 0.8 m and the cell diameter was varied to represent columns installed at replacement ratios of 15%, 25% and 35%. The relationship between replacement ratio and settlement reduction for a stone column installed in CIS using vibro-replacement is presented in Figure 3. To check the sensibility of the result, the FEM relationship was compared to results of commonly used design methods and testing of lightly compacted, vibro-replaced columns in soft clay, including:

- design curves based on the Priebe Method for $E_{column}/E_{clay}=10$ (Priebe, 1995)
- empirical curves for columns in clay with $c_u=20$ *kPa* (Greenwood & Kirsch, 1983)
- centrifuge test results on columns where $E_{column}/E_{clay}=7$ (Craig & Al-Khafaji, 1997)

As highlighted in Figure 3, the numerical model performance falls within the range generally expected for lightly compacted, vibro-replaced stone columns.

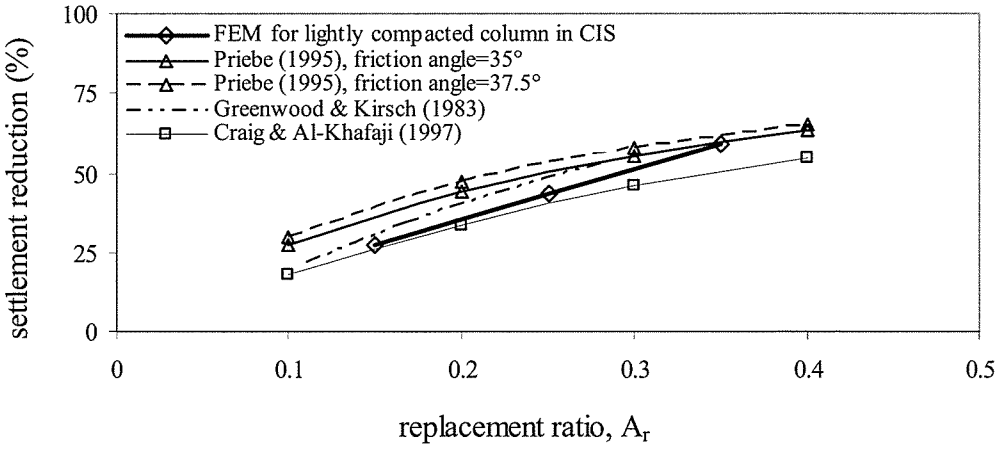

Figure 3: Comparison of numerical model to typical stone column performance

The properties of Secugrid® (produced by Naue GmbH) were used for the geogrid tensile elements in the numerical model. A Secugrid® material of medium stiffness and strength (ultimate tensile strength, UTS, of 100kN/m at a strain of about 6%) was adopted. Columns with 25%, 50% and 100% encasement were modelled and the behaviour compared to non-encased columns in Figure 4. The hoop forces within the geogrid for fully encased columns at different replacement ratios are also presented in Figure 4. Results of the full-scale study indicated similar reductions in vertical strain with increased encased length to small-scale tests.

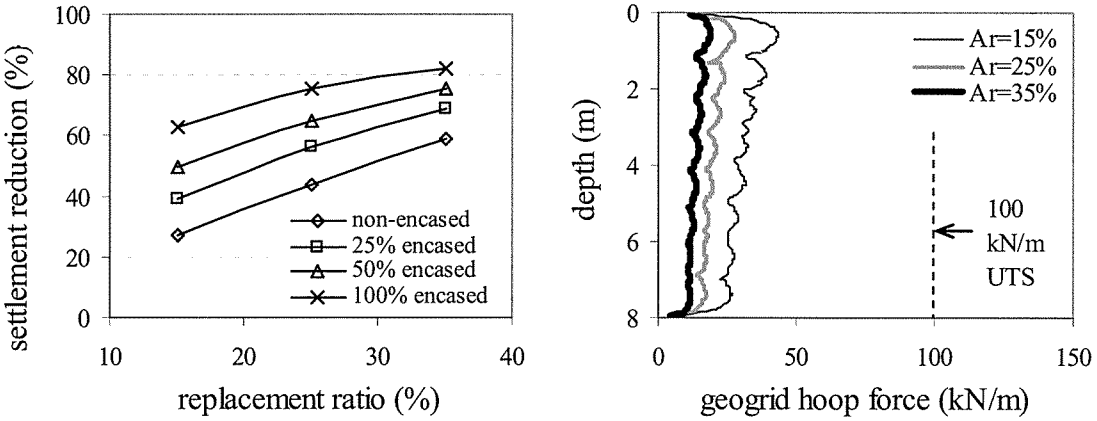

Figure 4: Results of numerical modelling for encased stone columns installed in CIS

3.4 Parametric Study

Parameters were varied to investigate their impact on column behaviour. Changes included:

- Increasing column stiffness and shear strength to that of a densely compacted column.
- Reducing clay stiffness to that of a very soft soil.
- Reducing/increasing geogrid stiffness.
- Lengthening/shortening column length and therefore encasement length.
- Increasing lateral earth pressures in the clay to model vibro-displacement.

Results of the study indicated that for a given replacement ratio, increasing the percent encased length produced the greatest reduction in vertical strain. Following this, vertical strain was reduced most effectively by increasing column stiffness, increasing the geogrid stiffness and using a displacement method of column installation. Reducing the clay stiffness appeared to have little impact on vertical strain, as did the column length. From this study, it was concluded that densely compacted columns, fully encased with a geogrid of high stiffness would provide the greatest reduction in vertical strain. In such cases and at replacement ratios of 25% to 35%, this reduction in vertical strain exceeded 90% of the untreated strain.

4 PRACTICAL APPLICATIONS

Like geotextile, it is expected that full-length geogrid encasement will provide the necessary confinement to extend the use of stone columns to very soft soils. However, unlike geotextile, the geogrid can be used with crushed rock and coarse gravel. Furthermore, geogrid encased columns can receive greater compaction during installation due to the robustness of the geogrid, reducing settlements associated with densification. For conventional stone column projects:

- Partial or full geogrid encasement could be used to reduce the number of stone columns needed. Research has indicated that by encasing the upper 50% of a column with geogrid, the number of columns required to provide the same settlement reduction could nearly be halved, providing a significant cost saving to a project.
- Settlement could be tailored to design requirements by adopting partial or full encasement or by varying the geogrid stiffness.
- Geogrid encasement could be used to reduce settlement by up to 90% (of the untreated settlement), making the technique competitive with other options such as soil mixing.

Furthermore, a common problem in soft soil engineering is the differential 'step' in creep settlement that can occur between areas of untreated soil and piled structures such as bridge abutments. The solution to such a problem generally involves maintenance of the interface and regular resurfacing if a motorway pavement or rail-line is involved. As stone columns reduce

creep settlement in the same manner as primary consolidation, partially encased columns could provide an innovative solution to this problem. By steadily increasing the encased length of columns leading up to the rigid structure, creep settlement could be tapered to meet design requirements, reducing the differential 'step' in settlement and eliminating maintenance needs.

5 CONCLUSIONS

Results from small-scale testing and a detailed numerical study have indicated that stone columns fully encased with geogrid could extend the ground improvement technique to extremely soft soils. The numerical study was calibrated to a deposit of soft, compressible clay (Coode Island Silt) and indicated that settlement reductions of up to 90% could be achieved for fully encased columns when compared to untreated settlements. This performance is similar to other methods of ground improvement including soil mixing. Furthermore, fully-encased or partially-encased columns could be used on stone column projects to reduce the number of stone columns used, reduce the settlement or tailor settlement to design requirements.

ACKNOWLEDGEMENTS

This work is funded by an Australian Research Council Linkage Grant and by Naue GmbH and Keller Ground Engineering. Their support is gratefully acknowledged.

REFERENCES

Barksdale, R. & Bachus, R. (1983) *Design and construction of stone columns: Final Report SCEGIT-83-104*. Federal Highway Administration, Washington D.C. 20590.

Craig, W. & Al-Khafaji, Z. (1997) Reduction of soft clay settlement by compacted sand columns. *Proceedings of 3rd International Conference on Ground Improvement Geosystems*, London, 219-224.

Day, R. & Woods, P. (2007) Verification of consolidation parameters of a near-normally consolidated clay by back analysis of an instrumented, wick-drained reclamation. *Proceedings of 10th ANZ Conference on Geomechanics,* Brisbane, Australia, (2) pp 105-111.

De Mello, L.G. et al. (2008) First use of geosynthetic encased sand columns in South America. *Proceedings 1st Pan-American Geosynthetics Conf.*, Cancun, pp.1332-1341.

Ervin, M. (1992) Engineering properties of Quaternary Age sediments of the Yarra Delta. *In: Engineering Geology of Melbourne*. A.A. Balkema, Rotterdam, pp 245-259.

Gniel, J. & Bouazza, A. (2008a) Model tests on geogrid encased stone columns. *Proceedings of 4th European Geosynthetics Conference*, Edinburgh.

Gniel, J. & Bouazza, A. (2008b) Numerical modelling of small-scale geogrid encased tests. *Proceedings of 2nd International Workshop on Geotechnics of Soft Soils*, Glasgow, Scotland, pp 143-149.

Greenwood, D. & Kirsch, K. (1983) Specialist ground treatment by vibratory and dynamic methods: State of the art. *Proceedings of Advances in Piling and Ground Treatment for Foundations*, Institute of Civil Engineers, London, 17-45.

McKelvey, D. et al. (2004) Modelling vibrated stone columns in soft clay. *Geotechnical Engineering*, 157(3), pp 137-149.

Priebe, H.J. (1995) Design of vibro replacement. *Ground Engineering*, 28(10), 31-37.

Raithel, M. et al. (2005) Foundation of construction on very soft soils with geotextile encased columns – state of the art. *Proceedings of GeoFrontiers*, Austin, USA.

Geotechnical Aspects of Engineering Design on Napier Hill

Paul Hayes
Tonkin & Taylor Ltd – Environmental and Engineering Consultants, Auckland, NZ

Keywords: Slope Stability, Napier

ABSTRACT

Tonkin & Taylor has developed an understanding of the geotechnical aspects of engineering design on Napier Hill through our landslide assessments for the Earthquake Commission and design and supervision of remedial works for land owners. Napier Hill is an uplifted limestone outcrop overlain by sandy siltstone, "Brickyard" clay and loess deposits. The soil mantle on slopes around the hill is subject to landslides triggered by saturation and erosion during heavy rainfall events. Typical remedial works include retaining walls and debris barriers at the top and bottom of slopes respectively and various slope face improvement options. Such solutions have been engineered to ensure slope stability in heavy rainfall events and when subject to the high seismic loads experienced in Napier, including an allowance for topographic amplification.

1 INTRODUCTION

Napier Hill is located in a prominent position immediately to the northwest of Napier city centre and overlooking the port. The hill (which actually comprises two hills; Hospital Hill to the south and Bluff Hill to the north) covers an area of 250 ha and is largely occupied by residential dwellings, together with three schools, a church, the Botanical Gardens and the disused hospital complex. There are very few areas of extensive flat land on Napier Hill and many of residences are located above, below or on steep slopes. Tonkin & Taylor's involvement on Napier Hill is largely based on work for the Earthquake Commission (EQC). In the last three years we have assessed land instability on 39 properties throughout Napier Hill and designed and supervised the construction of remedial works on 13 of these (Figure 1).

This paper outlines the lessons we have learnt from our work on Napier Hill, summarising the geology of Napier Hill, the geological hazards associated with development on the hill and methods of mitigating these hazards through engineering design. One brief case study is used to illustrate the application of these methods.

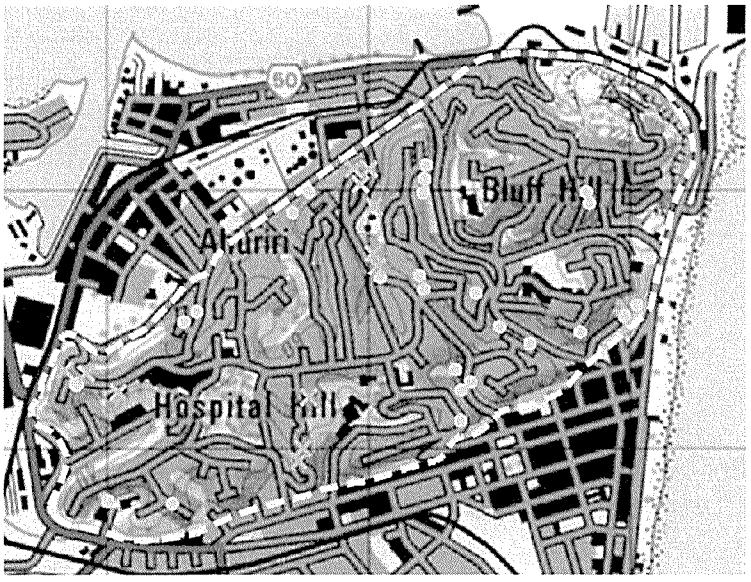

Figure 1. Location of assessments (circles) and construction works (crosses)

2 GEOLOGY OF NAPIER HILL

J.T. Kingma's geological mapping shows that the limestone outcrop which forms Napier Hill was once more extensive than it is at present. Following deposition of the Pleistocene Age limestone the area was uplifted and subjected to erosion, forming extensive gullying on the surface of the limestone. The drainage patterns formed by the erosion were then infilled as sea levels rose and a blanket of marine clays was deposited across the irregular topography until a reasonably flat surface was developed. Pumiceous deposits were later deposited on top of the clay. The strata, particularly the limestone, are frequently broken by folding, and Napier Hill itself is a remnant of the eastern flank of a very gentle syncline with a SW-NE axis. Kingma shows four main geological units present on the hill. They are, in increasing order of age:

- Brickyard clay (yellow-brown, very pumiceous, sandy clays)
- Sandy siltstone with sandy layers
- Upper Napier limestone
- Lower Napier limestone (recrystallised, often dark-blue, with shell-casts)

Observations of outcrops around the hill show that in many places this stratigraphy is overlain by several metres of wind blown loess. Today Napier Hill is characterised by steep perimeter cliffs (typically between 20 and 80 m high and inclined at up to 70°) and numerous internal slopes and gullies originating from the tectonic and erosion processes that have occurred.

3 EARTHQUAKE INDUCED SLOPE INSTABILITY

A magnitude 7.8 earthquake struck the Hawke's Bay region on 3 February 1931, killing 256 people (161 in Napier). Most of the damage in Napier was centred in the city centre where whole blocks of buildings collapsed. However, there was also extensive damage from landslides on Napier Hill. Sailors anchored offshore observed "'great clouds of dust from falling headlands', as if the shore was under bombardment" (Wright, 2001). The largest landslide came down at the northern end of the hill, blocking the road to the port (Figure 2), while smaller landslides scalloped large sections of Napier Hill. Few wooden houses completely collapsed, but most were damaged and a number fell down the hill when the ground failed beneath their foundations.

Fortunately, Napier has not experienced an earthquake that has caused significant damage since 1931. Neither of two recent moderate earthquakes (Gisborne, magnitude 6.8, 20 December 2007 and Hastings, magnitude 5.9, 25 August 2008) resulted in landslides on Napier Hill.

Figure 2. 1931 landslip blocking road to port © Napier City Council

4 TYPICAL FORMS OF NON-EARTHQUAKE INDUCED SLOPE INSTABILITY

4.1 General

Because of the steep topography and extent of residential development, nearly all landslides that occur on Napier Hill present a hazard to properties on and above the slope (loss of land, dwelling and/or potential loss of life) and/or below the slope (inundation of land, damage to dwelling and/or potential loss of life). The typical forms of slope instability encountered on Napier Hill in non-seismic events are drawn from observations and patterns noted during 39 EQC assessments on the hill. The large majority of the landslides we have assessed have occurred following heavy rainfall events, with the most common failure mechanisms summarised below.

4.2 Shallow landslides

The loess, Brickyard clay and sandy siltstone which overlay the Napier limestone are able to stand up very steeply, as evidenced by the steep perimeter cliffs encircling Napier Hill. However, there is typically a mantle of weathered soils at the top of slopes. Heavy rainfall induces shallow landslides (typically less than 4 m depth) by (i) saturating the near-surface soils, resulting in an increase in pore water pressure and corresponding reduction in effective strength, and (ii) causing surface erosion which can undermine the stability of the soil mantle (Figure 3). The majority of the shallow landslides encountered on Napier Hill are translational in nature, but some translational landslides have also been observed.

4.3 Block failures in jointed/fractured soils

Sub-vertical jointing and fracturing of exposed loess and sandy siltstone is frequently encountered around the perimeter of the hill and where slopes have been cut to facilitate development (Figure 4). Due to the high erodibility of the soils, particularly the loess, these joints are gradually opened as rainwater washes out soil from either side of the defect. This process is exacerbated in heavy rainfall events, triggering failure of soil blocks by either toppling, falling or sliding.

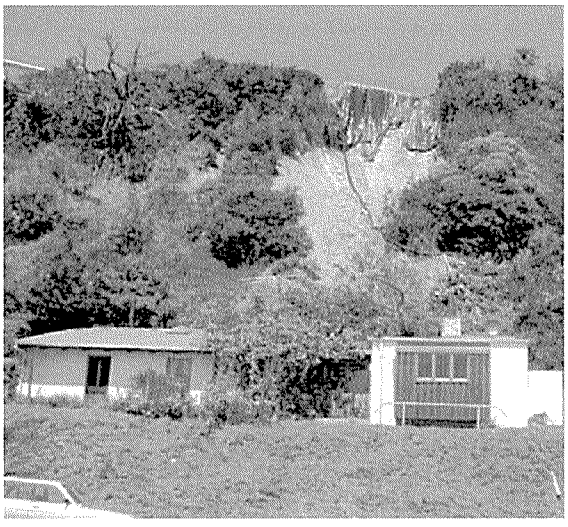

Figure 3. Shallow landslip after heavy rain

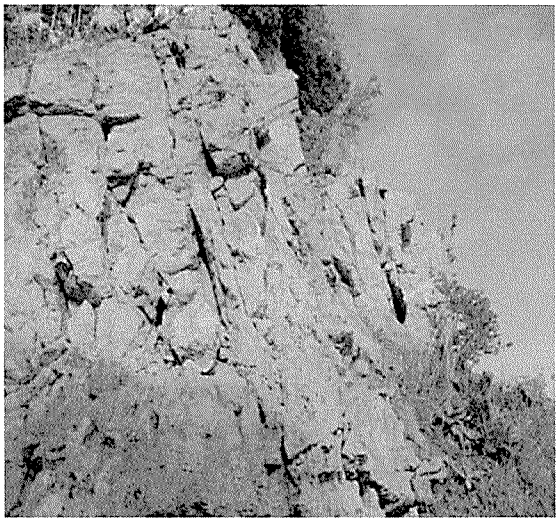

Figure 4. Sub-vertical defects

4.4 Rock falls

Rock falls and topples on Napier Hill typically occur on exposed limestone faces, where we have observed rocks up to 1.5 m in diameter that have been dislodged by the gradual weathering process. The onset of these rock falls is not particularly influenced by heavy rainfall and, on slopes where they do occur, rock falls are a fairly regular occurrence.

5 TYPICAL MITIGATION/REMEDIAL OPTIONS

5.1 Seismic design loading

Although the instability encountered on Napier Hill is typically shallow and triggered by heavy rainfall events, the high seismic accelerations for a 1:500 year earthquake govern the design of the remedial works. The seismic loading is derived from AS/NZS 1170:2002 which defines a "Z-value" hazard factor for Napier of 0.38. Due to the steep nature of the Napier Hill slopes, topographic amplification of the seismic wave up the slope is expected and may be estimated by either:

- **Eurocode 8, 1998** – Apply a standard topographic amplification factor of 1.4 for ridges with slope angle greater than 30°.
- **Ashford & Sitar, 2002** – Apply a topographic amplification factor of 1.5 and then modify this to account for the depth of the failure (h) in relation to the overall slope height (H). For example, a small failure at the top of a slope has an h/H modifier of 1 and a full depth failure has a modifier of 0.66, giving overall amplification factors of 1.5 and 1.0 respectively.

Remedial solutions have been designed for a high seismic acceleration and for the possibility of storms of increasing intensity and frequency as a result of climate change. Typical engineering solutions adopted on Napier Hill, design considerations and lessons learnt from their construction and subsequent performance are summarised below.

5.2 Retaining walls and debris barriers

Because residential dwellings are located above and below most slopes on Napier Hill, we have found that walls are frequently required at the top and bottom of slopes affected by landslides. Retaining walls have often been the best option to prevent additional loss of flat land at the top of steep slopes. As retaining walls are typically supporting and/or protecting residential dwellings they have been designed for the 1:500 year return period earthquake, meaning that walls are typically much deeper and stronger than is needed to prevent rainfall induced shallow slope failures. Frequently, the high seismic loading necessitates the use of reinforced concrete piles and restraint by grouted ground anchors through a reinforced concrete capping beam.

Because they do not protect land on the downslope side of the wall, which is typically erodible and subject to shallow landslides following heavy rainfall, it is prudent to allow for an evacuation of soil in front of the piles, even where other slope stabilisation measures are undertaken. Indeed, it has often proved desirable to excavate the top few metres of loose soil from in front of the piles and place timber lagging to restrain the soils behind, thus limiting the potential for unsightly and potentially damaging slippage of the unprotected near-surface soils immediately in front of the piles. This has been done in the wall at the top of Figure 5.

Debris barriers comprising solid and/or flexible walls and catch areas have been considered at the base of unstable slopes to prevent inundation of property, damage to dwellings and potential loss of life. Debris barriers have proved to be suitable for all the typical forms of slope failure encountered on Napier Hill and have worked best when undertaken in conjunction with works further up the slope to reduce the potential for further failures to occur.

For example, Figure 3 shows a shallow translational landslide that resulted in loss of land at the top of the slope and deposition of slope debris onto the roof of the house below. The remedial works shown in Figure 5 include a retaining wall at the top of the slope comprising 11 m long, 0.5 m diameter reinforced concrete piles at 1.5 m centres, tied back through a capping beam with 15 m long grouted anchors at 3 m centres. The top 3 m of soil in front of the wall was excavated and timber lagging installed between the piles. A cantilevered vehicle parking deck and a light weight building were incorporated into the design. A debris barrier and catch area protects the lower dwelling from further landslides.

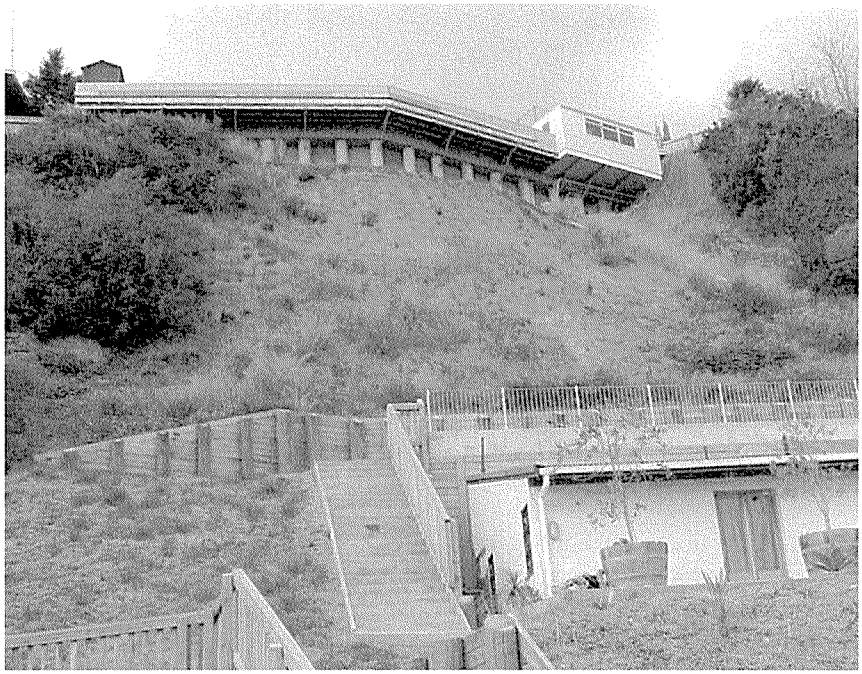

Figure 5. Anchored reinforced concrete retaining wall (top) and debris barrier (bottom)

5.3 Slope face improvements

Depending on the specific site circumstances, a number of measures have been used to improve the stability of slope faces, including:

- Grouted soil nails and rock fall protection mesh have proven to be an effective means of improving the integrity of the nailed soil mass and preventing surface soils from falling. Driven soil nails have also been adopted as a relatively rapid and cheap temporary measure to stabilise surface soils.
- The gradual weathering process of the exposed loess and sandy siltstone opens fractures in the soil, eventually leading to failure, particularly where joint orientation is unfavourable for stability. Imminent block falls can be observed in numerous locations around Napier Hill. Where possible, such blocks have been dislodged in a controlled manner to prevent the risk of uncontrolled falls causing damage to property and/or residents.
- Consideration has been given to trimming/felling large trees growing on steep slopes, while leaving their root system intact to hold soil and allow regrowth.
- Due to the high erodibility of the soil mantle, exposed slopes have been revegetated as quickly as possible to reduce erosion (which can trigger additional landslides), frequently with the help of coir matting or three dimensional geotextile. The maintenance of these plants in the dry Hawke's Bay climate, particularly until they become well established, should be carefully planned to increase plant survival.
- Because of the high erodibility of the loess and sandy siltstone, control of surface water is crucial for maintaining the stability of slopes on Napier Hill. Stormwater has

been collected to prevent it from discharging freely over the slope. Groundwater is not typically encountered on Napier Hill slopes, perhaps due to the high permeability of the underlying limestone. However, where groundwater is encountered, horizontal drains connected to a piped discharge system have enhanced slope stability.

Several of these face improvement options have been undertaken on the slope shown in Figure 5, including soil nailing areas at either end of the upper retaining wall, removing loose soil from the slope, planting with the aid of coir matting and piping stormwater to the base of the slope. This photograph was taken approximately two years after construction and there has been no significant erosion of the slope face.

6 CONCLUSIONS

Avoiding development on or adjacent to steep slopes on Napier Hill is not an option due to the extent of existing development and the scarcity of available land. Some of the key lessons learnt from our experience of geotechnical engineering design and construction on the slopes of Napier Hill are:

- The near certainty of another large earthquake governs the design of all engineering structures on the slopes of Napier Hill. Seismic accelerations for the design of retaining walls taken from AS/NZS 1170:2002 are modified for topographic amplification as appropriate.
- All of the slope failures we have observed on Napier Hill have been relatively shallow (less than 4 m) and triggered by saturation and/or erosion from heavy rainfall. However, the requirement to design for high earthquake loads means retaining wall piles are substantially deeper and stronger than would be required solely for the static situation, often necessitating the use of ground anchors.
- Ongoing shallow slope failures will continue to be experienced throughout Napier Hill due to the gradual weathering of exposed slopes, particularly those containing loess. This process is exacerbated by heavy rainfall which saturates and causes erosion of the near-surface soils, triggering shallow landslides and block slides.
- The control of surface water and the maintenance of a good vegetation cover is particularly important in reducing the occurrence of such failures, and stormwater should not be allowed to discharge over steep slopes.

ACKNOWLEDGEMENTS

- Earthquake Commission for granting permission to present this paper.
- Colleagues at Tonkin & Taylor, particularly Grant Loney and Andy Pomfret, with whom I work in the Hawke's Bay and who have reviewed this paper.

REFERENCES

Ashford, S.A. & Sitar, N. (2002) Simplified Method for Evaluating Seismic Stability of Steep Slopes. *Journal of Geotechnical and Geoenvironmental Engineering*. 119(1).

Fardis et al. (2005) *Designers' Guide to EN 1998-1 and EN 1998-5. Eurocode 8: Design of Structures for Earthquake Resistance*. Thomas Telford, London.

GNS Science and Earthquake Commission. www.geonet.org.nz [accessed 16 September 2008]

Kingma, J.T. (1971) *Geology of Te Aute Subdivision*. New Zealand Geological Survey, Wellington.

Wright, M. (2001) *Quake: Hawke's Bay 1931*. Reed Books, Auckland.

Seismic performance of geosynthetic-reinforced soil

Perry Jackson
College of Engineering, University of Canterbury, Christchurch, NZ

Keywords: Reinforced Soil, Shake-table, Geosynthetic-Reinforcement

ABSTRACT

Geosynthetic-Reinforced Soil (GRS) walls offer up to 50% in cost savings compared to conventional retaining wall structures. Additionally, large earthquakes of 1995 in Japan caused GRS walls to exhibit ductile behaviour, rather than failure, whereas their conventional retaining wall counterparts demonstrated significant damage. The behaviour of GRS walls under such seismic loadings however is not fully understood, resulting in engineering design inconsistencies.

GRS walls comprise geotextile or geogrid reinforcement layered into granular backfill. The wall is then typically faced by wrap-around geosynthetic or precast concrete segments. Design guidelines prepared by the British Standards Authority and US Federal Highways highlight acceptable lengths of reinforcement (L) in the retained backfill at 70% of the height (H) of the wall. The influence of this length on seismic performance has been investigated using shake-table and centrifuge tests previously, though with limited systematic variation of the reinforcement L/H ratio and limited attention to the pre-failure deformation behaviour of the walls.

Reducing the length of reinforcement can lessen the cost of GRS wall structures, mostly via a reduced cost of quality backfill – hence this is a desired outcome of research. However, the affect of relative length of reinforcement on GRS wall deformation performance during seismic loading is not well-understood. This is therefore to be further quantified by shake-table experiments at the University of Canterbury.

1 INTRODUCTION

Reinforced soil systems enable shortened construction time, lower cost, increase seismic performance and potentially improve aesthetic benefits over their conventional retaining wall counterparts such as gravity and cantilever type retaining walls (see Fairless, 1989; FHWA, 2001; Murahsev, 2003; El-Emam and Bathurst 2006 as examples).

Reinforced Earth (RE) was first developed in 1966 by the French Engineer, Henri Vidal, and is compared in Figure 1 with a conventional retaining wall. The RE system involved layering steel strips into engineering backfill, and connecting these to a stiff concrete facing. Through the incorporation of reinforcement into fill, it was found possible to steepen slopes above that which may occur naturally and to retain soil in a vertical or sub-vertical fashion. Alternative geosynthetic reinforcement was first used in 1971. Both RE and geosynthetic reinforcement are now part of a large family of reinforced soil systems that comprise different reinforcement, facing products and design methods. Reinforcement by geosynthetic geogrid inclusion is the focus of this paper.

This paper will first discuss the factors that require consideration for design, and focus on previous experimental work investigating one of these factors, namely the ratio of length of reinforcement, L, to wall height, H. A review of previous work is given that examines this parameter. Finally, an experimental setup and methodology for further investigation is

presented, with particular emphasis placed on the influence of the L/H ratio on the seismic stability of the geosynthetic-reinforced soil wall.

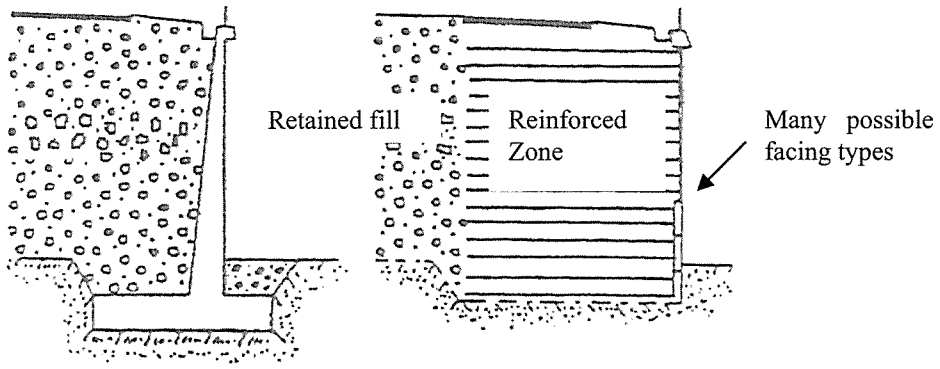

Figure 1: Conventional cantilever type retaining wall (left) and the alternative reinforced soil retaining wall (right). (Source FHWA (2001))

2 BACKGROUND

2.1 Geosynthetic-reinforced soil wall

In its original inception in 1966, the reinforcement used in reinforced soil walls was steel strips layered into the retained soil. Geosynthetic reinforcement was first used in 1971, in the form of geotextiles for embankment construction, followed by the development and introduction of geosynthetic geogrid in the 1980's. Geosynthetic reinforcement is a polymeric material and in contrast to steel, demonstrates complex load-time behaviour. It is considered an 'extensible' material (i.e. has a relatively low stiffness and extends under working loading), as opposed to 'inextensible' steel reinforcement (which, under the loads considered remains stiff and unyielding). For practical purposes, load application to extensible geosynthetic reinforcement induces a strain response that influences the formation of earth pressures within the wall. Design is thus different depending on the type of reinforcement selected.

GRS walls consist of two zones: the reinforced zone (where the reinforcement is layered into the backfill, and acts like a composite mass) and a retained backfill zone (the soil that is retained by the reinforced block), as shown in Figure 1. Within the reinforced zone there are four components that further determine the GRS wall's stability. These are the properties of the reinforcement and soil, the facing type, and connections between these. Facing is typically by pre-cast concrete segments, modular block dry cast units, or, as in the present study, is flexible; whereby the geosynthetic is used to wrap-around the face in layered lifts forming the wall.

Geosynthetic reinforcement provides soil with a tensile capacity generated from the soil-reinforcement interaction, allowing stress transfer to occur. The stress transfer occurs via either frictional or passive resistance. The stability of a GRS wall is thus governed by the soil-reinforcement interface, and for design purposes the length of reinforcement, L, is related to the reinforced soil wall height, H. This paper will focus on the L/H ratio interaction with deformation behaviour under seismic loading of walls with a wrap-around type facing.

2.2 Design procedures

The design methods presented in Federal Highways Administration (FHWA) (2001) and British Standard 8006:1995 differ in their design philosophy. The FHWA (2001) uses a limit equilibrium approach, while the BS8006:1995 uses a limit state approach, with some modifications. Limit equilibrium has traditionally been used in geotechnical design and involves

the use of a global factor of safety to prevent failure and implicitly limit deformation. Limit state design reflects the structural aspects of reinforced soil design and as a result, distributes factors of safety to where the uncertainty in the design analysis is found. The difference is important because during both self-weight and seismic loading, the structural and geotechnical components may endure different forces and strains, and thus their capacity to resist deformation may be mobilised at different times. An adaption of both standards is made by Murashev (2003) for New Zealand conditions, noting that the limit state approach is gradually being introduced into geotechnical design practice.

These methods, in addition to others in use, produce stable designs under static loading, more as a result of large factors of safety than explicit understanding of their behaviour under load. Such standards typically require for preliminary design purposes a minimal length of reinforcement to fit Equation 1. The Northridge earthquake of 1994 showed that this type of conservative static design, coupled with the inherently ductile nature of GRS walls, results in stable structures under seismic load as well (Sandri, 1997).

$$L = 0.7\ H \tag{1}$$

Across these different design methods, the consideration of failure modes is similar. First, the external stability of the reinforced composite block of soil and reinforcement is checked for possible failure. This can occur by the block sliding, overturning, exceeding its bearing capacity, or, failing via an external deep-seated slip formation. Next the internal stability of the previously assumed rigid, composite mass is considered. The possible failure modes that require checking are: reinforcement pullout, reinforcement rupture, the development of internal slip surfaces, or internal sliding of layers atop one another.

The above mentioned failure modes are checked to ensure stability under seismic loading in FHWA (2001), but this is omitted in BS 8006:1995. Procedures that do include seismic analysis differ significantly with regard to the consideration of magnitude and location of dynamic loads, acceleration amplification and application of factors of safety, as a result of inadequate understanding of GRS seismic response. These differences in design highlight a lack of understanding, hence a variety of scale model testing methods have been introduced to investigate GRS seismic behaviour.

2.3 Previous research

Various experimental approaches have been used to test deformation behaviour of GRS walls under static and dynamic loading, including Tilt-table, Shake-table and Geotechnical Centrifuge experimentation. Seismic excitation is conducted either pseudo-statically as in tilt-table tests, or dynamically as in shake-table and centrifuge testing. The following discusses experimentation using shake-table and centrifuge testing and its previous uses in attempts to quantify the L/H ratio influence on deformation behaviour under self-weight, and more recently, seismic loads.

In theory, to enable valid comparison between the full-scale real world situation and the shake-table scale model, the model must be constructed and tested such that geometric, kinematic and dynamic similitude is maintained. Iai (1989) proposed that the constitutive stress-strain law in soil holds if the confinement stress is scaled appropriately. At low strain levels (less than failure), and confining pressures 5 – 392 kN/m^2 this assumption seems to be applicable (Iai, 1989) – however these conditions are rarely held during scale model testing. Nova-Roessig and Sitar (2006) reports some research, that, to achieve similitude, included unpractical reinforcement lengths, such as L/H = 2.5, and unrealistically low soil-reinforcement interface friction angles. These actions could affect the location of failure surfaces, and are not indicative of full-scale behaviour (Nova-Roessig and Sitar, 2006). Additionally, the arrangement of reinforcement (length and vertical spacing) plays a role in the formation and location of failure

wedges , so it is important that this aspect is scaled appropriately (Watanabe et al, 2003 for example).

Sakaguchi (1996) looked at reduced scale shake-table and centrifuge experiments with reinforcement lengths set at L/H = 0.33, 0.66, and 1.0. Stiffness scaled geosynthetic geogrid was used in the centrifuge tests. An increase in L past 0.66H to L = 1.0H was found to be less effective at resisting deformation than as L increased from 0.33H to 0.66H. Sakaguchi (1996) suggests an optimum value of L = 0.67H.

Watanabe et al. (2003) conducted a series of reduced scale shake-table experiments. L/H was set to 0.4 and 0.7 using a stiffness scaled reinforcement of phosphor bronze strips. Extension of one of the upper layers of reinforcement was found to be effective at resisting wedge deformation, as tensile forces were activated to resist a failure surface that radiated out from the base of the rigid reinforced soil block. Takemura and Takahashi (2003) tested L/H = 0.27, 0.6 and 0.8 using a scaled geogrid in a geotechnical centrifuge to ensure greater similitude. Similar results were generated.

El-Emam and Bathurst (2005) used a geogrid with sand glued to its surface, and L/H = 0.6 and 1.0 in shake-table scale model experiments. Nova-Roessig and Sitar (2006) conducted geotechnical centrifuge tests on scale models with L/H = 0.7 and 0.9 and reinforcement comprising a geosynthetic sheet as well as wire mesh strips.

These investigations among others suggest an optimum reinforcement length, L, at which point any increase in length, is not met by a proportional increase in the interface shear resistance, and thus pullout capacity (Sakaguchi, 1996; Watanabe et al. 2003; Nova-Roessig and Sitar, 2006). However it is difficult to draw this conclusion precisely as reinforcement properties, approaches to similitude, and testing procedures vary greatly between test arrangements. Additionally, it is unclear as to the nature of this optimum length and how this relates to self-weight and seismic design. This is perhaps due to attempts during physical model testing to investigate other items of interest such as acceleration amplification, displacement prediction methods, and facing contribution, in addition to the effects of L/H. Thus there has been limited work on the systematic variation of L/H with the sole focus being its influence on deformation under seismic conditions, and hence on the underlying mechanisms of deformation. This is the main objective of the work proceeding from this literature review.

3 EXPERIMENTAL DESIGN

The chief objective of the study is to further investigate the effect of the L/H ratio on the seismic performance of GRS walls, during varying levels of shaking intensity. The experimental model wall is 1.0 m high, 2.6 m long and 0.8 wide, as shown in Figure 3. The plane-strain box will be mounted on a 4.0m by 2.0m shake-table which has a maximum velocity 240 mm/s, payload of 20T and a peak amplitude stroke of ±120 mm. Ang (1985) reviews the shake-table capabilities in-depth.

One side of the box is transparent acrylic (Perspex), allowing high speed imaging during testing and subsequent Particle Imaging Velocimetry (PIV) analysis to be undertaken. PIV will be used to examine the strain and displacement fields in the reinforced region, leading to an increased understanding of the soil-reinforcement interaction and deformation. Instrumentation is designed to effectively quantify the seismic response at varying intensity levels and is as shown in Figure 3. One additional accelerometer will be used against the transparent Perspex wall so that boundary effects can be quantified.

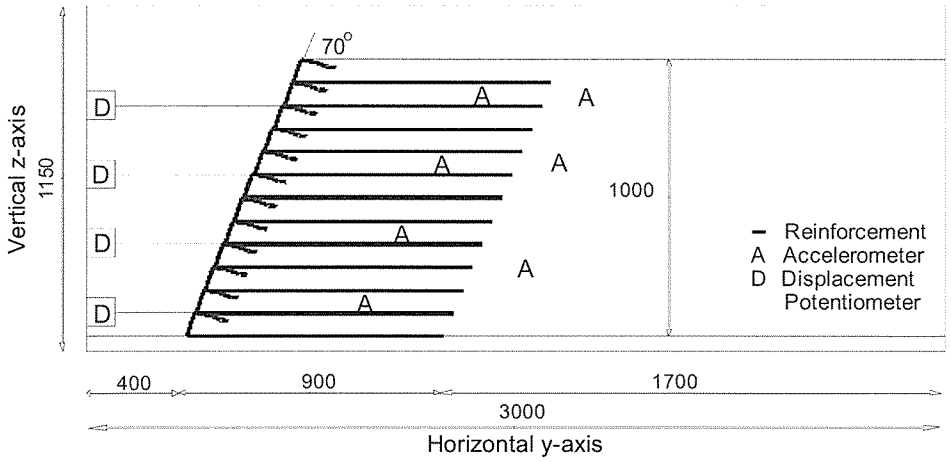

Figure 3: Proposed Experimental Setup in Shakebox

Scale model construction of the GRS wall will involve initial pluviation within a facing mould, followed by hand-held vibration compaction to create the desired in-situ soil properties. Scaled reinforcement will be layered into the soil at each layered lift

The shake table input motion will be separated into three distinct phases to investigate the seismic performance of GRS walls at various levels of intensity. The first phase will involve small shaking to cause negligible deformation and residual displacements, followed by an increase in shaking intensity to generate reinforced soil strains of 2 – 5%, and, finally, increasing agitation until wall collapse/failure.

Attention will be given to the effect of the L/H ratio on seismic wall performance. Therefore, over 4 test arrangements (including some repeat tests to examine repeatability), the L/H ratio will take the following values: L/H = 0.6, 0.7, 0.8, and 0.9. Measurements generated from the 8 accelerometers, 4 displacement transducers and PIV will be analysed and compared with that obtained in previous research to initially verify the model set up and experimental approach. The parameter L/H will be compared with the observed acceleration, displacement and strain responses across the range of seismic intensities. Acceleration and displacement data will be compared with that obtained by PIV analysis, providing data validation, as the use of PIV in GRS research has not been performed previously. The results will be compared with current design methodologies, and where appropriate, suggestions for design practice will be made.

4 SUMMARY AND CONCLUSIONS

The experimental set up is currently under construction and it is envisaged that preliminary results will be presented at the 8YGP Conference during November 2008. A summary as to the impetus for this study is given below:

- The historic focus on reinforcement by steel strip inclusion for reinforced soil is being challenged by an increase in the use of geosynthetic reinforcement.
- Previous research into the influence of GRS wall dimensions on deformation behaviour has illuminated trends, however has been relatively piece-meal due to differing experimental conditions.
- Design methodology is well established for self-weight and surcharge loading; however there are large discrepancies between design standards for seismic loading.
- Greater understanding of L/H during seismic excitation would be beneficial. There may be an optimum length of reinforcement beyond which extension may provide a reduced benefit to stability during seismic motion.

- An experimental setup and methodology has been presented that is intended to provide additional data to illuminate this matter further.

ACKNOWLEDGEMENTS

I would like to acknowledge the considerable support provided by my two supervisors Dr. Elisabeth Bowman and Assoc. Prof. Misko Cubrinovski. Additionally, the financial contribution towards the project made by the Earthquake Commission (EQC) and the University of Canterbury is gratefully appreciated.

REFERENCES

Ang, B. G. (1985) Seismic Response Shear Strength of Circular Bridge Piers, *PhD Civil Engineering*, University of Canterbury. Christchurch, NZ.

El-Emam, M. M. and R. J. Bathurst (2007) Influence of reinforcement parameters on the seismic response of reduced-scale reinforced soil retaining walls, *Geotextiles and Geomembranes* 25(1): 33-49.

British Standards Institute (1995) BS8006:1995 - *Code of Practice for strengthened/reinforced soils and other fills*.

Bathurst, R. J., Z. Cai, et al. (1996) Seismic design and the performance of reinforced segmental retaining walls, *Geotechnical Fabrics Report* 14(6): 48.

Koseki, J., Y. Munaf, et al. (1998) Shaking and tilt table tests of geosynthetic-reinforced soil and conventional-type retaining walls, *Geosynthetics International* 5(1-2): 73-95.

Ling, H. I., D. Leshchinsky, et al. (1997) Seismic design and performance of geosynthetic - reinforced soil structures, *Geotechnique* 47(5): 933-952.

Murahsev, A. K. (2003) *Guidelines for Design and Construction of Geosynthetic-Reinforced Soil Structures*, Transfund New Zealand.

Nova-Roessig, L. and N. Sitar (2006) Centrifuge model studies of the seismic response of reinforced soil slopes, *Journal of Geotechnical and Geoenvironmental Engineering* 132(3): 388-400.

Sakaguchi, M. (1996) Study of the seismic behavior of geosynthetic reinforced walls in Japan *Geosynthetics International* 3(1): 13-30.

Sandri, D. (1997) Performance summary of reinforced soil structures in the Greater Los Angeles area after the Northridge earthquake, *Geotextiles and Geomembranes* 15(4-6): 235-253.

US_Federal_Highways, F. (2001). *Mechanically Stabilized Earth Walls and Reinforced Soil Slopes Design and Construction Guidelines.*

Watanabe, K., Y. Munaf, et al. (2003) Behaviors of several types of model retaining walls subjected to irregular excitation, *Soils and Foundations* 43(5): 13-27.

Stress relaxation during K_0 compression of pumice sand

Naotaka Kikkawa
Faculty of Engineering, University of Auckland, NZ.

Keywords: pumice sand, stress relaxation, displacement rate, relative density, particle crushing

ABSTRACT

Previous research had shown that q_c values from cone penetration tests (CPT) on pumice sands were only marginally influenced by the density of the material. In this paper, data from K_o compression tests on dry pumice sand are presented. K_o triaxial compression tests on loose and dense specimens of pumice sand at various displacement rates were conducted to obtain further insight into the properties of this material. After compression, the maximum displacement was held constant for some time and relaxation of axial and lateral stresses were monitored with time. During testing, measurement of air permeability was conducted to monitor the temporal change in void ratio and the amount of particle crushing. Results indicated substantial decrease in air permeability. Moreover, stress relaxation increased with increasing displacement rate and the values for loose sample were generally larger than that for dense sample.

1 INTRODUCTION

Pumice deposits are found in several areas of the North Island of New Zealand. They originated from a series of volcanic eruptions centred in the Taupo and Rotorua regions of the central North Island. The pumice material has been distributed initially by the explosive power of the eruptions and associated airborne transport; this has been followed by erosion and river transport. Presently pumice deposits exist mainly as deep sand layers in river valleys and flood plains, but are also found as coarse gravel deposits in hilly areas. Although they do not cover wide areas, their concentration in river valleys and flood plains means they tend to coincide with areas of considerable human activity and development. Thus, they are frequently encountered in engineering projects and their evaluation is a matter of considerable geotechnical interest.

Pumice sand is known as a crushable material and the grains of pumice sand may be readily crushed against a hard surface by fingernail pressure because the particles have internal voids. Wesley (2001) investigated the specific gravity of pumice sand of various particle sizes by two methods, i.e., NZ standard method with and without vacuum air extraction. He observed that the specific gravity of pumice sand decreased with increasing particle size, indicating that the proportion of internal voids into which water penetrates increased with increasing particle size. In addition, he noted that because the specific gravity of the soil particles measured by both methods was not the same as that of quartz (about 2.65) even when the particle size was 0.04mm, some internal voids may not be interconnected to the outside surface. Therefore, it is necessary to distinguish between internal voids of particles and voids consisting of spaces between particles. Then, when a particle is crushed, the voids would increase because the internal voids would be exposed outside and manifest themselves as voids between particles.

Moreover, it is known that pumice sand is characterised by soft vesicular grains of low crushing strength, giving the material high void ratios and high compressibility. Previous research showed that the q_c values obtained from cone penetration tests (CPT) on pumice sand were only marginally influenced by the density of the material, as shown in Figure 1. It is also noted that pumice sand shows very gentle increase with confining stress as compared to normal (i.e. hard grained) sands (Wesley et al. 1999). Thus, conventional relationships between q_c value, relative density, and confining stress are not valid for these soils. Therefore, alternative relationships specifically for pumice sands need to be developed.

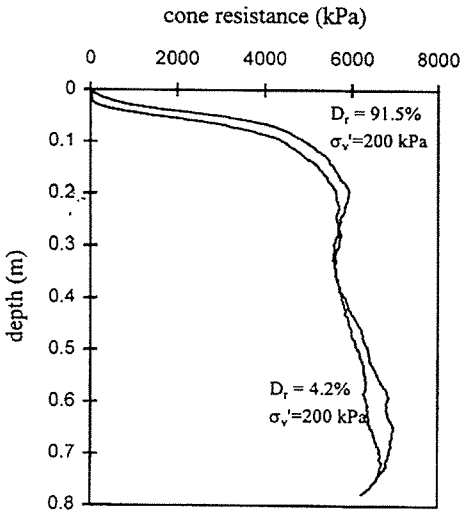

Figure 1: CPT resistance obtained from calibration chamber testing of loose and dense pumice sand (Wesley et al., 1999).

In this study, compression and stress relaxation testing were performed on loose and dense pumice sand using a simple K_o triaxial cell. In order to investigate the effect of density and particle crushing on compression and stress relaxation, the air permeability of the pumice sand was measured during testing. The effect of various constant displacement rates (0.5mm/min ~ 25mm/sec) on the response was also examined. This study was undertaken to supplement the test results obtained by Pender (2006).

2 SAND USED AND TEST PROGRAM

2.1 Sand used

Figure 2 shows the particle size distributions (PSD) of pumice sands used in this study, representing those before and after testing. Only sands passing through 1.18 mm sieve were used, with only 5.8% of the sand finer (by weight) than 63μm. Table 1 shows the maximum and minimum dry densities obtained using NZ standard method, but without surcharge in maximum dry density testing.

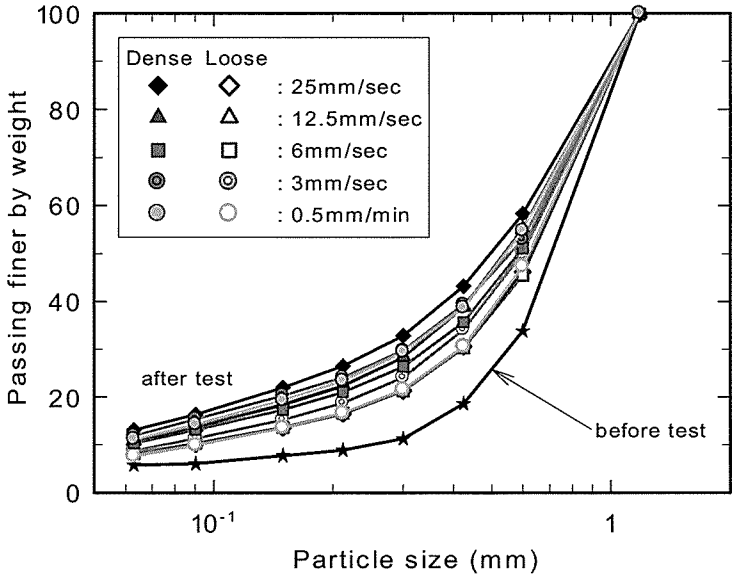

Figure 2: Particle size distributions (PSD) of pumice sand before and after testing

Table 1: Maximum and minimum dry densities of pumice sand

Maximum dry density kg/m^3	Minimum dry density kg/m^3	Maximum dry unit weight kN/m^3	Minimum dry unit weight kN/m^3
709	576	6.95	5.65

2.2 Test program

Figure 3 shows the schematic diagram of the K_0 triaxial cell used in this study. The concept of this test apparatus is based on that developed by Davis & Poulos (1964). The inside of the triaxial cell was filled with water and the diameter of loading ram and specimen were the same; therefore, the radial deformation was restricted because the cell water is incompressible.

The dimension of the specimen was 75mm in diameter and 150 mm high. The density of the specimen was varied by employing two specimen preparation methods. For both methods, the sand sample was split into 8 sub-specimens and each sub-specimen was pluviated into the mould lined with a rubber membrane. For loose specimens, the air pluviation method was used and each sub-specimen was pluviated from a height of 0 mm above the top end of the specimen using a funnel. For dense specimens, each sub-specimen was pluviated from a height of 100mm, and then densified by tapping the base of the triaxial cell with a rubber hummer. At the each end of specimen, two pieces of thin filter clothes and a porous metal were used in order to measure the air permeability. In addition, the specimen was dry during testing.

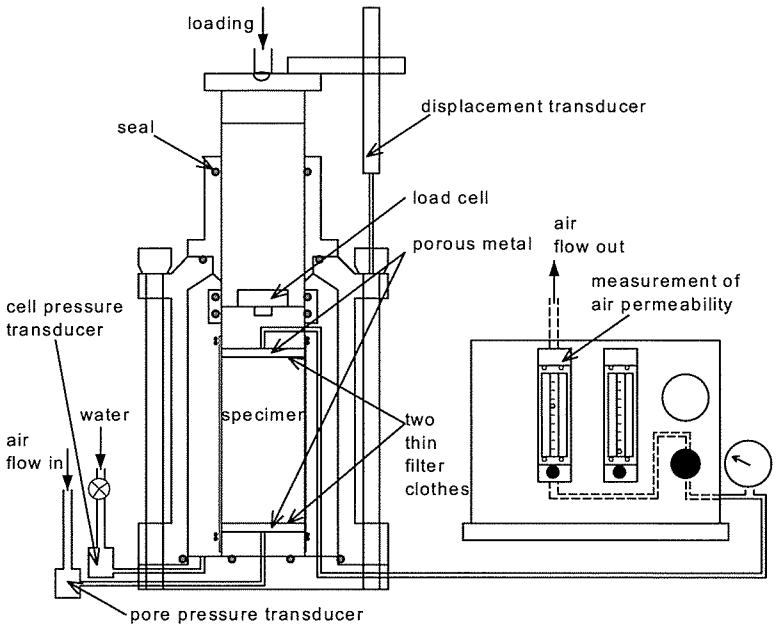

Figure 3: K_0 triaxial cell equipped with air permeability measuring device.

Next, the interior triaxial cell was filled with water and an initial cell pressure of 50 kPa was applied. The valve of the cell pressure was closed and air was allowed to flow into the specimen from the bottom under a constant air pressure of 10 kPa. The flow rate of the air from the top of specimen during testing was measured with a rotameter. The specimen was compressed at various displacement rates (0.5mm/min, 3mm/sec, 6mm/sec, 12.5mm/sec and 25mm/sec) until an axial deformation of 50mm was reached, which is equivalent to 33% axial strain. Immediately after, the 50mm axial deformation was kept constant and the decrease in axial stress and confining pressure was monitored with time. After the specified time, the specimen was unloaded and at the end of the test, the PSD of specimen was measured.

3 TEST RESULTS AND DISCUSSION

Firstly, the effect of displacement rate on axial stress is examined. The relation between axial strain and the logarithm of the axial stress is shown in Figure 4. The axial stress under similar axial strain seems to increase with increasing displacement rate during loading. However, it is noted that the maximum axial stress also increased with increasing initial relative density. Closer inspection of the results indicates that the maximum axial stress seemed to be affected more by the initial relative density rather than by the displacement rate.

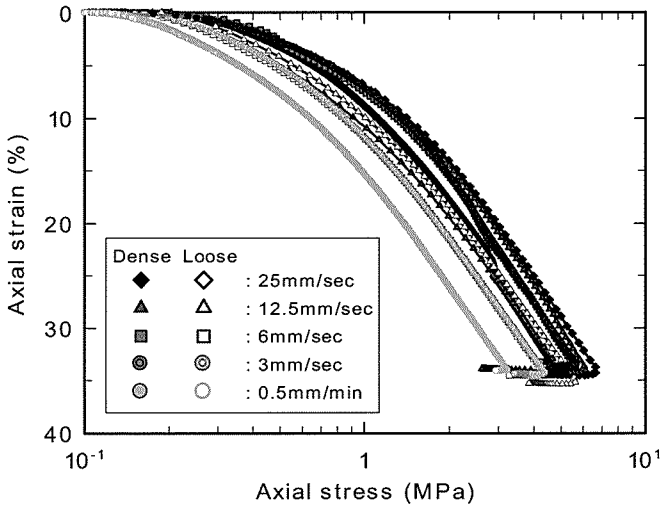

Figure 4: Relationship between axial strain and logarithmic axial stress.

Figure 5 shows the time history of axial stress normalised with respect to the maximum axial stress. There was not much difference between the curves during loading for dense and loose samples, but the curves during stress relaxation for loose samples shows higher drop in values than those for dense samples. These differences between the stress relaxation for loose and dense sample increased with increasing displacement rate. Such a trend is believed to be due to the excess axial stress which occurred during loading as a result of high displacement rate. Once the loading was stopped (stress relaxation), stress re-distribution followed and the excess stress tried to return to normal state, with higher excess stress resulting in larger stress relaxation.

Secondly, the change in air permeability is investigated. Figure 6 shows the void ratio plotted against the change in air permeability and axial stress for displacement rate of 0.5mm/min. The air permeability, k_a (expressed in units of milli Darcy (mD)), was calculated using Darcy's equation, which was modified for compressible fluids (Harpalani et al. 2006), and given as:

$$k_a = \frac{\mu L P_{out} Q}{1000 A (P_{in} - P_{out}) P_{mean}} \cdot \frac{1016}{9.87} \qquad (1)$$

where, μ: viscosity of air (Ns/m^2); L: length of specimen (m); A: area of specimen (m^2); Q: flow rate (m^3/s); P_{out}: $P_{atmosphere}$ (kPa); P_{in}: P_{gauge} + $P_{atmosphere}$ (kPa); and P_{mean}: (P_{out} - P_{in})/2 (kPa). It is interesting to observe that the void ratio vs axial strain relation showed a very similar trend to the void ratio vs change in air permeability relation.

Thirdly, particle crushing of pumice sand is studied. Based on the work of Hardin (1985), the total breakage, B_t, was calculated as the area enclosed by PSD curves before and after testing and the vertical line corresponding to 0.063mm (the line defined by Hardin was 0.074mm). The

effect of maximum axial stress on the value of B_t is examined. As shown in Figure 7, B_t increases with increase in the maximum axial stress.

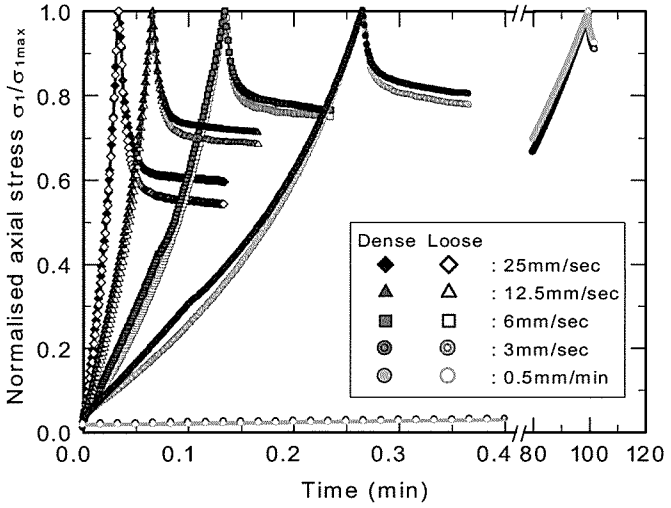

Figure 5: Relationship between normalised axial stress and time

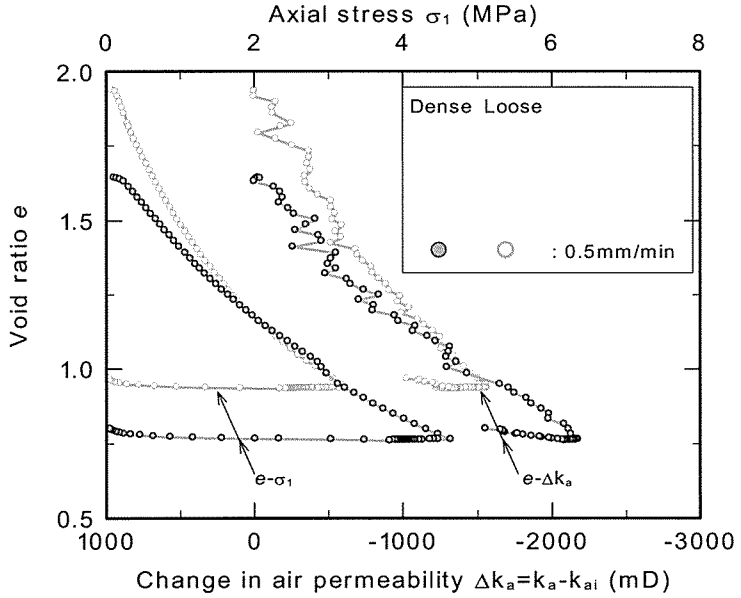

Figure 6: Void ratio plotted against change in air permeability and axial stress for displacement rate of 0.5mm/min (void ratio was calculated based on estimated G_s of 1.77).

Up to this point, attempts were made to explain why the stress relaxation was influenced by the displacement rate and the density of sample using maximum axial stress, void ratio and particle crushing. From the observations made, it was suggested that a high displacement rate could induce excess axial stress such that the K_o value would be less than the normal K_o value during loading. Such condition could induce larger stress relaxation when deformation is stopped. In addition, it was assumed that for loose sample, the available void space was larger than that for dense sample; thus, the stress relaxation for loose sample was observed to be larger than that for dense sample. The evidence of excess axial stress can be observed in terms of the total breakage shown in Figure 7, which indicates that if the displacement rate is faster, the maximum axial stress is larger, resulting in larger total breakage. Note that loose samples show lower maximum axial stress because they have more available void spaces in their structures.

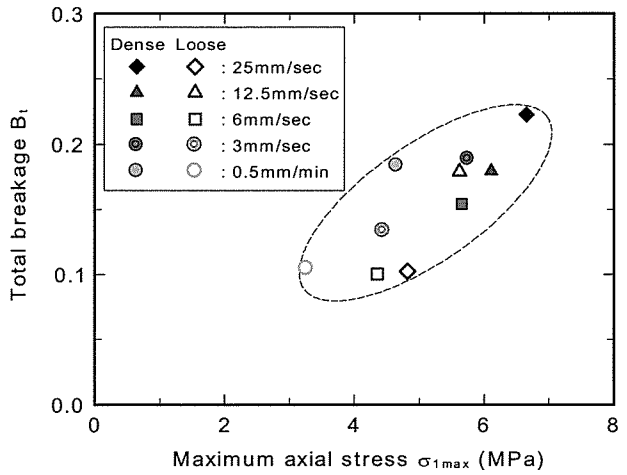

Figure 7: Relationship between total breakage and maximum axial stress

4 CONCLUSIONS

In this study, compression and stress relaxation testing were performed on loose and dense pumice sand using a simple K_o triaxial cell. The effects of density, displacement rate and particle crushing on compression and stress relaxation were investigated. From the test results, it was observed that stress relaxation increased with increasing displacement rate and the differences between the stress relaxation in loose and dense pumice sands increased with increasing displacement rate. This means that it might be possible to evaluate the density of pumice sand through the magnitude of stress relaxation during CPT sounding, e.g., since CPT testing is usually carried out at a displacement rate of 20mm/sec, CPT penetration can be stopped for a while and the decrease in q_c value recorded for several minutes to evaluate the magnitude of stress relaxation.

ACKNOWLEDGMENTS

I am very grateful to the New Zealand Earthquake Commission, Prof. Michael J Pender, Dr. Rolando P Orense and Dr. John D St. George for support and advice on this study.

REFERENCES

Davis, E. H. & Poulos, H. G. (1964) Triaxial testing and three-dimensional settlement analysis, *Proceedings Fourth Australian-New Zealand Conference on Geomechanics*, pp. 233-243.

Hardin, B. O. (1985) Crushing of soil particles, *Journal of Geotechnical Engineering*, Vol. 111, No. 10, pp. 1177-1192.

Harpalani, S., Singh, K. & Zutshi, A. (2006) CO_2/N_2 Flow Behavior of Deep Coal-Gas Reservoirs, *The 41st U.S. Symposium on Rock Mechanics (USRMS): "50 Years of Rock Mechanics - Landmarks and Future Challenges,"* Golden, Colorado, U.S.A., June 17-21

Pender, M. J. (2006) Stress relaxation and particle crushing effects during K_o compression of pumice sand, *International Symposium on Geomechanics and Geotechnics of Particulate Media*, Vol.1, pp. 91-96.

Wesley, L. D., Meyer, V. M., Pronjoto, S., Pender, M. J., Larkin, T. J. & Duske, G. C. (1999). Engineering properties of pumice sand. *Proc. 8th Australia-NZ Conference on Geomechanics*, Hobart, Vol. 2, pp. 901-908.

Wesley, L. D. (2001) Determination of specific gravity and void ratio of pumice materials, *Geotechnical Testing Journal*, **24** (4), pp. 418-422.

The Synthetic Rock Mass approach: from field data to rock mass constitutive behaviour

Cedric Lambert
CSIRO Exploration & Mining, Brisbane, Australia.

John Read
CSIRO Exploration & Mining, Brisbane, Australia.

Keywords: rock mass, strength characterisation, discrete element modelling

ABSTRACT

In the process of rock slope stability analysis, having a best estimate of the rock mass strength is of major importance. In the current state of practice, the rock mass strength is derived from various rock mass classification schemes (GSI, RMR, RQD...) that contain a series of well identified flaws and uncertainties. By combining the benefits of the particle flow code PFC3D to represent the rock and the benefits of a geostatistical tool to generate a full 3D discrete fracture network (DFN) of the domain, it is possible to create a Synthetic Rock Mass (SRM) representative of a geotechnical domain. The SRM is then submitted to a series of numerical tests (triaxial tests, UCS tests) using PFC3D to assess the constitutive behaviour of the rock mass, including the anisotropy and the scale effect. The strength envelopes derived from those tests can then be used in the different classical slope analysis tools. Using real and typical field data, this paper goes through the entire process of the rock mass strength characterisation, from the DFN generation to the SRM testing, giving an intelligible illustration of the methodology.

1 INTRODUCTION

One of the most challenging part of a design is to correctly assess the constitutive behaviour of our rock mass. A rock mass is made of two main ingredients: intact rock (or commonly named rock matrix) and discontinuities (joints, faults...). If it is possible to characterise each of these ingredients independently, many aspects of their combined effect in the deformation and failure of a rock mass remain indeterminate. The Synthetic Rock Mass approach, pioneered by Itasca (Pierce et al. 2007) , represents a jointed rock mass as an assembly of bonded particles where a joint network is introduced as a series of fractures (Figure 1). The SRM thus combines intact rock mechanisms (deformation and brittle fracture) with structural mechanisms (including slip and opening). Many different loading paths can be applied to the SRM sample to predict the mechanical behaviour of the rock mass. The methodology has proven its ability to reproduce a wide range of typical behaviour of a rock mass using exclusively measurable data.

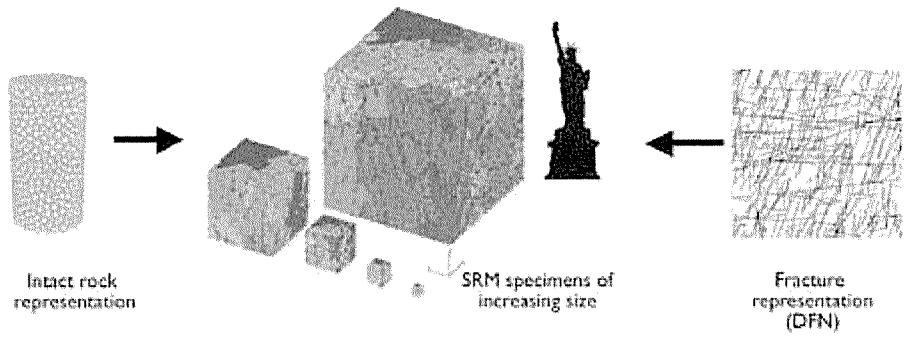

Figure 1: Concept of SRM sample generation (Pierce et al., 2007), intact rock represented as a bonded particle assembly and fracture representation introduced as a DFN

2 SYNTHETIC ROCK MASS CREATION

The SRM approach is a three step procedure. First a particle assembly is created in PFC3D to represent the intact rock of the considered rock mass. Then a discrete fracture network representative of the structural pattern of the rock mass is generated and imported into the particle assembly to create a large Synthetic Rock Mass sample. Finally, the sample is submitted to a variety of different loadings to assess the constitutive behaviour of the rock mass.

2.1 Intact rock representation

The Bonded Particle Model (BPM) as described by Potyondy & Cundall (2004) represents intact rock as a discrete assembly of spherical particles. The macroscale behaviour of such an assembly results from the interactions of microscale components. Unlike continuum models for which input properties such as deformation modulus and strength can directly be measured during laboratory experiments, the input microproperties remain unknown. The microproperties are adjusted following an iterative calibration process until the observed response of the numerical material matches the behaviour of the physical material. Three rock types have been modelled in this study (mafic intrusive, mafic volcanic and basalt), each of them exhibiting different macroproperties. The calibration process needs to be performed for each of them. A comparison between the obtained macroproperties of the synthetic samples and the target properties of the physical rock types (measured experimentally) can be seen in Table 1.

Table 1: Measured and simulated intact rock properties

	Mafic Intrusive		Mafic Volcanic		Basalt	
	Lab	PFC3D	Lab	PFC3D	Lab	PFC3D
UCS [MPa]	113.7	107.9	74.3	70	170	166.3
Young's modulus E [GPa]	96.6	98.0	28.8	29.5	30	30

2.2 Jointing system representation

The second step of the SRM construction process is the introduction of the fracture pattern. Using the Discrete Fracture Network modelling technique it is possible to represent the different structures of a rock slope from in situ measured data. The fracture network can then be imported into the SRM for an explicit representation of the joints of the rock mass.

For this study, a DFN of the domain has been developed using JK JointStats, a discontinuity data management system developed at the University of Queensland by the Julius Kruttschnitt Mineral Research Centre (JKMRC). The original software accepts standard structural data from a face mapping, borehole scanline or digital photogrammetry structure mapping software and organises the data hierarchically according to its orientation, length, spacing and persistence (trace length) attributes. Statistical analyses of those attributes are performed using maximum likelihood methods (Lyman, 2003). Estimates of joint set orientation, persistence and spatial density are provided, including confidence interval calculations. The DFN realisations that are generated are statistically representative of the domain, providing that the volume of study is large enough. Each joint set of the output DFN is in complete statistical agreement with the statistical description of the input data.

Examples of two-dimensional sections of the DFN realisation are shown in Figure 2. The example of DFN realisation contains 35,011 joints within the 100m x 100m x 100m volume. Sub-DFNs of different sizes can now be extracted and imported within PFC3D to create SRM samples of different shapes and/or sizes. The joints are represented using the Smooth Joint

Model proposed by Pierce et al. (2007). This new contact scheme allows the elimination of the roughness or bumpiness induced by the particles when simulating a joint by simply debonding the contact along a plane. Instead, a sliding plane is introduced through a dip and dip direction for each contact between particles that lie upon opposite sides of the specified plane.

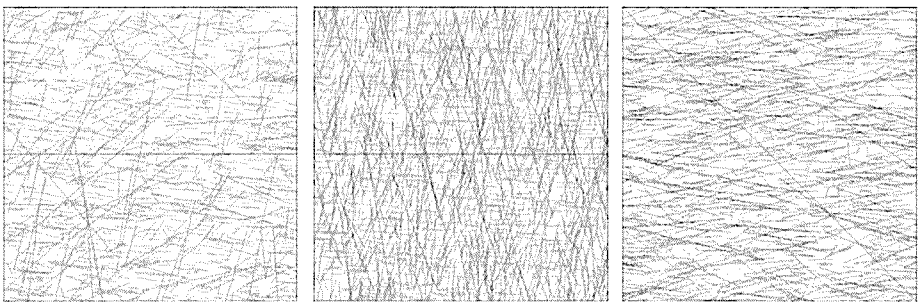

Figure 2: 100m x 100m 2D sections of the generated DFN

2.3 SRM testing

At this stage three 24m SRM cubes have been created, one for each of the rock type listed in Table 1 of the domain (mafic volcanic rock mass, mafic intrusive rock mass and basalt rock mass). The SRM samples are representative of the jointed rock mass as they combine the effect of discontinuities and of intact rock bridges. "Virtual" large scale laboratory tests can be numerically performed on the SRM samples for a characterisation of the mechanical behaviour of the jointed rock mass. Figure 3 shows the stress-strain curves of UCS tests performed on the three rock mass samples.

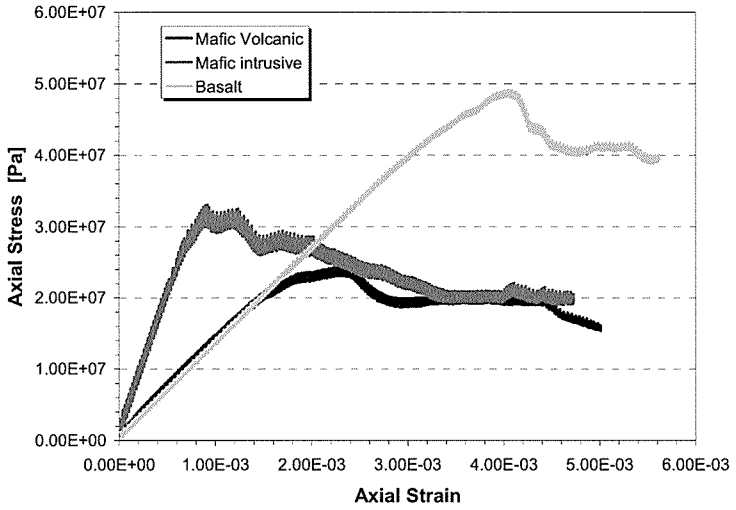

Figure 3: Stress-strain response of UCS tests tested numerically on three different rock mass (mafic intrusive, mafic volcanic and basalt)

3 ROCK MASS CONSTITUTIVE BEHAVIOUR

With the inherent versatility and flexibility of numerical modelling, the SRM samples offer the ability to characterise a wide range of constitutive behaviours of a rock mass, including attributes that cannot be obtained using empirical methods. Features such as scale dependency, anisotropy or uncertainty can now be characterised (Mas Ivars etal., 2008; Lambert, 2008) and will be briefly presented in this study. Pierce et al. (2007) have also applied the methodology to estimate the brittleness of the rock mass and to assess its fragmentation in a block caving environment. Lambert (2008) proposed an approach to characterise a rock mass containing various lithologies.

In order to study the scale dependency of rock mass strength, rock mass samples of different sizes can be constructed and tested. The samples of mafic volcanic rock mass samples and the results of UCS tests are presented on Figure 4. A clear reduction of the strength can be seen when increasing the sample size. The strength curve exhibits a possible asymptotic value for the rock mass strength as the rock volume increases that cannot be assessed by existing empirical techniques.

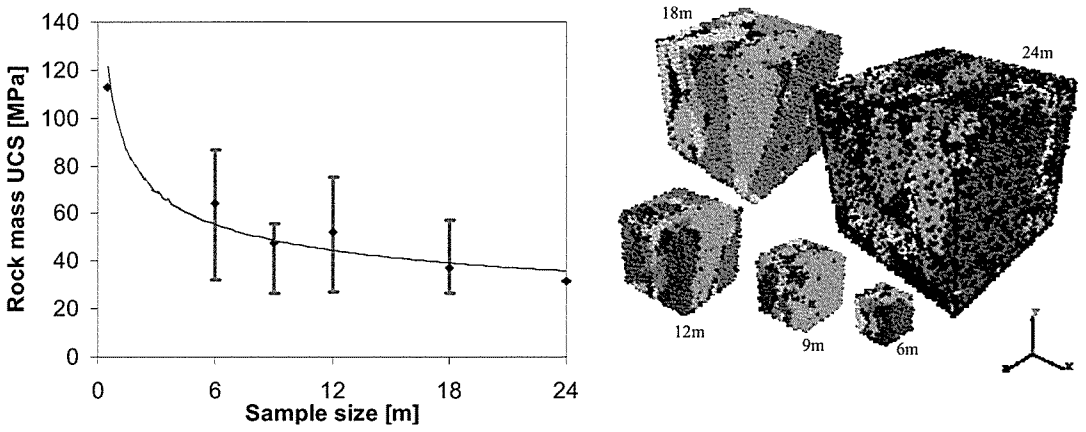

Figure 4: Mafic intrusive rock mass UCS as a function of sample size.

The strength of a rock mass is characterised by a non linear failure criteria. The strength envelope is obtained performing triaxial compression tests at different confining pressures. The strength envelope of the 24m rock mass can be built by performing numerical compression tests at different confining pressures (0 – 2MPa – 10MPa). The strength envelope can then be used to obtain the equivalent Mohr-Coulomb strength parameters (cohesion and friction angle) that can then be used in the conventional method of analyses. Of major interest is the possibility to predict the strength anisotropy of the rock mass, simply by changing the direction of loading. The 24m rock mass has been tested in three orthogonal directions (e.g. North-South, East-West and vertical) at different confining pressures. Figure 5 presents the strength envelopes of the mafic intrusive rock mass for those directions. Strong strength anisotropy is clearly seen, as a direct consequence of the joint set orientations. The equivalent Mohr-Coulomb parameters can thus be estimated according to the direction the most relevant for the design.

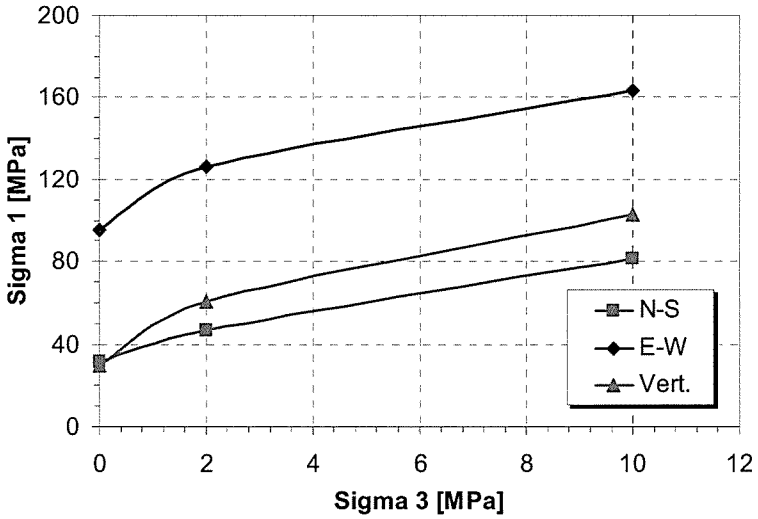

Figure 5: Strength envelopes of the 24m mafic intrusive rock mass in three directions

4 DATA UNCERTAINTY AND VARIABILITY

Dealing with scattered data is inevitable in large pit slope stability analysis mainly because variability is intrinsic to any rock mass (whether looking at intact rock strength or discontinuity attributes). Scattered values for intact rock strength or discontinuity attributes (e.g. orientation, trace length or spacing) result in uncertainties in the model parameters. These uncertainties can lead to an unreliable prediction of slope performance and thus need to be properly assessed through confidence interval estimates.

Whereas uncertainty of intact rock strength or discontinuity properties can be analysed performing statistical analysis on the database, the resulting uncertainty on rock mass strength remains unknown. To overcome the difficulty, a series of SRM samples have been created and numerically tested varying the intact rock strength. A linear variation of rock mass strength UCS_{rm} with intact rock strength UCS_i is obtained ($UCS_{rm} = 0.29 \times UCS_i$, Figure 6). In this case, the probability distribution of the rock mass UCS can easily be derived from the statistical description of intact rock UCS (assuming a normal probability distribution). The mean value μ_{rm} and standard deviation σ_{rm} of the rock mass strength is directly derived from the mean value μ_i and standard deviation σ_i of the intact rock UCS in the following way:

$$\mu_{rm} = 0.29 \times \mu_i \quad \& \quad \sigma_{rm} = 0.29 \times \sigma_i \tag{1}$$

The coefficient 0.29 of the linear regression is related to the DFN generated. Similar tests carried out on a similar rock mass but with a different DFN will result in a different value. The mean strength of the mafic intrusive intact rock has been evaluated from lab tests to 113 MPa. By assuming a standard deviation σ_i of 30 and using the equation of the trendline in Figure 6, the mafic intrusive rock mass strength is estimated to 32.5MPa ± 8.6. The variability of the rock mass strength can be derived from the previous equation and is presented on Figure 6.

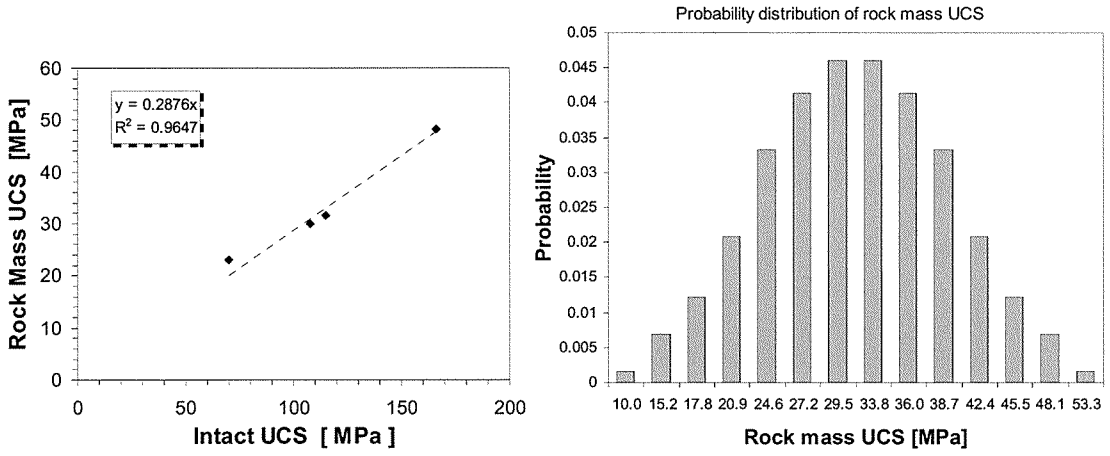

Figure 6: Rock mass UCS as a function of intact rock UCS (left) and probability distribution of rock mass UCS as a result of variability of intact rock UCS (right)

In the conventional methods of analysis, the variability of the rock mass strength is seldom introduced and the mean value is usually used for the design. Because of the variability of the UCS and of the limited number of tests that are usually performed for its estimate, a degree of uncertainty is associated with the mean value of UCS that can affect the reliability of the design. The Student's t-test offers a convenient way to assess this uncertainty.

$$\mu = \mu_{rm} \pm t \cdot \sigma_{rm} / \sqrt{N-1} \tag{2}$$

Where μ is the real mean strength of the rock mass, μ_{rm} and σ_{rm} the estimated mean strength and standard deviation of the statistical sample, N the number of values in the statistical sample and t a constant value depending on the required level of confidence. For example, estimating the intact mafic intrusive strength from three laboratory tests would lead to a 80% confidence interval on its rock mass strength of 32.5MPa ± 11.5, whereas an estimation from ten lab tests would reduce the 80% confidence level to 32.5MPa ± 4. Similar analyses can be performed to study the uncertainties coming from joint friction angle or joint size (Lambert, 2008)

5 CONCLUSIONS

The development of the Synthetic Rock Mass methodology has been a step forward in the rock mass characterisation process. It is now possible to generate a numerical equivalent rock mass of various shapes and sizes using only measurable field and/or lab data. The samples have proven their ability to capture typical behaviours of a rock mass such as anisotropy or scale dependency. The increasing number of applications of the SRM approach has lead to a significant improvement in the understanding of fundamental strength and deformation behaviours of a jointed rock mass.

The SRM can be used to quantify the variability and uncertainty on the rock mass strength resulting from data uncertainty, thus offering a new scope of application. The obtained confidence levels can be compared to the level of confidence required by the project and be implemented in a risk assessment tool.

ACKNOWLEDGEMENTS

The work presented in this paper was funded by the Sponsors of the Large Open Pit project and their support is acknowledged: the Sponsors are Anglo American plc, Barrick Gold Corporation, BHP Billiton Innovation Pty Limited, Corporacion Naciónal Del Cobre De Chile , Compania Minera Dona Inès de Collahuasi SCM, DeBeers Group Services (Pty) Limited, Newcrest Mining Limited, Newmont Australia Limited, Xstrata Queensland Limited, Debswana Diamond Company, the RioTinto Group, and Vale (formerly CVRD). The authors are grateful to BHPBilliton for providing data from the Nickel West project for this study, and to the Itasca Consulting Group for their technical and numerical contribution.

REFERENCES

Lambert, C. (2008) Variability and uncertainty on rock mass strength via a synthetic rock mass approach, *1st Southern Hemisphere International Rock Mechanics Symposium*, Perth, Australia

Lyman, G.J. (2003) Rock fracture mean trace length estimation and confidence interval calculation using maximum likelihood methods. *Int. J. Rock Mech. & Min. Sci. 40(6), pp. 825-832.*

Mas Ivars, D., Pierce, M., DeGagnné, D. & Darcel, C. (2008) Anisotropy and scale dependency in jointed rock-mass strength – A Synthetic Rock Mass Study. *Proceedings First International FLAC/DEM Symposium on Numerical Modeling*, Minneapolis, United States.

Pierce, M., Cundall, P., Potyondy, D. & Mas Ivars, D. (2007) A Synthetic Rock Mass Model for Jointed Rock. *In Rock Mechanics: Meeting Society's Challenges and Demands, 1st Canada-U.S. Rock Mechanics Symposium*, Vancouver, pp. 341-349.

Potyondy, D. O. & Cundall, P.A. (2004) A Bonded-Particle Model for Rock. *Int. J. Rock Mech. & Min. Sci. 41(8)*, pp. 1329-1364.

Landslide remedial works at 46 Taupo Bay Road

Idy C.W. Li
Tonkin & Taylor Engineering Consultants, Auckland, NZ

Keywords: Slope instability, retention design, stormwater management

ABSTRACT

This paper presents a case study involving the remediation of a residential property in the upper North Island of New Zealand located at 46 Taupo Bay Road, which was damaged by a landslide in July 2007. The dwelling was shunted from its foundations by debris, causing it to translate and rotate above a neighbouring dwelling. The cause of instability was attributed to reduced effective stresses in the slope soils due to rainfall. Proposed remedial works comprised two main components, (1) gravity retention at the toe of the landslide, and (2) a stormwater management system to divert surface runoff away from the affected area.

1 BACKGROUND

The eastern coast of Northland endured two severe rainstorm events on 29 March and 10 July 2007, both of which registered 100 to 150 year rainfall intensity exceedance probabilities (NIWA, GNS Science, 2007). The extreme weather resulted in widespread flooding and landslides, and caused damage to property, access roads and infrastructure in many parts of the upper North Island (NIWA, GNS Science, 2007) (Figure 1).

This paper looks at a case study of a residential property that was severely damaged due to a landslide, 46 Taupo Bay Road (Figure 1), and the remedial works designs proposed to reinstate the site and minimise the risk of similar slope failure. The project was funded by the Earthquake Commission (EQC), with the homeowner as the principal, and Tonkin & Taylor as the Engineer to the Contract.

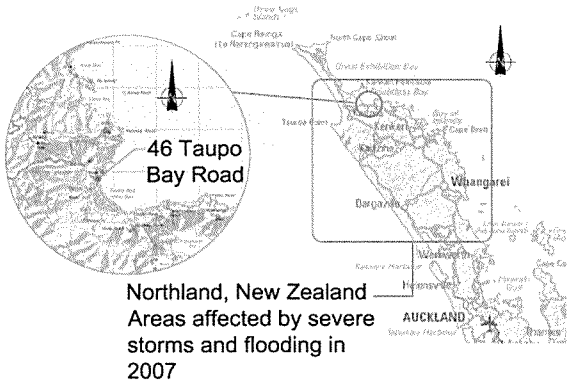

Figure 1: Map of Upper North Island, New Zealand

2 EXISTING SITE DESCRIPTION

46 Taupo Bay Road is located in the coastal embayment of Taupo Bay in the upper North Island. The property covers an approximate area of 0.116ha, comprising a predominantly flat lying topography. The western most extent of the property forms the base of a steep, densely vegetated, eastward dipping slope. The property fronts directly onto Taupo Bay and is set back approximately 10m west from the beach. The property contains a single storey, timber bach-

style dwelling founded on timber piles. The structure is located at the rear (western) extent of the property at the base of the steep slope.

3 LANDSLIDE DETAILS

3.1 Property Damage Details

Following the second extreme rainfall event in July 2007, a landslide from the steep slopes at the rear (west) of the property resulted in the evacuation of up to 1800m^3 of slip debris (Figures 2 and 3). Combined with the persistent rainfall, the evacuated materials formed a viscous debris flow that inundated the majority of the property under a layer of debris up to 2m deep, and 50m long. A Pohutukawa tree up to 15m tall was transported approximately 65m from the embankment and deposited in the centre of the property grounds.

The collision of the debris flow with the dwelling caused it to dislodge from its foundations and rotate approximately 50 degrees eastward. The structure remained generally intact only undergoing translational movement. The raised timber deck on the eastern perimeter of the dwelling had warped, and the force of the impact had distorted the building such that it was overhanging the neighbouring dwelling. The property was deemed unsafe to reside in by the Far North District Council (FNDC, 2007).

Immediate action was undertaken to remove the dwelling and loose debris from site due to the possibility of ongoing instability and risk to neighbouring properties.

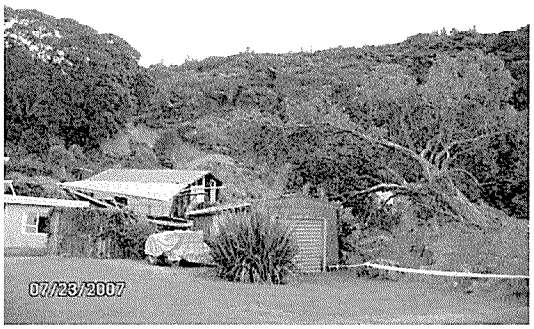

Figure 2: Site following landslide

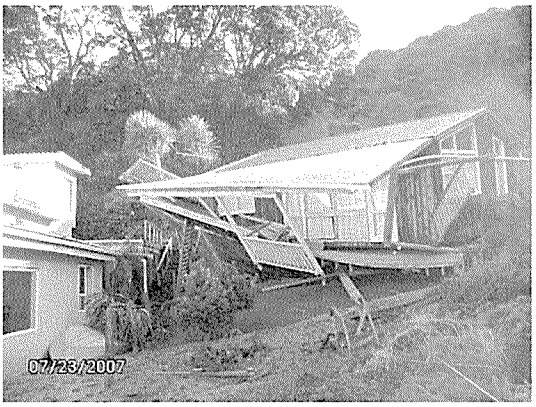

Figure 3: Damaged dwelling

3.2 Landslide Geometry

The landslide headscarp was approximately 3m in height and originated within a neighbouring property near the crest of the failed slope (Figure 4). The length of the landslide extended up to 60m to the base of the slope. The side scarps generally comprised stiff to very stiff, fine grained soils, with pockets of very weak rock exposed along the basal failure surface and up the side scarps. The geometry of the landslide formed a kidney shape contorted around a large rock exposure along the southern side scarp.

Figure 4: Looking west at headscarp of landslide

4 GEOTECHNICAL INVESTIGATION

Machine drilled auger holes were put down to determine the subsoil geology. A shallow weathering profile of Greywacke (Siltstone) rock origin was found, with stiff to very stiff residuals soils (clayey silts) recorded in the surficial layers. Within the basal surface and side scarps of the landslide, exposures of very weak and weathered Greywacke (Siltstone) rock were observed. Investigations carried out within the dwelling platform encountered a "fan" of very stiff, fine grained historic slip debris and colluvium deposits up to 4m depth.

5 LANDSLIDE MODE OF FAILURE

5.1 Pre-existing Conditions

The pre-existing geological conditions at the site provided evidence of landslide prone features, such as the persistence of hummocky slopes and small localised landslides observed on the surrounding bluffs, both indicative of historic instability. This was reinforced by the discovery of the "fan" of historic slip debris used for the dwelling platform. The topography of the failed area forms the centre of a shallow gully feature thereby attracting increased stormwater runoff, and increasing its susceptibility to slope failure.

5.2 Present Conditions

Although the pre-existing geological and topographical conditions provided increased susceptibility to slope instability, it is of interest to consider the additional factors specific to the subject failure and consequent failure mode.

The primary contributing factor to the subject landslide can be attributed to the extreme rainfall events, and consequent reduction of effective strength in the soil mass due to stormwater infiltration and increased pore pressures. The exposure of the weathered rock contact on the basal rupture surface indicates the landslide to have occurred on the soil-to-rock interface, and therefore can be described as a shallow seated failure occurring within surficial soils only. This failure mechanism is typical of rainfall-induced landslides due to the vulnerability of surface soils to pore pressure fluctuations caused by rainfall.

It is of interest to note that the rainfall intensities recorded in the first rainstorm event of March 2007 were higher than those for July 2007 (NIWA, GNS Science, 2007). If the failure was

attributed solely to stormwater infiltration (and consequent pore pressure increase), theoretical back analysis would conclude that the landslide should have taken place shortly after 29 March 2007. The author's hypothesis is that there were other contributing factors to the landslide, and both rainstorm events contributed to the failure. This is a complex subject that is subject to extensive international research (e.g. Rahardjo et al. 2007).
The significance of the rainfall event in March was that it occurred at the end of a dry Summer season; at a time when shrinkage cracking in the clay rich residual soils at this site would have been at their peak. The accumulation of stormwater in the shrinkage cracks would have generated destabilizing hydrostatic forces on the soil mass, forcing the slope towards failure. The increase in pore pressure due to stormwater infiltration in both rainstorm events would have further decreased the soils' resisting forces, to the point of catastrophic failure in July.

6 PERMANENT REMEDIAL WORKS DESIGN

Primary remediation objectives included the restoration of the site to re-establish the dwelling, and reduce the risk of similar slope instability in the future. Due to the landslide affecting multiple properties, it was necessary for remedial works designs to take place across property boundaries in order to be effective. Consent was required from the owners of the affected properties to ensure the success of the designs and recommendations. See Figure 5 for an illustration of the proposed designs.

6.1 Geotechnical/Structural Design

6.1.1 Retention structure

A concrete crib wall retaining wall was proposed near the base of the slope. The design was assessed for sliding, bearing and overturning failure for factors of safety under Ultimate Limit State conditions of 2.0, 3.0 and 2.0 respectively. Understanding the landslide failure mode was critical for retention design. A gravity wall was adopted as the retention solution as an embedded wall (normally suited for deep seated instability) was impractical due to the shallow rock level.

Due to the proximity of the retaining wall to the sea, micro silica additives were specified to improve the corrosion resistance to sea spray and ensure the longevity of the concrete.

6.1.2 Retention Geometry and Location

The location of the crib wall was proposed for the toe of the slope, immediately behind the location of the original dwelling. The location of the wall owed in part to building limitations placed on the eastern half of the property which had been identified by the District Council with Coastal Hazard Zones as an area prone to erosional and flooding hazards consistent with 100 year return periods (FNDC, 2007; Howse, 2007). Hence the area for redevelopment was confined to the western half of the property. The gravity wall was located as far west (up the slope) as possible to provide sufficient area for a dwelling platform to be located inland of the Coastal Hazard Zones.

6.1.3 Backfill

GAP 65 or similar free draining hardfill was specified as the backfill material behind the crib wall, filling almost the entire crevice left by the landslide. Introducing granular fill into the slope was intended to reduce the susceptibility of rainfall-induced failure, as pore pressures would be prevented from accumulating due to rapid dissipation. Installation of underfill drains beneath the hardfill would allow for the effective transportation of water to the base of the

slope. The use of concrete cribs with open, unrestrained facings also prevents the buildup of pore pressures.

Backfilling the crevice left by the landslide provided an additional function of retaining the unrestrained head scarps and side scarps with a form of buttressing.

6.2 Stormwater Design

Due to the inherent instability of the slopes, the control of stormwater runoff and rainfall infiltration was considered of primary importance. A stormwater collection and discharge system was proposed to divert water away from the affected slopes comprising the following components:

(1) Overlaying a 200mm thick, low permeability clay cap over the free draining backfill behind the wall. The clay cap was designed to perform dual functions,
   a. prevent infiltration of surface water into the slope
   b. form a contoured swale graded towards the centre of the slip crevice and into a sump/manhole behind the wall. A raised earth bund proposed downslope of the sump/manhole was intended to prevent overtopping of water

(2) A stormwater sump/manhole installed behind the crib wall was designed to collect surface runoff and pipe the discharge towards the beach. Discharging of stormwater onto the open, flat lying terrain on the site was not feasible as it was considered a flood risk to the properties and could potentially erode the slope, effectively undermining its stability. Sizing of the manholes and pipe systems took into consideration a catchment area accounting for the upslope neighbour's plans to subdivide the property and subsequent generation of impermeable ground. The system was conservatively designed for rainfall intensities consistent with 300 year return periods.

(3) Construction of a surface channel adjacent to the stormwater piping system, measuring 500mm wide and 400mm depth, was designed to provide a secondary discharge path in the event of pipe blockage or overflow of the primary stormwater system.

(4) Erosion preventative designs were proposed around the discharge outlet on the beach comprising:
   a. Installation of Enkamat (geotextile mat) on the sand dunes to prevent the erosion of sand and encourage the growth of dune preserving plants such as Spinifex.
   b. Installation of stones at the invert level of the outlet with a d_{50} of 200mm, designed to dissipate the energy of the discharge flow, thereby reducing scour effects.
   c. Installation of an open top manhole with scruffy dome lid approximately 10m upslope of the pipe outlet. The design was intended to provide a secondary outlet by allowing stormwater to accumulate in the manhole and overflow onto a vegetated spillway directed away from the properties.

(5) A series of horizontal drains installed into the bluffs adjacent to the affected slopes to reduce pore pressures.

7 REVEGETATION

Pohutukawa, Karamu, and native Cabbage Tree were among some of the plants chosen to re-vegetate the failed slopes. These plants were chosen for their suitability in the coastal environment and characteristics such as fast growth and spreading root balls which would assist with retaining surficial soils.

8 CONSTRUCTION

At the time of writing this paper, construction had not commenced for these works, pending consent approval from Far North District Council.

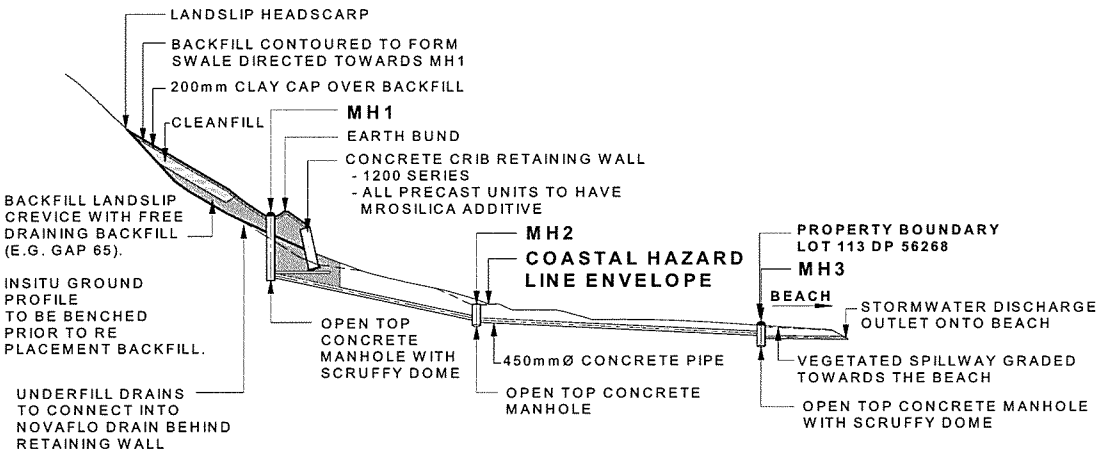

Figure 5: Proposed landslide remedial works

9 CONCLUSIONS

In July 2007, a landslide occurred upslope of the residential property at 46 Taupo Bay Road, inundating the site under approximately 2m of debris, and shunting the dwelling from its foundations. In addition to inherent slope instability, the subject landslide was attributed to,

(1) accumulation of stormwater in soil shrinkage cracks,
(2) the reduction of effective strength in the soil mass due to stormwater infiltration.

Remediation designs proposed for the restoration of the site included,

(1) A concrete crib retaining wall at the base of the affected slope intended to retain backfill and act as a debris barrier in the event of further instability. Free draining hardfill was specified as the backfill to, (a) reduce the susceptibility of rainfall-induced failure, as pore pressures are prevented from accumulating due to rapid dissipation and, (b) retain the unrestrained head scarps and side scarps formed by the landslide
(2) A stormwater management system was proposed to divert water away from the affected slopes consisting of a sump/manhole behind the crib wall, designed to collect surface runoff from the upper slopes and pipe the discharge towards the beach.

Construction is yet to commence for these works, pending District Council consent approval.

ACKNOWLEDGEMENTS

The author wishes to thank Tonkin & Taylor Ltd for the support in preparing this paper, and also the Earthquake Commission and the owners of the properties involved with the landslide, for their permission to publish this paper.

REFERENCES

Far North District Council (FNDC) (2007) *Land Information Memorandum – No. 7401: Lot 112 DP 56268 BLK II Whangaroa SD*. Far North District Council.

Howse (2007) Personal Communication.

NIWA and GNS Science (2007) *Natural Hazards 2007* joint publication by NIWA and GNS Science.

Rahardjo, H., Ong, T.H., Rezaur, R.B. and Leong, E.C. (2007) Factors controlling instability of homogeneous soil slopes under rainfall, *ASCE Journal of Geotechnical and Geoenvironmental Engineering*, Vol. 133, No. 12, December.

Implementation of Geotechncial Guidelines in Designing for the Road T3 and Associated Roadworks Project, Hong Kong

Jennifer Lo
URS New Zealand Ltd., Auckland, NZ

Keywords: Guidelines, landslide, slope, Hong Kong

ABSTRACT

Slopes are found everywhere amidst Hong Kong's urban developments. It is essential that they are properly maintained and landscaped to enhance the city outlook and ensure ongoing safety of people and property. In this respect, the Geotechnical Engineering Office (GEO) of the Civil Engineering and Development Department has developed an overall land risk reduction strategy with three main goals: (i) minimise risk arising from new developments, (ii) reduce risk by improving the stability of existing slopes, and (iii) reduce risk by minimising the possible consequences of landslides. This paper presents case studies from the project entitled "Road T3 and Associated Roadworks" in Hong Kong, indicating how the guidelines given by the GEO have been applied. The geotechnical engineering works for this project includes slope modification and improvement by filling or cutting with application of soil nails and construction of various types of retaining walls.

1 INTRODUCTION

1.1 History

Eighteenth June 1972 was called the most disastrous day for landslides in Hong Kong. It had been raining heavily in the past two days, more than 400mm of rainfall had been recorded. That resulted in the occurrence of two tragic landslides, causing a total of 138 deaths. Around one o'clock in the afternoon that day and one-and-a-half hours after high intensity rainfall, a 35m high fill slope liquefied at Sau Mau Ping Housing Estate (See Figure 1). In the evening of the same day, about nine o'clock, a large landside occurred on a steep natural colluvial slope above Po Shan Road in the Mid-level (See Figure 2).

Figure 1: Sau Mau Ping Landslide, 18 June 1972. Ground floors of the buildings were filled by debris, resulting in 71 deaths

Figure 2: Po Shan Road Landslide, 18 June 1972. A four-storey building and a 15-storey apartment block were demolished during the landslide, resulting in 67 deaths

Four years later in 1976, another landslide occurred on a fill slope behind Block 9 of the Sau Mau Ping Housing Estate. Seventy one people were killed in this failure. Research had shown that no fault was found "with the manner in which the design and construction of the embankment was carried out". The Government of Hong Kong therefore appointed an Independent Review Panel to evaluate and advise on the causes and implications of the Sau Mau Ping failure. The Panel reported that the triggers to this failure were intensive rainfall and appearance of loose fill. The Panel also recommended in the report "that a control organization be established within the Government to provide continuity throughout the whole process of investigation, design, construction, monitoring and maintenance of slopes in Hong Kong". Consequently, the Geotechnical Control Office (GCO) was established to regulate the design, construction, maintenance and monitoring of slopes in Hong Kong. Its name was changed to Geotechnical Engineering Office (GEO) in 1991 to more accurately reflect its expanded role and scope of responsibilities.

1.2 The Need of Guidelines – Landslide Risk Reduction Strategy

One of the GEO's tasks was to develop an overall landslide risk reduction strategy. The strategy can be categorised in three directions:-

i. Minimise risk arising from new developments by considering geotechnical impact at the early stage of land use planning and assessing all new slopes to ensure they are designed to current safety standards.
ii. Reduce risk by improving the stability of existing slopes under government maintenance responsibility and promote the maintenance of private slopes.
iii. Reduce risk by minimising the possible consequences of landslides, such as clearing squatters from hilly terrain and education to the public.

GEO understood that the risk of slope failure was aggravated by a lack of geotechnical guidelines or slope standards before the 1970's. Therefore, GEO has been putting tremendous effort on the production of geotechnical guidance documents and technical reports. One of the most notable publications, promoting good slope engineering practices is *Geotechnical Manual for Slope* (*Slope Manual*), which is widely used in the industry.

1.3 The Project

This paper will present the application of the GEO guidelines, especially the *Slope Manual*, on varies geotechnical engineering works in the project entitled "Road T3 and Associated Roadworks" (hereafter Road T3) in Hong Kong.

Road T3 forms part of the continuing programme for the development of Sha Tin New Town, Hong Kong. The trunk road mitigates the present traffic congestion at the Sha Tin Section and the Tai Wai Section of Tai Po Road. It also relieves the traffic congestion in the Tai Wai area and provides a connection to Route 8, which is a trunk road linking Chek Lap Kok and Sha Tin via Tsing Yi and Lai Chi Kok.

The project comprises the construction of an approximately 3km long mainline trunk road including 2km long dual 2-lane elevated carriageways and a 1km long slip road and at-grade roads; construction of approximate 150m long underpass; construction of footbridges and subways; 6.4km noise barriers and noise enclosures; realignment of existing roads; reconstruction of 200m long elevated carriageway over KCRC railway tracks; re-provision of rest gardens and sitting out areas; and associated slopeworks, drainage, waterworks and landscape works. The Contract Sum was approximately Hong Kong $1.48 Billion.

The site is typically underlain by slightly to moderately decomposed fine to coarse grained granite, with a cover of completely and highly decomposed granite (also known as saprolite soils). The granite bedrock is intruded locally by fine grained dyke rocks of rhyolite. The in-situ soils and rocks are overlain by an impersistent cover of colluvial debris flow deposits that range in composition from gravel to silt. Fill cover is generally found as fill bodies downslope of Tai Po Road.

The geotechnical engineering works in this project included slope modification and upgrading by filling or cutting methods with application of soil nails and construction of various types of retaining walls.

2 GUIDANCE ON SLOPE STABILITY

2.1 Assessing Existing or New Formed Slopes

In terms of Factor of Safety criteria (FoS), the *Slope Manual* suggested the consequence to life and economic consequence categories. Engineers should use professional judgement in assessing the "severity in terms of loss of life in the event of failure". In contrast, FoS against economic loss is a decision made by the owner upon the advice of engineers.

It is suggested in the *Slope Manual*, assessment should be made of all new formed, modified and existing slopes that could influence or be influenced by the new works. Assessment should also include slopes outside the immediate vicinity of the works. Engineers should design all aspects with consideration of the effects of the slopes on people and property.

Road T3 is enclosed by a concrete jungle, mainly surrounded by residential buildings of at least 15 storeys. According to the *Slope Manual*, all the slopes along Road T3 and slopes identified that could influence or could be influenced by the road should be formed with a FoS greater than 1.4. In some "occasional case", such as natural slope where the public and their property loss would be minimal if failure occurs, the required minimum FoS is reduced to 1.2.

The required minimum FoS for slopes in New Zealand is typically 1.5, while it is only 1.4 in Hong Kong. It is understood that the purpose of FoS is to allow uncertainty in design. The lower FoS value in Hong Kong may be due to less complexity of soil behaviour that engineers usually deal with.

2.2 Criteria on Designing New Slopes

The *Slope Manual* suggests forming new slopes with batters of maximum 7.5m high and berms of minimum 1.5m wide. The idea is to provide surface drainage channels so that it can reduce the volume and velocity of runoff on the slope surface. Secondly, formation of these slopes can

catch debris from slips occurring at a higher level and reduce the damage to the structures at slope toe. Thirdly, it also provides access for maintenance.

In Road T3, slopes at the uphill side were mostly soil-nailed cuts which followed the design criteria and have slope angles between 45° to 55° as shown in Figure 4. Similarly, fill slopes on the downhill side also followed these criteria and were formed with a slope gradient of 26°.

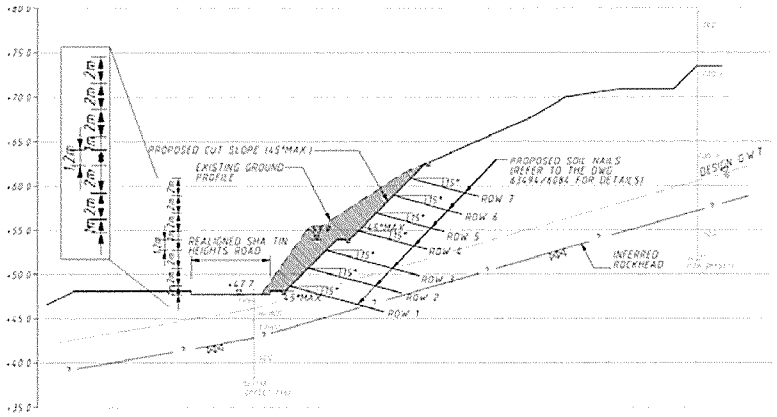

Figure 4: Example of Soil-nailed Cut Slope

2.3 Upgrading Existing Slopes

2.3.1 Substandard Cut Slopes

Soil nails on in-situ soil slopes have been the predominant method used in Hong Kong for upgrading works due to land availability. It was introduced to Hong Kong in the 1980s and gained popularity since the mid-1990s. According to *Geoguide 7: Guide to Soil Nail Design and Construction*, there are more than 200 slopes and retaining walls upgraded using soil nails each year in Hong Kong. GEO has consolidated all its Technical Guidance Notes regarding soil nails and projects studied in a newly released *Geoguide 7*, outlined the guidance of good practice in soil nail design, construction and monitoring.

Soil nails can be designed prescriptively or analytically. Prescriptive design is pre-determined, experience-based and conservative without having detailed ground investigations and design analyses. For a typical slope upgrading project, conventional analytical design may take 10 months longer than using prescriptive design. This is mainly due to the required review and approvals.

The soil nails used in Road T3 were designed analytically adopting the equations and literature on engineering judgement in the guidelines. Soil information was based on detailed ground investigation and laboratory testing. As discussed in the *Geoguide 7*, widely-spaced nails are not effective unless they are very long, large diameter and consist of high yield strength steel bar. Soil nail spacing of 1.5m to 2.0m is recommended and commonly used in Hong Kong soils. Therefore, soil nails in Road T3 were installed at a spacing of 1.5m to 2.0m as shown in Figure 4. In addition, pull-out tests were performed on site to simulate the assumed condition and verify the design.

2.3.2 Loose Fill Slope

Replacement and recompaction is the most effective way to enhance the stability of loose fill slopes. Performance of this method has been studied and measured. Firstly, remove vegetation, topsoil and unsuitable material. Then, bench to key the recompacted fill into existing slope. Unlike slope design in New Zealand, seismic assessment in Hong Kong can be omitted because it is located far from the seismic zones. However, slope failure in Hong Kong occurs due to soil

liquefaction after prolonged rainfall which results in loose fill achieving zero effective stress. One of the solutions is to alter the loose fill to compacted fill, commonly by vibratory rollers or hand-rammers in such a manner that structures or utilities are not disturbed or damaged. A drainage layer is required to be placed between the fill and natural ground to eliminate the possibility of high pore pressure developing behind the compacted face. Suitable drains should also be provided where springs and seepage-traces are found.

How much of the loose fill has to be removed? A minimum depth of 3m was recommended by the 1976 Independent Review Panel. The surface layers are stripped to a vertical depth of not less than 3m and replaced with fill compacted to a density of not less than 95% of BS maximum dry density. Long-term performance of this method has been reviewed and shows that the liquefaction potential of the underlying loose fill is reduced because of the increase strength of the recompacted surface and the addition of the drainage layer. The amount of rain water infiltration is reduced and watertable rise is restricted to 3m below the surface.

For the Road T3 project, the replace and recompact approach for the top 3m of loose fill was adopted in slope upgrading. Boulders or unsuitable materials such as topsoil and rubbish were screened out from the stripped loose fill. The screened materials were then compacted and reused in place. The Contractor was responsible to keep the fill. When the fill was adversely affected by rain, it was allowed to dry out under the sun. One of the upgraded slopes required 5m of replacement of recompacted rockfill for stability enhancement, due to the existing stream course, leakage of an aged box culvert underneath and its size.

2.4 Associated Facilities – Slope Surface drainage

Inadequate drainage is one of the biggest problems that leads to a landslide. As discussed, soils liquefy after prolonged rainfall causing one of the major issues in slope failure in Hong Kong. Therefore, GEO has promulgated guidance relating to slope surface drainage. Detailed guidance on the design of slope surface drainage systems is given in the *Slope Manual*, including guidance on assessment of return periods of rainstorms, design methodology and design charts. It is also recommended that a system of berm and stepped channels should be incorporated in the slope design. Furthermore, blockage by leaves and debris would reduce the performance of a drainage system and needs to be cleared. Occupational safety is of concern to GEO regarding slope safety in regular slope maintenance. Hence, handrails installed on berms are added to the requirement. It is an expensive approach; however, life is priceless.

The capacities of all the existing surface drainage along Road T3 were checked. New drainage systems were proposed where inadequacies were found. Similarly, new drainage systems were provided for new formed slopes and where slope modifications were required. In the project, the surface drainage systems were designed to cater for a 1 in 200 year rainstorm in accordance with the "rational method" suggested in the *Slope Manual*. The *Slope Manual* also emphasises the importance of a proper discharge of stormwater. Sand traps were used, accordingly, for filtering prior to discharging stormwater to streams or road drains.

2.5 Determination of Soil and Groundwater Properties

Some soil and material properties are recommended in the Guidelines. They are based on a large amount of factual data collected and past experience. For example, *Geoguide 1: Guide to Retaining Wall Design* suggests a range of parameters for several common soils in Hong Kong. This gives the geotechnical engineers a baseline reference to cross check the results of the project-specific ground investigation.

In addition, in the absence of groundwater records or wet season groundwater monitoring, the *Slope Manual* suggests using the wetting band method to estimate the groundwater level for acritical case. A rise of groundwater based on a wetting band analysis for a 10-year return

period rainfall has been assumed in Road T3 to estimate the probable rise in groundwater during the design rainstorm. A rise of 3m above the highest measured groundwater level was suggested using this method.

3 DISCUSSION

Setting up these guidelines is crucial for fast-track projects in a rapidly growing city. Some guidelines suggest prescriptive measures that can reduce a lot of design time and human resources by eliminating detailed ground investigation and design analyses. Prescriptive measures also save time during construction in the aspect of controlling workmanship when there are many slopes repairs occurring concurrently and urgent repairs required. This measure is suitable for a large number of small-scale slope repairs with limited available staff resources. In terms of non-prescriptive design, these guidelines provide a baseline for the parameters and solutions as reference. Apart from that, design engineers are provided with some commonly acceptable design methodologies and examples to follow, so that the time spent on reaching an "agreed design methodology" can be reduced. These guidelines also help the Government to grant approval to projects in an easier and faster way at the same time as ensuring a safe design.

A large database collected from research and previous projects is required for establishing these guidelines. In some other countries, guidelines may not be necessary because they may allow a longer project time. Besides, diversity of soil types and geotechnical properties may cause problems in generating a guideline for a specific design. Although guidelines suggest to engineers the proper practice to be followed, they also give constraints to engineers in creating innovative ideas. A strong justification may be needed to get approval for design not following the guidelines. Time for negotiation may cause delay of the project. In addition, the suggested data or information in the guidelines can only be relied on in the ordinary situation, and are not applicable for extreme cases or adverse conditions. Prescriptive measures can be designed easily and fast, however, they are often conservative and may not be the most cost-effective option.

4 CONCLUSIONS

Guidelines are required in Hong Kong because of the fast development. Previous lack of geotechnical guidelines or standards led to several fatal landslides in 1970's. Guidelines published by the GEO consolidated past experience and findings and suggest standards of good practice for design, construction, monitoring and maintenance of geotechnical activities in Hong Kong. Although the guidelines tend to be conservative and therefore may not able to provide the most cost-effective solution, the number of slope failures has decreased since the introduction of GEO guidelines and standards.

REFERENCES

Government of Hong Kong SAR (2000) *Geotechnical Manual for Slopes (2nd Edition)*. Geotechnical Engineering Office, Hong Kong.

Government of Hong Kong SAR (2000) *Guide to Retaining Wall Design (Geoguide 1, 2nd Edition)*. Geotechnical Engineering Office, Hong Kong.

Government of Hong Kong SAR (2008) *Guide to Soil Nail Design and Construction (Geoguide 7)*. Geotechnical Engineering Office, Hong Kong.

Maunsell Geotechnical Services Ltd (1998) *Sha Tin New Town – Stage II, Trunk Road T3 (Tai Wai) Geotechnical Appraisal Report*. Maunsell Counsultants Asia Ltd, Hong Kong.

Morgenstern, Norbert R (2000) Performance in Geotechnical Practice. *The Inaugural Lumb Lecture*, Hong Kong.

Wong, HN, Pang, LS, Wong, ACW, Pun, WK & Yu, YF (2000) *Application of Prescriptive Measures to Slopes and Retaining Walls (GEO Report 56, 2nd Edition)*. Geotechnical Engineering Office, Hong Kong.

Remediation of landslips in Northland Allochthon, Kaitaia, NZ

Hamish Maclean
Tonkin & Taylor, Auckland, NZ

Keywords: landslip, Northland Allochthon, slope modelling, shear surface

ABSTRACT

Two large progressive landslips in the Northland Allochthon materials underlying the slopes to the east of Kaitaia, in the Far North of New Zealand, represent a significant threat to life and property in the area. Investigation and monitoring results indicate both landslips are continuing to creep.

The first landslip, located on a moderate slope of around 10° at Allen Bell Drive, has a surface area of around 12,000m^2. It is proposed to construct a reinforced concrete palisade pile wall and undertake associated earthworks and drainage to stabilise the landslip. The second landslip is on Bell Hill near the northern bank of the Awanui River and affects an area of around 4000m^2. It is feared that catastrophic failure of this landslip may dam the river and flood nearby Kaitaia. The proposed solution is to install two fans of horizontal drains to lower the ground water table and stabilise the landslip.

1 INTRODUCTION

The landslips at Allen Bell Drive and Bell Hill are located in very close proximity to each other on the eastern side of the Awanui River at Kaitaia in Northland, New Zealand (Figure 1). The purpose of this paper is to overview the common mode of failure at both sites, the slope modelling methodology used and the proposed remedial works.

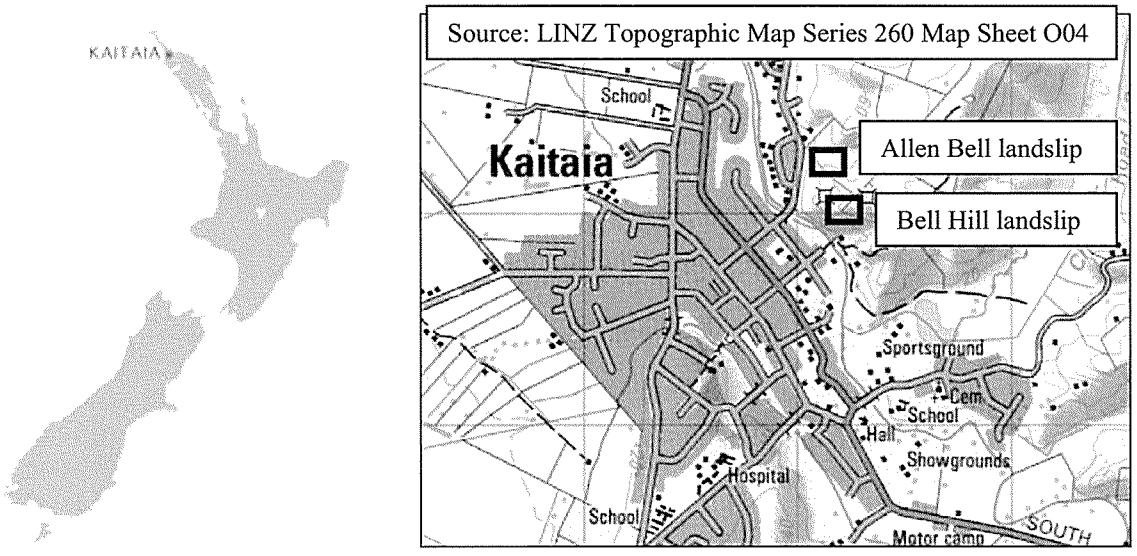

Figure 1: Landslip site locations, Kaitaia, New Zealand

2 SITE CONDITIONS

The large Allen Bell Drive landslip located on moderately sloping land to the east of Allen Bell Drive has been undergoing periodic, minor movement for a number of years (Figure 2). The landslip affects at least twelve properties and seven existing residential dwellings. The landslip measures around 120m across and extends at least 100m upslope to the east of Allen Bell Drive.

Damage to dwellings includes movement of timber pile foundations and minor racking of the structures as a result. Internal cracking in gib has predominantly occurred above window and door frames. Properties located closest to Allen Bell Drive appear to be worst affected as a result of landslip heave at the toe of the slope (Tonkin & Taylor, 2008).

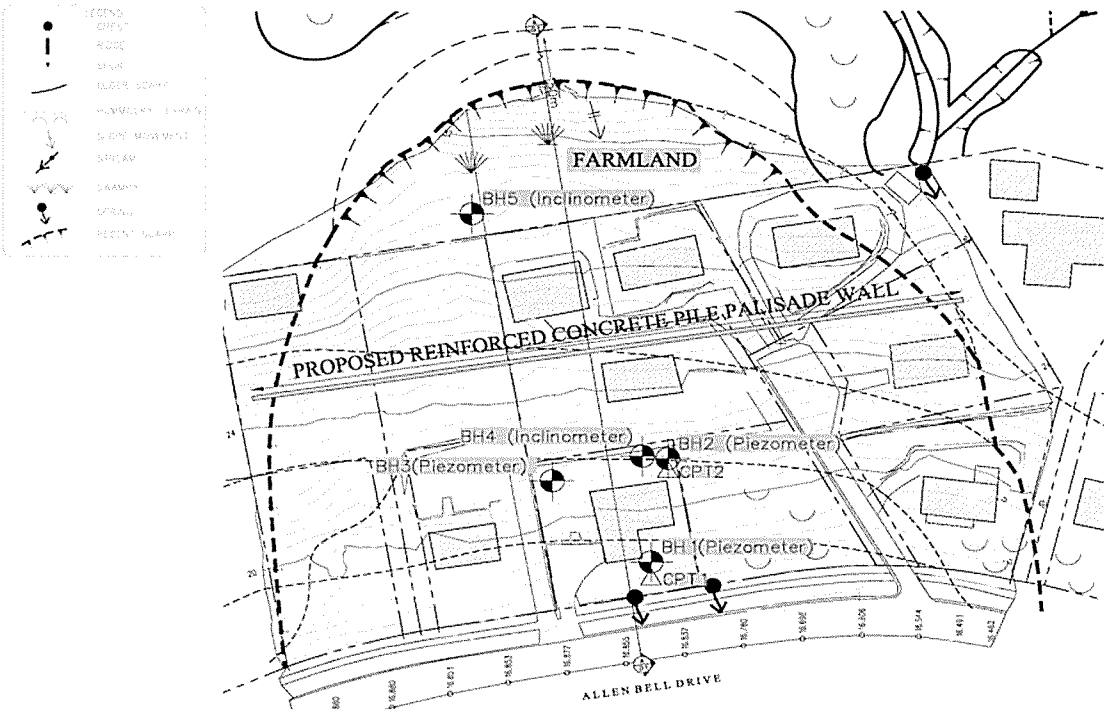

Figure 2: Site plan of the Allen Bell Drive landslip

The Bell Hill landslip, located off Korimako Lane on the northern bank of the Awanui River, first moved during heavy rain in July 1998. A large tension crack opened up 45m upslope of the river bank (Figure 3). The scarp measures around 85m long and an existing dwelling, located in close proximity, has been removed from the site. Complete failure of this landslip would pose a significant risk to Kaitaia as the landslip debris could dam the river, causing it to overflow the southern bank and flood into Kaitaia (Tonkin & Taylor, 1999).

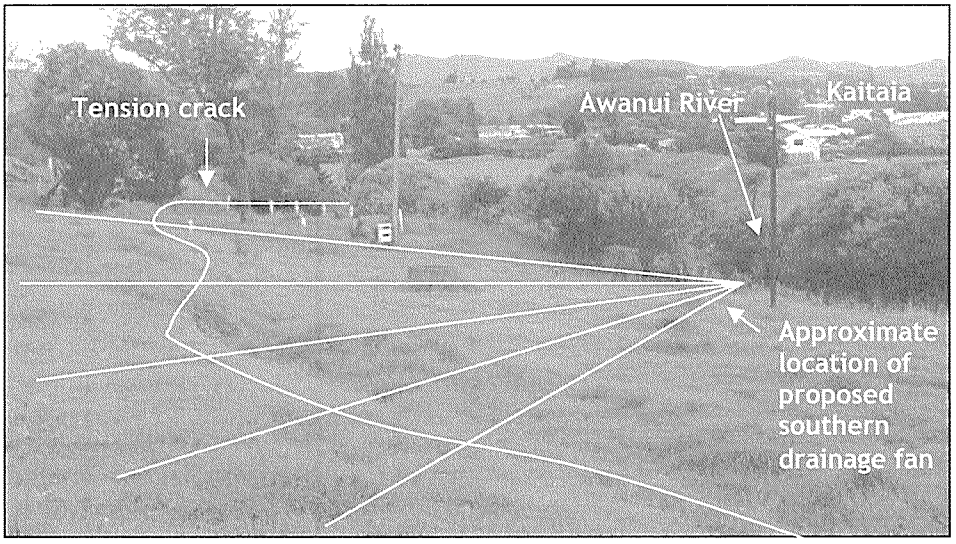

Figure 3: Photograph of the Bell Hill landslip with tension crack evident

3 FIELD INVESTIGATION

3.1 Site investigation

Geotechnical investigation for both sites has included the following:

- Visual inspection and geological mapping
- Review of aerial photographs
- Machine borehole and CPT investigations

Locations of the investigation holes for the Allan Bell Drive site are shown on Figure 2.

3.2 Monitoring

Monitoring of groundwater conditions and further landslip movement on both sites has included the following:

- Piezometer installation and monitoring
- Survey monitoring of known points
- Inclinometer installation and monitoring

Piezometers and inclinometers installed at the Allan Bell Drive site are shown on Figure 2.

3.3 Geology

Investigations show that both sites are underlain by Hukerenui Mudstone of the Mangakahia Complex, part of the Northland Allochthon. This material comprises pervasively sheared brown/grey/green mudstone and moderately sheared siltstone. Geotechnical investigations indicate that subsurface conditions at the two sites are generally consistent with the published geological information (Isaac, 1996 and Edbrooke, 2001). At Allen Bell Drive, weakly cemented dune sands of the Awhitu Group unconformably overlie the Allochthon basement rocks.

Topography developed on the Allochthon rock mass usually reflects the local lithologies, with steeper slopes on the igneous and cemented sediments and subdued slopes in the soft pervasively sheared mudstones.

3.4 Subsurface conditions

3.4.1 Allen Bell Drive subsurface conditions

The site at Allen Bell Drive is underlain by silty, grey sand (Awhitu Group) at the toe of the slope which interfingers with softened Northland Allochthon material from further upslope. This softened Allochthon is highly disturbed, having been subject to landslip movement in the past. The sand at the toe is similarly disturbed and contains several layers of highly organic brown peat.

Both the sand and softened Allochthon materials overlie more competent Allochthon basement rocks comprising grey, broken, blocky mudstone which becomes more competent with depth. A thin (approximately 0.5-1m thick) layer of highly disturbed, broken Allochthon was encountered at the interface between the softened Allochthon and the underlying, more competent Allochthon rock mass.

3.4.2 Bell Hill subsurface conditions

The Bell Hill site is underlain by softened Northland Allochthon comprising colluvium (slope transported debris) to a depth of around 3-4m and completely weathered, highly disturbed Allochthon beneath this material to a depth of around 9m. As with the Allen Bell site, this material is underlain by more competent Allochthon. Similarly, a thin layer of highly disturbed, blocky, broken Allochthon was encountered at the interface between the softened Allochthon and the more competent underlying Allochthon.

4 MONITORING RESULTS

4.1 Piezometer results

Piezometer monitoring indicates the groundwater beneath the Allen Bell Drive site is extremely high, being within 0.5-1.0m of the ground surface. Groundwater levels beneath the Bell Hill site are deeper at around 4-5m below the existing ground surface.

4.2 Inclinometer results

Inclinometer results indicate both landslips are continuing to move. The ongoing movement of the Bell Hill landslip is significant, with the inclinometer being completely sheared within six months of installation. Results indicate that at both sites, the shear surface is located at the interface between the upper, highly disturbed softened Allochthon and the underlying broken Allochthon.

Both landslips are translational with relatively shallow shear surfaces. At the Allen Bell Drive site the shear surface is around 5m below the existing ground surface. The shear surface is located slightly deeper at around 8.5m deep at Bell Hill.

5 SLOPE MODELLING AND PROPOSED REMEDIAL SOLUTIONS

5.1 Slope stability modelling

Material properties for both sites were determined by back analysis stability modelling, shear vane readings taken within the machine boreholes and the CPT results. A summary of the soil parameters used for the Allen Bell Drive site is given in Table 1 below.

Table 1: Material properties used in stability analyses for the Allen Bell Drive landslip

Geological unit	Unit Weight, γ (kN/m^3)	Effective cohesion c' (kPa)	Effective friction angle ϕ' (deg)
Sand	16	2	28
Peat	15	2	15
Softened mudstone	18	10	14
Shear surface	22	6	14
Broken mudstone	22	20	14

The SLIDE stability model output for the Allen Bell Drive landslip back analysis is shown below:

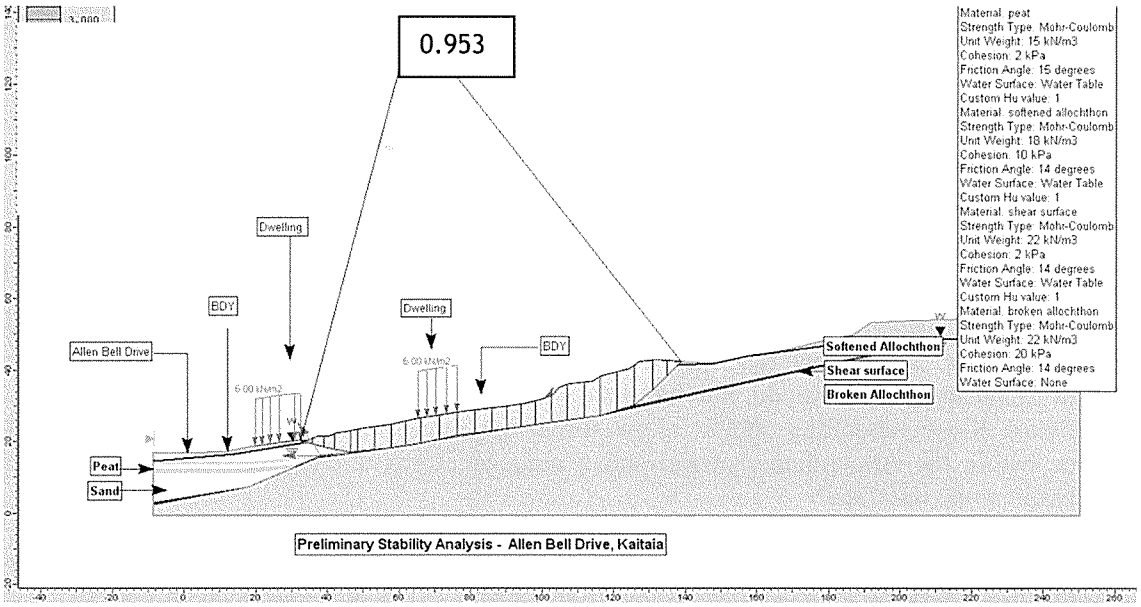

Figure 4: Stability model for Allen Bell Drive

5.2 Proposed remedial solutions

Preliminary design work has been undertaken to determine acceptable remedial solutions to stabilize the landslips at both sites.

5.2.1 Allen Bell Drive

Preliminary design of a remedial solution for this site has been undertaken. Proposed remedial works include the construction of a reinforced concrete pile wall through the centre of the landslip (as shown on Figure 2) and the installation of two fans of 5x100m horizontal drains in order to lower the extremely high ground water table. These remedial measures result in a calculated FOS in excess of 1.5. The proposed wall will stabilize failed material above by providing toe support and also stabilize down slope material by removing the driving force from the upslope slide mass. The wall is located mid-slope to ensure the upper material does not fail over the top of the wall.

5.2.2 Bell Hill

The following options were proposed as suitable for stabilizing this site.

- Palisade (inground) piles
- Toe buttressing
- Bulk earthworks to reduce potential slide mass volume
- Horizontal drains

The client (Northland Regional Council) decided to pursue the use of horizontal drains to stabilize the landslip. These drains are designed to increase the slope's FOS by intercepting and lowering the groundwater table below the shear surface. Design allowed for installation of two fans, each comprising five horizontal drains. These were to be drilled from the base of the river bank back into the slope, at an angle of around three degrees above the horizontal. The two proposed fans of drains are splayed over the extent of the landslip and are around 50-60m long. Stability modelling indicates that lowering the groundwater table to just below the shear surface results in a 30% increase in the FOS from 0.99 to 1.34.

The installation of two 'trial' horizontal drains was undertaken on 20 February 2008. This was done to determine whether the Allochthon material in this region has a suitable permeability for the proposed drainage to be effective. Results to date indicate that the material is suitably permeable with the trial drains producing a constant water flow of up to 0.3-0.6 L/min. The trial drains are currently continuing to be monitored with installation of the two full fans proposed for the near future.

6 CONCLUSIONS

Geotechnical investigations on the landslip sites at Allen Bell Drive and Bell Hill, underlain by Northland Allochthon, show that the surficial softened Allochthon is highly susceptible to shallow translational failure on the interface with the highly disturbed underlying broken Allochthon. Slope modelling should allow for a low effective friction angle of around 14 degrees within the Allochthon material and a reduced effective cohesion within the broken Allochthon at the interface.

Slope modelling and engineering design indicates that lowering the groundwater table, which is typically high, may be an effective means of stabilising existing landslips in this area but is unlikely to achieve a FOS>1.5. Trial drainage indicates that the permeability of the Allochthon should be sufficient to accommodate draining the slopes, however these drains will require periodic maintenance to ensure they do not become blocked. Because the failures are typically shallow, the use of palisade (inground) piles is also considered a feasible remedial measure for landslips of this nature.

Further development to the east of Kaitaia in the region of Allen Bell Drive and Bell Hill should account for the presence of landslip prone Northland Allochthon. Complete failure of the existing Bell Hill slip is considered possible, with potential for the slide mass to dam the Awanui River causing it to flood parts of Kaitaia.

ACKNOWLEDGEMENTS

The permission of the Earthquake Commission and the Northland Regional Council to publish this paper is gratefully acknowledged. The investigations have involved a team of individuals including Far North District Council representatives, land owners and machine operators. The author would like to thank these many contributors and especially Tonkin & Taylor geologists Kate Williams and Bernard Hegan.

REFERENCES

Edbrooke, S.W (2001) Geology of the Auckland area. Institute of Geological & Nuclear Sciences 1:250 000 geological map 3.1 sheet +74p. Graphic Press and Packaging, Levin.

Isaac, M (1996) Geology of the Kaitaia area. Institute of Geological & Nuclear Sciences 1:250 000 geological map 1.1 sheet +44p. Graphic Press and Packaging, Levin.

Tonkin & Taylor Ltd (2008) Geotechnical Investigation Report: Allen Bell Drive, Kaitaia (Ref: 17600.001). Unpublished report prepared for the Earthquake Commission.

Tonkin & Taylor Ltd (1999) Bell Hill Slip Geotechnical Report (Ref: 16946). Unpublished report prepared for the Far North District Council.

MASW profiling to obtain elastic moduli models for wind turbine foundation design – Te Rere Hau Windfarm

Dominic Mahoney
Connell Wagner, Christchurch, New Zealand

Key words: elastic moduli, greywacke, wind turbine, monopile foundation, MASW

ABSTRACT

The Te Rere Hau Windfarm, currently being constructed by NZ Windfarms Ltd, will eventually consist of 97 x 500kW, New Zealand designed and built wind turbines. The windfarm is situated on the ridgeline and the steep upper western slopes of the northern end of the Tararua Ranges, east of Palmerston North. The area as a whole is underlain by Mesozoic greywacke rock. A 2.4m diameter mono-pile foundation was adopted, as opposed to the more traditional pad foundation option. For structural design of the mono-pile foundation an accurate elastic modulus profile of the subsoil for each turbine site was required. To obtain the elastic moduli profiles with depth, the geophysical seismic method Multi-Channel Analysis of Surface Waves (MASW) testing was undertaken, and shear wave velocity profiles for each turbine site were obtained. These profiles were then compared to previously obtained geotechnical information such as test pit data and borehole logs, and elastic moduli profiles with depth were determined. This data was then used by the structural engineers to design the mono-pile foundation elements using FEM analysis. Data validation was obtained by observing pile shaft drilling. This paper sets out the need for MASW testing, and details the steps taken to convert test data to FEM analysis input data.

1 INTRODUCTION

The Te Rere Hau Windfarm is currently being developed by NZ Windfarms Ltd and will eventually feature 97 x 500kW, New Zealand made wind turbines. The site is located on the ridgeline and upper western slopes of the northern end of the Tararua Ranges, east of Palmerston North. Five turbines were installed in 2006 and these are operating satisfactorily. As part of the Stage II development of the windfarm a further thirty wind turbines are being installed in 2008.

The turbines for Stage II are designed with a 2.4m diameter mono-pile foundation, as opposed to a more traditional shallow pad foundation used in Stage I. FEM analysis was used to design the mono-pile foundation elements, and as such, an accurate elastic modulus profile with depth of each turbine location was required. Due to the highly variable nature of the underlying Mesozoic greywacke rock, (DSIR, 1962), a relatively tight construction schedule, the proposed number of wind turbines in the entire development, and the difficulty and cost in obtaining sufficient undisturbed samples for small strain tri-axial testing, it was decided that the geophysical method of MASW provided the best option for obtaining the required data. This raw data can then be used to provide in situ elastic moduli profiles for each wind turbine site. The seismic wave velocity profiles obtained from the MASW sounding were converted to elastic moduli profiles by constraining the results against known and previously obtained geotechnical and geological information. The elastic moduli profiles were then used by the nominated structural engineers in their FEM analysis for each turbine location to calculate the required minimum embedment depth for the mono-pile.

2 TESTING METHOD

Due to the gradational weathering profile of the underlying greywacke rock, MASW was selected as the most suitable geophysical test method from which to obtain velocity profiles with depth at each turbine location. An independent geophysical sub-consultant, Southern Geophysical Ltd, was engaged to carry out the MASW soundings and post-processing. The obtained dataset provided a 10-layer shear wave velocity profile for each turbine location.

3 DETERMINATION OF SHEAR WAVE VELOCITIES

Shear wave velocity (V_s) obtained from MASW testing was used to calculate the elastic moduli (E) with depth. A two-step computation related V_s and shear moduli (G) to determine G and E. The relationships between V_s and G, and G and E are detailed below (Kramer, S. 1996):

$G = \rho Vs^2$ where ρ is the material density (1)

$E = 2G(\upsilon+1)$ where υ is the Poisson's ratio of the material (2)

Therefore, relating V_s to E directly.

$$E = 2 \rho V_s^2 (\upsilon+1) \quad (3)$$

The elastic moduli value is dependent on both ρ and υ. In addition, ρ and υ for soil/rock are dependent on the intrinsic material properties, and to a great extent they are influenced by the extent of the weathering and jointing. In order to derive appropriate E profiles for the site, appropriate ρ and υ values that are representative of the extent of rock weathering must be selected. The process taken is outlined below.

As part of an earlier geotechnical investigation of the windfarm site, exploratory test pits were dug at each turbine location. These test pit logs provided the depth to the interface between soil and rock, and the degree of weathering of the underlying greywacke rock at each turbine location. In addition to the test pit excavations, six exploratory boreholes were drilled to depths between 10m and 15m. This was used to determine the rock weathering with depth. The material properties for individual soil/rock types were determined using the shear wave velocity values obtained at the residual soil/weathered rock and weathered rock/un-weathered rock interfaces for the six borehole locations. Thus, the depth to the residual soil/weathered rock interface, and depth to the weathered rock/un-weathered rock interface was determined for each turbine location using the velocity values at their interfaces. Due to the variability in shear wave data and inaccuracies in borehole data, a sensitivity analysis was subsequently undertaken as part of the elastic moduli modelling process. An upper and lower bound shear wave value at each of the above interfaces was measured and this resulted in four combinations of shear wave values at the interfaces (refer Table 1).

In order to convert the V_s profile to an elastic modulus profile for each turbine site, profiles of both ρ and υ with depth were required. By knowing the depth to the interface between residual soil/weathered rock, and weathered rock/un-weathered rock, limiting values of ρ and υ at these interfaces were allocated. Due to the variability of 'weathered greywacke', which ranges from completely-weathered soil type material to slightly-weathered rock, values of ρ and υ were then simply kept constant at a lower bound value in the residual soil and the slightly-weathered rock and varied linearly between the other interfaces.

Table 1: Combination shear wave velocity threshold values

	Residual Soil / Weathered Greywacke V_s Threshold Values (m/s)	Weathered Greywacke/Un-weathered Greywacke V_s Threshold Values (m/s)
Combination 1	275	380
Combination 2	275	500
Combination 3	300	380
Combination 4	300	500

The residual soil that blankets much of the windfarm site is derived from in situ weathering of greywacke rock to soil. This results in an essentially clayey-gravel material. For residual soils a value of υ was obtained from values published in Das and Wilun (2002), and Starzewski (1972), which provided a υ value of approximately 0.35 for clayey-gravel material, while an assumed value of ρ of 18kN/m^3 was used. Kleffmann et al (1998) was used to obtain values for ρ and υ at the un-weathered greywacke rock. In their deep seismic survey across the South Island, a ρ of 2.67t/m^3 (26kN/m^3) was used by Kleffmann et al (1998) for un-weathered greywacke, and during their analysis of their seismic data, a υ of 0.21 ± 0.03 was calculated.

With the depth to the interfaces being obtained from the test pit excavations, the calibration of seismic data against borehole logs, and the linear variation of ρ and υ between the interface points, the profiles of ρ and υ were calculated with depth. Small strain elastic moduli profiles for each turbine location can then be calculated from the provided V_s profiles using the above relationship and the calculated profiles of ρ and υ. This calculation was carried out for the four separate combinations of interface values based upon the different V_s at the interfaces. The sensitivity analysis indicated that there were minor variations in the determined elastic moduli profiles. Further shallow MASW soundings often exhibit unjustifiable elevated velocity profiles, which is generally a result of poor quality seismic data. Thus, geotechnical constraints were often used to justify truncating the elastic moduli values in the upper shallow soil layers. A typical calculated elastic moduli profile is presented in Figure 1.

The elastic moduli profiles were then provided to the structural engineer, who inputted them into a Finite Element Model (FEM), from which the required embedment length of the mono-pile foundation was calculated. The FEM results have been calibrated against full-scale load-deformation tests. The actual load-deformation response was compared to the FEM back-calculated load-deformation response. A load calibration factor was then determined to account for the difference between the measured and calculated load-deformation responses. This calibration factor was then applied to all the turbine FEM foundation models from which the initial pile embedment depths were calculated.

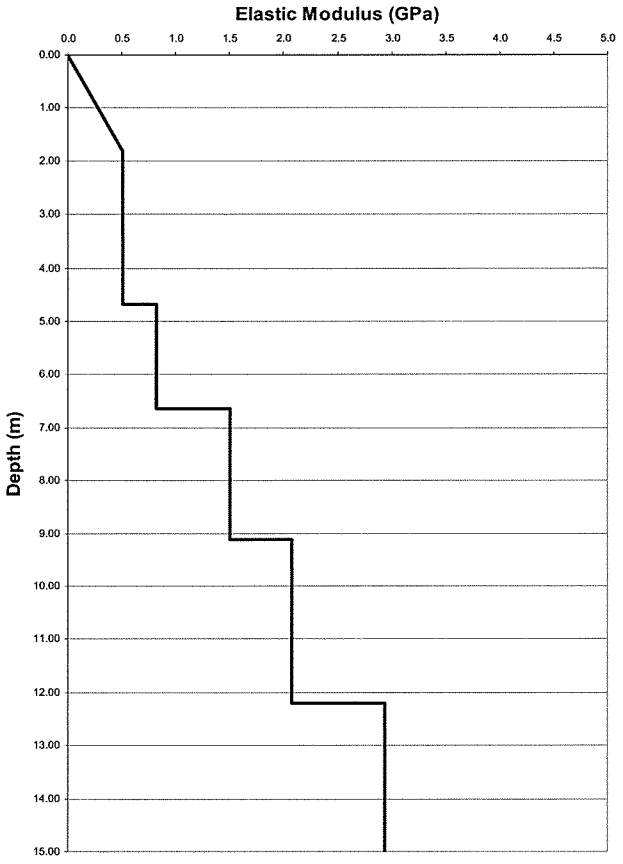

Figure 1: Typical Elastic Moduli Profile (Connell Wagner, 2008)

4 MODELLING ERRORS

Errors can arise when deriving an elastic modulus profile from MASW data. These errors need to be recognised, minimised and mitigated where possible in order to obtain higher accuracies for the elastic moduli profiles. As such, limitations are generally placed on the results. The main sources of errors are derived from the modelling process, as outlined below:

- The MASW method assumes an infinitely flat, discreetly layered, half-space. The windfarm site has steep and variable topography and has a continuous variation in material, not discretely layered, i.e. the interfaces can be indistinct.
- The edge effects caused by the steep topography on many of the turbine sites affects the inversion process, resulting in 3D spatial variation being represented as a 2D variation in depth at the site. To minimise these errors the author has relied upon the opinion and data quality gradings provided by the geophysical sub-consultant.
- Errors are associated with the conversion of velocity to elastic modulus that use only a simple linear variation in ρ and υ, which is reliant upon assumed interface depths. These depths in turn are based upon V_s interface values obtained from the borehole logs. By carrying out a sensitivity analysis using four combinations of interface velocity thresholds such effects were minimised and generally conservative elastic modulus profiles were chosen.
- Due to a lack of literature or research on in situ weathered residual greywacke rock elastic moduli, comparisons to established practice were difficult to achieve.

5 CONSTRUCTION MONITORING

In order to provide further constraints of the elastic moduli profiles, site inspections were undertaken to determine the exposed soil/rock strata on each mono-pile shaft once the initially determined founding depth was reached. Drill tailings were collected and logged at 1.5m intervals during the pilot hole drilling process. A visual inspection was then undertaken of the drilled pile shaft to confirm the assumptions made in the modelling process (refer Figure 2).

The logged and observed stratigraphic profile of the pile shaft was then compared to the modelled elastic moduli profiles as well as being compared to other sites that exhibited similar stratigraphical profiles. Several elastic moduli profiles required further modification to represent the conditions on site. The sites that needed modifying were generally those that had poor MASW data quality, or where MASW sounding was undertaken some distance away from the actual turbine pile shaft location.

Figure 2: Typical view of a 7m deep, 2.4m diameter pile shaft taken during a site inspection

6 DISCUSSION

Mono-pile wind turbine foundations are highly dependent on in situ small strain stiffness, a parameter that is generally difficult to obtain. In this study, MASW was used to obtain elastic moduli profiles for each turbine site in highly variable greywacke that underlies the Te Rere Hau windfarm location. Due to unavailability of elastic moduli values of in situ weathered New Zealand greywacke, the high number of turbine sites, and the cost and difficulty associated with obtaining undisturbed soil/rock samples for tri-axial testing, MASW was chosen as the most cost effective method from which to obtain elastic moduli with depth profiles for each turbine site.

Due to the topographical setting of the site and the underlying material, the MASW method of obtaining elastic moduli profiles had several shortcomings. These shortcomings were identified and where possible their effects limited during the modelling process. The MASW method was not ideally suited to the windfarm site due to the topographical and geological setting. Several simplifying assumptions were required and the inherent errors associated with these assumptions are presented in this paper. However, the data obtained was of sufficient quality to enable engineering design to be undertaken.

As such, visual inspections were undertake on each pile shaft once drilling was completed. The observed material properties were related to the modelled assumptions and the elastic

moduli profiles were adopted accordingly. Several sites required further embedment due to insufficient stiffness being available in the shallow soil layers. Carrying out site inspections of every pile shaft, prior to filling with concrete, provided an additional degree of certainty to the engineering process.

7 CONCLUSIONS

As part of the Stage II development at the Te Rere Hau Windfarm, located east of Palmerston North, 2.4m diameter mono-pile foundations embedded between 7m and 10m are being used to support the wind-turbines, as opposed to the more traditional pad foundation option. The site is underlain by highly variable greywacke rock, which varies across the site, from completely weathered clayey-silty-gravel material to essentially un-weathered (fresh) greywacke rock. In order to undertake engineering design and structural analysis of the foundations, the small strain elastic modulus profile with depth was required for each site. MASW was used to provide raw data in the form of seismic wave velocity profiles with depth for each turbine site. These velocity profiles were converted to elastic moduli profiles via their relationship to velocity and elasticity. Previously obtained geotechnical information from test pits and boreholes was used to constrain the modelling process and remove erroneous data sets. The resulting elastic moduli profiles were subsequently used by the structural engineers in their FEM analysis to calculate the embedment depth of each turbine foundation element.

In order to validate the initial assumptions and provide additional certainty each pile shaft was inspected after drilling, and the obtained data was used to back analyse the initial model.

As such, the MASW method was successfully used to obtain a large volume of data in a fast and economical manner. The mathematical model used was compared against and correlated with site observations and full scale testing. In summary, the test method achieved the set out requirements.

ACKNOWLEDGMENTS

The author would like to acknowledge the support of NZ Windfarms Ltd for allowing the discussion of the elastic moduli profile modelling undertaken as part of the mono-pile foundation design at Te Rere Hau Windfarm. Also, the author would like to acknowledge the assistance of Dr Jan Kupec in editing this paper.

REFERENCES

Connell Wagner (2008) *30616-001 Elastic Moduli Modelling, Te Rere Hau Windfarm, NZ Windfarms Ltd, 1 February 2008, Rev0.* Connell Wagner Ltd, Christchurch, NZ.

DSIR (1962) *Geological Map of New Zealand, 1:250,000, Sheet 11, Dannevirke.* Department of Scientific and Industrial Research, Wellington.

Das, B (2002) *Principles of Geotechnical Engineering, 5th Ed.* Wadsworth Group.

Kleffmann, S., Davey, F., Melhuish, A., Okaya, D., and Stern, T. (1998) Crustal structure in the central South Island, New Zealand, from Lake Pukaki seismic experiment. *New Zealand Journal of Geology and Geophysics, Vol. 41, 39-49.*

Kramer, S. (1996) *Geotechnical Earthquake Engineer.* Prentice Hall, New Jersey.

Southern Geophysical Ltd (2007) *Te Rere Hau Windfarm - MASW Geophysical Investigation of Turbine Site at Te Rere Hau Windfarm, 12 December 2007.* Southern Geophysical Ltd, New Zealand.

Wilun, Z. and Starzewski, K. (1972) *Soil Mechanics in Foundation Engineering – Volume 1.* Intertext Books, London.

Natural disaster events: Northland NZ, 2007

Rebekah A. McAteer
Tonkin & Taylor Ltd, Auckland, New Zealand

Keywords: Insurance, Landslip, Northland, EQC

ABSTRACT

This paper outlines the two storm events which occurred in the Northland region of New Zealand in 2007; the first in March and the second in July. The storm events both caused extensive flooding of the region which gave rise to civil defence emergencies as a result of the following natural disasters: landslips, land erosion, debris inundation and storm/flood damage.

The Earthquake Commission, New Zealand's primary provider of natural disaster insurance to residential property owners, was heavily involved in the assessment of the extent of damage to the region with natural disaster insurance claims numbering nearly 1000. This paper reviews both the greater than one in one hundred year storm events and resultant damage throughout the Northland region, focusing on the Whangarei area, as assessed by the Earthquake Commission consultant engineers. In addition, the paper investigates a number of claims that were inspected by the author, on behalf of the Earthquake Commission. The paper looks at the disaster that occurred, the mechanisms of failure, the impact the natural disaster caused and the proposed remediation of the natural disaster, as well as lessons learnt for a young geotechnical professional.

1 INTRODUCTION

As a young geotechnical engineer working for Tonkin & Taylor, there is a lot of "on the job" learning to be gained from assessing residential natural disaster damage claims for our client, the Earthquake Commission. The following sections of this report look firstly at the triggering mechanisms for a number of landslip claims lodged in 2007 and then at two specific case studies that the author assessed in the Whangarei area. The case studies outline a number of key lessons emphasised by assessing the specific claims.

2 STORM EVENT: MARCH 2007

From midnight of the 27th to approximately 5pm of the 29th March 2007, over 400mm of rain fell on the eastern coasts of Northland (Weston, 2007a). A cyclone in the Pacific, Cyclone Becky, caused moisture to be supplied to a low over New Zealand (NZWeather.net). The maximum recorded rainfall was at Glenbervie Hills, with a total of 438mm over the 2 days. The highest intensity rainfall recorded in Whangarei was 46mm/hr (Weston, 2007a). In Whangarei the storm return period was calculated as a 1:125 year event. The worst hit areas were in the Bay of Islands with a 1:150 year event (NIWA & GNS, 2007). Figure 1 (Niwa, 2007) illustrates the varying storm return periods across the region, with the highest return period on the north east coast in the Bay of Islands.

In Whangarei the storm water and waste water reticulation systems exceeded their capacities which resulted in surface flooding and sewerage contamination in the CBD during high tide.

3 STORM EVENT: JULY 2007

The storm event that occurred 10-11 July affected an even greater area than the March event, including much of the Northland, Auckland and Coromandel regions. Although significantly less rain fell over this period than during the storm in March, the ground was already saturated. The rainfall was accompanied by strong winds due to high pressure gradients between a high in the Southland region and two lows over the northern areas of New Zealand. Winds of up to 150km/hr

were recorded at the Tutukaka Coast. The maximum rainfall recorded in Whangarei was 180mm, with a maximum intensity of 40mm/hr (Weston, 2007b). This was classified as a 1:25 year event in Whangarei but was classified as being greater than a 1:100 year event in the Far North region (NIWA & GNS, 2007).

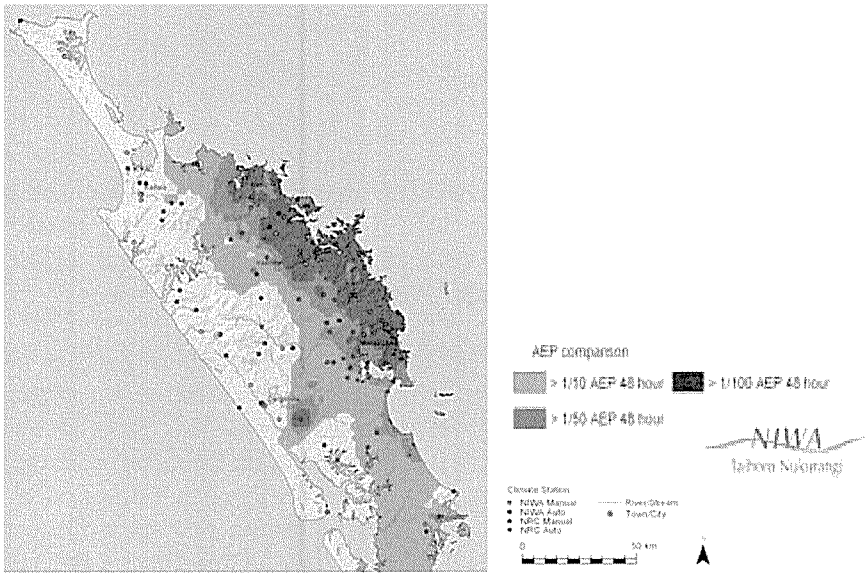

Figure 1: Annual Exceedance Probability Map: March Event (Niwa, 2007)

4 EQC COVER

The Earthquake Commission is New Zealand's primary provider of natural disaster insurance to residential property owners. The commission provides insurance in accordance with the Earthquake Commission (EQC) Act (1993) and covers the following natural disaster damage:

- Tsunami
- Earthquake
- Landslip
- Hydrothermal activity
- Storm/Flood damage to residential land
- Volcanic eruption
- Fire caused by any of the above

The general requirements of acceptance of a claim under the EQC Act are based on the criteria specified below (EQC, 2006):

- The property owner must have house insurance for the property, with a minimum of fire insurance; and
- the damage to land must be within 8m of the dwelling or appurtenant structure; or
- within 60m of the dwelling or appurtenant structure if the land is supporting the main access way or services; or
- within 60m of the dwelling or appurtenant structure if the damage involves a failed retaining wall supporting insured land.

Tonkin & Taylor Ltd, a New Zealand based environmental and engineering consultancy, was engaged by the EQC to assess the natural disaster damage claims that were lodged with the Earthquake Commission following the two storm events. Our role was to assess the validity and quantification of the claims within the confines of the EQC Act (1993).

A total of 968 claims were lodged as a result of the two storm events, of which Tonkin & Taylor assessed 829. The distribution of claims, as per the Tonkin & Taylor database, is illustrated in Figure 2. It can be seen from Figure 2 that the majority of claims were lodged by residents of the Bay of Islands and Kerikeri. This is consistent with the Annual Exceedance Probably (AEP) Map

shown in Figure 1, which indicates that the Bay of Islands experienced the greatest AEP in the Northland region during the March event.

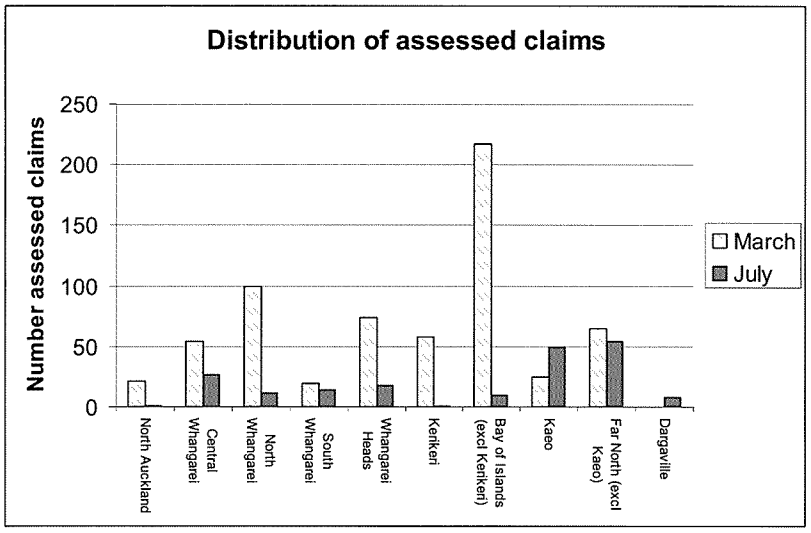

Figure 2: Geographical distribution of EQC claims assessed

5 CASE STUDIES

5.1 Parua Bay

This case study looks at a landslip that occurred at Parua Bay during the July 2007 event.

Parua Bay is located on the Whangarei Heads, to the south east of Whangarei City Centre. Published geology shows this area to be underlain by Hukerenui Mudstone (GNS, 1972). The site slopes moderately to the south west, where the two affected properties border the coast.

The landslip that occurred spans two neighbouring sections, over a width of 20m. The landslip extends to the contact with the shore platform (Figure 3), approximately 50m horizontally from the top of the landslip.

Borehole investigations undertaken in August 2007 indicate the site is underlain by a layer of fill. The depth of the fill ranges between 1.2m at the north eastern end of the site, near the building platform, to no fill at the south western end of the site, at the shore platform. Residual soils of the Hukerenui Mudstone underlie the fill to a depth of 4.4m below the ground surface at the north eastern end of the site. This depth becomes shallower towards the south west.

The failure surface was found to be at the contact between the residual soils and the underlying Hukerenui Mudstone. This is substantiated by the highly sheared clay layer at the top of the mudstone, which is consistent across all seven of the investigation boreholes undertaken.

The failure surface was pre-existing and had been creeping slowly for some time. This is evidenced by a previous claim by one of the property owners in 1999 for subsidence of land around their floor slab on the southern corner of the dwelling, in the direction of the current landslip. The creep movement was also evident in the visible damage on the properties such as slowly failing retaining walls. Further along from the subject properties, the contact between the Hukerenui Mudstone and the residual soils daylights onto the shore platform (Figure 3). It is apparent that the residual soils are sliding over the mudstone towards the coast. The presence of highly sheared surfaces, encountered during borehole investigation, at the contact between the residual soils and mudstone suggests historical and ongoing movement.

Figure 3: Residual soils sliding over mudstone as seen from shore platform

The most recent land movement was triggered by the high intensity storm event in July 2007 which reactivated the existing failure surface. Damage to the properties consisted of failure of retaining walls, extensive warping and displacement of a deck structure around the dwelling, tension cracks and hollows across the lawns, undermining of the concrete floor slabs and cracking of concrete paths and block work. This extensive warping of the ground surface and structures is consistent with a complex rotational failure mechanism.

Proposed remediation of the damage within the confines of the EQC Act consisted of an in-ground reinforced concrete palisade wall extending at least 5m into the mudstone unit and repair to the failed retaining walls on site. The intention of the palisade wall is to isolate the dwelling and services on the property and prevent further damage occurring to the property. Remediation of the land downslope of the proposed wall is not covered by the EQC Act as it is council reserve and not included in the Claimants' properties. Full stabilisation of the slope was not considered an economically viable solution.

This case study emphasises the need for investigation, even if only a site walkover, further away from the subject property and the immediate damage. The contact between the residual soils and the mudstone was only evident once investigation of the surrounding area was undertaken. The concept of *the bigger picture* and a good understanding of the geology and failure mechanisms are required in geological and stability models.

This case also shows the advantage of searching available data bases to research previous work undertaken on the property. By reading the previous reports from 8 years ago we were able to see what damage was historical and how much damage was as a result of the current landslip. We were able to see what repair work had previously been undertaken and could use this to predict further movement of the slip and damage to property.

5.2 Morningside

The second case study looks at a landslip that occurred in Morningside during the July 2007 event.

Morningside is a suburb of Whangarei, located 2 km south of Whangarei City Centre. Published geology shows this area to be underlain by Omahuta Sandstone of the Northland Allochthon (GNS, 1972). A hazard map of the area shows this area to be stability sensitive (WDC, 2000).

The site has been made level by the placement of fill around the building platform. This fill is retained by an un-engineered timber pole retaining wall, of 1.5m retained height with an embedment of 1.0m. Below the retaining wall the ground slopes steeply (~35°) to the south.

Borehole investigations show that the site is underlain by a layer of fill ranging from 0.5m at the base of the slope to 3.4m at the top of the slope. The fill is underlain by buried topsoil (highly plastic clays) and residual soils on weathered siltstone and sandstone. The weak rock occurs typically at a depth of 4m below the ground surface at the top of the slope.

The landslip that occurred after the July 2007 storm spans two properties, with a width of 35m and a horizontal length of 20m. Pressure ridges were observed at the toe of the slip, which is approximately coincident with the toe of the fill. The failure surface seems to follow the pre-filled land contour at the contact between the fill and the buried topsoil. This is illustrated in Figure 4.

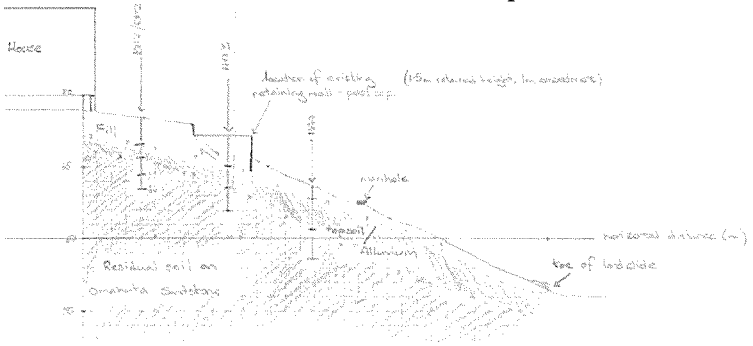

Figure 4: Cross section through landslip from north to south

Damage to the property included fence damage and land displacement, causing a 200mm head scarp and a vertical drop across the previously level section of approximately 1m (Figure 5). The head scarp runs perpendicularly through a sewer line connection, which was broken as a result of the landslip. This caused waste water to seep into the slope and resulted in contamination of the land. The embankment supporting the garage was undermined which posed threat of imminent risk to the garage. A number of appurtenant structures, including a garden shed and a washing line, were located on the landslip and were displaced downslope. The timber pole retaining wall remained intact but underwent vertical downward displacement of approximately 1m as the slip surface occurred beneath the embedment depth of the wall.

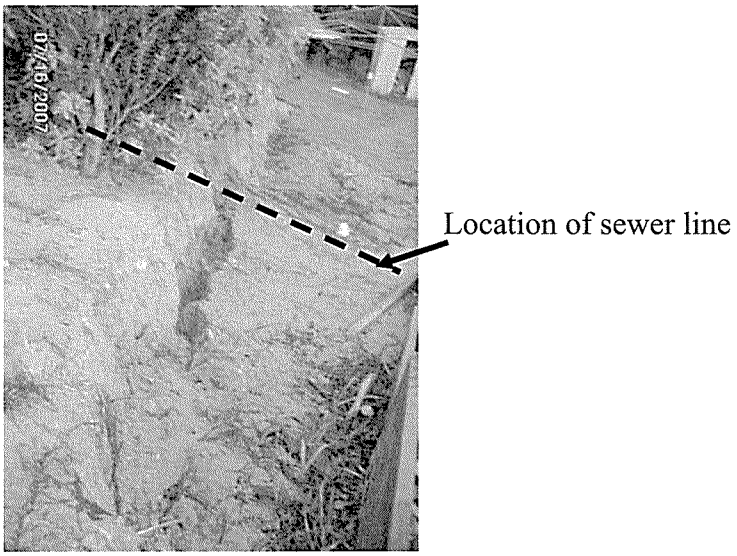

Figure 5: One metre vertical drop across section

Proposed remediation of the property included emergency works to fix the broken sewer line and remove contaminated land. Proposed permanent works consist of replacing the existing retaining wall with a properly engineered design. The total estimated cost to remediate the landslip and reinstate the evacuated land within the confines of the EQC Act (1993) was $84,000.

This case study emphasises the requirement for adequate subgrade preparation and fill placement. It also illustrates the need for sufficient geotechnical investigations for global stability of a retaining structure and design of adequate retaining structures to ensure the embedment is below any potential failure surfaces. We can also see the importance of researching published information, such as a regional hazard map or aerial photographs, to determine whether known historical failures have occurred in the area or are likely to occur in the future, given a triggering mechanism occurs. This is an important and easily accessed desk study tool when beginning geotechnical design.

6 CONCLUSIONS

The two storm events that hit the Northland region in March and July 2007 caused significant damage to residential properties, including a large number of landslips. The Earthquake Commission played a key role in the remediation of these residential landslips. Tonkin & Taylor was engaged to assess a number of the claims for the EQC within the confines of the EQC Act (1993). As a young geotechnical engineer a number of key lessons were learnt from assessing these claims, videlicet, the importance of the following aspects:

- adequate subgrade preparation and fill placement,
- looking at the surrounding area and *bigger picture* for evidence to indicate what geological mechanisms are occurring,
- utilising published information such as hazard maps and aerial photos,
- adequate drainage on slopes,
- having a good understanding of the geology and mechanism of the failure,
- properly engineered retaining systems, extending below potential global stability failure planes.

ACKNOWLEDGEMENTS

I would like to thank the Earthquake Commission for their permission in letting me use these case studies. I would also like to thank Tonkin & Taylor for supporting me and encouraging me in writing this paper and attending the 8th Young Geotechnical Professionals Conference.

REFERENCES

Earthquake Commission (1993) *Earthquake Commission Act.* Earthquake Commission.

Earthquake Commission (2006) *A Guide to Making a Claim with EQC.* Earthquake Commission.

GNS Science (1972) *Geological Map: North Island.* GNS Science

Niwa, GNS Science (2007) *Natural Hazards 2007.* A joint publication between Niwa and GNS Science.

NZ Weather (February 2007), *Tropical Cyclone Becky* [online] Available: http://www.nzweather.net/forum/international-weather/142-tropical-cyclone-becky.html

Weston, S (2007a) *Storm Event – March 2007.* Whangarei District Council

Weston, S (2007b) *Storm Event – July 2007.* Whangarei District Council

Whangarei District Council (2000) *Whangarei District Hazard Maps (Map 43) – 2000.*

NZ Weather (February 2007), *Tropical Cyclone Becky* [online] Available: http://www.nzweather.net/forum/international-weather/142-tropical-cyclone-becky.html

Rock socketed pile foundations - design methods for evaluating axial capacity

Paul McClean
Maunsell Limited, Auckland, New Zealand.

Keywords: rock socket, pile foundation, side resistance, base resistance.

ABSTRACT

Methods for determining the axial capacity of rock socketed pile foundations yield vastly varied results. While the theoretical basis for analysis is widely understood in terms of the mechanisms that govern rock-structure interaction, the methods of design are geologically dependent and widely dispersed throughout the literature relating to the subject. The application of this knowledge to design depends primarily on the structural characteristics of the rock mass. Design methods must consider all possible failure modes and this paper outlines the range of approaches that may be employed to ensure a rock socketed foundation design is compatible with geological conditions. Each method has limitations based on its underlying assumptions and perceived application. A sound design process will incorporate both a thorough geological investigation and field testing to ensure that the assumptions of the analysis reflect the practical constraints of the physical problem.

1 INTRODUCTION

Rock socketed pile or shaft foundations are commonly employed to transfer relatively large loads to an underlying rock mass as demonstrated in Figure 1. An appreciation of the mechanisms that govern the interaction between the rock and the structure may be grasped on the basis of simple physical principles. The challenge to the engineer however, lies in the application of these principles to geological conditions that are often derived from incomplete and imperfect data. It is the incorporation of this inherent uncertainty into the geotechnical design process that ultimately determines the effectiveness of the design. Historically, this process has lacked sophistication leading to crude and conservative estimates of capacity. This has been demonstrated by the rarity of failure even in the case of tests undertaken specifically to determine ultimate capacity. Recently, however there has been a concerted effort to both expand and interpret the database of load tests on rock socketed pile foundations and to apply the advances of the more general field of rock mechanics to the pile design process.

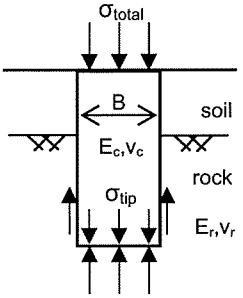

Figure 1: Axially loaded rock socket

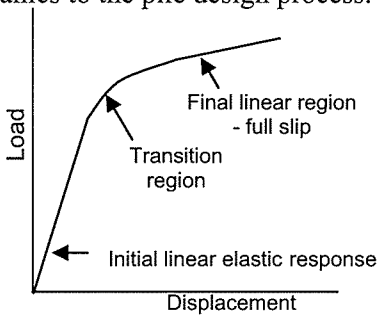

Figure 2: Generalised load-displacement behaviour

2 GENERALISED ROCK SOCKET BEHAVIOUR

The load displacement behaviour of an axially loaded rock socket foundation is generally characterised by the three distinct stages shown in Figure 2. Each of these stages reflects a slightly different interaction between the concrete structure and the rock. Initially the foundation responds in a linear elastic manner as relatively small loads induce shear stresses along the vertical shaft-rock interface. This first stage of loading is initially resisted by adhesive

cementation of the concrete to the rock but is also assisted by a frictional component that increases as greater vertical loads induce higher normal forces at the interface.

Following this, further load increase leads to a nonlinear transition region representing the onset and progression of slip at the rock-structure interface. As slip progresses a greater portion of load is transferred to the base until eventually the full side resistance is mobilised and the entire surface of the rock-structure interface begins to rupture. Rupture results from exceedance of the adhesive component of resistance resulting in greater mobilisation of the frictional sliding component and the onset of resistance due to mechanical dilatancy.

As displacement progresses more load is transferred to the base and side resistance decreases to a residual frictional state. The load-displacement behaviour of the pile again reverts to a linear response until a peak compressive strength is reached corresponding to a bearing failure of the rock beneath the base of the foundation.

3 SIDE RESISTANCE

3.1 General

Traditional approaches to the estimation of the available side resistance of rock socketed foundations have been described by a number of experts as 'unsophisticated' (Kulhawy et al 2005), 'crude' (Rowe & Armitage 1987) and 'overconservative' (Seidel & Collingwood 2001). This traditional approach is based on the empirical correlation of uniaxial compressive strength (q_u) to shaft resistance as measured by static load testing. The resulting data is widely scattered and it has been demonstrated that in addition to rock strength there are a number of other factors that influence the side resistance capacity. Essentially, the traditional approach represents the empirical derivation of a lower bound estimate of capacity and has emphasized construction observation to verify assumptions and allow refinement of the design. It can be argued that there is much to be gained by establishing a design procedure that incorporates all contributing factors into the earlier stages of design as this may reduce the reliance on costly load testing and provide greater certainty of the assumptions made at the preliminary design stages.

3.2 Analysis Methods

Since the mid 1970s a number of models have been developed for the evaluation of the side resistance of rock socketed pile foundations based on the empirical relationship with uniaxial compressive strength. The general design method has developed iteratively as the database of recorded load tests has expanded and the proposed relationships have been reviewed. A significant development in this process was the incorporation by Kulhawy & Phoon (1993) of the Bloomquist & Townsend (1991) and McVay et al. (1992) databases into the database developed by Rowe & Armitage (1987). For consistency, Kulhawy & Phoon (1993) normalised all stresses by atmospheric pressure (p_a) and averaged the data for each test site. A general relationship between uniaxial compressive strength and ultimate side resistance (f_{su}) was derived Eq.(1). Linear regression analysis suggests that a value of 2 for the coefficient C correlates to the mean behaviour and a value of 1 to the lower bound. This is consistent with the correlations previously suggested by Rowe & Armitage (1987).

$$\frac{f_{su}}{p_a} = C \times \left(\frac{q_u}{2p_a} \right)^{1/2} \qquad (1)$$

Recent re-examinations of this relationship (Kulhawy et al. 2005) (Kulhawy & Prakoso 2007), have provided further validation for the model but emphasize the importance of direct uniaxial compressive testing rather than derivation from simpler tests. It has also been noted that artificially roughened sockets or foundations constructed in rock with known and quantified roughness characteristics may allow C values greater than 1. The use of such values should however be substantiated by load testing or local experience.

The method outlined above is limited to the empirical relationship between intact rock strength and side resistance and neglects all other factors that could influence socket behaviour. Therefore, in the absence of load testing or local knowledge it should be applied conservatively.

There have however, been some attempts to identify and quantify all of the factors that influence shaft resistance, and incorporate these into a coherent design method. In particular, Seidel & Collingwood (2001) have derived a parameter known as the shaft resistance coefficient (SRC) that incorporates socket roughness, rock mass modulus, Poisson's ratio, socket diameter, construction processes and insitu stress into the analysis procedure. It relates these to an adhesion factor that can then be applied to the uniaxial compressive strength to estimate the ultimate side resistance. However, due to the limitations in accurately quantifying some of these factors it is not currently feasible to directly apply these methods to design and they should only be utilised within the limitations of accepted empirical relationships. As records of the application of this method are still somewhat limited, verification through load testing and local experience remains a necessity and any economic advantage of applying these more complex design procedures will be dependent on developments within the field of rock mass characterisation, and the growth and application of a load test database.

4 BASE RESISTANCE

4.1 General

The proportion of axial working load that is transmitted from the top to the base of a rock socketed pile foundation is highly variable and primarily dependent on the embedment and modulus ratios. The progressive behaviour of the rock-structure interaction, as described in previous sections, is also significant as base resistance is typically mobilised at greater displacements than side friction. This means that the bearing strength of the rock beneath the tip of the pile can not be fully utilised until slip has occurred and side resistance reduced to a residual value. This has led some authors to suggest that base resistance should only be relied on to resist a fractional portion of the total axial load (Carter & Kulhawy 1988).

Methods for determining the base resistance of rock socketed pile foundations are generally based on the bearing capacity equation for soil with appropriate modifications made for geological conditions. In particular rock mass properties, and discontinuity spacing, orientation and condition have a significant influence on ultimate base resistance. It is imperative that these variables are adequately characterised to ensure the appropriate analysis method is employed.

4.2 Intact or Massive Rock Mass

The failure mode for massive or intact rock is dependent on ductility. Brittle rock will typically undergo a local shear failure with crushing at the foundation edge developing into patterns of wedges and slip surfaces as shown in Figure 4a. These surfaces terminate within the rock mass rather than propagating to the ground surface. Bearing failure in ductile rock exhibits a similar failure mechanism however the slip surfaces develop into well defined wedges that extend to the ground surface leading to a general rather than local shear failure. This failure mode is illustrated in Figure 4b. Theoretically, these cases can be evaluated by applying the general bearing capacity equation which for foundations bearing on intact rock reduces to Eq. (2).

Rowe & Armitage (1987) recommend limiting the value of N_c to 2.5. This is based on field test data and the pressure required for the onset of first failure according to incipient failure theory. For the design of rock socketed foundations on intact or massive rock, Eq. (3) is recommended:

$$q_{ult} = N_c q_u \quad (2)$$

$$q_{ult} = 2.5 q_u \quad (3)$$

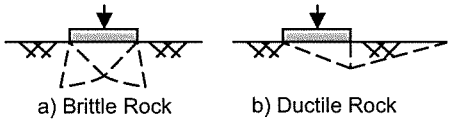

Figure 4: Bearing capacity failure mode for intact

4.3 Jointed Rock Mass

The behaviour of a rock socketed foundation constructed on a jointed rock mass is dependent on the properties of both the rock material and the discontinuities. The response of the foundation to loading may be anisotropic, non-linear or stress-dependent and it is imperative that the design method accounts for the particular geological conditions that dictate the mode of response.

For rock masses with near vertical joints the failure mode is dictated by the spacing and aperture of the discontinuities. If the discontinuity spacing (s) is less than or equal to the foundation diameter (b) and the joints are open, failure is likely to occur by unconfined compression of the rock columns as shown in Figure 5a. The ultimate bearing capacity is then estimated according to the Mohr-Coulomb failure criterion. With the assumption of zero minor principle stress or uniaxial compression, this reduces to Eq. (4).

Alternatively, if these steeply dipping joints are closed a general wedge failure may develop as shown in Figure 5b and the bearing capacity equation Eq. (5)[1] provides a more appropriate method of analysis.

$$q_{ult} = q_u = 2c \tan(45° + \varphi/2) \quad (4)$$

$$q_{ult} = cN_c s_c + (B/2)\gamma N_\gamma s_\gamma + \gamma D N_q s_q \quad (5)$$

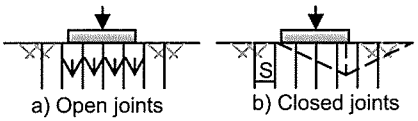

Figure 5: Bearing capacity failure mode for closely spaced steeply dipping jointed rock masses

For cases where steep discontinuities are present at spacing greater than the foundation diameter, failure will occur by splitting which will lead to a general shear failure as shown in Figure 6. Again, based on the Mohr-Coulomb failure criterion a modified version of the bearing capacity equation has been derived for this case Eq.(6). This incorporates a correction factor (J), refer to Figure 7, for the thickness of the foundation rock (H) and the width of foundation (B), and a bearing capacity factor (N_{cr}) which is derived with the assumption that no stress is transmitted across the vertical discontinuity Eq. (7) and (8) (Kulhawy & Goodman 1980).

$$q_{ult} = J\, c\, N_{cr} \quad (6)$$

$$N_{cr} = [2N_\varphi^{0.5} / (N_\varphi - 1)] \times [N_\varphi (S/B)^{(1-1/N_\varphi)} - 1] \quad (7)$$

$$N_\varphi = \tan^2(45 + \varphi/2) \quad (8)$$

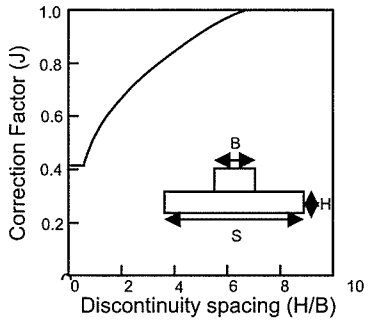

Figure 7: Correction factor (J)

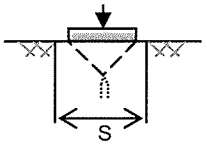

Figure 6: Bearing capacity failure mode for widely spaced steeply jointed rock masses

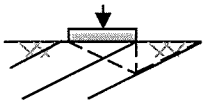

Figure 8: Bearing capacity failure mode for moderately dipping jointed rock masses

For cases of moderately dipping discontinuities, failure is likely to occur along the discontinuity plane as shown in Figure 8. The strength of the discontinuity will be considerably less than that of the rock mass. An assessment of the base resistance capacity is still conducted in terms of the

[1] Shape factors for Eq.5 are: $s_c = 1+N_q/N_c$
$s_\gamma = 0.6$
$s_q = 1+\tan\varphi$

general bearing capacity equation (Eq. 5), however strength parameters should be representative of the joints and the first term neglected due to the uncertainty of the cohesion component of shear strength along joint surfaces.

4.4 Fractured Rock Mass

A fractured rock mass will also fail in general shear as shown in Figure 9, but the failure surface is likely to be irregular as a result of the closely spaced joint sets and variable rock strength. The bearing capacity equation may be applied to this case but the shear strength parameters (c', φ') must be representative of the rock mass. This is further complicated by the non-linearity of the fractured rock mass failure envelope and in this situation it is advisable to apply some of the more recently developed principles of rock mechanics to the rock socketed pile design process.

In particular, the Hoek-Brown failure criterion (Hoek et al. 2002) provides an approach that incorporates geological observation into the quantitative foundation design process. By generally quantifying rock mass and discontinuity characteristics the Hoek-Brown strength criterion Eq. (9) is derived. The Hoek-Brown strength parameters (m_b, s, a) can then be correlated to the Mohr-Coulomb parameters (c', φ') for a given stress range or utilised directly in the foundation design process.

The incorporation of the Hoek-Brown strength parameters into rock socketed foundation design assumes that the failure mode can be approximated by active and passive wedges as shown in Figure 10. Within the active zone, σ'_1 at failure is equivalent to the ultimate bearing capacity. According to equilibrium conditions σ'_3 in the active zone is assumed to be equal to the σ'_1 in the passive zone. σ'_3 in the passive zone may be conservatively assumed to be zero. For the passive zone these assumptions reduce Eq. (9) to Eq. (10).

$$\sigma'_1 = \sigma'_3 + q_u [(m_b \sigma'_3/q_u)+s]^a \quad (9)$$

$$\sigma'_1 = q_u s^a = \sigma'_H \quad (10)$$

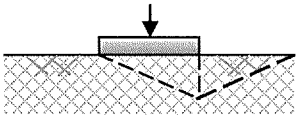

Figure 9: Bearing capacity failure mode for a fractured rock mass

Again, to satisfy equilibrium the horizontal stress in the passive zone must be equivalent to that of the active zone, or rather the active zone σ'_3 must be equal to $q_u s^a$. The ultimate bearing capacity of a foundation can then be determined according to Eq. (11). In the case of rock socketed foundations where the bearing elevation is often relatively deep, the insitu vertical stress ($\sigma'_{v,b}$) may be significant and it may be overly conservative to assume that it is zero. This can be incorporated into the above derivation by assuming that σ'_1 in the passive zone is equal to Eq (12). Substituting this into the Hoek-Brown failure criterion for the active zone gives the ultimate bearing capacity Eq. (13).

$$q_{ult} = q_u [s^a + (m_b s^a + s)^a] \quad (11)$$

$$A = \sigma'_{v,b} + q_u [(m_b \sigma'_{v,b}/q_u)+s]^a \quad (12)$$

$$q_{ult} = A + q_u [(m_b A/q_u)+s]^a \quad (13)$$

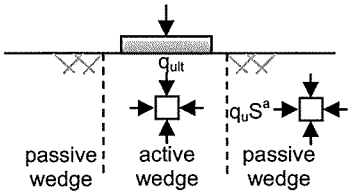

Figure 10: Active and passive wedges beneath a foundation on a fractured rock mass

5 CONCLUSIONS

The traditional approach to estimating the side resistance of rock socketed pile foundations is inherently conservative and emphasizes the observational phase of design. This is due to the fact that the method is empirically based on only one of several independent variables. While recent developments have made optimistic advances towards incorporating all contributing factors it is still recommended that design is conducted within accepted empirical limits unless verified by load testing or local experience. Immediate advances in this field of foundation

engineering may be more forthcoming from local and regional based research that builds on the accepted empirical relationships within the framework of wider global developments. The expansion of local load test databases and the subsequent correlation to rock mass characteristics may eventually shift the relative weighting in the design process from construction verification to geological investigation and characterisation allowing greater certainty in preliminary design assumptions.

The general bearing capacity equation provides a rational basis for the estimation of the base resistance of rock socketed pile foundations however it must be applied in accordance with the geological conditions of the site. Accurate geological characterisation of rock mass and discontinuity properties allows assumptions to be made about the expected bearing failure mode. These assumptions lead to the derivation of alternative forms of the bearing capacity equation and the adoption of certain strength parameters depending on the specific geological conditions. Analysis and design should address all of the possible failure modes and it is evident that a more detailed investigation phase will narrow the range of applicable design methods.

To ensure that real engineering value is added to the development of structures that are constructed on rock socketed pile foundations, it is imperative that a thorough geological investigation is undertaken to define the nature of the problem and allow the appropriate design method and strength parameters to be applied. Load testing or local experience is also necessary for both verification and refinement of the design. Failure to incorporate these aspects into the progressive process of rock socketed pile design necessitates a conservative solution.

REFERENCES

Bloomquist, D. & Townsend, F.C. (1991) Development of insitu equipment for capacity determinations of deep foundations in Florida Limestones. *Report to Florida Department of Transportation*, University of Florida, Gainesville, Florida.

Carter, J.P. & Kulhawy, F.H. (1988) Analysis and design of drilled shaft foundations socketed into rock. *Report EL-5918, Electric Power Research Institute*, Palo Alto, California.

Hoek E., Carranza-Torres, C. & Corkum, B. (2002) Hoek-Brown failure criterion – 2002 edition. *Proceedings of the North American Rock Mechanics Society Meeting*, Toronto.

Kulhawy, F.H. & Goodman, R.E. (1980) Design of foundations on discontinuous rock. *Proceedings of the International Conference on Structural Foundations on Rock*, Sydney, Australia.

Kulhawy, F.H. & Phoon, K.K. (1993) Drilled shaft side resistance in clay soil to rock. *Geotechnical Special Publication No. 38: Design and Performance of Deep Foundations*, New York.

Kulhawy, F.H., Prakoso, W.A. & Akbas, S.O. (2005) Evaluation of capacity of rock foundation sockets. *Alaska Rocks 2005, Proceedings of the 40th U.S symposium on Rock Mechanics*, Anchorage, Alaska.

Kulhawy, F.H. & Prakoso, W.A. (2007) Issues in evaluating capacity of rock socket foundations. *Proceedings of the 16th Southeast Asian Geotechnical Conference*, Kuala Lumpur.

McVay, M.C. (1992) Design of socketed drilled shafts in limestone. *Journal of Geotechnical Engineering*, Vol. 118, No. 10.

Rowe, R.K. & Armitage, H.H. (1987) A design method for drilled piers in soft rock. *Canadian Geotechnical Journal*, Vol. 24.

Seidel, J.P. & Collingwood B. (2001) A new socket roughness factor for prediction of rock socket shaft resistance. *Canadian Geotechnical Journal*, Vol. 38.

Impacts of pond leakage on stability of a 20m outwash gravel terrace in Mid Canterbury

Mandy Mills
Beca Infrastructure Ltd, Auckland, NZ

Keywords: liner material, low permeability layers, outwash gravel terrace, pond leakage, slope stability, storage ponds.

ABSTRACT

Ponds capable of storing 4,500,000m^3 of water are required to service the largest privately operated irrigation scheme in New Zealand. The ponds will be located on an outwash gravel terrace, some 20m above the Rangitata River plain in Mid Canterbury.

A challenge was identifying suitable liner material available locally to limit leakage and costs. A suitable material was identified in the surficial weathered alluvial soils on site, which has a sufficient percentage of clay to achieve a hydraulic conductivity of 4 x 10^{-9}m/sec, limiting leakage from the total pond area to less than 40l/s.

A concern was that low permeability layers might exist at depth and water leaked from the ponds would perch above these layers, potentially reducing the stability of the terrace slope. A suitable set-back would therefore be required to minimise risk to the ponds.

Geotechnical investigations identified the presence of such low permeability layers. Computer modelling using SEEP/W and SLOPE/W was used to predict the amount of leakage from the ponds and the effect on stability of the terrace under both static and seismic scenarios.

1 INTRODUCTION

The Mayfield Hinds irrigation scheme is the largest community irrigation scheme in New Zealand with an irrigable area of 32,000ha. The scheme is owned and operated by Mayfield Hinds Irrigation Society Ltd (MHIS). The scheme is permitted to take up to 16.5m^3/sec from the Rangitata Diversion Race (RDR), however, fluctuating flows in the Rangitata and Ashburton Rivers mean 16.5m^3/sec is not always available. Consequently, there are periods during the year when the scheme cannot meet demand and other times when consented water is not fully utilised by irrigators.

Currently, only small private storage facilities are available as part of the RDR to store unutilised water for use when water demand exceeds supply. MHIS proposes to develop an irrigation storage scheme on a block of land located on the Canterbury Plains some 1,500m east of Arundel, Mid Canterbury. The site is 172.58ha in area and located on a relatively flat terrace, some 20m above the Rangitata River bed (Figure 1).

Three ponds are proposed, with a total nominal storage capacity of 4.5Mm^3. The ponds will be of equal size, up to 3.7m deep and will step down to suit the sloping topography.

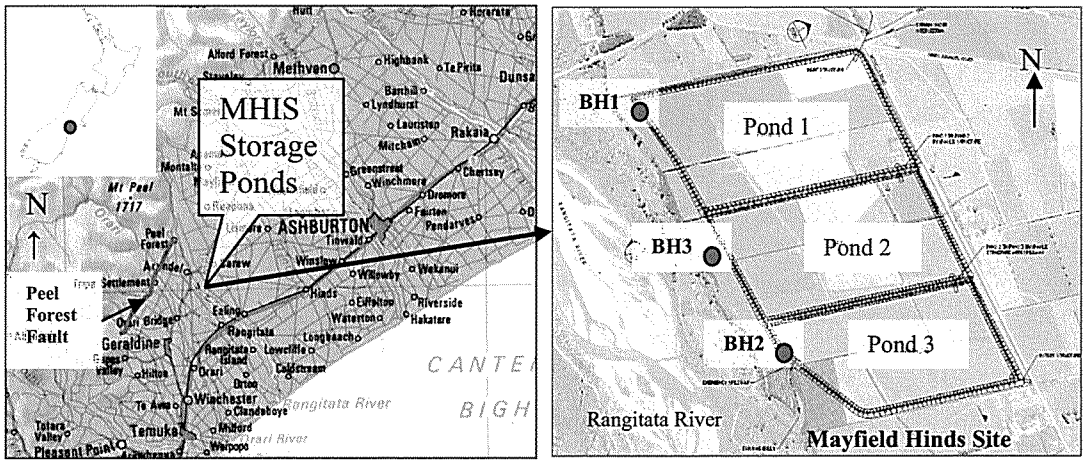

Figure 1: Location map of Mayfield Hinds site

2 SITE GEOLOGY

The basement rock is Torlesse Group greywacke and argillite, unconformably overlain by younger multiple glacial and interglacial deposits. The glacial deposits are unsorted gravels deposited during ice advances on the inner-most margins of the Canterbury Plains. The interglacial deposits result from periods of climatic warming where rivers cut down through the glacial deposits developing terraces. The interglacial deposits comprise mainly alluvial sandy silts and loessic clayey soils developed on each glacial terrace.

The closest mapped active fault is the SW-NE trending Peel Forest Reverse Fault located some 7km NW of the site. The fault trace is some 18km long, extending from Four Peaks to Peel Forest (Figure 1).

3 POND LINER

The suitability of site surface and subsurface soils for use as a liner to the ponds was investigated by excavating 19 test pits.

The generalised soil profile (Figure 2) comprises:

- Up to 0.32 m of topsoil; dark brown organic SILT with minor clay, minor gravel and trace sand (Layer 1); over
- Up to 0.55 m of Burnham Formation gravelly SILT with some sand and trace clay (Layer 2); over
- Tightly packed, non-plastic sandy GRAVEL (Burnham Formation), at least 0.5 m thick in the test pits (Layer 3).

Bulk samples were collected from each pit and taken to the laboratory for hydrometer, wash grading and triaxial permeability testing for the purpose of determining whether the soils are suitable for use as a liner for water retention. A suitable liner requires a soil with a high percentage of fines (clay and silt size particles) and a low permeability (i.e. preferably down to 1 x 10^{-9}m/sec).

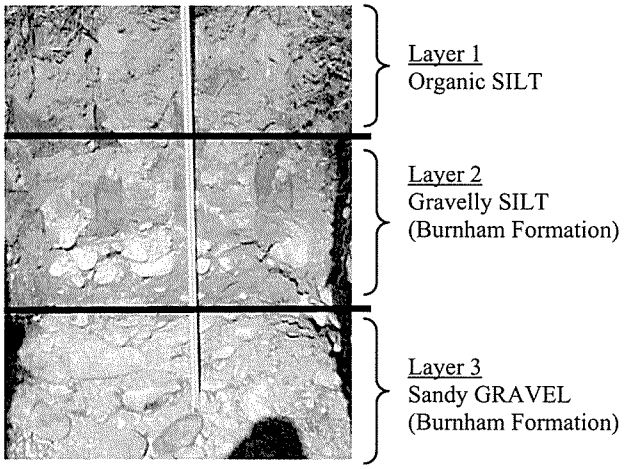

Figure 2: Generalised soil profile

3.1 Laboratory testing results

The following summarises laboratory testing results:

Table 1: laboratory testing results

Layer	Hydrometer (%)		Wash Grading (%)		Triaxial Permeability Testing
	Clay	Silt	Clay	Silt	
1	Range: 12 - 16 Mode.: 12	Range: 55 - 65 Mode.: 61	-	-	4×10^{-9} m/s (12 % clay; 65% silt)
2	Range: 0 – 18 Mode: 1	Range: 1 - 62 Mode: -	-	-	3.3×10^{-9} m/s (12 % clay; 45 % silt)
3	1	4	Range: 0 - 1 Mode: 0	Range: 0 - 5 Mode: 4	-
1 & 2	13	62	-	-	Range: 1.6 - 2.5 x 10^{-9} m/s

3.2 Liner design

On average a thickness of about 500mm of low permeability material from Layers 1 and 2 could be collected for use as a liner. This material could achieve a permeability of the order of 4×10^{-9}m/sec if carefully compacted in two layers of not less than 250 mm thickness, which could maintain leakage to less than 40l/s for a maximum pond depth of 3.7m.

Layer 3 has a low percentage of fines and is therefore not recommended for use in a liner and should not be mixed with Layers 1 and 2.

4 SLOPE INSTABILITY & SUITABLE SETBACK DISTANCE

The identification of low permeability material at the surface suggests that similar layers or lenses may exist at depth. The presence of these layers could encourage additional water, leaked from the ponds, to perch above these layers, eventually resulting in horizontal flow towards the terrace slope leading to instability and thus threatening the storage ponds.

Three machine boreholes to a depth of 25m were drilled along the terrace slope edge to determine whether low permeability layers exist at depth (Figure 1).
The investigation identified layers (up to 2m in thickness) of gravel in a plastic matrix of silt, sand and clay (aquiclude) at different depths in each borehole. Saturated zones (ranging from 0.1m to 1.8m in thickness, typically 1.2m) were identified above the aquicludes. The random irregular depth distribution of the layers between boreholes suggests they are likely to be discontinuous.

4.1 SEEP/W analysis

Steady state seepage modelling was undertaken using the computer software SEEP/W to provide an assessment of the existing hydrogeological conditions (Model 1) and the effect of the proposed irrigation ponds on groundwater levels, particularly mounding above low permeable layers part way up the bank (Model 2). The following parameters were used for seepage modelling.

Table 2: Hydrogeological parameters

Unit		K^1 (m/s)	Kv/Kh	Comments
1	Topsoil	1×10^{-7}	1.0	Allows for the discontinuous nature of this unit.
2	Non Plastic Gravel (Burnham Formation)	1×10^{-4}	1.0	Takes into account presence of low permeability lenses within the unit.
3	Low permeability lens (Burnham Formation)	1×10^{-9}	1.0	Used to model the "worst case scenario".
4	Water Race Liner	5×10^{-9}	1.0	Calibration modelling suggests that the existing liner is this order of K. This is reasonable given there is minimal water loss from the water race.
5	Pond Liner	4×10^{-9}	1.0	Takes into account contractor faults e.g. inclusion of minor permeable material when mixing Layers 1 & 2 and locally poor liner compaction.
[1.] K = Hydraulic Conductivity				

Model 1 was calibrated to the measured regional groundwater level of 22mBGL. The model was also calibrated to the saturated zone identified 1.0m above the aquiclude formed some 8.0mBGL in MB3. The saturated zones appear to be largely caused by seepages already in the system from distant sources NW of the site. Leakage from an unlined water race, which flows through the site, contributes a measurable volume of water however contribution from rainfall or irrigation would be relatively less.

Model 1 was modified to include the proposed irrigation pond (Model 2). The pond embankment was set 50m back from the terrace crest. The maximum water depth in the pond was assumed to be 3.7m. Modelling indicates that the presence of the irrigation pond would raise the saturated zone above the modelled aquiclude by around 1.2m. The regional groundwater level remains the same; this is expected because additional water entering the system from pond leakage would mostly flow laterally above the aquaclude with minor seepage progressing down to the regional groundwater table. In reality, the lenses appear discontinuous

and therefore a similar rise in the regional groundwater table may occur with a smaller rise in the saturation zones above the aquicludes.

4.2 SLOPE/W stability analysis

4.2.1 Model setup

A slope stability analysis using the computer software SLOPE/W was undertaken to provide an assessment of the current slope stability of the terrace under existing conditions and post-pond construction; and under seismic loading with the ponds in place. The slope and soil profile and groundwater levels used for this slope stability analysis were obtained from the SEEP/W output files. It is assumed that the slope consists mainly of non-plastic gravels.

Table 3: Soil parameters for stability analysis

Description	Unit Weight (kN/m3)	Ø' (degrees)	c' (kPa)	Undrained Shear Strength (kPa)
Non plastic GRAVEL	19	34	0	N/A

The following cases were analysed using SLOPE/W:

Table 4: Cases analysed using SLOPE/W

Case	Analysis	Static	Seismic
1	Slope stability under existing conditions	✓	
2	Post-pond construction	✓	
3	Ponds in place and a horizontal acceleration of 0.2 g (1 in 500 year return period)		✓
4	Ponds in place and a horizontal acceleration of 0.3 g (1 in 1000 year return period)		✓
5	Sensitivity analysis; ponds in place with 0.2 g (1 in 500 year return period) plus an elevated regional groundwater level		✓
6	Ponds in place plus a saturated toe of the terrace slope	✓	✓

4.2.2 Results

Modelling suggests that shallow surficial failures within 10m of the terrace edge could be expected (Table 5). This is confirmed by the numerous debris fans along the toes of the gravel terrace face, which indicate marginal stability. The bank stands at present due to the reinforcing effects of the vegetation and the tree roots on the surface. Increasing the saturation zone by 1.2m above the low permeability lens would decrease the factor of safety (FOS) of the existing slope by a small margin to a FOS < 1.5.

A seismic event with a horizontal acceleration (PGA) of up to 0.3 (1 in 1000 yr return period) will decrease the FOS and slumps may occur within about 25m of the terrace face. However, such movements would be unlikely to affect the ponds set back 50m from the top edge of the terrace.

As a sensitivity analysis, the regional water table was artificially elevated by about 3.0m to saturate the bottom of the terrace; this appears to have a minor effect on the overall slope stability.

Modelling demonstrates that a setback distance of 50m from the terrace edge to the pond embankment is considered sufficient to avoid a major bank failure causing a breach of the pond walls.

Table 5: Results from SLOPE/W analysis

Case	FOS - Distance[1]			Distance to back-scarp at FOS = 1.5
	10 m	20 m	25 m	
Static				
Case 1: Existing Conditions	0.98	1.44	>2.0	20 m
Case 2: Post Pond Construction	0.98	1.45	>2.0	20 m
Seismic				
Case 3: 500/year return period	0.68	1.02	>2.0	20 m
Case 4: 1000/year return	0.58	0.84	>2.0	21 m
Case 5: Sensitivity	0.69	1.09	>2.0	20 m
[1]Distance to back-scarp of slip measured from terrace crest edge.				

5 CONCLUSION

MHIS is proposing to construct a new irrigation water storage pond on their 174ha property on a relatively flat terrace, some 20m above the Rangitata River.

Suitable material for use as a pond liner is available from the top 0.5m of soil on site, which is capable of achieving an average permeability of 4 x 10^{-9}m/s when compacted into a liner 0.5m thick and is expected to maintain pond leakage to less than 40l/s.

Aquicludes up to 2m in thickness were identified at various depths in 3 boreholes drilled to 25m depth along the terrace edge. Resting above these aquicludes are saturated zones (perched water tables), typically around 1.2m thick. Seepage modelling identified an increase in thickness of the saturated zones by around 1.2m during pond operation. Analyses suggest that slope instability along the terrace edge is unlikely to pose a risk to the ponds at the proposed set-back distance of 50m.

REFERENCES

Beca (2007a) *Mayfield Hinds Irrigation Storage – Geotechnical Report.* Prepared for Mayfield Hinds Irrigation Society Ltd.

Beca (2007b) *Mayfield Hinds Geotechnical Report 2 – Groundwater & Slope Stability Modelling.* Prepared for Mayfield Hinds Irrigation Society Ltd.

Earthworks design & construction monitoring for the Macarthur Resource Recovery Park

Peter Oitmaa
Douglas Partners Pty Ltd, Sydney, Australia

Keywords: earthworks, excavation, filling, stabilisation, subsidence

ABSTRACT

The Macarthur Resource Recovery Park is a state of the art waste recovery facility currently being commissioned in south-western Sydney. The processing facility is adjacent to an existing landfill operation which will soon become redundant. The plant is the first step towards greatly improved waste handling for Sydney.

A lack of useable space on the site meant extensive earthworks were required to construct a building platform for the plant. The location of the plant presented numerous geotechnical challenges including 35 m high cuts in weathered rock, rock-slope stabilisation, 25 m high reinforced filling emplacements, earthworks testing and control, and remedial pressure grouting of storm-damaged subsidence areas.

This paper provides a case history of the project and presents some of the challenges faced during planning, design and construction.

1 INTRODUCTION

The Macarthur Resource Recovery Park is a $50M state of the art waste recovery facility currently being commissioned in south-western Sydney. The facility is being developed by WSN Environmental Solutions, a state-owned corporation that operates Australia's largest waste management network. The landfill space at Jack's Gully Waste Management Centre (WMC) was running out when it was decided to construct a new facility to better handle waste that may otherwise have been sent directly to landfill.

The new plant has been designed to divert 85% of household waste from landfill using the latest technology to better recover components of the waste that can be reused or recycled (WSN, 2008). The site for the proposed plant required extensive earthworks in order to meet the design requirements. Douglas Partners Pty Ltd was commissioned to provide earthworks design and construction monitoring services for the project.

2 SITE DESCRIPTION

2.1 Location and topography

The client selected a site for the facility which was adjacent to an existing landfill area at Jack's Gully WMC near Narellan in south-western Sydney. The site was bounded by a landfill cell and leachate collection ponds to the north, a small former quarry to the east, a coal washery and machinery sheds to the south, and the Nepean River to the west. The platform required for the facility was to be approximately 360 m by 80 m and relatively level.

At the commencement of the design works the topography of the site included:

- A tree-lined gully at the western end of the site which was up to 25 m below the proposed platform level;
- A steep rock slope up to 35 m above the proposed platform level along the southern edge of the site; and
- Steep rock slopes between 10 m and 25 m high along the northern side of the proposed platform against which engineered filling would be required to extend the platform boundary.

2.2 Geology

Published information (Department of Mineral Resources, 1985) indicated that the site is generally underlain by the Bringelly Shale which is a fine-grained sedimentary rock of Triassic age. Bringelly Shale typically comprises shale, carbonaceous claystone, laminite and some coal. Bands of lithic sandstone are also often present within the shale unit.

Field observations confirmed this geological setting. There was also a deep filling embankment supporting an access road to the west of the site.

3 INVESTIGATION PHASE

Investigation initially involved a detailed site inspection and mapping of the existing rock slopes and bench areas of the site. Photographic montages of the rock faces were prepared before, during and after excavation so relevant features could be documented (e.g. Figure 1). Rock strength, weathering profiles and joint/parting orientations were of particular interest for excavation design.

The assessment phase of the investigation was followed by borehole drilling at specific locations on the site to determine foundation conditions in the areas of the proposed structures. Ten boreholes were drilled using NMLC-sized diamond coring equipment fitted to truck-mounted drilling rigs. Several test pits were also excavated on the platform area of the site to collect soil and rock samples for laboratory testing purposes. This included physical testing to determine suitable design California bearing ratio (CBR) values and chemical testing to assess the salinity potential of the site.

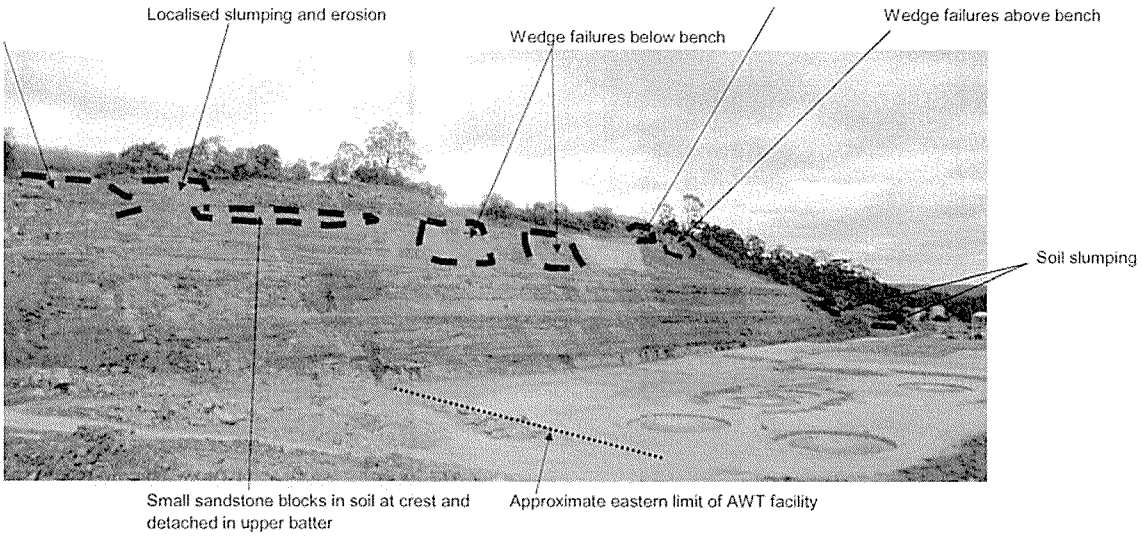

Figure 1: Example of a post-excavation photo montage

4 DETAILED DESIGN PHASE

4.1 Rock slopes

Following consultation with the client it was decided that the design should incorporate unsupported rock slopes where at all possible to keep construction costs down. The topography of the site and area required for the facility resulted in cuts of up to 35 m height in weathered shale. The design incorporated 55° batters with 3 m wide horizontal benches at each 10 m elevation to provide an overall slope of about 45°.

The incorporation of benches was aimed at providing a catch area for minor slips and rock falls, access to the batters for maintenance, and room to construct concrete dish-drains to reduce the volume of stormwater running over and eroding the slopes. Although an individual batter slope of 55° is probably considered relatively steep for an unsupported slope in the Bringelly Shale, the overall slope of 45° was considered adequate for the jointing patterns observed in the existing faces.

4.2 Engineered filling

Two main areas of the site required filling – the gully on the western side of the platform and the area along the north-eastern edge of the site. These areas required filling to depths of up to 25 m and 10 m respectively. To ensure the filling emplacements did not significantly encroach into the adjacent landfill area it was decided that reinforced filling was to be used on the site.

Analysis was undertaken using STARES v4.2 (Balaam, 1999), a computer software package which analyses circular slip within a reinforced soil mass using a modification of Bishop's simplified method (Bishop, 1955). The program was used to design the primary and secondary reinforcement requirements for both emplacement areas.

The design incorporated 45° batters with primary reinforcement at 1 m elevations to increase the factor of safety of the slope to approximately 1.5. Secondary reinforcement was to be provided at 0.3 m elevations between the primary layers to provide support for small slip failures at the face of the slope. A 3 m wide horizontal bench was provided midway down the face of the deeper emplacement to allow a dish-drain to be constructed. The slope face itself was covered with a grass-seed and topsoil mix to reduce erosion potential. Drainage was also provided below and behind the filling to reduce hydrostatic pressures acting on the rear of the emplacement and provide an avenue for seepage removal.

4.3 Geometry

The cut and fill requirements were developed into a three-dimensional model using AutoCAD (Autodesk, 2005), a design and drafting software package. The model was designed to real coordinates (i.e. life size) and provided to the earthworks contractor whose machinery has differential global positioning system (DGPS) capability. This negated the need to use conventional survey and set-out techniques and allowed the contractor to accurately construct in accordance with the latest geometric design. Any design modifications were simply updated in the AutoCAD file and emailed to the contractor for download into their DGPS software.

5 SPECIFICATION AND TENDERING PHASE

A technical specification for the earthworks phase of the project was developed to allow the client to request tender submissions for the work. The specification provided detailed information and requirements for setting out, stripping and subgrade works, site geometry,

filling works, excavation works, inspection and testing requirements and the responsibilities of the geotechnical testing authority.

At the completion of the tendering period an assessment process was undertaken to evaluate the submissions. The assessment included interviewing potential contractors, analysis of different scenarios for financial comparison and comparison of available equipment and construction methodology.

6 CONSTRUCTION PHASE

Construction monitoring of the filling works was undertaken by an experienced technician who was present on site during all filling activities. The monitoring included inspections of stripping works and subgrade conditions, observations of material quality, and observations of the placement of soil reinforcement and drainage media. The technician was also responsible for undertaking density testing within each layer of filling to check compliance with the specification. This work was undertaken to a Level 1 responsibility as described in the then current AS 3798 earthworks standard (Standards Australia, 1996).

Monitoring of the excavation works included regular inspections of the rock faces by experienced geotechnical professionals to check for the presence of unfavourable jointing. One small wedge failure occurred during early stages of excavation in the upper section of weathered shale. This was assessed immediately following the failure and support was provided by installing soil nails and provided reinforced shotcrete facing to the affected area of the slope. Detailed design was undertaken using STARES v4.2 (Balaam, 1999) and a specification for the works was prepared to enable support to be provided as soon as possible. The stabilisation work was undertaken before excavation works had progressed significantly further so there was a wide platform from which to install the soil nails and shotcrete.

A report was provided at the completion of the earthworks activities (Douglas Partners, 2007) which assessed the monitoring regime, provided a summary of all test results, provided an assessment of the risk of further slope failures, and an opinion on the quality of the works in accordance with the engineering specification.

7 SELECTED ADDITIONAL PROJECT COMPONENTS

7.1 Rock slope stabilisation

Weathering of the upper portion of the Bringelly Shale and several significant rainfall events contributed to further slope failures in the same area as the initial failure. This zone of rock contained bands of claystone which appeared to weather more rapidly than the surrounding rock. The rainfall events are likely to have contributed to the failure by increasing erosion of the rock face as well as increasing seepage through the face of the rock mass and encouraging failure of the weathered outer layers.

Excavation had already been completed and it was therefore necessary to undertake stabilisation works from a bench in the rock slope and from the crest of the slope itself. Detailed design was again undertaken using STARES v4.2 (Balaam, 1999) and a specification was prepared. Consultation with the stabilisation contractor resulted in the need to design working platforms to provide a safe foundation for the required machinery. These platforms consisted of reinforced concrete slabs supported on vertical mini-piles. A wire mesh fence was also provided along the outside edge of the bench.

Another significant rainfall event during the stabilisation works resulted in an additional slip at the location of one of the elevated work platforms. The presence of the foundation platform and

the catch fence minimised damage to the machine and prevented significant loss of spoil material to the area below the slope. An experienced geotechnical engineer monitored the installation of the soil nails and shotcrete to check compliance with the engineering specification.

Figure 2: Stabilisation works in progress

7.2 Rectification of subsidence

The significant rainfall events also coincided with subsidence of a large concrete slab that had been constructed on the western portion of the site. Detailed survey of the slab was commissioned and the results were overlain on the geometric design model. It was evident from the survey that up to about 190 mm of subsidence had occurred close to the transition between existing 'uncontrolled filling' which could not be removed for boundary support reasons and the recently placed engineered filling.

Cone penetrometer tests (CPTs) were undertaken in a grid pattern across the affected area of the slab. Analysis of the CPT data indicated zones of lower density material close to the assumed interface between the existing and recently placed filling. A review of site photographs and site inspections at the time of the subsidence suggested that stormwater infiltration through a trench excavated along the southern side of the slab had probably caused erosion of some filling material at depth.

A number of options were considered for repair of the slab and it was decided that injecting URETEK polymer would create the best result from a programme perspective if successful. Polymer injection was undertaken on a closely spaced grid pattern and the slab levels were corrected close to the design levels. Some 120 m^3 of polymer were used to correct the subsidence which provides an indication of the magnitude of internal erosion experienced on the site. Ongoing monitoring since stabilisation suggests this technique was successful.

Simple site works such as erecting earth bunds and excavating shallow dish-drains were undertaken to redirect stormwater and prevent further erosion and subsidence.

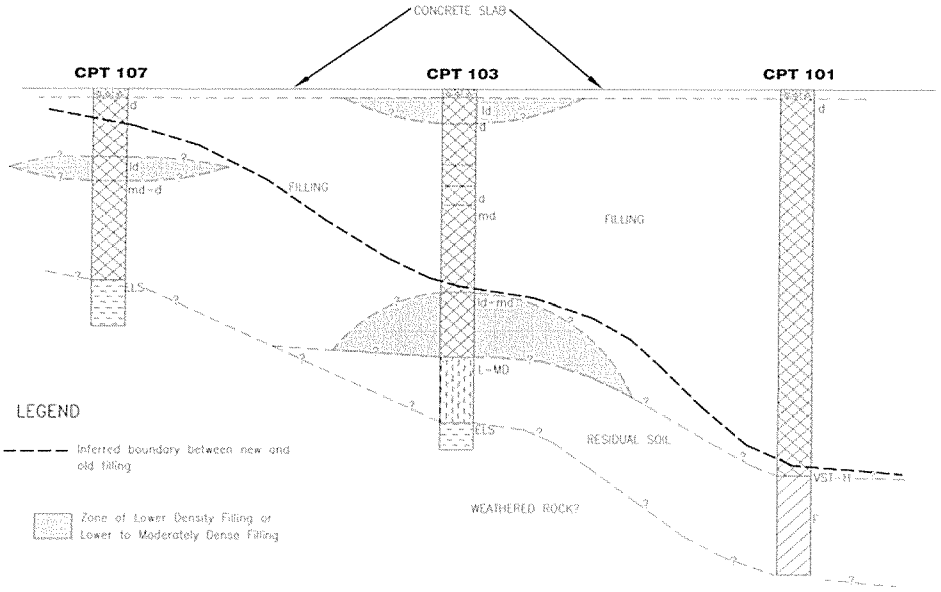

Figure 3: Example of cone penetration test results

8 CONCLUSIONS

This paper describes several aspects of the investigation, design, specification, tender and construction phases of a relatively large earthworks project. Geotechnical involvement throughout the various stages enabled a coordinated approach to be undertaken and allowed for an appropriate response to issues that arose during construction. As with most geotechnical design projects it was necessary to undertake detailed inspections during construction to enable design modifications and timely responses to address issues that arise during the construction process.

ACKNOWLEDGEMENTS

The author would like to thank Mr Grahame Wilson, Mr Michael Thom and Dr Terry Wiesner for their assistance with the project and in the preparation of this paper. The author also acknowledges the good working relationship with WSN Environmental Solutions and in particular Mr Virinder Singh.

REFERENCES

Autodesk Inc. (2005), *AutoCAD LT 2006*, United States of America.

Balaam, N P (1999), *STARES v4.2 (Stability Analysis of Reinforced Soil)*, Centre for Geotechnical Research, The University of Sydney.

Bishop, A W (1955), The Use of the Slip Circle in the Stability Analysis of Earth Slopes, *Geotechnique*.

Department of Mineral Resources (1985), *Wollongong-Port Hacking 1:100 000 Geological Series Sheet 9029-9129 (Edition 1)*, Sydney.

Douglas Partners Pty Ltd (2007), *Report on Completion of Earthworks Activities*, Project 43746 dated 28 April 2007.

Standards Australia (1996), *Guidelines on earthworks for commercial and residential developments*, Sydney.

WSN Environmental Solutions (2008), *Making Waste Work*, Sydney.

Engineering geology and debris flow hazards at Matata

Annette O'Leary
Maunsell Ltd, Auckland, NZ

Keywords: Matata, debris flow, debris avalanche, landslide, stream, rainfall.

ABSTRACT

On 18 May 2005, prolonged and intense rainfall triggered numerous landslides and debris flows throughout the steep terrain south of Matata. Flooding destroyed 27 homes, damaged a further 87 properties, washed away 100 m of railway, closed the state highway for 12 days, and cost in excess of $30 million in damages. Erosion associated with the debris flow events has created fresh exposures throughout the catchments which provide a unique opportunity to study the geological and geotechnical aspects of the area. The geology consists of weak/unconsolidated deposits which have created a landscape dominated by deeply incised stream valleys and debris. As a result the region is highly susceptible to landslides and streambeds are littered with boulders and debris. Further debris flows are possible whenever there is rainfall with high enough intensity to trigger landslides on the steep slopes.

1 INTRODUCTION

Matata is a small coastal settlement located in the Bay of Plenty, in the North Island, New Zealand (Figure 1). It is situated on the north western edge of the Taupo Volcanic Zone (TVZ), a region of active extension and volcanism associated with the oblique subduction of the Pacific plate beneath the Australian plate. Behind the settlement steep, predominantly normal faults dissect the > 300 m high Matata Fault Block (MFB), which hosts the two catchments (Awatarariki and Waitepuru) associated with the 18 May 2005 debris flows.

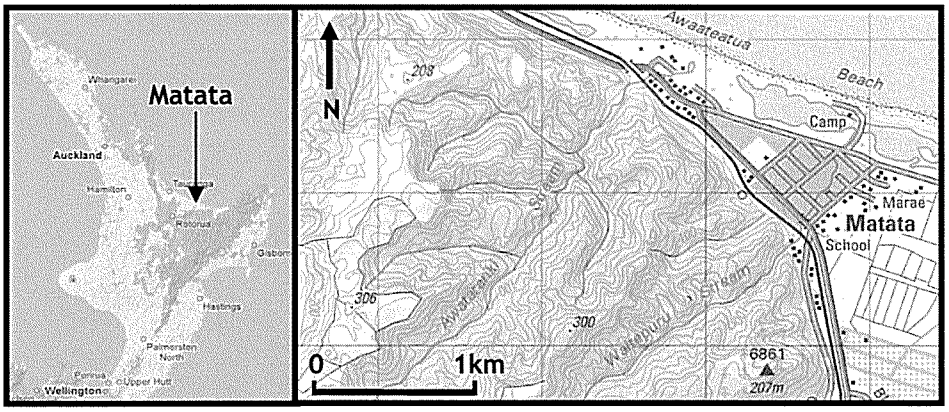

Figure 1. Map of North Island (left), and location of Awatarariki and Waitepuru Streams (right)

The TVZ is heterogeneous with respect to the geotechnical properties of rocks (porosity, permeability, density, strength, cohesion). This, coupled with fast rates of tectonic deformation (~ 10 mm/yr extension), creates a landscape that is vulnerable to erosion in periods of high rain fall. Ancient debris flow deposits sourced from the Awatarariki and Waitepuru catchments are interbedded within the stratigraphy of Matata. Erosion associated with the 18 May 2005 debris flows has resulted in many fresh exposures within the catchments, littering the stream bed with boulders in the process. Over 300,000 m^3 of debris was deposited on Matata (McSaveney et al., 2005) during the 2005 debris flows, and possibly up to 650,000 m^3 (Costello, 2007). This event provided a unique and time-limited opportunity to investigate the processes that created the debris flow in order to better understand why they occur, and when they are likely to happen again in the future.

The stratigraphic units throughout the catchments are comprised of vertically and laterally heterogeneous mid to late Pleistocene fluvial gravels, overlain by marine and non-marine sequences with interbedded pyroclastic fall deposits. Interbedded within the stratigraphy of the Matata area are polymictic, matrix supported debris flow deposits, sourced from the catchment areas of Awatarariki, and Waitepuru Streams. These deposits are capped by the 280-ka Matahina ignimbrite, and range in thickness from a few centimetres to tens of metres. The Matahina ignimbrite varies considerably in colour, density and texture, depending on thickness, degree of welding and crystallisation. It is the source of the harder boulders in the stream beds and forms the jointed bluffs in the upper catchments of Awatarariki and Waitepuru streams.

2 GEOLOGY AND GEOMORPHOLOGY

Awatarariki and Waitepuru streams form broadly branching dendritic drainage networks cut down through the Matahina ignimbrite into the weakly cemented quaternary sediments. Sediments eroded from the streams have been deposited as gently sloping fans along the Matata coast, in front of the ancient coastal cliffs. The catchments comprise steep, heavily vegetated cliffs surrounded by farmland with narrow, deeply incised stream channels. Cliff heights range from 3 m up to 40 m above the stream bed, rising to >300 m throughout the catchments.

Numerous north east oriented, eastern dipping normal faults are present throughout the catchments and range from micro to macro scale with vertical offsets of centimetres to tens of metres. Multiple joint sets occur in areas of faulting and exert control on the stream channel (Figure 2). They are predominantly closely spaced next to the fault plane, and become more widely spaced further away from the plane of movement (O'Leary, 2007).

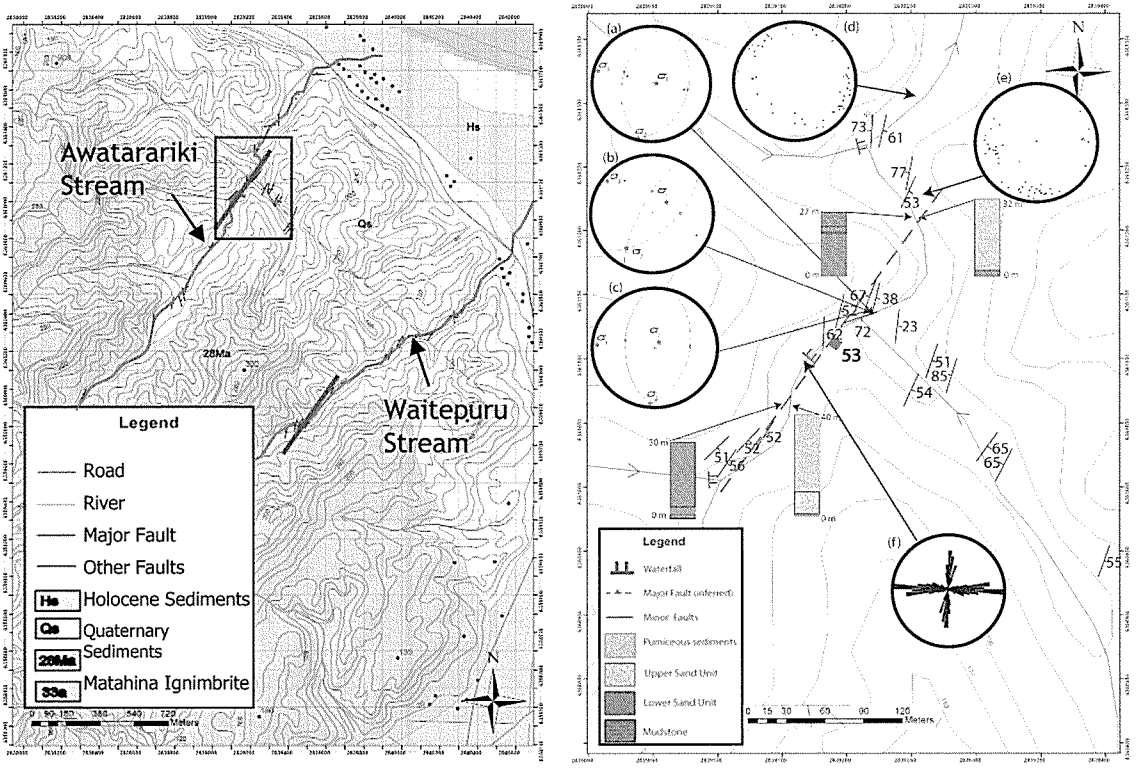

Figure 2. Geological Map of Matata (left), and (right) Map of Awatarariki stream with stereonets a – c show fault orientations, stereonets d & e show poles to joints. Rose diagram shows orientation of joints from a platform at stream level. Location shown on geological map.

The Awatarariki catchment is twice the size of the Waitepuru catchment with a wide flood plain near the stream mouth. During the debris flow, boulders, sediment and vegetation were deposited at the stream mouth where the channel widens slightly and decreases in gradient. The decrease in gradient allows the debris to drop out of suspension in this area. Minimal debris was present in the Waitepuru stream channel, which is very narrow (<1m), forming a box canyon in places.

Joints throughout the streams show an east-west trend, are steeply dipping and predominantly occur throughout the more cohesive mudstone and muddy sandstone units. All joint sets are systematic, undulating to planar, closely to moderately spaced and almost always occur in sets of parallel joints (O'Leary, 2007). The joints facilitate collapse of the stream walls and widening of the stream channel (Figure 3). This affects the local and regional geomorphology, with distinctive areas of large scale rockfall occurring along the valleys where joint sets are present, indicating a relationship between areas of cliff instability and jointing.

Figure 3. Parallel joints in Waitepuru stream cause erosion of the cliff face and exert controls on the morphology of the stream.

2.1 Description of Deposits

Ancient debris flow deposits have built up much of the land beneath Matata for the last 7,000 years (McSaveney et al., 2005) when sea level stabilised at the current level. The debris flow deposits are primarily sourced from the catchment areas of Awatarariki and Waitepuru Streams. The gravel deposits are poorly sorted, polymictic, matrix supported, and moderately weathered with some limonite staining. Clasts of mudstone, greywacke gravels, and Matahina ignimbrite are loosely packed in a sandy matrix. Clasts range in size from 20 mm to 7 m in diameter with large boulders entrained throughout the deposits.

Most debris flows travel in pulses of material characterised by boulder fronts. The debris flow deposits exposed throughout the streams support this, with the larger pulses of material reaching as far as the lowland plain. The debris flow deposits are very weak and completely disaggregate upon hammer blow. The Matahina ignimbrite is the source of the hard to very hard (welded) ignimbrite boulders that dominate the debris flow deposits in Awatarariki, and Waitepuru Streams, whilst previous debris flows delivered the huge boulders that have been used as landscaping features on the fan of Awatarariki Stream.

The density, porosity and water content of the lithologic units throughout the catchments are typical of weak rocks. The bulk densities are very low and reflect the high porosities and clay content of the units. The slaking behaviour shows that overall the mudstone is slightly more prone to slaking than the sandstone, although the sandstone eventually breaks down into a silty residue. This is thought to be one of the causes for accelerated erosion throughout the

Awatarariki catchment. The mudstone is relatively strong as a rock mass but when broken down into smaller blocks it becomes weak. Laboratory testing has shown that the water content affects the strength of the mudstone and sandstone units, which decrease in strength as the units become more saturated.

The geotechnically weak marine mudstone and siltstone units in the Awatarariki Stream appear to be more resistant to erosion than the pumiceous sediments and unconsolidated sand units observed throughout the rest of the catchment, and they generally form the beds and banks of the stream channel. The siltstone at the mouth of Awatarariki stream exhibits higher strength values than the rest of the units tested, however it is important to note that this unit only outcrops in a small percentage of the study area. The units in Waitepuru stream were found to be marginally stronger than the lithologic units in Awatarariki stream. These Quaternary sediments are able to absorb, to some extent, the impacts of large boulders scoured out of the headwaters during periods of intense rainfall.

3 THE MAY 18TH DEBRIS FLOW

On 18 May 2005, a band of intense rainfall passed over the catchments behind the coastal settlement of Matata. As a result a massive torrent of sediment laden water swept through parts of Matata with immense power, carrying boulders and trees. In its wake it left 27 destroyed homes, and 87 considerably damaged properties. SH2 was closed for 12 days, and the railway for more than 20 days. Sediment up to 1 m deep was deposited within houses in front of the stream mouths and total costs are estimated to be over $30 million in damages. The debris flow struck in the early evening when residents were awake, which meant that no lives were lost. However, if the event occurred in the middle of the night it may have been a different outcome.

3.1 Sequence of Events

The debris flow occurred at the end of a day of moderately heavy rain (302 mm in 24 hrs at Awakaponga, McSaveney et al., 2005), which included a particularly heavy downpour from 4.45 pm to 5 pm in which 30.5 mm was recorded. These measurements were taken from the closest automatic rain gauge at Awakaponga about 5 km SSE of Matata. The rainfall event that occurred in Matata in May 2005 has been described as a 1 in 200 to 1 in 500 year event. Such an intense rainfall event indicates a strongly convecting storm cell, typically associated with lightening and thunder. Earlier rainfall during the day had already saturated the ground in all catchments. When the heavy rainfall occurred on the slopes during May 18th 2005, the natural subsurface drainage system could no longer cope and was overwhelmed. This caused the pore-water pressure in the slope to increase rapidly, which resulted in landslips or 'debris avalanches' cascading down from the steep slopes into the stream channel.

The cause of events that led to the destruction in Matata were 'debris avalanches'. Evidence in the upper catchments indicates that the debris flows were direct consequences of these avalanches which were triggered by exceptionally heavy rain. Debris avalanches occur when thin slabs of rock detach from the slope, and slide down to stream level taking all the surrounding vegetation with them. When these reach the stream channel they become so fluid that they do not stop at the foot of the slope, but continue down the channel picking up more debris along their path to form a debris flow.

Debris flows are defined as dense fluid mixtures of rock, soil, vegetation and water which move rapidly in a confined channel and are capable of carrying large boulders. They contain a much higher volume of rock and sediment than floods and are much more powerful. Debris flows are denser and travel faster than normal floods, which results in increased erosion throughout the stream channels. As they travel downstream they entrain more debris, boulders and vegetation from within the stream bed. The stream bed is eroded in this process often down to bedrock.

When the debris flows encounter wider channels with a gradient < 6° (McSaveney et al. 2005), such as those at the stream mouths, they begin to deposit the sediment and boulders entrained within the flow. When this occurs, the debris flow ceases to become a debris flow, and becomes a debris flood which extends beyond the debris flow depositional area.

The sediment-laden water draining from the debris flow becomes so highly charged with sand and silt that it no longer behaves like normal water and is capable of moving boulders up to 7 m in diameter. The debris floods that occurred on May 18 2005 extended beyond the streams out onto the coastal plains inundating several houses and sweeping away anything in the flow path (Figure 4). Although some damage was caused by the debris flows directly, other houses and property were more severely damaged by the debris floods that extended beyond the debris flows.

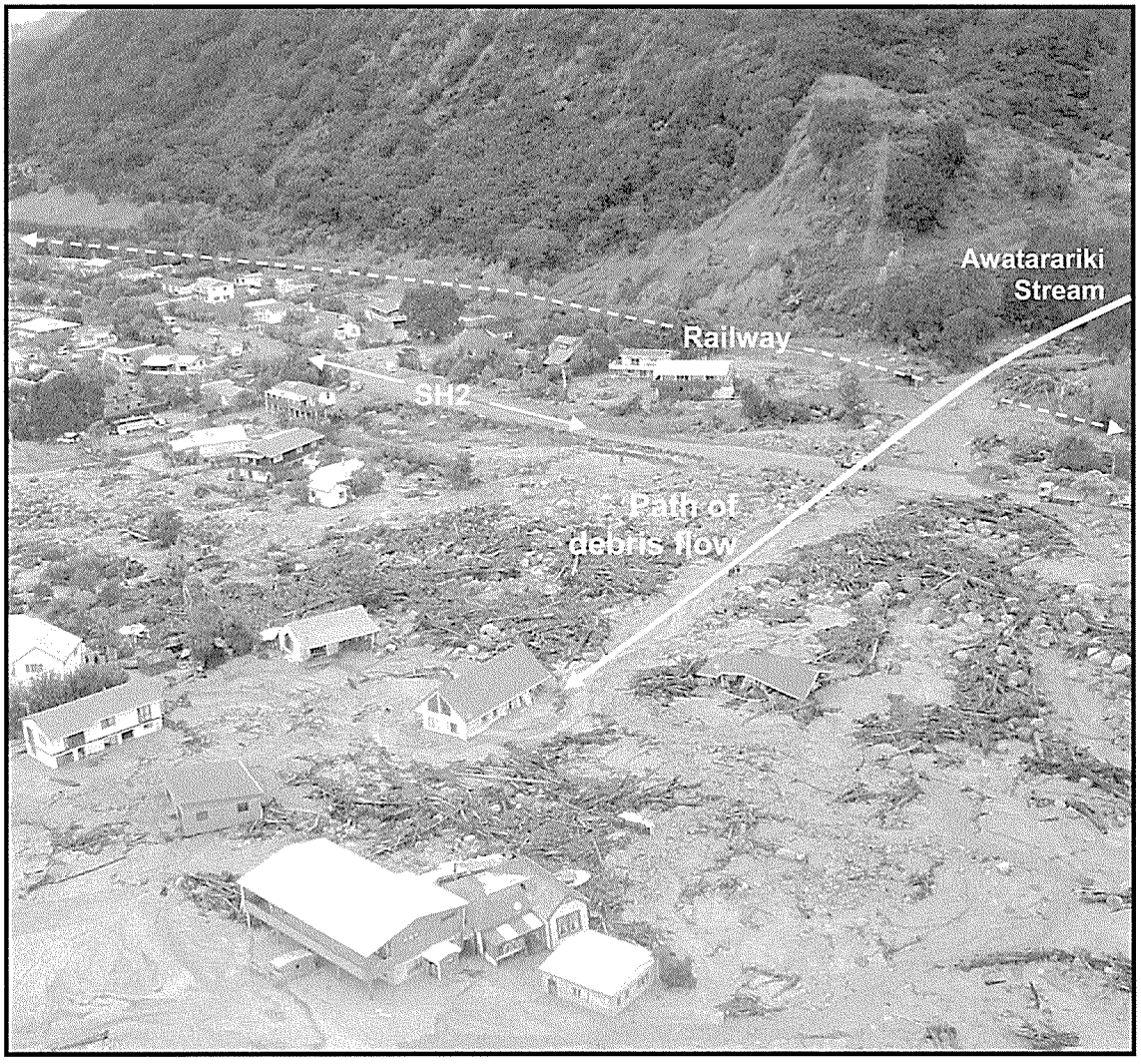

Figure 4. The debris flow on May 18 extended beyond Awatarariki stream (top right) onto the coastal plain, depositing boulders and debris at the mouth of the stream. Debris floods also damaged numerous houses on the coastal flood plain and deposited silt up to 1 m thick inside some houses.

4 DEBRIS FLOW HAZARDS FOR THE FUTURE

Debris flows are frequent occurrences in New Zealand but are rarely understood as they occur in areas of low population density. As a result debris flow hazards are not always recognised,

particularly on alluvial fans that are subject to low frequency, high impact events like that at Matata. Evidence for past debris flows at Matata can be seen in the boulders used as landscaping features on the alluvial fan, boulders unearthed during the excavation of foundations, and boulders seen 1.6km offshore by divers. Boulders of this size can only be moved by the debris flows responsible for building up the land on which Matata sits.

Numerous landslides have fallen since the 2005 event and the catchments are badly scarred as seen in aerial photographs. As more time elapses from the May 18 2005 debris flow, the unconsolidated Quaternary deposits in the catchments continue to supply sediment to the stream channel. As a result the stream is classed as 'supply unlimited' and is capable of producing debris flows whenever hydrological thresholds are exceeded (Jacob & Hunger, 2005). Accurately predicting future events is not possible, however it is likely that debris flows will continue to occur in this catchment system on a regular basis.

5 CONCLUSION

Debris avalanches triggered by heavy rain were responsible for the 2005 destruction in Matata. As the avalanches reached the stream channel they transformed into a debris flow or a rapid flow of surging water highly charged with debris. Although some damage was caused by the debris flows directly, other houses and property were more severely damaged by the debris floods that extended beyond the debris flows.

Matata has been subject to intense rainfall events and erosional processes over thousands of years, resulting in punctuated, long-standing instability throughout the major catchments. Large prehistoric debris flows have built the land beneath Matata over the last 7000 years with historical records indicating that debris flows have occurred on at least eight occasions since 1891 (McSaveney et al., 2005). The unconsolidated Quaternary sediments within the catchments are easily eroded, resulting in a supply unlimited system. Therefore whenever rainfall of high enough intensity exceeds the critical hydrological threshold, further debris flows are possible.

REFERENCES

Bailey, R.A, and Carr, R.G (1994) Physical geology and eruptive history of the Matahina Ignimbrite, Taupo Volcanic Zone, North Island, New Zealand. *New Zealand Journal of Geology and Geophysics*, 37: 319-344

Costello, D (2007) Slope failures and debris flow assessment at Matata, Bay of Plenty, New Zealand. *MSc Thesis*. The University of Auckland.

Jacob, M (2005) Debris flow hazard analysis. In M Jacob and O Hunger (eds.) *Debris-flow Hazards and Related Phenomena,* (17) pp 411 – 443. Praxis. Springer Berlin Heidelberg.

Lamarche, G, Barnes, P.M, and Bull, J.M (2006) Faulting and extension rate over the last 20,000 years in the offshore Whakatane Graben, New Zealand continental shelf. *Tectonics*, 25(4) TC4005 doi:10.1029/2005TC001886

McSaveney, M.J. Beetham, R.D. Leonard, G.S (2005) The 18 May 2005 debris flow disaster at Matata. Causes and mitigation suggestions. *IGNS client report 2005/71* prepared for the Whakatane District Council.

O'Leary, A.K (2007) Geology of the Matata Fault, Block, Taupo Volcanic Zone. *MSc Thesis.* The University of Auckland.

Integration of geotechnical database software with GIS for effective data management on the Northern Expressway

Chad Parken
Parsons Brinckerhoff (PB), Adelaide, Australia

Keywords: knowledge management, GIS, GDMS, spatial display, geotechnical information

ABSTRACT

The work required in collating geotechnical information and passing it on to the interested parties can be a significant undertaking for even the smaller projects involving several geotechnical investigations. One way of handling this task is through the use of a Geotechnical Database Management System (GDMS) and displaying it using a Geographical Information System (GIS). Using a commercially available GDMS and GIS, storing, sorting and managing geotechnical data can be achieved efficiently and easily. By linking the GDMS to a GIS, the data becomes readily available, through a mapping interface, to all parties involved in a project, including project managers, contractors, tenderers and clients. Through the GIS, all users are able to find and use the data which is available, for each particular geographical area of a project. The information that can be displayed in this manner includes borehole and test pit logs, electric friction cone logs, laboratory results, plans and reports. The GIS operator is able to customise the way the data is viewed and to control access to the data. The software programs gINT and ESRI ArcGIS have been used together in managing the geotechnical data collected for the biggest road project in South Australia since the 1960's. The benefits of this process are that it can be utilised with low expenditure and results in productivity gains within a team.

1 INTRODUCTION

The Northern Expressway is a 23 km, $564 million, four-lane, two-way road linking the Gawler Bypass with Port Wakefield Road, Waterloo Corner, 25 km north of Adelaide, South Australia (Engineers Australia 2008). This paper outlines the work PB undertook on behalf of and in conjunction with South Australia's Department for Transport, Energy and Infrastructure (DTEI). This paper discusses the importance of data management, the technology used, data input and output and the lessons learned in collating and preparing the geotechnical information.

1.1 PB's role

The work PB undertook included compiling all site investigation information. The information was placed in a geotechnical data management system (GDMS), which was linked to a site-specific GIS. The GDMS was used to provide the framework for the GIS to access the geotechnical information relating to the Northern Expressway project. The GIS was compiled on a DVD that was distributed to tenderers for the construction of the project.

The information on the disc included geotechnical site investigation data, laboratory results and reports. It also included geotechnical cross sections, basic geology and relevant photographs of key areas. During the tender period the disc was revised a number of times as the design was optimised and new data became available.

2 THE PROJECT

The Northern Expressway project was awarded as a design and construct contract in June 2008. The method undertaken to award the design and construct contract involved an expression of interest tendering process that began in July 2007, leading to a short list of three consortia in

November 2007. The short-listed consortia were required to submit preliminary designs and costs for construction, with the final tender given to the party that best satisfied the criteria.

3 DATA MANAGEMENT SYSTEM

DTEI had undertaken a number of in-house geotechnical investigations along the proposed route of the Northern Expressway, dating back to 1985. These included numerous boreholes, test pits, electronic friction cone tests, laboratory tests and related reports. DTEI was also conducting further in-house geotechnical investigations during the tender period. PB advised DTEI that a database could be set-up to store the geotechnical data and that it could be linked to a GIS to display the data spatially.

The advantage of using a GIS was that it could display the boreholes in context to related spatial information, such as the latest road alignments, cadastral information, aerial photographs and the geotechnical data, as they became available. Producing a disc that was a stand-alone product, with the software and instructions included, meant that tenderers did not have to attend special training in order to have access to the geotechnical data. By distributing the information on a disc, the data was accessible and could be saved on multiple computers, enabling knowledge sharing within the tendering consortia.

4 TECHNOLOGY

The field and laboratory testing was initially entered into gINT Professional Version 8.1, a commercially available GDMS and ESRI ArcGIS Version 9.2, commercially available GIS software. ArcReader, a free GIS data viewer and was provided on each DVD produced with instructions on how to install the software and gain access to the database and GIS.

All the site investigation data points and relevant information was entered into gINT. These points all had GPS co-ordinates, in MGA zone 54. Extra fields were added to the main data input page in gINT, which allowed hyperlinks to be included. The hyperlinks were used to identify the paths to the corresponding reports, laboratory results, photographs, fence diagrams and borehole logs. In this manner, gINT was used to store the data, while a GIS was used to access the hyperlinks and interrogate them with the information in the GIS. This method was adopted because it displayed the data in a user-friendly way and made the data available with the use of readily available free GIS software (ArcReader).

A software tool called "gINT for ArcGIS" was used to enable ArcGIS to interrogate the gINT database file and access spatial information and references. This automated the process of displaying the database information in the GIS with existing layers. By using the tool, the GIS became the interface for the spatial and aspatial geotechnical data.

The finished DVD had a self-launching title page which gave instructions on how to access the data stored on the disc. The introduction page of the DVD was used to outline the contents of the disc and highlight the changes for each edition.

5 DATA

Multiple borehole data fields and hyperlinks had to be entered directly into the GDMS. These were all referenced spatially by their GPS co-ordinates. Table 1 lists the geotechnical fields that were entered into the GDMS and the additional data entered into and displayed by the GIS.

The GDMS input screen was straightforward to use and enter data. It allowed important information such as borehole depth and number to be easily navigated (Figure 1). The GDMS was able to display all of the data points spatially (Figure 2), making it easy to create long sections. The GDMS input allowed boreholes and associated data to be incorporated quickly

and efficiently. It also had the advantage of being compatible with MS Excel, which allowed users to enter information into a spreadsheet in the field computer and later update the GDMS in the office.

Table 1: GDMS (gINT) Data Inputs

Data System	Group	Name (Number of data points)
GDMS	**Site Investigation Information**	Borehole logs (314)
		Test Pit logs (96)
		CPT logs (15)
	Hyperlinks	Long Sections (60)
		Site Photographs (44)
		Falling Head Tests (3)
		Laboratory Results (500+)
		Reports (19)
GIS	**Design Information**	GDMS Data Points (425)
		Road Designs (2)
		Sites of Interest (17)
	Geographical Information	Aerial Photography
		Spot Heights
		Contours
		Cadastral Boundaries
		Suburbs
	Infrastructure	Major Roads
		Minor Roads
		Railways
	Geological Information	Seismic Events
		Fault Lines
		Detailed Geology

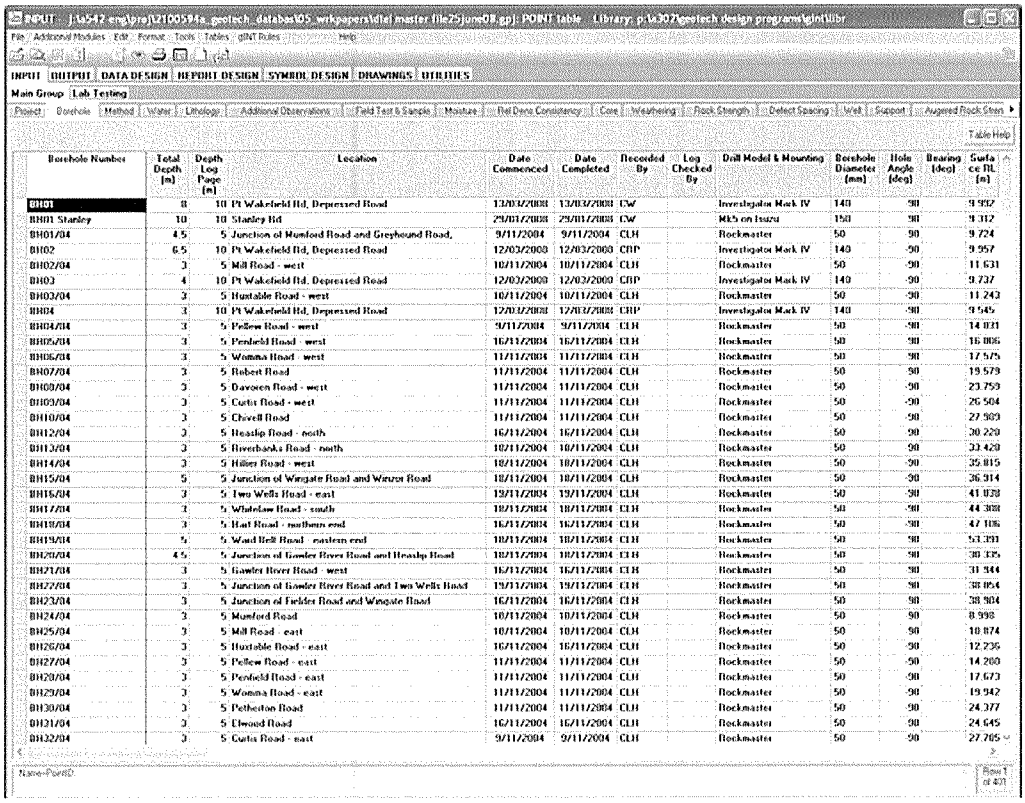

Borehole Number	Total Depth (m)	Depth Log Page (m)	Location	Date Commenced	Date Completed	Recorded By	Log Checked By	Drill Model & Mounting	Borehole Diameter (mm)	Hole Angle (deg)	Bearing (deg)	Surface RL (m)
BH01	0	10	Pt Wakefield Rd, Depressed Road	13/03/2008	13/03/2008	CW		Investigator Mark IV	140	90		9.992
BH01 Stanley	10	10	Stanley Rd	29/01/2008	29/01/2008	CW		Mk5 on Isuzu	150	90		9.312
BH01/04	4.5	5	Junction of Mumford Road and Greyhound Road,	9/11/2004	9/11/2004	CLH		Rockmaster	50	90		9.724
BH02	6.5	10	Pt Wakefield Rd, Depressed Road	12/03/2008	12/03/2008	CBP		Investigator Mark IV	140	90		9.957
BH02/04	3	5	Mill Road - west	10/11/2004	10/11/2004	CLH		Rockmaster	50	90		11.631
BH03	4	10	Pt Wakefield Rd, Depressed Road	12/03/2008	12/03/2008	CBP		Investigator Mark IV	140	90		9.737
BH03/04	3	5	Huxtable Road - west	10/11/2004	10/11/2004	CLH		Rockmaster	50	90		11.243
BH04	3	10	Pt Wakefield Rd, Depressed Road	12/03/2008	12/03/2008	CBP		Investigator Mark IV	140	90		9.545
BH04/04	3	5	Pellew Road - west	9/11/2004	9/11/2004	CLH		Rockmaster	50	90		14.021
BH05/04	3	5	Penfield Road - west	10/11/2004	10/11/2004	CLH		Rockmaster	50	90		16.006
BH06/04	3	5	Womma Road - west	11/11/2004	11/11/2004	CLH		Rockmaster	50	90		17.575
BH07/04	3	5	Robert Road	11/11/2004	11/11/2004	CLH		Rockmaster	50	90		19.579
BH08/04	3	5	Dawson Road - west	11/11/2004	11/11/2004	CLH		Rockmaster	50	90		23.759
BH09/04	3	5	Cutts Road - west	11/11/2004	11/11/2004	CLH		Rockmaster	50	90		26.504
BH10/04	3	5	Chivell Road	11/11/2004	11/11/2004	CLH		Rockmaster	50	90		27.989
BH12/04	3	5	Heaslip Road - south	16/11/2004	16/11/2004	CLH		Rockmaster	50	90		30.220
BH13/04	3	5	Riverbanks Road - south	10/11/2004	10/11/2004	CLH		Rockmaster	50	90		33.429
BH14/04	3	5	Hiller Road - west	10/11/2004	10/11/2004	CLH		Rockmaster	50	90		35.815
BH15/04	5	5	Junction of Wingate Road and Winzer Road	10/11/2004	10/11/2004	CLH		Rockmaster	50	90		36.914
BH16/04	3	5	Two Wells Road - east	19/11/2004	19/11/2004	CLH		Rockmaster	50	90		41.078
BH17/04	3	5	Whitelaw Road - south	10/11/2004	10/11/2004	CLH		Rockmaster	50	90		44.388
BH18/04	3	5	Hart Road - northern end	16/11/2004	16/11/2004	CLH		Rockmaster	50	90		47.106
BH19/04	5	5	Wood Hill Road - eastern end	10/11/2004	10/11/2004	CLH		Rockmaster	50	90		53.391
BH20/04	4.5	5	Junction of Gawler River Road and Heaslip Road	10/11/2004	10/11/2004	CLH		Rockmaster	50	90		38.125
BH21/04	3	5	Gawler River Road - west	16/11/2004	16/11/2004	CLH		Rockmaster	50	90		31.544
BH22/04	3	5	Junction of Gawler River Road and Two Wells Road	19/11/2004	19/11/2004	CLH		Rockmaster	50	90		38.054
BH23/04	3	5	Junction of Fielder Road and Wingate Road	16/11/2004	16/11/2004	CLH		Rockmaster	50	90		38.504
BH24/04	3	5	Mumford Road	10/11/2004	10/11/2004	CLH		Rockmaster	50	90		8.998
BH25/04	3	5	Mill Road - east	10/11/2004	10/11/2004	CLH		Rockmaster	50	90		10.874
BH26/04	3	5	Huxtable Road - east	16/11/2004	16/11/2004	CLH		Rockmaster	50	90		12.236
BH27/04	3	5	Pellew Road - east	11/11/2004	11/11/2004	CLH		Rockmaster	50	90		14.200
BH28/04	3	5	Penfield Road - east	11/11/2004	11/11/2004	CLH		Rockmaster	50	90		17.673
BH29/04	3	5	Womma Road - east	11/11/2004	11/11/2004	CLH		Rockmaster	50	90		19.942
BH30/04	3	5	Petherton Road	11/11/2004	11/11/2004	CLH		Rockmaster	50	90		24.377
BH31/04	3	5	Elwood Road	16/11/2004	16/11/2004	CLH		Rockmaster	50	90		24.645
BH32/04	3	5	Cutts Road - east	9/11/2004	9/11/2004	CLH		Rockmaster	50	90		27.705

Figure 1: Example of GDMS (gINT) data input

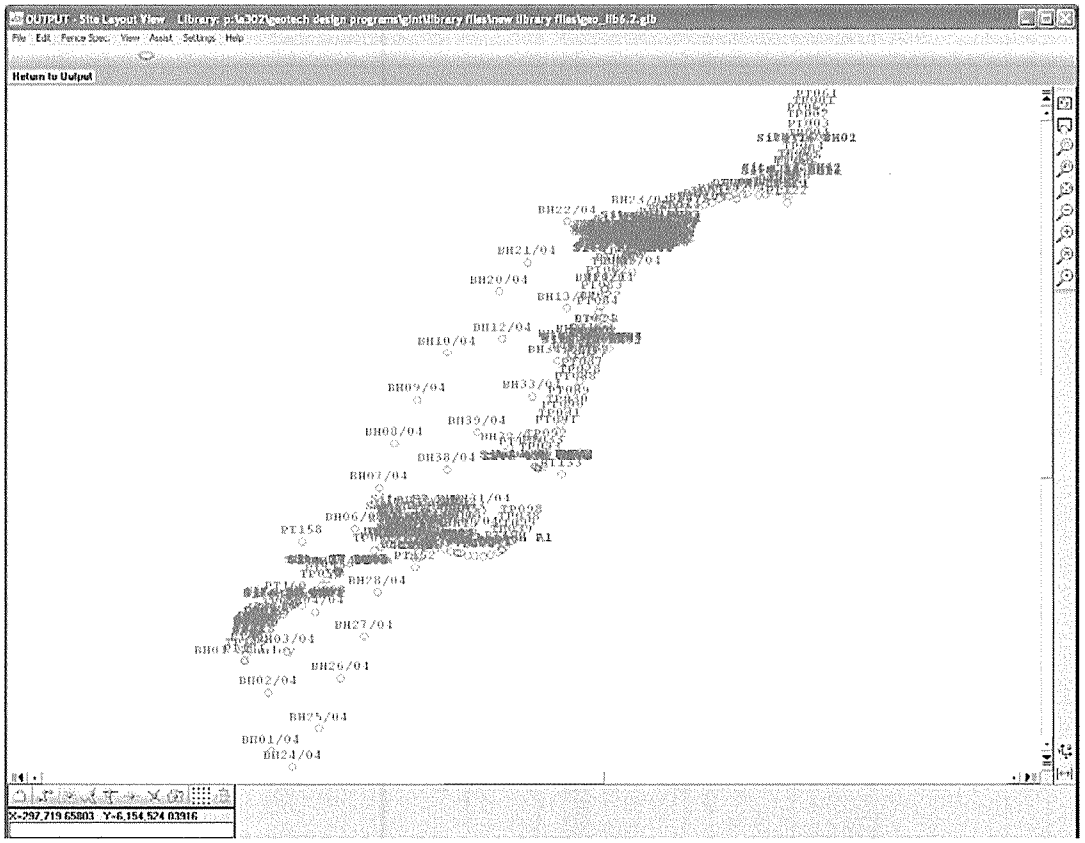

Figure 2: GDMS (gINT) spatial data display

6 OUTPUT

The output of the GDMS was presented in the GIS as an attribute accessible through interrogating the boreholes represented as a point in the GIS. It included information such as hole depth, drilling date, borehole diameter, co-ordinates, elevation and links to the borehole log, cross sections, laboratory results, site photographs and reports which were relevant to that area (Figure 3). The GIS was able to display an existing library of spatial data including topography, roads, geology and aerial photography, as well as displaying the project specific road designs, cadastral parcels and sites of interest. The use of GIS enabled users to customise the amount of information they wanted to view, as well as providing fast and easy access to spatial geotechnical data.

7 LESSONS LEARNED

As this was the first time DTEI and PB had worked together on a project of this nature, the process produced some challenges. We found it was important to carefully plan the names of files and locations of folders containing linked material, otherwise much time could be expended by having to change hyperlinks. It was also important to actively update the GDMS as data became available, in order to not omit information or fall behind.

The main shortcoming of the GDMS being linked to GIS in this way was due to the map grid zones. The Map Grid of Australia (MGA) is a projection which divides the Australian continent into eight zones of six degrees of longitude in width The current parameters of the "gINT to ArcGIS" tool mean that the GIS reads the co-ordinates from the GDMS however it could not distinguish which zone the co-ordinates were in. Therefore, if a project spanned more than one MGA zone, the co-ordinates would be plotted in one zone only. Thankfully the Northern Expressway project was only within zone 54, however had it been in more than one zone, a separate GDMS and GIS would have been required for each zone. It is expected that this functionality will be made available as the "gINT for ArcGIS" tool evolves.

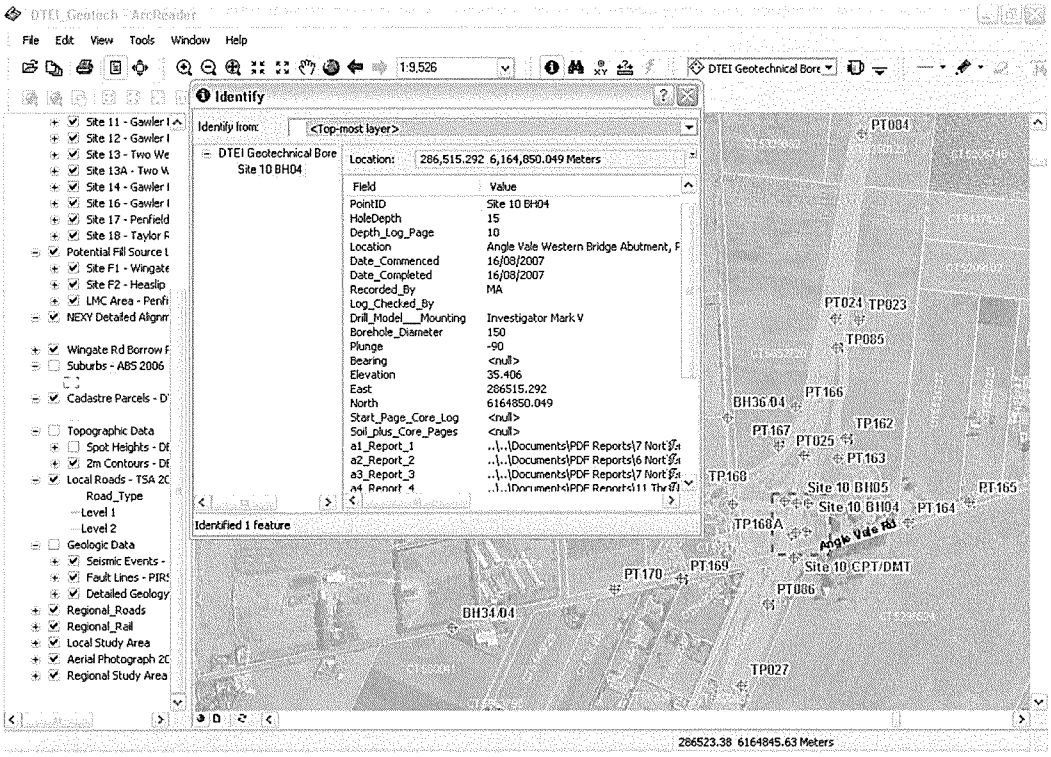

Figure 3: GIS spatial data display and GDMS output

8 CONCLUSIONS

Knowledge management is an important consideration when working on large projects, which can be made more efficient with the use of a GIS. Linking a GDMS to GIS allowed multiple users access to spatially presented geotechnical data. Distributing the systems on a stand alone DVD also gave wide coverage to the project tenderers and allowed them to drill down into the relevant information. With some careful planning, distributing the data within the GIS onto a DVD, had significant cost savings in terms of time spent searching for data. The reduction in paper usage also had environmental benefits.

ACKNOWLEDGEMENTS

The author would like to thank Justin Nottage of PB for creating the GIS and providing GDMS integration support and Michael Anchor of DTEI for giving PB the opportunity to assist with this aspect of the Northern Expressway project.

REFERENCES

Engineers Australia (2008) "Major contract let for Northern Expressway", Volume 80, Number 7, pp. 37 (July 2008)

Howell, C. & Smith, M (2004) *Enhanced Profitability Through Effective Knowledge Management and Communication – A Proposed System for PB*. Submission for the 2004
Emerging Professional Paper Competition, World Paper Category, PB.

Wade, P. et al (2007) Geotechnical Data Management of the New Doha International Airport Platform Reclamation. *Proceedings of the 10th Australia New Zealand Conference on Geomechanics*. Australian Geomechanics Society

Geotechnical investigations in the rugged and remote Waipa Valley

Rebecca Poole, BSc
Beca Infrastructure Ltd, Auckland, NZ

Keywords: site investigations, remote areas, instability

ABSTRACT

This paper presents the complex geological model of a very isolated part of the Central North Island, New Zealand (Waipa Valley) and sets out a methodology for undertaking geotechnical site investigations in remote locations.

Using helicopter support, five boreholes, were drilled on the steep slopes of a deep gorge, over an elevation change of 200 m, and correlated with a sixth borehole drilled to a depth of 220 m deep at the top of the slope. The 600 m long bush-covered steep slope (1H:1V in places) was covered in bouldery slope debris and lined locally with terraces of pumiceous sands representing historical eruptions from the Taupo Volcanic Zone.

The boreholes identified the deposits as comprising Mesozoic Manaia Hill Group greywacke overlain by Te Kuiti Group sandstone and limestone, flanked by ignimbrite flows of the Pakaumanu Group and overlain by bouldery slope movement debris. Until now, the presence of the Te Kuiti Group between the ignimbrite deposits and basement rock was unknown.

Currently this project has not proceeded beyond concept design.

1 INTRODUCTION

Undertaking geotechnical investigations in remote areas is challenging due to the environmental limitations imposed by access and mobilisation. Geotechnical investigations were undertaken in rugged terrain within the deeply incised and forested Waipa Valley approximately 40 km south east of Te Kuiti township, to establish a geological model of the site so that aspects of development, such as slope stability and effects of potential earthworks could be assessed. Geological and geotechnical data was obtained during the investigation. This paper presents the overall logistics of undertaking geotechnical investigations in remote areas and the complex geological conditions encountered.

2 PLANNING

Detailed planning prior to an investigation should always be undertaken. The following systematic steps are recommended prior to beginning investigations in remote environmentally significant locations: desk top study, initial scope of investigations, contractor commissioning, a preliminary site visit and consent applications.

2.1 Desk Top Study

Prior to planning or scoping any site investigation a desk top study and site visit should be completed. This includes review of published geological and topographical maps, previous investigations and aerial photography. This desk top study is not always required to be submitted to the client, but is usually undertaken to provide information pertaining to geology

you are likely to encounter, the estimated depth of the lithological units, and the topography of the site . For remote site investigation these desk top studies may include availability of water (for drilling), geological and culturally protected areas, as well as evidence of slope instability and other hazards associated with the site

2.2 Scope of Investigation

For investigations undertaken in remote areas it is important to clearly understand the purpose of the site investigation. This is to enable the design of the investigation programme to be relevant and complete, so that at the end of the investigation all the information required for the design has been obtained.

Remote sites, generally have limited (if any) means of communication (e.g. out of cell phone range) and changes to the scope will not be timely as calling the site representative is not practical. Changes in scope can be costly and time consuming to implement.

Items that should be considered in preparing a scope are: location, borehole depth, amount of in-situ testing and sampling for laboratory testing.

2.3 Contractor Commissioning

Once the objective of the job is understood and a scope of investigation is developed it is important to obtain quotations from contractors. Requests for quotation should detail the scope such as type of investigation and sampling test requirements, expected ground conditions, and client requirements. A site plan indicating borehole locations is preferred by most contractors. When requesting contractors for a quote, it should be made clear that the site is in a remote location and drillers are encouraged to visit the site to determine access and environmental conditions.

When choosing a drilling contractor for investigations in remote areas, it is important to review track records and request proof that they have been able to successfully complete jobs which may incorporate some of the same challenges envisaged for the job. Items may include but are not limited to:

- Working in remote locations;
- Building platforms;
- Helicopter lifting/setting down;
- Dismantling and reassembling drilling rig;
- Geotechnical Drilling; and
- Geotechnical Testing (Standard Penetration Tests (SPT), shear vane, push tubes)

2.4 Initial Site Visit

It is good practice to visit any site prior to beginning investigations and ideally prior to completing an initial desk top study or appraisal. The site visit will allow yourself and the contractor(s) clear vision of the site and the extent of preparation required to undertake the site investigation. Some issues that the site visit would confirm are:

- Site access;
- Availability of water and permits to take and discharge drilling water;
- The topography;
- Suitable borehole equipment
- Suitable sites for borehole placement;

- Platforms/scaffolding required and permit to carry out earthworks in a forested area;
- Vegetation clearing required and permit if necessary;
- Geology (stability, outcrops, slope debris, stream beds, vegetation, steepness/angle of hills); and
- Environmental limitations and consent conditions

Scope and cost may need to be tailored to suit site conditions.

2.5 Environmental Consents

The Resource Management Act (RMA) of 1991 was passed to protect New Zealand's environment and allow input from stake holders. The RMA contains rules and guidelines to manage natural and physical resources. Depending on where the site is located, various resource consents may be required. The type of consents required for most geotechnical jobs fall under the category of 'Land use Consents'. Land use consents identify, control and minimise the impacts of activities on people and the environment. The following are usual activities requiring a resource consent prior to site investigations in remote areas:

- Advance/construct a borehole;
- Carry out earthworks, roading or tracking;
- Plant or clear vegetation; and
- Take water from discharge to a stream, river or lake

Further to the land use activities requiring resource consent, an environmental plan is required. The environmental plan is needed to identify any potential or actual environmental aspects of the project and the effects the investigation activities may have and provide procedures to manage, monitor and mitigate any potential or actual effects.

It's not uncommon to come across culturally significant areas in remote areas of New Zealand. These areas should be located prior to the investigations so that measures can be made to avoid the sites.

3 HEALTH AND SAFETY

Health and Safety is an important aspect for all site investigations, and in particular within remote locations. Legislation requires an individual be made responsible for health and safety in the workplace. That person should be the person in charge of activities in the workplace, generally the contractor's representative on site, or a person delegated specific health and safety responsibility by that person. Prior to any site investigations a health and safety procedure needs to be developed. In the event of an emergency everyone who is on site should be aware of what procedures to take in order to overcome any incident the safest way possible. Generally in remote locations there is no cell phone reception and one may have to drive or walk some distance before obtaining cell phone coverage. It is encouraged to have a satellite phone.

4 CASE STUDY

The site is located in the isolated and steep Waipa Valley approximately 40 km south east of Te Kuiti township. The site is a gorge some 200 m in height with a steep 600 m long native bush covered slope (1H:1V in some places) dropping down into the Waipa River bed. The ridge is covered in boulder debris as well as elevated volcanic terraces of ash and pumice sands typically featuring recent slope failures both down and transverse to the ridge line.

Due to the remoteness of the site and the steep contour, it was not possible for a drill rig to access the site by normal vehicular ground methods. Drill platforms were constructed and the drill rigs had to be flown in by helicopter to perform subsurface investigations. Each borehole site required helicopter support for mobilisation.

A total of six boreholes were advanced during the investigations. Five boreholes, 17 to 45m were drilled progressively down the slope, with the shallowest being at the river bed. A sixth borehole was drilled at the top of the slope to find the likely overall profile and check the depth to basement greywacke rock.

4.1 Desk top study

Prior to site investigations a basic desk based study was conducted for the site and concluded the following:

- The Geological Map of Waikato indicated that the site was underlain by Mesozoic Manaia Hill Group (Greywacke) flanked by ignimbrite flows of the Pakaumanu Group.
- The topographical map indicated that the topography of the land contained very steep gradients.
- Water from the Waipa River was a potential source of water for boreholes at the bottom of the slope.
- The site was located within Department of Conservation (DOC) land; environmental consents would need to be obtained.
- Study of stereo-pair photos indicated that there was evidence of historical and recent slope instability.

4.2 Scoping Investigations

The scope included five machine boreholes spaced along the slope up to 40 m depth with SPT's undertaken at 1.5m centres. Site access was down a track that had been created, however the gradient was very steep in some places. The work scope included two options for site access either, 4WD vehicular or helicopter mobilisation. Request for drilling quotations were sent out to various drillers.

4.3 Contractor Commissioning

Request for quotations were sent out to various drilling contractors, which included the scope, location and options for accessing the site (at this time heli-transport was assumed for some of the locations). Two contractors responded positively to the proposed work.

4.4 Preliminary Site Visit

A preliminary site visit was arranged and included the client and two drilling contractors. Access by 4WD motorbike and tractor rigs were agreed to access the top three boreholes, with only two boreholes located at the bottom of the slope and river bed requiring helicopter mobilisation.

Water was to be supplied from a farmer's pond at the top of the slope for the first two boreholes and from the Waipa River for the bottom three boreholes.

The site visit confirmed the extent of slope instability found during the desk top study. The steep gorge was littered with large ignimbrite boulder debris. Borehole depth was reassessed to reach in-situ rock during investigations.

The drilling company accepted was highly recommended and the crew's track record and experience indicated they had the expertise to complete the work envisaged. The crew had experience working in remote locations, building platforms, helicopter lifting, and disassembling/reassembling rigs.

4.5 Environmental Consents

Consents were required from DOC and Environment Waikato (EW). An Environmental Management plan had to be put in place by the contractors. EW made visits to the site to conduct environmental audits to ensure all rules were being abided.

4.6 Mobilisation Difficulties

On the first day of the investigation it was discovered that the slope was too steep to drive a tractor rig down the slope and that helicopter support would be needed for all sites. This change resulted in additional cost and slowed the programme down. The helicopter could only operate under certain conditions (no heavy rain or high wind). Each helicopter had limited lift capacity. The weight of the drill rig was underestimated and larger helicopters had to be brought in. Due to time limitations and the slow rate of progress being made, an additional contractor was brought in to finish the work and mobilisation of this rig required assistance from the largest helicopter in New Zealand.

4.7 Geological and Geotechnical Results

After advancing five boreholes down the boulder debris littered slope, it became apparent that distinguishing in-situ welded ignimbrite rock from colluvium/slope debris would be difficult, as the majority of the ignimbrite was unwelded and had the same appearance as sand when it was recovered in the core barrel.

A sixth borehole was drilled at the top of the slope to find the depth to the basal greywacke rock and confirm the stratigraphy.

According to The Geological Map of Waikato, the geology of the Waipa Valley only comprised Mesozoic Manaia Hill Group greywacke overlain by variable welded ignimbrite flows of the Pakaumanu Group.

Subsurface investigations identified welded, partially welded and non-welded ignimbrites of the Pakaumanu Group interbedded with ashfall/tephra deposits and alluvium (alluvium identified as silty clay, with decomposing organics). Shelly sandstone and pebbly shelly limestone was encountered interceding the Pakaumanu Group and the Manaia Hill Group. The greywacke bed rock was encountered at 215m the top of the gorge and 12m below the river bed. Along the slope approximately 10.5 m of Pakaumanu Group ignimbrite colluvium/debris material was found (Figure 1).

The investigation identified a 70 m thick sequence of Te Kuiti Group sandstones and limestones separating Manaia Hill Group greywacke and the Pakaumanu Group ignimbrites. Before the investigations the presence of the Te Kuiti Group and alluviual sediments at this site was unknown.

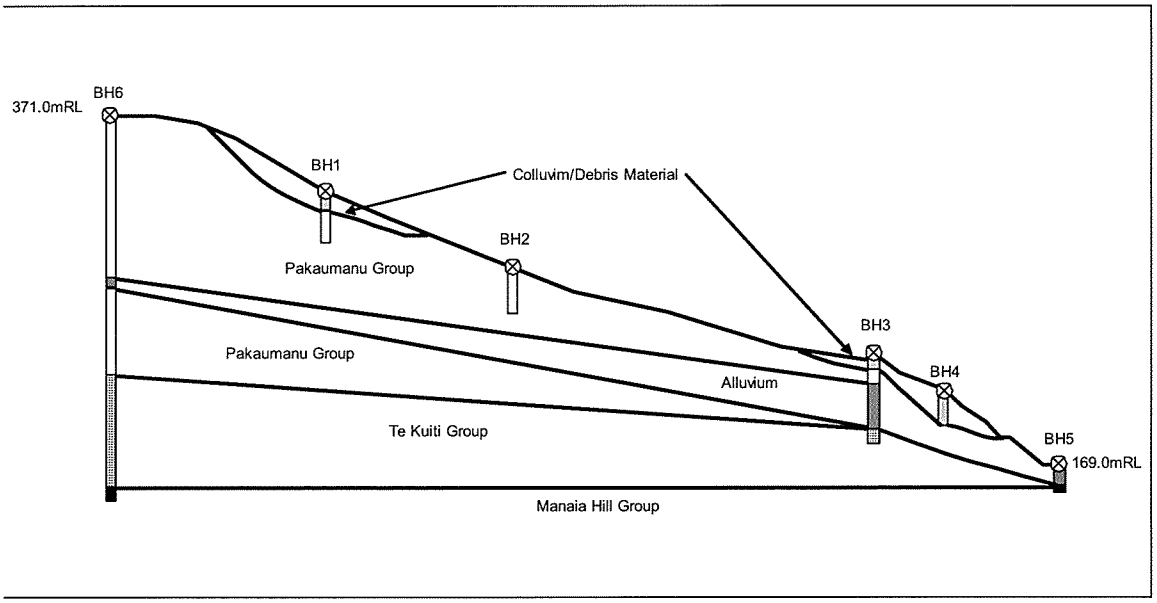

Figure 1: Subsurface stratigraphy

5 CONCLUSIONS

- Undertaking any site investigation requires detailed planning and preparation, even more so in remote locations. Although there may be time constraints, the following steps should be completed prior to investigations: desk top study, contractor commissioning, preliminary site visit, environmental consents.
- Be prepared and have heightened awareness of need for scope changes due to site constraints.
- Having a health and safety plan in place is important during all investigations. When in remote locations the level of risk increases therefore additional steps should be taken to ensure safety such as a health and safety procedure and access to a satellite phone.
- It is good practice to refer to published geological maps prior to investigations to know what the expected underlying geology is for the site. As demonstrated in the case study above, when undertaking investigations in remote locations the underlying stratigraphy may be different from what is presented on published geological maps.

ACKNOWLEDGEMENTS

The author would like to thank the many staff within the Geotechnical team at Beca Infrastructure for their willingness to provide constructive suggestions during the writing of this paper.

Deterministic seismic hazard analysis in central and southeast Viti Levu, Fiji

Tariq I.H. Rahiman
Golder Associates Pty Ltd, Brisbane, Australia

Keywords: faults, seismic hazard, maximum credible earthquakes, Suva City, Monasavu Dam, Viti Levu, Fiji

ABSTRACT

Newly identified crustal faults representing earthquake source structures are used to evaluate the seismic hazard at the hydroelectric Monsavu Dam and at Suva City on Viti Levu, the main island of Fiji. Viti Levu occurs within the Fiji Platform seismotectonic source zone. Forty seven fault strands on Viti Levu are identified and their activity evaluated using fault displacements of Quaternary geological or geomorphological features and well located epicentral distribution of large and micro earthquakes. The Mavuvu Fault Lineament Zone, Naqara Fault, Sovi/Yalavou Fault, Nasivi Fault, Suva Canyon Fault and the Nakorotubu Fault are classified as potentially or tentatively active. The maximum credible earthquakes capable on these structures range from M_W 6.8 to 7.6 and their surface rupture lengths from 20 to 127 km.

The seismic hazard analysis shows that the Mavuvu Fault Lineament Zone and the Suva Canyon Fault provide the controlling maximum credible earthquakes at Monasavu Dam and Suva City respectively. The estimated horizontal peak ground acceleration (PGA) value estimated for Suva City ranges from 0.40g to 0.62g and for Monasavu Dam from 0.39g to 0.51g. The spectral accelerations at a period equal to 0.2 seconds are comparable to accelerations that have return periods of over 1000 years based on a regional probabilistic seismic hazard study by Jones (1998).

1 INTRODUCTION

Past seismic hazard studies in Fiji have relied solely on instrumental seismicity data and historical records of earthquakes (Everingham, 1986; Jones, 1998). One of the limitations of using such data uniquely in seismic hazard analysis is that historical and instrumental records of seismicity are incomplete with respect to much longer repeat times of large earthquakes on major faults. Recently completed geological studies on crustal fault earthquake sources in Fiji (e.g. Rahiman & Pettinga, 2006; 2008) provide impetus for re-evaluating seismic hazards at critical sites in Fiji.

Suva City, (pop. 77 000) the capital of Fiji, and the hydroelectric Monasavu Dam are two critical sites located on Viti Levu, within a seismically active zone of Fiji and are vulnerable to large earthquakes (Figure 1). In southeast Viti Levu, important infrastructures of Fiji are located in Suva and considerable infrastructure development is being planned here for the future. The Monsavu Dam, in central Viti Levu, is an 82 m high earthfill dam, with lake capacity of 133 million cubic metres and power capacity of 80 MW and supplies 70% of the country's electricity.

This paper presents the result of a deterministic seismic hazard analysis of Suva City and the Monasavu Dam using newly identified crustal fault source structures. The results of this study have applications in the design of new engineering structures in Suva and in the review of dam safety levels at Monasavu.

2 SEISMOTECTONIC SETTING OF FIJI

The Fiji islands lie in a complex region of the active boundary between the Australian and Pacific plates in the SW Pacific (Figure 1 inset). Plate convergence at the Tonga and Vanuatu subduction zones changes to a broad zone of extension and diffused shearing deformation in the Fiji region. Ongoing plate tectonic deformation induces seismicity both within and along the margins of the remnant Fiji arc crust, the Fiji Platform (Figure 1).

Updated seismicity data, earthquake focal mechanisms, submarine topography, and the tectonic model of the Fiji Platform define five principal seismotectonic source zones within 500 km of Viti Levu. The principal seismotectonic source zones identified are: 1) Fiji Fracture Zone; 2) West Viti Levu Seismic Zone; 3) Peggy Ridge Seismic Zone; 4) Kadavu/Hunter Fracture Zone; and 5) the Fiji Platform (Figure 1). Source zones 1 to 4 are fracture zones/spreading ridges at the margins of the Fiji Platform, while the fifth represents a diffuse source zone within the Fiji Platform itself.

Due to its close proximity to the critical sites, the Fiji Platform source zone centred on Viti Levu is considered to be the most important in terms of relevance to strong earthquake shaking in Viti Levu. Earthquakes in the Fiji Platform have generated Modified Mercalli Scale intensities up to MMX (~1.2g) in Suva and up to MMVII (~0.2g) in central Viti Levu. Individual source structures in Viti Levu were examined further to provide the basis for a quantitative evaluation of seismic hazard of Suva City and Monasavu Dam.

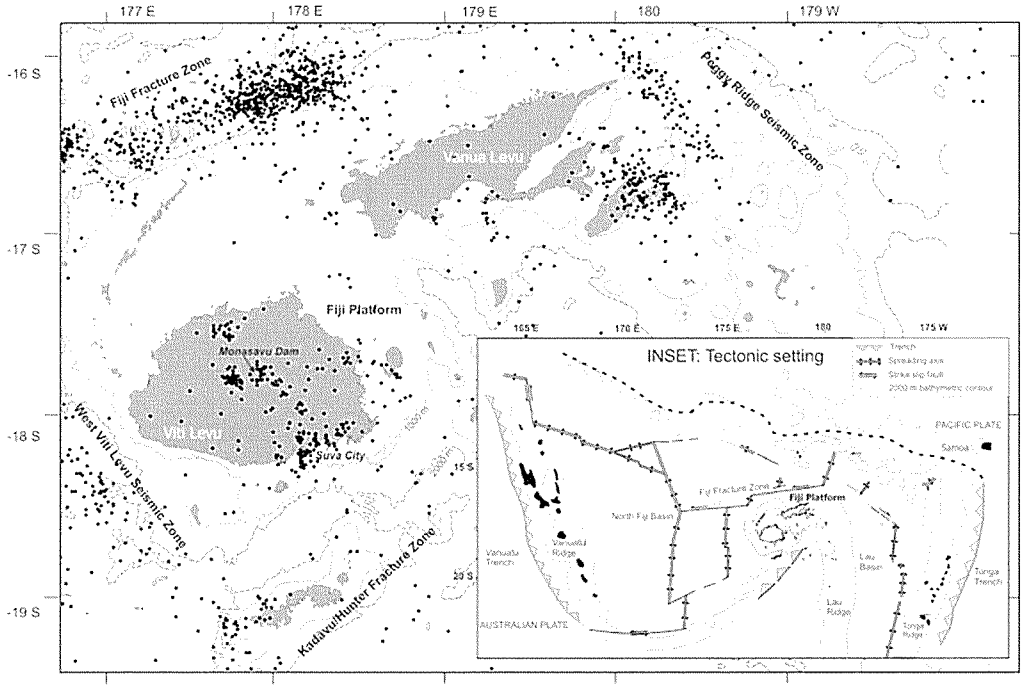

Figure 1: Map of the main islands of Fiji, showing the principal seismotectonic source zones defined by earthquake epicentres (black dots) and regional bathymetry. The critical sites: Suva City and Monasavu Dam, are labelled on Viti Levu. Inset: The tectonic setting of the Fiji Platform.

3 FAULT SOURCES IN VITI LEVU

A comprehensive fault/lineament map was compiled for Viti Levu in order to identify potential earthquake source structures (Figure 2). This map integrates fault data previously published by the Geological Survey of Fiji/Mineral Resources Department with new onshore and offshore fault/lineament mapping described in Rahiman & Pettinga (2008) and Rahiman & Pettinga (2006) respectively.

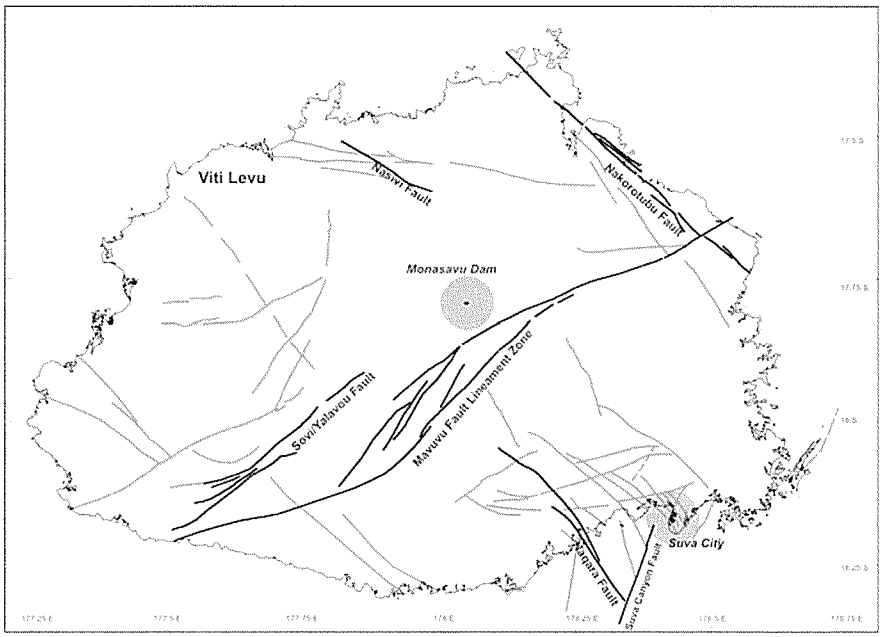

Figure 2: Fault/lineament map of Viti Levu, with locations of critical sites

Forty-seven major faults were identified, all within 70 km of the critical sites. The activity on these faults was evaluated using classification categories of Cluff et al. (1972) which included: active; potentially active; tentatively active; and inactive. The activity categories were assigned based on evidence for historical coseismic surface fault rupture, displacement of Quaternary geological or geomorphological features, and geographic association of the faults with strong earthquakes and well located epicentral data (± 1 to 3 km) on micro to small earthquakes.

None of the faults were classified as active as there were no historical coseismic surface fault rupture records on any. Six faults, however, were classified as potentially active or tentatively active and were investigated further to determine their potential for generating strong ground motions at the critical sites. These faults are the Mavuvu Fault Lineament Zone, Nakorotubu Fault, Sovi/Yalavou Fault, Nasivi Fault, Suva Canyon Fault and Naqara Fault. They are labelled in Figure 2.

4 THE DETERMINISTIC METHOD

The deterministic method involves evaluating and quantifying seismic hazards based on the development of earthquake scenarios. The scenarios assume the occurrence of the largest single earthquake event of known magnitude that appears conceivable on each fault recognised in the region, regarded as the maximum credible earthquake (MCE). The effects of MCEs are compared by calculating ground motions at the site of interest using attenuation relations and the source to site distances. The controlling MCE earthquake or earthquakes (CMCE) are those that produce the worst-case or most severe ground motions and are selected as the design earthquake. This method is time invariant and does not provide the likelihood of the event occurring over a finite period of time.

5 MAXIMUM CREDIBLE EARTHQUAKES

The MCE of the six faults selected in this study were estimated using the empirical relations between earthquake magnitude (M_w) and fault parameters of Wells & Coppersmith (1994) and Stirling et al. (2002). Parameters in the analysis included surface rupture length and rupture area. The longest uninterrupted surface length of a fault was assumed to represent the surface rupture length of the fault and was measured directly off the fault/lineament map. The rupture

area can be calculated using the product of either the surface rupture length (Stirling et al. 2002), or the subsurface rupture length (Wells & Coppersmith, 1994), and the down dip rupture width. The surface rupture is on average equal to 75% of the subsurface rupture length for earthquakes with magnitudes (M_w) between 5.5 to 8.0 (Wells & Coppersmith 1994). The down dip rupture width was constrained by the dip of fault planes, the seismogenic zone depth and the hypocentral depths of large earthquakes within the Fiji Platform. A seismogenic depth of 20 km was adopted to calculate the rupture area.

Table 1 summarises the fault parameters and the calculated MCEs of the six selected faults. Since there are uncertainties in the length, dip and seismogenic depth of faults, a sensitivity analysis of the MCE was carried by changing each of these parameters ± 20% while holding others constant. It was assumed that the true fault parameter value would fall within at least 20% of the estimated adopted value. Changes in the surface rupture length and seismogenic depth by 20% of the adopted values produced variations in magnitudes of only 0.1 magnitude units. Variation in fault dip by 20% resulted in changes in magnitude by 0.02 to 0.04 magnitude units. The variations in the MCE due to uncertainties in the fault parameter data are very small. They are in fact, much smaller than the standard deviation inherent in the regression of the magnitude to fault parameter relationships used here.

The estimated MCEs are half an order of magnitude greater than the magnitudes of large historical earthquakes in the Fiji Platform over the last 150 years, which have been in the range M_w 6.6 to 7.0. Given the low rates of occurrence of large earthquakes within the Fiji Platform, it is reasonable to assume that the maximum historical earthquake would have a magnitude slightly lower than the maximum earthquake potential within the Platform. It is therefore plausible that the estimated maximum capability of the Mavuvu Fault/Lineament Zone of M_w 7.6 would be close to the upper limit of earthquakes within the Fiji Platform. The selected MCEs shown in Table 1 are an average of the results provided by all methods and reflect the best estimate of earthquake potential for each of the sources based on the currently known characteristics of the faults.

Table 1: Maximum Magnitude Earthquakes

Earthquake source	SRL (km)	Fault dip	SSRL^ (km)	RW (km)	(Wells & Coppersmith 1994) [1](M_W)	(Wells & Coppersmith 1994) [2](M_W)	(Stirling et al 2002) [1](M_W)	(Stirling et al 2002) [2](M_W)	**Selected MCE (M_W)**
Mavuvu Fault/ Lineament Zone	127[&]	vertical	169	20	7.5	7.5	7.6	7.6	**7.6**
Naqara Fault	39*	70	52	21	6.9	7.0	7.2	7.2	**7.1**
Sovi/Yalavou Faults	37	vertical	49	20	6.9	7.0	7.1	7.2	**7.1**
Nasivi Fault	20	vertical	27	20	6.6	6.7	6.9	7.0	**6.8**
Suva Canyon Fault	25	75	33	21	6.7	6.9	7.0	7.1	**6.9**
Nakorotubu Fault	60[&]	vertical	80	20	7.1	7.2	7.3	7.3	**7.2**

Abbreviations: SRL - surface rupture length, SSRL - subsurface rupture length, RW - rupture width

[&] Minimum length- continues offshore ^ 1.33 SRL (Wells & Coppersmith 1994)

* Combined onshore-offshore length [1]using SRL [2]using rupture area

6 ESTIMATION OF GROUND MOTIONS

In seismic hazard analysis, ground motion parameters are estimated using attenuation relationships. In the absence of a local attenuation model for Fiji, recently updated attenuation relationships developed from shallow crustal earthquakes from active tectonic (interplate) regions of the world were considered suitable for Fiji conditions. The models of Abrahamson & Silva (1997), Sadigh et al. (1997), Campbell & Bozorgnia (2003) and Spudich et al. (1999) were used in this study. The style of faulting factor was taken as strike slip for all the earthquake sources. As most faults are steeply dipping, the hanging wall factor is not considered significant

for most faults. Owing to the near-field condition of Suva City relative to the Suva Canyon Fault, the directivity effect and the hanging-wall factor were considered to be significant at this site. Both the critical sites were classified as "rock" sites for the models of Abrahamson & Silva (1997) and Sadigh et al. (1997) and as "soft rock" sites for the model of Campbell & Bozorgnia (2003). Monasavu Dam was classified as "shallow soil" site for the model of Spudich et al. (1999).

7 CONTROLLING MAXIMUM CREDIBLE EARTHQUAKES

The estimated horizontal PGA at the two sites produced by all the six source structures using each of the four attenuation relationships are given in Table 2. All the horizontal PGA estimates are median values. The MCE of the source structure that produced the largest horizontal PGA value at a site was selected as the CMCE for that site. The CMCE PGA values are shown in bold in Table 2. The horizontal acceleration response spectra (S_a) for all sites were determined using the CMCEs and the spectral attenuation relationship of Abrahamson & Silva (1997). The 5% damped horizontal acceleration response spectra for each site is shown in Figure 3.

The Suva Canyon Fault and the Mavuvu Fault Lineament Zone are identified as the controlling structures for Suva City and the Monasavu Dam respectively. The CMCE PGA value at Suva City ranges from 0.40g to 0.61g and is produced by an earthquake of magnitude M_w 6.9 on the Suva Canyon Fault at a distance of 4 km from Suva City. The hazard calculated for the Monasavu Dam is a horizontal PGA of 0.39g to 0.51g produced by a CMCE of M_w 7.6 on the Mavuvu Fault/Lineament Zone. The Mavuvu Fault/Lineament is identified as the most relevant seismic source structure to Monasavu Dam as it occurs only 11 km from the dam embankment. This structure was not previously identified in past seismic hazard evaluations of this dam.

Table 2: Horizontal PGAs of MCE at Suva City and Monasavu Dam

Source Structure	Suva City MCE PGA Value (g)				Monasavu Dam MCE PGA Value (g)			
	1	2	3	4	1	2	3	4
Mavuvu Fault/ Lineament Zone	0.12	0.12	0.12	0.1	**0.41**	**0.42**	**0.39**	**0.51**
Naqara Fault	0.27	0.29	0.25	0.32	0.14	0.16	0.14	0.15
Sovi/Yalavou Fault	0.06	0.05	~	0.05	0.12	0.13	0.12	0.13
Nasivi Fault	0.04	0.03	~	0.03	0.16	0.17	0.15	0.16
Suva Canyon Fault	**0.62**	**0.55**	**0.46**	**0.4**	0.07	0.06	0.06	0.07
Nakorotubu Fault	0.09	0.08	0.09	0.07	0.11	0.11	0.11	0.12

Attenuation relationships used:
1 - Abrahamson & Silva (1997)
2 - Sadigh et al. (1997)
3 - Campbell & Bozorgnia (2002)
4 - Spudich et al. (1999)
Note: Values in bold represent CMCE PGAs

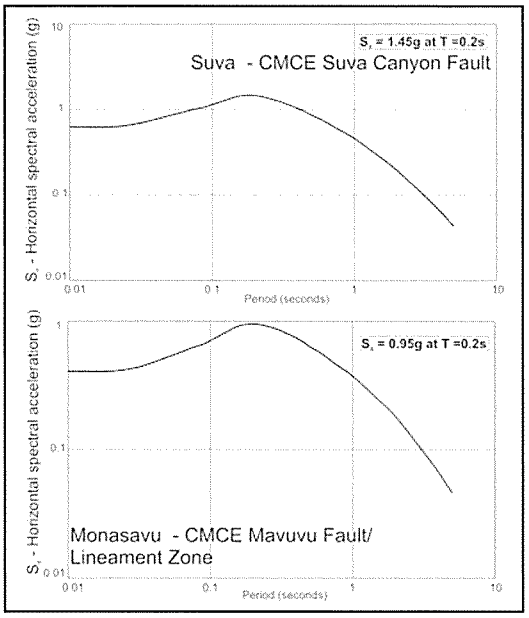

Figure 3: Response spectra for Suva City and Monsavu Dam

8 COMPARISON TO PROBABILISTIC HAZARD MODEL

The 5% damped spectral acceleration at period equal to 0.2 seconds for the two sites were compared to the results of a probabilistic seismic hazard analysis of Fiji by Jones (1998) (Table 3). Spectral accelerations similar to those calculated here using the deterministic approach have return periods of over 1000 years in the probabilistic analysis. Large return periods at these two sites are due to the low rate of occurrence of large magnitude events in Viti Levu in the seismicity model used in the probabilistic analysis. Comparatively larger earthquake loading values at the Suva and Monasavu sites estimated in the present study are due to the closer

proximity of the source structures of large earthquakes than was considered likely in the probabilistic analysis.

Table 3: Deterministic and probabilistic estimates of horizontal, 5% damped spectral acceleration at T = 2 s

Site	Probabilitistic Seismic Hazard (Jones 1996)				This study
	50 yrs	150 yrs	450 yrs	1000 yrs	(Deterministic)
Suva City	0.28	0.45	0.68	0.87	1.45
Monasavu Dam	0.2-0.3	0.4-0.5	0.6-0.7	0.8-0.9	0.95

All values are horizontal, 5% damped spectral acceleration (g) at T = 2 s.

9 CONCLUSIONS

Forty-seven possible crustal fault earthquake source structures are identified and evaluated within 70 km of Suva City and Monasavu Dam in Viti Levu. Six of these structures are recognised as potentially active and tentatively active and are considered capable of producing large ground accelerations at the two critical sites. The deterministic hazard analysis indicates that the Mavuvu Fault Lineament Zone and the Suva Canyon Fault provide the CMCE at Monasavu Dam and Suva City respectively. The CMCE PGA value at Suva City ranges from 0.40g to 0.62g and at Monasavu Dam from 0.39g to 0.51g. The spectral accelerations of the CMCEs at a period equal to 0.2 seconds are comparable to accelerations that have returns periods of over 1000 years in a regional probabilistic seismic hazard study by Jones (1998).

REFERENCES

Abrahamson, N.A. & Silva, W.J. (1997) Empirical response spectral attenuation relations for shallow crustal earthquakes. *Seismological Research Letters* 68, 94-127.

Campbell, K.W. & Bozorgnia, Y. (2003) Updated near-source ground-motion (attenuation) relations for the horizontal and vertical components of peak ground acceleration and acceleration response spectra. *Bulletin of the Seismological Society of America* 93, 314-331.

Cluff, L.S., Hansen, W.R., Taylor, C.L., Weaver, K.D., Brogan, G.E., McClure, F.E., Idriss, I.M. & Blayney, J.A. (1972) Site evaluation in seismically active regions; an interdisciplinary team approach. *Proceedings, First International Conference on Microzonation,* Seattle, Washington, 2, 957-987

Everingham, I.B. (1986) A note earthquake risk zoning in Fiji. *Fiji Mineral Resources Department Note* BP33/14, 6 p.

Jones, T. (1998) Probabilistic earthquake hazard assessment for Fiji. *Australian Geological Survey Organisation Record* 1997/46.

Rahiman, T.I.H. & Pettinga, J.R. (2006) The offshore morpho-structure and tsunami sources of the Viti Levu Seismic Zone, SE Viti Levu, Fiji. *Marine Geology* 232, 203-225.

Rahiman, T.I.H. & Pettinga, J.R. (2008) Analysis of lineaments and their relationship to Neogene fracturing, SE Viti Levu, Fiji. Geological Society of America Bulletin (in press).

Sadigh, K., Chang, C.Y., Egan, J.A., Makdisi, F. & Youngs, R.R. (1997) Attenuation relationships for shallow crustal earthquakes based on California strong motion data. *Seismological Research Letters* 68, 180-189.

Spudich, P., Joyner, W.B., Lindh, A.G., Boore, D.M., Margaris, B.M. & Fletcher, J.B. (1999) SEA99; a revised ground motion prediction relation for use in extensional tectonic regimes. *Bulletin of the Seismological Society of America* 89, 1156-1170.

Stirling, M., Rhoades, D. & Berryman, K. (2002) Comparison of earthquake scaling relations derived from data of the instrumental and preinstrumental era. *Bulletin of the Seismological Society of America* 92, 812-830.

Wells, D.L. & Coppersmith, K.J. (1994) New empirical relationships among magnitude, rupture length, rupture width, rupture area, and surface displacement. *Bulletin of the Seismological Society of America* 84, 974-1002.

Innovative Highway Stabilisation on Rimutaka Hill Road

Selvem Raman
Opus International Consultants, Wellington, New Zealand

Keywords: Slope Stability, Soldier Pile, Ground Improvement Piles, Rock Anchors

ABSTRACT

A section of the SH2 Rimutaka Hill Road was affected by a dropout caused by storm events. Transit New Zealand let a "design and build" tender for the design and construction of a 70 m long retaining structure supporting the road formation to reinstate the affected traffic lane. The instructions for tendering indicated that the specimen design which was a contiguous bored pile wall does not meet the principal's requirements.

A cost effective design solution consisting of a combination of unanchored and anchored (rock anchors) soldier pile wall, and ground improvement piles was developed to provide the required performance. This considers the varying depth of bedrock level below existing ground. A shotcrete facing was provided to support the ground between the piles to transfer the load to the piles.

Trench cut-off drains, sub-horizontal drainage holes, additional sumps, discharge culverts with extended flexible hoses, weepholes and stripdrains were installed to reduce the groundwater pressures and improve stability.

The design considered the importance of the highway as a key arterial road and also Transit's desire for a 50 year design life and 0.2g peak ground acceleration earthquake design.

1 INTRODUCTION

In February 2004, the Wellington Region was hit by a number of major storm events that had a significant impact on the state highway network. The Rimutaka Hill Road on State Highway 2 suffered a number of dropouts. Of these sites, Site 7, which is located at RP 921/9.55 approximately 850 m east of the Rimutaka Summit, is a large dropout with a surface area of approximately 850 m^2. The total length of highway affected was about 70 m.

Following heavy rainfall in June 2005, a larger slip occurred immediately east of the February 2004 slip. The head scarp of this slip encroached to the edge of the road. Tension cracks within the east bound lane developed above the slip and into the carriageway. Both slips converged downslope leaving a large potentially unstable wedge of soil between the two.

Transit New Zealand (Principal) let a "design and build" (DB) tender, for the design and construction of a 70 m long retaining structure and all the necessary ancillary works in supporting the road formation at Site 7. MWH, the region's network management consultant, was the Principal's Advisor, and had undertaken the site investigations and preliminary design.

Fulton Hogan (FH) approached Opus International Consultants (Opus) to be the Designer for the project. Subsequently, FH with Opus collaboration, won the DB contract.

2 PRINCIPAL'S REQUIREMENT

A specimen design was made available in the tender document for contractor's information. However, the tender document clearly stated that the Specimen Design does not meet the

Principal's requirements. The DB contractor was required to prepare and submit a new tender design which meets all the principal's requirements (Transit New Zealand, 2006).

The design had to be in compliance with the Transit New Zealand Bridge Manual. The design was required to be carried out for a design durability life of 50 years. The Principal's requirement specified that the retaining system should be designed for a reduced seismic load corresponding to a 100 year return period earthquake with a peak ground acceleration of 0.2g. The reduced PGA was due to Transit's expectation that this section of the Rimutaka Hill road would be realigned in about 20 years time.

3 LOCATION AND SITE TOPOGRAPHY

The slip site is shown on Figure 1. The slip and site features are shown on Figure 2. The slips are located on a north facing slope, downhill from the summit. A large soil wedge remains intact between two north facing headscarps, immediately below the road. The site is mostly covered with thick bush and shrubs both uphill and downhill from the road. At this section SH2 is a two lane road with a west-bound passing lane. The passing lane was closed following the slips, and two lane access was maintained. Rock exposures can be observed on the cut batter flanking the road on the south side.

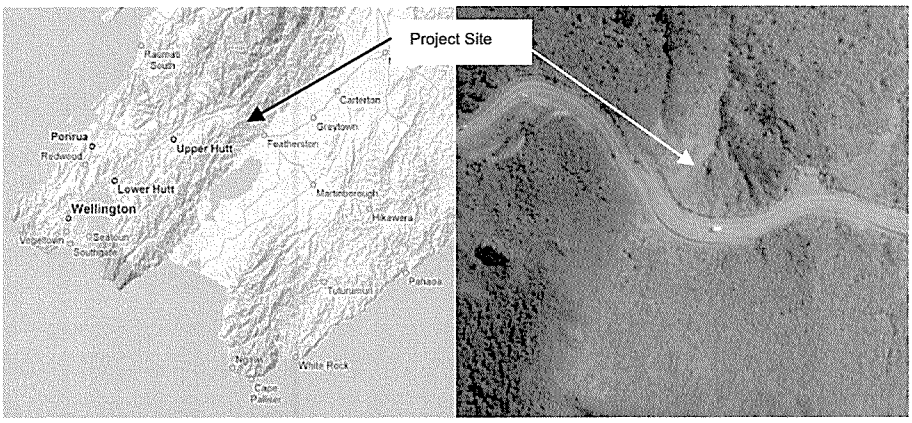

Figure 1: Project Site Location

There are two culverts located below the existing road at both northern and southern ends of the section to discharge the water from the roadside stormwater drain at the southern side of the road. The culvert outlets were discharging on to the slope below the road through the use of drainage socks. Cracking in the pavement extending approximately 2 metres into the carriageway was noted in August 2005. Further cracking in the road pavement was observed in February 2006 and was located along the eastbound lane/middle lane white line.

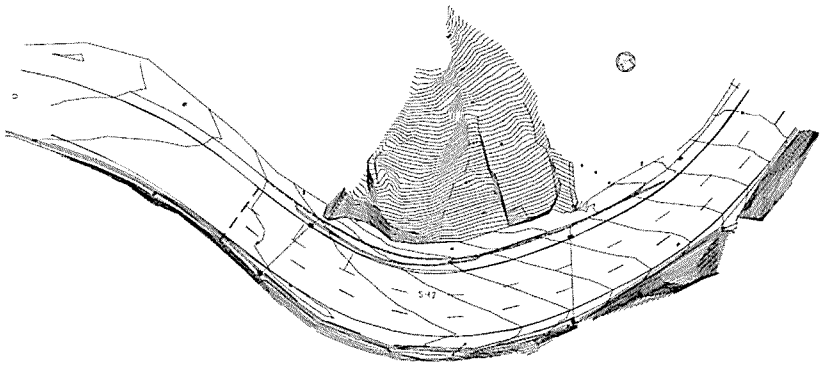

Figure 2: layout of the Slip and Site Features

4 GEOLOGY & GROUND CONDITIONS

The bedrock in this area is the Esk Head belt formation of the Torlesse Supergroup (Institute of Geological and Nuclear Sciences, 2000). This deformed rock belt consists of Greywacke sandstone and argillite dominated sequence with varying degrees of deformation.

The ground conditions at the site comprise generally medium dense to loose silty sandy gravel and gravely silt, underlain by very dense gravely silt and silty gravel with some cobbles and boulders. The overburden soils are underlain by slightly to moderately weathered interbedded sandstone and mudstone, weak to very strong. The bedrock depth is generally up to 13 m with a deeper section up to about 18 m at eastern side of the section. Groundwater monitoring indicated that the groundwater is at or up to a metre above the overburden-bedrock interface.

5 GEOTECHNICAL ASSESSMENT

The fill slope supporting the eastbound lane was found to be of marginal stability, as indicated by the cracking within the pavement. The slip on the slope below the road has created oversteepened head scarps, with a large potentially unstable wedge of soil between two slip headscarps. The site therefore is vulnerable to failure in future storm or earthquake events. The slip is within the fill and colluvium on which the road is constructed. The slip is a shallow translational type failure that occurred within the fill.

The slip is presumed to have occurred during prolonged and intense rainfall events that saturated the soils in the steep slope resulting in failure. The uncontrolled discharge from the two stormwater culverts, directly onto the slope may have also contributed to the erosion and undercutting of the slope. The thick loose overburden soils, the highly fractured and sheared greywacke bedrock and a significant variation in bedrock level presented challenging geotechnical issues.

6 REMEDIAL DESIGN CONCEPTS

Various remedial design concepts were explored and discussed with the DB contractor during the tender stage. The involvement of the contractor helped in evaluating cost effectiveness of different proposals. The following concepts were considered during tender stage:

- Contiguous bored piles with 2 levels of rock anchors (specimen design),
- Soldier piles with rock anchors,
- Soldier piles with deadman anchors,
- Soil nailing of the slope below the road and
- 3 rows of concrete columns along the edge of the road.

The final remedial concept was chosen to accommodate large variations in the bedrock level (from existing ground level to 18 m depth), and allow construction from within the limited space available. The final remedial design concept comprised a combination of:

- Unanchored Soldier Pile wall, where depth to bedrock is up to 3 m
- Anchored Soldier Pile wall, where depth to bedrock is 3 m to 13 m
- Ground Improvement Piles, where depth to bedrock is greater than 13 m

The design concept will support the road formation, and isolate the highway from any potential future slope instability below. Figure 3 presents the longitudinal section along the retaining wall showing the inferred bedrock profile and the combination of different options within the wall section.

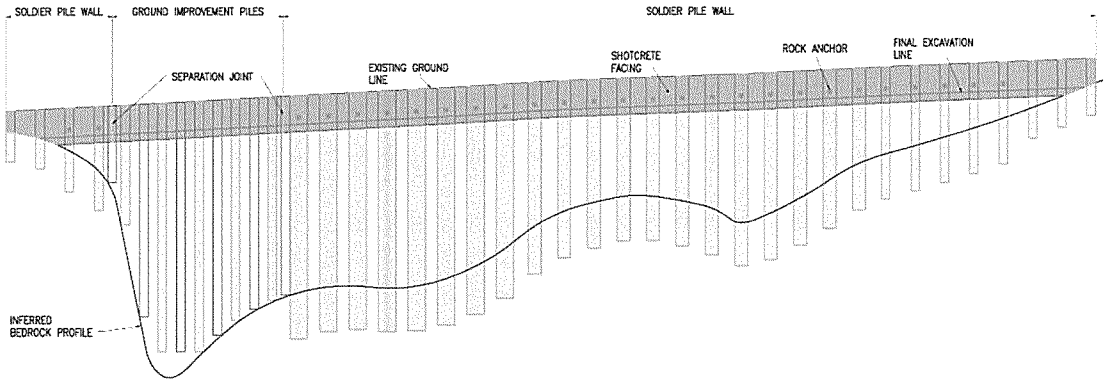

Figure 3: Longitudinal Section of the Wall

7 DETAILED DESIGN

7.1 Tender Award

FH sumitted the tender based on the final remedial concept. Based on the robust and cost effect design concept, the DB contract was awarded to FH with Opus as its designer. Subsequently, Opus developed the detailed design which was reviewed both internally (within Opus) and externally (by an independent consultant), and approved for construction.

7.2 Detailed Design

7.2.1 Soldier Pile Wall

The soldier piles comprised:

- 600 mm diameter piles at 2 m centres, for bedrock depths of up to 8 m
- 900 mm diameter piles at 2 m centres, for bedrock depths between 8 m and 10 m
- 1200 mm diameter piles at 2 m centres, for bedrock depths between 10 m and 13 m

The soldier piles are reinforced concrete bored piles socketed into bedrock. The soldier piles supporting more than 3 m height of overburden (above bedrock) were tied-back with a rock anchor at 1.5 m below the top of the wall. Figure 4 shows a typical detail of the anchored soldier pile. A shotcrete facing is provided for the upper 2.5 m height of the soldier pile wall below road level to support the ground between the piles and to transfer the local earth pressure to the piles.

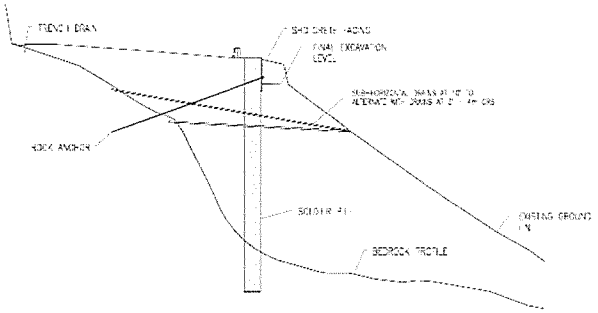

Figure 4: Typical Detail of the Anchored Soldier Pile Wall

7.2.2 Rock Anchors

The rock anchors were installed at 1.5 m below road level to enable practical construction, without having to excavate too far below the road and also to minimise bending moments in the pile. The rock anchors were installed through the bored piles.

The rock anchors comprise of 500 MPa multiple Strand Anchors. The anchors were designed to transfer the wall loads to the bedrock through a fixed bond length in the slightly weathered rock. Three anchor pull-out tests were undertaken before installation of production anchors, to confirm the grout-rock bond capacity. The anchors were designed for a grout-rock ultimate bond capacity of 900 kPa based on the pull-out test results. All the anchors were subjected to acceptance testing prior to lock-off. Figure 5 shows a typical detail of the rock anchor installed.

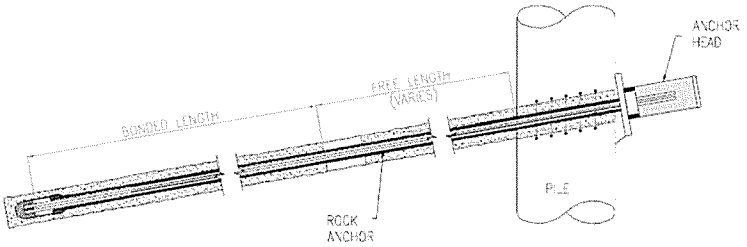

Figure 5: Typical Rock Anchor Details

7.2.3 Ground Improvement Piles

Ground inprovement piles were installed in the section where the bedrock depth is greater than 13 m. Ground improvement piles are 600 mm diameter reinforced concrete bored piles installed in a triangular grid pattern. The ground improvement piles were chosen due to the deep bedrock level. A soldier pile solution would have required larger piles with higher capacity multiple level anchors to withstand the large loads. Figure 5 shows a schematic section through the ground improvement piles.

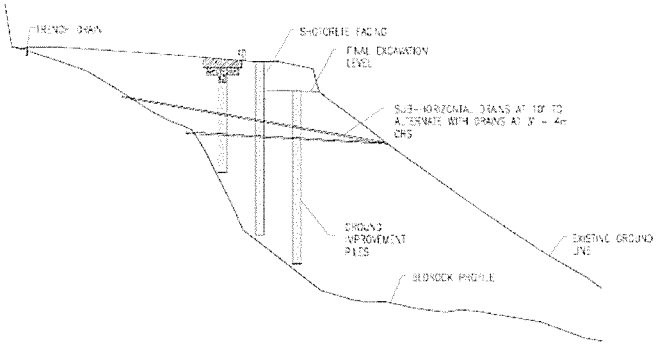

Figure 5: Typical Ground Improvement Piles Details

The ground improvement piles were found to be more cost effective and practical than the large diameter soldier piles and multiple anchors. Soil-pile interaction was considered in the design of ground improvement piles. The reinforcement in the piles improved the bending capacity of the piles and provided confinement to the concrete so that the piles will behave in a ductile manner and withstand displacements, even in a earthquake events larger than the design earthquake event.

A shotcrete wall was installed along the middle pile for the road above to be supported. Movement joints were provided in the shotcrete wall between the soldier piled section and the section strengthened by ground improvement piles, to allow for differential movement during earthquake.

7.3 Drainage Measures

Various drainage measures were provided to reduce the groundwater pressures on the retention systems and improve the overall stability of the slope below. Strip drains and weep holes were installed behind and through the shotcrete face. A trench cut-off drain was installed at the uphill

side of the highway and connected to the existing culverts to intercept the large seepage flows from the hillside into the road formation. Sub-horizontal drainage holes were installed at 4 m spacing in the slope to penetrate into bedrock at a level about 5 m below the road level. These will intercept the groundwater flow above the bedrock interface. The sub-horizontal drainage holes were installed with alternate holes having different inclinations to target different depths where the drains enter bedrock. The discharge from the culverts flow through flexible hoses connected to the outlets and secured down the slope using warratah stakes.

8 CONSTRUCTION

The construction of the remedial works was carried out between April and November (2007). Sufficient quality control measures proposed for wall elements during the detailed design stage were executed to ensure that the design requirements are met.

A new "W" section guardrail was installed and connected to the existing guardrail at the uphill end (Upper Hutt end) and terminates in a terminal end at the downhill end (Featherston end) of the wall. The slope immediately below the road section was hydroseeded to minimise further erosion and discharge of sediments down the slope. The road within the wall section was resurfaced prior to completion of the works.

The completed wall is shown in Figure 6.

Figure 6: Photograph of the Completed Wall

9 CONCLUSIONS

The innovative design concepts provided a cost effective and robust solution to the dropout repair at Rimutaka Hill Road. The DB procurement method adopted facilitated close cooperation between the contractor (FH) and designer (Opus) during tender design, detailed design and construction. The design recognised Transit's performance expectations for this section of highway and provided an innovative, practical and cost effective solution.

REFERENCES

Institute of Geological and Nuclear Sciences (2000) *Geology of the Wellington area, scale 1:50,000*. Geological Map 22. Prepared by Begg, J.R. and Johnston, M.R.

Transit New Zealand (2006) *Contract 494PN, SH2 Rimutaka Dropout Site 7 Remedial Works*. Contract Documents.

Transit New Zealand (2003) *Bridge Manual*. Prepared by Opus International Consultants.

Undrained cyclic tests on silty sands compared using intergranular and equivalent granular void ratio

Sean Rees
Department of Civil and Natural Resources Engineering, University of Canterbury, NZ.

Keywords: liquefaction, sand, fines, undrained cyclic behaviour, equivalent granular void ratio

ABSTRACT

It is well recognised that liquefaction due to seismically-induced cyclic loading can occur in silty sands as well as clean sands. This has led to a significant amount of research into the undrained behaviour of silty sands and the effect that the fines have on this behaviour, although there is still conflict as to the nature of these effects. This issue was investigated by performing undrained cyclic triaxial tests on a silty sand (FBM) sourced from Christchurch, NZ, and a review of cyclic triaxial data from the literature. Two characterisation parameters for silty sand comparisons were assessed – the intergranular void ratio (e_S) and the equivalent granular void ratio (e_C). It was found that e_C was more useful for characterising the cyclic resistance of the tested and reviewed materials, due to a sand-dependant influence factor b accounting for some level of fines participation in the soil force-chain. When comparing materials, lower values of e_C showed higher cyclic resistances.

1 INTRODUCTION AND BACKGROUND

Seismically-induced liquefaction in clean and silty sands has been well documented following the occurrence of historical earthquakes (Chang et al. 1982). This led to research on this phenomenon utilizing both in-situ field testing and laboratory experimental work, which initially focused on the undrained behaviour of clean sands (Shen et al. 1977). It soon became recognised that many instances of liquefaction were occurring in sand deposits containing some amount of fines (Yamamuro & Lade, 1999) and thus research has been undertaken to understand the undrained behaviour of silty sands. This has proven to be more complex (Thevanayagam et al. 2002) than that of clean sands, due in part to the larger range of grain sizes and the potential plasticity of the fines within these silty sands. It has also led to conflict in the literature as to the influence the fines have on the undrained cyclic behaviour, in terms of increasing (Amini & Qi, 2000) or decreasing (Thevanayagam et al. 2000) resistance to cyclic liquefaction.

One of the major difficulties in assessing the effect of such fines is the lack of a reliable parameter for comparing the undrained behaviour across different silty sand materials. Common parameters used when characterising clean sands such as void ratio (e) and relative density (D_r) may not be appropriate for use with silty sands. Research (Thevanayagam, 1998) has suggested that this may be due in part to the fine particles not actively participating in the force-chain of the soil skeleton, but instead sitting in the void space between the sand particles. This led to an intergranular void ratio (e_S) being defined, whereby the fines are considered to be voids.

$$e_S = \frac{e + f_C}{1 - f_C} \tag{1}$$

Further research using this intergranular void ratio determined that the fines were not always inactive in the force-chain, and that some percentage of the fines could in fact participate in providing shear resistance. This insight was used to again adjust the void ratio (Thevanayagam

et al. 2000), taking into account the potential participation the fines, and is defined in Equation 2 as the equivalent granular void ratio e_c, where b = fines influence factor:

$$e_c = \frac{e + (1-b)f_c}{1-(1-b)f_c} \tag{2}$$

This equivalent granular void ratio is dependant on the influence factor for the fines, b, and the fines content. Recent undrained monotonic tests have suggested this parameter ranges between b = 0 – 1.0 for low plasticity fines and b < 0 for plastic fines, for fines contents up to the threshold fines content (Ni et al. 2004). Note that b = 0 corresponds to $e_C = e_S$. Data from a series of laboratory tests was used to examine the usefulness of e_c, along with data presented in literature.

2 MATERIALS AND TESTING

A series of triaxial tests were carried out on a silty sand named the Fitzgerald Bridge Mixture (denoted FBM followed by the fines content) sourced from a site investigation in central Christchurch, NZ. Each material was created by mixing a sand base with varying amounts of fines (the fines were determined to be non-plastic). The triaxial tests included both monotonic and cyclic undrained tests as part of an investigation into the behaviour of silty sands. The material properties are given in Table 1, and the particle size distributions are shown in Figure 1.

Table 1 – Tested material properties

Material	F_C (%)	G_S	e_{max}	e_{min}	$e_{max} - e_{min}$
FBM-1	1	-	0.907	0.628	0.279
FBM-10	10	2.664	0.945	0.597	0.348
FBM-20	20	-	0.895	0.511	0.384
FBM-30	30	-	0.860	0.527	0.333

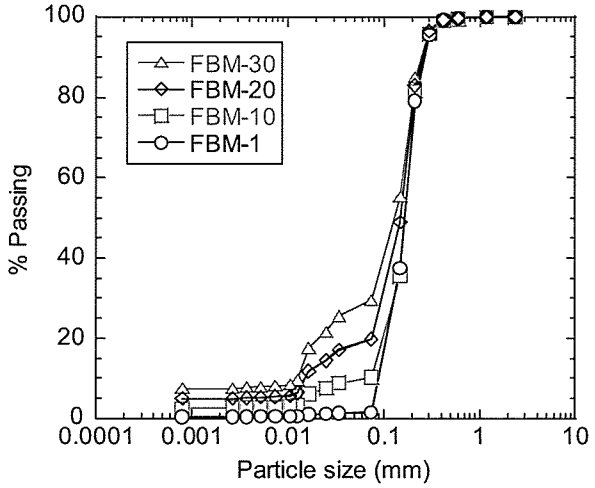

Figure 1 – Material particle size distributions

All cyclically tested specimens were created using a moist tamping placement method and were 100mm in height by 50mm in diameter. The specimens were saturated to a Skempton's B-value ≥ 0.95 and isotropically consolidated to an initial mean effective stress of 100kPa. Undrained cyclic loading was carried out by applying a cyclic stress ratio (CSR) at a rate of 2 min/cycle, with multiple tests performed for a given specimen density to define cyclic liquefaction curves.

3 UNDRAINED CYCLIC TEST RESULTS

Typical undrained stress path and stress-strain curves from the undrained cyclic tests on FBM-10 are shown in Figure 2.

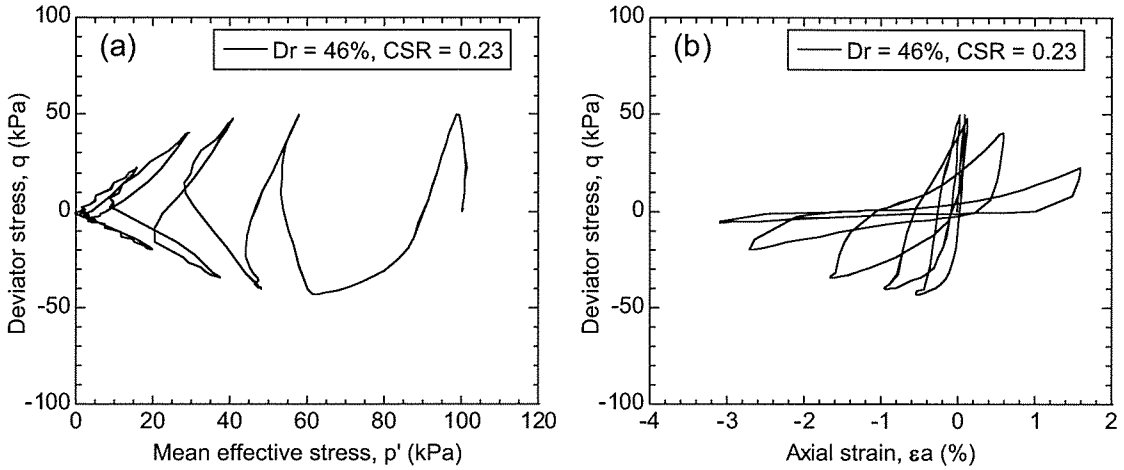

Figure 2 – Cyclic stress path (a) and stress-strain curve (b) for FBM-10.

The stress path in Figure 2 moves towards the condition of zero mean effective stress as the test progresses, reaching initial liquefaction after 4 cycles. The stress-strain curve is typically skewed, with the specimen reaching larger strains in extension. It also shows the onset of cyclic liquefaction, which is defined in this paper as the number of cycles to reach 5% double amplitude (DA) strain. This required some extrapolation of the stress-strain curve peaks as the testing apparatus would not reach the desired level of CSR as the mean effective stress approached zero. Note that the number of cycles to initial liquefaction and cyclic liquefaction coincided in most tests (if this was not the case there was ≤ 1 cycle difference). All cyclic tests were reviewed to determine the number of cycles to reach 5% DA strain for each tested level of CSR. This allowed cyclic liquefaction curves to be created, such as those in Figure 3.

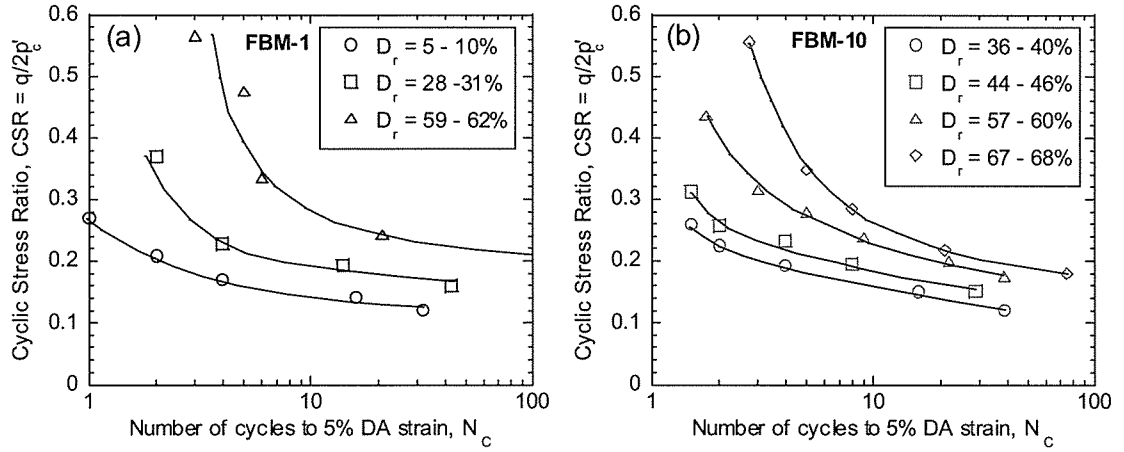

Figure 3 – Cyclic liquefaction curves for FBM-1 (a) and FBM-10 (b)

The curves shown in Figure 3 demonstrate how increasing the specimen density increases the resistance to cyclic liquefaction, as the curves shift upwards with increasing D_r. However they also highlight issues when comparing materials with different fines contents. The lowest strength curves for FBM-1 and FBM-10 are practically coincident in CSR – N_C space, yet the relative densities of the curves are significantly different (D_r = 5 – 10% for FBM-1 and D_r = 36 – 40% for FBM-10). In this case reporting the relative density of a specimen does not give a good indication of the undrained cyclic behaviour, as higher relative densities may perform at lower cyclic strengths compared with other materials, depending on the fines content.

4 INTERGRANULAR & EQUIVALENT GRANULAR VOID RATIO COMPARISONS

4.1 FBM Comparisons

The cyclic resistance (CSR at N_C = 15 cycles) at each specimen density for all materials was evaluated from the cyclic liquefaction curves. This was then compared with the intergranular void ratio e_S to determine the usefulness of considering the fines simply as voids with no participation in the force-chain. These results are shown in Figure 4a.

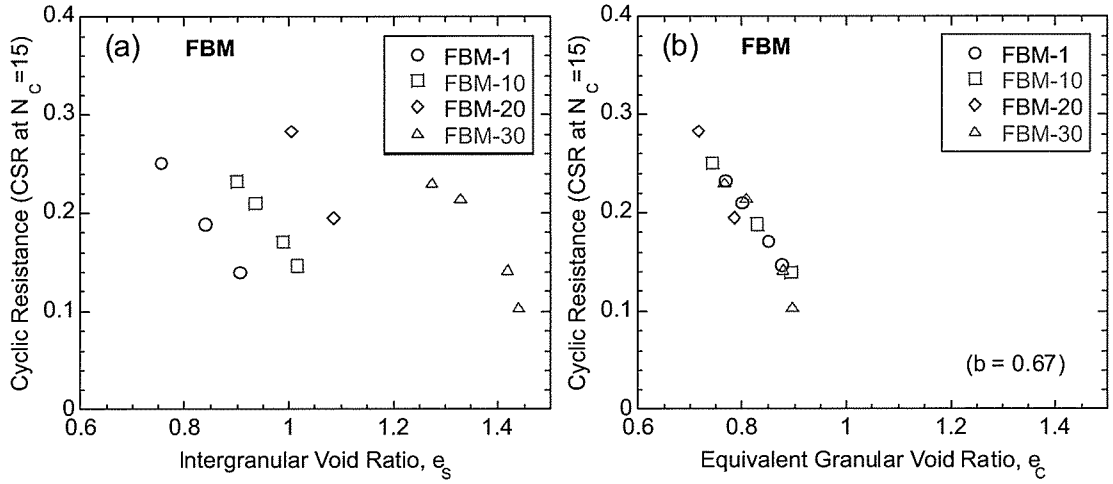

Figure 4 – Cyclic resistance of FBM materials using intergranular void ratio (a) and equivalent granular void ratio (b)

Figure 4a shows a trend of increasing e_S with increasing fines content for a constant cyclic resistance level. This demonstrates that the assumption of the fines not participating in the force-chain to be incorrect for these materials, as all points should in theory fall on the same line (that of FBM-1, which has essentially no fines) if the fines were not participating in the behaviour.

Recognising that the fines influence the undrained cyclic behaviour, the cyclic data was reanalysed to evaluate the equivalent granular void ratio e_C. This accounts for the participation of the fines by incorporating an influence factor, b, into the void ratio equation. Previous work (Ni et al. 2004) has suggested that this factor may be constant for a given sand base and fines up to the threshold fines content, and between 0 – 1.0 for low plasticity fines. Therefore to assess b for the FBM materials, the e_C values were firstly calculated for all tested densities using $0 \leq b \leq 1.0$. These values were then compared to the trend line passing through the FBM-1 cyclic resistance points, with a sum of least squares method being used to determine the best fit from all calculated equivalent granular void ratios. This determined that e_C with b = 0.67 provided the best fit, and the results are plotted in Figure 4b.

Figure 4b shows how the use of the influence factor b for the fines collapses the cyclic resistance points onto a single trend line, which allows for direct comparison of cyclic behaviour between the FBM materials. In this case, a specimen with a lower e_C will have a larger cyclic resistance, regardless of the fines contents of the materials being compared.

4.2 Literature Comparisons

The concept of using the equivalent granular void ratio to characterise the undrained cyclic behaviour of silty sand was extended to incorporate triaxial test data from the literature. This was done to assess how the influence factor b varies with different sands and examine trends

that may allow the prediction of b as opposed to back calculation. Four different sands were used for this assessment, each with a number of different materials created by varying the fines content (all with low plasticity fines). The cyclic resistances were again evaluated using the cyclic liquefaction curves, and Figure 5 shows these resistances for Monterey 0/30 sands (Polito & Martin, 2001) and Yunlin sands (Chien et al. 2002).

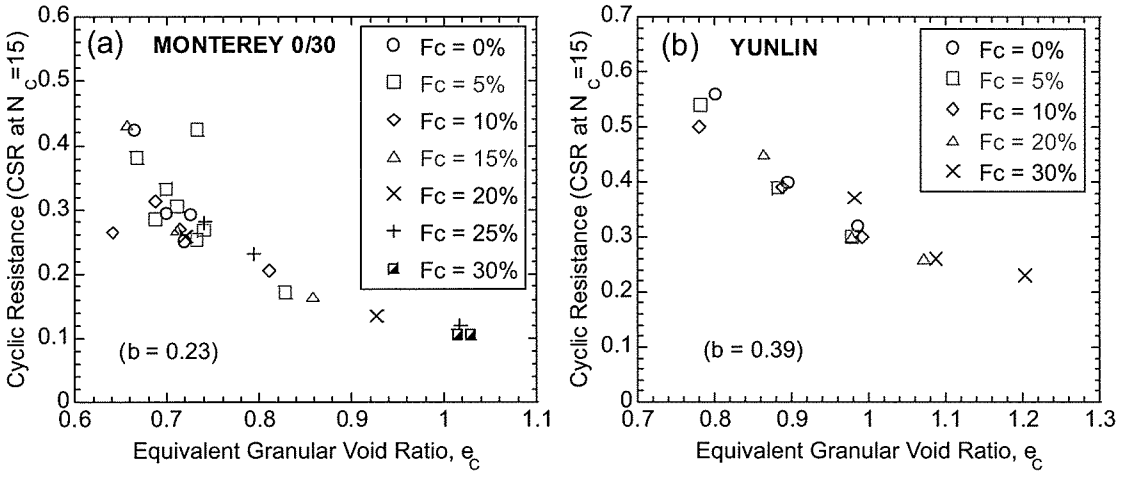

Figure 5 – Cyclic resistance of Monterey 0/30 sands (a) and Yunlin sands (b) using e_C

The plots in Figure 5 again show the cyclic resistances collapsing onto a single line (with some outliers) when using e_C to characterise the materials for up to 30% fines content. Similar trends were seen for Mai Liao (Huang et al. 2004) and Ottawa (Carraro et al. 2003) sands, with b calculated using the same method as for the FBM materials. Results from this assessment are summarised in Table 2, and show a significant range of influence factor values between the examined sands ($0.23 \leq b \leq 0.70$). Also note that two different types of specimen preparation methods were used in these tests (moist tamping and slurry deposition).

Table 2 – Materials and corresponding influence factors

Material	Tested F_C Range (%)	Deposition method	b
Mai Liao	0 - 30	Moist tamping	0.70
Monterey 0/30	0 - 35	Moist tamping	0.23
Ottawa	0 - 15	Slurry	0.31
Yunlin	0 - 30	Moist tamping	0.39

The results from the triaxial testing and literature data suggest that there may be a single influence factor b for a given sand and fines type that will allow good characterisation of the cyclic resistance using the equivalent granular void ratios. This essentially means that a lower specimen e_C value will show higher cyclic resistance when comparing amongst materials within a sand and fines type, regardless of fines content. It also may allow comparison of influence factors between soils to further understand the effects of fines, but this will require more research. Note that results are based on sands with low plasticity fines up to 30% fines content.

5 CONCLUSIONS

A number of results were obtained from the undrained cyclic triaxial testing program on FBM materials (fines contents from 1% – 30%) and the review of literature test data. It appears that a different parameter to those used for clean sands, such as e and D_r, needs to be defined for silty sands. Two potential parameters were examined using the FBM materials and four sands from the literature. These parameters were the intergranular void ratio e_S (assumes no fines

participation in the soil force-chain) and the equivalent granular void ratio e_C (assumes some fines participation in the soil force-chain). These were assessed using the cyclic resistance for given specimen densities of each material, and produced the following conclusions:

(1) e_S did not provide a unique relationship with the cyclic resistance for the FBM materials. Analysis showed that e_S increased with increasing fines content for a given level of cyclic resistance.

(2) e_C did provide a good correlation with cyclic resistance for the FBM materials. All points collapsed onto a single curve when using a single influence factor value of b = 0.67. A similar trend was observed when using data from the literature, but with varying b factors.

(3) When comparing specimens of a given sand, a lower e_C will correspond to a higher cyclic resistance.

ACKNOWLEDGEMENTS

The author would like to acknowledge the help from his supervisors, Dr Misko Cubrinovski and Dr Elisabeth Bowman, and the financial support provided by the Earthquake Commission (EQC), New Zealand.

REFERENCES

Amini, F. & Qi, G. (2000) Liquefaction Testing of Stratified Silty Sands. *Journal of Geotechnical and Geoenvironmental Engineering.* ASCE.

Carraro, J. et al (2003) Liquefaction Resistance of Clean and Nonplastic Silty Sands Based on Cone Penetration Resistance. *Journal of Geotechnical and Geoenvironmental Engineering.* ASCE.

Chang, N. et al (1982) Liquefaction Potential of Clean and Silty Sands. *Proceedings of the 3rd International Earthquake Microzonation Conference.*

Chien, L. et al (2002) Effects of fines content on liquefaction strength and dynamic settlement of reclaimed soil. *Canadian Geotechnical Journal.*

Huang, Y. et al (2004) A laboratory study on the undrained strength of a silty sand from Central Western Taiwan. *Soil Dynamics and Earthquake Engineering.*

Ni, Q. et al (2004) Contribution of fines to the compressive strength of mixed soils. *Geotechnique.*

Polito, C. & Martin, J. (2001) Effects of Nonplastic Fines on the Liquefaction Resistance of Sands. *Journal of Geotechnical and Geoenvironmental Engineering.* ASCE.

Shen, C. et al (1977) The Effects of Fines on Liquefaction of Sands. *Proceedings of the 9th International Conference on Soil Mechanics and Foundation Engineering.*

Thevanayagam, S. et al (2000) Effect of Non-Plastic Fines on Undrained Cyclic Strength of Silty Sands. *Proceedings from Soil Dynamics and Liquefaction 2000.*

Thevanayagam, S. et al (2002) Undrained Fragility of Clean Sands, Silty Sands, and Sandy Silts. *Journal of Geotechnical and Geoenvironmental Engineering.* ASCE.

Yamamuro, J. & Lade, P. (1999) Experiments and modelling of silty sands susceptible to static liquefaction. *Mechanics of Cohesive-Frictional Materials.* John Wiley & Sons, Ltd.

Micropiling in Karstic Rock

Anne Rosborg
Golder Associates (NZ) Ltd, Auckland, New Zealand

ABSTRACT

Golder Associates Pty Ltd was employed by the construction group at Sepon Gold Mine, SPDG, in Laos to assist in the design and construction supervision for bridge foundations, whose superstructure would eventually support pipelines carrying tailings across the Namkok River, a tributary to the Mekong River in Southeast Asia. Following an options study and initial bored pile works, conventional bored piles were discounted due to the karstic landscape in favour of micropiles, a relatively uncommon approach in large parts of Asia. This particular type of piling provided greater flexibility in variable ground conditions and allowed the use of smaller, more portable plant but also presented added complexity to the site work, which was made more demanding due to the remoteness of the area. This paper outlines the geotechnical aspects of the project with focus on the construction phase of the piling, where flooding, cultural diversity and language difficulties were part of the daily routine in addition to the technical and logistical challenges encountered during the installation process.

1 INTRODUCTION

Access to communist Laos has been restricted until 1990, at which time the country saw an influx of tourists and foreign investors. The Australian mining company Oz Minerals Ltd formerly known as Oxiana Ltd established a base in southern Laos in a joint venture with the Lao government and formed Lane Xang Minerals Ltd with the intention of extracting gold and copper from the hills surrounding Sepon. The project started in 2000 when the area was purchased from Rio Tinto with the plant completed in 2001 and the first gold and copper produced in 2002 and 2005, respectively. Oz Minerals Ltd has since expanded the operation to form a well established mining community that employs 2000 workers at present. Golder has provided on-going consultancy services for the mine over a number of years in the form of exploration advice and engineering assistance on infrastructure projects.

Plans for a pipeline carrying tailings contaminated with cyanide to a newly established tailings dam were proposed in 2005 as part of an upgrade to the mine and Golder was contracted to design the piles supporting two bridges over the Namkok and Namkieng Rivers. This paper will focus on the construction of the foundations for the bridge crossing the Namkok River. The bridge measures a total of 144m in length and features two piled abutments and two intermediate piers, each supported by a group of approximately 20 micropiles.

Commissioning of the entire pipeline relied on timely completion of the bridges and with the construction period leading up to the monsoon season in Asia, it was critical that the construction went as smoothly as possible with priority given to the works in the river bed.

1.1 Geological Setting

The subsurface profile comprises 10m to 15m of interbedded alluvium and clay underlain by high weathered karstic dolomite. Fill from the mining operation was encountered overlying the alluvium on the eastern abutment.

The stratigraphy can be divided into three main geotechnical units of varying thickness:

- Overburden material in the form of surface fill and / or fluvial deposits along the river bed. The fill comprised silt with varying amounts of gravel and boulder sized fragments up to

18m depth below ground level. The fluvial deposits consisted of soft clay surface sediments and a combination of sand, gravel and boulders to 14m depth.

- Karstic grey dolomite was typically encountered below 10m to a depth of 30m to 70m below the surface level with multiple infilled cavities estimated up to 6m in height. The infill material was typically soft silt and very loose fine grained sand. The strength of the intact rock between the cavities was moderately strong to very strong with UCS values ranging from 30MPa to 150MPa.

- The karstic features of the dolomite reduced at depth. This unit was referred to as fresh dolomite, although the interface between the fresh rock and the overlying chemically weathered zone was gradual and determined using a degree of judgement. The fresh dolomite was described as dark grey, strong to very strong with some quartz veins and silica staining.

Typical core samples and a geological cross section of the subsurface conditions summarising the findings are provided below on Figures 1 and 2, respectively:

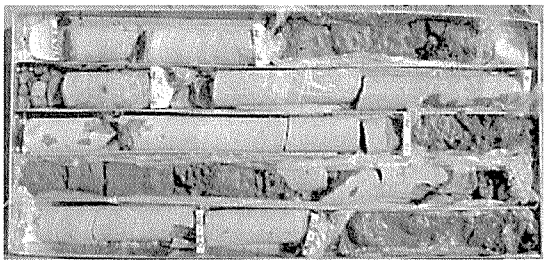

Figure 1a: Karstic highly weathered dolomite showing open cavities with silty sand infill

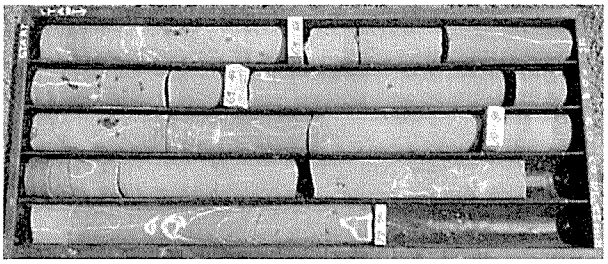

Figure 1b: Fresh strong dolomite

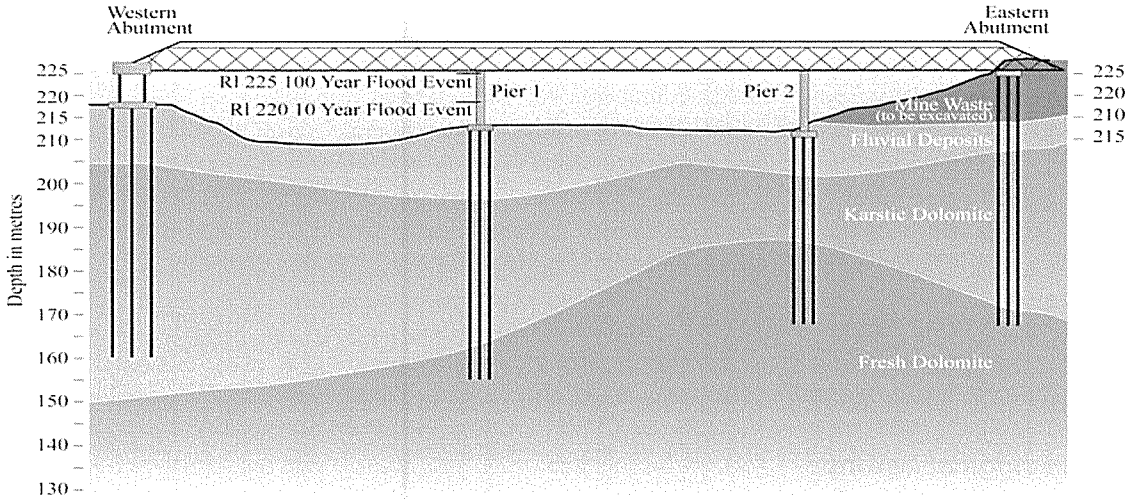

Figure 2: Geological cross section at Namkok site in relation to the bridge location

1.2 Aspects of Karstic Rock

Karstic topography is a landscape shaped by chemical weathering and is generally the result of mildly acidic water acting on soluble calcareous bedrock such as limestone or dolomite. The carbonic acid that causes these features is formed as rain passes through the atmosphere picking up CO_2, which dissolves in the water. Once the rain reaches the ground, it may pass through soil that provides further CO_2 to form a weak carbonic acid solution: $H_2O + CO_2 \rightarrow H_2CO_3$.

Over time, the rock develops distinctive features such as sinkholes, caves, enclosed depressions, pinnacles, floating boulders and caverns within otherwise competent rock strata. Overburden soils above such cavities can collapse into the voids forming sinkholes. The term refers to a type of hummocky terrain found in the Karst area of Slovienia but has been adopted to describe any area that has similar features (Traylor et al, 2001).

2 INITIAL APPROACH

2.1 Design and Methodology

Bored piles were initially adopted, in part due to the remoteness of the area and the contractor's familiarity with traditional bored piles. The Thai contractor, Siam Tone, utilised commonly adopted construction practices involving large diameter bored piles using casing and drilling mud for support in the unstable upper ground. The design comprised six piles per pier in the form of 800mm diameter friction piles with the socket within competent rock zones containing the lowest risk of karstic features. The design toe level for the bored piles was about 25m below ground level. The construction of such piles proved difficult due to the unstable nature of the subsurface conditions at many elevations above the competent rock.

The construction method consisted of using a tricone drill bit to advance the holes with a reverse circulation pump to lift the cuttings from the base of the hole. The bentonite drilling fluid was stored in holding tanks and continuously reconditioned for recirculation. In order to stabilise the overburden soil strata, a casing was vibrated into the ground prior to mucking out excess material from within the casing.

2.2 Summary of Learnings during the Construction Period

A few teething issues were experienced with the suction pump, piping and rig. This was partly due to the state of the equipment, which demanded a high level of maintenance. In addition to the problems experienced with the plant, the casing method became a problem as it could only be vibrated to the top of the karstic rock stratum. However, when drilling through a cavity, collapses in the unstable clay infill material were common. Loose boulders were also present as well as sizeable fragments of strong rock sheared off during the drilling process, which lead to very slow progress as the rotation of the drill string was obstructed by the larger objects.

Even worse were instances where cavity material collapsed on top of the drill string causing the drill head to shear off, resulting in further delay while the trapped length of the string was retrieved from the hole. Delays were also experienced sourcing a hard formation drill bit required to penetrate high strength intact rock due to the remoteness of the area. Extra weights were added to the drill string to increase the bit pressure, however this triggered further problems as it increased torque on the bit, causing it to shear more frequently down the hole.

Multiple attempts were made to lower the casing to avoid collapsing of the hole. This had to be done by letting a weight in the shape of a chisel free fall within the casing to the bottom of the hole in order to loosen material. The spoil was then picked up by a crane operated grab. Once the hole was clear of debris, the casing was pushed down. The process was repeated until the casing was lowered sufficiently, although this was again a very time consuming exercise. In addition, the grab occasionally became wedged in the pile hole due to boulders loosened by the chiselling and drilling activities falling on top, thus jamming the grab in place within the hole.

The delays associated with using relatively large diameter casing and mud drilling methods became significant and alternative methods more suitable to the karstic conditions were assessed. After four weeks with drilling difficulties on site, the pile design and installation methodology were changed to smaller diameter rotary percussive methods which were better able to penetrate the ground and confirm rock quality.

3 REVISED DESIGN ADOPTING MICROPLIES

3.1 Concept

It was decided that micropiles would offer an appropriate solution to the construction problems experienced on site. Micropiles are structural elements which have a small overall diameter, typically less than 300mm. At this site, they comprise steel pipes acting as reinforcement surrounded by pressure injected grout. A typical cross section of a micropile is shown on Figure 3. They are usually designed to transfer load by skin friction, acting in a similar manner to soil nails. The main difference between micropiles and standard piles is that a micropile is basically a steel section grouted into the ground as opposed to a reinforced concrete structure. This allows for small diameter drilling using smaller rigs capable of advancing the hole using percussive, coring or auguring techniques.

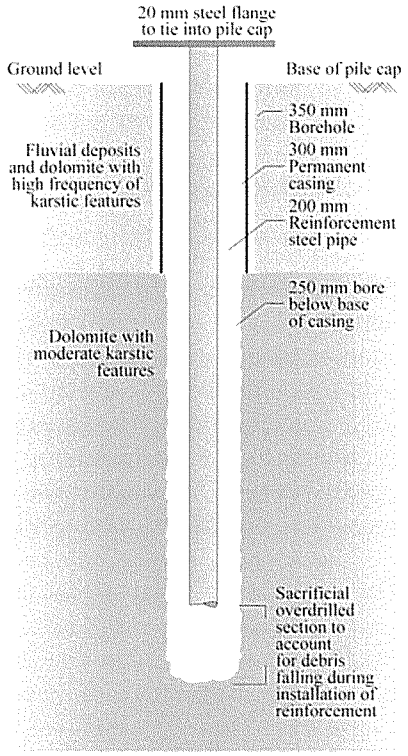

Figure 3: Typical cross section of a micropile

An advantage of this type of pile is that the existence of a major karstic feature just under the pile tip has a low risk of compromising the performance of the micropile, as it would have the potential to do in the case of a large-diameter end bearing pile. The design implication is that if a certain thickness of competent rock is encountered, then the available pile capacity can be more reliably assessed. There is therefore dramatically reduced risk of piles "punching through" into a solution feature as would occur in the case of an end-bearing pile.

Since the material types used to provide pile capacity in karst can range from relatively poor quality rock and weathered materials that behave as sands and gravels to very strong rock, construction observations are an important tool when ensuring that the design requirements for bond lengths are satisfied in each pile.

3.2 Design of Bridge Foundations at Namkok

In addition to the four cored boreholes drilled during the geotechnical investigation for the bridge, an additional air percussive drill hole was drilled at the each of the abutments and pier locations to gain an appreciation of drilling rates, frequency of cavities, suitability of drilling equipment and stability of small 150mm holes in the karstic zone.

The abutments and piers were designed to be supported by fourteen 300mm micropiles transferring the axial loading of 750kN per pile and eight shorter piles intended to provide lateral support due to relatively high river flow forces acting on the bridge (55kN per pile). The fourteen main micropiles extended to depths up to 70m and the secondary micropiles for the lateral loading were 12m long. Subsequent load testing of a pile to 1000kN indicated a deflection in the order of 6mm.

4 CONSTRUCTION CONSIDERATIONS

4.1 Projectwide Factors

The micro piling works were delegated to two contractors: Siam Tone was employed to carry out the grouting of the piles and the drilling operation was undertaken by the exploratory drilling company associated with the mine, Boart Longyear Asia. As soon as specialist drilling

equipment, such as stabilisers, bits and adapters sourced from South Africa, India and Thailand were brought to site, the micro piling work began.

Due to the timing of the project and the delays experienced during the attempts to construct large diameter bored piles and the setup time for the micropiling operation, it was unlikely that the micropile installation would be complete before the onset of the monsoon. Contingency plans were made for a rapid demobilisation of the site, as the water level of the river was known to rise quickly following intense rainfall. These were put into effect twice during construction, each time resulting in a one week delay to the project. The crane on site was critical to the success of the operation, as this was responsible of lifting most of the plant onto dry land.

4.2 Ground Improvement

Ground improvement measures were undertaken to preconcolidate the areas immediately under the piers to ensure the lateral stiffness of the soils was sufficient and to prevent buckling of the micropiles. A 12m by 12m area was excavated to 1.5m depth and replaced with a low strength concrete. This exercise also prevented scouring to occur adjacent to the pier location during periods of flooding. In addition, grout was injected to bind the riverbed deposits in order to facilitate drilling through the gravel strata. Furthermore, boreholes were drilled at the pier and abutment locations to further map the presence of major voids and grouted by gravity to stabilise the karstic rock and pre-fill existing voids.

The eastern embankment contained substantial amounts of non-engineered fill, which was removed and replaced with compacted fill through an earthworks operation exposing a 12m deep excavation in three tiers covering an area of 40m by 60m in plan view. This work was carried out while the piles for the piers were drilled.

4.3 Drilling

The drilling company was managed by expatriates from Australia, who oversaw the operation to ensure the local Lao drillers carried out the drilling as intended. The approach involved drilling of 350mm diameter holes to the interface between the overburden material and the karstic rock, installing 300mm diameter sacrificial casings and drilling 250mm diameter sockets below the base of the casing. In some instances the length of the cased segment was increased to key the casing into the fresh dolomite in order to reduce grout consumption and prevent collapse of infill material in areas with large cavities.

Installation records were kept for each pile, logging the quality of the rock, the depths of any cavities and composition of the infill material. The exploratory air percussive and cored borehole logs were used for planning the pile installation, but in karst conditions, the rock quality varied greatly within short distances and each pile was considered unique in overall length, un-bonded length, depth to rock head and sequencing of the bearing strata. For this project, cumulative sections in excess of 3m of moderately strong rock were recorded towards a total of 30m of competent rock, at which point the design bearing capacity was reached. In addition to the pile logs, one pile was successfully test loaded to confirm the overall design parameters as mentioned in Section 3.2 of this paper.

The micropile drilling component was difficult and required good control of the rig due to the risk of breaking the drill string on contact with the uneven base of a cavity. This lesson was learnt relatively early into the drilling programme, when the drill string sheared, leaving the newly purchased drill bit and stabilisers in the ground. Despite several attempts to retrieve the equipment, the undertaking was abandoned. However, SPDG foresight during the equipment sourcing stage proved invaluable as a second set of stabilisers and drill bit was available.

4.4 Grouting

The grouting process is critical to the integrity of the micropile. Due to the presence of cavities and the connection between the pile locations through the cavities, the grout consumption for the first piles in a pier or abutment location amounted to several times the volume of the pile, as grout filled the surrounding cavities. It was not uncommon to inject ten to fifteen cubic metres of grout into a pile location when completing the first pile, despite the theoretical volume of the pile being approximately $0.2m^3$. The total volume of grout injected equated to $200m^3$.

It is important to ensure that the grout will fully encapsulate the reinforcement of the micropile to provide adequate bonding between the pile and the rock. The flange bolted onto the top of the reinforcement pipe would function as a pressurised tremie during the grouting process (refer Figure 3). As a result, the grout would be forced to the base of the hole through the reinforcement pipe and surround the outside of the reinforcement and the casing before daylighting at surface level, thus ensuring that the pile was fully grouted. Post grouting of the outside of the casing would take place as a final measure before the pile was complete.

6 CONCLUSIONS

Essentially, a micropile is a steel section grouted into the ground, allowing for the use of small diameter drilling with small rigs. This technique was adopted for the foundations for the Namkok Bridge at the Oz Minerals Mine Site in Sepon, Laos. The micropiling commenced in July 2007 and was completed in December 2007 with the bridge launched later the same month. The experience gained from the design process and construction of the micropiles is valuable and proves that micropiles are an efficient and advantageous solution to piling in karstic rock or similar conditions, where traditional bored piles cannot be constructed. In particular, the benefits of micropiling were noticeable when advancing the drill hole to depths up to 70m with only minor collapses of the hole walls experienced during drilling.

It is worth acknowledging the risk involved in implementing relatively uncommon construction practices within the mining industry. It was gratifying that Oz Minerals Ltd (under the guidance of SPDG) chose to adopt the micropile design. In general, it is our experience that decision makers on mine sites seem more open-minded and willing to try new techniques if there is a potential to finish sooner or possible cost savings, than managers of conventional building projects. This is partly because of the dynamic environment of the mining business and the nature of mining, where financial risk taking is an integral part of the scene when it comes to establishing a mine, assessing ore bodies and predicting the life span of the mine.

Micropiles are presently rarely used in New Zealand. It is considered to be a matter of time before micropiles are routinely implemented in projects here as they are suitable in a variety of applications, typically in situations requiring underpinning or stabilisation of roads or structures. They are a practical alternative pioneered in Italy to resolve site constraints such as restricted access, complicated ground conditions and geology or difficulties with conventional construction methodologies. By raising awareness of this type of piling it is anticipated that there will be projects incorporating micropiles in the near future in this part of the world.

REFERENCES

Bruce, D.A. Member; Cadden, A.W. Member; & Sabatini, P. J. (2005) *Practical Advice for Foundation Design – Micropiles for Structural Support.*

Jennings, J.N. (1985) *Karst Geomorphology*, 2nd Edition.

Traylor, R.P.; Cadden, A.W.; Bruce, D. A.; MASCE (2001) *High Capacity Micropiles In Karst: Challenges and Opportunities.*

Quantifying the influence of rolling dynamic compaction

Brendan Scott
School of Civil, Environmental and Mining Engineering, The University of Adelaide, Australia

Mark Jaksa
School of Civil, Environmental and Mining Engineering, The University of Adelaide, Australia

Keywords: compaction, ground, improvement, impact, rolling

ABSTRACT

Rolling dynamic compaction (RDC) is a commonly used ground improvement technique. A key feature of RDC is the ability to provide deep layer compaction when compared to conventional rollers. This greater zone of influence makes it a productive and cost-effective option in earthworks applications. Whilst RDC has been used successfully on many projects in Australia and overseas in applications such as roads, airports, construction and land reclamation projects, there are cases where the expected ground improvement has not occurred. There is a lack of information indicating what the zone of influence of the roller is, and how much input energy is required for different soil conditions. The methods of testing the effectiveness of RDC need improvement. Relationships are needed that relate the input energy and the ground improvement that can be expected for different soil types.

1 INTRODUCTION

Rolling dynamic compaction (RDC) consists of a non-circular module of 3, 4 or 5 sides, that rotates about its corners as it is towed, causing it to fall to the ground and compact it dynamically. A square impact rolling module is shown in Figure 1. A cross section of this 4-sided module, which is concrete filled and encased with steel, is shown in Figure 2. The module is towed at a speed typically in the range of 10-12 km/h (Pinard 1999).

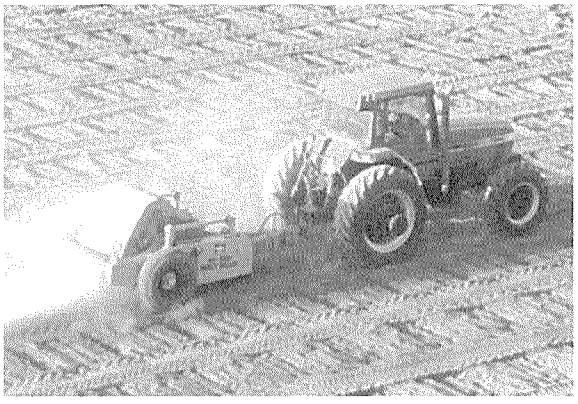

Figure 1: 4-sided impact roller

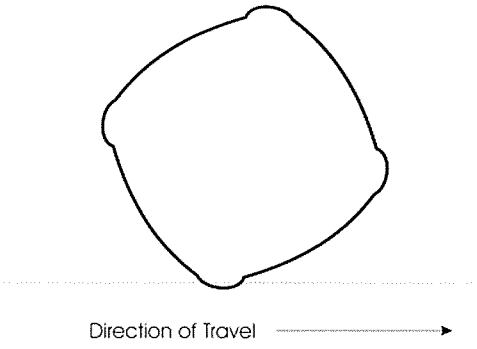

Figure 2: Cross-section of 4-sided module

2 NEED FOR GROUND IMPROVEMENT

One of the major functions of geotechnical engineering is to design, implement and evaluate ground improvement schemes for civil engineering infrastructure projects. Since the 1970s an increasing number of new technologies and ground improvement methods have been developed and implemented to assist the geotechnical engineer in providing cost-effective solutions for construction on marginal or difficult sites. The available methods and techniques to improve the geotechnical characteristics of soils are described in detail by Terashi & Juran (2000), Munfakh & Wyllie (2000) and Munfakh (2003). The general consensus from the

aforementioned authors is that ground improvement using surface dynamic compaction techniques such as RDC can be successfully undertaken to improve a soil's shear strength and stiffness, or reduce its permeability.

RDC has been used successfully in many earthworks applications in Australia and overseas including the improvement of poor quality ground insitu, the compaction of thick layers for in-filling deep excavations, the proof rolling of road and subgrade materials and the compaction of reclaimed land. In recent years, RDC has been used to construct haul roads in the mining industry, as well as in agriculture, where it is used to compact soil in irrigated areas to reduce soil permeability and conserve water.

3 WHAT IS THE DEPTH OF INFLUENCE OF RDC?

RDC has demonstrated improvements in soil density to depths of more than one metre below the ground surface for clay soils and 2-3 m or more in sands (Avalle, 2004, Avalle & Carter, 2005). This zone of influence is far deeper than conventional static or vibratory rolling techniques (Clegg & Berrangé 1971, Clifford 1976, 1978), which are generally limited to depths of less than 0.5 m. This ability to provide deep layer compaction, as well as its relatively fast operating speed (when compared to conventional rollers) makes RDC a productive and cost-effective option in earthworks applications. This view is supported by Pinard (1999) who stated that in most open-field situations, RDC is able to compact soil, crushed rock and landfill waste cost-efficiently and to greater depths when compared to other available compaction methods.

Whilst RDC has the proven ability to improve a variety of soil types, for example sand (Figure 3) and clay (Figure 4), not all site conditions lend themselves to using RDC. Small or restricted sites are not suitable, as the roller is not able to maintain an operating speed in the vicinity of 10-12 km/h. Clifford & Bowes (1995) predicted the impact energy of the square roller and concluded that the speed of the module striking the ground was the most significant parameter contributing to the energy imparted by the impact roller. In the author's experience, careful assessment (e.g. the use of an impact rolling trial) is highly recommended in soil conditions where non-engineered fill material is present, particularly if the site contains large oversized material; depending upon the nature and depth of the material it may be able to be broken down and compacted, however, there is also the potential for it to bridge underlying soil that would otherwise be improved (Scott & Suto 2007). Cases have also been observed where the high energy impacts of RDC have caused existing inter-particle bonds to break within the soil; hence careful assessment of the suitability of RDC is needed in such soil conditions.

The depth of influence of RDC varies, depending upon factors such as the soil material type, moisture, groundwater conditions and the input energy (Avalle 2004). There is currently little information on predicted depths of treatment for varying soil conditions, and it is often up to the project engineer to predict if the use of RDC will improve the ground sufficiently for the project application. This prediction as to whether to adopt RDC for ground improvement at a site, may or may not prove to be cost-effective, as RDC has the potential to save significant time and construction costs (or otherwise). In applications where deep layers of imported fill material are being compacted it is common for cost benefits to still be obtained whilst limiting the layer thicknesses to well within the capability of the machine, however, the variable depth to which ground improvement can be achieved is one of the biggest limitations on the use of RDC when improving insitu material, as a back-up plan may need to be implemented if ground improvement is not achieved to the required (or expected) depths. The variable depth of treatment using RDC also has the potential to cause damage to existing services, culverts or bridges (via load transfer) if an insufficient thickness of soil is not placed over such structures. Broons (2008) recommends that at least 1.5 metres of soil cover is required to prevent such damage, however, further research is warranted to verify or refine this requirement.

4 HOW IS GROUND IMPROVEMENT USING RDC VERIFIED?

There are currently no guidance documents to provide the engineering profession with recommended testing methods to use for various soil conditions so that appropriate decisions and assessments can be made on the ground improvement undertaken by RDC. Whilst the latest edition of the Australian Earthworks Code, AS 3798 (Standards Australia 2007) now recognises deep compaction by impact rolling as an alternative procedure for earthworks, it offers little guidance as to how to determine if ground improvement has been achieved, only stating that "trial programs may be required to develop the most appropriate testing regime for any particular project or site". As explained by Avalle (2004) there is no simple rule that outlines what the scope and nature of trial programs should be, as this depends on factors such as budget, efficiency, risk and site conditions.

Field density testing (in order to comply with AS 3798) is commonly undertaken to verify thick-lift filling or ground improvement using RDC. The determination of field density testing using a nuclear surface moisture-density gauge (Standards Australia 1995), is the current industry standard, and involves determining the in situ density at discrete locations within 300 mm below the tested surface, making it an ideal testing method where conventional surface compaction techniques and relatively thin layers (lifts) are used. However, RDC applications involving thicker lifts or where surface improvement of in situ ground is undertaken, verification using field density testing requires excavation through compacted material to the desired test levels. Scott & Suto (2007) used this method to help quantify ground improvement using RDC, and cited limitations such as lengthy test durations and the difficulty with the testing process for mixed soils, particularly where oversized particles are present.

The cone penetration test (CPT) involves statically pushing a cone penetrometer and associated drilling rods into the ground and continuously recording the resistance to penetration mobilised in the soil (Lunne et al. 1997). The CPT has been shown to be one of the most accurate in situ test methods available in routine geotechnical engineering practice (Jaksa et al. 1997), and has been successfully used in RDC applications to verify the ground conditions prior to, and after impact rolling. Avalle & Carter (2005) reported the verification of RDC in sandy soils; with improvement evident to at least 3 metres below the ground surface (refer Figure 3). Budget constraints, availability of equipment and the presence of heterogeneous fill material often dictate as to whether the CPT can be used to verify impact rolling applications.

For sites containing significant quantities of mixed soils or oversized particles that are not conducive to traditional (intrusive) geotechnical investigation methods, the use of seismic methods is becoming increasingly common. The use of seismic methods such as MASW (Multi-Channel Analysis of Surface Waves) and CSWS (Continuous Surface Wave System) as reported by Scott & Suto (2007) and Avalle & Mackenzie (2005), respectively, enable correlations of Young's modulus to be made from measuring seismic velocity. Avalle & Mackenzie (2005) reported the verification of RDC in a clay landfill capping overlying refuse using CSWS; with improvement evident to approximately 2 metres below the ground surface (refer Figure 4). Budget constraints and the use of highly specialised equipment are factors that may limit the use of seismic methods to verify RDC.

The use of on-board sensing equipment to measure density, stiffness, subgrade strength or modulus based on the response of the roller as it travels across the ground surface is becoming increasingly common. This technology (known as Intelligent Compaction or Continuous Compaction Control) was first used on vibrating drum rollers the mid 1990s to help identify soft spots and to create more uniform pavement and subgrade layers (Petersen & Peterson 2006). Similar technology, known as the Continuous Impact Response (CIR) system, has recently been introduced into RDC applications and is discussed in detail by McCann & Dix (2007) and Landpac (2008). The CIR system involves measuring ground decelerations from

accelerometers that are placed on the impact rolling module. With increasing passes, ground decelerations increase as the soil density and stiffness increase. A GPS system is employed to spatially monitor the movements of the impact roller, thereby enabling soft spots to be identified from both ground decelerations and spatial data. Due to the inherent heterogeneity of soils in terms of their material properties and moisture contents, technology such as Intelligent Compaction and CIR will become more prevalent in the future, and are good examples of how advances in technology are helping to improve confidence in achieving uniform compaction.

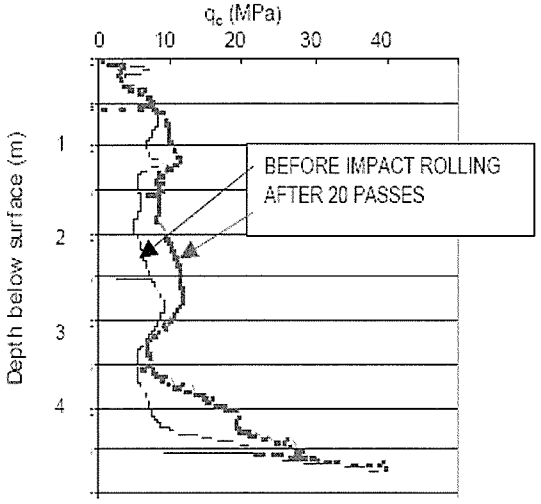

Figure 3: Verification using CPT (Avalle & Carter 2005)

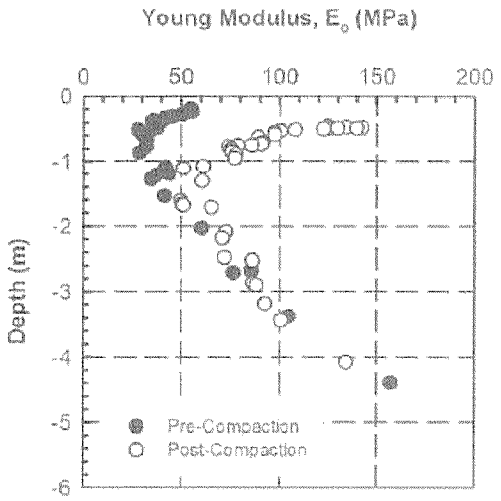

Figure 4: Verification using seismic methods (Avalle & Mackenzie 2005)

Measuring surface settlements is commonly adopted; this can be undertaken in a number of ways, ranging from the use of accurate robotic total station equipment to the use of simple string lines and tape measures (Avalle 2004). Whilst settlement monitoring output can generally be obtained in an efficient and cost-effective manner, care needs to be taken to account for the effect of surface undulations caused by the periodic impacts of the module on the ground (as observed in Figure 1). Such surface undulations can typically have up to 200-300 mm height difference between the high and low points, meaning that if accurate surface settlements are to be obtained, a grader and smooth-drum roller are often required to produce a finished level surface. Alternatively, embedded steel plates can be placed beneath the surface to help overcome the effect of surface undulations. This method has been adopted in recent trials undertaken by the authors, whereby central vertical tell-tale rods of variable lengths can be bolted to the steel plates prior to embedment to measure settlement at various depths below the ground surface. The use of magnetic extensometers installed within boreholes has also been trialled for this purpose, and is the more promising method for determining settlement in targeted soil layers, especially as installing and removing embedded steel plates can become quite cumbersome when placed greater than 300 mm below the ground surface.

Further to the methods discussed previously, Avalle (2004) offers a comprehensive list of testing methods that have been adopted prior to, and after impact rolling to quantify ground improvement. As stated by Avalle (2004) the different test methods chosen often depend on factors such as the geotechnical engineer's preference of field testing methods and experience with impact rolling, available testing equipment, budget constraints, site location and ground conditions. It is the author's opinion that site specific field trials are the most appropriate and efficient way of assessing factors and considerations such as: will RDC be suitable for the site conditions? How many passes are required? What testing methods are appropriate to quantify and validate the performance of RDC? With a large variation in current approaches, there is a need for some direction and guidance.

5 NEED FOR FURTHER RESEARCH INTO RDC

Currently, a key limitation that restricts the use of RDC is the reluctance by the engineering profession to specify the use of impact rolling. This is largely due to the theory behind RDC generally not being well understood, particularly as the use of RDC is often guided by intuition, or based on experience in similar soils and applications. Whilst RDC is a commonly used technique to improve poor or marginal ground, there is little published information on what the zone of influence is for different soil types, or to indicate what testing methods should be adopted to quantify its effectiveness.

In order to develop, calibrate and validate a suitable model for RDC applications, field and laboratory measurements are needed in a variety of site conditions. A database containing testing data from previous RDC projects is being used to assist with this research; however, further field testing and measurements are required to complement existing data. This will involve conducting field testing both prior to, and after impact rolling to compare and evaluate a number of different testing methods. Commonly specified testing methods on impact rolling projects (such as those discussed in Section 4), as well as insitu permeability and porewater pressure testing will be trialled in a variety of soil conditions. Laboratory tests to classify soil types and to determine shear strength and compressibility parameters will also be undertaken so that accurate and efficient testing and verification techniques and protocols can be recommended to quantify the improvement of RDC in the field.

To determine the zone of influence of RDC on different soil conditions, commonly used testing methods will be combined with instrumentation that is embedded into the ground to quantify the zone of influence of RDC. The transfer of energy of the impact rolling module to the underlying ground will be measured at various depths, using load cells and accelerometers that will be embedded into the ground. The impact roller will pass over the embedded instrumentation whereby the force measured in the load cell, and the ground deceleration measured using accelerometers can be used to determine the energy recorded. By measuring the energy at various depths below ground level, and for differing soil types, it will enable the zone of influence of the roller to be quantified.

6 CONCLUSIONS

Although RDC has been used on many projects in Australia and overseas, there is little published information quantifying what the zone of influence is, or how much energy is required in order to improve soils of different types. There is also little guidance on how RDC should be verified to quantify its effectiveness.

It is anticipated that the outcomes of this work will enable RDC to be applied and validated more appropriately for a range of soil conditions. More accurate assessments of RDC, as well as improved testing regimes, are expected to reduce design conservatism and construction costs. In addition, perhaps most significantly, quantifying the effectiveness of RDC in terms of the energy imparted into the ground and the zone of influence for various soils will lead to a greater understanding of its theory, which will enable RDC to be used more effectively and with greater confidence in a range of engineering applications.

ACKNOWLEDGMENTS

The authors wish to acknowledge Broons Hire (SA) Pty Ltd., a South Australian company that owns and manufactures the square impact roller for their support of this research. The first author also wishes to acknowledge Dr Mark Jaksa, Dr William Kaggwa, Dr Peter Mitchell and Mr Derek Avalle for their ongoing support in undertaking this research.

REFERENCES

Avalle, D.L. (2004) Impact Rolling in the Spectrum of Compaction Techniques and Equipment. *Earthworks Seminar Proceedings,* Australian Geomechanics Society, Adelaide, 1-4.

Avalle, D.L. & Carter, J.P. (2005) Evaluating the Improvement from Impact Rolling on Sand. *6th International Conference on Ground Improvement Techniques,* Coimbra, Portugal.

Avalle, D.L. & Mackenzie, R.W. (2005) Ground improvement of landfill site using the "square" impact roller, Australian Geomechanics, Vol. 40, No. 4.

Broons (2008) Website: *http://www.broons.com/*, accessed 25 July 2008.

Clegg, B. & Berrangé, A.R. (1971) The Development and Testing of an Impact Roller. *The Civil Engineer in South Africa,* Vol. 13, No. 3, 65–73.

Clifford, J.M. (1976) Impact Rolling and Construction Techniques. *Proceedings ARRB Conference,* Vol. 8, 21–29.

Clifford, J.M. (1978) *Evaluation of Compaction Plant and Methods for the Construction of Earthworks in Southern Africa,* Masters Thesis, University of Natal, South Africa.

Clifford, J.M. & Bowes G. (1995). Calculating the Energy delivered by an Impact Roller. *A trilogy of Papers for the September 1995 Lecture Tour and International Seminars to commemorate the tenth anniversary of the BH 1300 Standard Impact Roller,* Paper Two, pp 1-15.

Jaksa, M.B., Brooker, P.I. & Kaggwa, W.S. (1997) Inaccuracies Associated with Estimating Random Measurement Errors. *Journal of Geotechnical and Geoenvironmental Engineering,* ASCE, Vol. 123, No. 5, 393–401.

Landpac (2008) Website: *http://www.landpac.co.za/*, accessed 25 July 2008.

Lunne, T., Robertson, P.K. & Powell, J.J.M. (1997) *Cone Penetration Testing in Geotechnical Engineering Practice,* Blackie Academic and Professional, New York.

McCann, K. & Dix, S. (2007) Engineered impact compaction of un-engineered fills. *Earthworks Symposium,* Australian Geomechanics Society, Sydney, 83-92.

Munfakh, G.A. & Wyllie, D.C. (2000) Ground Improvement Engineering - Issues and Selection. *Proceedings International Conference on Geological and Geotechnical Engineering, GeoEng2000,* Melbourne, CD-ROM.

Munfakh, G.A. (2003) Ground Improvement in Transportation Projects: From Old Visions to Innovative Applications. *Ground Improvement,* Thomas Telford, Vol. 7, No. 2, 47-60.

Petersen, L. & Peterson, R. (2006) *Intelligent Compaction and In-Situ Testing at Mn/DOT TH53.* Minnesota Department of Transportation, Report No. MN/RC-2006-13, Minnesota.

Pinard, M.I. (1999) Innovative Developments in Compaction Technology Using High Energy Impact Compactors. *Proceedings, 8th Australia New Zealand Conference on Geomechanics,* Hobart, Australian Geomechanics Society, Vol. 1, 775-781.

Scott, B.T & Suto, K (2007) Case study of ground improvement at an industrial estate containing uncontrolled fill. *Proceedings 10th Australia - New Zealand Conference on Geomechanics,* Brisbane, Vol. 2, 150-155.

Standards Australia (1995) Soil Compaction and Density Tests – Determination of Field Density and Field Moisture Content of a Soil Using a Nuclear Surface Moisture-Density Gauge – Direct Transmission Mode, *AS 1289.5.8.1,* Sydney, NSW.

Standards Australia (2007) Guidelines for earthworks for commercial and residential developments, *AS 3798,* Sydney, NSW.

Terashi, M. & Juran, I. (2000) Ground Improvement-State of the Art. *Proceedings International Conference on Geological & Geotechnical Engineering, GeoEng2000,* Melbourne, Vol. 1, 461–519.

Comparison of lateral loads due to surcharge with particular reference to the Australian Standard AS4678 (2002)

Bernard Shen
Pells Sullivan Meynink, Sydney, Australia

ABSTRACT

The Donaldson open pit coal mine is located in Blackhill, New South Wales. Three water pipelines, supplying approximately 100,000 people in the Cessnock and Maitland areas, traverse the mine site. A design for a crossing over the pipelines was required in a short time frame to allow access to the western part of the site for mining purposes. The crossing had to accommodate 300 t hydraulic mining shovels and 250 t mining trucks.

The design led to a requirement to assess the lateral loads imposed on the crossing structure by a fully loaded CAT785B mining truck. The paper presents a comparison of six methods of assessing lateral loads due to surcharge with particular reference to the Australian Standard AS4678 (2002), Earth-retaining structures. The six methods are line load, Rankine active earth pressure theory, surcharge, semi-infinite load with elastic theory, loaded strip with elastic theory and finite element method.

The comparison demonstrates that the methods provided in AS4678 (2002) are either too conservative or not conservative enough. Therefore, where large surcharges are involved, other methods for assessing lateral loads from surcharge should be considered during design and the methods presented in AS4678 (2002) not simply adopted.

1 INTRODUCTION

The Donaldson open pit coal mine is located in Blackhill, New South Wales. Three Hunter Water Corporation (HWC) water pipelines, supplying approximately 100,000 people in the Cessnock and Maitland areas, traverse the mine site. A design for a crossing over the pipelines was required in a short time frame to allow access to the western part of the site for mining purposes.

The design led to a requirement to assess the lateral loads imposed on the crossing structure by a fully loaded CAT 785B mining truck with a maximum rear axle load of 167 t. The paper presents a comparison of six methods of assessing lateral loads due to surcharge with particular reference to the Australian Standard AS4678 (2002), Earth-retaining structures.

2 DESIGN

The design criteria for the crossing required it to carry loads from 300 t hydraulic mining shovels and 250 t mining trucks and a design life of 5 years. Also, a requirement for a 2 m high by 5 m wide access space around the pipes was imposed by HWC to have access to the pipes for minor works if required. The crossing was also designed such that it could be dismantled within 24 hours should emergency access to the pipes be required.

The crossing comprised cast in situ reinforced concrete vertical walls on either side of the pipes and precast reinforced concrete top slabs supported by the walls, as shown in Figure 1. Footings for the structure comprised 450 mm diameter piles founded on bedrock spaced at 1.0 m centres. The walls were backfilled with engineered fill to provide a ramp approach for the mine vehicles.

3 LOADS

The load considered during design is that due to a fully loaded CAT 785B mining truck. The truck imposes a lateral load on the structure as it approaches the structure and a vertical load on the top slab as it crosses the pipes. The paper discusses the lateral loads imposed on the structure.

The actual truck loads and distributions are referenced from the Caterpillar Performance Handbook, Edition 37.

Total load of CAT 785B (fully loaded)	= 250 t (2453 kN)
Load on rear axle	= 167 t (1640 kN)

Some methods of assessing lateral loads require simplification of the actual loading geometry. The load was therefore simplified in the following two ways:

- Equivalent uniformly distributed load (UDL)
- Line load

3.1 Equivalent uniformly distributed load (UDL)

The UDL was calculated based on the load distribution shown in Figure 2 (a) and (b). A tyre pressure of 700 kPa was adopted for the assessment of tyre contact area.

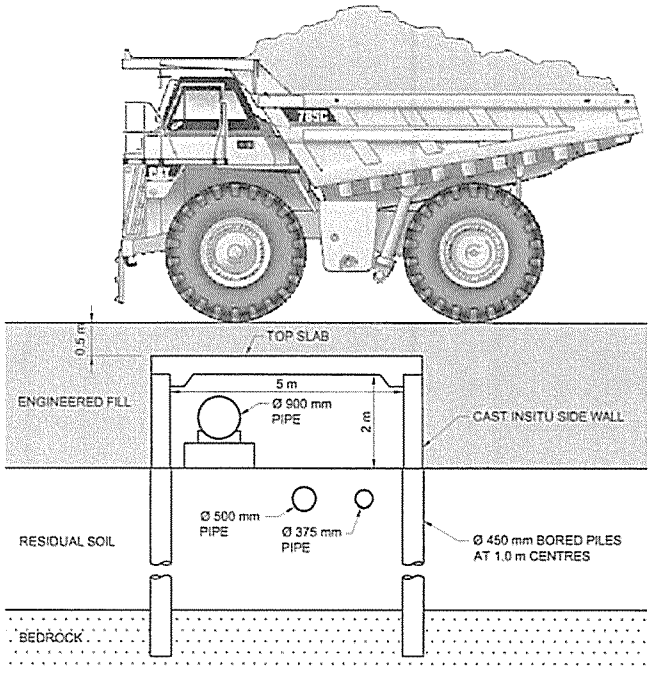

Figure 1: Pipeline crossing design

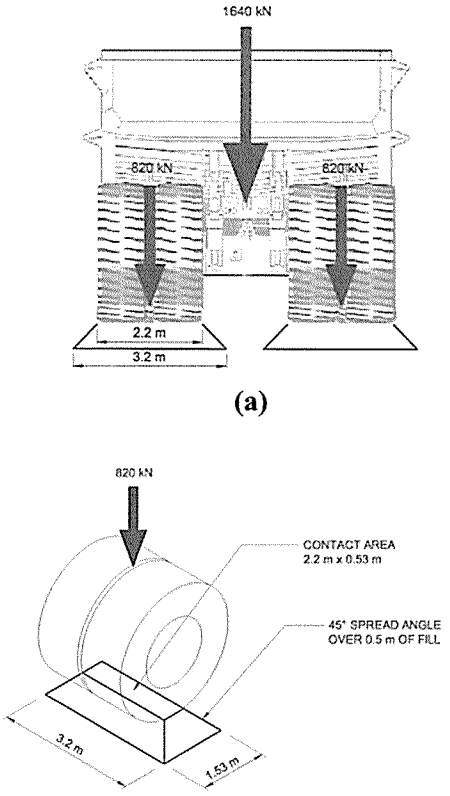

Figure 2: Load distribution

Load per pair of wheels on the rear axle	= 1640 kN / 2	= 820 kN
Contact area per pair of wheels	= 820 kN / 700 kPa	= 1.17 m^2
Contact area at 0.5 m depth with load spread	= 1.53 m x 3.2 m	= 4.9 m^2
∴ Service load	= 820 kN / 4.9 m^2	= 168 kPa

The calculated service load is treated as a semi-infinite UDL applied at the slab level as shown in Figure 3. Note that the service load actually extends 1.53 m away from the structure and 3.2 m into the third dimension, therefore treating it as a semi-infinite UDL is conservative.

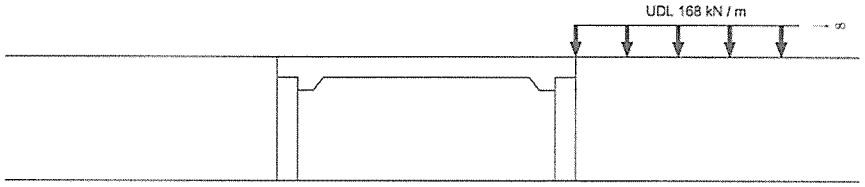

Figure 3: Equivalent uniformly distributed load

3.2 Line load

Load per pair of wheels on the rear axle	= 820 kN	
Width of pair of wheels	= 2.2 m	
Line load	= 820 kN / 2.2 m	= 373 kN / m

The calculated line load is applied at the surface, 0.5 m above the slab level.

4 ENGINEERED FILL PARAMETERS

The Engineered Fill specified comprised of a compacted cohesive and frictional fill. The following parameters were adopted:

- Cohesion (c') = 5 kPa
- Friction angle (ϕ') = 35°
- Young's modulus = 15 MPa

5 LATERAL EARTH PRESSURE

The lateral earth pressure on the loaded side of the structure was assessed using six methods. Clause J10.3 in Appendix J of AS4678 (2002), allows the following approaches to assess the magnitude and distribution of lateral pressures induced by surcharge loading:

- Rankine active earth pressure theory
- Elasticity theory supported by experimental measurements
- Numerical modelling

5.1 Method 1 - Line load

This method is provided in AS4678 (2002) and the Hong Kong Geoguide 1 (1994) which originates from a paper by Terzaghi (1954). The truck load is treated as a vertical line load (Q_l) applied at a distance (x) away from the structure. The lateral earth pressure distribution is shown in Figure 4. The lateral earth pressure (σ_h) and horizontal force (P_h) is calculated with equations (1) and (2).

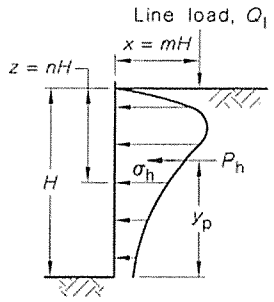

For $m \leq 0.4$

$$\sigma_h(\frac{H}{Q_l}) = \frac{0.20n}{(0.16+n^2)^2} \quad (1)$$

$$P_h = 0.55Q_l \quad (2)$$

Figure 4: Lateral earth pressure distribution

Following a literature review, Morgan (1988), Bowles (1996) and NavFac Design Manual 7.2 (1982) all note that this method produces high lateral earth pressures and caution against its use without specific consideration. Terzaghi and Peck (1967) and Terzaghi, Peck and Meshri (1996) do not adopt this method. British Standard BS8002 (1994), Code of practice for earth retaining structures, does not adopt this method but recommends characterising the load as a surcharge (see Method 3).

5.2 Method 2 - Rankine active earth pressure theory

This method is provided in AS4678 (2002). The truck load is treated as a semi-infinite UDL and the Rankine's coefficient of active earth pressure (K_a) is adopted. The increase in lateral earth pressure ($\Delta\sigma_h$) is calculated by equation (3).

$$\sigma_h = K_a\sigma_v - 2c'(K_a)^{0.5} \qquad \text{where } K_a = \frac{1-\sin\phi'}{1+\sin\phi'}$$

Thus, $\Delta\sigma_h = K_a\Delta\sigma_v$ (3)

5.3 Method 3 - Surcharge

This method is recommended by BS8002 (1994), which is more conservative than the Rankine approach (Method 2) suggested by AS4678 (2002). The truck load is treated as a semi-infinite UDL and adopts a coefficient of earth pressure at rest (K_0). The increase in lateral earth pressure ($\Delta\sigma_h$) is calculated by equation (4).

$$\Delta\sigma_h = K_0\Delta\sigma_v \qquad \text{where } K_0 \approx 0.95 - \sin\phi' \quad (4)$$

5.4 Method 4 - Semi-infinite load with elastic theory

This method is provided in Poulos and Davis (1974), equation 3.10b. The truck load is treated as a semi-infinite UDL and the lateral earth pressure is assessed using elastic theory. The increase in lateral earth pressure ($\Delta\sigma_x$) is calculated by equation (5) with reference to Figure 5.

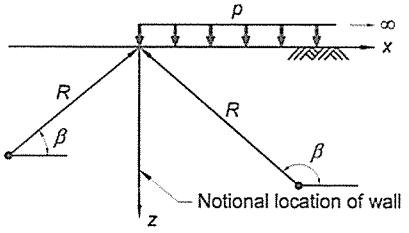

$$\Delta\sigma_x = \frac{p}{\pi}(\beta - \frac{xz}{R^2}) \quad \text{where } \beta \text{ is in radians} \quad (5)$$

Thus, $\Delta\sigma_h = 0.5\Delta\sigma_v$

Figure 5: Semi-infinite UDL

The method does not explicitly include Poisson's ratio as part of the solution. A finite element analysis was performed using Phase^2 by Rocscience Inc. to observe the effects of varying Poisson's Ratio. The analysis indicated a Poisson's ratio of 0.5 has been assumed in the Poulos and Davis equation. Note that it is conservative to assume 0.5 for Poisson's ratio.

5.5 Method 5 - Loaded strip with elastic theory

This method is provided in Poulos and Davis (1974), equation 3.1b and Clayton et al (1993), table 5.1. The truck load is treated as a loaded strip immediately adjacent to the structure with an assumed width (L) of 2.0 m. The increase in lateral earth pressure ($\Delta\sigma_h$) is calculated by equation (6) with reference to Figure 6. It is likely that this method also assumes, but does not state, a Poisson's ratio of 0.5.

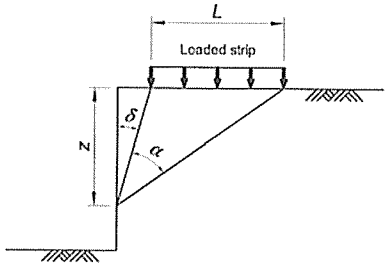

$$\Delta\sigma_h = \frac{\Delta\sigma_v}{\pi}\left[\alpha - \sin\alpha\cos(\alpha + 2\delta)\right] \qquad (6)$$

where α and δ vary with depth (z) and are in radians

Figure 6: Loaded strip

5.6 Method 6 - Finite element method

A 2D finite element analysis software, Phase^2 by Rocscience Inc. was used to assess the lateral earth pressure applied on the structure. The truck load is treated as a semi-infinite UDL in the finite element model to model the service load case. Note that numerical modelling is allowed by AS4678 (2002).

6 RESULTS

The lateral earth pressure distributions resulting from the six assessment methods are summarised in Figure 7.

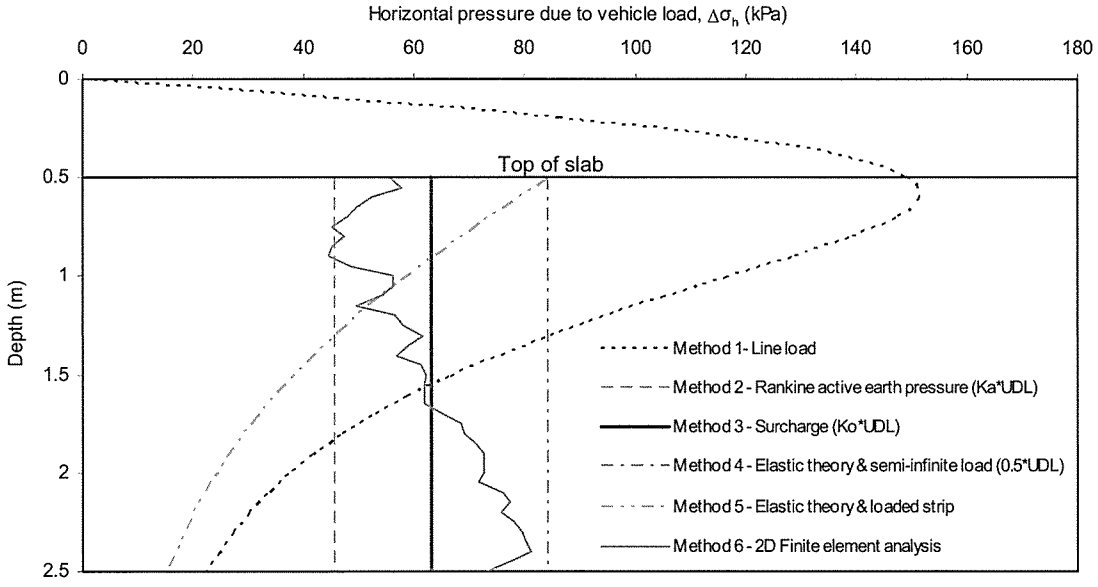

Figure 7: Lateral earth pressure distributions

Figure 7 shows that the lateral earth pressure distribution assessed with Rankine, surcharge and elastic theory with semi-infinite load methods remains constant with depth. The line load method gives a pressure distribution with a high peak pressure near the top and decreasing rapidly with depth. The elastic theory with loaded strip method gives a pressure distribution that

decreases with depth. The finite element method gives a pressure distribution that increases with depth.

The lateral earth pressure assessed with the line load method is considerably higher that that assessed by the other methods. Over the upper half of the structure, in the area of interest for overall stability and structural design of the walls, the surcharge method and finite element method give similar assessments and are approximately 75% of that given by elastic theory with a semi-infinite load.

Based on the above comparison, assessment of lateral earth pressure with the finite element method was adopted to check the overall stability of the structure and the surcharge method was adopted for the structural design of the walls. Further analyses performed with the finite element method indicated that, provided the structure is constructed in accordance with the design, it is stable under loads several times the applied service load.

7 CONCLUSION

The comparison demonstrates that the methods provided in AS4678 (2002) are:

- Too conservative in the case of the line load method (Method 1). The higher lateral earth pressure assessed by this method over the upper half of the structure would increase the overall structural cost.
- Not conservative enough in the case of the Rankine method (Method 2), for a structure with a high consequence of failure.

Therefore, where large surcharges are involved, other methods for assessing lateral loads from surcharge should be considered during design. Simply adopting the methods in AS4678 (2002) can lead to either a conservative or unconservative design.

REFERENCES

Australian Standard AS4678 (2002) *Earth-retaining structures*. Standards Australia, Sydney.

Bowles, J.E. (1996) *Foundation analysis and design*, fifth edition. McGraw-Hill, New York.

British Standard BS8002 (1994) *Code of practice for earth retaining structures*. British Standard Institution, London.

Clayton, C.R.I., Milititsky, J. and Woods, R.I. (1993) *Earth pressure and earth-retaining structures*, second edition. Blackie Academic and Professional, London.

Hong Kong Geoguide 1 (1994) *Guide to retaining wall design*, second edition. Geotechnical Engineering Office, Civil Engineering Department, Hong Kong.

Morgan, J. (1988) *Basement excavations workshop notes*. Department of Civil Engineering, University of Queensland, Brisbane.

Poulos, H.G. and Davis, E.H. (1974) *Elastic solutions for soil and rock mechanics*. John Wiley and Sons, New York.

Terzaghi, K. (1954), Anchored Bulkheads, Transactions, ACSE, vol. 119, pp. 1243-1280, New York.

Terzaghi, K. and Peck, R.B. (1967) *Soil mechanics in engineering practice*, second edition. John Wiley and Sons, New York.

Terzaghi, K., Peck, R.B. and Mesri, G. (1996) *Soil mechanics in engineering practice*, third edition. John Wiley and Sons, New York.

U.S. Department of the Navy NAVFAC Design Manual 7.2 (1982) *Foundations and earth structures*. Naval Facilities Engineering Command, Alexandria.

Aspects of Engineering Geology of a Dam in South East Asia

Chris Soutar
Maunsell Limited, Auckland, NZ

Keywords: dam, valley de-stressing, rock mass, rock strength

ABSTRACT

The engineering geology of a dam site in South East Asia is presented. The author was involved in the design investigations for the dam and spent one year on site. The project is located in a narrow gorge created by the downcutting of a river through a syncline limb and de-stressing of the valley walls. Geology consisted of bedded siltstone and sandstone and occasional conglomerate with bedding parallel shear zones caused by flexural slip. The engineering properties of the materials and their relationship to the engineering geology are discussed.

1 INTRODUCTION

A proposed hydropower dam is to be constructed on a river in South East Asia. The proposed dam is approximately 180m tall and during investigation design stages was designed as a Roller Compacted Concrete (RCC) mass dam, with a 1km long diversion tunnel and 2 power tunnels approximately 400m long. Investigations in 2007 consisted of 35 boreholes, adits and test pits across the site. Testing on samples included UCS, lugeon, point load, cross hole seismic, seismic lines, ring shear and down hole hydraulic fracturing testing. The author was involved with the site investigations and controlled the testing and site works during the design phase.

2 GEOLOGICAL SETTING

The project site is located in a narrow gorge created by the river down-cutting through the western limb of a NW/SE orientated syncline. The limb forms a prominent strike ridge that has a very steep scarp slope to the southwest and gentler dip slope to the northeast. The ridge rises approximately 700 m above the adjacent plains to the west and it is possible that the ridge is faulted along its south-western flank, creating the high escarpment. The syncline structure is formed in Mesozoic sedimentary rocks dominated by non-marine fine to coarse sandstone with mudstone and siltstone. The sediments were folded in the Cenozoic into relatively open synclines and anticlines, the axes of which are oriented northwest/southeast.

The river valley at the dam site is narrow (50 m) and valley slopes are steep (35°) with cliff sections up to 50 m high. About 1 km downstream the valley opens onto alluvial plains. Alluvial terraces flank the river at the mouth, but these diminish upstream and are of very limited extent at the dam site. The slopes at the site are forested and slabs of rock occur as a talus ramp at river level. Bedding dips upstream at approximately 10° with strike perpendicular to river valley axis and parallel to the dam axis.

A feature of the dam site is a thick unit of resistant sandstone that forms a prominent cliff on the valley slopes. From high on the valley slopes at the southern end of the site, it dips northward to river level just north of the proposed dam axis. The dip is conformable with the synclinal bedding dip.

Overlying and underlying the resistant sandstone are bedded sandstone, siltstone and mudstone. Sandstone beds are typically 10 m to 20 m in thickness and siltstone/mudstone units less than 10 m. The sandstone is moderately strong to strong and the finer lithologies are weak to moderately strong. Weathered rock (i.e. completely and highly weathered grades) ranges in depth to 25 m and to an extent is controlled by the rock types close to ground surface. Siltstone and mudstone tend to weather more deeply.

3 ROCK MASS DEFECTS

Defects on site include bedding plane shears, vertical joints parallel with the valley and slickensided joints. It is likely that many of the defects occurring at the site may have been caused by regional folding and development of the regional syncline and or valley bulging caused by valley de-stressing. Bedding plane shears are present along lithological boundaries at the site. They may have been caused by any one or combination of the above mechanisms. General examples of stress states and effects associated with de-stressing of sedimentary rock by incised valley formation, which are similar to the site condition, are discussed.

A river cutting though shallow dipping moderate to low strength sedimentary rocks may cause valley bulging or valley rebound due to stress unloading. This can result in a gentle anticline developing across the valley axis, manifesting as a gentle raising of the valley walls, and bulging of the valley floor. Other features that may develop as a result of valley de-stressing include bedding plane shears, thrust faulting, and steeply dipping open joints developing in the valley walls parallel to the valley axis (Figure 1).

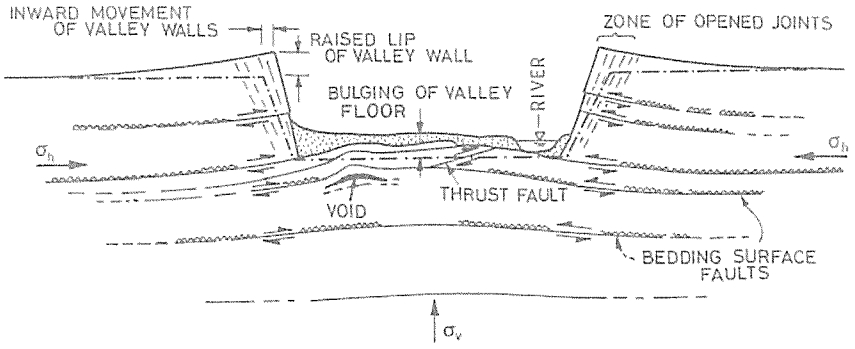

Figure 1: Valley De-stressing and stress release in weak, flat-lying rocks (based on Hendron and Patton, 1972)

Bedding plane shears often develop within shallow dipping bedded mudrocks (such as siltstone and shale) when they have been disturbed by regional folding or stress relief such as valley bulging. Thin seams of crushed rock typically develop at the interface of stiffer rocks (Figure 2). They develop due to interbed slippage during movement as a result of differing moduli of the different lithologies. These bedding plane shears are typically planar slickensided surfaces that may only be a few millimetres thick, but cover wide areas.

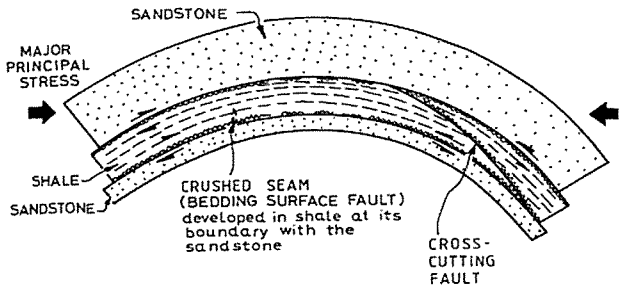

Figure 2: Bedding Plane shears formed in mudrocks

Rocks at the site generally fall within the weak to strong category (5 to 100 MPa). Therefore the effects of both valley-floor bulging and concentration of horizontal stresses within the valley

sides and floor is expected. Many of the features described in valley floor bulging are evident at the site (Figure 3) along with the effects of regional folding.

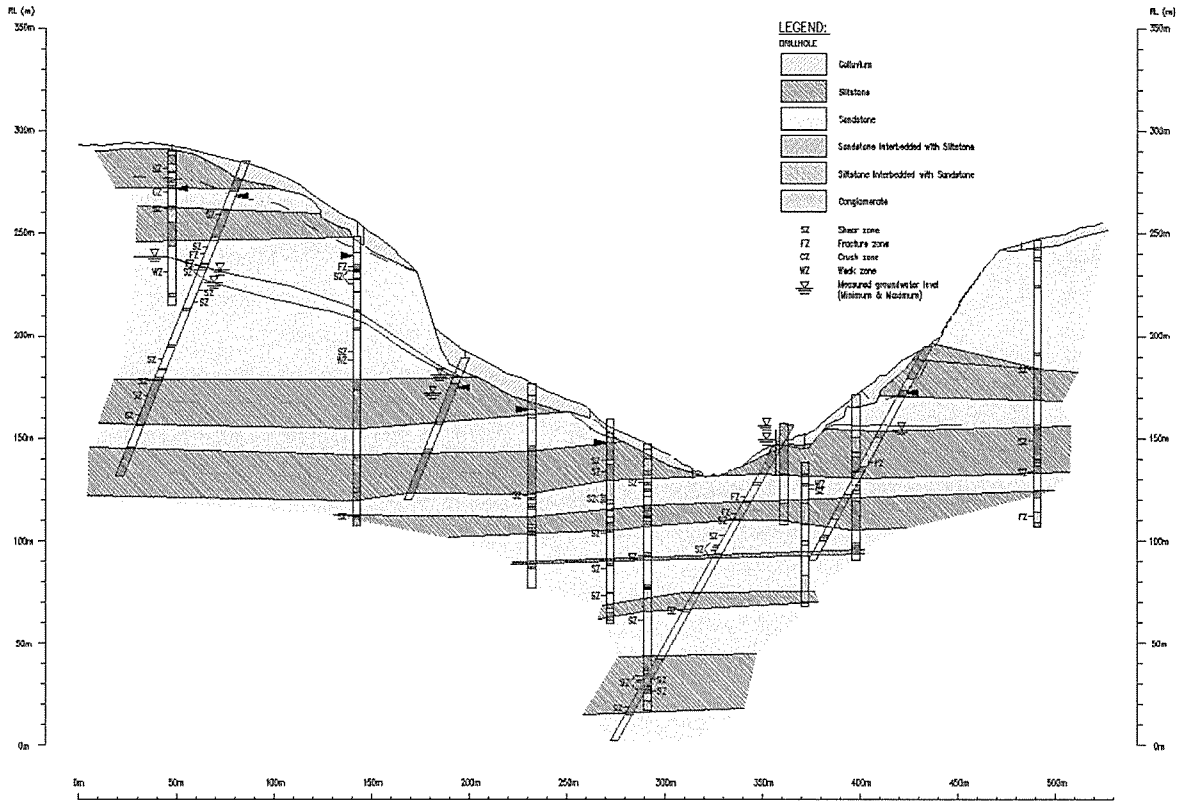

Figure 3: Cross section of geology of dam site showing valley de-stressing

4 DISCONTINUITIES IN CORE

4.1 Stereonet Analysis of Drillcore Joints

There are three dominant joint sets J1, J2 and J3. A limited number of mapped joints do not fit the three dominant sets; these dip either at 30° to 50° or at low angle downstream (i.e. oblique to bedding). It is likely that the latter joints include low angle thrust faults. Table 1 presents the results.

Table 1: Joint Sets from Drillcore and Field Mapping

Joint Set	Dip Direction	Dip Angle	Defect Type	Typical Continuity of Joint	Typical Spacing	Typical Defect Roughness
J1	360° to 50° north and 160° to 230° south	75° to 90°, average of 78°	Joints	2m to 5m	1 – 5m	Planar to smooth, some rough
J2	280° o 330° west and 90° to 130° east	75° to 90°, average of 80°	Joints	1m to 5m	0.5 – 5.0m	Planar to rough
J3	10° to 40° north	0° to 25°, average of 10°	Bedding plane partings /bedding joints	1m to 20m	0.5 to 1.0m	Planar to smooth, occasionally rough

The stereonet on the left in Figure 4 plots the great circle of each defect; the stereonet on the right plots the pole of each defect. Both stereonets clearly show three dominant joint sets.

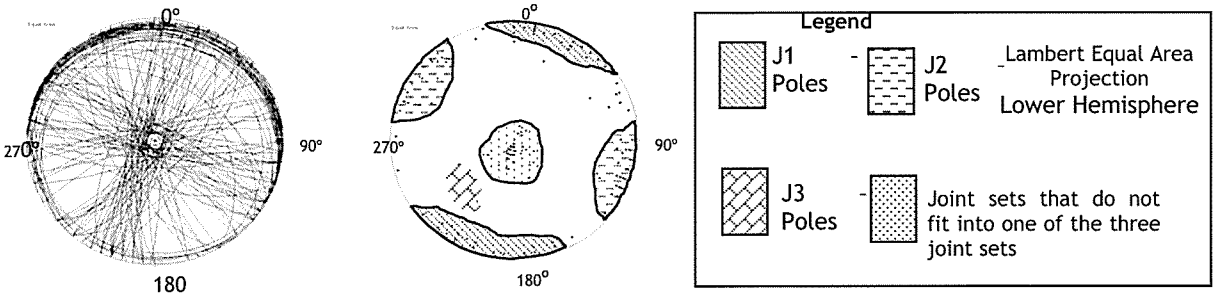

Figure 4: Discontinuities: Exposed Defect Stereonets

Slickensided joints logged in core are typically tight, planar to undulating with the majority of JRC values ranging between 1 and 12. Approximately 40% of logged slickensided joints have infill less than 1mm in thickness, the infill typically being iron stained, calcite, carbonised material or clay. The remaining slickensided joints are tight. Bedding plane partings / bedding joints are typically tight, clean to iron stained, planar to undulating and occur throughout both sandstone and siltstone. Other joints described in core range from subhorizontal to subvertical and are typically undulating to planar. For open joints a wide range of infill material is described such as calcite, clay, iron, pyrite, chlorite and manganese. They occur throughout all geological units.

4.2 Shear Zones in Drillcore at Base of Resistant Sandstone

Approximately 230 shear zones were identified and described in drillcore. Persistence of these shear zones could not be established in drillcore, with the exception of the shear zone at the base of the resistant sandstone. The main reason for this is that distance between boreholes is too great to confidently correlate shear zones, which may or may not change characteristics between holes. It is also possible that a single shear zone in one borehole splinters into many in another borehole. Small scale thrust faulting or parasitic folding may also offset these shear zones.

A prominent zone of shearing is evident in drillcore and adits at the base of the resistant sandstone. This zone of basal shearing was found in all twelve boreholes that were drilled through the base of the resistant sandstone and in both adits. This shear zone occurs at the contact between the resistant sandstone and the underling siltstone. It is typically described as firm, slightly to moderately plastic clay occasionally with some fragmented siltstone, and interpreted as breccia with gouge material.

5 MATERIAL STRENGTH

Material strength was assessed using UCS, point load and a number of other techniques. The site has two main lithologies, sandstone and siltstone and the results are presented in Figure 5.

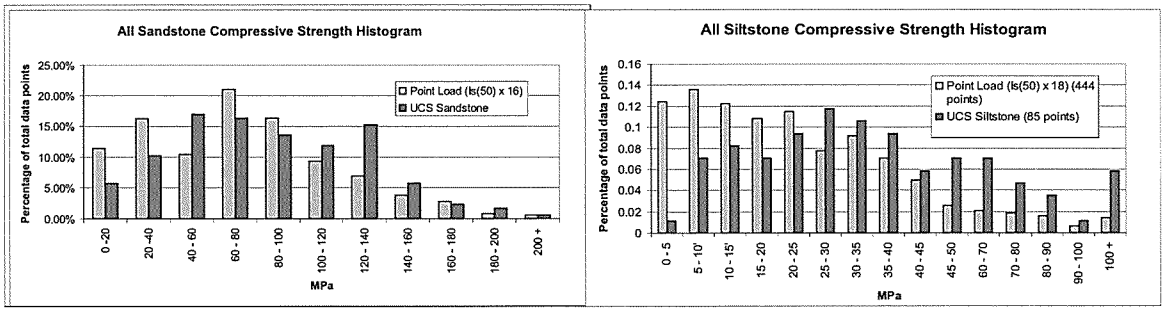

Figure 5: UCS and corrected point load test for sandstone and siltstone

6 ROCK MASS CLASSIFICATION

Q system, GSI and Rock Mass Rating (RMR) were used to determine rock mass for the site and are presented. Q system for rock mass classification was based on the method of Barton et al (1974). Results (Table2) indicated a poor to fair rating for rock mass for this method. GSI values (Table 3) reflect the quality of the rock mass as a whole for the evaluation of its bearing capacity and shearing resistance against potential failure through the mass. It however does not account for any well developed weak zones or planes which are evident on site. Evaluation of RMR follows the procedure developed by Bieniawski (1984). Results of RMR (Table 4) indicate that the rock on average is good for sandstone and fair for siltstone.

Table 2: Q System Rock Mass Results

Lithology	Data Points	Drilled Length (m)	Rock Mass Condition		Extremely Poor	Very Poor	Poor	Fair	Good
			Q Range	Min	0.00	0.08	0.40	2.0	10.0
				Max	0.08	0.40	2.0	10.0	1000
Sandstone	301	2351	Percentage occurrence		3	8	44	38	7
Siltstone	164	1158			10	9	39	38	4
Conglomerate	32	88			2	16	31	40	11
Total	497	3726			8	8	41	37	6

Table 3: GSI Rock Mass Results

GSI Items	Sandstone	Siltstone
Minimum	34	34
Mean – SD	45	39
Mean	55	49
Mean + SD	65	58
Maximum	100	86

7 ROCK MASS MODULUS OF DEFORMATION

Rock mass modulus of deformation has been evaluated using the procedure reported by Hoek and Diederichs, 2006. This procedure utilises GSI, intact rock modulus (E_i) and disturbance factor (D). This evaluation is recommended in place of alternative methods involving Q and RMR. Hoek and Diedericks (2006) recommend utilising UCS data to determine E_i in place of laboratory measured E_i due to sample disturbance effects. Three disturbance factors (D) were considered 0, 0.1 and 0.5. For instance for the dam foundation, which will be blasted, disturbance is likely to be limited to the upper few metres, which represents a small proportion of the affected foundation rock mass and consequently a low D factor will apply. The same would not apply for tunnels where near surface disturbance zone has direct bearing support requirements. Results of rock mass modulus of deformation are presented below in Table 5.

Table 4: Rock Mass Rating (RMR) results

Material	Min Average RMR	Rock Quality Rating	Average RMR	Rock Quality Rating	Max Average RMR	Rock Quality Rating	Std. Dev	Range
Siltstone	41	Fair	57	Fair	77	Good	14	19 – 84
Sandstone	51	Fair	69	Good	83	Very Good	10	35 – 89
Combined	56	Fair	65	Good	83	Very Good	13	19 - 89

Table 5 Rock Mass Modulus of Deformation Results

E_{rm} Rock Mass Modulus of Deformation (GPa)		
Material	Sandstone	Siltstone
UCS Mean	86	45
MR*	200-350	350-400
Ei	18-31	9-16
D=0	9-15	3-6
D=0.1	8-13	3-6
D=0.5	4-7	2-3

* From table 3 of Hoek and Brown, 1996

8 CONCLUSIONS

Numerous material parameters were developed to characterise the rock mass. It is essential however that discreet defects are not overlooked as these control stability in certain cases depending on geometry (e.g. day lighting, slide planes, wedges etc) and type of works (e.g. open surface excavations, slopes, tunnels and foundations). The dam stability is controlled by the bedding plane shears while the rock mass properties such as strength and modulus of deformation are utilised in dam foundation bearing and deformation. Determining which properties to apply for any particular design problem requires careful consideration of what is critical. The combination of these rock mass and defect properties has significantly influenced the selection of the dam type and its design.

REFERENCES

Barton, N.R., Lien, R. and Lunde, J. (1974) Engineering classification of rock masses for the design of tunnel support. *Rock Mech.* 6(4), 189-239

Bieniawski, Z.T. (1984) Rock Mechanics Design in Mining and Tunnelling, 121 – 126. A.A. Balkema Publishers, Netherlands

Heddron , A.J. & Patton, F.D. (1985) The Vaiont slide, a geotechnical analysis based on new geologic observations of the failure surface. US army corps of Engineers, Technical Report GL- 85 – 5

Hoek, E., Brown, E.T. (1996) Underground Excavations in Rock, 27 - 35

Hoek, E. & Diederichs, M.S. (2006) Empirical Estimation of Rock Mass Modulus, IJRM&MS, 203-215.

Construction of a Reinforced Soil Slope in the Northland Allochthon, Silverdale, Auckland

Chris Thompson
Coffey Geotechnics (NZ) Limited, Orewa, NZ

Phil Chapman
Coffey Geotechnics (NZ) Limited, Auckland, NZ

Keywords: northland allochthon, reinforced soil slope, silverdale, whangai formation

ABSTRACT

Recent papers have highlighted the challenging nature of the Northland Allochthon, both in terms of investigation and modelling and also construction. This paper looks at the issues relating to construction of a reinforced soil slope within the Whangai Formation of the Northland Allochthon. It gives an overview of the Northland Allochthon, reasons for development of geotechnically complex land, why a reinforced soil slope was chosen, a review of construction and post construction issues relating to building development on the site.

1 INTRODUCTION

1.1 Reasons for Development

A lack of knowledge about the behaviour of the Northland Allochthon soils has resulted in both developers and local councils becoming increasingly wary of developments within this geology. There is an increase in costs associated with design, investigation and construction on sites underlain by these soils. In spite of these extra costs, land within this geology has been developed. This is mainly due to there being a shortage of suitable alternative industrial land in the wider Silverdale area.

In addition, there are physical limits to expansion imposed by the Weiti River and State Highway 1. However, the most important constraint on development is the presence of the Northland Allochthon geology.

Silverdale is the industrial hub on the Hibiscus Coast and therefore it was considered that expansion within this area would best suit Council's, the developers' and end users' needs. The block of land that this case study focuses on is located immediately to the south of the main industrial area.

1.2 Overview of the Northland Allochthon

The Northland Allochthon underlies much of Northland, New Zealand, extending as far south as Silverdale on the northern outskirts of Auckland City (Edbrooke, 2001). Many references have highlighted the extent of the Northland Allochthon; however this paper only provides a brief overview of the lithologies encountered within close proximity to the study area. A review of published geological maps for the study area indicated that the site was underlain by the Mangakahia Complex, with the two main units being the Hukerenui Mudstone and the Whangai Formation. The third unit within the Mangakahia Complex, the Punakitere Sandstone, was not expected to be encountered on site.

The Whangai Formation and Hukerenui Mudstone both tend to have very clayey overburden soils, with a sheared and shattered transition zone comprising silts, clays and rock fragments, which has a greater permeability than either the underlying rockmass or overburden. This leads to the predominant failure mechanism within these lithologies being translational sliding. Once investigation began on site it became clear that the Whangai Formation was the predominant geology present. A summary of the important aspects of this lithology is presented below. Isolated pockets of Hukerenui Mudstone were encountered on site but these were removed where present in critical areas.

1.3 Whangai Formation

The residual soils of the Whangai Formation weather to form firm to very stiff silts and clays with minor traces of sand (Lentfer, 2007). Overburden soil depths on site ranged from 1.6 to 2.5 metres (FEL, 2005). Due to the high clay content of these overburden soils, permeability rates are usually very low (in the range of 10^{-8}m/s), which limits the inflow of water into the transition zone materials, essentially capping and protecting these materials.

The complex nature of the transition zone, comprising variable amounts of partially weathered highly fractured, sheared and slickensided rock fragments and a variable clay matrix means that the soil mass frequently behaves as a cohesionless material with a very low friction angle. It swells and shrinks readily as a result of changes in seasonal moisture content, causing downhill soil creep movement and areas of translational planar slumping on slopes less than 10° (FEL, 2005). The low permeability of the overburden soils leads to a build up of excess pore water pressure within the transition zone which can cause translational landsliding.

The unweathered parent rockmass remains relatively stable unless it is subjected to either changes in ground geometry, such as high loading on a slope, exposure in a cut batter, removal of toe support, or changes in groundwater conditions which may lead to shrinking and swelling, which in turn destroys the integrity of the rock mass (FEL, 2005).

1.4 Design

The design of the industrial subdivision was based on the need to maximise the available land for building development. Accordingly, the most effective way to use the land was to construct reinforced soil slopes. In this case the batter slopes were designed to be at an angle of 45° (1V:1H). A geogrid reinforcing system comprising predominantly Fortrac 55M and also Fortrac 80M from Maccaferri was utilised for this project.

Internal stability of the reinforced soil slope (RSS) was confirmed by Maccaferri, however global stability analyses carried out for the site indicated that a shear key excavated approximately 10 metres wide and excavated into competent Whangai Formation bedrock would be required to provide appropriate stability conditions. A chimney drain comprising self filtering scoria (SAP50) was installed up the rear face of the shear key to intercept any groundwater seepage. This shear key was deepened significantly in the eastern portions due to the construction of large retaining walls in the adjacent property. In addition, the majority of the overburden soils were excavated out underneath fill areas to remove the transition zone soils and enhance overall site stability.

The rear face of the reinforced soil block had a chimney drain installed to provide additional control over groundwater seepage and to protect the block. In addition to this drain, mid height drainage was installed in the higher slopes (greater than 10 metres) to reduce the build up of pore water pressure. These drains were connected into the chimney drain on the rear face of the reinforced block and were installed at regular intervals where required. The drains were connected into the chimney drain as exiting the drains through the face of the RSS would have

been difficult and would potentially increase scour on the face. The geogrid product utilised for this project was Fortrac 55M. This was selected as it allowed the use of lime stabilised materials if required by the construction programme and to ensure the fill material was at the appropriate water content within the very narrow range as shown in Figure 1.

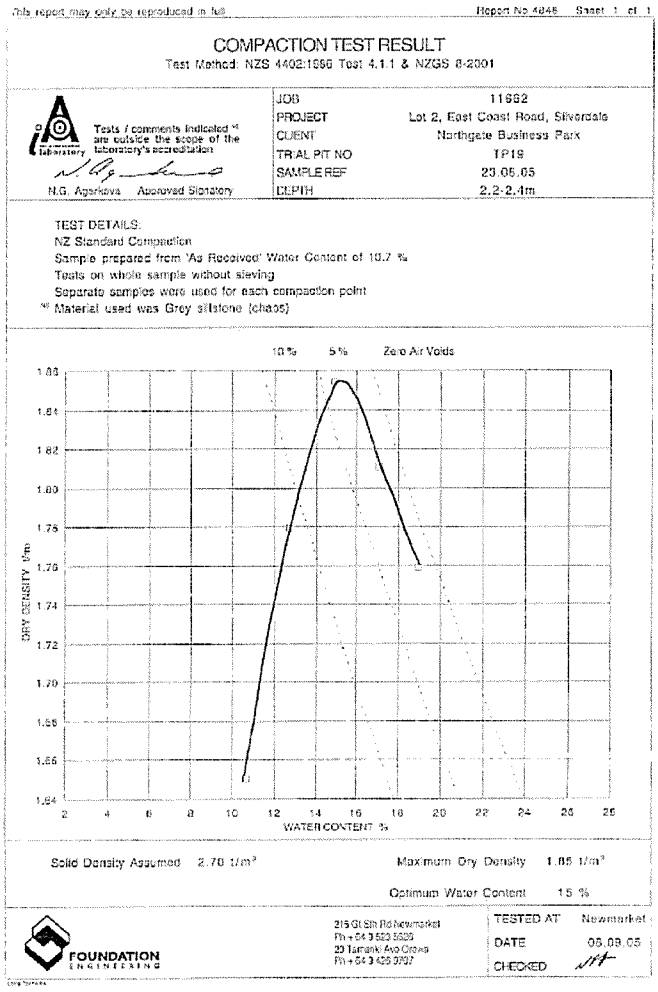

Figure 1: Compaction Curve for Northland Allochthon Bedrock as sampled on site.

One of the critical aspects of the design process was to optimise the use of the geogrid in relation to the fill material chosen for the RSS, as the length of embedment for the geogrid was dependent on the effective stress parameters of the backfill materials. On this site the options for the fill material were clayey overburden soils, a combination of overburden soils and bedrock or bedrock only.

Each of the options came with a different set of problems in terms of constructability and wall stability considerations. Initially it was proposed to construct the RSS using imported hardfill material but this was discounted due to the high cost of the raw materials and the quantities required for the project. The option of using only overburden soils for the RSS was limited by the amount of available material on site due to the relatively shallow depths of overburden soils encountered. The natural water content of the overburden soils was also higher than the optimum and this indicated that significant drying would be required for these materials to achieve compaction specifications.

A combination of the clayey overburden soil mixed with bedrock was also considered for the RSS, however testing to confirm the effective stress parameters for this material proved difficult due to the varying percentages of soil and bedrock in each sample. It is likely that the effective

friction angle for this combination would be the friction angle of the clay materials so the use of bedrock materials would only add volume and not necessarily decrease the embedment depth for the geogrid.

The third option comprised Northland Allochthon bedrock. This material was considered the most appropriate due to the depth of cut proposed over much of the site. It was the dominant cut material and it had the highest effective friction angle available. Triaxial testing of the bedrock revealed typical effective stress parameters of c' = 4kPa and Ø' = 30°. However over the design life the level of cohesion is likely to decrease and has therefore been ignored for the analysis (of the RSS design). This follows standard practice and recommendations contained in International publications and guidelines (Stevens, 2004). The use of Northland Allochthon bedrock as the fill material decreased the embedment depth for the geogrid due to the higher friction angle of the bedrock and this typically reduced overall embedment depths leading to a significant cost saving.

2 CONSTRUCTION ISSUES

The most problematic issue with the use of Northland Allochthon bedrock as the fill material for the RE slope was its very narrow acceptable water content range as shown in Figure 1. Undisturbed, this material is drier than desirable for compaction to engineered standards so some wetting up was required to achieve compaction specifications. However, the addition of too much water resulted in the material becoming too wet to achieve compaction standards. The location of the water addition was also critical in ensuring a consistent mix of fill. At the start of construction water was added on the fill area which resulted in layers of drier material and layers of wetter material which was not satisfactory.

The solution was to add water in the cut area prior to loading into the earthmoving plant, but even so it was difficult to arrive at the optimum application rate that resulted in the soil staying within the desired water content range. Once these issues were resolved, the development of a test specification for confirmation of compaction standards was implemented. The use of hand-held shear vane devices was not considered practical as the bedrock fill material was typically too stiff for an accurate measurement. A test specification using an Impact Hammer along with a Nuclear Densometer (NDM) for confirmation of strength and compaction was developed with an impact value of 8 and an average air voids ratio of 8%. This test specification was developed after plotting field data on dry density and gauge moisture content on the laboratory derived compaction curves. The data was then compared with the impact values recorded nearby to confirm appropriate compaction specifications.

Once the test specification had been developed, the next construction issue was the placement of the facing system. The facing system for the RSS was to comprise a mixture of topsoil and clay to encourage grass growth over the geogrid face to protect the north facing slopes from increased ultraviolet light degradation and to satisfy the conditions of Resource Consent. The Contractor decided that this method of facing with the geogrid wrapped around the face would be the easiest way to construct this area. Other facing systems were available, such as Terramesh Green or degradable socks filled with a mix of topsoil, mulch and grass; however these were not utilised on this project. The method of compaction for this face area proved to be difficult as the large construction machinery were not to be used within 1 metre of the face of the RSS. In hindsight, the use of a degradable sock facing system would have greatly improved ease of construction.

Placement of the geogrid layers around corners created some difficulties as overlapping or cutting of the geogrid were not permitted. Ensuring appropriate tensioning within corner and cross wall sections was essential as these areas needed to be constructed to minimise any untensioned geogrid allowing scour on the face of the RSS. Where corners and cross walls were

located it was necessary to place the geogrid in a hit and miss method with a minimum of 100mm of fill between each of the geogrid layers. Another issue was the long lead time with ordering from Europe and the quantity of product required to complete the job. In one section, a higher and alternative specification of geogrid (Fortrac 80M) was utilised due to a delay in ordering and uncertainties in the quantities required to complete the project.

Management of on-site materials was one of the major construction issues as the volume of overburden soils was limited, compared with the abundance of bedrock material due to the depth of cuts undertaken. The key reason for the need for a well managed operation was to ensure the exposed bedrock and rock fill could be capped with a 1 metre thick layer of clayey soils to limit degradation of those materials and the relaxation of the undisturbed rockmass. This required stockpiling of the overburden materials away from the main fill areas and ensuring that this stockpile was sufficient to cover all the required areas to the appropriate depth.

3 POST CONSTRUCTION ISSUES

The main aim of the subdivision was to create large industrial platforms for building development. At the initial design stage it was advised that a geotechnical ultimate bearing capacity of 300 kPa should be available for shallow strip and pad foundation systems in conjunction with a live floor load up to 10 kPa.

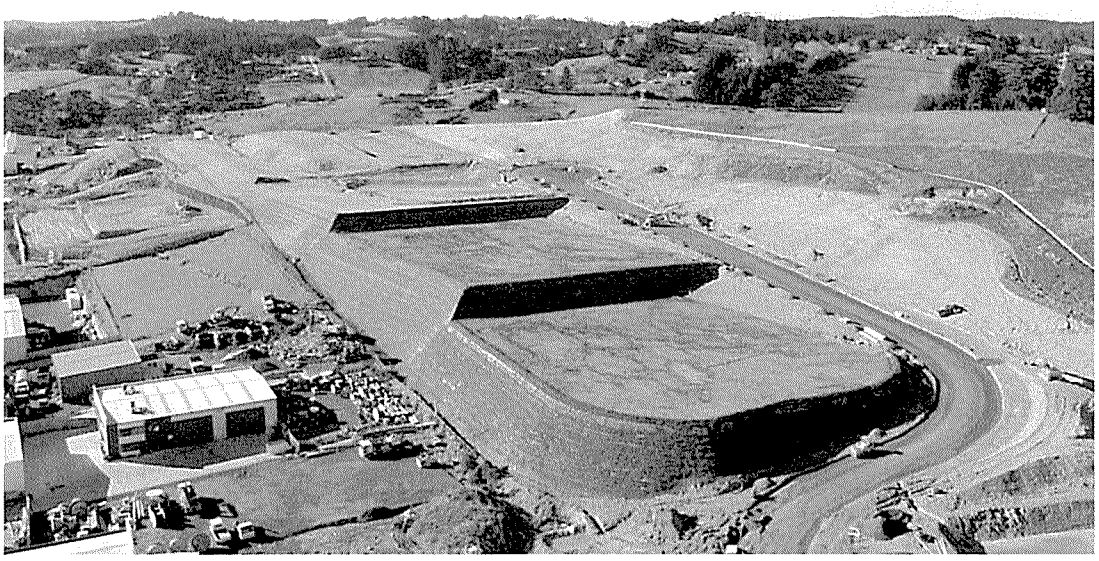

Figure 2: Reinforced Soil Slope during construction.

Following the preparation of the Geotechnical Completion Report (GCR) for the subdivision, these values were confirmed. Building restriction zones were also imposed on all platforms due to the steepness of the RSS and also to limit interference with the reinforcing system. A no-build zone was identified within 1.5 metres from the crest of the RSS due to the facing system employed to ensure grass strike. The building restriction zones were significant and on some lots were up to 50% of the lot sizes due to the height of the RSS within that lot.

The GCR identified that interference with the geogrid could detrimentally affect the overall stability of the RSS for that lot. The location of the chimney drain as shown in Figure 3 imposed restrictions on building development as in some cases it was up to 5 metres behind the end of the geogrid reinforcing due to the construction methodology. Poor grass strike on the face of the RSS also proved that the use of a different facing system may have been more appropriate. The method of placement did not allow the grass seed to germinate well, which necessitated hydroseeding the face of the RSS several times in places to ensure adequate grass coverage.

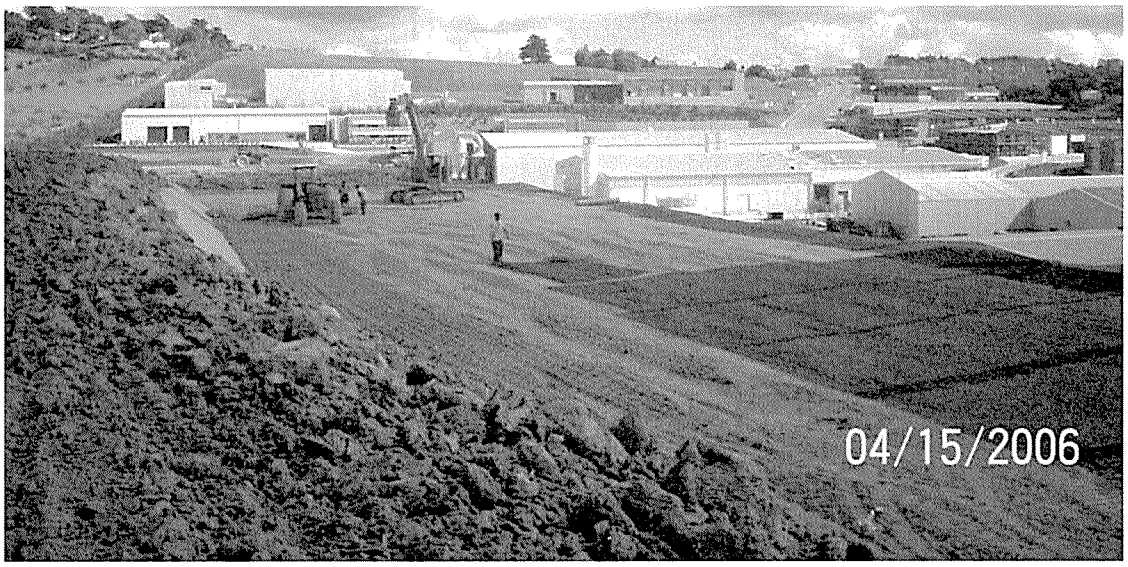

Figure 3: Setback of chimney drain from back of reinforcing grid.

4 CONCLUSIONS

The construction of a large reinforced soil slope in the Northland Allochthon provided many geotechnical and construction challenges. The key challenges were the use of Northland Allochthon bedrock as the fill material for the RSS, optimisation of the RSS design to best utilise on site materials, the implementation of the facing system and the resolution of the post construction issues relating to the restrictions imposed by the reinforced soil slopes. The additional industrial and commercial land developed has been well utilised by local businesses to further serve the greater Silverdale area.

ACKNOWLEDGEMENTS

The author would like to acknowledge Brent Glover for permission to discuss the Northgate Business Park development, Phil Chapman and Adam Akehurst for their special insights into the project and Coffey Geotechnics staff for encouraging the preparation of this paper.

REFERENCES

Coffey Geotechnics (NZ), (2007). *Geotechnical Completion Report on Northgate Business Park Stage 1*. Unpublished Consultants report No. 11662.

Edbrooke, S. (Compiler) (2001). *Geology of the Auckland Area.* Institute of Geological and Nuclear Sciences 1:250,000 Geological Map 3.

Foundation Engineering Limited. (2005). *Geotechnical Investigation Report on Northgate Business Park Stage 1*. Unpublished Consultants report No. 11662.

Lentfer, K. (2007). *Engineering Geology of the Northland Allochthon, Silverdale, North Auckland, New Zealand.* Unpublished MSc Thesis, University of Auckland, Auckland.

Stevens, G. (2004). Benefit of Soil Testing for the Design of Reinforced Soil Structures. *Proceedings of the 9th ANZ Conference on Geomechanics*. NZGS & AGS, Auckland.

Radial consolidation equation with variable load, material and drain efficiency parameter

Rohan Walker
Coffey Geotechnics Pty. Ltd., Sydney, Australia

Keywords: consolidation, vertical drains, analytical solution

ABSTRACT

Numerous complex analytical solutions are available for analysis of consolidation problems involving radial drainage, yet the most common solution used for determining the rate of consolidation is the equal strain solution presented by Hansbo (1981). Maintaining the simplicity of Hansbo's (1981) solution this paper presents radial consolidation equations that capture the versatility of the more complex methods. Material and geometry properties vary piecewise-constant with time while loading/unloading varies piecewise-linear with time. A new drain efficiency parameter is introduced to model the detrimental effects of drain clogging and kinking. Drain clogging/kinking is simulated by specifying the excess pore pressure in the drain, normally set to zero, as a fraction of the average excess pore pressure in the soil. The new equations are easily implemented in a spreadsheet or computer program providing a simple yet versatile tool for analysis of consolidation problems dominated by radial drainage. Computer code for implementing the new approach in a Microsoft Excel is provided.

1 INTRODUCTION

Many analytical solutions to consolidation problems with radial drainage are available (Walker, 2006) but they are rarely used owing to their complexity and difficult implementation. In the authors experience the most common method used, especially for quick calculations, is the simplest, that of Hansbo (1981). Hansbo's (1981) method assumes constant soil properties and constant, instantaneously applied load, both of which are rarely encountered in the field. The radial consolidation equations presented in this paper build on the simplicity of Hansbo's (1981) approach but have the flexibility to account for varying load and material properties.

The equations presented can also roughly account for long term degradation of wick drain performance, sometimes associated with kinking or partial drain clogging. The only existing way to account for drain efficiency is to introduce a well resistance term related to the permeability and length of the drain. Modern wick drains usually have potential to become ineffective only after large deformations lead to kinking and partial blockage. Using a well resistance term like Hansbo (1981) tends to slow consolidation at the start of analysis not at the end. When drains are 100% efficient then the excess pore pressure in the drain is zero. If flow out of the drain is retarded then the excess pore pressure in the drain is non-zero. Exactly what the non-zero value is remains uncertain. As an approximation it may be appropriate (and mathematically convenient) to assume that the pore pressure in the drain is a fraction of the average pore pressure in the soil. In such a case pore pressure will still decay to zero but at a slower rate than if the drain pore pressure was always zero. The piecewise treatment of this drain efficiency parameter with time allows the clogging/kinking effects to be 'switched on' at a certain time. Indeed it is the piecewise treatment of all properties in the equations below that provide great flexibility. The equations are not 'hard wired' with a constitutive relationship and so it is up to the user to exercise judgment as to what period of time a soil or drain property is appropriate for. Thus the user can quickly assess many 'what if' scenarios: what if load gradually decreases due to submergence of fill? What if for a period the consolidation coefficient of a structured soil approaches zero? What if the smear effect decreases over time? What if I install more wick drains between existing drains?

2 DERIVATION

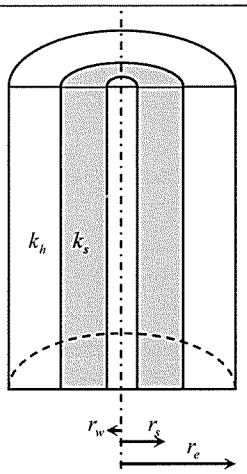

Figure 1 Axisymmetric unit cell

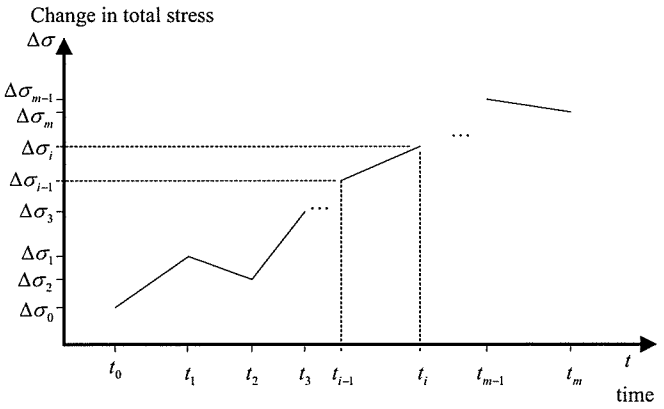

Figure 2 Multiple ramp loading/unloading

Hansbo (1981) presented the following radial consolidation equations for equal strain conditions in an axisymmetric unit cell (Figure 1):

$$\overline{u} = \overline{u}_0 \exp\left[\frac{-8T_h}{\mu}\right] \tag{1}$$

where, $\overline{u}$ = average excess pore water pressure,
$\overline{u}_0$ = initial excess pore water pressure and
T_h = horizontal time factor defined by:

$$T_h = \frac{c_h t}{4r_e^2} \tag{2}$$

c_h = horizontal coefficient of consolidation,
r_e = equivalent drain influence radius,
t = time
μ = geometry and smear zone parameter.

For a smear zone with constant permeability μ is given by:

$$\mu = \frac{n^2}{n^2-1}\left(\ln\frac{n}{s} + \kappa \ln s - \frac{3}{4}\right) + \frac{s^2}{n^2-1}\left(1 - \frac{s^2}{4n^2}\right) + \frac{\kappa}{n^2-1}\left(\frac{s^4-1}{4n^2} - s^2 + 1\right) \tag{3}$$

$$n = r_e / r_w \tag{4}$$

$$s = r_s / r_w \tag{5}$$

$$\kappa = k_h / k_s \tag{6}$$

where, r_w = equivalent drain radius,

r_s = smear zone radius,

k_h = horizontal permeability in the undisturbed zone,

k_s = horizontal permeability in the smeared zone.

Other expressions for μ can be found for non-constant smear zone permeability distributions Walker and Indraratna (2006), Walker and Indraratna (2007).

The penultimate step in the derivation of Equation (1) is the differential equation:

$$\overline{u} = \frac{4r_e^2\mu}{8c_h}\left(\frac{\partial\Delta\sigma}{\partial t} - \frac{\partial\overline{u}}{\partial t}\right) + w \tag{7}$$

where, $\Delta\sigma$ = change in load or total stress. w = excess pore water pressure in the drain. Equation (1) is produced when Equation (7) is solved with $\partial\Delta\sigma/\partial t = 0$ (i.e. constant loading), $w = 0$ (i.e. excess pore pressure in the drain is zero) and the initial condition of $\overline{u} = \overline{u}_0$ at $t = 0$ (i.e. instantaneous loading).

The somewhat limiting assumptions described above need not be followed. Consider the ith loading stage in a multiple ramp loading/unloading scenario as in Figure 2. The load varies in a linear fashion from $\Delta\sigma_{i-1}$ at time t_{i-1} to $\Delta\sigma$ at time t_i. Assume that between loading stages soil and drain properties may vary but are constant within each stage. Furthermore, assume that the excess pore pressure in the drain is not zero but a constant multiple of the excess pore water pressure in the soil (i.e. $w = \overline{u}\theta$). With the modified assumptions Equation (7) can be written:

$$\overline{u}(1-\theta) = \Delta\dot{\sigma}_i - \frac{\partial\overline{u}}{\partial\widetilde{T}\eta_i} \tag{8}$$

where

$$\Delta\dot{\sigma}_i = \frac{\Delta\sigma_i - \Delta\sigma_{i-1}}{(\widetilde{T}_i - \widetilde{T}_{i-1})\eta_i} \tag{9}$$

where $\widetilde{T}$ = a reference time factor given by:

$$\widetilde{T} = 8\overline{c}_h t / 4\overline{r}_e^2\overline{\mu} \tag{10}$$

The soil/drain parameters that make up $\widetilde{T}_h$ are any convenient reference values.

η_i = the ratio of soil/drain properties in the ith loading stage to the reference values of properties in $\widetilde{T}_h$. That is:

$$\eta_i = \frac{c_{hi}}{r_{ei}^2\mu_i} \Big/ \frac{\overline{c}_h}{\overline{r}_e^2\overline{\mu}} \tag{11}$$

If soil properties remain constant throughout analysis then η will always be unity. c_h might change due to different loading and unloading stiffness. r_e might change if extra drains are installed between existing drains. μ might change if the smear zone becomes less pronounced

during consolidation. Using the initial condition $\overline{u} = \overline{u}_{i-1}$ at $t = t_{i-1}$ Equation (8) can be solved to give the excess pore pressure in the i th loading increment:

$$\overline{u}_i = \exp\left[-\left(\widetilde{T}_{is} - \widetilde{T}_{if}\right)\left(1-\theta_i\right)\right]\left[\overline{u}_{i-1} + \frac{\Delta\dot{\sigma}}{\left(1-\theta\right)}\left(\exp\left[\left(\widetilde{T}_{is} - \widetilde{T}_{if}\right)\left(1-\theta_i\right)\right]-1\right)\right] \tag{12}$$

where

$$\widetilde{T}_{is} = \min\left[\widetilde{T}_{i-1}, \widetilde{T}\right]\eta_i \tag{13}$$

$$\widetilde{T}_{if} = \min\left[\widetilde{T}_i, \widetilde{T}\right]\eta_i \tag{14}$$

By taking the pore pressure at the end of a loading increment as the initial condition at the start of the following loading increment the pore pressure at any time is found to be:

$$\overline{u} = \sum_{i=1}^{m} \overline{u}_i \tag{15}$$

where

$$\overline{u}_0 = \Delta\sigma_0 \tag{16}$$

and u_i is from Equation (12).

The formulation of $\widetilde{T}_{is}$ and $\widetilde{T}_{if}$ prevents the need to determine which loading step the current time falls in. Contributions from future loading steps will evaluate to zero. Computer code for implementing the above equations in Microsoft Excel is given in APPENDIX A.

3 EXAMPLE

Consider a wick drain configuration where r_e=0.8 m, n=32, s=5, κ=5 (giving μ=9.07) under the loading scheme: load to 100 kPa over 5 weeks, wait for 4 months, load to 150 kPa over 3 weeks, wait for 6 months, unload to 100 kPa over 1 week, wait 6 months. For a constant c_h=7 m^2/yr the excess pore pressures and effective stress increase under the above loading scheme is shown in Figure 3 as CASE A. The effective stress increase is the excess pore pressure subtracted from the load. CASE B is similar to CASE A but it is assumed that until the effective stress increases by 30 kPa the soil is overconsolidated (i.e. preconsolidation stress is 30 kPa above the insitu effective stress) and so has a higher c_h of 49 m^2/yr (i.e. η=7). By trial and error, with the higher c_h 30 kPa of excess pore pressure was dissipated in 3.5 weeks. Also, upon unloading the soil again becomes overconsolidated with η=7. CASE C is as per CASE B but when the load reaches 150 kPa the wick drains are assumed to become partially clogged and are 50% efficient (θ=0.5).

Effective stress increase is important when considering undrained shear strength gain and hence stability of embankments. CASE B and C have more rapid effective stress gain at early times and so will have faster strength gain than CASE A. The second loading stage may be able to be brought forward if this faster strength gain is sufficient. If the wick drains become clogged then the highest effective stress increase experienced, and thus strength gain, may be less than that predicted without clogging (CASE C vs CASE B) which may lead to stability issues. Finally if the c_h is not adjusted for unloading (CASE A vs CASE B) then the time for the end of primary consolidation is unrealistically long.

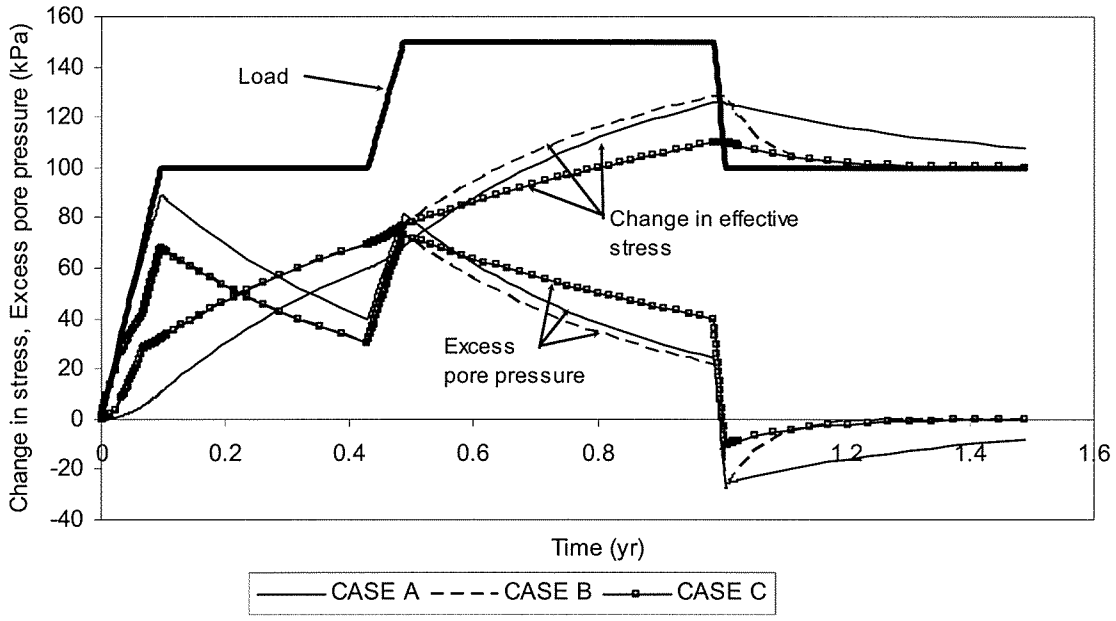

Figure 3 Excess pore pressure and effective stress change vs time

4 CONCLUSION

A flexible, easy to implement approach for investigating consolidation problems involving radial drainage has been presented (including computer code, see APPENDIX A). Material and geometry properties vary piecewise-constant with time while loading/unloading varies piecewise-linear with time. A new drain efficiency parameter was introduced to model the detrimental effects of drain clogging and kinking that may occur in the latter stages of consolidation. The consolidation equations build on the simplicity of Hansbo's (1981) approach, with the ability to more realistically assess of a wide range of radial consolidation problems.

REFERENCES

Hansbo, S. (1981). Consolidation of fine-grained soils by prefabricated drains. Proc. *10th International Conference Soil Mechanics and Foundation Engineering*, Stockholm, 677-682.

Walker, R. (2006). "*Analytical solutions for modeling soft soil consolidation by vertical drains.*" PhD thesis, University of Wollongong, NSW, Australia.

Walker, R. & B. Indraratna (2007). *Vertical drain consolidation with overlapping smear zones. Geotechnique*, 57(5), 463-467.

Walker, R. & B. Indraratna (2006). Vertical drain consolidation with parabolic distribution of permeability in smear zone. *Journal of Geotechnical and Geoenvironmental Engineering, ASCE*, 132(7), 937-941.

APPENDIX A – COMPUTER CODE

The above equations can be implemented in Microsoft Excel, and then used like any other Excel function, by copy and pasting the code shown below into a VBA module (Tools…Macro…Visual Basic editor…Insert…Module). Note that the variables 'times' ($t_0, t_{1,...}$), 'loads' ($\Delta\sigma_0, \Delta\sigma_{1,...}$), 'etas' ($\eta_0, \eta_{1,...}$) and 'ws' ($\theta_0, \theta_{1,...}$) must be input as columns.

```
Function MultiRampConsol(ch, re, mu, t, times, loads, etas, ws) As Double
   Dim F As WorksheetFunction
   Set F = Application.WorksheetFunction
   Dim eta0, A1, u, term, The1, The2, I
   timesA = times: loadsA = loads: etasA = etas: wsA = ws
   eta0 = 8 * ch / (4 * re ^ 2 * mu)
   u = loadsA(1, 1)
   For I = LBound(timesA, 1) To UBound(timesA, 1) - 1
      A1 = (loadsA(I + 1, 1) - loadsA(I, 1)) / _
         (timesA(I + 1, 1) - timesA(I, 1)) / eta0 / etasA(I, 1)
      The1 = F.Min(timesA(I, 1), t) * eta0 * etasA(I, 1)
      The2 = F.Min(timesA(I + 1, 1), t) * eta0 * etasA(I, 1)
      term = A1 / (1 - wsA(I, 1)) * (Exp((The2 - The1) * (1 - wsA(I, 1))) - 1)
      u = (u + term) * Exp(-(The2 - The1) * (1 - wsA(I, 1)))
   Next I
   MultiRampConsol = u
End Function
```

Raiseboring through deeply weathered profiles in the Yilgarn, WA

Shonagh Walker
AMC Consultants, Melbourne, Aus.

Vadim Louchnikov
OZ Minerals, Golden Grove Operations, WA, Aus.

Keywords: raiseboring, deep weathering, saprolite, stability issues, site investigations, shaft design

ABSTRACT

Large diameter raisebored ventilation shafts (>4m) are required for most high-tonnage modern underground mines, but their unsupported stability can be an issue if the large diameter raiseboring heads are to be pulled through to the surface. In Western Australia's Yilgan, deeply weathered zones (30m – 100m) are common and are the product of water table fluctuations and stable, low-relief topography. Over millions of years the two have culminated in weak, wet and clay-rich saprolite, which poses a significant geotechnical design issue when raiseboring. This paper discusses the design issues using an example from OZ Minerals' (formerly Oxiana) Golden Grove Operations, where a 4.5m diameter, 1000m deep raisebored ventilation shaft was proposed. Site investigations located a deeply weathered saprolite profile to a depth of 110m. The geotechnical assessment showed the weathered section had to be conventionally sunk, but economic considerations dictated the shaft could be constructed quicker and more cheaply by finding – if possible – a site with either a shallower weathering profile or more competent rock. Design and site investigation strategies are discussed which mitigate the stability risks caused by deep weathering profiles and which provide alternative solutions to site planning, dictated by underground layouts / accesses. This is an Australia-wide problem, exacerbated by the need for stable large-diameter raisebored ventilation shafts.

1 INTRODUCTION

Raiseboring describes the process in which a vertical circular shaft is excavated between an existing level in an underground mine and the surface or between two existing underground mine levels. The excavation is done using a raisebore head, the diameter of the desired excavation, with multiple cutters on its upper surface (Figure 1a). Initially a pilot hole is drilled, through which rods for the raisebore head are fed. The rods link the raisebore machinery, on the higher level, to the raisebore head below. Once attached the raisebore head is rotated and pulled upwards, cutting away the material above it and producing fine tailings (Figure 1b). Single pass raiseboring is the preferred method for vertical circular shaft construction because of the faster advance rates, decreased disturbance of the rock or material around the head, reduced labour costs and greater safety for operating personal.

Oz Minerals (formerly Oxiana) Golden Grove operations, located in the Western Australia, required an intake ventilation shaft for their Gossan Hill orebody. The shaft proposed was a 4.5m diameter, 1000m deep vertical shaft, to be constructed using conventional raiseboring techniques. The mine extracts zinc, copper, lead and lesser amounts of gold and silver, at depths of 1000m and more. The mineralisation is hosted in the volcanogenic sedimentary rocks and volcanic intrusions of the Gossan Hill volcanic-hosted massive sulphide (VHMS) deposit. It sits in the Warriedar Fold Belt, on the eastern limb of a N-S (approximately) striking fold. The strata of the area strike NW-SE and dip steeply (sub-vertical) to the south west. The Warriedar Fold Belt comprises the southern half of the Yalgoo-Singleton greenstone belt, in the Yilgarn Craton Murchison Province.

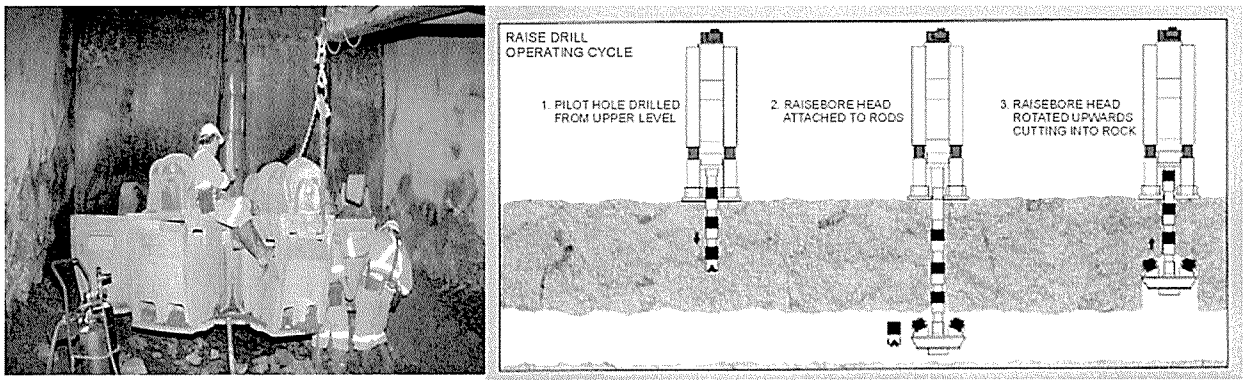

Figure 1a. Raisebore head cutters b. Method of raiseboring (after Atlas Copco, 2007)

2 YILGARN

The Yilgarn Craton (2.94 – 2.63 Ga) makes up a large portion of Western Australia. The geology comprises Archean granite-gneiss metamorphic terrains that are crossed by several north-northwest trending greenstone belts. Accretion of the craton as well as regional metamorphism and deformation has endowed the Yilgarn with significant recoverable reserves of iron ore, gold, nickel-platinum group metals, copper-lead-zinc base metals, rare earth elements and uranium.

The landsurface of the Yilgarn Craton forms a partial etchplain with deep gentle undulations and low-relief topography (Arand and Paine, 2002). The relatively flat landscape has been attributed to a complex history of valley development, minimal to no glaciations (minor erosion) and aggradation (general levelling of the Earth's surface by means of deposition). Deep weathering has resulted from this "stable" environment and affects most lithologies and geological provinces across the Craton.

Studies by Arand and Paine (2002) have found the depth of weathering varies considerably across the craton, in some places extending down to 150m. The main factors that influence the extent of weathering are rock type, mineralization and deformation. A typical profile grades from fresh bedrock upwards into saprock or saprolite that is commonly bleached towards the top of the horizon. Bleached saprolite is most prevalent in regolith formed from felsic or sheared mafic parent material. The saprolite horizon is overlain by a clay rich and/ or quartz-rich layer that is in turn overlain by a mottled horizon and then a ferruginous, bauxitic or siliceous upper horizon. A thin layer of transported soil may top the profile.

Deeply weathered profiles consist of a combination of the most resistant primary minerals (quartz, zircon, chromite, muscovite and talc) and the least soluble secondary minerals (kaolinite, hematite, goethite, maghemite, gibbsite, anatase and boehmite) (Arand and Paine, 2002). The saprolite, out of all the profile horizons, poses the greatest challenge in geotechnical design. Saprolite forms *in situ* by chemical weathering of igneous or metamorphic rocks during humid climate conditions. In the Yilgarn it is believed the saprolites developed in the tropical paleo-climate conditions of the Paleocene (65 – 55 Ma). The saprolite horizon is typically a soft, earthy, red or brown, clay-rich unit capable of holding significant quantities of water. The water table commonly sits within this horizon because it lies immediately above the fresh rock. Consequently the clay-rich material is generally wet, exacerbating the poor geotechnical stability performance of the material.

3 GOLDEN GROVE, OZ MINERALS – A CASE STUDY

A stability assessment based on site specific the drill core for the proposed raisebored ventilation shaft was performed. The location of the proposed shaft is shown in Figure 2 with respect to the Gossan Hill deposit, mined out areas, reserves and development. The stability

assessment looked at the characteristics of the weathered profile and primary geotechnical features within it. The assessment also considered the strengths of the weathered and fresh material, blockiness of the ground, interblock shear strength and in situ stresses. Attention was paid to the orientation of structures, mixed face conditions, probability and depth of stress induced breakout. Finally, estimated stand up times (unsupported and supported) were derived using Peck and Lee (2008).

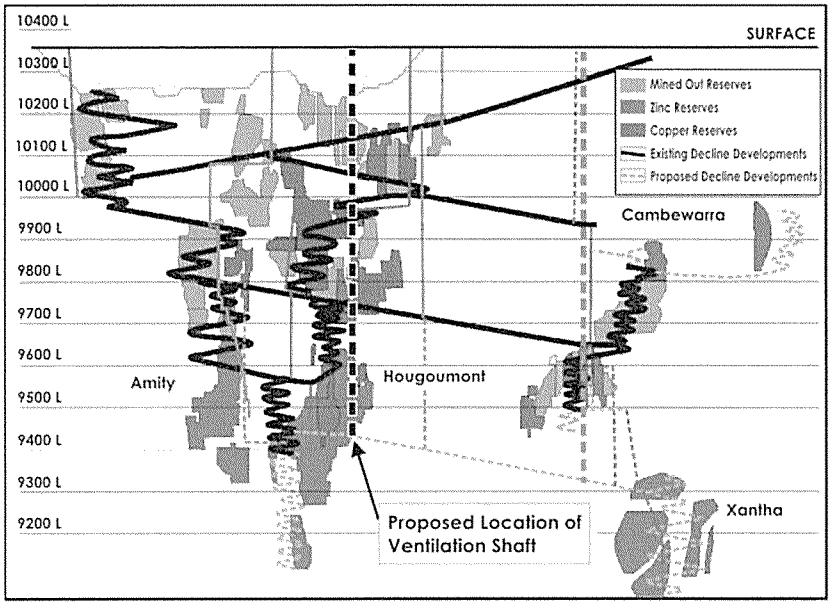

Figure 2. Location of the proposed raisebored ventilation shaft in long section

The drill core confirmed the weathering profile matched that of the typical Yilgarn weathering profile. Complete, partial and slightly weathered material extended to depths of 0m - 91m, 91m – 105m and 105m – 110m, respectively. Weathering effects on the surface of discontinuities were observed to a depth of 146m and only thereafter was the rock classified as fresh. This deeply weathered profile of 110m is almost double the expected depth of weathering on site, which is generally 60m. Nineteen major rock units and a number of smaller units were intersected by the vertical drill hole. However these units only comprised three rock types (dolerite, dacite and rhyolite). The degree of weathering lessened from unrecognisable completely weathered saprolite, to partially weathered dolerite and dacite.

Two critical intervals were identified in which stability issues were likely to occur. The first was the interface between the fresh material and the weathered material above it. The second was a long zone of low interblock strength predicted in the face and walls. Results indicated the shaft did not meet the OZ Minerals 1 in 20 probability of failure criteria for stability. The shaft was also predicted to fall within the 1 in 4 failure-zone in the AMC Australian raisebore case history database. From the assessment it was concluded that either:

- the location of the site should be changed to a site where the weathering profile was thinner or there was more competent rock
- alternatively the ventilation shaft had to be conventionally sunk through the weathered profile and raisebored in the fresh material at a smaller diameter. The smaller diameter shaft could then be expanded from surface down, using conventional shaft strip-and-line techniques, and the smaller shaft as a muck chute for the debris formed during the second pass expansion.

Economic and functionality requirements dictated the proposed site of the intake ventilation shaft be abandoned, in favour of a site where it could be constructed quicker and more cheaply, in an area of shallower weathering.

Due to the geology of the Gossan Hill deposit, choosing an alternative site with shallower weathering and better quality rock for raiseboring a shaft was a viable and easy option. The deposit sits within strata that dip sub-vertically and are not thick (hence the 19 major rock units intersected in the single vertical drillhole). Therefore different rock types outcrop at the surface with relatively little lateral movement across the site.

An investigation into the depth of complete and partial weathering versus the rock type for all surface drill holes across the Gossan Hill deposit confirmed that some rock types were notably more susceptible to weathering than others. The results of the comparison (Figure 3) show which of the main rock types at Gossan Hill may be expected to have the greatest depth of weathering. Rhyolite is predicted to be the most susceptible to deep weathering out of all the rock types and the range between weathering depths for different rock types may be expected to be as large as 40m. Maximum depths of weathering for each rock type far exceed the predicted depth, with a difference of some 15m – 55m. The results confirm the weathering of the dacite at the site for the proposed shaft was extreme.

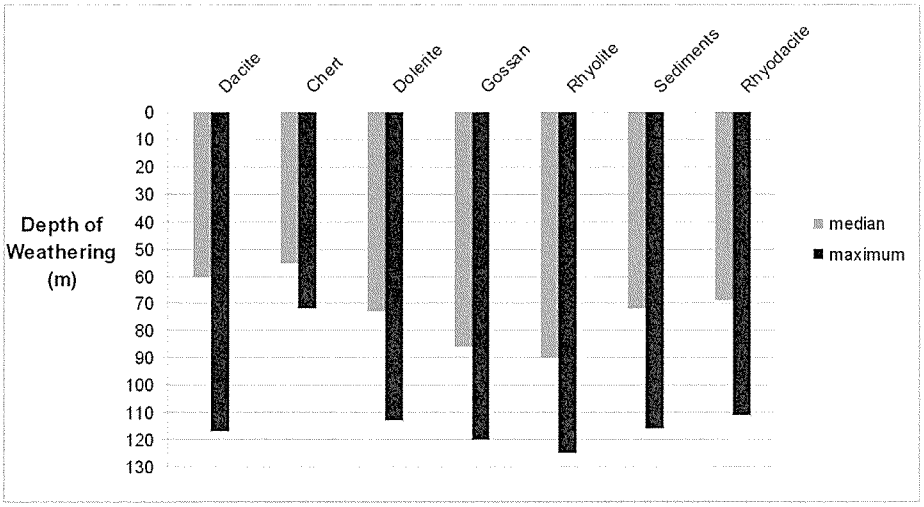

Figure 3. Depth of weathering versus rock type at Gossan Hill Deposit, Golden Grove Operations.

Site personnel cautioned that weathering of the dacite could be highly variable and, though not represented in this comparison, experience noted the rhyodacite was typically more affected by weathering than pure dacite. Site observed that the thickness of a unit had an affect on the depth of weathering, experience noting the thinner units tend to be more weathered to a greater depth than the thicker units (especially for dolerite units). Furthermore, site experience noted the depth of weathering in the gossan may be misleading. This is because the sulphides in the gossan preferentially weather during the development of the rock unit, thus giving a completely weathered appearance to the unit when the host rock in not significantly weathered (pers. comm. B. Laws, 2008).

4 SITE INVESTIGATION AND ALTERNATIVE DESIGN STRATEGIES

Whilst using conventional raiseboring techniques to construct a shaft is generally the cheapest, fastest and safest method, it is not always the most appropriate method of construction with respect to the geotechnical ground and rock mass conditions. (This was shown to be the case for the Golden Grove – case study). The expense of a collapsed raisebored shaft can easily extend beyond the cost of the repair or replacement of equipment (rods and the raiseboring head) to knock on expenses such as delays in mine production and reduced processing plant throughput. A worst case scenario could involve unachieved production because a planned mining area needed to be abandoned due to lack of access or adequate ventilation.

Numerous large diameter raises have collapsed during the reaming of wet and weak weathered rocks (Peck and Lee, 2008). In highly weathered saprolite units, failure and subsequent collapse of the raisebore can occur as a result of the wet and weak material swelling and/or squeezing into the void as the raisboring head moves through and past the unit. Water and the presence of swelling clays or unstable minerals (e.g. smectite group clay minerals or brucite respectively) in the weathered profile exacerbate the weakness of the material. The swelling and squeezing can also often mean support is ineffective or cannot be installed fast enough to prevent collapse.

Preventative solutions for such causes of raisebore shaft collapse are naturally more desirable than corrective measures. These can be achieved by locating stable sites through clearly defined site investigation and analysis techniques, as well as flexibility to use alternative shaft construction designs.

4.1 Raisebore Site Investigation

The site investigation of ground conditions must include drilling a site specific borehole on the centre-line coordinates of the proposed raisebored shaft, which follows the alignment of the raise. To maintain the *in situ* integrity of the core, especially the weathered material, triple tube diamond drill core (min. 50 mm diameter) should be drilled. As soon as is possible the weathered material should be bagged, to maintain the *in situ* moisture content, photographed, as weathered material can often deteriorate quickly and then sampled for *in situ* moisture content, plasticity and liquid limit index as well as triaxial shear strength. Samples for x-ray diffraction or particle size distribution testing may also be collected, if required.

In Australia the geotechnical assessment of raisebored shaft stability has typically been performed using the McCracken and Stacey (1998) analysis method. But this method is limited in its application to the weathered portion of a raisebore because:

- RQD (used as a factor in the McCracken and Stacey assessment) applies only to "hard and sound" sticks of core, which excludes highly and partially weathered material. Deere and Deere (1989) regard moderately weathered rock as being "hard and sound".
- Completely and partially weathered material will behave differently to the moderately weathered to fresh rock mass.

The site investigation and stability assessment of deeply weathering profiles must pay attention to the primary geotechnical features likely to result in stability issues in the weathered profile, as well as include recognised empirical methods. Primary geotechnical factors to look for include depth of weathering, composition of weathered material, the weathered material's sensitivity to time-dependent deterioration resulting from changes in moisture and mining induced stresses, past and present water table levels and likely sources of ground water inflows.

4.2 Alternative Design Strategies

In most cases, if a proposed shaft is located in an area of deeply weathered material the best solution to prevent risk of failure is to relocate the shaft onto an outcrop with better weathered ground conditions (shallower depth of weathering, different composition etc.). However, this is not always possible. Constraints in the mine schedule and resources (equipment, labour and budget) often mean there is no time to investigate alternative sites or investigate construction options. An ideal situation would see the site planning of a shaft dictated by the geotechnical properties of the ground, as opposed to underground layout and access, which is normally the case.

If a proposed shaft cannot be relocated there are a range of construction options that can be considered. Often raisebore contractors have the expertise and experience to give advice on

alternative design options. They should therefore be consulted regarding viable alternatives early in the planning process of a proposed shaft. Some such design options which can improve ground stability and allow the majority of a shaft to be raisebored include:

- Dewatering the weathered material, which will substantially increase the stability. Ideally the site should be continuously pumped until adequate support and drains have been installed.
- Excavating beyond the completely and partially weathered material, to rock that can be grouted and have piles installed around the final shaft perimeter.
- Raiseboring at a smaller diameter through the completely weathered material. Thereafter expanding the raisebored shaft using either conventional shaft strip-and-line techniques or the alimak and a smaller diameter shaft as a muck chute (as suggested for the Golden Grove case study). The advantage to using the alimak is that it does not need a head frame, winder driver nor slip form liner.
- Large diameter piling through the weathered zone. Piling can be performed with large pile boring machines (up to 5 m in diameter) generally used in civil engineering projects.
- Using small diameter reinforced bored piles in the weakest zones of the weathered profile to increase the support. A case study using this method was done at the Avoca Resources Ltd., Trident Gold Mine (Sexton, *et. al.* 2008).
- Depending on the planned use of the raisebored shaft it could be stepped or staggered to avoid the deepest weathering zones (a viable option for Golden Grove case study).

5 CONCLUSIONS

OZ Minerals, a large underground zinc, copper and lead mine, proposed the construction of a 4.5m diameter, 1000m deep ventilation shaft, using conventional raiseboring techniques. The stability assessment concluded deep weathering (110m) at the site and other fresh-rock related stability issues required alternative site investigation strategies and shaft design options. The Golden Grove site provides a good case study of shaft construction in the deeply weathered profiles in the Yilgarn and the alternative site and design strategies. The similarity of the weathering profile to the typical Yilgarn weathering profile and the differences in the depth of weathering, for sub-vertical dipping rock types across the site, meant that changing the location to one with more favourable weathering and ground conditions was a viable option. This paper shows that if there is flexibility within mine scheduling and construction design, as well as adequate time-planning, shafts can be constructed faster, cheaper and without the potential risks associated with raiseboring through thick deposits of highly weathered material.

REFERENCES

Arand, R. R. and Paine, M. (2002) Regolith Geology of the Yilgarn Craton, Western Australia: implications for exploration. *Australian Journal of Earth Sciences*, **49**, pp 3 – 162.

Atlas Copco (2007) Mining Methods in Underground Mining, Ulf Linder Publishers, Sweden.

Deere, D. U. and Deere, D. W. (1989) Rock Quality Designation (RQD) after Twenty Years. *US Army Corps of Engineers, contract report GL-89-1.*

Laws, B. Senior Exploration Geologist, OZ Minerals – Golden Grove Operations (2008) Personal Communication.

McCracken, A. and Stacey, T. R. (1989) Geotechnical Risk Assessment of Large Diameter Raise-bored Shafts. Shaft Engineering, *Inst Min Met*, pp 309 – 316.

Peck, W. A. and Lee, M. L. (2008) Stability of Raise Bored Shafts in Australian Mines. *13th Australian Tunnelling Conference*, Melbourne, VIC., pp 331 – 337.

Sexton, M., Mikula, P. A. and Lee, M. F. (2008) Trident Mine Raisebore – A Bored Pile Case Study. *SHIRMS*, Perth, WA. (In Press).

INVESTIGATION, DESIGN AND CONSTRUCTION OF CSH217 GOLD PROJECT, INNER MONGOLIA, CHINA

Bill Wang
Golder Associates Pty Ltd, Melbourne, VIC, Australia

ABSTRACT

The Chang Shang Hao (CSH) Gold Project is located 650 km northwest of Beijing, in the Nei Mongol Autonomous Region of Northern China (Inner Mongolia). From its discovery during 1980's, the low grade ore was considered to be uneconomical to mine. However, the Joint Venture Partnership (JVP) Canadian-Chinese consortium introduced new engineering standards, methods, technology and approaches to allow the CSH217 gold project to become fully operational by mid 2007.

This paper presents the challenges faced and methods used during the investigation, design and construction of the project in the extreme climate of the Gobi Desert. An integral part of the project is the heap leach process. During the design and construction phases, both Chinese and International (ASTM) standards were implemented and enforced. The heap leach facility will be one of the largest in China on its completion. The JVP introduced new expertise into China in the areas of design and construction methods for the compacted clay/geosynthetic lined solution collection and drainage systems, leak detection systems, solution ponds and stormwater diversions.

1 INTRODUCTION

CSH Gold Project is located near the Gobi desert in Wulatezhongqi county of Inner Mongolia. The Mine and Heap Leach Pad sites are approximately 8 km north of Xinhure, a small village which is located about 650 km northwest of Beijing. The site is part of the vast arid grasslands of Inner Mongolia, sheep and goat herding is the most common method of subsistence employed by the nomadic people living in the area today.

The CSH Gold Project is also known as the CSH 217 Gold Project or the 217 Project. It is operated by the Ningxia Pacific Mining Co. Ltd., a joint venture between Jinshan Gold Mines and Brigade 217 of the Northwest Geological Bureau of the China National Nuclear Corporation. Golder Associates (Australia and USA) were the principal geotechnical engineers for the project, KD Engineering Company (USA) were the project managers and process engineers.

To meet Chinese design regulations, Beijing General Institute of Mining and Minerals (BGIMM) were the Chinese design institute and project superintendents who were responsible for the issuing and approval of detailed construction documentation. Baogang Geological Exploration Institute (Baogang) of Baotou were the geotechnical engineers during the site investigation stage.

The project consists of an open pit mine, mined using shovels and haul trucks, placement of waste rock in waste rock dumps, and processing of ore using cyanide heap leaching techniques with recovery of gold and silver from cyanide solution using a carbon-desorption recovery (ADR) process plant. Initial plans were to process 52 million tonnes of ore to produce 1.25 million ounces of gold at an average grade of 0.74 grams per tonne. The planned mine life is about 8 to 10 years. Ore will be placed and processed run-of-mine (ROM) on the heap in the first and second years. A crushing plant constructed in the second year of operation will crush

ore to nominally less that 12 mm particle size prior to placement on the leach pad. The planned ore production rate is 7.1 million tonnes per year and the peak material movement (ore plus waste) is 18.3 million tonnes per year during the first three years of operation.

2 CLIMATE

The site topography ranges in elevation between 1610 m above sea level in the south to about 1650 m in the north. The climate at the site is a semi-desert climate characterised by warm summers and cold, dry winters, combined with low rainfall and high evaporation. During summer (June, July and August) daytime temperatures range from 20 °C to 35 °C. Winters are long, cold and windy, based on available records from Wulatezhongqi weather station between 1979 and 2000, the minimum recorded temperature was -32 °C. The freezing weather runs from October through the winter until April, with an average of about 160 days per year below freezing and frost penetrates to typically 2.0 m below ground. Strong winds are common throughout most of the year, a northwest wind is most common during the spring season. During snow blizzards and sandstorms, onsite wind speed can reach up to 40 m/s. Summer is the wet season, characterised by large storms with heavy rain in a short period of time, creating high velocity stormwater runoff across the site.

3 GEOLOGY

The ore body is located within the North China Gold Belt in the central area of the Bayan Obo Depression near the edge of the North China Craton. Low grade metamorphosed Proterozoic quartzites, shale and limestone, as well as unmetamorphosed Palaeozoic rocks, occur as accretionary complexes surrounding the Early Proterozoic and older basement rocks.

South of the mine ore body, Aeolian deposits and granite bedrock predominate Phase 1 of the heap leach facility site. In areas where bedrock was not exposed at the ground surface, Aeolian soils at the ground surface support small sparse grass turfs with fine roots extending to depths of up to 0.4 m. Aeolian soils consisting of blends of loess, low plasticity silt, clay and fine sand soils blanket the site to a typical depth of 0.5 m to 1.5 m, and locally as deep as 3 m to 4 m. As typical with most Aeolian deposits in grassland areas, the silt has a porous structure that, when eroded by water, cleaves vertically to create free-standing, vertical faces. The granite bedrock encountered in boreholes generally consists of fine to coarse grained, green, brown and white, extremely to moderately weathered, low strength rock.

4 HEAP LEACH FACILITY DESIGN

4.1 Design Criteria

The leach pad site was selected based on the availability of a sufficiently large area to contain the 52 million tonnes of ore, in close proximity to the ore deposit and to soils used as bedding fill for pad liner construction. The site also needs to be relatively flat terrain for ease of construction and ease of ore stacking during mine operations. Additionally, the leach pad site should provide sufficient slope for gravity solution flow and should be outside of major drainages to reduce the impact from stormwater runoff during operation and after closure of the mine.

Field investigation works were carried out during the spring of 2005 in conjunction with Baogang Geological Exploration Institute. The aim of the program was to characterise the geological conditions of the founding materials for the facility and process plant area, and to locate available quantities of borrow materials for use as liner bedding fill for the leach pad and pond construction. In total, 64 boreholes and 80 test pits were completed across the site.

4.2 Heap Leach Design

The heap leach facility is known as the "South Leach Pad", and is located approximately 3 km south of the mine ore body. The purpose of the south leach pad, constructed in two phases, is to contain the currently identified economical ore reserve of 52 million tonnes. Phase 1 construction included the installation of approximately 460,000 m^2 of heap leach pad, the pregnant pond, the overflow pond, process plant, administration buildings and living quarters for the staff. Phase 2 construction will expand the leach pad by an additional 360,000 m^2 to the north of Phase 1. The "Pregnant Pond" is capable of storing 35,000 m^3 of cyanide solution to supply the process plant. The "Overflow Pond" is capable of storing up to 80,000 m^3 of cyanide solution as an emergency measure during large storm events and power outage within the process plant. A series of stormwater diversion channels were also designed to divert stormwater runoff around the pad during large storm events. Figure 1 shows the Phase 1 South Leach Pad during construction.

Figure 1: Heap Leach Pad

The design of lining systems, leak detection systems, solution collection systems and stormwater diversion channels for the heap leach facility used environmental protection regulations developed by the State of Nevada, USA, as formal regulations for heap leach design were not available in China. Geotechnical laboratory testing was carried out in accordance with ASTM standards.

The design intended to achieve zero discharge of process solutions through the following:

- A lining system composed of a composite geomembrane (2 mm thick HDPE geomembrane) and soil bedding layer with a permeability of 1 x 10^{-5} cm/s or less;
- A coarse granular fill and gravity piping system placed over the composite liner to collect and convey solution and to reduce fluid pressure on the composite lining system;
- A leak detection system beneath the composite lining system, in areas where cyanide solution flow above the lining system is concentrated;
- A double lining system (1.5 mm and 2.0 mm HDPE geomembrane) within the pregnant pond fitted with a continuous leak detection layer between the geomembrane;
- A lining system within the overflow pond; and
- Stormwater diversion channels to divert stormwater flow from natural drainage tributaries around the heap leach facility.
- An 8 metre wide perimeter access road/soil bund around the leach pad and the ponds.

The pregnant pond was constructed within the leach pad as an "internal pond". Mine ore placed within the pond served to insulate pregnant cyanide solution during the cold winter months to prevent freezing. The pregnant pond solution capacity was provided by the pore space within the ore placed in the pond. The pregnant pond has 3H:1V side slopes, is 10 m in depth with 1 m

of freeboard and has been designed with a maximum combined ore and solution capacity of 107,000 m^3 or a solution capacity of 35,000m^3 assuming ore porosity of 0.33. Figure 2 shows the final stages of pregnant pond construction.

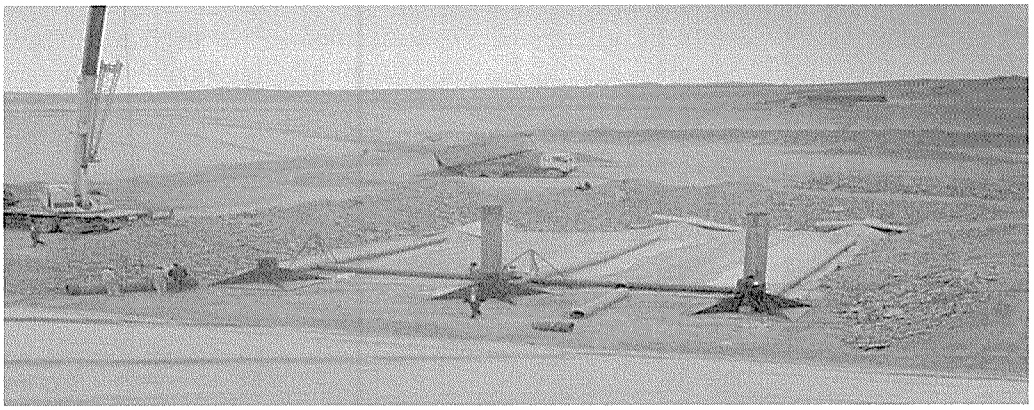

Figure 2: Pipe Installation and Backfilling of Pregnant Pond

5 GEOTECHNICAL ASPECTS AND CHALLENGES

The extreme weather conditions of the Gobi desert including large stormwater runoff during storms and extremely high velocity winds presented challenges to be overcome during the earthworks and installation of the geomembrane. The following discusses two geotechnical issues encountered during the construction of the heap leach facility.

5.1 Bedding Fill Material

Licensing and other requirements required all fill materials used for construction to be sourced within the mine property boundary. A liner bedding of 300 mm thickness placed in two layers is required beneath a 2.0 mm thick HDPE geomembrane liner across the leach pad. Locating adequate volumes of suitable bedding fill material was an initial challenge faced during construction of the south leach pad. During the investigation stage, surficial deposits of suitable material that extend to depths of 3 m along valleys between the rocky outcrops consisting of low plasticity silty clay and clay overlying silty sand were identified.

Flexible-wall saturated permeability testing (ASTM D 5084) was conducted on four re-compacted soil samples to assess the potential for use as liner bedding fill. Three samples of silty clay and clay met the project specification of 1 x 10^{-5} cm/s, the fourth sample consisting of silty sand achieved a result of 3.1 x 10^{-4} cm/s. The permeability testing verified that the silty clay and clay were suitable as bedding fill material. The project specification also stated that the bedding fill material used for construction is to have a minimum of 50% passing the No. 200 sieve, 0.075 mm opening (ASTM D 422). The placed bedding fill material also required to be compacted to achieve a 92% maximum density ratio in accordance with ASTM D 1557 – Modified Proctor, with a compaction moisture content in the range of -2% to +3% of the optimum moisture content.

The construction contract for the heap leach facility was awarded to local Chinese contractors, experienced with road construction works as well as Chinese testing standards and specifications. Earthwork machinery used for construction ranged between 10 to 20 tonne front end loads, road truck, dozers, excavators, dynamic and static compactors. For the heap leach pad and pond construction, the contractors were tutored and mentored on the requirements of the CSH heap leach facility specification and the requirements of ASTM standards, in particular, the requirement for compaction of fill material to achieve a 92% maximum dry density ratio in accordance with ASTM D 1557 – Modified Proctor.

During the construction of three trial areas, it was found that the Aeolian silts and clays were unstable and heaving occurred beneath the 20 tonne smooth drum dynamic compactor when the moisture content exceeded 2% wet of the optimum moisture content. Through many discussions and meetings with the earthworks contractor, a set method of moisture conditioning techniques (using drip bars and water cannons) were utilised to more evenly distribute moisture within the fill materials.

Surface cracks up to 5 mm wide developed during compaction of the trial area when the vibratory compactor had undergone more than 8 passes on the bedding fill material. Within the trial areas, it was found that to achieve the required compaction of the Aeolian fill, a combination of vibratory and non-vibratory compaction was required. A vibratory smooth drum compactor was first used to compact the loosely spread fill, then to "seal" the surface of the compacted bedding fill layer, an 18 tonne non-vibratory smooth drum compactor was used. The combination of 4 passes of the vibratory compactor and 6 passes of non-vibratory compactor typically achieved 5 % to 8 % higher compactive efforts than using dynamic compaction alone. To meet the project specification, this method of compaction was adopted to construct the bedding fill layer.

5.2 Pregnant pond

Construction of the pregnant pond was undertaken over a period of two years, and completed in July 2007. During the first stage of pond construction, blasting was used to excavate the granite bedrock to the pregnant pond's design levels. In June 2006 the excavation was completed and the construction of the dual composite lining system followed.

The extreme weather conditions presented construction difficulties following excavation works. The construction season (in order to avoid working in freezing conditions) is generally between the warmer months of April and September. This period is also the wetter part of the year, often with large unpredicted thunderstorms and sandstorms. Stormwater runoff from the constructed leach pad damaged the placed liner bedding fill of the pregnant pond at the end of the 2006 construction season. A decision was made by Ningxia Pacific that the pregnant pond was to be repaired and completed as early as possible in 2007, without delaying the schedule for gold production.

When construction recommenced in March 2007, bedding fill material in the pregnant pond was found to be severely damaged. Frozen bedding fill material was removed from the base of the pond. Subsequently, a pond underdrain was designed and constructed to remove groundwater beneath the new bedding fill material. Figure 3 shows a typical section through the pregnant pond's underdrain, leak detection sump and pipe as well as the dual composite layer.

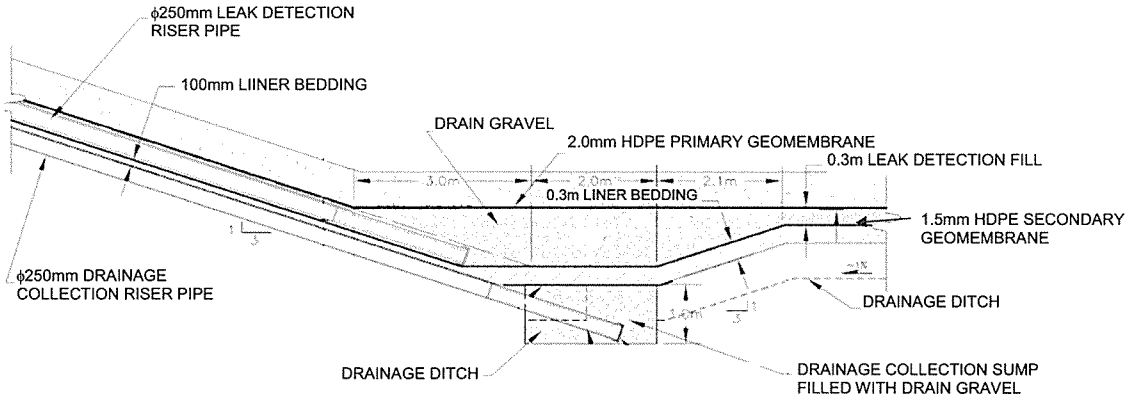

Figure 3: Sump and Riser Section of Pregnant pond

Stormwater runoff from the leach pad had created erosion channels within the bedding fill along the slopes of the pond. More than five storms at different stages of construction damaged the pond. The erosion channels ranged from 0.1 m to 1.8 m deep and up to 2.5 m wide. Final surface of the bedding fill were compacted using conventional smooth drum compactors. A single front wheel of a front end loader was employed to compact the bedding fill materials placed in thin layers within the deeper erosion channels where access for the smooth drum compactors was not available. Figure 4 shows examples of eroded bedding fill and the exposed granite bedrock on the slopes of the pregnant pond after a storm event.

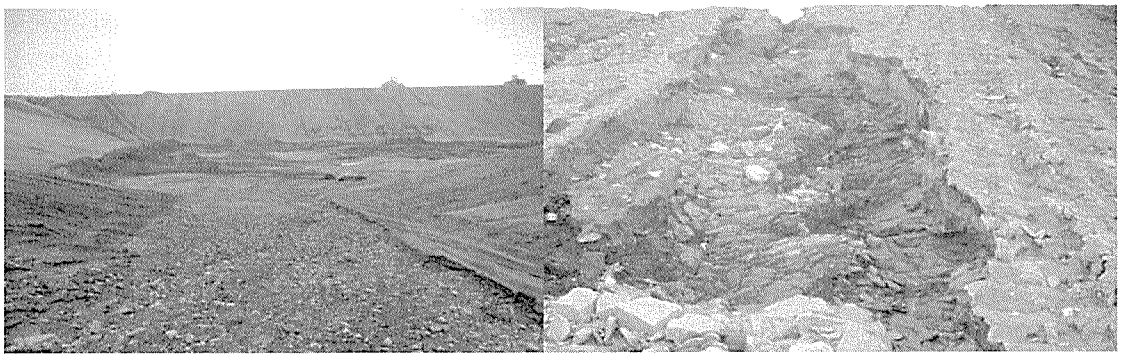

Figure 4: Eroded Bedding Fill along Pregnant Pond's entrance ramp (left) and side slope (right)

6 CONCLUSIONS

Golder Associates performed construction monitoring and construction quality assurance from April 2006 to July 2007, during the heap leach facility earthworks (Level 1 supervision) and installation of geosynthetics. The lead geotechnical engineer and CQA monitors were from Australia and USA. A team of Chinese engineers and technicians supported the lead personnel during the construction programme. Chinese and ASTM regulations were met as the heap leach facility was constructed in general accordance with the project design and project specification.

The heap leach facility was fully operational during July 2007, and gold production commenced in August 2007. The construction of the heap leach facility faced many obstacles and challenges such as extreme inclement weather conditions, geotechnical issues, technical differences and language barriers. The collaborative effort between the contractors, designers, engineers, managers and the client showed that through careful planning and management, new techniques and design measures can be successfully implemented and constructed.

ACKNOWLEDGEMENTS

The author wishes to acknowledge the assistance of staff from, Beijing Geotechnical Institute, Ningxia Pacific, BGIMM, Baogang and Golder Associates (Australia, China and USA) who assisted with the project during the investigation and construction stages is greatly appreciated.

REFERENCES

Rossi, M.E, Tutton D.A, Nilsson, J.W., (2005), *Preliminary Assessment of the Chang Shan Hao 217 Gold Project, Nei Mongol, People's Republic of China,* Prepared on behalf of Jinshan Gold Mines, Inc., April 15, 2005

Golder Associates Inc, (2005), Report on *South Heap Leach Facility, CSH Gold Project, Inner Mongolia, China,* Reference 053-2515 Prepared on behalf of Jinshan Gold Mines, Inc., October, 2005

Evaluation of empirical strength-suction relationships for a Northern Adelaide Plains Clay

Christopher Ward
Parsons Brinckerhoff, Adelaide, Australia

Keywords: soil water characteristic curve, suction, undrained, drained, shear strength, electrical conductivity.

ABSTRACT

Unsaturated shear strength of soils forms an important engineering property in the geotechnical design of engineering structures. Soils in arid and semi-arid climates often do not become saturated during the design life of the structures and in these cases, the geotechnical properties of soils in the unsaturated state are more relevant than the traditional design principles for saturated soils. Methods were investigated for finding the unsaturated shear strength when the soil can not be sampled at the desired moisture state. Primarily, the relationship between soil suction and shear strength was investigated. In autumn 2007, thin-walled push tube samples were obtained from a northern Adelaide road project over a range of land uses in order to obtain samples at representative soil suctions. It became clear that a method was needed for conditioning soil samples to a lower moisture state, which was subsequently developed.

A relationship was obtained between unconsolidated undrained triaxial shear strength and total suction. An empirical soil water characteristic curve (SWCC) was determined, which was verified by pressure plate testing. Solute suctions, which were estimated by conductivity testing, were corrected on the basis of the SWCC and measured total suctions. Upon consideration of the solute suctions, a better relationship was found between shear strength and matric suction, which compared favourably with theoretical models.

1 INTRODUCTION

The objective of this study is to investigate methods for evaluating the relationship between soil strength and moisture content for stiff clays in the Northern Adelaide Plains region. There is a known relationship between soil moisture content and suction values, and also between soil suction and shear strength. Our goals were to further understand these relationship and investigate simple testing methods.

A site with homogenous soil and three different suction profiles was found and push tube samples were obtained. Unconsolidated undrained (UU) triaxial compression tests, dewpoint psychrometer suction, moisture content, electrical conductivity, percentage passing 75 μm sieve and Atterberg limits were performed.

2 LABORATORY TEST METHODS

There is a range of tests applicable to unsaturated soils and there are several empirical methods for estimating the properties of unsaturated soils which, if validated, could prove useful in reducing the need for testing. The empirical methods and the proposed tests are discussed in the following sections.

2.1 Soil suction

Total Suction (u_t), is composed of osmotic, or solute (u_s) and matric (u_m) suctions, and can be expressed approximately as follows (Fredlund & Rahardjo, 1993):

$$u_m = u_t - u_s \quad (1)$$

Total suction can be measured indirectly by measurement of relative humidity of air near, and in equilibrium with, the sample using a dewpoint hygrometer or similar device.

2.2 Solute suction from Electrical Conductivity

Shaw (1994) details a method of obtaining the electrical conductivity of a sample. The sample is passed through a 425 μm sieve and mixed with demineralised water at a ratio of 1:5 by weight. An approximate solute suction value (u_s) can be derived for a given field moisture content:

$$u_s = 36EC_{1:5}\ \frac{500}{w} \tag{2}$$

Where;

EC1:5 = electrical conductivity in deci-siemens

w = field moisture content in %

2.3 Soil Water Characteristic Curve (SWCC)

The SWCC defines the relationship between the soil suction (total or matric) and gravimetric or volumetric water content, and is a tool by which the behaviour of unsaturated soils can be understood (Fredlund & Rahardjo, 1993). Commonly, small soil samples are conditioned over a high air entry ceramic plate in a pressure chamber (pressure plate). Since matric suction is the difference between the air pressure in the soil voids (u_a) and the negative pore water pressure (u_w), increasing u_a while u_w is kept constant increases the matric suction. The process is known as the axis translation technique (Nelson and Miller 1992). Typically, a soil sample which follows a drying path in the pressure plate performs as if the soil is saturated up to a certain matric suction, known as the air entry value, $(u_a - u_w)_b$. Further drying sees an acceleration of desaturation.

2.4 SWCC from basic soil properties

Fredlund et al (1996) present the method of showing a soils SWCC expressed as volumetric water content against matric suction, where the volumetric water content is given by:

$$\theta_w = C(h) \times \left[\frac{\theta_s}{\left(\ln\left(\exp(1) + \left(\frac{h}{a} \right)^b \right) \right)^c} \right] \tag{3}$$

$$C(h) = \left[1 - \frac{\ln\left(1 + \frac{h}{h_r} \right)}{\ln\left(1 + \frac{10^6}{h_r} \right)} \right] \tag{4}$$

Θ_s = saturated volumetric water content.

h = matric suction in kPa.

a = a soil parameter which is primarily a function of the air entry value of the soil in kPa.

b = a soil parameter which is primarily a function of the rate of water extraction from the soil, once the air entry value has been exceeded.

c = a soil parameter which is primarily a function of the residual water content.

h_r = a soil parameter which is primarily a function of the suction at which residual water content occurs in kPa.

Zapata et al (2000) presented a method for estimating the SWCC for a soil with PI > 0, where the constants required for Equations 3 and 4 are derived from the soil's Plasticity Index (PI) and the percentage of dry mass passing a 75 μm sieve. Providing the following equations:

$$a = 0.00364(wPI)^{3.35} + 4(wPI) + 11 \quad (5)$$

$$\frac{b}{c} = 2.313(wPI)^{0.14} + 5 \quad (6)$$

$$c = 0.0514(wPI)^{0.465} + 0.5 \quad (7)$$

$$\frac{h_r}{a} = 32.44e^{0.0186(wPI)} \quad (8)$$

The wPI parameter in equations 5 to 8 is defined as:

$$wPI = Passing75\mu m \times PI$$

Where:

Passing75μm = proportion of sample passing the 75μm Sieve expressed as a decimal

PI = Plasticity Index(%) = Liquid Limit – Plastic Limit

In those cases where the saturated volumetric water content (θ_s), is unknown, the user can make use of the following correlation:

$$\theta_s = 0.0143(wPI)^{0.75} + 0.36 \quad (9)$$

2.5 Undrained unsaturated cohesion

Using the SWCC and saturated stress state variables, Vanapalli (2001) propose the following equation for estimating the undrained, unconfined shear strength:

$$c_u = \frac{c'\cos\phi' + (u_a - u_w)\{(\Theta^\kappa)\tan\phi'\}\cos\phi'}{1 - \sin\phi'} \quad (10)$$

κ = fitting parameter used for obtaining a best-fit between the measured and predicted values.

Θ = θw/θs = ratio of volumetric water contents, actual to saturated, or degree of saturation.

Vanapalli (2001) propose that κ can be estimated from the PI, in this instance, the estimated value would be κ = 3.0. The author goes on to show that the κ value found by fitting Equation 10 to c_u test results is a suitable approximation for use in Equation 11.

2.6 Unsaturated drained shear strength

Unsaturated drained shear strength can be estimated using the SWCC and saturated stress state variables, using the equation proposed by Fredlund et al (1996).

$$\tau = [c' + (\sigma_n - u_a)\tan\phi'] + [(u_a - u_w)(\Theta^\kappa)\tan\phi'] \quad (11)$$

3 APPROACH

3.1 Sampling

Borehole samples were taken from three locations to depths of up to 4 m with thin walled push tube at 0.5m intervals. Three borehole locations where chosen because of their identical geomorphology but different anticipated suction profiles. Borehole 1 was in an open paddock, borehole 2 was across the road in a field irrigated with reclaimed sewage water, and borehole 3 in the root zone of a stand of trees. All boreholes were within a 20 m radius.

3.2 Testing

Initial testing involved extruding the samples from the push tubes from borehole 2 (BH2) and trimming two to three sub-samples of 100 mm lengths for undrained triaxial testing. Tests were undertaken at two confining pressures (75 & 300 kPa). Moisture content, total suction, % passing 75 μm sieve, $EC_{1:5}$ tests were undertaken on all samples and a sample from each BH2 push tube was reserved for Atterberg limit testing.

After analysing the test results from BH2, the decision was made undertake all triaxial testing of BH1 and BH3 samples at a confining pressure of 75 kPa, maximising meaningful results for the shear strength-suction relationship. Furthermore, while the samples obtained from BH3 were extremely dry and provided meaningful values at lower moisture contents, it became desirable to develop a method to condition BH1 samples to a higher moisture content.

It was established that the device would need to confine the soil to one-dimension expansion, as expected in-situ. A vertical load was required to simulate the weight of soil at depths, and restrict any uncontrolled expansion. An arbitrary surcharge pressure of 13 kPa was used, which is equivalent to a depth of 0.6 to 0.8 m, within the depth range of field seasonal moisture variation.

4 FINDINGS

4.1 Test results

From Atterberg testing of BH2, the soils were characterized as red-brown highly plastic clay. Soil from push tubes two to five had very similar properties in the depth range of 1.0 to 2.9 m (Plasticity Index 38 to 44). Subsequently this soil was treated collectively as homogeneous material. From visual observations soil from BH1 and BH3 over the same depth range were the same material.

For samples from BH02 with a total suction (u_t) range of 3.8 to 3.9 pF, the undrained cohesion (c_u) and the undrained angle of friction (ϕ_u) were measured at 19 kPa and 16° respectively.

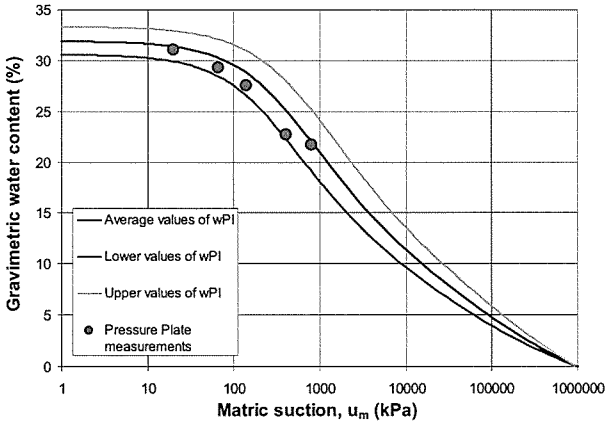

Figure 1: Estimated SWCC verified with Pressure Plate matric suction measurements

4.2 Comparison of measured matric suctions with predicted SWCC

Using Equation 3 for estimating the SWCC from the weighted plasticity index (wPI), upper, lower and average SWCC's were derived.

A high air entry Pressure Plate (PP) was used to study the drying curve SWCC of soils from BH2. The agreement with the estimated SWCC's calculated using the range of wPI values obtained was encouraging (refer Figure 1).

4.3 Undrained shear strength and matric suction

To derive u_m from $EC_{1:5}$ measurements of samples triaxial tested at 75 kPa confining pressure, Equation 2 was used, with u_m calculated from Equation 1. To obtain a best fit it was necessary to change the constant value of Equation 2 from 36 to 30:

$$u_s = 30 \times EC_{1:5} \frac{500}{w} \tag{13}$$

The additional strength from the confining pressure of 75 kPa (σ_3) was added to Equation 10, resulting in:

$$\tau = c_u + (\sigma_3) \tan\phi_u \tag{12}$$

As c' and ϕ' were not experimentally derived a sensitivity analysis was performed with the best fit being achieved with reasonable values of c' = 5 kPa, ϕ' = 26° and κ = 2.3.

Figure 2 shows the good agreement between the experimental result and best fit curve and the empirical estimation from Equation 12.

4.4 Estimated drained shear strength and matric suction

Equation 11 was used to estimate the unsaturated drained shear strength at 75 kPa confining pressure. Both the experimentally derived κ = 2.3 and Vanapalli (2001) recommended value of κ = 3.0 are shown in Figure 3.

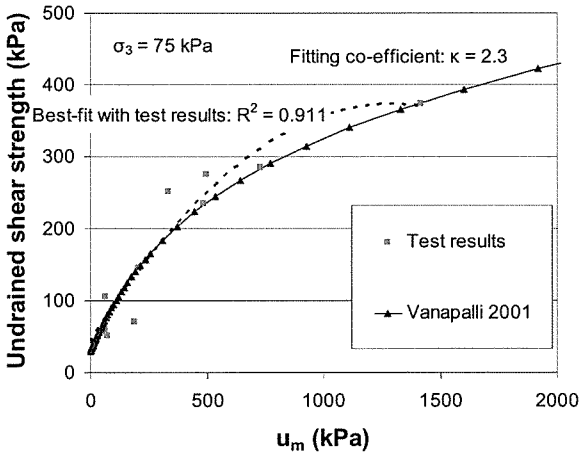

Figure 2: Undrained shear strength against matric suction (confining pressure of 75 kPa)

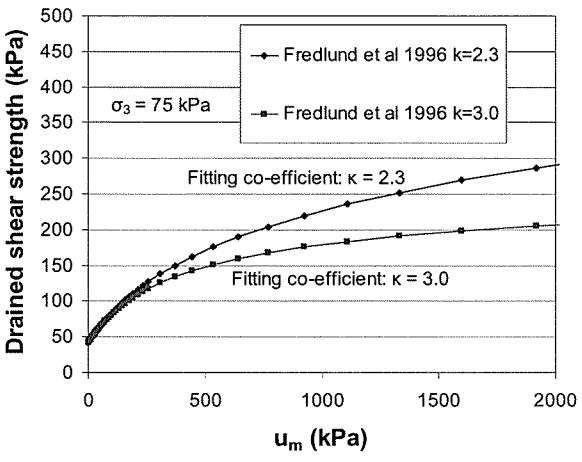

Figure 3: Estimated drained shear strength against matric suction (confining pressure of 75 kPa)

5 DISCUSSION

The investigation has shown that it is possible to obtain shear strength at any matric suction using relatively simple methods. First, a soil water characteristic curve (SWCC) must be established. In this project it was found that the level of agreement was encouraging between the estimate of the SWCC (Zapata et al 2000) and the drying SWCC measured using the high air entry pressure plate.

From the SWCC, a relationship between undrained shear strength and matric suction was developed by Vanapalli (2001). Measured shear strengths and matric suctions derived from total suctions of samples in the current study were plotted against the empirical relationship, and it was seen that the Vanapalli (2001) relationship provides a useful estimate of the variation of strength with suction (refer Figure 2). Using the Fredlund et al (1996) method it was possible to estimate the drained shear strength, however this was not verified through testing. Furthermore the effect of the different values of κ seemed to have a negligible impact upon the lower range of shear strength where the greatest interest to designers lies.

6 CONCLUSION

There is a clear relationship between soil matric suction and shear strength of the soils tested. This is of interest to designers undertaking long term drained analysis with unsaturated soils, where saturated stress state variables significantly underestimate analysis results.

Solute suction derived through electrical conductivity testing ($EC_{1:5}$) may be dependent on the particular soil, and the constant may not have a universal value due to electrolyte composition. In this project conductivity readings had to be reduced to achieve sensible levels of solute suction. In hindsight, it would have been preferable to have measured matric suction using the filter paper technique.

The results reinforce the existing literature on unsaturated soils, but are of particular interest as the samples were obtained in-situ, were not manufactured to be identical, and produced an outcome which is the possible application of simple test methods for common unsaturated geotechnical design tasks.

REFERENCES

Fredlund, D.G., Rahardjo, H., (1993). *Soil Mechanics for Unsaturated Soils.* John Wiley & Sons.USA

Fredlund, D.G. Xing, A. Fredlund M.D. & Barbour S.L., (1996). *The Relationship of the Unsaturated Soil Shear Strength Function to the Soil-Water Characteristic Curve.* Canadian Geotechnical Journal, Vol. 33, No.3, pp.440-448.

Nelson, J. D. and Miller, D. J. (1992). *Expansive Soils: Problems and Practice in Foundation and Pavement Engineering.* John Wiley & Sons.

Shaw, R.J. (1994). *Estimation of the Electrical Conductivity of Saturation Extracts from the Electrical Conductivity of 1:5 Soil:Water Suspensions and Various Soil Properties.* Queensland Department of Primary Industries Project Report QO94025.

Vanapalli S. K. (2001) *A Simple Experimental Procedure for Determining the Fitting Parameter, κ for Predicting the Shear Strength of an Unsaturated Soil.* 54th Canadian Geotechnical Conference, Calgary, pp. 622-629.

Zapata, C.E., Houston, W. N., Houston, S. L., and Walsh, K. D. (2000). *Soil-Water Characteristic Curve Variability.* Advances in Unsaturated Geotechnics, GEO-Institute, ASCE, Shackelford et al. (eds.), pp 84-124.

Experimental replication of The Lost Valley rock-fall (Glencoe, Scotland): with or without a glacier?

Sarah J Williams
URS New Zealand Ltd., Auckland NZ.

Keywords: The Lost Valley, rockfall, glacial ice.

ABSTRACT

Glencoe Caldera Volcano (GCV) in the Scottish Highlands comprises Silurian-Devonian Rock Units of rhyolitic and andesitic lavas and rhyolitic ignimbrites. Coire Gabhail, also known as The Lost Valley (LV), is eroded into these caldera rocks. The western wall of the valley has suffered slope failure and the debris accumulation can be traced down the northwestern valley side, across the valley floor and onto the opposing (southeastern) valley side to an elevation of approximately 60m above the valley floor. Rockfall debris blocking the valley consists of boulders and sands ranging from tens of millimetres to meters in diameter. The run-out distance and nature of this rockfall is unusual and reasons for this are explored in this paper. How could an estimated debris volume of 1.42×10^6 m^3 (assuming 30% void space) run 'up' such a height? Could this run-out distance have been achieved if glacial ice existed on the valley floor? Experimental replication of the Lost Valley rockfall was undertaken to evaluate the physical effects of a rockfall in ice and ice-free conditions, demonstrating that debris was deposited on remnants of valley glacial ice, not on the current topography.

1 INTRODUCTION

This paper documents research undertaken to demonstrate debris from the LV rockfall was deposited on remnants of glacial ice on the valley floor, not, on current topography. The hypothesis of this study was largely developed from field observations which indicated the following; unusually high elevations of coherent rockfall material on the opposing valley side and rockfall debris present 100's of meters from the failure scarp in the drainage channel of the alluvial basin.

The objective was to design, construct and utilize a scaled replica valley profile to carry out rockfall simulations in ice and ice free conditions. The investigation compared and evaluated the physical effects of materials in these conditions including, lithological distributions, effects of differing debris mass and density, fragmentation, fluidization, run-out, roll-back, grain over-passing and sorting. If rockfalls simulated onto ice corresponded to the cross-sectional profile of the current topography, it can be assumed glacial ice was present in the base of Core Gabhail during the failure event. Findings may lead to re-evaluation of the last known ice cover in the Scottish Highlands. This paper will discuss how the integration of field data, desk study and laboratory experimentation has lead to an assessment of mass movements in glacial terrains.

2 GEOGRAPHICAL AND GEOLOGICAL SETTING

Coire Gabhail is situated within the Three Sisters mountain range of Glencoe, Scotland. Known as a 'steep sided hanging valley', it is a tributary of the River Coe comprising an alluvial basin approximately 600m long and 150m wide. It was carved during periods of glaciation and has a 'U' shaped profile. The valley is blocked by rockfall debris which has lead to the appellation 'The Lost Valley'. This area of the Scottish Highlands was subject to growth of glacial ice and deglaciation during the Loch Lomond Readvance. Radiometric dating of sediments suggests the last ice sheet existed around 13 ka BP, (Ballantyne, 1997).

Glencoe Caldera is renowned for being one of the world's largest caldera super eruptions forming a 450 to 500Ma Silurian-Devonian volcanic sequence (Figure 1). The caldera is

thought to have collapsed due to "incremental haphazard subsidence of numerous crustal blocks" (Kokelaar and Moore, 2006,) prior to the development of a ring fault. Glacial erosion into the GCV formed the Coire Gabhail. These rocks have been bought in to contact with metamorphic basement rocks along the ring fault.

Figure 1: Geological map of field area.

3 POSSIBLE ROCKFALL EMPLACMENT MECHANISMS

3.1 Background

The 'wedge' like failure scar prominently cuts the northwestern valley side; dipping steeply at 56° and ~70 m in width. The majority of debris material accumulates on the failure slope as a debris cone that can be traced down the western valley side, across the valley floor onto the opposing (southeastern) valley side. Debris blocks the valley and consists of boulders and sands ranging from tens of millimetres to meters in diameter. Boulders of coherent rockfall material, approximately 7-10m in diameter are emplaced at approximately 60 m above the valley floor on the opposing valley side, segregated from the debris cone.

Ballantyne (2004), obtained an age of 1.8 ka for the rockfall implying failure occurred 9,000 years post glaciation. Ballantyne suggests slope failure occurred due to deglacial unloading and stress release caused by glacially-steepened rock slopes at Glencoe, and other mountain ranges within the Scottish highlands. Although a large amount of the debris toe has accumulated at an altitude of around 400masl on the opposing valley side from the initial failure point, Ballantyne proposes the morphology of debris is due to run-up and rebound mechanisms.

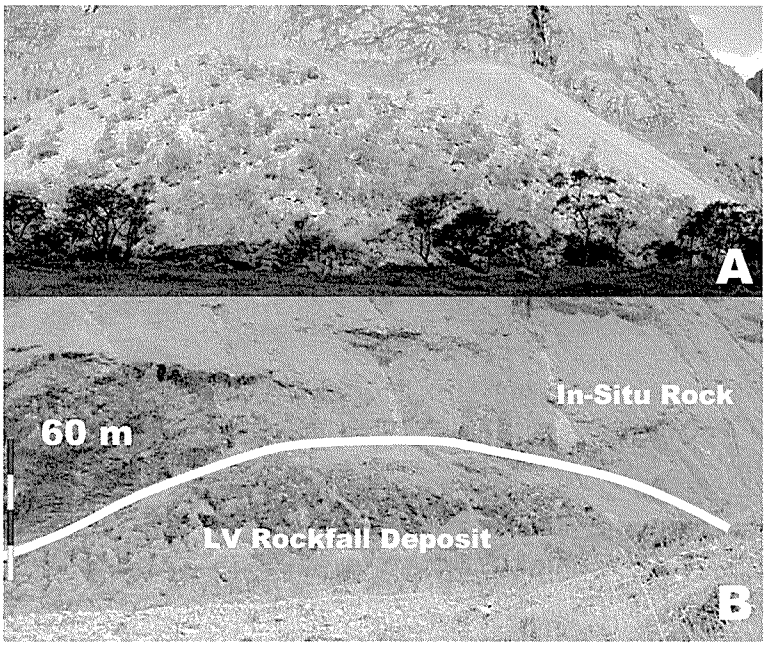

Figure 2: A – Lost Valley Rockfall; The debris cone and accumulation on failure slope (northwestern). B – Coherent debris deposit on opposing (southeastern) slope.

The debris deposit profile (Figure 2) evokes curiosity due to its unusual emplacement for a rockfall of this size in such a steep sided valley. Some of the principal considerations are;

- Coherent rockfall debris 'stuck' at considerable elevations on the opposing valley side.
- The volume of rockfall material has been identified as $1.42 \times 10^6 m^3$ (assumed 30% void space). Large velocities and energy transfers would have occurred to displace this mass. Would these have been efficient enough to thrust a non-fluidized mass to such a height without a large run-out platform, in such a narrow valley?
- Mobile rockfalls achieve run-up due to the amount of energy input, transfer and consumption (Davies, 1999). Extensive run-out distances can be achieved by large mass movements and are dependent on topographical and morphological features (Hungr, 1995). Run-up can often be achieved over neighbouring mountain sides ('obstacles'). This is largely dependant on the failure height, volume and density of rockfall debris and available run-out distance. (In-line with this research, run-up could not be achieved at Glencoe, due to the morphological features of Coire Gabhail valley).
- Heim (1932) assessed that debris masses partly or completely deflect and decelerate when impacting against an opposing mountainside and the effects are a function of the angle of impact. If the impact angle is 90°, a subdivision of the mass into two equal parts will occur. Oblique impact would produce unequal parts and acute impact results in no partition or deflection; therefore, run-up would occur. This would have occurred at Glencoe if glacial ice were present.
- Slump features were identified in debris material on the opposing valley side with a NW axial movement, indicating the deposit has undergone post depositional erosion. If the rockfall occurred on glacial ice, glacier retreat would evoke slumping toward the valley axis.
- Rock avalanches and slope failures are common within mountainous areas that have been modified by glacial processes. Glaciers have the capability to initiate slope instability and evoke future slope failures by freeze-thaw erosive action, debuttressing, stress concentrations, and valley over-steepening (as seen at Glencoe).
- Boulders up to 11 m in diameter can be traced several 100's of metres down the valley channel. It is likely boulders of this size have not been transported by alluvial processes but rather the result of a retreating glacial moraine.

The existence of glacial ice would have elevated the valley floor thus allowing a more archetype run-out, dispersion and lateral spread of the rockfall therefore providing a rational relationship between the slope angle, height and distance travelled.

3.2 Research

Avalanche Lake in the Mackenzie Mountains, Canada is considered an analogous case study. Kaiser and Simmons (1990), used field evidence, numerical flow modelling and run-up relationships to conclude debris was deposited on glacier ice 400-500 m above the valley bottom. This suggested that parts of the travel distances of the debris, as seen today, were provided by the movement and melting of glacier ice (Figure 3). Evidence given to support this theory included: the presence of debris in ephemeral drainage channels, zones of rare-fraction, debris 'ramps' and super-elevated and disrupted masses. In contrast, Evans et al. (1994), suggested the avalanche occurred in 'ice-free' conditions, dating the mass movement much younger than Kaiser and Simmons. Evans presented the following evidence: the nature of detachment, morphology of debris deposit, shelf lobe architecture, alluvial deposits and extraneous material entrained within the body of the deposit (Figure 3).

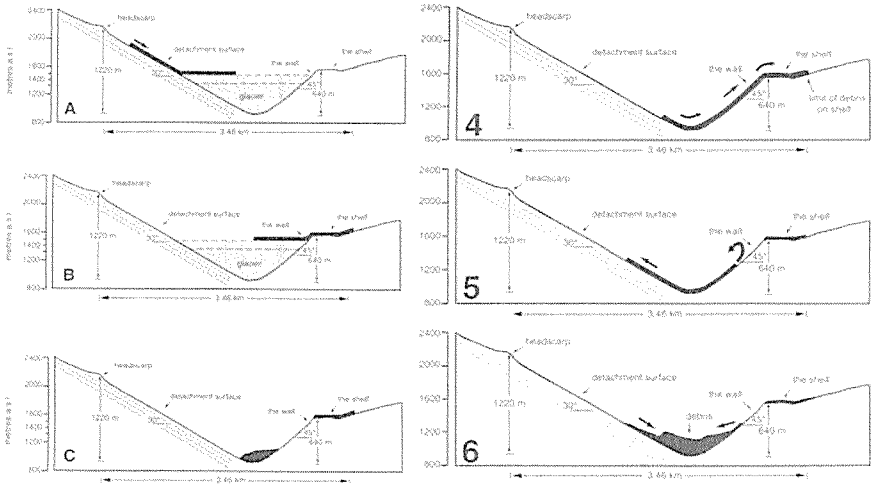

Figure 3: A-C Kaiser and Simmons Model; presence of glacial ice. 4-6 Evans et al., Model; No glacial interaction - slab detachment, run-up & roll-back.

4 EXPERIMENTATION

4.1 Model Construction

A scaled model was constructed from particle board, chicken wire and fibreglass matting based on an average valley cross-sectional profile (Figure 4). The model was supported by considerable field work including geological mapping, valley sectional profiling, grain size analysis, slope angle analysis and rockfall debris cone strike and dip orientations. Digital Elevation Mapping (DEM) and volume calculations using Petrel were also completed.

The objective of the experimentation was to prove debris run-out distances were modified due to the presence of glacial ice on the valley floor. The assessment was to determine run-up of materials tested in ice and ice free conditions. Materials used to simulate rockfalls were chosen based on varying grain size, density, and cohesion. Fragments used were <20 mm in diameter to closely represent grain size of the debris deposit. Materials used were as follows; wet sand and basalt aggregate, glass beads, coarse granite, packed and non-packed plastic blocks, plastic blocks and sugar solution, plastic blocks with a sand matrix and granite gravel with a sand matrix. Density of materials ranged from 0.52 (plastic blocks) to 1.53 g/m^3 (granite gravel with sand matrix). Data recorded from each experiment included depth of material along the valley

axis, run-up height, lateral dispersion (width) of the deposit and the angle of repose on both the failure slope and opposing valley side. Each experiment was filmed from an aerial and aspect perspective and cross-sectional photos were taken of the rockfall deposits. Movies were digitally enhanced and reduced to $^{1}/_{8}^{th}$ of the overall speed to analyse the fragmentation, roll back, granular collision and dispersion of grains.

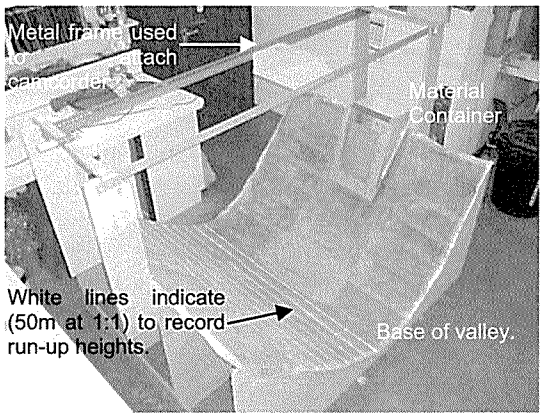

Figure 4: The Lost Valley model.

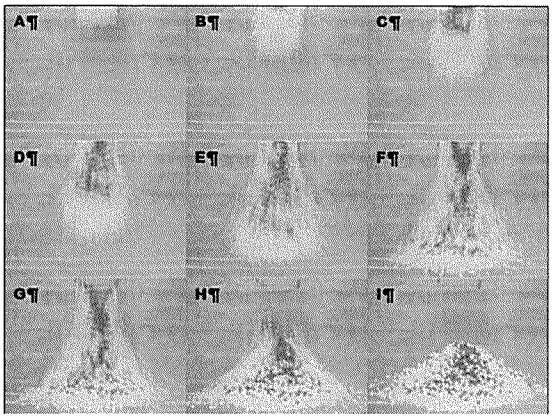

Figure 5: Screen shots of 'plastic block' simulation.

5 RESULTS

5.1 Ice free Conditions – Physical Effects

5.1.1 Lithological Distributions

Stacked brown and white plastic blocks were used to represent stratification of the UER and USA rock units in the field area to identify distributions of stratigraphically higher rocks in the debris of a rockfall. White blocks formed the lower stratigraphic units and the brown blocks formed the upper units. Brown blocks appeared to 'ride' on the surface of the stratigraphically lower white blocks during transportation (Figure 5).

5.1.2 Mass and Density

Less dense materials such as the plastic blocks had a greater run-up height and greater lateral spread. The depth of the deposit was also shallower. Materials of greater density (i.e. granite gravel) demonstrated opposite characteristics; greater run-up was achieved and the deposition of debris was concentrated along the valley axis. The middle of the deposit comprised the majority of the material, becoming shallower towards the limits of the deposit. On average the maximum depth of material along the section was 6.48cm and had an average density of 1.29g/cm^3.

5.1.3 Fragmentation

Fragmentation processes generate high velocities in all directions of a moving rockfall deposit, resultant forces of the mass act in the direction of least mass depth and causes the rear of the debris flow to decelerate and eventually stop, increasing velocities at the front of the moving deposit. This is an important constraint on run-up potential. During the simulations of plastic blocks and sugar solution (to form cohesion between blocks), impact with the slope resulted in greater dispersion of blocks, slightly greater run-up and a thinner depth along the valley axis. This is due to the plastic blocks failing as one 'complete' mass (greater density) as opposed to separate blocks.

5.1.4 Roll back, grain overpassing and sorting.

Each experiment demonstrated varying degrees of roll-back. The basalt aggregate with a wet sand matrix generated the highest amount of granular rollback, reaching a height of 28 cm on

the opposing valley side before returning to the valley axis. The less dense plastic blocks appeared to generate elastic collision and resultant rebound between blocks, therefore generating a smaller degree of rollback.

The degree of sorting was dependent on the type of material. Larger grains mixed with a sand matrix demonstrated a poorly sorted deposit. The larger, denser grains fell faster and the less dense material (sand) flowed behind them. The less dense sand collected underneath the larger grains and to the back of the deposit on the failure side.

5.2 Ice Conditions

Due to time constraints basalt aggregate with a coarse sand matrix (density 1.34g/cm^3) was the only medium chosen to run in ice conditions. Ice was frozen in plastic bags and trays and placed along the valley axis. Ice lay at variable height on the modelled valley floor (between 8 and 28 cm), to assess the possibility of variable run-up heights. Rockfalls were initiated onto the ice and filmed overnight until ice had fully melted. The following observations were made;

- The sand and basalt did not reach the opposing valley side. As a result no material was 'stuck' on the opposing valley side once ice had melted.
- A back slope angle of 74.3°, was recorded, 40° steeper than in ice free conditions. This is due to a decreased run-out distance.
- Once ice had melted the cross-sectional profile was similar to that of the Lost Valley. Material was observed in the 'drainage path' of the model.

6 SUMMARY/CONCLUSIONS

Controlled rockfall experiments were conducted in ice and ice-free conditions to illustrate the Lost Valley rockfall was deposited on the last remnants of valley glacier ice, *not* on the current topography. A manufactured artificial slope and a range of materials were used to conduct the experiments. Initial experiments in ice conditions appear to replicate characteristics seen in the field area. Experimental results suggest failure occurred during late stages of glaciation where debris from the rockfall accumulated on ice and the opposing valley side.

ACKNOWLEDGEMENTS

I would like to thank my Masters Supervisor, Dr. Peter Kokelaar at the University of Liverpool for allowing me to further utilise this data. I am thankful to my colleagues Debbie Fellows and Paul Salter for their constructive comments and support while writing this paper.

REFERENCES

Ballantyne, C.K. (2004) Coire Gabhail. *Draft from the Geological National Conservation Review of The Quaternary of Scotland Press*. Scotland Press, Scotland.

Davies, et. el. (1999) A fragmentation-spreading model for long run-out rock avalanches. *Canadian Geotechnical Journal*, 36: 1096-1110.

Evans, S.G., Hungr, O. and Enegren, E.G. (1994) The Avalanche Lake rock avalanche, Northwest Territories, Canada: description, dating and dynamics. *Canadian Geotechnical Journal,* 31: 749-768.

Heim, A. (1932) Bergsturz und Menschenleben. Fretz&Wasmuth Verlag, Zurich: 218pp.

Hungr, O. (1995) A model for the runout analysis of rapid flow slides, debris flows and avalanches. *Canadian Geotechnical Journal*, 32: 610-623.

Kaiser, P.K. and Simmons, J.V., 1990. "A reassessment of transport mechanisms of some rock avalanches in the Mackenzie Mountains, Yukon and Northwest Territories, Canada." *Canadian Geotechnical Journal*, 27 (1): 129-144.

Settlement prediction under fill embankments using finite element modeling, a case history

Jodi Wooding
Golder Associates (New Zealand) Ltd, Christchurch, New Zealand

ABSTRACT

The New Zealand Transport Agency, (NZTA) [formerly TransitNZ] has commissioned a design build contract for the construction of the SH20 Manukau Extension project. The almost 5-kilometre-long motorway includes of the order of 1 million m^3 of earthworks over complex geology comprising a mixture of weak alluvial soils to approximately 20 m depth interbedded with basaltic flows.

As part of the detailed design process, an assessment was made to predict settlements along a stream culvert as a result of the placements of a 6 m high embankment fill over soft ground. The sections of the soft ground were improved by stone columns to increase both the stiffness of the soil mass and to accelerate the rate of consolidation (Tan et al, 2008).

Modeling to predict settlements was carried out using the finite element software PLAXIS. One particular feature of the program is its ability to analyses a staged construction sequence by adding layers of fill over a specified length of time as would occur in the field. This paper includes a discussion of the subsurface conditions, the selection of the input engineering parameters and a presentation of results.

1 INTRODUCTION

Constructing embankments on soft soil is challenging in itself and when utilities are present this can considerably add to the complexity.

An existing stream crosses the proposed SH20 extension alignment in an area of soft soils and basalt flows. The flows occur under part of the embankment giving highly variable foundation conditions. An approximately 4 m wide by 6 m high culvert is required under the proposed 6 m high road embankment in order to maintain the existing stream. A temporary diversion of the stream was necessary for the construction works to proceed. The fill load on the soft soil promotes the potential for large settlements along the culvert alignment.

Stone columns have been installed at the site to improve the soil strength and permeability, which should reduce settlements and consolidation time. Modeling the expected embankment behavior and prediction of settlements is a critical step in the culvert design and can be carried out using numerical analysis including finite element models. Monitoring of the construction is also important to confirm that the predictions are close to the site behavior and updates can be made to the initial model if required.

2 GEOLOGY AND LOCATION

The geology of the project area can be separated into four main geologic units:

1. Holocene Alluvium: comprising recent stream deposits consisting of very soft clays and loose to very loose sands (and silts) extending up to 8 m depth.
2. Tauranga Group Sediments: comprising estuarine and terrestrial sediment consisting of very soft to very stiff pumiceous silts, sand, clay and peat. These materials are typically erodable and highly variable along the proposed motorway alignment.

3. Quaternary Basalt: comprising the northern extent of basalt flows from the Manurewa Volcano, and consisting of between 3 m to 8 m thickness of slightly weathered to fresh and typically high strength basalt rock.
4. Kaawa and Waitemata Group Sandstone/Siltstone: comprising weathered siltstone and sandstone bedrock with some gravel. The Waitemata Group rocks are effectively the basement rock along the majority of the alignment.

The location of the culvert is shown below in Figure 1. All of the geological units are present in varying layers under the site.

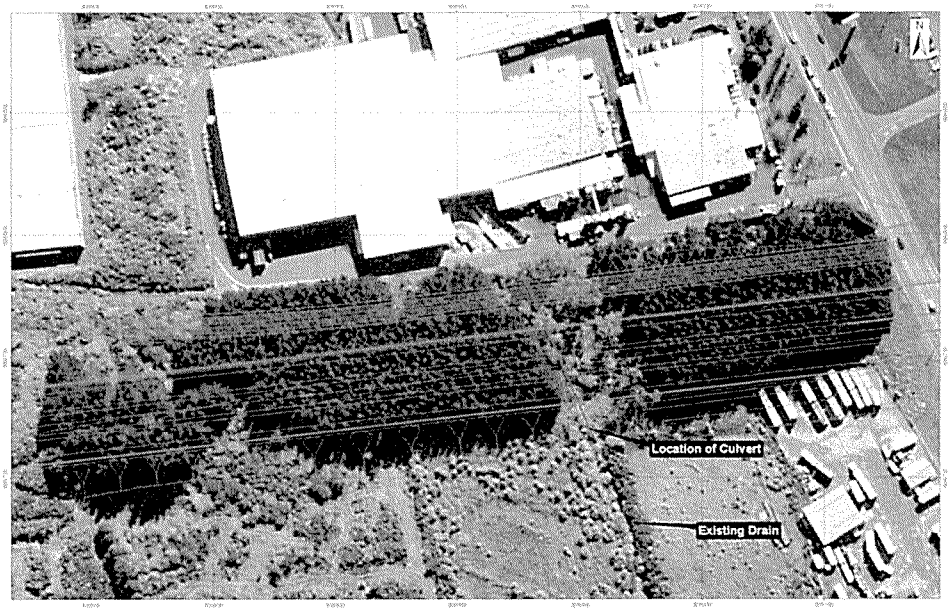

Figure 1: Location of culvert

3 SOIL PARAMETERS

Site investigations were undertaken included; boreholes, Cone Penetration Tests (CPT), and test pits. Selected samples collected from these investigations were tested to access parameters such as compressibility, particle size distribution, rock strength and permeability. The laboratory data was combined with experienced engineering judgment to develop parameters for use in the analysis.

4 PLAXIS BACKGROUND AND MODEL USED

PLAXIS is a finite element modeling software package that provides analysis of a large range geotechnical problems. PLAXIS was chosen as the preferred software to model this site as it is capable of calculating consolidation times, stability and deformations from the same model.

A Mohr-Coulomb (M-C) elastic - plastic model and drained soil types were adopted for the fill basalt, sand and culvert material.

A soft soil model similar to a Cam-clay model was used for the soft soils as it is generally considered to model normally-consolidated, highly compressible soft soils more accurately than the Mohr-Coulomb model. The soft soil model was used for the soft clay, silty clay and desiccated clay materials in the profile using undrained parameters.

Features of the soft soil model:

- stress dependent stiffness (logarithmic compression behavior)

- distinction between primary loading and unloading-reloading
- memory for pre-consolidation stress
- failure behavior according to the Mohr-Coulomb criterion

Basic parameters required for the modeling are:

- E = Young's modulus – M-C modeling
- ν = Poisson's ratio – M-C modeling
- λ^* = Modified compression index – soft soil modeling
- κ^* = Modified swelling index – soft soil modeling
- c = Cohesion – both M-C and soft soil modeling
- φ = Friction angle – both M-C and soft soil modeling
- Ψ = Dilatancy angle – both M-C and soft soil modeling

λ^* and κ^* can be obtained from the one-dimensional consolidation test.

Stone columns were used on this site to improve the soft soils and provide two major benefits:
1. The columns improve the strength of the soil mass.
2. The columns are significantly more permeable than the surrounding soil and therefore improve the drainage of the soil mass and reduce the time required for consolidation.

There are two commonly adopted methods for modeling the stone columns:
1. Alter the permeability and soil strength of the whole soil mass that incorporates the stone columns to reflect the improved soil characteristics due to the presence of the stone columns.
2. Model the stone columns as individual rigid elements.

Method 1 (improving the soil mass) was adopted to model the changed soil conditions due to the installation of stone columns. This method provides a more time efficient model, both in initial setup of the input model and calculation times.

5 MODEL DEVELOPMENT

The soil model was developed from the boreholes and CPT tests within the vicinity of the culvert. Basalt intrudes under part of the culvert alignment as shown in Figure 2 and was included in the model.

Stone columns were installed at 2.0 m centre to centre spacing under the extent of the embankment over the culvert. The soil improvement method was used for simplicity and stone columns were installed on a 2.0 m x 2.0 m square grid. With the inclusion of stone columns the surrounding soils is anticipated to improve by a factor of $\eta = 1.65$ (Priebe, 1995).
The model was constructed using points and lines with a mesh created from either 6-noded or 15-noded triangular elements. The line elements define the physical boundaries of the geometry and differing soil layers (Waterman, 2008).

The sides and base of the model must have boundary conditions. In this case standard fixities were selected. As a result PLAXIS automatically generates a full fixity along the base, i.e. no displacement in the horizontal and vertical directions with horizontal fixity along the sides allowing vertical movement.

The initial conditions of the modeled subsurface zone must now be generated and these include groundwater conditions, the physical geometry and initial effective stress state. The pore pressures in the model were generated based on the phreatic surface. The initial stresses were created using the K_0-procedure, where K_0 is selected according to Jaky's formula ($K_0 = 1\text{-sin } \varphi'$)

(Waterman, 2008). This initial stress generation only applies to horizontal soil layers as inclined surfaces are not in equilibrium for the K_0-procedure. This is resolved in the first calculation phase by running a plastic calculation followed by complete consolidation. The balanced stress state created in this stage then provides the basis for the following phases.

In the analysis surcharge is placed over the proposed culvert location in order to consolidate the soft foundation soils prior to construction of the culvert. The surcharge load is removed, the culvert constructed and the fill subsequently replaced to final height. This construction method reduces possible damage to the culvert as primary consolidation takes place under the surcharge load and minimal further displacement occurs following reloading of the final fill material.

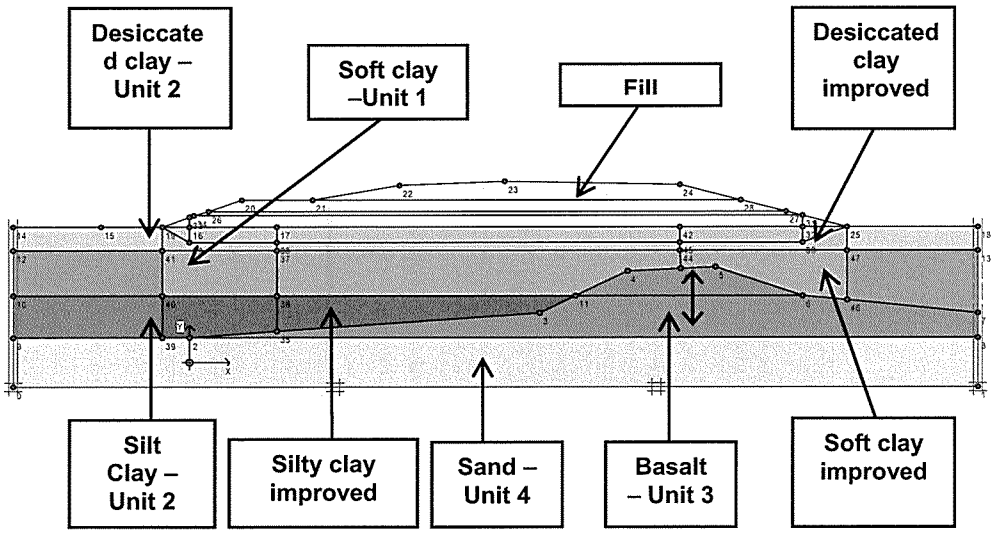

Figure 2: Input model

6 CALCULATION PHASES

The staged construction calculation steps were used in the model as this enables the placement of fill in layers with a set amount of consolidation before the next layer is placed. This was critical at this site due to the potential instability of the embankment and soft founding soils if the embankment was constructed in a single lift. After each consolidation stage had been completed, a stability analysis was undertaken to assess the safety factor. This calculated safety factor controlled the amount of consolidation and associated strength gain required prior to placing more fill. Utilizing PLAXIS in this way reduces the construction time as predictions can be made as to minimum pause period required and maximum fill layer thicknesses allowable.

The updated mesh feature was used in the calculations as this allows the deformations from one stage to become the starting point for the next. It is generally considered good practice to use updated mesh analysis and this approach is important if more than 10 % strains are generated.

The fill was left in place until sufficient excess pore dissipation had occurred, indicating that primary consolidation had been largely completed. At this point the fill was removed, reducing the stress on the soil and the model showed a small amount of rebound. The culvert was installed in the model and the fill material placed to its final height. This last step was achieved in one calculation phase as the soil had already been consolidated. Figure 3 shows the construction site with the temporary diversion of the stream.

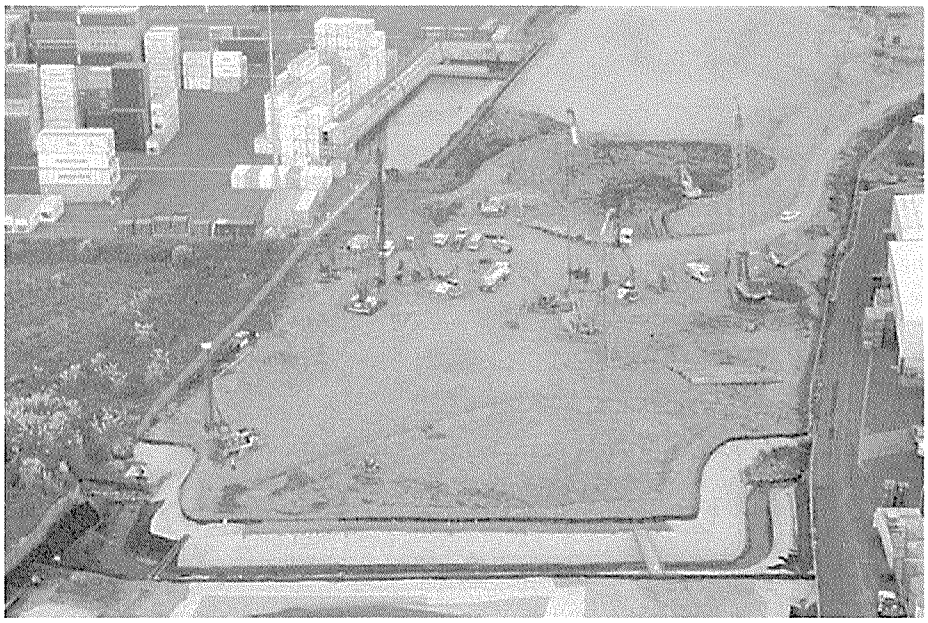

Figure 3: Construction site

7 RESULTS

The specified consolidation required to be completed for each stage prior to continuing filling is shown in Table 1 below:

Table 1: Set consolidation achieved in each fill stage

Construction stage	Maximum excess pore water pressure (kN/m^2)	Days to achieve maximum excess pore water pressure
First lift – 1.8 m	30	94
Second lift – 1.8 m	15	87
Third lift – 2.2 m	1	174
Unloading – 5.8 m	1	63
Final fill – 5.8 m	1	149

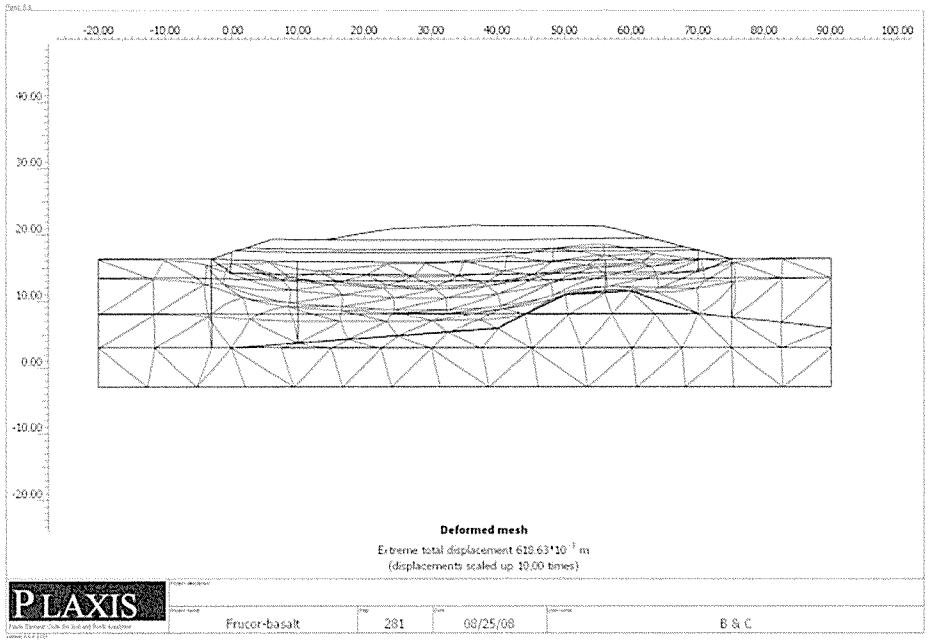

Figure 4: Final deformed mesh

The minimum factor of safety against embankment failure as calculated by PLAXIS for each stage was 1.9, this occurred following construction of the third fill layer.

Final calculated displacements along the culvert alignment were 620 mm with total phase displacement post consolidation of the final fill of 100 mm. It is this final stage displacement that will affect the hydrologic performance of the culvert in the long term.

As shown above in Figure 4, the displacement varies over the culvert alignment due to differing fill heights. The positive effects of the improved soil and the presence of the basalt can be seen.

8 CALIBRATION OF MODEL AND FIELD MONITORING

The PLAXIS modeling is beneficial in terms of actual field behavior when monitoring is also undertaken to measure settlements and the dissipation of excess pore pressures. Monitoring was carried out under the embankment using settlement plates and vibrating wire piezometers. These instruments allow the embankment behavior to be monitored and compared with the predications calculated in PLAXIS.

Monitoring is important, as the modeling is only a first step to obtain baseline expectations. The observed behavior will probably differ from the predictions due to variable soil conditions and other inconsistencies that are always present in the ground. Data obtained from monitoring allows the PLAXIS model to be updated and new predictions developed to improve the accuracy of the analysis.

9 CONCLUSION

The use of stone columns for soil improvement works provides two benefits; improving the soil stiffness and increasing the permeability of the soil which accelerates the rate of consolidation. PLAXIS is an effective finite element tool to model this behavior and provides a method of predicting excess pore pressures and expected settlements.

The modeling of stone columns can be carried out either by modeling them as individual columns or by modeling the overall improvement in the soil mass.

The staged construction feature allows specific design as to when and how much fill is placed on the soft soils within a set timeframe. This reduces potential stability concerns that may occur with placing the fill too rapidly and predictions can be made of expected consolidation times.
As with all geotechnical models, the calculated data must be correlated with field behavior and monitoring is an important part of the whole process.

ACKNOWLEDGEMENTS

This paper was written with the support of Golder Associates (NZ) Ltd. The author also acknowledges the assistance of the New Zealand Transport Agency and Leighton Works.

REFERENCES

Priebe, H.J. (1995) Design of vibro replacement, *Ground Engineering,* 28(10), 31-37.

Tan, S.A, Tjahyono, S., Oo, K.K. (2008) Simplified Plane-Strain Modeling of Stone-Column Reinforced Ground, *Journal of Geotechnical & Geoenvironmental Engineering*,134:2,185-194.

Waterman, D. (2008) Introduction to Plaxis, Workshops and Hands on Training: *Geotechnical Engineering Practice via Plaxis.*

Monitoring of William Street Station Box – Perth, Western Australia

Owen Woodland
Golder Associates, Perth, Western Australia.

Keywords: inclinometer, station box, diaphragm wall, monitoring

ABSTRACT

William Street Station is an underground station in the Perth central business district associated with the recently opened Perth southern suburbs railway. The station box was built top-down using diaphragm walls and supporting slabs. An adjacent multi-storey building, currently under construction, was designed with basement levels well below the top of the station box. Construction of such a building could potentially lead to movement of the station box resulting from unequal earth pressure and hydrostatic loading. Design approval was granted with strict conditions about the movements of the station box. This paper discusses the modelling of the station box movements as a result of the construction, the monitoring program implemented during construction and the outcomes of the monitoring program.

1 INTRODUCTION

1.1 William Street Station

William Street Station was constructed leading up to the opening of the Perth southern suburbs railway in December 2007. The underground station is housed within a station box as indicated in Figure 1. The station is built over two levels, with elevations as shown in Table 1.

The station box was constructed top-down with diaphragm walls formed from reinforced concrete. Excavation was carried out between the walls. Lateral support was provided in the permanent case by slabs at the base level, concourse level and top of the station box.

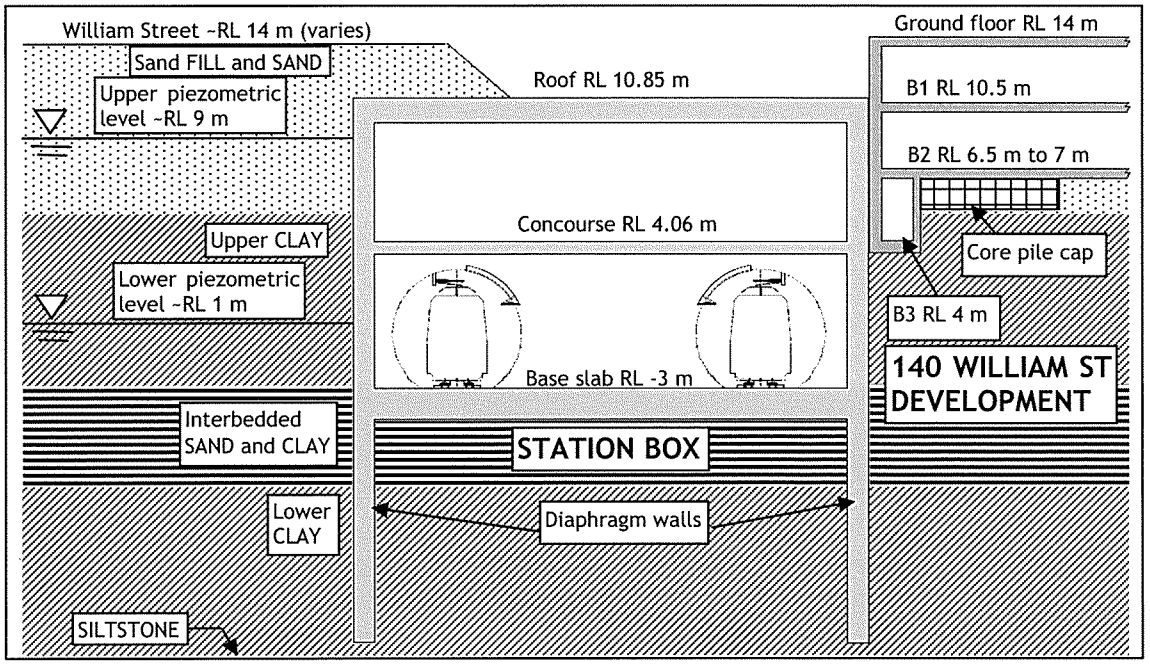

Note: AHD – Australian Height Datum

Figure 1: Typical section through station box and 140 William Street Development

1.2 140 William Street Site

After construction of the structure of William Street station was complete, the adjacent site was made available for development. The site had previously been occupied by a heritage building and a former department store, including a basement.

The new building at 140 William Street (currently under construction at the site) comprises a 21 storey tower with a basement up to 3 levels deep. Basement levels 1 and 2 cover most of the site. Basement level 3 is restricted in plan area to a small area immediately adjacent to the station's east diaphragm wall, where a connection to the station through the diaphragm wall is made at the concourse level (as indicated on Figure 2). The levels of the lower floors of the development and the corresponding levels in the station box are as indicated in Table 1 and Figure 1. The section is taken through the section of the site where B3 is present.

As the 140 William Street development is being built bottom-up, excavation is necessary against the eastern side of the station box. This requires dewatering and removal of lateral restraint from the eastern side of the box, while the western side continues to experience lateral pressures from soil and groundwater. The resulting imbalance was expected to lead to lateral movements of the station box towards the excavation.

The owner of the station, the Public Transport Authority (PTA) specified that movements of the station box diaphragm wall must be limited to the values nominated by the designer as shown in Table 1. The PTA required that pre-construction modelling and monitoring during construction be undertaken to demonstrate that deflections would not exceed these limits. The PTA required that propping be undertaken for any excavation adjacent to the station box. A limit on excavation of RL 7 m AHD was also imposed by PTA.

Table 1: 140 William Street and station box levels and lateral deflection limits

140 William St Floor Level [RL (m AHD)]	Station Box Floor Level [RL (m AHD)]	Maximum allowable lateral deflection of station box (mm)
Ground floor [14.0]	-	-
Basement B1 [10.5]	Roof level [10.85]	10
Basement B2 [6.5 to 7.0]	-	-
Basement B3 [4.0]	Concourse level [4.06]	5
-	Base slab [-3.0]	Not specified

2 PRE-CONSTRUCTION DESIGN AND MODELLING

Golder Associates undertook modelling to assess the effects of the 140 William Street construction on the station box. The most detailed modelling was undertaken using PLAXIS 2D. The modelling accounted for the construction sequence of the 140 William Street development in assessing deflections of the station box. The stratigraphy used in the modelling is indicated on Figure 1. Soil properties were adopted as used by the designers of the station box, in order to limit conflicting opinions.

Short-term soil strength was not considered to be an issue during construction for deflection of the station box. Accordingly, modelling was undertaken using drained (effective strength) parameters using the Mohr Coulomb soil model, with the exception of the siltstone, which was taken as undrained.

Pore water pressures were modelled as hydrostatic, with two water tables (upper and lower, separated by an aquiclude clay layer). The upper water table was modelled at RL 9 m and the lower at RL 1 m AHD.

The structural elements (diaphragm walls and slabs) were modelled as plate elements. Moment connections were included at the roof and base levels between the slabs and the diaphragm walls. Pinned connections were used at the concourse level. Lateral restraint to the roof level of the station box was provided by three large, pre-loaded I-section props (see Figure 2). The props were supported by special additional barrettes and tie beams. Modelling included an allowance for the restraint expected because of the three-dimensional effects of the longitudinal stiffness of the station box acting as an effective beam between lateral restraint locations.

The expected movements of the station box wall were assessed at two excavation stages. The results are summarised in Table 2 as the calculated maximum lateral deflections at each stage. Also shown is the expected overall maximum lateral deflection allowing for disturbance caused by demolition, earthworks, prop installation and bulk excavation. These calculated movements were expected to be conservative due to the conservative three-dimensional effects incorporated into the 2D analysis and the conservative soil stiffness parameters used.

Table 2: Summary of station box maximum lateral deflection predictions

Floor level [RL (m AHD)]	Bulk Excavation to B2 Level (RL 7 m)	Bulk Excavation to B3 Level (RL 4 m)	Overall including all demolition and construction
Roof [10.85]	5	5	8 to 10
Concourse [4.06]	4	7	8 to 9
Base [-3.00]	2	4	4 to 5

The above deflections account for the presence of props, which were installed prior to the B2 level bulk excavation. The maximum calculated deflections were greater at the concourse level than specified by PTA but were accepted (in part, because of the modelling conservatism). Construction was allowed to proceed, subject to undertaking a detailed monitoring program.

3 MONITORING PROGRAM

3.1 General Description

A monitoring program was implemented to monitor the lateral movements of the station box and the piezometric levels on the west side of the station box. A list of the monitoring equipment installed, the objectives of monitoring and the monitoring frequency is presented in Table 3. Figure 2 indicates the plan locations of monitoring equipment relative to the station box and the 140 William St construction site.

Table 3: Summary of monitoring equipment

Item [Count]	Installation Method	Monitoring Objective	Typical Reading Frequency
Inclinometers [5]	In grouted boreholes 3 west of station box 2 east of station box	Assessment of lateral deflection profile of station box along excavated interval	Weekly to fortnightly
Tilt Plates [8]	Glued to station box walls at concourse level	Assessment of angular rotation of station box wall at around RL 5 m	Weekly to fortnightly
Piezometers [2]	Standpipes in boreholes on west of station box	Assessment of piezometric levels in the upper aquifer on the retained side of the station box	Weekly to fortnightly
Survey points [12]	Survey nails installed into station box roof	Three-dimensional measurement of station box movements (particularly laterally)	Weekly
Strain gauges [3]	Bonded to I-beam props	Assessment of load in props	Continuous after prop installation

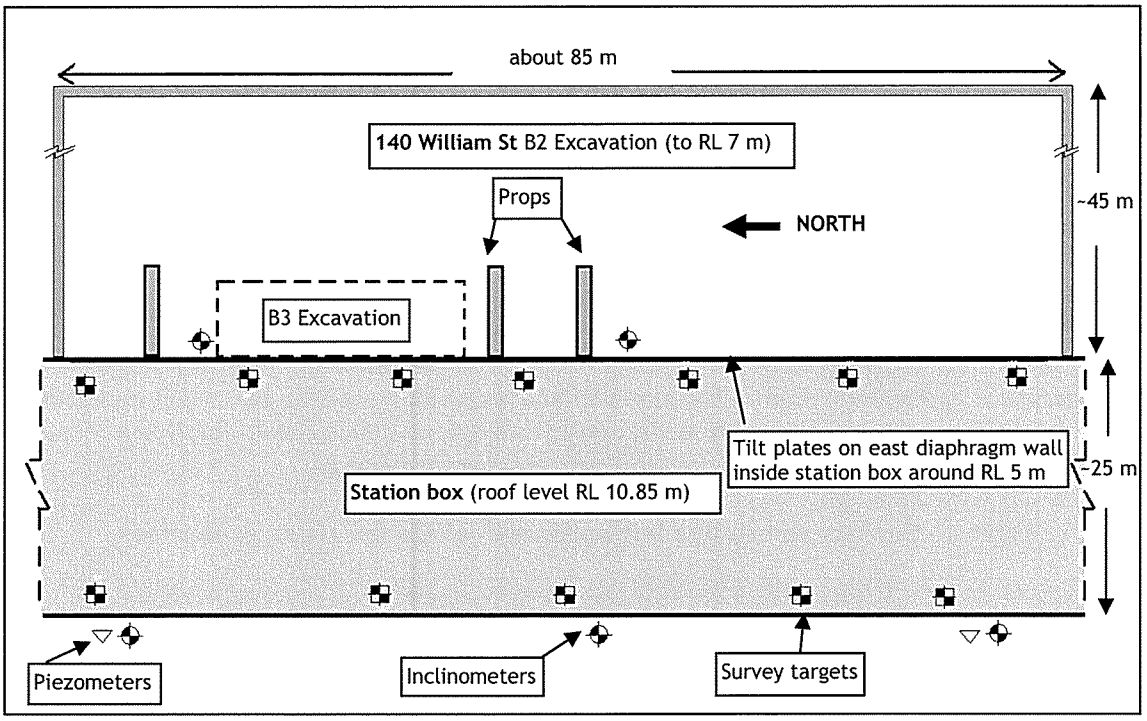

Figure 2: Plan locations of monitoring equipment

3.2 Results of Monitoring

Monitoring results were presented to the client on an ongoing basis throughout construction, with an emphasis on timing monitoring periods to coincide with major construction activities, such as installation of the props, excavation to B2 level, excavation to B3 level and tying-in of the basement slabs (after which time, the station box was supported by the basement slabs and external restraint from the props became redundant). The results of the monitoring equipment are considered individually in the following sections.

3.2.1 Inclinometers

Typical results of inclinometer monitoring are presented in Figure 3 as cumulative displacement versus time since first monitoring for levels corresponding to the station box roof, concourse level and base slab. I2 is the central inclinometer on the west side of the station box and is representative of all inclinometers, including those on the east side of the station box.

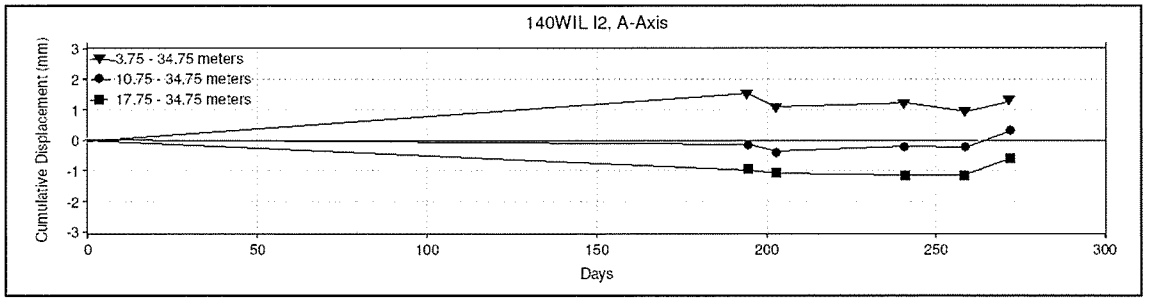

Figure 3: Time Displacement, I2, A-axis

The inclinometer results generally indicated less than 2 mm of movement at the station box roof and concourse levels. Minor variations during the different monitoring rounds indicate that the effective accuracy of the inclinometers was no better than 3 mm to 4 mm at the top of the station box (consistent with manufacturer guidelines).

3.2.2 Tilt Plates

Within the accuracy of the tilt meter used to read the tilt plates, essentially zero rotation of the east wall of the station box during construction was recorded.

3.2.3 Piezometers

The piezometers indicated that the piezometric level in the upper aquifer on the east side of the station box fell from around RL 9.2 m at the commencement of excavation to around RL 8.5 m at the completion of excavation. Seasonal variation is likely to have been responsible for most of this fall. Piezometric levels were consistently lower than the design level.

3.2.4 Survey

Results of the conventional surveying (typically accurate to around 3 mm in each dimension) showed zero displacement at each of the 12 monitoring points over the monitoring period.

3.2.5 Strain Gauges

An example of the results of the strain gauge monitoring is presented in Figure 4 as prop load versus time for the south prop. Also shown is the prop temperature. The strain gauge output is corrected for temperature and bending effects through use of longitudinal and lateral strain gauges connected via a Wheatstone bridge. The intended preload for each prop was around 2,500 kN, or around 50% of the calculated working loads. Hydraulic difficulties were encountered during preloading of the props and none achieved the full preload. Each prop indicated an overall fall in load over the construction period, which appears to be due largely to a fall in the ambient temperature. None of the props appeared to take significant additional load arising from movement of the station box.

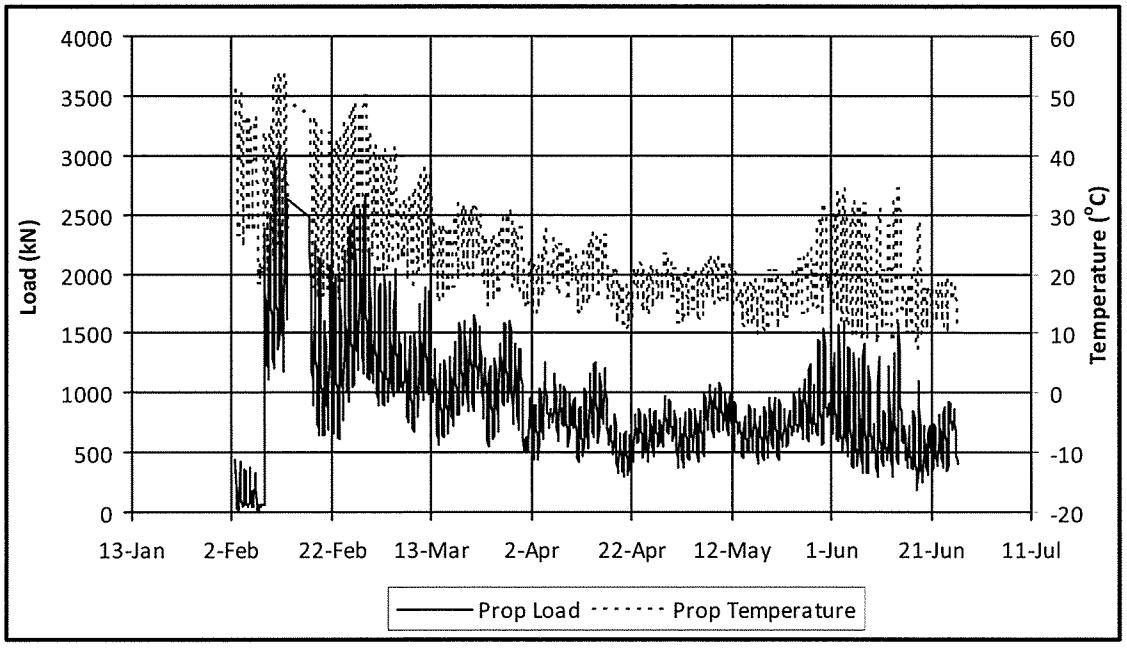

Figure 4: Prop loads and temperature - south prop

4 DISCUSSION

The displacement monitoring equipment installed, particularly the inclinometers, indicated that the movements of the station box were either zero or less than 2 mm to 3 mm at the station box roof level. Based on the results and previous experience, methods of monitoring lateral displacements of the station box other than the inclinometers were considered to be less reliable,

that is the inclinometers were viewed to be the most accurate measure of the station box lateral displacements within the site constraints. None of the methods of monitoring showed clear evidence of lateral displacement of the station box. The location and density of measurement was considered adequate to pick up significant lateral movements, had they occurred.

Accuracy of the inclinometer readings could potentially have been improved by using an in place inclinometer (IPI) system. However, the system available at the time of installation was not considered to have sufficient resolution to monitor movements of the station box accurately.

The fact that the direct measurement of strain (and hence load) on the props showed essentially no increase in load (and generally a decrease) during the bulk excavation program supports the contention that the station box did not move significantly laterally toward the excavation. Concrete and grout shrinkage around the ends of the props may have influenced this outcome somewhat, but preload of the props was expected to account for such factors.

Various scenarios were run in the PLAXIS 2D modelling in which model parameters were changed from those used in the original station box design to assess the impact on the lateral movements of the station box. None of these models indicated zero lateral station box displacements. The displacements were expected to reduce if:

- the station box diaphragm walls were stiffer than accounted for;
- moment transfer occurred at concourse level between the diaphragm walls and slab;
- shear in the roof and base slabs was accounted for (in a more sophisticated 3D analysis);
- the soils (particularly the upper soil sequence) were stiffer than modelled;
- the at-rest lateral earth pressure coefficients of the upper soil sequences were reduced; and
- the piezometric level on the west side of the station box was reduced.

The analyses carried out were two-dimensional and ignored some mitigating three-dimensional effects, e.g. restraint of the return diaphragm walls at the north and south of the 140 William Street excavation and the finite length of the excavations (85 m for B2 and 25 m for B3).

The fact that the monitoring equipment indicated near-zero lateral displacement is probably a consequence of a mixture of all the above factors. It is difficult to assess a specific cause for the discrepancy between the preliminary displacement estimates and those observed as theory (and logic) would suggest that at least *some* movement would be expected. Some lateral movement probably did occur, but so small that it could not be measured reliably within the limits of the available equipment.

5 CONCLUSION

Lateral restraint of the station box and a construction monitoring program were requirements set down by PTA for the 140 William Street Development. The adopted monitoring program was considered adequate to demonstrate that the deflection limits specified by PTA were met.

The monitoring program undertaken indicated that the station box experienced near-zero lateral displacements during construction. However, given the value of the assets being protected by restraint of the station box and potential impacts of loss of its serviceability, the conservative construction approach is considered to be warranted.

The outcomes of the monitoring program have confirmed that deflections were generally less than the lateral displacement estimated before construction. The outcomes of the monitoring program will be considered when undertaking future modelling, particularly by undertaking three-dimensional soil-structure interaction analyses and removing some of the conservatisms in the analysis.

Implementation of Soil Ageing in Liquefaction Assessment for the Tauranga Harbour Link Project

Carol Yan
Tonkin & Taylor Ltd - Engineering and Environmental Consultants, Auckland, New Zealand

Keywords: earthquake; liquefaction; cyclic mobility; soil ageing; pumiceous soils; cementation; densification; Standard Penetration Test; Atterberg Limits; Cyclic Triaxial test

ABSTRACT

The geologic age of soil deposits is a factor that is considered to increase its liquefaction resistance, however these effects are difficult to quantify and incorporate into typical quantitative liquefaction assessment methods such as SPT and CPT-based assessments. Soil ageing processes such as particle cementation and densification are often destroyed or not fully captured in SPT and CPT sampling methods. Similarly, pumiceous soils which tend to crush and compress under bearing can result in misinterpretation of the soil characteristics when using conventional correlations of SPT and CPT data.

The liquefaction assessments for the Tauranga Harbour Link (THL) project had to consider the results of relatively low SPT and CPT penetration resistances of Pleistocene aged and pumiceous soils. In isolation these low penetration resistances would indicate the soils to be susceptible to liquefaction, however laboratory test results indicated low liquefaction potential. This paper presents the results of a sensitivity assessment of the effects of soil ageing on the liquefaction potential of the soils within the Chapel Street Viaduct (CSV) section of the THL project, based on the state-of-the-art method by Leon et al. 2006.

1 PROJECT BACKGROUND

The Tauranga Harbour Link (THL) project by Transit New Zealand aims to expand and develop the existing traffic route between Takitimu Drive and Tasman Quay in Tauranga. Stage 2, currently under construction, begins with the construction of Chapel Street Viaduct (CSV), linking the Takitimu Drive Expressway to a new harbour bridge (NHB) across Stella Passage. The carriageway expansion continues along side the existing route over the reclamation causeway adjacent to the Tauranga Harbour Marina, towards Aerodrome Bridge (AB) which will also be duplicated.

2 SITE DESCRIPTION

2.1 Geotechnical Investigations

In total, the geotechnical site investigation for the project comprised 60 CPT profiles, and over 80 machine drilled boreholes, with SPT tests and associated laboratory testing of retrieved samples. Two of the CPT probes were seismic CPTs, yielding shear wave profiles. Laboratory testing included Atterberg Limit classification, triaxial tests, cyclic triaxial tests, particle size distributions and electron microscopic examination. The majority of the investigations were completed at the specimen design phase, with SPT and CPT data used in preliminary liquefaction assessments. Based on these assessments, "Minimum Depths of Liquefaction" were evaluated along the route alignment and included in the Principal's Requirements, stating that above these depths soils were required to be assumed as liquefiable in a design event. A further round of borehole investigations was undertaken in mid 2007 for detailed design, which formed proof-drilling for piles. This data was included, where possible, in the liquefaction potential assessments at detailed design.

2.2 Site Geology

The site geology reflects the marine and volcanic environs, with generally Ignimbrite basement rock at depth, overlain by various deposits of estuarine, fluvial and volcaniclastic origins. The depositional processes are complex, with interbedding and reworking of the various materials resulting in a highly variable geological profile, including indistinguishable strata boundaries, variable strata thicknesses and discrete lenses of deposits apparently out of sequence with the general depositional processes.

The stratigraphy of the route corridor can generally be summarised as reclamation fill, overlying Holocene aged sediments comprising loose sandy Beach Deposits and soft, silty, organic rich Estuarine Deposits. Beneath this were Pleistocene aged sediments, with Ignimbrite material at depth. The Pleistocene deposits were sub-divided into interbedded Airfall and Sand units. The Airfall deposits by nature were finer grained and comprised silts, often sandy, generally soft and highly sensitive with varying plasticity. The Sand deposits were generally fine sand, loose to dense though becoming denser with depth and in local zones. These deposits were typified by some fine pumice gravel inclusions.

The Ignimbrites, generally encountered below RL -20 m, are also of the Pleistocene age, though they are estimated to be significantly older than the shallower Pleistocene deposits. Generally, the Ignimbrite deposits exhibited a trend of becoming denser with depth, which was reflected in the SPT N values; however there were also several uncharacteristic test data points, with uncorrected N values below 10, which is very unusual for such sand deposits at depths. The depths and characteristics of all the stratigraphical units varied considerably along the route alignment, however a summary is compiled in Table 1 below.

Table 1: Summary of Site Geology

Geological Unit	RL (m) range	Sub-units	General Soil Description	SPT 'N' range	CPT q_c (MPa)
Fill	down to RL-4m	Fill	Variable, derived from local marine sediments	5 – 10	1 – 5
Holocene Aged Deposits	down to RL-20m	Beach Deposits	Loose fine sands, trace pumice gravels	0 – 10	1 – 12
		Estuarine Deposits	Very soft silt, trace gravels, organic rich, non to moderately plastic	0 – 17	0 – 1
Late Pleistocene Aged Deposits	RL-5m to RL-50m	Upper Airfall	Soft sandy silt to very loose sand, variable plasticity, highly sensitive	0 – 35	1 – 2
		Upper Sands	Loose to dense, fine to medium sands, sometimes silty and pumiceous	0 – 50	2 – 8
		Lower Airfall	Soft sandy silt to loose sand, variable plasticity, sensitive	1 – 38	4 – 5
		Lower Sands	Medium dense fine sand, sometimes silty, becoming locally dense to very dense	5 – 11	3 – 20
Older Pleistocene Aged Deposits	from RL-20m	Ignimbrite Mantle	Very stiff silt with minor clay, to sandy silt	0 – 50+	-
		Ignimbrite	Medium dense to dense sand, medium grained, minor pumice gravels	0 – 50+	-
		Basal Sands	Very dense sand, fine to medium grained, minor silt	10 – 50+	-

2.3 Pumiceous Soils

The Tauranga region is typified by its pumiceous deposits, a soil which is noted for following classical soil behaviour mechanisms. Pumice particles are characterised by fine vesicles which can lead to low relative densities and high air voids, but relatively high strengths. Recent research investigated the mechanisms by which pumiceous soil particles tend to crush and compress under bearing, even at relatively low overburden stresses, rather than displace and consolidate by particle re-orientation (Pender et al. 2006). The pumiceous nature of the soils encountered was considered as a possible explanation for the uncharacteristically low SPT N values (N<10) recorded for some of the deposits at significant depth and high confining stress.

2.4 Chapel Street Viaduct East

This paper will focus on a section of the alignment known as Chapel Street Viaduct East (CSV East) to provide an example of the SPT based liquefaction assessments undertaken for the THL project. The site investigations within this area comprised 19 boreholes with a total of 560 SPT samples used for liquefaction assessment, and also 14 CPT probes.

The stratigraphy of CSV East is characterised by an infilled paleo-historic channel of Estuarine Deposits. This buried channel extends to RL -17m at its deepest, with other deposits being encountered deeper than typical of the rest of the route. The Upper Airfall unit is locally displaced by the Estuarine Deposits, with the Lower Airfall and Lower Sands units generally found below RL -20m. The Ignimbrite derived deposits are encountered from RL -30m downwards, though the Ignimbrite Mantle unit is locally absent. SPT samples showed a general trend of becoming denser with depth, from approximately RL -16m; however some uncharacteristically low SPT samples with N values less than 10 were noted between RL -25m and -31m (Figure 3a).

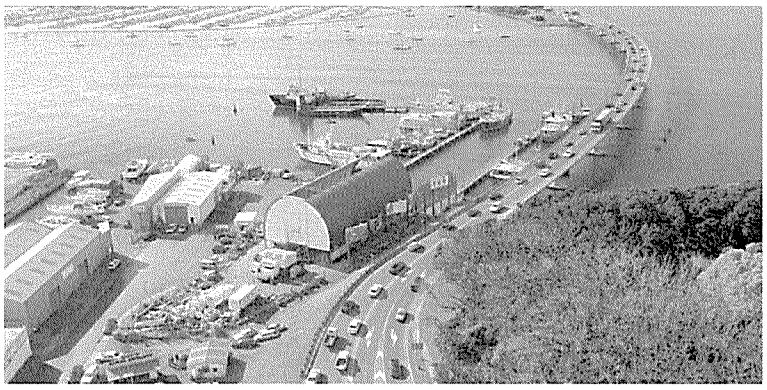

Figure 1: Looking east over CSV East, towards Stella Passage. The existing Harbour Bridge will be duplicated to the north (left)

3 LIQUEFACTION ASSESSMENT

3.1 A Unified Approach to Liquefaction Potential Assessment

A unified approach to liquefaction assessment was adopted for the THL project to permit a more complete understanding of the liquefaction potential for the site. Different techniques were undertaken and results incorporated together, including SPT, CPT, laboratory data and shear wave based assessments. In accordance with the Principal's Requirements, NCEER Technical Report 97-022 (Youd et al. 2001) was adopted as the base reference for liquefaction assessments undertaken. This publication summarises what is now established as current practice for liquefaction potential assessment, evolved from Seed and Idriss' pioneering "simplified procedure". The deterministic, originally SPT based approach, yields a Factor of Safety against liquefaction from empirical correlations for the cyclic demand of a design earthquake (CSR) and the cyclic resistance of the soil (CRR). More recent developments, including the publication by Seed et al. (2003) which aims to provide a "unified and consistent framework" to liquefaction assessment, were also included.

3.2 Laboratory data based Liquefaction Potential Assessment

Laboratory data, particularly Atterberg Limits classification, is typically used as an initial assessment of liquefaction potential, based an overview of a soil's inherent material properties, without consideration to factors such as overburden, groundwater and strength parameters which are obtained from in-situ SPT and CPT investigations. For the Tauranga Harbour Link project, laboratory based assessment was critical from an engineering perspective to provide a general rationalisation and interpretation of the variable deposits. The Modified Chinese

Criteria by Andrews and Martin (Seed et al. 2003) was adopted, for which the results are presented below in Figure 2. Generally, it can be concluded that the finer grained soils are of low liquefaction potential. This assessment was supported by the cyclic triaxial tests undertaken. Of the 5 cyclic triaxial samples, representing Estuarine Deposits, Upper Airfall and Upper Sand units, none liquefied at the design earthquake Cyclic Stress Ratio (CSR).

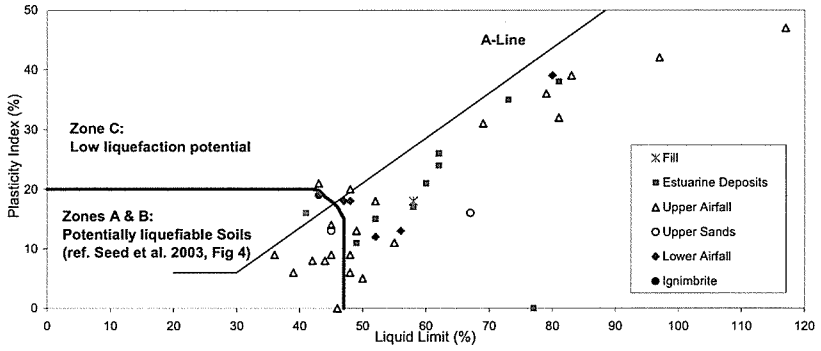

Figure 2: Liquefaction Potential Assessment by Modified Chinese Criteria

3.3 Soil Ageing in Liquefaction Assessment

It is generally accepted in principle though difficult to evaluate numerically, the argument that sediments deposited prior to the Holocene age are generally immune to liquefaction, most probably due to cementation and particle re-orientation processes which develop with age. Often, these processes and their effects on soil properties are not fully captured in SPT and CPT penetrations. Current research is at a stage of developing state-of-the-art relationships and methodologies to incorporate soil ageing into liquefaction assessment, of which the method proposed by Leon et al. 2006 was considered in the assessment for the THL project.

The proposed method incorporates empirical correlations which firstly back-ages a soil to when it was initially deposited, calculates the $CRR_{freshly\ deposited}$ of the soil, then utilises a "strength gain correction factor" to consider the improvement due to age on the CRR of the soil. It considers that the original CRR relationships developed (Youd et al. 2001) are not relevant for Pleistocene aged soils or older, since they were derived from younger Holocene deposits. As such, a correction factor is applied to those original correlations, to account for the older age. This $CRR_{aged/current}$ is then used in calculating the Factor of Safety against liquefaction for the soil.

Based on the principle that a soil begins ageing processes after it has been "freshly deposited", then a liquefied soil can be considered as freshly deposited, or re-deposited. Any earthquake which causes a soil to liquefy essentially freshly deposits the material again, from which point in time it recommences the ageing processes. As such, the "age" of the soil in liquefaction analysis should not be its true geologic age, but should conservatively be assessed as the time since the material most recently liquefied, or the period since the last liquefaction inducing earthquake. The soil ages conservatively used for liquefaction assessment are presented below in Table 2.

Table 2: Soil Ages used for Aged Liquefaction Potential Assessment

Geological Unit	Geologic Age	Liquefaction Assessment Age
Fill	< 100 years	not aged
Holocene Aged Deposits	~ 10,000 years	not aged
Late Pleistocene Aged Deposits	10,000 – 350,000 years	100 years
Older Pleistocene Aged Deposits	> 350,000 years	1000 years

Liquefaction assessment undertaken at CSV East was primarily interested in reviewing liquefiable materials below RL -20m, which was stipulated in the Principal's Requirements as

the Minimum Depth of Liquefaction for this alignment section. The design earthquake for the assessment was a 1000 year return event, with a Peak Ground Acceleration (PGA) of 0.29g, under an earthquake magnitude of 6.5. A statistical approach to assessing SPT results within sample clusters was adopted. SPT samples were visually assessed and clustered based on the known stratigraphy and similarities in SPT N values over an RL range. The sensitivity results of the liquefaction assessment incorporating soil ageing are presented below in Figure 3.

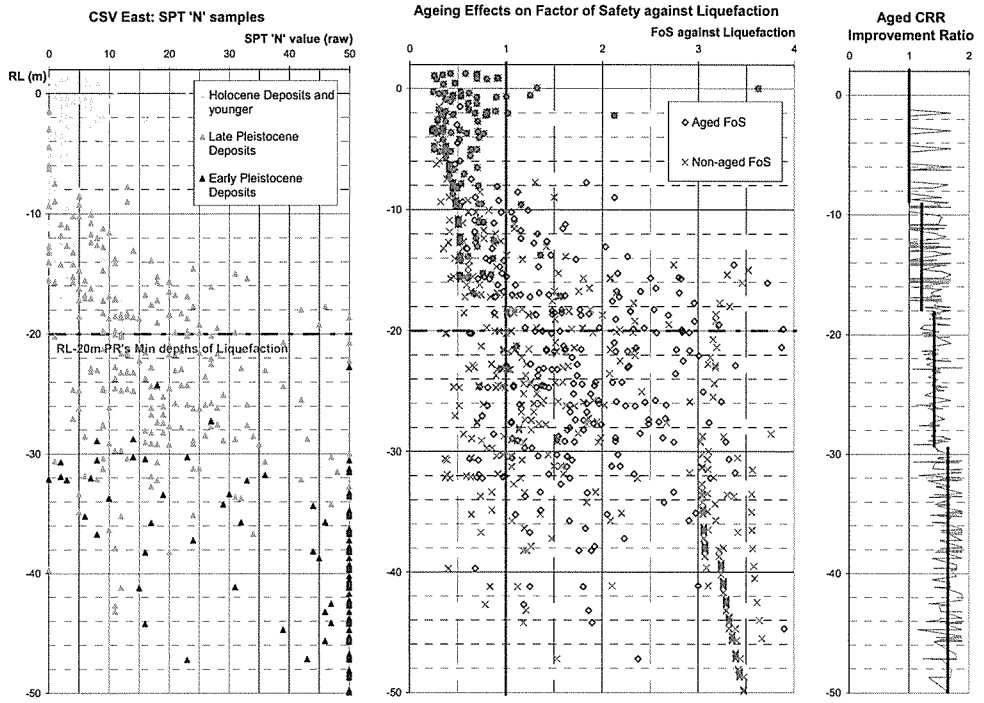

Figure 3: Soil ageing improvement effects on Liquefaction Potential at CSV East
(3a) (3b) (3c)

Under the design event, some low SPT samples between RL -25m and -37m, showed theoretical liquefaction potential with Factor of Safety against liquefaction less than 1.0 (Figure 3b). The use of soil ageing allowed the CRR of these samples to increase, and confirmed these to be non-liquefiable under a design event. The samples down to RL -30m were predominantly of the Late Pleistocene deposits, and improved in CRR by an average factor of 1.4 for 100 years ageing (Figure 3c). The SPTs from RL -30m to -37m included both samples aged 100 years (Late Pleistocene deposits) and samples aged 1000 years (Early Pleistocene deposits), and showed a slightly higher Aged CRR improvement in the order of 1.6.

Figure 3c summarises the effect of ageing on CRR and highlights the importance of selecting an appropriate soil age in liquefaction assessment. The Aged CRR Improvement Ratio is highly sensitive to the soil age considered, ranging from 1.0 for no soil ageing considered, up to a maximum of 1.8 at depth for the Early Pleistocene deposits, aged 1000 years. The sensitivity to soil age is illustrated in the Aged CRR Improvement Ratio down to RL -9m (Figure 3c). This depth range is dominated by Holocene deposits (Figure 3a), which were not aged, as the existing non-aged correlations (Youd et al. 2001) are considered appropriate for these soils. For no ageing, the Improvement Ratio remains at 1.0, however note how it spikes up to 1.7 for the few interdispersed Late Pleistocene deposits aged to 100 years.

It is tentatively considered that an Aged CRR Improvement Ratio up to a maximum value of 2.0 may be an appropriate limit for incorporating soil age benefits in liquefaction assessment. Soil age must be conservatively assessed to consider only the ageing processes which are not captured in SPT or CPT sampling, to ensure the Aged CRR is not artificially overestimated. Whilst this paper has focused on soil ageing of SPT based liquefaction assessment, the technique is also applicable to CPT analyses.

4 CONCLUSIONS

- A unified approach to liquefaction assessment between different assessment methods is critical to a broader understanding of soil behaviour and their liquefaction potential
- Laboratory data based liquefaction assessment is a critical technique to getting an overall understanding of a soil's behaviour and liquefaction potential
- Pumiceous soils by nature do not exhibit typical soil behaviour, with low relative densities and particles which tend to crush or compress under bearing, rather than consolidating and re-aligning as per classical soil mechanisms
- These atypical mechanisms can lead to misinterpretation of low SPT and CPT penetration in pumiceous soils and falsely indicate a liquefaction potential, despite their often high strength
- Implementation of soil ageing methods into liquefaction assessment is a possible means of improving these interpretations
- Further research is required into understanding pumiceous soil mechanisms and correlating pumice soil parameters to typical soil tests such as SPT and CPT
- Soil age is an important consideration for assessing liquefaction potential of a material
- Generally, soils of the Pleistocene age and older can be considered non-liquefiable
- To date, there are few techniques to which allow quantitative assessment of this theory
- Leon et al. have proposed a method to account for soil age in liquefaction assessment by increasing the soil's CRR
- This method, which when used appropriately, can effectively confirm liquefaction resistance in SPT and CPT based assessments
- Aged CRR improvement is highly sensitive to the soil age considered
- The Aged CRR Improvement Ratio is an appropriate tool to assess the effects of considering soil age in liquefaction assessment
- A maximum limit of 2.0 is tentatively proposed for Aged CRR Improvement Ratio, to allow soil age benefits to be conservatively implemented
- Soil age must be assessed appropriately to ensure the CRR is not artificially over evaluated, leading to inaccurate assessment of liquefaction resistance
- Holocene aged deposits and younger should not be aged for liquefaction assessment, as established correlations (Youd et al. 2001) are generally appropriate for these soils
- Pleistocene aged deposits and older may be conservatively aged for liquefaction assessment
- The soil age used in liquefaction assessment should consider both the soil's geologic age, as well as when the soil last experienced a liquefaction inducing earthquake

REFERENCES

Leon et al. (2006) "Accounting for Soil Aging When Assessing Liquefaction Potential" *Journal of Geotechnical and Geoenvironmental Engineering.* Vol. 132, No. 3, p.363-377. ASCE, United States of America.

Pender et al. (2006) "Geotechnical Properties of a Pumice Sand" *Soils and Foundations.* Vol. 46, No. 1, p.69-81. Japanese Geotechnical Society, Tokyo.

Seed et al. (2003) *Recent Advances in Soil Liquefaction Engineering: A Unified and Consistent Framework. Report No. EERC 2003-06* University of California Earthquake Engineering Research Center, United States of America.

Youd et al. (2001) "Liquefaction Resistance of Soils: Summary Report from the 1996 NCEER and 1998 NCEER/NSF Workshops on Evaluation of Liquefaction Resistance of Soils" *Journal of Geotechnical and Geoenvironmental Engineering.* Vol. 127, No. 10, p.817-833. ASCE, United States of America.